National Research Council Canada

Conseil national de recherches Canada

NRC · CNRC

Canadian Journal of Fisheries and Aquatic Sciences

Journal canadien des sciences halieutiques et aquatiques

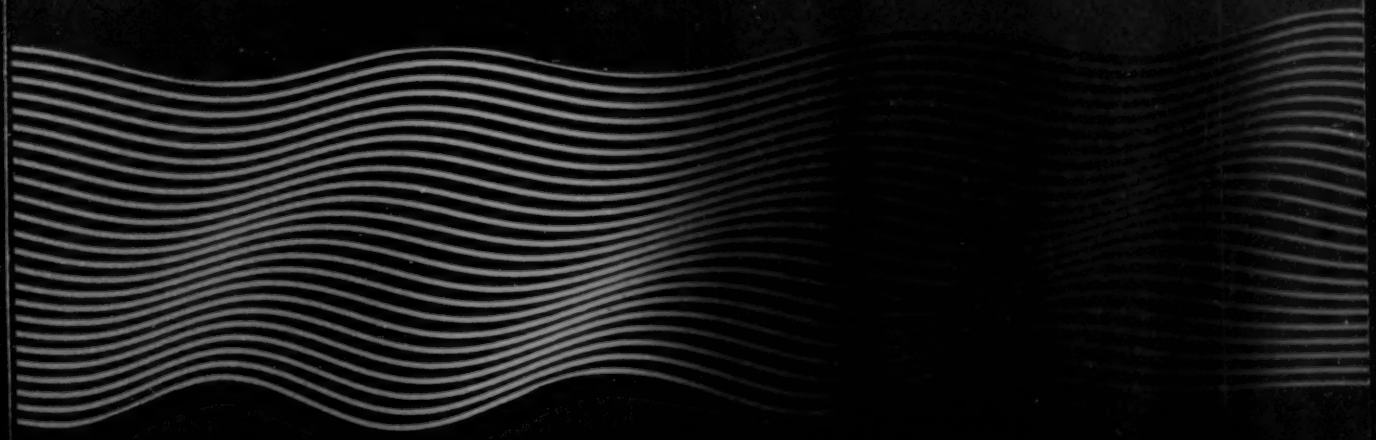

http://cjfas.nrc.ca

http://jcsha.cnrc.ca

ISSN 0706-652X / CJFSDX 59(3) 405–585 (2002)

The *Canadian Journal of Fisheries and Aquatic Sciences*, previously published as *Contributions to Canadian Biology* 1901–1925, *Contributions to Canadian Biology and Fisheries* 1926–1934, *Journal of the Biological Board of Canada* 1934–1937, and *Journal of the Fisheries Research Board of Canada* 1938–1979, is issued monthly to form annual volumes of 12 numbers plus supplements.

Editorial policy: The Journal publishes original research articles, perspectives (syntheses, critiques, re-evaluations), discussions (comment and reply), and rapid communications. Manuscripts may concern cells, organisms, populations, communities, ecosystems, or processes that affect aquatic systems. They may cover a range of disciplines including biology and ecology of marine and freshwater organisms, limnology, oceanography, physiology, toxicology, genetics, economics, disease, and management. Preference will be given to manuscripts that emphasize understanding of observed phenomena and interpretation of experimental results. The Journal encourages papers that lead from clearly stated purpose or rationale and from testable hypotheses, concepts, or questions to identifiable conclusions or syntheses. Such papers may amplify, modify, question, or redirect accumulated knowledge embodied in contemporary perceptions of a particular state of aquatic sciences. The Journal discourages papers that are essentially descriptive, except in emerging disciplines; have only site-specific or local applications (a certain year, place, taxon, chemical compound, etc.); only confirm previously established principles; or apply standard techniques without breaking new methodological ground.

Manuscripts for publication should be submitted to the Editors, *Canadian Journal of Fisheries and Aquatic Sciences*, Department of Zoology, University of Guelph, Guelph, ON N1G 2W1, Canada (519-824-4120 ext. 2646; fax: 519-767-9798; e-mail: cjfas@uoguelph.ca).

Submissions in either English or French are acceptable. The information must be original, that is, not copyrighted, published, or submitted elsewhere except in abstract form or unless by written consent of the Editor. NRC accepts no responsibility for statements or opinions expressed by a contributor. Acceptance of an advertisement, announcement, or other material does not imply endorsement by either the Journal's Editors or NRC. The use of proprietary names does not imply endorsement of the product or company.

Correspondence concerning accepted manuscripts and corrected proofs should be sent to NRC Research Press, National Research Council of Canada, Ottawa, ON K1A 0R6, Canada (fax: 613-952-7656; e-mail: research.press@nrc.ca).

Instructions to Authors are published once a year in the first issue of each volume. Copies are available from NRC Research Press or at http://cjfas.nrc.ca. The **Publication Policy** of NRC Research Press is available at http://cjfas.nrc.ca.

The National Research Council of Canada accepts no responsibility for statements or opinions expressed by a contributor. Acceptance of an advertisement, announcement, or other material does not imply endorsement by either the Journal's Editors or NRC.

Microfilm: Issues from 1934 through the current volume can be purchased on 16- or 35-mm microfilm. Photocopies of individual articles or issues can be purchased from University Microfilms International, 330 North Zeeb Road, Ann Arbor, MI 48106, U.S.A.

U.S. periodical postage paid at Champlain, N.Y., and at additional mailing offices. Attention U.S. POSTMASTER: Send address changes to **Canadian Journal of Fisheries and Aquatic Sciences**, c/o USACAN Media Distribution Center, P.O. Box 2888, Plattsburg, NY 12901, U.S.A.

Publié sans interruption depuis 1901, le *Journal canadien des sciences halieutiques et aquatiques* a paru sous plusieurs titres : *Contributions to Canadian Biology* 1901–1925, *Contributions to Canadian Biology and Fisheries* 1926–1934, *Journal of the Biological Board of Canada* 1934–1937, et *Journal of the Fisheries Research Board of Canada* 1938–1979. Le Journal paraît tous les mois, formant ainsi un volume de 12 numéros, et offre en plus jusqu'à deux suppléments par année.

Politique éditoriale : On publie, dans le Journal, des articles rendant compte de recherche originale, des perspectives (synthèses, critiques et réévaluations), des discussions (commentaires et réponses) et des communications rapides. Les documents peuvent porter sur les cellules, organismes, populations, communautés, écosystèmes ou processus qui affectent les systèmes aquatiques. Ils peuvent relever de divers domaines y compris la biologie et l'écologie des organismes marins et d'eau douce, la limnologie, l'océanographie, la physiologie, la toxicologie, la génétique, l'économie, la pathologie et la gestion. On accorde la préséance aux articles qui contribuent à la compréhension de phénomènes observés et à l'interprétation de résultats expérimentaux. On invite les auteurs à soumettre des articles ayant des objectifs précis ou relevant d'hypothèses, de concepts ou de questions vérifiables et se terminant par de solides conclusions ou d'utiles synthèses. Ces articles enrichissent, changent, mettent en question ou réorientent les connaissances acquises sur divers aspects des sciences aquatiques. On décourage toutefois la soumission d'articles simplement descriptifs (à moins qu'il ne s'agisse de nouvelles disciplines), d'application très limitée (applicables à une seule année, une seule région ou un seul taxon, portant sur un unique composé chimique, etc.); d'articles qui ne font que reprendre les principes énoncés dans des articles précédents; et d'articles rendant compte de l'application de normes sans gain de méthodologie.

Les auteurs voudront adresser leurs **manuscrits** aux directeurs scientifiques, *Journal canadien des sciences halieutiques et aquatiques*, Department of Zoology, University of Guelph, Guelph, ON N1G 2W1, Canada (519-824-4120 poste 2646; télécopieur : 519-767-9798; courriel : cjfas@uoguelph.ca).

Les contributions peuvent être en anglais ou en français. Elles doivent être originales, c.-à.-d. qu'elles ne doivent pas avoir fait l'objet d'un copyright, avoir été publiées ou soumises ailleurs, sauf sous forme abrégée ou avec le consentement du rédacteur. Le CNRC ne se tient en aucune façon responsable des opinions exprimées par un collaborateur ou des déclarations qui pourrait faire ce dernier. La publication d'annonces publicitaires, d'avis et autres n'implique pas l'endossement de leur contenu par les directeurs du Journal ou du CNRC. L'utilisation des noms de marques de commerce ne signifie aucunement une sanction du produit en question ou de la compagnie qui le fabrique.

La correspondance ayant trait aux manuscrits acceptés et les **épreuves corrigés** doivent être envoyées aux Presses scientifiques du CNRC, Conseil national de recherches du Canada, Ottawa, ON K1A 0R6, Canada (télécopieur : 613-952-7656; courriel : presses.scientifiques@cnrc.ca).

Les Recommandations aux auteurs sont publiées une fois par année dans le premier numéro de chaque volume. Des copies sont disponibles auprès du Bureau de la rédaction aux Presses scientifiques du CNRC ou au http://jcsha.cnrc.ca. **La Politique de publication** est disponible auprès des Presses scientifiques du CNRC ou au http://jcsha.cnrc.ca.

Le Conseil national de recherches du Canada ne se tient en aucune façon responsable des opinions exprimées par un collaborateur ou des déclarations que pourrait faire ce dernier. La publication d'annonces publicitaires, d'avis et autres n'implique pas l'endossement de leur contenu par les directeurs de la Revue ou du CNRC.

Microfilms : On peut acheter sur microfilms de 16 ou 35 mm tous les numéros depuis 1934. Des photocopies d'articles ou de numéros individuels sont aussi en vente auprès de University Microfilms International, 330 North Zeeb Road, Ann Arbor, MI 48106, É.-U.

This Journal is indexed or abstracted in / Cette revue est signalée ou résumée dans

ABSEARCH, Aquatic Sciences and Fisheries Abstracts, Biological Abstracts, Biological & Agricultural Index, CAB Abstracts, Chemical Abstracts, Current Contents, Elsevier BIOBASE, Environmental Abstracts, Environmental Periodicals Bibliography, GEOBASE, GeoRef, Internationale Bibliographie der Zeitschriftenliteratur, Life Sciences Collection, Meteorological and Geoastrophysical Abstracts, Oceanic Abstracts, PASCAL Database, and Science Citation Index.

Volume 59, Number 3, March 2002

Canadian Journal of Fisheries and Aquatic Sciences

Published by the National Research Council of Canada

Volume 59, numéro 3, mars 2002

Journal canadien des sciences halieutiques et aquatiques

Publié par le Conseil national de recherches du Canada

Editors / directeurs scientifiques John C. Roff and Moira M. Ferguson

Assistant to the Editors / adjointe aux directeurs scientifiques **Holly Foster**

Associate Editors / directeurs scientifiques associés

M.T. Arts, *Environment Canada, Burlington*
D. Boisclair, *Université de Montréal*
U. Borgmann, *Environment Canada, Burlington*
S.E. Campana, *DFO/MPO, Dartmouth*
R. Carignan, *Université de Montréal*
D.G. Dixon, *University of Waterloo*
A.E. Dizon, *National Marine Fisheries Service, La Jolla, Calif.*
J.J. Dodson, *Université Laval*
J.A. Downing, *Iowa State University*
K.T. Frank, *DFO/MPO, Dartmouth*
D.F. Houlihan, *University of Aberdeen, Aberdeen, Scotland*
F.A. Huntingford, *University of Glasgow*
J.A. Hutchings, *Dalhousie University*
G.S. Jamieson, *DFO/MPO, Nanaimo*
B. Jonsson, *Norwegian Institute for Nature Research, Oslo, Norway*
D.M. Mason, *NOAA-Great Lakes Environmental Research Laboratory, Ann Arbor, Mich.*
A. Mazumder, *University of Victoria*
D.L. Parrish, *Vermont Cooperative Fish and Wildlife Research Unit (USGS/BRD), University of Vermont*
P. Pepin, *DFO/MPO, St. John's*
T.M. Powell, *University of California, Berkeley, Calif.*
E.E. Prepas, *University of Alberta*
T.J. Quinn II, *University of Alaska–Fairbanks, Juneau, Alaska*
T.P. Quinn, *University of Washington*
R.D. Robarts, *Environment Canada, Saskatoon*
B. Sainte-Marie, *DFO/MPO, Mont-Joli*
D.W. Schindler, *University of Alberta*
S.J. Smith, *DFO/MPO, Dartmouth*
W.G. Sprules, *University of Toronto*
R.J. Thompson, *Memorial University of Newfoundland*
C.J. Walters, *University of British Columbia*
R.D. Ward, *CSIRO Marine Research, Australia*
C.M. Wood, *McMaster University*
B. de Young, *Memorial University of Newfoundland*

NRC Research Press / Presses scientifiques du CNRC

Editor-in-chief / directeur général **Bruce P. Dancik**

Assistant Editor-in-chief / directeur général adjoint **Iain E.P. Taylor**

Journals Program / Programme des revues

(Fax / télécopieur : 613-952-7656; e-mail / courriel : research.press@nrc.ca;
URL: http://researchpress.nrc.ca)

Director / directrice **Aldyth Holmes**

Business Manager / gestionnaire des affaires **Paul McClymont**

Managing Editor / rédactrice administrative **Cecily M. Pearson (613-993-9099)**

Publication Officers / agentes de publication **Jennifer McColl and Lee Murphy**

Advertising / annonces publicitaires **Judy Heyman (613-993-0151)**

Reprints / tirés à part **Roxanne Landriault (613-990-2254)**

Subscriptions / abonnements **Helen Goulet (613-993-9084)**

© National Research Council of Canada 2002. World rights reserved.
No part of this publication may be reproduced, stored, or transmitted in any form or by any means, without the written permission of the publisher, except as stated below.

The National Research Council of Canada grants **permission*** to individuals to make single copies of articles for personal use. Any person may reproduce short excerpts from articles in the journal for any purpose that respects the moral rights of authors, provided that the source is fully acknowledged. As a courtesy, the consent of authors of such material should be obtained directly from the author.

Authorization to reproduce items for other than personal use, as stated above, is granted by the National Research Council of Canada provided that the copyright fee of $7.00 per copy is paid directly to CANCOPY, One Yonge Street, Suite 1900, Toronto, ON M5E 1E5, Canada.

*The above permission does not extend to other kinds of copying, such as copying for general distribution, for advertising, or promotional purposes, for creating new collective works, or for resale. For such copying, arrangements must be made with the publisher, National Research Council of Canada, Ottawa, ON K1A 0R6, Canada.

© Conseil national de recherches du Canada 2002. Tous droits réservés.
Il est interdit de reproduire, de sauvegarder ou de transmettre quelque partie de la présente publication dans quelque format ou de quelque façon sans le consentement écrit de l'éditeur, à l'exception des conditions suivantes.

Le Conseil national de recherches du Canada accorde aux particuliers le droit de faire des copies individuelles pour leur usage personnel. Toute personne peut reproduire de courts extraits des articles de la Revue pour autant que les droits moraux de l'auteur soient respectés et que la mention de provenance soit clairement indiquée. Il est de convenance de demander le consentement de l'auteur avant de faire mention de son travail.

On obtiendra l'autorisation de reproduire des articles à d'autres fins que l'usage personnel (tel qu'on l'a décrit ci-dessus) auprès du Conseil national de recherches du Canada pour autant que des redevances de droits d'auteurs de 7,00 $/copie soient versées au CANCOPY, 1, rue Yonge, bureau 1900, Toronto, ON M5E 1E5, Canada.

*La permission ci-dessus ne s'applique pas à la reproduction à grande échelle, telle que la reproduction aux fins de distribution générale, publicitaire ou promotionnelle, de compilation de nouveaux ouvrages collectifs ou de revente. Dans de tels cas, il faudra ratifier une entente particulière avec l'éditeur, le Conseil national de recherches du Canada, Ottawa, ON K1A 0R6, Canada.

Subscription information

The *Canadian Journal of Fisheries and Aquatic Sciences* (ISSN 0706-652X) is published monthly by the National Research Council of Canada. 2002 annual subscription rates (second class postage) for Canada are $732CAN institutional and $227CAN personal, for US & foreign $732US institutional and $227US personal. For air mail add $175US to foreign rate. Canadian customers please include 7% GST (business no. 12149 1807 RT 0275). Subscriptions are entered for the calendar year. Remittances should be made payable to the Receiver General for Canada credit NRC. Price for regular single issues: institutional, $95.00; personal, $30.00. Supplements will be priced separately. Special rates apply to members of Canadian scientific and engineering societies if they subscribe through their respective societies.

There are no refunds on cancelled subscriptions once delivery has begun. Claims for missing issues should be made within four months (N. America) or six months (outside N. America) following the date of publication. The publisher expects to supply missing issues only when losses have occurred in transit and when the reserve stock will permit. For change of address and subscription enquiries: Subscription Office, NRC Research Press, National Research Council of Canada, Ottawa, ON K1A 0R6, Canada; tel.: 613-993-9084; fax: 613-952-7656; e-mail: research.press@nrc.ca.

Microform backfiles are available from UMI, P.O. Box 1346, Ann Arbor, MI 48106-1346, U.S.A., and Micromedia Ltd., 20 Victoria St., Toronto, ON M5C 2N8, Canada.

All issues of the *Canadian Journal of Fisheries and Aquatic Sciences* since 1996 are available on the Web. Pricing information can be found at http://cjfas.nrc.ca.

Renseignements sur l'abonnement

Journal canadien des sciences halieutiques et aquatiques (ISSN 0706-652X) est une publication mensuelle du Conseil national de recherches du Canada. Le prix de l'abonnement annuel au Canada (courrier de deuxième classe) est de 732 $CAN pour les organismes et de 227 $CAN pour les particuliers. À l'étranger (y compris les É.-U.), le prix de l'abonnement est de 732 $US pour les organismes et de 227 $US pour les particuliers. L'expédition par avion exige des frais de 175 $US en sus du prix d'abonnement à l'étranger. Les clients du Canada doivent ajouter la TPS de 7% (numéro d'entreprise 12149 1807 RT 0275). Les abonnements sont pour l'année civile. Tout paiement doit être adressé au Receveur général du Canada, crédit du CNRC. Le prix par numéro est de 95 $ pour les organismes et de 30 $ pour les particuliers. Le prix des hors-série varie. Les membres des sociétés canadiennes de sciences et de génie bénéficient de taux préférentiels en s'abonnant via leurs sociétés respectives.

Aucun remboursement ne sera accordé ni aucune annulation acceptée une fois que les livraisons auront commencé. Les réclamations de numéros manquants devront être soumises dans les quatre mois (Amérique du Nord) ou dans les six mois (à l'extérieur de l'Amérique du Nord) suivant la date de publication. L'éditeur ne fournira de numéros manquants que si le document a été perdu pendant l'expédition et que si le stock le permet. Adressez tout changement d'adresse ou toute question quant à l'abonnement au : Bureau des abonnements, Presses scientifiques du CNRC, Conseil national de recherches Canada, Ottawa, ON K1A 0R6, Canada; téléphone : 613-993-9084; télécopieur : 613-952-7656; courriel : presses.scientifiques@nrc.ca.

On peut obtenir les fichiers rétrospectifs sur **microforme** auprès de UMI, P.O. Box 1346, Ann Arbor, MI 48106-1346, É.-U., et auprès de Micromedia Ltée, 20 rue Victoria, Toronto, ON M5C 2N8, Canada.

À partir de 1996, tous les numéros de *Journal canadien des sciences halieutiques et aquatiques* sont accessibles sur le Web. On trouvera des renseignements sur les tarifs à http://jcsha.cnrc.ca.

Modelling the effects of establishing a marine reserve for mobile fish species

P. Apostolaki, E.J. Milner-Gulland, M.K. McAllister, and G.P. Kirkwood

Abstract: We present a model of the effects of a marine reserve on spawning stock biomass (SSB) and short- and long-term yield for a size-structured species that exhibits seasonal movements. The model considers the effects of protecting nursery and (or) spawning grounds under a range of fishing mortalities and fish mobility rates. We consider two extremes of effort redistribution following reserve establishment and analyze the effects of a reserve when the fishery targets either mature or immature fish. We apply the model to the Mediterranean hake (*Merluccius merluccius*) and show that a marine reserve could be highly beneficial for this species. We demonstrate benefits from reserves not just for overexploited stocks of low-mobility species, but also (to a lesser extent) for underexploited stocks and high-mobility species. Greatly increased resilience to overfishing is also found in the majority of cases. We show that a reserve provides benefits additional to those obtained from simple effort control. Benefits from reserves depend to a major extent on the amount of effort redistribution following reserve establishment and on fishing selectivity; hence, these factors should be key components of any evaluation of reserve effectiveness.

Résumé : On trouvera ici un modèle qui décrit les effets d'une réserve marine sur la biomasse du stock des reproducteurs et sur les rendements à court et à long termes chez une espèce à structure de taille définie qui fait des déplacements saisonniers. Le modèle examine les effets de la protection des zones d'alevinage et (ou) de fraye sur une gamme de mortalités dues à la pêche et de taux de mobilité des poissons. Nous considérons deux extrêmes dans la redistribution de l'effort de pêche à la suite de l'établissement d'une réserve et nous analysons les effets de la réserve quand la pêche cible les poissons immatures ou alors les poissons adultes. Nous appliquons le modèle au merlu commun (*Merluccius merluccius*) et démontrons qu'une réserve marine lui serait très bénéfique. Les bénéfices d'une réserve s'appliquent non seulement aux stocks surexploités d'espèces à mobilité réduite, mais aussi, bien que dans une plus faible mesure, aux stocks sous-exploités et aux espèces très mobiles. Dans la majorité des cas, il existe aussi une résilience fortement accrue à la surpêche. La réserve apporte des bénéfices additionnels à ceux que génère le simple contrôle de l'effort de pêche. Ces bénéfices dépendent en grande partie de l'importance de la redistribution de l'effort de pêche après l'établissement de la réserve et de la sélectivité de la pêche; ces facteurs devraient donc être les éléments essentiels de toute évaluation de l'efficacité d'une réserve.

[Traduit par la Rédaction]

Introduction

There has been much recent interest in the potential of marine reserves as a fishery management tool, based on the perception that conventional fishery management techniques have failed to prevent overexploitation of target species (FAO 1995; Beverton 1998; Buckworth 1998) and the depletion of nontarget species, habitat degradation, and associated disruption of the food chain (Roberts and Polunin 1993; Dayton et al. 1995; Pitcher and Pauly 1998). Marine reserves have been proposed as an easily enforced management method that could reduce the impacts of fishing on marine populations and habitats and help managers to cope with the inherent irreducible uncertainty in stock assessments (e.g., Allison et al. 1998; Lauck et al. 1998; Roberts 1998). In this paper, we consider a marine reserve to be an area that is permanently closed to all fishing.

Compared to other methods, marine reserves have not been considered to be a widely applicable fishery management tool. However, they have long been used for particular problems; for example, the protection of river mouths for homing Atlantic and Pacific salmon; Mediterranean coastal area closures for the protection of immature fish; and protection of coral reefs. Increases in fish abundance and size in reserves have been widely reported (Mosqueira et al. 2000), although whether these benefits are exported to surrounding areas is less clear. Some of the reasons why marine reserves have not been more widely used include the uncertainties concerning the yield improvements that reserves can offer, issues concerning the placement and size of reserves, and opposition to prohibiting fishing in areas that are currently fished (Ballantine 1995; Sant 1996).

Given these uncertainties and the lack of empirical data, much recent modelling has focused on the effects of establishing a reserve on fishery yields and spawning stock biomass (SSB). So far, these studies have shown that yield

Received 27 February 2001. Accepted 8 February 2002. Published on the NRC Research Press Web site at http://cjfas.nrc.ca on 21 March 2002.
J16241

P. Apostolaki,[1] E.J. Milner-Gulland, M.K. McAllister, and G.P. Kirkwood. Renewable Resources Assessment Group, Department of Environmental Science and Technology, Imperial College of Science, Technology and Medicine, Royal School of Mines, Prince Consort Road, London SW7 2BP, U.K.

[1]Corresponding author (e-mail: y.apostolaki@ic.ac.uk).

 DOI: 10.1139/F02-018 © 2002 NRC Canada

enhancement is possible only if the fishery is initially overexploited, although the predicted degree of enhancement varies from minimal (e.g., Polacheck 1990; Die and Watson 1992) to considerable (Sladek Nowlis and Roberts 1999; Mangel 2000*a*, 2000*b*). In contrast, yields have been predicted to decline if a reserve is instituted for an underexploited fishery. The effect of reserves on SSB has always been found to be positive.

The assumptions made about the biology of the target species, reserve size, and fisher behaviour are key to predicting the effectiveness of marine reserves. The early models tended to assume random movement and spawning throughout the area under study, and no population structure (Table 1). More recent models have increased realism by including population structure, directional movement of larvae or adults, and protection of key areas such as spawning grounds. However, a major gap in modelling is the interaction between spatial and temporal heterogeneities in fish abundance and fishing selectivity. This is important because many exploited fish species exhibit seasonal movement and have distinct spawning and (or) nursery grounds, combined with size-selective fishing. Here, we present a general model of the effects of a marine reserve on yield and SSB for such species. We also consider the effects of the extent of effort redistribution that occurs following the establishment of a marine reserve on its effectiveness, both in the short and long term. We apply the model to the Mediterranean hake (*Merluccius merluccius*).

Materials and methods

The general model

Population dynamics

We assume a size-structured population with overlapping generations to capture the effects of both size-related fishing selectivity and size-related fish movement. It is assumed that the area inhabited by the fish population is divided into two. One of the areas (area *a*) is a spawning and (or) nursery ground, and the marine reserve is created by closing this area to fishing. Model parameters are defined in Table 2. The first size category is recruits to the fishery, R, numbers of which depend on the number of eggs, E, according to the Beverton–Holt egg–recruit relationship (Beverton and Holt 1957),

$$(1) \qquad R = \frac{E}{\alpha + \beta E}$$

where α and β are constants (see Appendix A).

The number of fish spawning in time period t depends on the number of mature fish in the spawning area, since it is assumed that fish spawn only in the spawning area. This number is calculated as

$$(2) \qquad N_{\mathrm{sp},t} = \sum_{S \geq S_{\mathrm{mat}}} \sum_{I \subseteq \mathrm{spawn}} N_{I,S,t} Q_{S,t} (1 - \mathrm{e}^{-(F_{I,S} + M_S)}) \frac{1}{F_{I,S} + M_S}$$

following Quinn and Deriso (1999), where S is a particular size class (mature fish only, $S > S_{\mathrm{mat}}$), I is the area (the spawning area only, which is area *a* if it is assumed to be the spawning area or area *b* otherwise), and $N_{I,S,t}$ is the number of fish in size class S and area I at the beginning of period t. $F_{I,S}$ is the fishing mortality rate per time period for fish in size class S and area I, M_S is natural mortality rate per time period for fish in size class S, and $Q_{S,t}$ is the proportion of mature fish (size class S) in the spawning area that spawn in time period t. A time period of 1.5 months has been used in the calculations.

We assume that all mature females spawn once each year. When spawning occurs in area *a* (hence fish must migrate into this area to spawn), we assume that Q varies with S, but not with t. We set Q_S to the value at which all the fish in each mature age class spawn once during a year. When spawning occurs in area *b*, fish do not migrate into a spawning area. In this case, we assume that Q varies only with t, but not with S. We vary Q_t over the eight time periods that make up a year such that the proportion of fish spawning in each period is the same as when fish must move to area *a* to spawn. This requires a reduction in Q_t to account for the fact that all mature fish are in area *b*.

The number of eggs spawned in time period t, E_t, is $f_S N_{\mathrm{sp},t}$, where f_S is the fecundity of fish in size class S (Table 3). The spawning stock biomass, SSB, is $\overline{W}_S N_{\mathrm{sp},t}$, where $\overline{W}_S$ is the mean weight of fish in a size category. $\overline{W}_S$ is determined as the mean of the weights corresponding to the minimum, maximum, and mean length of a fish in this size class using a weight–length relationship. Fish weight, W, is assumed to scale exponentially with length, L (Abella et al. 1995; Table 3).

The biomass of fish caught during time period t, Y_t, is the sum of the numbers of fish caught from each size category multiplied by the corresponding mean weights (Quinn and Deriso 1999),

$$(3) \qquad Y_t = \sum_{S,I} \frac{F_{I,S}}{F_{I,S} + M_S} N_{I,S,t} (1 - \mathrm{e}^{-(F_{I,S} + M_S)}) \overline{W}_S$$

The probability, $P_{S-1,S}$, of a fish in size class $S - 1$ growing to the next size class during a time period depends on the mean growth, $\overline{\Delta L}_{S-1}$, of fish in this size class:

$$(4) \qquad P_{S-1,S} = \frac{\overline{\Delta L}_{S-1}}{L_{\mathrm{min},S} - L_{\mathrm{min},S-1}}$$

where $L_{\mathrm{min},S}$ denotes the minimum length of fish in category S and $L_{\mathrm{min},S-1}$ is the minimum length of fish in size category $S - 1$. The size intervals are chosen such that fish move at most one size class in a time period but do not remain in any size class (except the last) for a long period. The mean growth, $\overline{\Delta L}_{S-1}$, is calculated as the mean of the growth per time period of fish of the minimum, mean, and maximum size in the class. Growth declines with length such that fish belonging to the last size class barely increase in size.

Fish movement

Fish are distributed across the study area over time using movement coefficients. These coefficients describe the proportion of a given size class that moves from one area to another in each time period. Movement between areas *a* and *b* is seasonal and directional, comprising movement of recruits out of the nursery area and adults into and out of the spawning area. The model can be run with different patterns of

© 2002 NRC Canada

Table 1. A categorization of models of marine reserve effectiveness, showing the major assumptions made in each case.

Source	Model structure	*F* modified?	Movement	Other characteristics
Beverton and Holt (1957)	Age	Yes	Random	Per-recruit analysis
Polacheck (1990)	Age	Yes	Random	Per-recruit analysis
Mangel (2000*a*)	Age	N/A	Pelagic juvenile phase	Effects of reserve on catch variability
Mangel (2000*b*)	Age	No	Uniform distribution	Distinct spawning ground
Die and Watson (1992)	Age	N/A	Age- and area-dependent	Per recruit analysis, area-dependent recruitment
Guénette and Pitcher (1999)	Age	Yes	Area-dependent	Comparison of egg–recruit functions, stochastic recruitment
Sladek Nowlis and Roberts (1999)	Size	No	Larval dispersal	Short- and long-term effects, stochastic survivorship
Lauck et al. (1998)	Logistic	N/A	Uniform distribution	Stochastic harvesting
This paper	Size	Yes	Directed, seasonal & size dependent	Distinct spawning and nursery grounds, short- and long-term effects.

Note: *F* modified refers to whether the fishing effort is redistributed following reserve creation. N/A, not applicable.

Table 2. A list of the parameters used in the model.

Parameter	Symbol	Units
Age	A	year
Recruits to the fishery	R	number of individuals
Number of eggs	E	eggs × 10^3
Constants	α, β	—
Number of fish	N	—
Size class	S	—
Area (divided into *a*, *b*)	I	—
Time period	t	1.5 months
Proportion of mature fish spawning	Q	—
Natural mortality rate for a given size class	M	$year^{-1}$
Fishing mortality rate for a given size class and area	F	$year^{-1}$
Fishing mortality multiplier	$\hat{F}$	—
Fecundity of an individual female	f	eggs × 10^3
Fish weight	W	g
Fish length	L	cm
Biomass yield (of fish caught)	Y	g
Probability of moving into the next size category	P	—
Movement coefficient (between areas)	θ	t^{-1}
Size of area *a* as a proportion of total study area	ρ	—
Steepness of the egg–recruit curve	h	—

Table 3. Values of the parameters used in the model.

Parameter	Symbol (units)	Value and function	Source
Growth model	L (cm)	$L = L_\infty(1 - e^{-kt})$ $L_\infty = 79.1$ cm, $k = 0.185$ $year^{-1}$	Abella et al. (1995)
Fecundity (by size and age)	f (× 10^3)	$\log_{10} f = 3.33 \log_{10} L - 3.52$ $\log_{10} f_A = 2.06 \log_{10} A - 0.4$	Papaconstantinou et al. (1986)
Fish weight	W (g)	$W = 0.0041 L^{3.192}$	Abella et al. (1995)
Constants in egg–recruit relationship (eq. 1)	α, β	$\alpha = 1512.04$ $\beta = 7.87 \times 10^{-7}$	Calculated from simulation
Steepness of egg–recruits function	h	0.7	—
Age at reproductive maturity	A_{mat}	4 years	Oliver and Massutí (1995)
Size class at reproductive maturity	S_{mat}	7	Recasens et al. (1998)
Area *a* as a proportion of the total area	—	0.35	—

Note: The model is parameterized for the Mediterranean hake (*Merluccius merluccius*) where data are available, otherwise, reasonable values and sensitivity analyses are used.

© 2002 NRC Canada

Table 4. Natural mortality rate (M) and fishing mortality rate (F) per size class for Mediterranean hake (*Merluccius merluccius*).

Size interval (cm)	M (year^{-1})	F (year^{-1}) (*i*)	F (year^{-1}) (*ii*)
7–8.5	2.6	0.35	0.05
8.5–11	2.1	1	0.1
11–16.5	1.55	1.4	0.1
16.5–22	1.1	0.73	0.1
22–28.5	0.8	0.37	0.3
28.5–36	0.65	0.2	0.5
36–43	0.52	0.15	0.7
43–50	0.43	0.15	0.8
50–55	0.4	0.2	0.8
55–60	0.4	0.2	0.8
60–65	0.4	0.2	0.8
65–70	0.4	0.2	0.8
70–75	0.4	0.2	0.8
75–79	0.4	0.2	0.8

Note: Three assumptions about fishing mortality are modelled: selectivity for small fish (*i*), no selection by size (fishing mortality constant at 0.5), and selectivity for larger fish (*ii*). The values of natural mortality and of fishing mortality (case *i*) are from Caddy and Abella (1999) up to 50 cm and are our assumptions from 50 cm onwards. Actual fishing mortalities on each size class (F_S) are calculated by multiplying these values by the fishing mortality multiplier, F.

movement and different locations for the spawning and nursery areas and can also be used to represent traditional closed areas (which are closed only for part of the year). In the realizations presented here, area a is assumed to be a nursery and (or) a spawning area. If it is a nursery area only, fish recruit into the population in the nursery area and are distributed across the study area in subsequent time periods, and all spawning is assumed to occur in area b. If area a is a spawning area only, then fish recruit in area b. We assume that in all cases, area a contains either all or none of the spawning or nursery ground; partially overlapping areas are not considered. We also assume that the whole area a is protected once a marine reserve is established. The model can easily be extended to the case where only a proportion of area a is protected. However, because the results obtained are intermediate between those obtained when area a is fully protected, or not protected, we do not present them here.

In the absence of fishing, the number of fish in area a in size class S in the beginning of period t is assumed to be (Hilborn 1990)

$$(5)\quad N_{a,S,t} = (N_{a,S-1,t-1}P_{S-1,S}\,e^{-M_{S-1}} + N_{a,S,t-1}P_{S,S}\,e^{-M_S})(1-\vartheta_{a,b}) + (N_{b,S-1,t-1}P_{S-1,S}\,e^{-M_{S-1}} + N_{b,S,t-1}P_{S,S}\,e^{-M_S})\vartheta_{b,a}$$

where $\vartheta_{b,a}$ and $\vartheta_{a,b}$ are movement coefficients (from area b to a and a to b, respectively). For ease of presentation, eq. 6 does not show the dependence of the movement coefficients on fish length and time period. The number of fish in a given size category and area is calculated, accounting for growth, movement, and mortality (Appendix B).

Fishing effort

When a marine reserve is instituted, an assumption has to be made concerning the redistribution of fishing effort into the reduced area that is now available. The usual assumption is that effort previously expended within the reserve relocates to the nonreserve area. In this case, and assuming that fishing mortality is proportional to fishing effort, fishing mortality in the remainder of the study area after the reserve is instituted (F^{mr}; mr = marine reserve) increases to (Guénette and Pitcher 1999)

$$(6)\quad F^{mr}_{I,S} = F_{I,S}\frac{1}{(1-\rho)}$$

where F is fishing mortality prior to the reserve and ρ is the size of area a as a proportion of the total area. Hence, $1-\rho$ is the proportion of the total area available to fishing. Equation 6 cannot realistically be used for all values of ρ, since for very large marine reserves, the exploited area becomes so small that it cannot sustain the fishing effort that operated prior to reserve establishment. Also, eq. 6 gives the fishing mortality needed to achieve catches equal to those before reserve establishment if fish are uniformly distributed. However, the distribution of fish in our model is not uniform because we have segregation of fish in different areas during different time periods, so the use of eq. 6 results in catches that are not exactly equal to pre-reserve levels. Therefore, we also investigate two cases in which effort limitation is instituted along with the marine reserve: either effort in the nonreserve area is held at the previous level (i.e., effort that was expended in the reserve is not redistributed), or F^{mr} is set at a value producing an initial annual catch that is the same as that immediately prior to the institution of the reserve, so that the reserve does not initially lead to a loss in catch. In practice, this last assumption gave results intermediate between full redistribution of effort and no redistribution, so the results are not presented.

The Mediterranean hake

Many Mediterranean fisheries are multispecies and multigear, characterized by heavy exploitation of demersal fish at small sizes (Caddy 1990; Papaconstantinou and Stergiou 1995). The variety of target species results in small individual catches, a considerable proportion of which are small fish (Caddy 1990). The preference for small fish can be attributed to the high value of fish of that size in many Mediterranean markets (Abella et al. 1997). Hake is one of the most commercially important of these species. It is caught mainly with bottom trawls, and to a lesser degree with gillnets and longlines. Each fishing technique exploits particular sections of the population; bottom trawls target recruits and juveniles, whereas adults are mainly caught with gillnets and longlines (Oliver and Massuti 1995). Immature fish make up the largest proportion of the catch and have the highest fishing mortality (Oliver and Massuti 1995; Abella et al. 1997; Caddy and Abella 1999).

Hake occur at depths from approximately 50 m to more than 700 m (Papaconstantinou and Stergiou 1995; Recasens et al. 1998). Mature hake move inshore to spawn and then return to deeper waters; immature fish remain for the first period of their lives in the nursery area and then exhibit sim-

© 2002 NRC Canada

Fig. 1. (*a*) Values of the movement coefficients that describe movement between area *a* and *b* for fish of size 55–60 cm and moderate mobility. $\vartheta_{a,b}$, movement from area *a* to area *b* (○); $\vartheta_{b,a}$, movement from area *b* to area *a* (△). (*b*) Number of mature fish in area *a* (when it is a spawning ground) expressed as a percentage of the total number of mature fish per time period (1.5 months) for the three types of movement. A full year is shown (8 time steps). High mobility is shown as open, moderate mobility as shaded, and low mobility as solid bars.

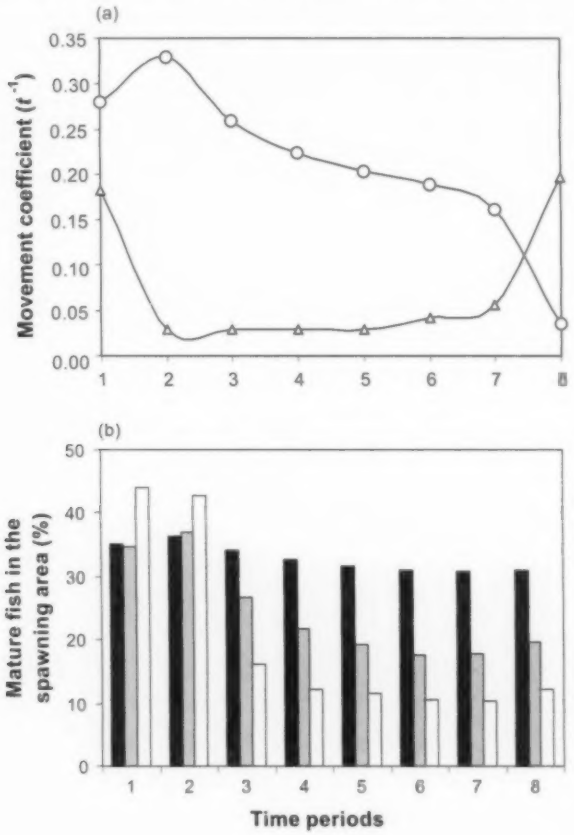

ilar migratory behaviour (Zupanovic and Jardas 1986; Recasens et al. 1998). In some cases, the spawning and nursery areas are known to overlap. Size at maturity varies regionally and by sex; the length at which 50% of the specimens examined have spawned at least once is 26–36 cm for males and 34–43 cm for females, depending on the location (Orsi Relini et al. 1989; Recasens et al. 1998). Spawning takes place all year, but is more intense during particular time periods, depending on the location; peak spawning has been reported either in autumn and early winter or in summer (Oliver and Massuti 1995; Papaconstantinou and Stergiou 1995; Recasens et al. 1998). Recruitment to the fishery occurs approximately six months after hatching, at a size of 6–9 cm (Orsi Relini et al. 1989; Papaconstantinou and Stergiou 1995). Myers et al. (1995) present data suggesting that recruitment in Mediterranean hake is independent of the number of eggs produced for a wide range of egg values. Males grow more slowly and to a smaller maximum length than females, with size differentiation being more marked after male maturation (Oliver and Massuti 1995; Recasens et al. 1998).

The Mediterranean hake is an ideal species for evaluating the effectiveness of marine reserves for species that carry out directional migration. It uses specific nursery grounds, has seasonally defined periods of peak spawning and recruitment, and is heavily exploited. The segregation of immature fish into a restricted inshore area probably makes them an easy target and facilitates their intense exploitation (A.J. Abella, Agenzia Regionale per la Protezione Ambientale della Toscana, Via dell'Ambrogiana 2, 57127 Livorno, Italy, personal communication). Hence, marine reserves are a potentially useful management option for this species.

Model implementation

The parameter values used in the model were taken from the literature on the Mediterranean hake (Table 3). The values of a and β (eq. 1) were calculated for a given number of eggs, E_0, and steepness, h (Appendix A). Two values of h were tested, 0.7 and 0.9. The latter was based on the results obtained by Myers et al. (1995) (i.e., stock–recruitment curve characterized by steepness which is close to 1); the former represents a greater level of dependence of E on SSB. Model results did not depend strongly on h, and results are presented only for $h = 0.7$; this value gives larger benefits from spawning stock protection.

Only females were modelled; a full model also including males was found to give very similar results. There were 14 size classes, with natural mortality rates for the majority of size classes taken from Caddy and Abella (1999); the values for the largest size classes were assumed (Table 4). A 1.5-month time step was used, such that each year consisted of eight time steps. Recruitment into the first size class occurs six months after hatching. The time step was chosen so that all fish in the first size class enter the second class after one time step, and to allow seasonality to be modelled.

We assumed that fish spawn only once per year, but that spawning can occur at any time throughout the year. The largest proportion of adults was assumed to enter the spawning area in autumn and winter and to leave in the spring and summer. Recruits were assumed to stay in the nursery area (when area *a* is a nursery area) for one time period and then follow the movement pattern into and out of area *a*, as described by the movement rates in Fig. 1. Slow-moving fish remained for longer in the spawning area than fast-moving fish. Because data on hake movement are not available, and to allow model results to be generalized, three sets of movement coefficients were examined, representing high, moderate, and low levels of mobility. The movement coefficient $\vartheta_{a,b}$ that characterizes fish of size 55–60 cm and describes moderate mobility is high for the first two time steps of the year and then decreases, while the value of $\vartheta_{b,a}$ is high in the first time period of the year, becomes smaller afterwards and increases again in the last time step of the year (Fig. 1*a*). Movement coefficients characterizing fish of other sizes are similar. Each set of movement coefficients results in a different distribution of fish in the study area (Fig. 1*b*).

© 2002 NRC Canada

Table 5. Results of the model under assumptions that best represent the situation for Mediterranean hake (*Merluccius merluccius*).

		Change from nonreserve value (%)			
Redistribution	Exploitation	SSB	Equilibrium yield	Year 1 yield	Recovery time (years)
Full	Under	+1	+38	+32	—
	MSY	+10	+42	+28	—
	Over	+16	+50	+24	—
None	Under	+26	**+9**	−11	6
	MSY	+54	**+25**	−13	4
	Over	+87	**+47**	−14	3

Note: Assumptions are that fish have moderate mobility (Fig. 1), there is selectivity for small fish (Table 4), and the marine reserve protects the nursery area. Results are presented as the long-run equilibrium spawning stock biomass (SSB) and yield as well as the yield in the first year after the reserve is instituted, all as percentages of the pre-reserve yield. We also show the number of years required for yield to recover to at least pre-reserve levels. Three levels of pre-reserve fishing mortality are shown (underexploited, $\hat{F} = 0.3$; maximum sustainable yield (MSY), $\hat{F} = 0.5$; and overexploited, $\hat{F} = 0.7$). Fishing effort from the reserve area is either fully redistributed to the rest of the fishing area (full) or not redistributed at all (none). For comparative purposes, the values in bold are for the situation shown in Fig. 2*d*.

The model was run under unexploited conditions until the population reached equilibrium. Starting from this point, the model was run for different levels of fishing pressure under a no-reserve regime, which allowed the maximum sustainable yield (MSY) fishing effort and the lowest fishing mortality resulting in fish extinction to be found. Three assumptions about fishing selectivity were modelled: selection for smaller size classes, which was based on estimated fishing mortalities for Mediterranean hake (Caddy and Abella 1999); no selection by size class; and selection for larger fish (Table 4). Fishing mortality by size class was obtained by multiplying the reference values given in Table 4 by a fishing mortality multiplier, $\hat{F}$.

Three values for $\hat{F}$ were chosen, representing a fishery that was underexploited prior to reserve establishment, the MSY level, and an overexploited fishery. The institution of a marine reserve was assumed to occur after the fished population had reached equilibrium for a given value of $\hat{F}$, and was accompanied by a redistribution of fishing effort. After the institution of the reserve, no fishing took place in area *a*. The post-reserve value of $\hat{F}$ depended on the assumption made about effort redistribution. A number of assumptions were also tested concerning fish movement patterns, spawning behaviour, and use of area *a*.

Results are presented in terms of biomass yield and SSB. To capture both short- and long-term effects of the reserve, the time required for yields to reach pre-reserve levels is presented. Another possible advantage of instituting a reserve is increased resilience to high fishing mortalities. Hence, we also present the fishing mortality at which population extinction would occur before and after reserve establishment.

Results

Under the movement and selectivity assumptions that best represent the situation for Mediterranean hake (moderate fish mobility, which results in movement patterns that are closest to available descriptions of hake movement, and selectivity for small fish), the institution of a marine reserve always has beneficial results. The reserve leads to increases in both SSB and long-term equilibrium yield (Table 5). Greatest long-term benefits from the reserve occur if the fishery is overexploited before its institution. Yield increases are obtained even in the first year after the reserve is instituted if effort is redistributed. If a more precautionary approach is taken, by not redistributing effort following reserve creation (instead keeping $\hat{F}$ at the pre-reserve level in area *b*), short-term losses in yield are incurred. However, yields recover rapidly, particularly if the fishery was initially overexploited. The advantage of not redistributing effort is that SSB shows a marked increase, whereas long-term yields are still improved over the pre-reserve level.

The benefits obtained from a marine reserve depend on fish mobility and on the interaction between fishing selectivity and the placing of the reserve area (Fig. 2). As would be expected, the greatest benefits are obtained if the area protected is both a spawning and a nursery area (Figs. 2*a*, 2*b*). If the spawning and nursery areas are separate, benefits are highest when the area used by the size classes that are the main target of the fishery is protected. Hence, protecting the nursery area has greatest benefits if immature fish are targeted, whereas protecting the spawning area is most beneficial if mature fish are targeted (Figs. 2*d* and 2*f*, 2*c* and 2*e*). The more mobile the fish are, the lower are the yield improvements from the marine reserve. Nonetheless, under the assumptions in Fig. 2, the protection of a nursery area leads to long-term yield improvements at all fishing mortalities and mobilities, whatever the size selectivity of the fishery. On the other hand, if the spawning area is protected, yield improvements are obtained at higher fishing mortalities, but not for underexploited fisheries (Figs. 2*e*, 2*f*). Underexploited fisheries also do not show yield improvements if the area protected is both a spawning and a nursery area, despite the much higher yields obtained for overexploited fisheries (Figs. 2*a*, 2*b*).

Another potential benefit of marine reserves is increased resilience to high fishing mortalities (leading to a shift in $\hat{F}_{MSY}$ to the right), and hence protection against overexploitation and uncertainty in stock assessments. Our results suggest that the marine reserve gives a resilience benefit, such that the fishing mortality at which stock extinction is predicted ($\hat{F}_{ext}$) is much higher when a reserve is in place (Fig. 2). The fishing mortality on area *b* that is required to drive the stock to extinction when area *a* is pro-

© 2002 NRC Canada

Fig. 2. The sustainable yield from fishing with a marine reserve that protects the whole of area *a*, shown for a range of fishing mortalities. The sustainable yield per fishing mortality curves before the establishment of the reserve are also given for comparative purposes. The maximum sustainable yield (MSY) fishing mortality coefficients without a reserve can be found from these curves. Sustainable yield with and without a marine reserve is normalized to the MSY without a reserve in each case. It is assumed that there is no redistribution of effort from area *a* to *b* when the reserve is instituted. Broken line and solid triangle, no reserve; with reserve: open diamond, high mobility; ×, moderate mobility; solid circle, low mobility fish. Note the different scales on the *y* axis when immature fish are targeted (*b*, *d*, *f*) and mature fish are targeted (*a*, *c*, *e*). (*a*) Selectivity for mature fish; area *a* is a spawning and nursery area. (*b*) Selectivity for immature fish; area *a* is a spawning and nursery area. (*c*) Selectivity for mature fish; area *a* is a nursery area. (*d*) Selectivity for immature fish; area *a* is a nursery area. (*e*) Selectivity for mature fish; area *a* is a spawning area. (*f*) Selectivity for immature fish; area *a* is a spawning area.

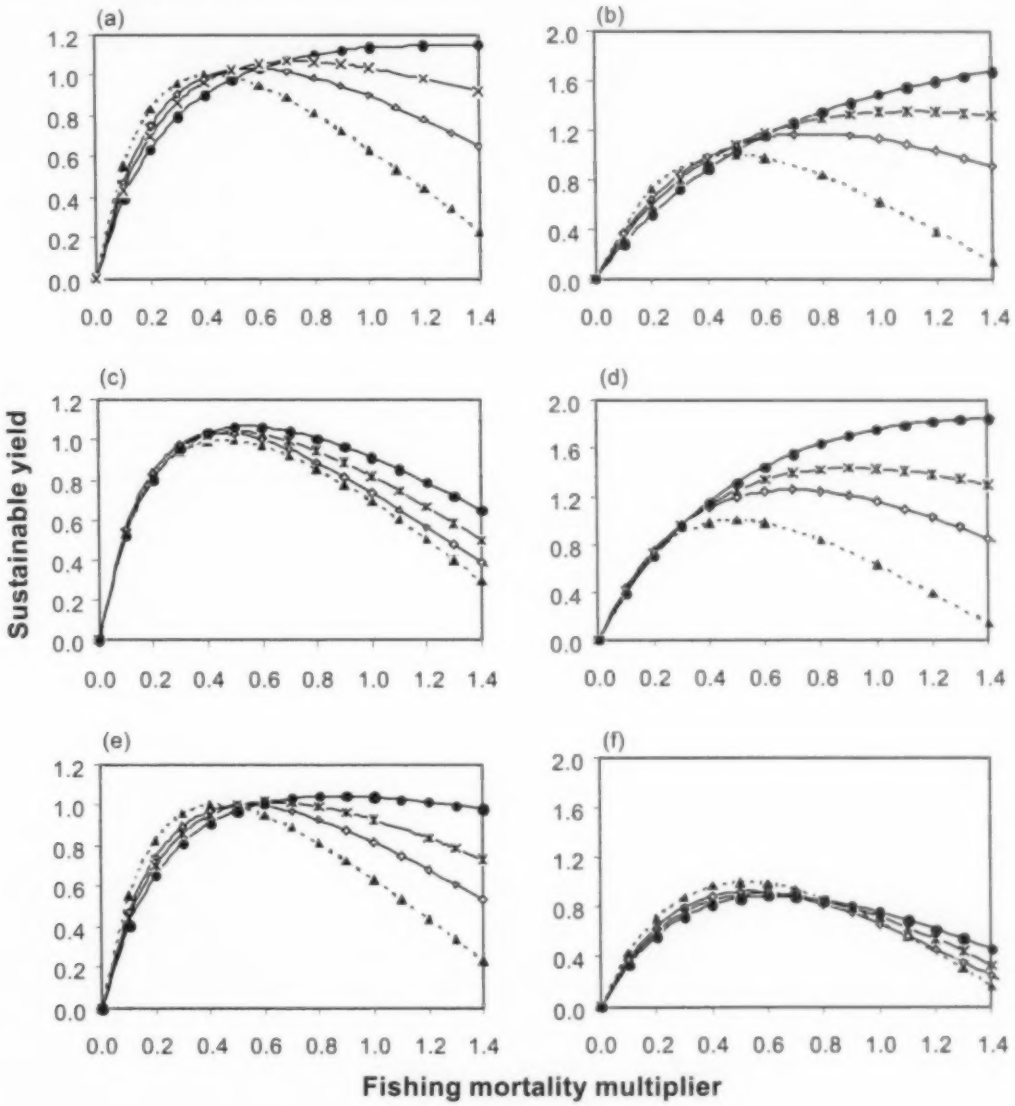

tected is considerably higher than that required when the entire area is fished (Table 6); the gains are substantial when the area protected is biologically important (hence the benefits are much higher if the nursery ground is protected and immature fish are targeted in the fishery), and for less mobile fish. If spawners get incidental protection because the nursery ground is also a spawning ground, the benefits are even more pronounced. $\bar{F}_{ext}$ would be expected to be higher on the remaining area if a part of the area is not fished, although this may not constitute an overall benefit to the fish-

© 2002 NRC Canada

Table 6. The resilience of a fish population to overexploitation when protected by a marine reserve.

	Actual $\hat{F}$			Comparative $\hat{F}$		
	L	M	H	L	M	H
Spawning	33	20	13	–13	–20	–27
Nursery	300	107	53	160	33	0
Spawning & nursery	>500	213	73	>500	100	13

Note: Results are shown as the percent difference between the value of the fishing mortality multiplier causing extinction of the population when area *a* is fully protected as a marine reserve and when there is no reserve. The fishing mortality multiplier leading to extinction without a reserve is $F_{ext} = 1.5$. It is assumed that fishermen are targeting small fish. Once the reserve is instituted, fishing mortality takes place only in area *b*. Results are shown for three levels of fish mobility (L, low; M, moderate; H, high). Area *a* is assumed to be either a spawning ground, a nursery ground, or both. Actual $\hat{F}$ is based on the fishing mortality on area *b* that produces extinction; comparative $\hat{F}$ is based on this value multiplied by the proportion of the total area that area *b* makes up, thus showing the effect on overall fishing effort of instituting a reserve.

ery if this fishing mortality corresponds to an overall fishing effort that is lower than that immediately prior to reserve establishment. But overall benefits can also be substantial, particularly when the fish are not mobile and the reserve protects both the spawning and nursery areas (Table 6).

As well as long-term benefits, an important consideration is whether a marine reserve can provide short-term benefits. This depends on the type of effort redistribution and fish mobility. The quantitative dependence of the short-term effects of reserve establishment on these factors is presented for a situation in which the nursery area is protected and there is no size selectivity (Table 7*a*). The general patterns shown here are similar to those found under other assumptions about selectivity and the status of area *a*. Long-term benefits (increases in equilibrium SSB and yield) are inversely related to fish mobility, whereas short-term benefits (yield in the first year after reserve creation and yield recovery rate) are positively related to mobility.

The type of effort redistribution also affects reserve effectiveness: full redistribution leads to SSB reductions compared with the situation before reserve establishment (except in some cases of lower mobility fish), whereas SSB is always increased by a reserve if effort is not redistributed. Conversely, full redistribution generally leads to yield increases in both the short and long terms, (except in the case of highly mobile overexploited stocks, for which the large reduction in SSB leads to long-term yield reductions). If effort is not redistributed, yield does increase in the long term (by very little if the fishery was previously underexploited), although reductions in yield are experienced in the short term.

A marine reserve without effort control (full redistribution) is beneficial in some cases, whereas a reserve with effort control is always beneficial in terms of SSB and long-term yield (Table 7*a*). However, some of that benefit is likely attributable to the effort control itself, rather than to the act of limiting access to a distinct area. For this reason, the effect of effort control alone, in the absence of a marine reserve, is also given (Table 7*b*). For comparability, fishing effort was reduced to the level that gives the same yield in the first year after control as is obtained when a reserve is instituted and effort is not redistributed. Effort control alone produces an increase in SSB for both under- and overexploited fisheries and in long-term yield for overexploited fisheries, although substantially less than when a marine reserve is also created. Hence, the marine reserve leads to a substantial improvement in fishery performance over effort control alone.

Discussion

Our study has evaluated a broad range of assumptions concerning fish mobility, the status of the area being protected (spawning ground and (or) nursery ground), effort redistribution, and fishing selectivity. Previous studies have shown that each of these factors separately could be significant for the effectiveness of a reserve (e.g., movement rate, Polacheck 1990; fishing effort control, Sladek Nowlis and Roberts 1999), but we have shown how these factors affect reserve effectiveness in combination, thereby moving towards an approach that combines realistic assumptions about both the biology of the target species and the response of the fishery to area closure. Previous studies of the effectiveness of marine reserves have generally concluded that they are beneficial only for overexploited fisheries (e.g., Guénette and Pitcher 1999; Sladek Nowlis and Roberts 1999). Those studies that have considered mobility have found yield improvements only for species that are not highly mobile, although Guénette and Pitcher (1999) noted that SSB and resilience of mobile species were improved by a reserve. Our results concur with those of some recent modelling studies regarding overexploited fisheries (Guénette and Pitcher 1999; Sladek Nowlis and Roberts 1999), but we have found that yield and SSB benefits can be obtained through the use of a marine reserve even for highly mobile fish and underexploited fisheries. Thus, marine reserves could be used for the protection of a larger range of marine species than previously thought. However, our model showed that the establishment of a reserve is not always beneficial, and could lead to both yield and SSB reductions. To avoid this, it is important to designate reserves only in appropriate areas and to consider the regulatory measures needed in conjunction with the reserve (see Roberts and Hawkins 2000).

Generally there are trade-offs to be made between the short-term and long-term effects of a marine reserve. The short-term effects of reserve establishment are not usually considered in modelling studies (but see Sladek Nowlis and Roberts 1997); however, they are of crucial importance in practical implementation. Our study has shown that the short-term losses associated with reserve establishment are less severe for highly mobile fish. If effort from the reserve area is redistributed to the rest of the fishing area on establishment of a reserve, short-term losses can be minimized or avoided, although this can lead to a concomitant reduction in long-term benefits from the reserve both in terms of yield and SSB, and even to decreases in SSB. Although our study does not address the important and overlooked issues of the economic and social impacts of reserve establishment, it does address effort redistribution following reserve creation, albeit in a highly simplified manner. Changes in effort levels following the closure of a fished area can be due to the reactions of individual fishers or to management actions accompanying reserve creation. The results suggest that

© 2002 NRC Canada

Table 7. (*a*) The effects of the type of effort redistribution (full or none) and fish mobility on spawning stock biomass (SSB), equilibrium biomass yield, yield in the first year (Year 1), and the time taken for yield to recover to the pre-reserve level (time), shown for two levels of initial fishing mortality; an underexploited stock and an overexploited stock. (*b*) The effect of effort limitation without a marine reserve, with effort being reduced such that yields in the first year are the same as those obtained for a marine reserve with no effort redistribution.

(*a*) Effort redistribution.*

		Underexploited				Overexploited			
Redistribution	Mobility	SSB	Equilibrium yield	Year 1	Time	SSB	Equilibrium yield	Year 1	Time
Full	Low	–5	+30	+32	—	+9	+39	+15	—
	Moderate	–14	+27	+40	—	–3	+6	+28	—
	High	–19	+23	+42	—	–46	–14	+32	—
None	Low	+19	+4	–12	5	+90	+49	–18	3
	Moderate	+12	+4	–6	6	+53	+34	–9	3
	High	+9	+3	–5	6	+39	+27	–6	3

(*b*) Effort limitation.

	Underexploited				Overexploited			
Mobility	SSB	Equilibrium yield	Year 1	Time	SSB	Equilibrium yield	Year 1	Time
Low	+8	–6	–12	∞	+50	+11	–18	6
Moderate	+4	–3	–6	∞	+24	+7	–9	6
High	+3	–2	–5	∞	+17	+6	–6	6

*Results are presented as the percentage change compared with the equilibrium value before the institution of the reserve, except time, which is given in years. It is assumed that the reserve is protecting the nursery area. The effect of selectivity is removed from the results by assuming no selectivity by size.

consideration of the extent to which effort is redistributed following reserve creation will be a key determinant of management success, and thus should be a priority for future modelling work.

Another major benefit that has been suggested for marine reserves is improved resilience to overexploitation (e.g., Lauck et al. 1998). We have shown that this is indeed a benefit in most cases, particularly for less mobile fish, except when the area protected does not shelter the size classes primarily targeted by the fishery.

Our study has shown that reserves could be beneficial in the specific instance of Mediterranean hake, because there is a defined area in which the sought-after immature fish are mostly found. If this area also happens to coincide with the spawning ground, as is sometimes the case, benefits from a reserve can be greater still. These benefits are found for underexploited as well as overexploited fisheries. Benefits also depend on the assumptions made concerning effort redistribution; if effort is not redistributed, short-term yields are reduced but SSB is higher. It should be noted, however, that these conclusions are preliminary for Mediterranean hake, because of the uncertainty in parameter estimation (particularly with respect to movement rates), and because we have not considered sociopolitical barriers to reserve creation. Nevertheless, the use of area closures for the management of red mullet (*Mullus barbatus*) fisheries in the Mediterranean and the protection of part of the Gulf of Castellammare (Sicily), where many juvenile hake are caught (C. Pipitone, National Research Council, Istituto di ricerche sulle Risorse Marine e l'Ambiente, Laboratorio di Biologia Marina, Castellammare del Golfo, Italy, personal communication), have produced positive results, supporting our predictions (Garcia and Demetropoulos 1986; Caddy 1990; Pipitone et al. 2002).

The model investigates some of the potential benefits of marine reserves for a single species. However, marine reserves also have broader benefits. The establishment of a reserve in an area offers protection to all species inhabiting the area (Allison et al. 1998) and could protect habitats from destructive fishing techniques (Roberts 1998). They also contribute to the protection and enhancement of biodiversity and could benefit tourism (Lauck et al. 1998; Roberts and Hawkins 2000).

We have shown here how important it is to account correctly for the biological characteristics of an exploited species and the dynamics of the fishery targeting it when considering the benefits of a marine reserve. By increasing model realism, we have shown that marine reserves that take spatial and temporal variation in fish population dynamics into account (e.g., by protecting nursery areas) could be beneficial even for underexploited stocks and for highly mobile species. The modelling framework presented here is likely to be useful for the many other species that, like hake, exhibit seasonal migrations and defined spawning and nursery areas. Our analysis suggests that reserves may well also be of value for these species. However, the theoretical models presented here now need to be tested by application to fisheries in practice.

Acknowledgements

We would like to thank A.J. Abella, J.F. Caddy, Callum Roberts, and two anonymous referees for the information and the valuable comments they provided, and R.I.C.C. Francis for his help with the construction of some of the equations used in the model. C. Cunningham and I. Mosquera are thanked for their comments on earlier versions of the manuscript. This work was partly funded by the Wildlife Conservation Society.

© 2002 NRC Canada

References

Abella, A.J., Auteri, R., and Serena, F. 1995. Some aspects of growth and recruitment of hake in the Northern Tyrrhenian sea. Rapport Commision International Mer Méditerranée, **34**: 235.

Abella, A.J., Caddy, J.F., and Serena, F. 1997. Does natural mortality decline with age? An alternative yield paradigm for juvenile fisheries, illustrated by the hake *M. merluccius* fishery in the Mediterranean. Aquat. Living Resour. **10**: 257–269.

Allison, G.W., Lubchenco, J., and Carr, M.H. 1998. Marine reserves are necessary but not sufficient for marine conservation. Ecol. Appl. **8**(1)(Suppl.): S79–S92.

Ballantine, W.J. 1995. The New Zealand experience with 'no-take' marine reserves. *In* Review of the use of marine fishery reserves in the U.S. southeastern Atlantic. *Edited by* C. Roberts et al. NOAA Tech. Memo. NMFS-SEFSC-376. pp. C15–C31.

Beverton, R.J. 1998. Fish, fact and fantasy: a long view. Rev. Fish Biol. Fish. **8**: 229–249.

Beverton, R.J., and Holt S.J. 1957. On the dynamics of exploited fish population. Her Majesty's Stationary Office, London.

Buckworth, R.C. 1998. World fisheries are in crisis? We must respond. *In* Reinventing fisheries management. *Edited by* T.J. Pitcher, P.J.B. Hart, and D. Pauly. Fish and Fisheries Series 23. Chapman and Hall. pp. 3–14.

Caddy, J.F. 1990. Options for the regulation of Mediterranean demersal fisheries. Natural Resources Modeling, **4**: 427–475.

Caddy, J.F., and Abella, A.J. 1999. Reconstructing reciprocal M vectors from length cohort analysis (LCA) of commercial size frequencies of hake, and fine mesh trawl surveys over the same grounds. Fish. Res. **41**: 169–175.

Dayton, P.K., Thrush, S.F., Agardy, M.T., and Hofman, R.J. 1995. Environmental effects of marine fishing. Aquat. Conserv. Mar. Freshwater Ecosyst. **5**: 205–32.

Die, D.J., and Watson, R.A. 1992. A per-recruit simulation model for evaluating spatial closure in an Australian penaeid fishery. Aquat. Living Resour. **5**: 145–153.

Food and Agriculture Organization (FAO). 1995. The state of the world fisheries and aquaculture. FAO Fisheries Department, Rome.

Francis, R.I.C.C. 1992. Use of risk analysis to assess fishery management strategies: a case study using orange roughy (*Hoplostethus atlanticus*) on the Chatham Rise, New Zealand. Can. J. Fish. Aquat. Sci. **49**: 922–930.

Garcia, S., and Demetropoulos, A. 1986. Management of Cyprus fisheries. FAO Fish. Rep. No. 253.

Guénette, S., and Pitcher, T.J. 1999. An age-structured model showing the benefits of marine reserves in controlling overexploitation. Fish. Res. **39**: 295–303.

Hilborn, R. 1990. Determination of fish movement patterns from tag recoveries using maximum likelihood estimators. Can. J. Fish. Aquat. Sci. **47**: 635–643.

Lauck, T., Clark C.W., Mangel, M., and Munro, G.R. 1998. Implementing the precautionary principle in fisheries management through marine reserves. Ecol. Appl. **8**: S72–S78.

Mangel, M. 2000*a*. On the fraction of habitat allocated to marine reserves. Ecol. Lett. **3**: 15–22.

Mangel, M. 2000*b*. Trade-offs between fish habitat and fishing mortality and the role of reserves. Bull. Mar. Sci. **66**: 663–674.

Mosqueira, I., Côté, I.M., Jennings, S., and Reynolds, J.D. 2000. Conservation benefits of marine reserves for fish populations. Anim. Conserv. **3**: 321–332.

Myers, R.A, Bridson, J., and Barrowman, N.J. 1995. Summary of worldwide spawner and recruitment data. Can. Tech. Rep. Fish. Aquat. Sci. No. **2024**: 120–124.

Oliver, P., and Massuti, E. 1995. Biology and fisheries of eastern Mediterranean hake (*M. merluccius*) *In* Hake: fisheries, ecology and markets. *Edited by* J. Alheit and T.J. Pitcher. Fish Fish. Ser. 15. Chapman and Hall, London. 181–202.

Orsi Relini, L., Cappanera, M., and Fiorentino, F. 1989. Spatial-temporal distribution and growth of M. merluccius recruits in the Ligurian Sea. Observations on the 0 group. Cybium, **13**: 263–270.

Papaconstantinou, C., and Stergiou, K.I. 1995. Biology and fisheries of eastern Mediterranean hake (*M. merluccius*) *In* Hake: fisheries, ecology and markets. *Edited by* J. Alheit and T.J. Pitcher. Fish Fish. Ser. 15. Chapman and Hall. pp. 149–180.

Papaconstantinou, C., Petracis, G., and Vassilopoulou, V. 1986. The fecundity of hake (*Merluccius merluccius*) and red Pandora (*Pagellus Erythrinus*) in Greek seas. Acta Adriat. **27**(1–2): 85–95.

Pipitone, C., D'Anna, G., Badalamenti, F., Scotti, G., Coppola, M., Di Stefano, G., and Kienzle, M. 2002. Fishery reserves as a management tool: the case of the Gulf of Castellammare. Fishery Exclusion Zones Internet Conference, 21 January – 4 February 2002. http://www.valfez.org/internet_conf/ (accessed 27 January 2002).

Pitcher, T.J., and Pauly, D. 1998. Rebuilding ecosystems, not sustainability, as the proper goal of fishery management. *In* Reinventing fisheries management. *Edited by* T.J. Pitcher, P.J.B. Hart, and D. Pauly. Fish Fish. Ser. 23. Chapman and Hall, London. pp. 311–325.

Polacheck, T. 1990. Year around closed areas as a management tool. Nat. Resour. Model. **4**: 327–354.

Quinn, T.J., and Deriso, R.B. 1999. Quantitative fish dynamics. Oxford University Press, New York.

Recasens, L., Lombarte, A., Morales-Nin, B., and Torres, G.J. 1998. Spatio-temporal variation in the population structure of the European hake in the NW Mediterranean. J. Fish Biol. **53**: 387–401.

Roberts, C.M. 1998. No-take marine reserves: unlocking the potential for fisheries. Marine Environmental Management: Review of Events in 1997 and Future Trends, **5**: 127–132.

Roberts, C.M., and Hawkins, J.P. 2000. Fully-protected marine reserves: a guide. WWF Endangered Seas Campaign, 1250 24th Street NW, Washington, DC 20037, U.S.A., and Environment Department, University of York, York, YO10 5DD, U.K.

Roberts, C.M., and Polunin, N.V.C. 1993. Marine reserves: simple solutions to managing complex fisheries? Ambio, **22**: 363–368.

Sant, M. 1996. Environmental sustainability and the public: responses to a proposed marine reserve at Jervis Bay, New South Wales, Australia. Ocean Coast. Manag. **32**: 1–16.

Sladek Nowlis, J., and Roberts, C.M. 1997. You can have your fish & eat it too: theoretical approaches to marine reserve design. Proc. 8th Int. Coral Reef Symp. (Issue 2), 24–29 June 1996, Panama City. *Edited by* W. Holland. pp. 1907–1910.

Sladek Nowlis, J., and Roberts, C.M. 1999. Predicted Fisheries Benefits and Optimal Marine Fishery Reserves Design. Fish. Bull. **97**: 604–616.

Zupanovic, S., and Jardas, I. 1986. A contribution to the study of biology and population dynamics of the Adriatic hake, *M. merluccius*. Acta Adriat. **27**(1–2): 97–146.

Appendix A. Calculation of stock–recruitment parameters.

The values of α and β in eq. 1 depend on the steepness, h, of the egg–recruits curve and on the number of eggs, E_0, produced under natural mortality

© 2002 NRC Canada

$$(A1.1)\quad a = \sum_{A \geq A_{mat}} n_{0,A} f_A \frac{(1-h)}{4h}$$

$$(A1.2)\quad \beta = \sum_{A \geq A_{mat}} n_{0,A} f_A \frac{(5h-1)}{4h \cdot E_0}$$

where A denotes the age of the fish, A_{mat} is the age at maturity of female fish, and f_A is fish fecundity at age (see Table 3 for the values of A_{mat} and f_A). The steepness, h, is equal to the fraction of the recruits under virgin conditions, R_0 (the recruitment corresponding to E_0), that are expected when the number of eggs is reduced to 20% of E_0. The parameter $n_{0,A}$ is the exponential factor that determines the proportion of fish at age A that survive under virgin conditions (Francis 1992),

$$(A1.3)\quad n_{0,A} = \begin{cases} e^{-\left(\sum_{j=1}^{A} M_j\right)} e^{\frac{1}{2}M_A} e^{-\frac{1}{2}M_{A=0.5}} & A < A_{max} \\ \dfrac{e^{-\left(\sum_{j=1}^{A_{max}} M_j\right)} e^{\frac{1}{2}M_{A_{max}-1}} e^{-\frac{1}{2}M_{A=0.5}}}{1 - e^{-M_{A_{max}}}} & A = A_{max} \end{cases}$$

The natural mortality at age, M_A, as well as the maximum age of fish, A_{max}, are necessary for the estimation of $n_{0,A}$. The expression for $n_{0,A_{max}}$ was derived assuming that M of fish at age A_{max-1} or older remains constant. M of six-month-old fish, $M_{A=0.5}$, is needed, since recruitment is assumed to take place six months after spawning. Because this formulation was developed for age- rather than stage-structured models, we must assume that all spawning takes place in a single time period. Then, once the virgin biomass is found, the model is run without fishing until the equilibrium for the size-structured model is found.

Appendix B. Calculation of the number of fish in a given size category and area.

To calculate the number of fish in an area that belong to size category S at the beginning of time period t, it is necessary to account for fish that have grown from size category $S-1$ at the beginning or time period $t-1$ to size category S at the beginning of time period t, as well as fish that have remained in size category S between the two time periods. It is also necessary to account for fish that have remained in area a or b or moved into or out of each area between the two time periods. As an example, we show the calculation for the number of fish in area a that belong to size category S at the beginning of time period t.

First, consider the fish that have remained in area a. The number of these is given by

$$(A2.1)\quad N_{a\to a,S,t} = N_{a,S-1,t-1} e^{-(F_{a,S-1}+M_{S-1})} P_{S-1,S}(1-\vartheta_{a,b,S-1,t-1}) + N_{a,S,t-1} e^{-(F_{a,S}+M_S)} P_{S,S}(1-\vartheta_{a,b,S,t-1})$$

The number of fish that moved from area a to area b is given by

$$(A2.2)\quad N_{a\to b,S,t} = N_{a,S-1,t-1} e^{-(F_{a,S-1}+M_{S-1})} P_{S-1,S} \vartheta_{a,b,S-1,t-1} + N_{a,S,t-1} e^{-(F_{a,S}+M_S)} P_{S,S} \vartheta_{a,b,S,t-1}$$

The number of fish that moved from area b to area a is given by

$$(A2.3)\quad N_{b\to a,S,t} = N_{b,S-1,t-1} e^{-(F_{b,S-1}+M_{S-1})} P_{S-1,S} \vartheta_{b,a,S-1,t-1} + N_{b,S,t-1} e^{-(F_{b,S}+M_S)} P_{S,S} \vartheta_{b,a,S,t-1}$$

Thus, the number of fish in area a that belong to size category S at the beginning of time period t is given by

$$(A2.4)\quad N_{a,S-1,t-1} = N_{a\to a,S,t} + N_{b\to a,S,t} - N_{a\to b,S,t}$$

Similar formulas apply for calculating the numbers of fish in area b. When area a is a marine reserve, $F_{a,S} = 0$ for each size class, S, because fishing does not take place in the area.

© 2002 NRC Canada

Natural mortality estimates of juvenile Pacific herring (*Clupea pallasi*) in Prince William Sound, Alaska

Kevin D.E. Stokesbury, Jay Kirsch, E. Vincent Patrick, and Brenda L. Norcross

Abstract: The densities of young-of-the-year and 1-year-old Pacific herring, *Clupea pallasi*, in Prince William Sound, Alaska, were estimated using acoustic surveys from June 1996 to March 1998. Four bays were surveyed with acoustic transects that were repeated three times in 24 h. Species composition and size structure were determined from net collections. Averaging over the 24-h period allowed the best use of all data, as observations between the three replicates were similar but sporadic, possibly resulting from the different seasonal day–night cycle in these northern latitudes. The average instantaneous natural mortality rates for young-of-the-year Pacific herring were 0.009 (standard deviation (SD) = 0.002) and 0.016 (SD = 0.012) for the 1996 and 1997 cohorts, respectively. The average instantaneous natural mortality rates for 1-year-old Pacific herring were 0.003 (SD = 0.007) and 0.008 (SD = 0.005) for the 1995 and 1996 cohorts, respectively. Combining our estimates with those in the primary literature for other life history phases of Pacific herring indicated a progressive decrease in instantaneous natural mortality with age. This study presents the first direct estimates of natural mortality for juvenile herring.

Résumé : Des inventaires acoustiques faits de juin 1996 à mars 1998 ont permis d'estimer les densités des petits de l'année et des poissons de 1 an chez le hareng du Pacifique, *Clupea pallasi*, dans le détroit du Prince-William en Alaska. Quatre baies ont été inventoriées à l'aide de transects acoustiques réitérés trois fois en 24 heures. La composition spécifique et la structure en taille ont été déterminées à l'aide de récoltes au filet. L'établissement de la moyenne sur une période de 24 heures a permis une utilisation optimale des données, parce que les observations lors des trois inventaires réitérés étaient semblables mais sporadiques, sans doute à cause de différences saisonnières dans le cycle nycthéméral à ces latitudes nordiques. Les taux instantanés moyens de mortalité naturelle pour les jeunes de l'année chez le hareng du Pacifique étaient de 0,009 (écart-type, SD = 0,002) et de 0,016 (SD = 0,012) pour les cohortes de 1996 et de 1997. Les taux instantanés moyens de mortalité naturelle pour les harengs du Pacifique de 1 an étaient de 0,003 (SD = 0,007) et de 0,008 (SD = 0,005) pour les cohortes de 1995 et de 1996. L'intégration de nos résultats à ceux de la littérature primaire concernant d'autres étapes du cycle biologique du hareng du Pacifique montre une décroissance progressive de la mortalité instantanée naturelle avec l'âge. C'est la première fois que l'on estime directement la mortalité naturelle chez de jeunes harengs.

[Traduit par la Rédaction]

Introduction

Pacific herring (*Clupea pallasi*) dominate the near-shore ichthyofauna of Prince William Sound, Alaska (Stokesbury et al. 2000). They provide primary forage for piscivorous fishes, birds, and marine mammals and support commercial bait, sac-roe, and roe-on-kelp fisheries (Livingston 1993; Paine et al. 1996; Pearson et al. 1999). Mature Pacific herring spawn in late April over 23–268 km of coastline primarily in the eastern portion of Prince William Sound (Norcross et al. 2001). The embryos suffer high mortality owing to wave exposure and predation (McGurk and Brown 1996; Rooper et al. 1999). After hatching, the larvae are advected away from the spawning areas (Norcross et al.

Received 17 May 2001. Accepted 25 January 2002. Published on the NRC Research Press Web site at http://cjfas.nrc.ca on 21 March 2002.
J16356

K.D.E. Stokesbury[1,2] **and B.L. Norcross.** Institute of Marine Science, School of Fisheries and Ocean Sciences, University of Alaska–Fairbanks, Fairbanks, AK 99775-7220, U.S.A.
J. Kirsch[3] **and E.V. Patrick.**[4] Institute of Marine Science, School of Fisheries and Ocean Sciences, University of Alaska–Fairbanks, Fairbanks, AK 99775-7220, U.S.A., and Prince William Sound Science Center, P.O. Box 705, Cordova, AK 99574, U.S.A.

[1]Corresponding author (e-mail: kstokesbury@umassd.edu).
[2]Present address: School for Marine Science and Technology, University of Massachusetts Dartmouth, 706 South Rodney French Boulevard, New Bedford, MA 02744-1221, U.S.A.
[3]Present address: Harman Music Group, 8760 South Sandy Pkwy., Sandy, UT 84070, U.S.A.
[4]Present address: Advanced Visualization Laboratory and Institute for Systems Research, University of Maryland, College Park, MD 20742, U.S.A.

 DOI: 10.1139/F02-017 © 2002 NRC Canada

2001). Larval pacific herring metamorphose from the water column in June and July. The juvenile Pacific herring then aggregate at the heads of bays and are rarely observed along the open coastline (Stokesbury et al. 2000). Within each bay, juvenile Pacific herring have a distinct short-term growth pattern (Stokesbury et al. 1999). These data suggest that once Pacific herring enter the bays of Prince William Sound, they are isolated until the end of their 2nd year (Stokesbury et al. 1999, 2000). Pacific herring move out of the bays, joining the adult schools in the southern portion of Prince William Sound in June of their 2nd year (Stokesbury et al. 2000).

Presently, no reliable estimates of Atlantic or Pacific juvenile herring natural mortality exist (Blaxter and Hunter 1982; McGurk 1993; Tanasichuk 1997). Pacific herring larval mortality rates have been estimated from laboratory experiments and plankton field samples (Wespestad and Moksness 1990; McGurk 1993; McGurk et al. 1993). Adult herring natural and fishery mortality rates have been estimated using fishery data and age structure analysis (Beverton 1963; Tanasichuk et al. 1993). Juvenile herring mortality must be estimated from direct observations; it cannot be estimated from life history models that require gonadosomatic indices or von Bertalanffy growth parameters (Gulland 1988). An accurate estimate of natural mortality would be useful to fishery management as it facilitates determining the various components of total mortality, such as fishing and incidental mortality (Ricker 1975; Cushing 1981).

We estimated instantaneous natural mortality rates of juvenile Pacific herring in Prince William Sound, Alaska, from June 1996 to March 1998. Measuring isolated juvenile Pacific herring aggregations directly using acoustic techniques allowed us to construct life tables for the 1995, 1996, and 1997 cohorts. The critical assumption for these calculations is that juvenile Pacific herring aggregations are isolated within the bays, or that immigration and emigration are equal, and that the acoustic survey provides a relative estimate of density that reflects the changes in density actually occurring within the population.

Materials and methods

Prince William Sound, Alaska, is a large body of water separated from the Gulf of Alaska by a series of mountainous islands (Fig. 1). The rocky coastline is irregular with numerous islands, passages, bays, and deep fjords. Four bays (Simpson, Zaikof, Whale, and Eaglek) were selected as study sites because they are spatially segregated and contain isolated aggregations of juvenile Pacific herring (Stokesbury et al. 1999, 2000). These four bays were acoustically surveyed between June 1996 and March 1998. During each 7-day cruise, each bay was surveyed three times over 24 h beginning at 0000, 0800, and 1600 hours until October 1997 when the survey was reduced to a single transect per bay beginning at 1600 hours.

The acoustic survey vessel (commercial fishing seiner, ≈17 m) followed a continuous parallel transect pattern; total transect distances were 31.2 km (Simpson Bay), 35.0 km (Zaikof Bay), 31.2 km (Whale Bay), and 43.8 km (Eaglek Bay) (Fig. 1). The acoustic vessel surveyed at 9–11 km·h^{-1} with a 120 kHz BioSonics 101 echosounder (BioSonics Inc., Seattle, Wash.) using a preamplified dual-beam transducer towed ≈1 m below the water surface. The acoustic system was calibrated both with a hydrophone and with a standard target. The acoustic signals were processed in real time using the BioSonics ESP 221 echo square integration software and ESP 281 dual-beam software, and the raw signal was stored on digital audio tape (MacLennan and Simmonds 1992; Stokesbury et al. 2000). Latitude and longitude were recorded simultaneously for each data cell using the GPS navigational system. There are two types of cells in acoustic data sets; insonified volume increases with depth but is not numerically known and was therefore removed mathematically during the density calculations. Echo integration measurements were converted into the second data cell type with 22.2-m lengths (16 pings per cell, 2 pings·s^{-1}) and 1-m width and depth.

Once a fish school was measured with the acoustic equipment, it was sampled to determine species composition and size structure. Fish were captured using a modified bottom trawl in deep water (1.52 m × 2.13 m Nor'Eastern Astoria V trawl doors, head rope 21.3 m, foot rope 29.0 m, estimated 3 m × 20.0 m mouth, 10.2-cm-mesh wings, 8.9-cm middle, and a 32.0-mm cod-end liner deployed by the Alaska Department of Fish and Game R/V *Pandalus*, ≈20 m), one of two anchovy seines (250.0 m × 34.0 m or 20.0 m, 25.0 mm stretch mesh deployed by a commercial fishing seiner, ≈17 m), or a small salmon fry seine in shallow water (50.0 m × 8.0 m, 3.0 mm stretch mesh deployed from a 6-m skiff equipped with a 70-horsepower engine). The fish from each sample were identified, after which 1000 of the dominant fish species were randomly subsampled. Fork length (mm) was measured for the 1000 fish, and a subsample of 450 fish were measured for wet weight (g). From these data, length–weight regressions were calculated for each bay during each survey to account for the wide seasonal and spatial variation in weight-to-length relationships of Pacific herring observed in Prince William Sound (Stokesbury et al. 1999). Size modes of Pacific herring, representing young-of-the-year, 1-year-old, or adult fish, were identified (Stokesbury et al. 1999, 2000). Juvenile Pacific herring age cohorts are easily identified by length frequencies because the herring metamorphose from the water column in June and July, creating distinct size modes per cohort until after their 2nd year when they have completed about 75% of their somatic growth (Iles 1971; Winters and Wheeler 1994; Stokesbury et al. 2000).

A length-dependent scaling constant, based on a target strength-to-biomass ratio, was used to convert the acoustic signal (TS – 10log$w$) from units of reflected acoustic energy (dB) to units of biomass density (kg·m^{-3}):

$$(1) \qquad TS - 10\log w = -6.0\log L - 24.2 \text{ dB m}^2/\text{kg}$$

where L is the mean fork length (cm) of the fish collected in the area (Thorne 1977; Stokesbury et al. 2000). The species proportions, based on the number of individuals per fish species in the net collections, were multiplied by the echo integration densities (kg·m^{-3}) and then converted using the length–weight regression estimated for each bay during each survey into number of Pacific herring per size mode (Stokesbury et al. 2000). Pacific herring dominated the fish collections, and there appears to be little spatial overlap

© 2002 NRC Canada

Fig. 1. Location of the acoustic transects used to survey the four bays in Prince William Sound, Alaska, U.S.A., from June 1996 to March 1998: A, Prince William Sound; B, Eaglek Bay; C, Simpson Bay; D, Whale Bay; E, Zaikof Bay.

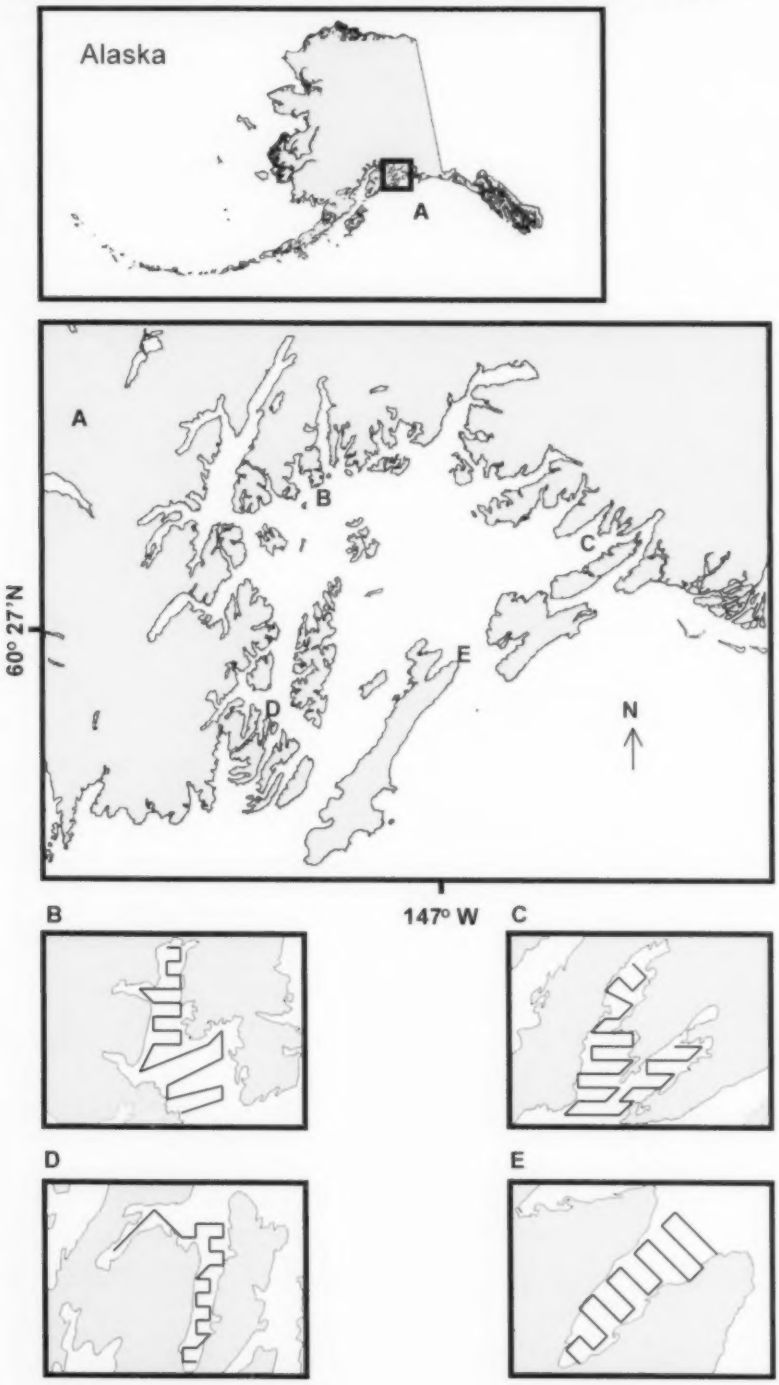

between Pacific herring and juvenile walleye pollock, *Theragra chalcogramma*, the second most abundant species in the nearshore water column (Stokesbury et al. 2000). For our analysis, adult Pacific herring and any other species observed were removed from the acoustic signal. Based on frequency distributions of the data, cells containing the

© 2002 NRC Canada

Table 1. Life tables estimating instantaneous natural mortality rates[a] of Pacific herring, *Clupea pallasi*, observed from June 1996 to March 1998 within the four bays in Prince William Sound.

Bay	Date	Age	$t_{x+1} - t_x$	0000	0800	1600	Mean	SD	$\ln(a_x)$	M
1995 cohort										
Simpson	Aug. 1996	431	274	355.9	199.7	59.1	204.9	148.5	5.323	0.005
Simpson	May 1997	705		28.6	9.3	123.1	53.6	60.9	3.982	
Zaikof	Aug. 1996	430	276	59.2	147.0	199.0	134.9	70.5	4.905	–0.005
Zaikof	May 1997	706		578.5	658.5	556.6	378.8	327.1	5.937	
Whale	Aug. 1996	428	280	24.1	129.3	130.7	94.7	61.2	4.551	0.003
Whale	May 1997	708		10.3	49.0	78.3	45.9	34.1	3.826	
Eaglek	Aug. 1996	429	280	294.7	4468.7	2245.0	2336.1	2088.5	7.756	0.011
Eaglek	May 1997	709		169.1	74.4	45.2	96.2	64.8	4.567	
1996 cohort										
Simpson	Aug. 1996	66	373	16 352.7	1747.2	2339.0	6813.0	8266.9	8.827	0.010
Simpson	Aug. 1997	439	218	113.9	174.8	260.4	183.0	73.6	5.210	0.003
Simpson	Mar. 1998	657				99.0	99.0		4.595	
Zaikof	Aug. 1996	65	341	0.0	0.0	601.9	200.6	347.5	5.301	0.011
Zaikof	July 1997	406	103	12.3	0.0	0.0	4.1	7.1	1.411	0.006
Zaikof	Mar. 1998	656							0.000	
Whale	Aug. 1996	63	373	3 294.3	978.7	0.0	1424.3	1691.7	7.261	0.010
Whale	Aug. 1997	436	218	77.8	0.0	20.7	32.8	40.3	3.491	0.013
Whale	Mar. 1998	654				2.0	2.0		0.693	
Eaglek	Aug. 1996	65	372	17.3	261.6	131.4	136.8	122.3	4.918	0.006
Eaglek	July 1997	437	218	5.1	39.1	2.8	15.6	20.4	2.750	0.013
Eaglek	Mar. 1998	655							0.000	
1997 cohort										
Simpson	Aug. 1997	74	218	9 253.0	890.7	4258.6	4800.8	4207.5	8.477	0.016
Simpson	Mar. 1998	292				158.0	158.0		5.063	
Zaikof	Aug. 1997	69	219	0.0	0.0	271.2	90.4	156.5	4.504	0.002
Zaikof	Mar. 1998	288				53.0	53.0		3.970	
Whale	Aug. 1997	71	218	880.1	0.0	233.9	371.3	455.8	5.917	0.033[b]
Whale	Mar. 1998	289				0.0	0.3		–1.204	
Eaglek	Aug. 1997	76	214	444.0	0.0	0.0	148.0	256.4	4.997	0.015
Eaglek	Mar. 1998	290				6.0	6.0		1.792	

Note: Age is estimated in days with 1 June = day 1. The means and standard deviations (SD) are for the 24-h sample. Blank spaces represent unobserved transects (refer to the text).

[a] $M = \ln(a_{x+1}/a_x)/(t_{x+1} - t_x)$ with the sign changed.

[b] There were no observations of 1997 young-of-the-year Pacific herring in March 1998 (only four fish were observed in October 1997), but this observation was given a value of 1 fish to allow for the calculation of the instantaneous mortality rate.

equivalent of <0.5 fish·m^{-3} were probably zooplankton and were removed from the data set (MacLennan and Simmonds 1992). Finally, all cells were summed to calculate the density estimate of Pacific herring observed within each transect. Many physical and biological variables affect the reflection strength of the acoustic signal, including the morphology of the fish (physostomic, physoclistic, fat content), the orientation of the fish, structure of the fish school, and water temperature and depth (MacLennan and Simmonds 1992; McClatchie et al. 1996). Therefore, our estimates of density are relative and we assume that their fluctuations reflect those of the absolute densities of Pacific herring within each bay.

To calculate instantaneous natural mortality rates, a cohort of fish is followed over a time series (Ricker 1975; Krebs 1989). The time period used to calculate instantaneous mortality was based on the young-of-the-year herring recruiting into the bays during June and July. The 1995 cohort was observed only as 1-year-old fish. The first observation for the 1995 Pacific herring cohort was taken in August 1996 after full recruitment of the 1996 cohort into the bays. The final observation for the 1995 cohort was May 1997 as these fish appeared to leave the bays to join the adult herring schools in June. The 1996 cohort was observed as young-of-the-year and 1-year-old fish. The young-of-the-year observations began in August 1996 after full recruitment into the bays, and the final young-of-the-year observation and, simultaneously, the first 1-year-old observation were made in August 1997 after full recruitment of the 1997 cohort into the bays. The 1997 cohort was observed as young-of-the-year, with the first observation occurring in August 1997 after full recruitment into the bays and the final observation in March 1998, which was our final survey. Thus, for each of the four bays, there are two observations of young-of-the-year and 1-year-old natural mortality rates (Table 1).

The number of fish observed (a_x) during one survey was compared to the subsequent survey (a_{x+1}) approximately 1 year later for each bay. Instantaneous natural mortality rates (day^{-1}) were calculated using the equation

$$(2) \qquad M_x = \ln(a_{x+1}/a_x)/(t_{x+1} - t_x)$$

© 2002 NRC Canada

Fig. 2. Average density ($\log_e$ transformed) of Pacific herring, *Clupea pallasi*, acoustically observed over a 24-h period within each of the four bays from June 1996 to March 1998 in Prince William Sound, Alaska (◇, Simpson Bay; □, Zaikof Bay; Δ, Whale Bay; ×, Eaglek Bay): (*a*) 1995 cohort; (*b*) 1996 cohort; (*c*) 1997 cohort. Slopes of the line segments are the young-of-the-year and 1-year-old estimated instantaneous natural mortality rates for each cohort within each bay.

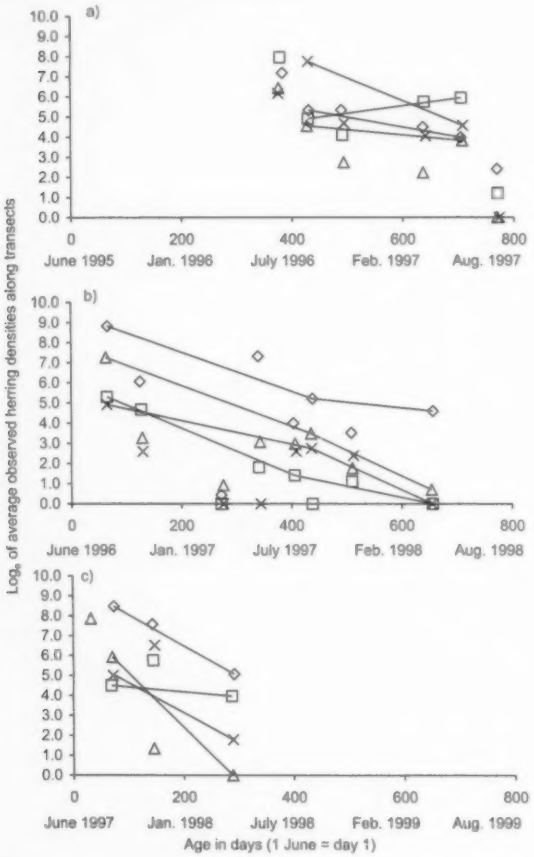

where $t_{x+1} - t_x$ equals the time interval between surveys in days (Ricker 1975; Krebs 1989).

Two repeated measures of the same transect during the same time period in the same bay during the same survey were completed within a 4-day period twice during our study. Density estimates from these replicate transects were compared using a χ^2 test at the 5% level of significance (Sokal and Rohlf 1981). Yate's correction, which subtracts 0.5 from the numerator before it is squared in the χ^2 test, was applied because of the low number of degrees of freedom.

Results

The juvenile Pacific herring densities measured during the three replicates (transects) within a 24-h period were similar. For the survey period with all bays combined, 36.5, 31.6, and 31.9% of Pacific herring were observed on the 0000-, 0800-, and 1600-hour transects, respectively. This pattern was observed in each bay; therefore, the average of number of Pacific herring observed during the three transects was used to calculate instantaneous mortality (Table 1). Averaging over 24 h allowed the best use of all data, as observations could be sporadic, possibly resulting from the different seasonal day–night cycle in these northern latitudes. Our sampling design allowed us to collect samples during sunrise, sunset, and darkness; however, these did not occur during the same transects throughout the year. Further, although Pacific herring moved vertically in the water column with the light cycle, the acoustics still measured them unless they flattened against the sea floor or the water surface.

Life tables were constructed for each of the four bays in Prince William Sound where the 1995, 1996, and 1997 Pacific herring cohorts were acoustically observed (Table 1). The average instantaneous natural mortality rates for young-of-the-year Pacific herring were 0.009 (standard deviation, SD = 0.002) and 0.016 (SD = 0.012) for the 1996 and 1997 cohorts, respectively. The instantaneous natural mortality for the 1997 young-of-the-year cohort was influenced by a high measurement in Whale Bay (0.033), and if this value is removed, the average becomes 0.011 (SD = 0.007). However, there is no logistical or biological reason to remove this observation. The average instantaneous natural mortality rates for 1-year-old Pacific herring were 0.003 (SD = 0.007) and 0.008 (SD = 0.005) for the 1995 and 1996 cohorts, respectively. The 1995 1-year-old cohort contained a negative measure for Zaikof Bay (Table 1), and if this is removed, the average becomes 0.006 (SD = 0.005).

Instantaneous mortality rates varied between bays, between cohorts, and with age (Fig. 2). Young-of-the-year Pacific herring instantaneous mortality rates were always higher than 1-year-old rates in Simpson Bay, which also had the highest densities (Table 1). The initial densities of 1995 1-year-old Pacific herring were higher than the densities for the 1996 1-year-old herring, suggesting better young-of-the-year survival. The 1-year-old instantaneous mortality rates for the 1996 cohort in Zaikof, Whale, and Eaglek bays were calculated from very low densities and these rates are higher than the estimates for the same bays but with the higher densities of the 1995 cohort (Table 1). The density estimates collected in March were always low, possibly because of difficulties, such as ice, during the field sampling (Fig. 2). These lower estimates in March may cause an overestimate in the young-of-the-year 1997 cohort instantaneous mortality rates (Table 1).

During two cruises, it was possible to repeat a transect in the same bay at the same time of day within a 4-day period, enabling an estimate of the precision of the acoustic samples. Similar Pacific herring counts of the dominant age cohorts were observed (Table 2).

Discussion

This study presents the first direct estimates of instantaneous natural mortality rates for juvenile Pacific herring. The juvenile life history stage of Pacific herring was spent within the bays of Prince William Sound and was divided into two 1-year periods. The first period was the young-of-the-year, which began with metamorphose from the larval phase in June and July until the following year when the

© 2002 NRC Canada

Table 2. The number of observed Pacific herring, *Clupea pallasi*, within each year cohort along a continuous acoustic measured at the same time of day in the same bay within a 4-day period in Prince William Sound, Alaska.

Zaikof Bay, 0800 hours					
	5 Oct. 1996		9 Oct. 1996		
Cohort	Observed	Percentage	Observed	Percentage	χ^2
1995	55	94	3	6	78.01*
1996	48	46	56	54	0.51
Simpson Bay, 0000 hours					
	13 Aug. 1997		14 Aug. 1997		
Cohort	Observed	Percentage	Observed	Percentage	χ^2
1995	96	49	98	51	0.00
1996	114	28	297	72	18.96*
1997	9253	53	8286	47	0.20

*$p < 0.01$. Comparisons are between each observation for each age cohort.

next cohort metamorphosed. The 1-year-old period extended from June and July until the following June when the 1-year-old fish became 2-year-old fish and left the nursery bays. The highest natural mortality occurred when the Pacific herring were young-of-the-year, although the rates vary greatly between years. There are probably several sources of this natural mortality, including predation and overwintering starvation. At the same time as Pacific herring metamorphose from the larval phase, both marine mammals and birds are actively feeding their young as well as increasing their own energy supplies in preparation for migrations (Hatch and Sanger 1992; Livingston 1993; Suryan et al. 2000). The largest predator influx is the returning wild and hatchery salmon, numbering 8.4 million wild + 20.4 million hatchery and 4.6 million wild + 23.7 million hatchery for 1996 and 1997, respectively, occurring in early August (Morstad et al. 1997). Herring and sand lance are the most frequently consumed prey (fish represented 80% to 97% of the total diet volume) by marine adult chinook and coho salmon (Scott and Crossman 1973). Newly recruited young-of-the-year Pacific herring are small and abundant and aggregated in bays (Stokesbury et al. 1999, 2000). The mouths of salmon-spawning streams are also located primarily in bays. Thus, these Pacific herring may be the last prey that the salmon encounter before entering their spawning streams. Simpson and Whale bays have large wild salmon runs, whereas Eaglek Bay has both a strong wild salmon and hatchery salmon run (M. Willette, Alaska Department of Fish and Game, Cordova, Alaska, U.S.A., 99574, personal communication).

Pacific herring natural mortality is probably also high during their first winter as a result of starvation and predation. Young-of-the-year Pacific herring must store a critical amount of energy during the summer or they will starve during the winter (Paul and Paul 1998; Paul et al. 1998; Foy and Paul 1999). Smaller fish have the least amount of surplus energy and their survival rate is probably low (Paul and Paul 1998; Paul et al. 1998). Further, Pacific herring may be highly vulnerable to predators during the winter (Stokesbury et al. 1999). Hunger suppresses the herring's antipredator behavior, resulting in loosely packed schools of mixed size-classes (Robinson and Pitcher 1989*a*, 1989*b*; Robinson 1995). The Pacific herring cohort would still be the most frequently encountered prey until the new young-of-the-year cohort recruits in June.

The hypothesis that predation causes a high proportion of the natural mortality of juvenile Pacific herring differs from other studies that conclude that food quality and supply appear to be the primarily determining factors in herring survival and population size in Prince William Sound (Pearson et al. 1999). Further research examining the seasonal patterns of natural mortality is required to test and compare these hypotheses.

The assumption of our analyses is that bays within Prince William Sound were isolated nursery areas, or that immigration and emigration were equal. Therefore, changes of relative densities reflect shifts in the absolute densities of the juvenile Pacific herring. The spatial distribution and growth patterns of juvenile Pacific herring with these bays support this assumption (Stokesbury et al. 1999, 2000). Our observations of density also support this assumption, although if emigration occurred, this may result in an overestimation of mortality rates that would be undetected. Our observations of juvenile Pacific herring differ from those of other herring species where the juveniles appear to range over large areas (Iles 1971; Iles and Sinclair 1982; Sinclair et al. 1985).

There is a progressive decrease in instantaneous natural mortality as the Pacific herring passes through each of its life history stages. Egg–larval instantaneous natural mortality rates were estimated as 0.186 day^{-1} and 0.446 day^{-1} form unoiled and oiled sties, respectively, in Prince William Sound, Alaska, after the *Exxon Valdez* oil spill (McGurk and Brown 1996). The mean natural instantaneous mortality rate was 0.139 day^{-1} for larval Pacific herring (McGurk 1993). Our estimates of mean young-of-the-year and 1-year-old Pacific herring instantaneous natural mortality rates were 0.009–0.016 day^{-1} and 0.003–0.008 day^{-1}, respectively. The mean natural instantaneous mortality rate was 0.0016 day^{-1} for adult Pacific herring (McGurk 1993). Instantaneous natural morality rates of 0.0024 day^{-1} and 0.0030 day^{-1} for adult Pacific herring from the Beaufort Sea and Strait of Georgia, Canada, respectively, were estimated using catch curves (Tanasichuk et al. 1993).

The total mortality rate of an exploited fish population is made up of natural and fishing mortality (Ricker 1975). Instantaneous natural mortality rates are critical to many popu-

© 2002 NRC Canada

lation dynamic models including virtual population analysis, which is commonly used in many temperate fisheries (Hilborn and Walters 1992). Our estimates of instantaneous natural mortality in juvenile Pacific herring will be useful when combined with herring fisheries models as it provides estimates of the number of herring recruiting into the adult fishery.

Acknowledgments

We thank R. Foy, M. McEwen, N. Peters, G.B. Steinhart, S. Moreland, and M. Vallerino for assistance in collecting and processing the data. C. Campbell assisted with the map. J. McLelland, D. Mason, and P. Rago provided statistical advice. Critical comments by M. McGurk and several anonymous reviewers greatly improved the manuscript. We also thank the captains and crews of the F/V *Temptation*, F/V *Miss Kayley*, F/V *Kyle David*, M/V *Pacific Star*, F/V *Pagan*, F/V *Cape Elrington*, R/V *Pandalus*, and the Alaska Department of Fish and Game, Cordova, for their help. This project was funded by the *Exxon Valdez* Oil Spill Trustee Council through the Sound Ecosystem Assessment (SEA) project to the University of Alaska–Fairbanks and the Prince William Sound Science Center. However the findings presented by the authors are their own conclusions and not necessarily the Trustee Council position.

References

Beverton, R. 1963. Maturation, growth and mortality of clupeid and engraulid stocks in relation to fishing. Papp. P-v. Réun. Cons. Int. Explor. Mer, **154**: 44–67.

Blaxter, J.H.S., and Hunter, J.R. 1982. The biology of clupeoid fishes. Adv. Mar. Biol. **20**: 1–223.

Cushing, D.H. 1981. Fisheries biology. The University of Wisconsin Press, Madison.

Foy R.J., and Paul, A.J. 1999. Winter feeding and changes in somatic energy content for age 0 Pacific herring in Prince William Sound, Alaska. Trans. Am. Fish. Soc. **128**: 1193–1200.

Gulland, J.A. 1988. Fish population dynamics. John Wiley & Sons, Ltd, Bath.

Hatch, S.A., and Sanger, G.A. 1992. Puffins as samplers of juvenile pollock and other forage fish in the Gulf of Alaska. Mar. Ecol. Prog. Ser. **80**: 1–14.

Hilborn, R., and Walters, C.J. 1992. Quantitative fisheries stock assessment: choice, dynamics and uncertainty. Chapman & Hall, New York.

Iles, T.D. 1971. Growth studies on North Sea herring. III. the growth of East Anglan herring during the adult stage of the life history for the years 1940 to 1967. J. Cons. Int. Explor. Mer, **33**: 386–420.

Iles, T.D., and Sinclair, M. 1982. Atlantic herring: stock discreteness and abundance. Science (Washington, D.C.), **215**: 627–633.

Krebs, C.J. 1989. Ecological methodology. Harper & Row Publishers, Inc., New York.

Livingston, P.A. 1993. Importance of predation by groundfish, marine mammals and birds on walleye pollock *Theragra chalcogramma* and Pacific herring *Clupea pallasi* in the eastern Bering Sea. Mar. Ecol. Prog. Ser. **102**: 205–215.

MacLennan, D.N., and Simmonds, E.J. 1992. Fisheries acoustics. Chapman & Hall, London.

McClatchie S., Alsop, J., and Coombs, R.F. 1996. A re-evaluation of relationships between fish size, acoustic frequency, and target strength. ICES J. Mar. Sci. **53**: 780–791.

McGurk, M.D. 1993. Allometry of herring mortality. Trans. Am. Fish. Soc. **122**: 1035–1042.

McGurk, M.D., and Brown, E.D. 1996. Egg–larval mortality of Pacific herring in Prince William Sound, Alaska, after the *Exxon Valdez* oil spill. Can. J. Fish. Aquat. Sci. **53**: 2343–2354.

McGurk, M.D., Paul, A.J., Coyle, K.O., Ziemann, D.A., and Haldorson, L.J. 1993. Relationships between prey concentration and growth, condition, and mortality of Pacific herring, *Clupea pallasi*, larvae in an Alaskan subartic embayment. Can. J. Fish. Aquat. Sci. **50**: 163–180.

Morstad, S., Sharp, D., Wilcock, J., and Johnson, J. 1997. Prince William Sound management area 1996 annual finfish management report. Alaska Department of Fish and Game, Commercial Fisheries Management and Development Division, 333 Raspberry Rd., Anchorage, AK 99518, U.S.A. Regional information report 2A97-17.

Norcross, B.L., Brown, E.D., Foy, R.J., Frandsen, M., Gay, S., Kline, T.C.J., Mason, D.M., Patrick, E.V., Paul, A.J., and Stokesbury, K.D.E. 2001. A synthesis of the life history and ecology of juvenile Pacific herring in Prince William Sound, Alaska. Fish. Oceanogr. **10**(Suppl. 1): 42–57.

Paine, R.T., Ruesink, J.L., Sun, A., Soulanille, E.L., Wonham, M.J., Harley, C.D.G., Brumbaugh, D.R., and Secord, D.L. 1996. Trouble on oiled waters: lessons from the *Exxon Valdez* oil spill. Annu. Rev. Ecol. Syst. **27**: 197–235.

Paul, A.J., and Paul, J.M. 1998. Comparisons of whole body energy content of captive fasting age zero Alaskan Pacific herring (*Clupea pallasi* Valenciennes) and cohorts over-wintering in nature. J. Exp. Mar. Biol. Ecol. **226**: 75–86.

Paul, A.J., Paul, J.M., and Brown, E.D. 1998. Fall and spring somatic energy content for Alaskan Pacific herring (*Clupea pallasi* Valenciennes 1847) relative to age, size and sex. J. Exp. Mar. Biol. Ecol. **223**: 133–142.

Pearson, W.H., Elston, R.A., Bienert, R.W., Drum, A.S., and Antrim, L.D. 1999. Why did the Prince William Sound, Alaska, Pacific herring (*Clupea pallasi*) fisheries collapse in 1993 and 1994? Review of hypotheses. Can. J. Fish. Aquat. Sci. **56**: 711–737.

Ricker, W.E. 1975. Computation and interpretation of biological statistics of fish populations. Bull. Fish. Res. Board Can. **191**: 1–382.

Robinson, C.J. 1995. Food competition in a shoal of herring: the role of hunger. Mar. Behav. Physiol. **24**: 237–242.

Robinson, C.J., and Pitcher, T.J. 1989*a*. Hunger motivation as a promoter of different behaviours within a shoal of herring: selection for homogeneity in fish shoal? J. Fish. Biol. **35**: 459–460.

Robinson, C.J., and Pitcher, T.J. 1989*b*. The influence of hunger and ration level on shoal density, polarization and swimming speed of herring, *Clupea harengus* L. J. Fish. Biol. **34**: 631–633.

Rooper, C.N., Haldorson, L.T., and Quinn, T.J.I. 1999. Habitat factors controlling Pacific herring (*Clupea pallasi*) egg loss in Prince William Sound, Alaska. Can. J. Fish. Aquat. Sci. **56**: 1133–1142.

Scott, W.B., and Crossman, E.J. 1973. Freshwater fishes of Canada. Bull. Fish. Res. Board Can. **184**: 1–966.

Sinclair, M., Anthony, V.C., Iles, T.D., and O'Boyle, R.N. 1985. Stock assessment problems in Atlantic herring (*Clupea harengus*) in the Northwest Atlantic. Can. J. Fish. Aquat. Sci. **42**: 888–898.

Sokal, R.R., and Rohlf, F.J. 1981. Biometry—the principles and practice of statistics in biological research. Freeman, San Francisco.

Stokesbury, K.D.E., Foy, R., and Norcross, B.L. 1999. Spatial and temporal variability in juvenile Pacific herring (*Clupea pallasi*) growth in Prince William Sound, Alaska. Environ. Biol. Fish. **56**: 409–418.

Stokesbury, K.D.E., Kirsch, J., Brown, E.D., Thomas, G.L., and Norcross, B.L. 2000. Seasonal variability in Pacific herring,

© 2002 NRC Canada

Clupea pallasi, and walleye pollock, *Theragra chalcogramma*, spatial distributions in Prince William Sound, Alaska. Fish. Bull. **98**: 400–409.

Suryan, R.M., Irons, D.B., and Benson, J. 2000. Prey switching and variable foraging strategies of Black-legged Kittiwakes and the effect on reproductive success. Condor, **102**: 375–385.

Tanasichuk, R.W. 1997. Influence of biomass and ocean climate on the growth of Pacific herring (*Clupea pallasi*) from the southwest coast of Vancouver Island. Can. J. Fish. Aquat. Sci. **54**: 2782–2788.

Tanasichuk, R.W., Kristofferson, A.H., and Gillman, D.V. 1993. Comparison of some life history characteristics of Pacific herring (*Clupea pallasi*) from the Canadian Pacific Ocean and Beaufort Sea. Can. J. Fish. Aquat. Sci. **50**: 964–971.

Thorne, R.E. 1977. A new digital hydroacoustic data processor and some observations on herring in Alaska. J. Fish. Res. Board Can. **34**: 2288–2294.

Wespestad, V.G., and Moksness, E. 1990. Observations on growth and survival during the early life history of Pacific herring, *Clupea pallasii*, from Bristol Bay, Alaska, in a marine mesocosm. Fish. Bull. **88**: 191–200.

Winters, G.H., and Wheeler, J.P. 1994. Length-specific weight as a measure of growth success of adult Atlantic herring (*Clupea harengus*). Can. J. Fish. Aquat. Sci. **51**: 1169–1179.

© 2002 NRC Canada

An improved method for estimating individual growth variability in fish, and the correlation between von Bertalanffy growth parameters

Graham M. Pilling, Geoffrey P. Kirkwood, and Stephen G. Walker

Abstract: A new method for estimating individual variability in the von Bertalanffy growth parameters of fish species is presented. The method uses a nonlinear random effects model, which explicitly assumes that an individual's growth parameters represent samples from a multivariate population of growth parameters characteristic of a species or population. The method was applied to backcalculated length-at-age data from the tropical emperor, *Lethrinus mahsena*. Individual growth parameter variability estimates were compared with those derived using the current "standard" method, which characterizes the joint distribution of growth parameter estimates obtained by independently fitting a growth curve to each individual data set. Estimates of mean von Bertalanffy growth parameters from the two methods were similar. However, estimated growth parameter variances were much higher using the standard method. Using the random effects model, the estimated correlation between population mean values of L_∞ and K was –0.52 or –0.42, depending on the marginal distribution assumed for K. The latter estimate had a 95% posterior credibility interval of –0.62 to –0.17. These represent the first reliable estimate of this correlation and confirm the view that these parameters are negatively correlated in fish populations; however, the absolute correlation value is somewhat lower than has been assumed.

Résumé : On trouvera ici une nouvelle méthode pour estimer la variabilité individuelle des paramètres de croissance de von Bertalanffy chez les espèces de poissons. La méthode utilise un modèle non-linéaire à effets aléatoires qui présuppose de façon explicite que les paramètres de croissance d'un individu représentent des échantillons tirés d'une population multidimensionnelle de paramètres caractéristiques d'une espèce ou d'une population. La méthode a été utilisée sur des mesures de longueur à une taille donnée obtenues par rétro-calcul chez le bec de cane, *Lethrinus mahsena*. Les estimations de la variabilité des paramètres individuels de croissance ont été comparées à celles générées par la méthode « standard » courante qui caractérise la distribution commune des estimations des paramètres de croissance en ajustant de façon indépendante une courbe de croissance à chaque série de données individuelles. Les estimations des paramètres de croissance de von Bertalanffy obtenues par les deux méthodes sont semblables. Cependant les variances estimées des paramètres de croissance sont beaucoup plus élevées lorsqu'on utilise la méthode standard. Le modèle à effets aléatoires produit une estimation de corrélation de –0,52 ou de –0,42 entre les valeurs moyennes de L_∞ et de K de la population, selon la distribution marginale présupposée de K. La seconde estimation a un intervalle de crédibilité a posteriori de 95 % allant de –0,62 à –0,17. C'est la première fois que l'on obtient une estimation fiable de cette corrélation et cela confirme que ces paramètres sont en corrélation négative chez les populations de poissons, bien que la valeur absolue de la corrélation soit inférieure à ce qu'on avait supposé.

[Traduit par la Rédaction]

Introduction

Most fisheries population dynamics models assume that population growth in length (or weight) can be described adequately through mean growth parameters (Sainsbury 1980). Indeed, the overwhelming majority of growth parameter estimates in the literature describe such "average" growth. However, considerable variation around this mean growth pattern can be seen in most length-at-age plots, and an individual's growth trajectory may be quite different from the population average.

Individual variability in growth can strongly influence the accuracy of estimates of population parameters. For example, variability can strongly bias estimates of growth param-

Received 6 February 2001. Accepted 12 December 2001. Published on the NRC Research Press Web site at http://cjfas.nrc.ca on 21 March 2001.
J16206

G.M. Pilling[1,2] **and G.P. Kirkwood.** Renewable Resources Assessment Group, Department of Environmental Science and Technology, Imperial College of Science, Technology and Medicine, RSM Building, Prince Consort Road, London, SW7 2BP, U.K.
S.G. Walker. Department of Mathematical Sciences, University of Bath, Bath, BA2 7AY, U.K.

[1]Corresponding author (e-mail: g.m.pilling@cefas.co.uk).

[2]Present address: Centre for Environment, Fisheries, and Aquaculture Science (CEFAS), Fisheries Laboratory, Pakefield Road, Lowestoft NR33 0HT, U.K.

 DOI: 10.1139/F02-022 © 2002 NRC Canada

eters derived through length-based methods (Rosenberg and Beddington 1987; Isaac 1990) or through tagging (Kirkwood and Somers 1984; Wang and Thomas 1995), and hence affect management based on stock assessments using these parameter estimates as inputs. Incorporating knowledge on the level of individual variability in growth may improve assessments (Wang and Ellis 1998). A measure of the degree of individual growth variability is also essential for models that attempt to simulate exploited fish stock behaviour realistically at an individual level (Parma and Deriso 1990; Lowerre-Barbieri et al. 1998; Martinez-Garmendia 1998).

There are several ways in which individual variability in growth could be estimated. Ideally, one would wish to observe the growth of individual fish directly, throughout their lives. Such measurements, usually obtained through captive studies or sometimes through tagging programmes, allow a growth curve to be estimated for each individual (Shackell et al. 1997). However, for captive studies, it is usually unclear whether the growth rates achieved really are representative of those in wild populations. Tagging programmes, especially those with the multiple recaptures needed to determine individual growth curves, undoubtedly cause additional stresses to the fish. These factors may alter individual growth rates from their natural state, biasing the estimates. The only realistic method of obtaining the required data for marine fishes is to obtain information on individual growth histories through the backcalculation of lengths-at-age using increment width information contained in fish hard parts (Fossen et al. 1999). This is the approach taken in the current study.

Considering the potential importance of individual growth variability in fisheries assessments (Sainsbury 1980), and despite the increasing number of studies that have generated data from which estimates of individual variability in growth could have been derived, the number of published studies that have quantified this variability for populations is extremely low. The only comprehensive examination of individual growth variability in fish of which we are aware is that of Isaac (1990). However, the method used by Isaac (henceforth called "Isaac's method"), which analyzes sets of growth parameter estimates for individual fish, has a potentially serious source of bias. This arises because estimates of growth parameter variability among individuals may be inflated by the inevitable estimation errors associated with the growth parameter estimates for each individual. For example, where data are confined to young ages and growth is slow, there is very little information on the true value of L_∞. In such cases, L_∞ is often estimated to be very much larger than estimates that have been obtained for the same species using data with a much wider range of ages. Clearly, such large differences in estimates of L_∞ would not be representative of the true variability in individual growth.

In this study, an alternative method is presented, based on the use of a nonlinear random effects model (e.g., Smith and Wakefield 1994; Davidian and Giltinan 1995; Walker 1996). Nonlinear random effects models have been used in a number of fields, including the assessment of individual and population growth in humans (Susman et al. 1998). The key advantage presented by a random effects growth model is that it explicitly assumes that the growth parameters for each individual represent samples from a multivariate population of growth parameters characteristic of the fish species or population. The main parameters estimated are the mean vector and the covariance matrix of the population of growth parameters, and these are precisely the parameters needed to assess individual growth variability.

Given an estimate of the covariance matrix, it is trivial to estimate, for example, the correlation between the von Bertalanffy growth parameters L_∞ and K. These two parameters are frequently assumed to be negatively correlated when simulations of individual fish growth are carried out (e.g., Hampton and Majkowski 1987). However, there is little, if any, direct evidence to suggest that this is actually true. Regrettably, it is quite common for the ubiquitous negative correlation between estimates of L_∞ and K to be mistakenly interpreted as evidence that these parameters are negatively correlated in the population. Use of the random effects model should allow this issue to be clarified.

The aim of this paper is to demonstrate the new method for assessing individual variability in growth, using backcalculated length-at-age data from the tropical emperor, *Lethrinus mahsena*. Estimates of the population means and of the covariance matrix of the von Bertalanffy growth parameters are compared with estimates derived using Isaac's method. As already mentioned, one of the reasons for estimating individual variability in growth parameters is to allow realistic individual-based simulations of fish populations to be carried out. The distributions of estimates of each von Bertalanffy growth parameter were compared for the two approaches. Finally, estimates of the correlations between the growth parameters derived using the two approaches are compared.

Methods

Length-at-age data

Otoliths of *L. mahsena* were collected from Nazareth Bank on the Mascarene Ridge of the Indian Ocean. Using the methods described in Pilling et al. (2000), lengths-at-age were backcalculated over the life span of a number of individuals. This involved taking measurements of the total otolith radius, from nucleus to the tip of the dorsal lobe, and of the distance along this growth axis between annual increments, using the approach described in Millner and Whiting (1996).

Following the recommendations of Francis (1990) and Ricker (1992), the geometric mean regression (GMR) of fork length at capture on otolith radius at capture was calculated. Backcalculated lengths-at-age for each individual were then derived using the formula (Ricker 1992)

$$(1) \qquad Fl_i = \left(\frac{Fl_c - b}{O_c} O_i \right) + b$$

where Fl_i is the estimated fork length at age i, Fl_c is the fork length at capture, O_c is the otolith radius at capture, O_i is the otolith radius at age i, and b is the intercept of the GMR calculated using the Ricker procedure.

Equation 1 assumes that the relationship between fork length and otolith radius is consistent. However, studies have indicated that the fish–otolith size ratio can vary systematically with somatic growth rate (Mosegaard et al. 1988; Secor

© 2002 NRC Canada

and Dean 1989). This can result in relatively large otoliths in slow-growing (and hence relatively small at age) fish, confounding the direct relationship between length and otolith size (Campana 1990). To identify whether the assumption underlying eq. 1 was valid, the relationship between *L. mahsena* fork length and total otolith radius was examined.

Isaac's method

This method was based on the procedures described in Isaac (1990). A von Bertalanffy growth curve was fitted to the backcalculated length-at-age data for each *L. mahsena* individual, using the method described by Allen (1966). This produced least-squares estimates of the three von Bertalanffy growth parameters. For each growth parameter, the mean, variance, and coefficient of variation were calculated from the individual estimates. A covariance matrix for the estimates of all three parameters L_∞, K, and t_0 was also calculated.

Nonlinear random effects model

The backcalculated length-at-age data represented measurements of lengths L_{ij} at ages T_{ij}, $j = 0, 1, 2,\ldots,n_i$ for $i = 1, 2,\ldots,N$ fish. The basic model to be fitted to these data was

$$(2) \qquad L_{ij} = L_{\infty i}(1 - e^{-K_i(T_{ij} - t_{0i})}) + \varepsilon_{ij}$$

where $L_{\infty i}$, K_i, and t_{0i} are the von Bertalanffy growth parameters for the ith fish, and the ε_{ij} are assumed to be independent identically normally distributed error terms. The growth parameters for each individual were assumed to be sampled independently from a trivariate distribution.

Two alternative assumptions were made about the form of this trivariate distribution. The first was that the individual growth parameters were sampled independently from a trivariate normal distribution

$$(3a) \qquad \begin{pmatrix} L_{\infty i} \\ K_i \\ t_{0i} \end{pmatrix} \sim N_3(\mu, \Sigma) \qquad \text{for } i = 1\ldots,N$$

The alternative assumption was that $L_{\infty\, i}$, $\ln(K_i)$ and t_{0i} were sampled independently from a trivariate normal distribution

$$(3b) \qquad \begin{pmatrix} L_{\infty i} \\ \ln(K_i) \\ t_{0i} \end{pmatrix} \sim N_3(\mu, \Sigma) \qquad \text{for } i = 1\ldots,N$$

In both cases, μ and Σ represent the population mean and population variance–covariance matrix of the appropriate trivariate normal distributions. The model therefore corresponds to the form of a nonlinear random effects model.

As noted earlier, there is no reliable evidence available to guide the choice of an appropriate distribution for the individual growth parameters. The trivariate normal has the advantage of simplicity, but it also has the unfortunate feature that even for plausible values of their means and variances, it can allow negative values of K_i. Theoretically, negative values can also occur for $L_{\infty i}$, but this almost never happens in practice. It was this point that led Sainsbury (1980) to assume a gamma distribution for K. In practice, the computer software used for the parameter estimation (see below) very easily allows estimation of posterior credibility intervals for each of the elements of the correlation matrix of the untransformed growth parameters when the distribution in eq. 3a is assumed, but not as far as we can determine when the distribution in eq. 3b is assumed. For this reason, we present and compare results for both assumptions.

Table 1. Mean backcalculated length-at-age, number of observations (n), variance, and coefficient of variation (CV) by age for *Lethrinus mahsena*.

Age (years)	n	Mean fork length (cm)	Variance	CV (%)
1	72	11.3	6.3	22.3
2	72	17.7	6.9	14.8
3	72	22.1	7.1	12.1
4	72	25.3	7.0	10.5
5	68	27.6	7.5	9.9
6	60	29.6	7.0	8.9
7	43	30.6	7.5	8.9
8	27	31.5	8.1	9.0
9	15	32.0	11.4	10.6
10	8	31.4	11.3	10.7
11	3	33.1	19.2	13.2
12	2	36.2	15.3	10.8

Fig. 1. Geometric mean regression of fork length from otolith radius for *Lethrinus mahsena* (n = 222).

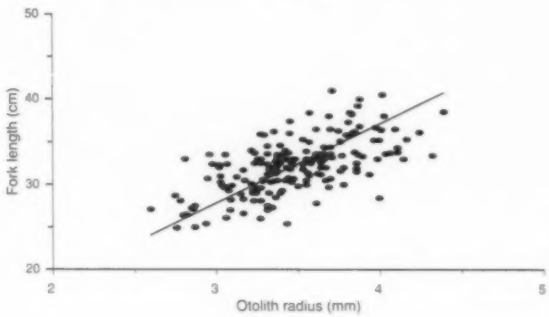

Table 2. Means and variances of estimated von Bertalanffy growth parameters and correlations between them estimated for individual *Lethrinus mahsena* length-at-age data using Isaac's method.

Parameter	Estimate
Mean(L_∞)	36.81
Mean(K)	0.30
Mean(t_0)	–0.40
Variance(L_∞)	50.51
Variance(K)	0.013
Variance(t_0)	0.36
Correlation(L_∞, K)	–0.69
Correlation(L_∞, t_0)	–0.62
Correlation(K, t_0)	0.04

Note: Units: L_∞, cm; K, year^{-1}; t_0, year.

© 2002 NRC Canada

Table 3. Means, standard deviations (SD), and lower and upper 2.5 percentiles of growth parameters, calculated from individual *Lethrinus mahsena* length-at-age data, using the Bayesian nonlinear random effects models.

	K normal				*K* lognormal			
Parameter	Mean	SD	2.5%	97.5%	Mean	SD	2.5%	97.5%
Mean(L_∞)	35.57	0.59	34.42	36.74	35.94	0.64	34.67	37.17
Mean(K)	0.30	0.01	0.28	0.33	0.28	0.01	0.26	0.31
Mean(t_0)	–0.37	0.06	–0.48	–0.26	–0.40	0.06	–0.53	–0.28
Variance(L_∞)	17.98	3.88	11.64	26.66	19.47	4.23	12.54	28.95
Variance(K)	0.009	0.002	0.006	0.014	0.01			
Variance(t_0)	0.17	0.04	0.11	0.26	0.20	0.05	0.13	0.31
Correlation(L_∞, K)	–0.42	0.12	–0.62	–0.17	–0.52			
Correlation(L_∞, t_0)	0.09	0.15	–0.21	0.39	0.02	0.16	–0.29	0.32
Correlation(K, t_0)	0.32	0.12	0.06	0.54	0.45			
σ^2	0.52	0.04	0.44	0.61	0.51	0.04	0.44	0.60

Note: Results are shown for the model where L_∞, K, and t_0 are jointly normally distributed (K normal) and the alternative model where L_∞, ln(K), and t_0 are jointly normally distributed (K lognormal). For the latter model, the variance of K and the three correlations were estimated from 10 000 simulated observations from the estimated distribution of L_∞, ln(K), and t_0. Estimates of standard deviations and posterior credibility percentiles for variances and correlations involving K are not available for the K lognormal model. Units: L_∞, cm; K, year^{-1}; t_0, year.

To fit the model to the data, a Bayesian approach was used. Prior probability distributions for σ, μ, and Σ and their parameters were selected with the criterion of being as noninformative as possible, i.e., to ensure that the likelihood dominates the prior (e.g., Smith and Wakefield 1994; Wakefield et al. 1994). Accordingly, the prior for μ was a noninformative multivariate normal distribution, with zero mean and covariance matrix with diagonal elements equal to 200, and off-diagonal elements equal to zero. The prior for Σ was an inverse Wishart distribution (VonRosen 1997), with precision parameter 3, and mean

$$\begin{bmatrix} 0.1 & 0.0 & 0.0 \\ 0.0 & 0.2 & 0.0 \\ 0.0 & 0.0 & 0.1 \end{bmatrix}$$

Finally, the prior distribution for σ (specifically, for $\frac{1}{\sigma^2}$) was taken to be a gamma distribution, with parameters ½ and ½. In these last two distributions, small values of their parameters are associated with nearly flat priors, as is the value selected for the precision parameter of the inverse Wishart distribution.

Using these prior distributions, the random effects model was fitted to the backcalculated length-at-age data using a software package developed for Bayesian inference using Gibbs sampling (BUGS; Thomas et al. 1992; Spiegelhalter et al. 1999). This allowed estimation of the posterior distributions of each of the main parameters (σ, μ, and Σ), and selected functions of them (e.g., when prior distribution 3a was used, the elements of the correlation matrix for the growth parameters). It also allowed estimation of posterior distributions for the von Bertalanffy parameters for each individual fish in the sample, thus further facilitating a comparison of the results of fitting the random effects model with those obtained using Isaac's method. An example of the use of the BUGS software when fitting surplus production models to fisheries data is given by Meyer and Millar (1999).

Fitting the random effects model to simulated data

Whereas the use of random effects models is now common in the wider statistical literature and the BUGS software is well tested, this does not guarantee that the parameter estimates obtained using them will have acceptable levels of bias and precision in any particular application. For the data set analyzed in this paper, we were reasonably confident that the estimates of the population means of the growth parameters would be reliable. However, given the restricted size of the data set, it was by no means obvious that their estimated correlation matrix would have low bias and reasonable precision. This is an important point, since particular significance was to be given to the estimated correlations between the growth parameters.

Accordingly, we simulated a set of individual length-at-age data similar to the original *L. mahsena* data, using the model in eqs. 2 and 3a. Parameter values for the simulations were set equal to those estimated for that model using BUGS on the *L. mahsena* data, except the off-diagonal elements of the covariance matrix were set to zero, thus ensuring that the true growth parameters were uncorrelated. Mirroring the *L. mahsena* data, length-at-age data for 72 individual fish were simulated, with the number of data for each individual being set equal to the average number of length-at-age observations per individual for the *L. mahsena* data (7). The same random effects model was then fitted to these simulated data using BUGS and the resulting parameter estimates and their posterior confidence intervals were compared with their known values.

Comparison of Isaac's and random effects model estimates

Obviously, the first comparison to be made between results of use of Isaac's method and fitting the random effects model to the *L. mahsena* data is between the estimates of the population means and covariance matrices for the growth parameters. Such a comparison, however, does not provide much insight into how each has interpreted the individual length-at-age data.

By its very nature, Isaac's method generates estimates of

© 2002 NRC Canada

Fig. 2. Marginal frequency distributions of 10 000 L_∞, K, and t_0 values sampled from Bayesian mean vectors and accompanying covariance matrix with K normally distributed (solid line) or lognormally distributed (dashed line).

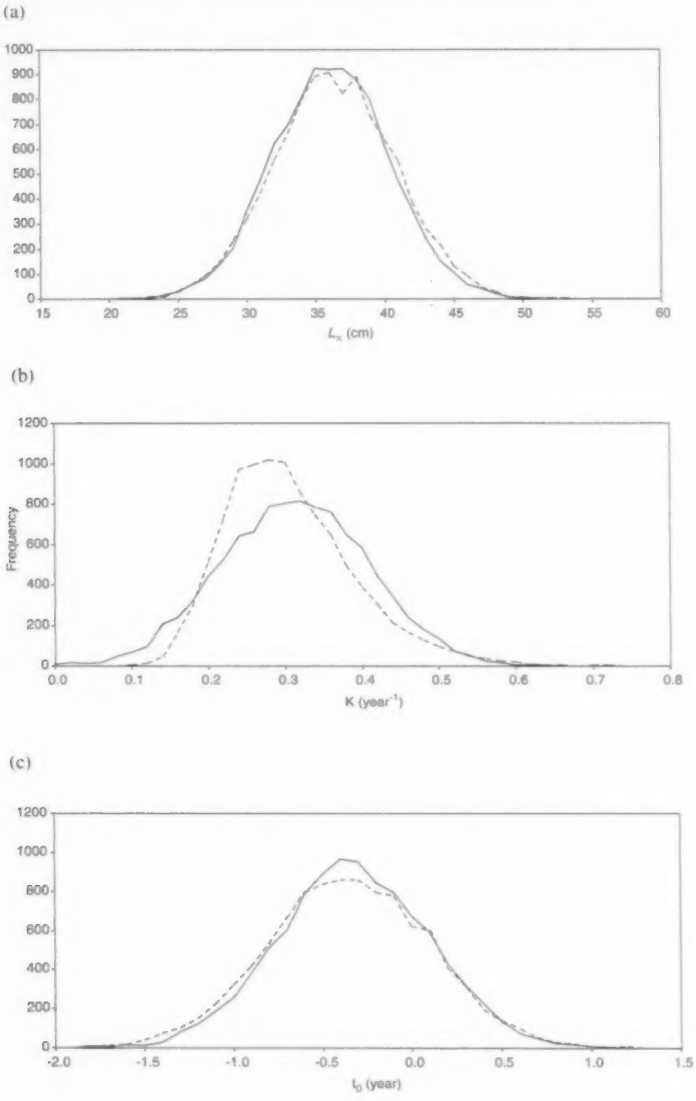

the growth parameters for each individual fish. Fortunately, as noted above, it is also possible to obtain posterior mean estimates of the individual fish growth parameters when fitting the random effects model. Accordingly, histograms of estimates of each von Bertalanffy growth parameter were compared for both Isaac's method and the two random effects models.

Results

Length-at-age data

Backcalculated lengths-at-age were successfully obtained for 72 *L. mahsena* individuals from Nazareth bank, including the means, variances, and coefficients of variation (CV) of the length at each age (Table 1).

Overall, the variance in length-at-age increased with age. The estimated CV of length-at-age, however, was highest at age 1, decreasing to around 9% by age 6 years. The estimated CV then increased slightly with further increases in age; however, it should be noted that the sample sizes for older ages were rather small.

There was a linear relationship between the fork length and otolith total radius in *L. mahsena* across the range sampled (Fig. 1). Variability around the regression line was generally normally distributed for a given otolith radius, although there was a tendency for larger and smaller lengths to correspond with smaller and larger otolith radii, respec-

© 2002 NRC Canada

Table 4. Comparison of true and estimated parameters for simulated data. For estimated parameters, the mean, standard deviation (SD), and lower and upper 2.5 percentiles of the posterior distribution are shown.

		Estimated			
Parameter	True value	Mean	SD	2.5%	97.5%
Mean(L_∞)	35.54	36.28	0.63	35.08	37.52
Mean(K)	0.30	0.29	0.02	0.26	0.33
Mean(t_0)	–0.36	–0.35	0.06	–0.47	–0.23
Variance(L_∞)	17.82	17.97	4.03	11.54	27.32
Variance(K)	0.009	0.015	0.003	0.010	0.022
Variance(t_0)	0.17	0.20	0.04	0.13	0.30
Correlation(K, t_0)	0	0.12	0.13	–0.14	0.36
Correlation(L_∞, K)	0	–0.09	0.15	–0.37	0.21
Correlation(L_∞, t_0)	0	–0.09	0.14	–0.37	0.20
σ^2	0.52	0.50	0.04	0.43	0.59

Note: Units: L_∞, cm; K, year^{-1}; t_0, year.

tively, at the very extremes of the otolith radius sample range. However, this may be a result of the relatively small sample sizes at these extremes. Overall, therefore, there is little evidence for allometry in the relationship, at least over the range of sample data available for this study.

Isaac's method

The estimated means and variances of the individual von Bertalanffy growth parameter estimates, and correlations between them, were derived using Isaac's method (Table 2).

Nonlinear random effects models

Means, standard deviations (SD), and lower and upper 2.5 percentiles of growth parameters were calculated from individual *L. mahsena* length-at-age data using the two alternative Bayesian nonlinear random effects models (Table 3). Using the estimated mean vectors and covariance matrices for the two trivariate distributions, marginal frequency distributions of 10 000 individual von Bertalanffy growth parameter estimates were simulated (Fig. 2).

The sets of parameter estimates obtained for the two alternative random effects models are very similar (as shown in Table 3). The simulated marginal distributions of L_∞ and t_0 are almost identical for the alternative models, but the distributions for K are notably different, reflecting the different distributional assumptions made (Fig. 2).

Fitting to simulated data

The results of fitting the random effects model (eqs. 2 and 3a) to simulated data are shown in Table 4, along with the parameter values used to generate the simulated data.

With the exception of the variance of K, var(K), all the estimated mean values of the parameters were close to the true values, and the true values lay well within the estimated posterior 95% credibility intervals for those parameters. The mean of the posterior distribution for var(K) was higher than the true value, which lay just below the estimated lower 2.5 percentile of the posterior distribution. Pleasingly, the true values of the correlations between the growth parameters lay well inside their estimated posterior 95% credibility intervals. However, it is clear that the precision of these estimates is not high for the simulated data set.

Comparison of estimation methods

The estimated mean von Bertalanffy growth parameters were very similar between estimation methods (see Tables 2 and 3). However, the estimated variances of the growth parameters were far higher when Isaac's method was used than when the random effects model was fitted. Both methods suggested a substantial negative correlation between L_∞ and K, which was significantly less than zero, judging by the posterior 95% credibility interval estimated using the random effects model with K having a marginal normal distribution. Issac's method results also suggested a substantial negative correlation between L_∞ and t_0, but the random effects model indicated that this correlation was not significantly different from zero. Conversely, the random effects model suggested a significant positive correlation between K and t_0, whereas the Issac's method estimate was close to zero. It is also of interest to compare the marginal frequency distributions of growth parameter estimates for the 72 individual sets of length-at-age data obtained using the two methods (Fig. 3).

The frequency distributions for the Isaac's method results and the two random effects model results have very similar central tendencies. It is very clear from Fig. 3 that the much higher variances for the Isaac's method results stem from the highly skewed distributions of growth parameter estimates, especially for L_∞ and t_0. Inspection of the individual sets of estimates revealed that the outlying large estimates of L_∞ almost invariably corresponded with outlying low estimates of t_0 and also with low estimates of K. These, in turn, corresponded to data sets typically with a smaller number of observations exhibiting nearly linear growth from a relatively high length at age 1. As noted much earlier, it is precisely such data sets that are known to produce anomalous estimates of von Bertalanffy growth parameters.

Discussion

The main potential drawback with Isaac's method is that estimation error associated with the individual growth parameter estimates is incorporated into the estimates of the mean growth parameters and of their variability. The random effects model does not suffer from this problem; by pooling the data rather than working with each individual data set in-

© 2002 NRC Canada

Fig. 3. Frequency distributions of individual growth parameter estimates resulting from the application of Allen's estimation method to 72 sets of individual *Lethrinus mahsena* length-at-age data (solid bars), and the random effects model with K normally (shaded bars) or lognormally (open bars) distributed.

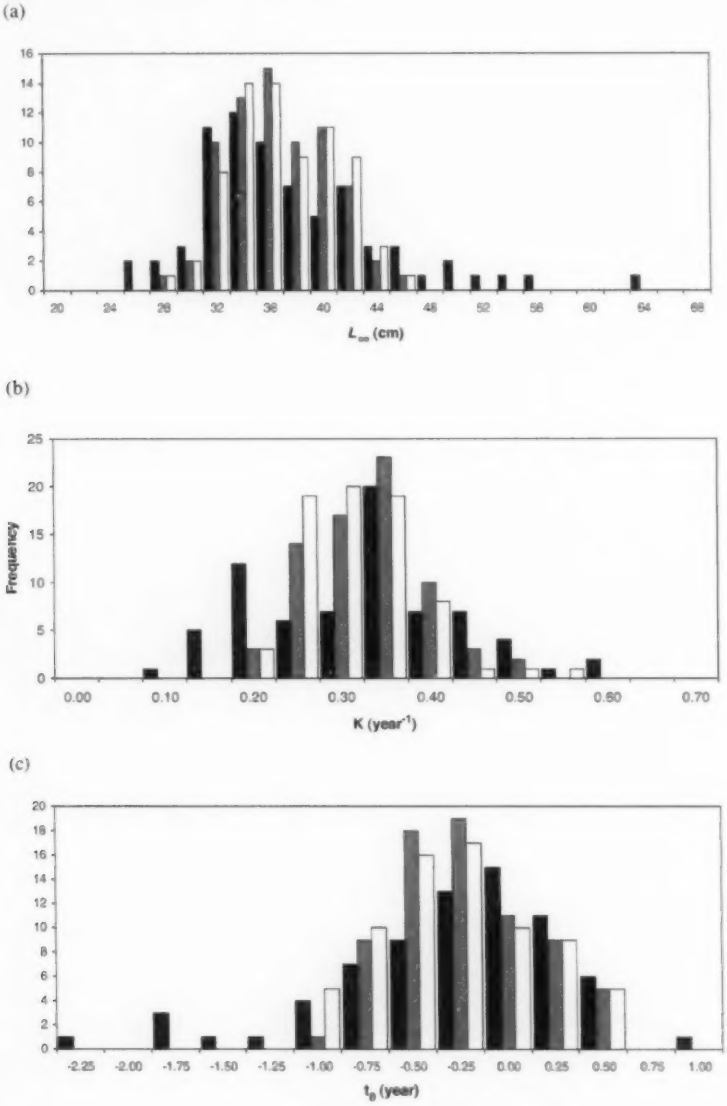

dependently, it improves estimates by a process of shrinking, combining population averages with the individual data. In theory, therefore, use of the random effects model should result in more reliable and generally lower estimates of growth parameter variability.

In practice, for the *L. mahsena* data the estimates of the means of all three von Bertalanffy growth parameters and of the coefficients of variation of L_∞ and K calculated using the two methods were very similar. The backcalculation method produced estimates of length-at-age for *L. mahsena* individuals down to age one, and many of the data sets included individuals of sizes relatively close to the estimated mean L_∞. Consequently, it is likely that the estimation error associated with the individual estimates of the growth parameters for such data sets was relatively small. This would imply that for these data sets, the potential biases associated with Isaac's method should be low, and therefore the similarity in mean growth parameter estimates was not too surprising. As noted earlier, however, this was not true of all of the individual growth data sets. Rather, some exhibited restricted ranges of ages with apparently near-linear growth, which are known typically to produce large estimates of L_∞, low estimates of K, and often low estimates of t_0. The presence of such sets of growth parameter estimates led to the much higher variances of growth parameters obtained for Isaac's method. Although there is no absolute standard with which

© 2002 NRC Canada

to make the judgement, we believe the estimates obtained using the random effects model to be much more reliable.

The advantages of using the Bayesian random effects model do carry a potential price: a considerably greater computational burden. There has been a feature of most Bayesian assessment methods described in the recent fisheries literature (e.g., Hilborn et al. 1994; Hoenig et al. 1994; McAllister and Kirkwood 1998). Fortunately, models such as the one described in this paper are very easy to implement in the BUGS software package developed for Bayesian inference using Gibbs sampling (BUGS; Thomas et al. 1992; Spiegelhalter et al. 1999). This should bring Bayesian fitting of the nonlinear random effects model within the ambit of most readers.

The random effects model as currently implemented still relies on the assumption that the backcalculated lengths correspond to ages that have been measured without error. Such an assumption is obviously false. First, the original age estimated from the initial otolith reading will include observation error, and the backcalculation process will introduce both additional errors and probably correlated errors. Although the model could have been extended to include such additional complexity, for a first presentation of the model, and for the relatively small data set, this was not felt warranted. Further investigation of the application of this method using a much larger data set for a different species is underway, and it will also allow exploration of the impacts of potential errors in backcalculated lengths-at-age on derived estimates of individual growth variability.

The correlation between L_∞ and K estimated using the random effects model (−0.52 using the K lognormal model, −0.42 using the K normal model) was a little lower in absolute value than that estimated using Isaac's method (−0.69). This was not unexpected, since the latter estimate is likely to be inflated by the negative correlation between the estimates of L_∞ and K for each of the individual data sets. The estimates from the random effects model appear to represent the first reliable assessment of this correlation. Although the correlation is negative, as expected, its absolute value is lower than the general perception of this relationship identified in the literature. For example, the correlation between these parameters that was selected for the length frequency simulations of Hampton and Majkowski (1987) was −0.8. Obviously, however, many further studies would be required to determine whether this correlation was consistent among different populations of this species or among different species.

The variance of *L. mahsena* backcalculated lengths-at-age increased with age. Other studies have noted that such increases can be modelled by individual variation in L_∞ alone (Jones 1987; Rosenberg and Beddington 1987). However, these studies assumed that the growth parameters were independently distributed. As suggested in the current study, this assumption is almost certainly false. All three parameters will therefore contribute to the variability in length-at-age.

Finally, a note of caution on the specific growth parameter estimates for *L. mahsena*. Whereas the backcalculated length-at-age data set has served well to illustrate the application of the random effects model for estimating growth parameters and their individual variability, as already mentioned, the data set was relatively small. It was also unavoidably restricted; subsequent catch sampling indicated that the backcalculated data set lacked individuals from the oldest age classes in the population. Distributions of length-at-age simulated for such older age classes were skewed toward lengths smaller than those found in the actual catch samples. This suggests that the true mean value of L_∞ may be larger than that estimated using the constrained data set. This will be examined further in a later paper.

Acknowledgements

We would like to thank Carl Walters and an anonymous reviewer for helpful comments on the manuscript. The project to which this paper relates was funded by the Department for International Development through the Fisheries Management Science Programme.

References

Allen, K.R. 1966. A method of fitting growth curves of the von Bertalanffy type to observed data. J. Fish. Res. Board Can. **23**: 163–179.

Campana, S.E. 1990. How reliable are growth backcalculations based on otoliths? Can. J. Fish. Aquat. Sci. **47**: 2219–2227.

Davidian, M., and Giltinan, D.M. 1995. Nonlinear models for repeated measurement data. Chapman and Hall, London.

Fossen, I., Albert, O.T., and Nilssen, E.M. 1999. Back-calculated individual growth of long rough dab (*Hippoglossoides platessoides*) in the Barents Sea. ICES J. Mar. Sci. **56**: 689–696.

Francis, R.I.C.C. 1990. Back-calculation of fish length—a critical review. J. Fish. Biol. **36**: 883–902.

Hampton, J., and Majkowski, J. 1987. An examination of the reliability of the ELEFAN computer programs for length-based stock assessment. *In* Length-based methods in fisheries research. *Edited by* D. Pauly and G.R. Morgan. International Centre for Living Aquatic Resources Management, Manila, Philippines, and Kuwait Institute for Scientific Research, Safat, Kuwait. pp. 203–215.

Hilborn, R., Pikitch, E. K., and McAllister, M.K. 1994. A Bayesian estimation and decision analysis for an age-structured model using biomass survey data. Fish. Res. **19**: 17–30.

Hoenig, J.M., Warren, W.G., and Stocker, M. 1994. Bayesian and related approaches to fitting surplus production models. Can. J. Fish. Aquat. Sci. **51**: 1823–1831.

Isaac, V.J. 1990. The accuracy of some length-based methods for fish population studies. International Centre for Living Aquatic Resources Management (ICLARM) Tech. Rep. 27.

Jones, R. 1987. An investigation of length composition analysis using simulated length compositions. *In* Length-based methods in fisheries research. *Edited by* D. Pauly and G.R. Morgan. International Centre for Living Aquatic Resources Management, Manila, Philippines, and Kuwait Institute for Scientific Research, Safat, Kuwait. pp. 217–238.

Kirkwood, G.P., and Somers, I.F. 1984. Growth of the two species of tiger prawn, *Penaeus esculentus* and *Penaeus semisulcatus*, in the western Gulf of Carpentaria. Aust. J. Mar. Freshw. Res. **35**: 703–712.

Lowerre-Barbieri, S.K., Lowerre, J.M., and Barbieri, L.R. 1998. Multiple spawning and the dynamics of fish populations: inferences from an individual-based simulation model. Can. J. Fish. Aquat. Sci. **55**: 2244–2254.

Martinez-Garmendia, J. 1998. Simulation analysis of evolutionary response to size-selective harvesting with the use of an individual-based model. Ecol. Model. **111**(1): 37–60.

© 2002 NRC Canada

McAllister, M.K., and Kirkwood, G. P. 1998. Bayesian stock assessment: a review and example application using the logistic model. ICES J. Mar. Sci. **55**: 1031–1060.

Meyer, R., and Millar, R.B. 1999. BUGS in Bayesian stock assessments. Can. J. Fish. Aquat. Sci. **56**: 1078–1086.

Millner, R.S., and Whiting, C.L. 1996. Long-term changes in growth and population abundance of sole in the North Sea from 1940 to the present. ICES J. Mar. Sci. **53**: 1185–1195.

Mosegaard, H., Svedang, H., and Taberman, K. 1988. Uncoupling of somatic and otolith growth rates in Arctic char (*Salvelinus alpinus*) as an effect of differences in temperature response. Can. J. Fish. Aquat. Sci. **45**: 1514–1524.

Parma, A.M., and Deriso, R.B. 1990. Dynamics of age and size composition in a population subject to size-selective mortality: effects of phenotypic variability in growth. Can. J. Fish. Aquat. Sci. **47**: 274–289.

Pilling, G.M., Millner, R.S., Easey, M.W., Mees, C.C., Rathacharen, S., and Azemia, R. 2000. Validation of annual growth increments in the otoliths of the lethrinid *Lethrinus mahsena* and the lutjanid *Aprion virescens*, with notes on the nature of growth increments in *Pristipomoides filamentosus*. Fish. Bull. **98**: 600–611.

Ricker, W.E. 1992. Back-calculation of fish lengths based on proportionality between scale and length measurements. Can. J. Fish. Aquat. Sci. **49**: 1018–1026.

Rosenberg, A.A., and Beddington, J.R. 1987. Monte-Carlo testing of two methods for estimating growth from length–frequency data with general conditions for their applicability. *In* Length-based methods in fisheries research. *Edited by* D. Pauly and G.R. Morgan. International Centre for Living Aquatic Resources Management, Manila, Philippines, and Kuwait Institute for Scientific Research, Safat, Kuwait. pp. 283–298.

Sainsbury, K.J. 1980. The effect of individual variability on the von Bertalanffy growth equation. Can. J. Fish. Aquat. Sci. **37**: 241–247.

Secor, D.G., and Dean, J.M. 1989. Somatic growth effects on the otolith–fish size relationship in young pond-reared striped bass, *Morone saxatilis*. Can. J. Fish. Aquat. Sci. **46**: 113–121.

Shackell, N.L., Stobo, W.T., Frank, K.T., and Brickman, D. 1997. Growth of cod (*Gadus morhua*) estimated from mark-recapture programs on the Scotian Shelf and adjacent areas. ICES J. Mar. Sci. **54**: 383–398.

Smith, A., and Wakefield, J.C. 1994. The hierachical Bayesian approach to population pharmokinetic modelling. Int. J. Bio-med. Comput. **36**(1–2): 35–42.

Spiegelhalter, D.J., Thomas, A., and Best, N.G. 1999. WinBUGS Version 1.2 User Manual. Medical Research Council Biostatistics Unit, Institute of Public Health, Cambridge, U.K.

Susman, E.P., Murphy, J.R., Zerbe, G.O., and Jones, R.H. 1998. Using a nonlinear mixed model to evaluate three models of human stature. Growth Dev. Aging, **62**: 161–171.

Thomas, A., Spiegelhalter, D.J., and Gilks, W.R. 1992. BUGS: a program to perform Bayesian statistical inference using Gibbs sampling. *In* Bayesian statistics 4. *Edited by* J.M. Bernardo, J.O. Berger, A.P. Dawid, and A.F.M. Smith. Oxford University Press, Oxford, U.K. pp. 837–842.

VonRosen, D. 1997. On moments of the inverted Wishart distribution. Statistics, **30**: 259–278.

Wakefield, J.C., Smith, A.F.M., Racinepoon, A., and Gelfand, A.E. 1994. Bayesian analysis of linear and nonlinear population models by using the Gibbs sampler. Appl. Stat. **43**: 201–221.

Walker, S. 1996. An EM algorithm for nonlinear random effects models. Biometrics, **52**: 934–944.

Wang, Y.-G., and Ellis, N. 1998. Effect of individual variability on estimation of population parameters from length–frequency data. Can. J. Fish. Aquat. Sci. **55**: 2393–2401.

Wang, Y.-G., and Thomas, M.R. 1995. Accounting for individual variability in the von Bertalanffy growth model. Can. J. Fish. Aquat. Sci. **52**: 1368–1375.

© 2002 NRC Canada

Estimating salmon stock–recruitment relationships from catch and escapement data

Jon T. Schnute and A.R. Kronlund

Abstract: This paper presents an analysis of stock–recruitment data that takes account of natural variation in stock productivity (process error) and inaccurate escapement counts (measurement error). We formulate the model using dynamic state variables and take advantage of related techniques for parameter estimation, such as an extended Kalman filter. Our recruitment function depends explicitly on parameters relevant to management and includes various cases of historical interest. We adopt Bayesian methods for assessing uncertainty and use Markov chain Monte Carlo (MCMC) techniques to obtain posterior samples. A worked example, based on simulated data, illustrates geometric relationships among model choices, estimated recruitment curves, and data interpretations.

Résumé : Notre analyse des relations stock–recrutement tient compte de la variation naturelle de la productivité des stocks (erreurs de traitement) et des mesures erronées d'échappements (erreurs de mesure). Nous avons élaboré le modèle à l'aide de variables d'état dynamique et avons utilisé des techniques apparentées pour l'estimation des paramètres, telles que le filtre de Kalman étendu. La fonction qui décrit le recrutement est explicitement reliée à des paramètres pertinents à la gestion et inclut divers cas d'intérêt historique. Des méthodes bayésiennes ont servi à déterminer l'incertitude et des méthodes de Monte Carlo par chaîne de Markov (MCMC), à produire les échantillons a posteriori. Un exemple détaillé, basé sur des données simulées, illustre les relations de type géométrique qui existent entre les choix de modèles, les courbes estimées de recrutement et l'Interprétation des données.

[Traduit par la Rédaction]

Introduction

For nearly fifty years, Ricker's (1954) analysis of stock and recruitment has provided a conceptual framework for salmon management, based on a functional relationship

$$(1) \qquad R_{t+1} = f(S_t; \theta)$$

between stock S_t in year t and future recruitment R_{t+1}. The time scale in (1) depends on the stock. One time unit corresponds to the number of years from birth to maturity, after which an adult salmon returns to its natal stream, spawns, and dies. For example, pink salmon (*Oncorhynchus gorbuscha*) require two calendar years to proceed from generation t to $t+1$. A parameter vector θ determines the curve appropriate for a given stock, and a sequence of observed data points (S_t, R_{t+1}) leads to an estimate $\hat{\theta}$. Ricker (1958) specifically proposed the functional form

$$(2) \qquad f(S; \theta) = \alpha S e^{-\beta S}$$

with $\theta = (\alpha, \beta)$.

Walters and Ludwig (1981) and Ludwig and Walters (1981) investigated the consequences of introducing realistic statistical error into the analysis of (1)–(2). They considered two potential sources of error: natural variation in stock productivity (process error) and inaccurate fish counts (measurement error). They concluded (Walters and Ludwig 1981, p. 704), "Errors in measuring spawning stocks can have a profound effect on the appearance of stock–recruitment relationships." The effect is particularly acute when the measurement error in S_t is log normal (Schnute 1993). For example, if the data contain incorrect low measurements of large spawning stocks, then an estimation model based only on process error can underestimate the system carrying capacity.

This paper presents an analysis of the stock–recruitment problem that incorporates three recent theoretical developments. First, we formulate the model using dynamic state variables (Harvey 1989; Schnute 1994) and take advantage of related techniques for parameter estimation, such as an extended Kalman filter. Second, we use a generalized version of the recruitment function (2) that depends explicitly on parameters relevant to management (Schnute and Kronlund 1996). Third, we adopt Bayesian methods for assessing uncertainty, as illustrated for salmon stocks by Schnute et al. (2000). Their results considered only process error; we extend their analysis by including measurement error as well.

A state–space model requires assumptions about the observed data. For salmon stocks, the data typically include measurements of catch C_t and escapement E_t in year t (Schnute et al. 2000). We assume that catch from the fishery is relatively well known but that escapement counts from field programs on natal streams contain significant measurement error. The model uses a state variable S_t to represent the true, but unknown, spawning stock. This also determines the true recruitment $R_t = C_t + S_t$.

Received 21 August 2001. Accepted 30 January 2002. Published on the NRC Research Press Web site at http://cjfas.nrc.ca/ on 22 March 2002.

J.T. Schnute[1] **and A.R. Kronlund.** Fisheries and Oceans Canada, Science Branch, Pacific Biological Station, 3190 Hammond Bay Road, Nanaimo, BC V9T 6N7, Canada.

[1]Corresponding author (email: schnutej@pac.dfo-mpo.gc.ca).

 DOI: 10.1139/F02-016 © 2002 NRC Canada

Table 1. Two parametric forms of the recruitment function, with associated parameter constraints and relationships.

Parameters

(T1.1) $\phi = (\alpha, \beta, \gamma),\ \theta = (h^*, S^*, \gamma)$

Functional forms

(T1.2) $$f(S;\phi) = \begin{cases} \alpha S(1-\beta\gamma S)^{1/\gamma}; & \gamma \neq 0 \\ \alpha S e^{-\beta S}; & \gamma = 0 \\ 0; & \gamma > 0,\ S \geq \dfrac{1}{\beta\gamma} \end{cases}$$

(T1.3) $$f(S;\theta) = \begin{cases} \dfrac{S}{1-h^*}\left[1+\gamma h^*\left(1-\dfrac{S}{S^*}\right)\right]^{1/\gamma}; & \gamma \neq 0 \\ \dfrac{S}{1-h^*}\exp\left[h^*\left(1-\dfrac{S}{S^*}\right)\right]; & \gamma = 0 \\ 0; & \gamma > 0,\ S \geq S^*\left(1+\dfrac{1}{\gamma h^*}\right) \end{cases}$$

Parameter constraints

(T1.4) $1 < \alpha,\ 0 < \beta$

(T1.5) $$0 < S^*,\ 0 < h^* < \begin{cases} 1; & \gamma \geq -1 \\ -1/\gamma; & \gamma < -1 \end{cases}$$

Parameter relationships

(T1.6) $$\alpha = \begin{cases} \dfrac{(1+\gamma h^*)^{1/\gamma}}{1-h^*}; & \gamma \neq 0 \\ \dfrac{e^{h^*}}{1-h^*}; & \gamma = 0 \end{cases}$$

(T1.7) $$\beta = \frac{h^*}{(1+\gamma h^*)S^*}$$

Measurement and process error occur in the two transitions

(3) $S_t \mapsto E_t$

and

(4) $S_t \mapsto C_{t+1} + S_{t+1}$,

respectively, where the mapping arrow indicates a functional relationship and the function (1) governs (4). We can contrast this scenario with the observed transition

(5) $E_t \mapsto C_{t+1} + E_{t+1}$

commonly used to estimate stock–recruitment relationships. As measurement error increases in (3), the observed recruitment process (5) becomes a poor representation of the actual process (4).

The paper begins with an analysis of the recruitment function (1). Following Schnute and Kronlund (1996), we derive various reference points for biological interpretation and stock management. The recruitment function, combined with the measurement and process error outlined in (3)–(5), defines a corresponding state–space model. This allows us to simulate a data series $\{C_t, E_t\}_{t=1}^n$, based on known parameters, and to construct algorithms for estimating these parameters from observed data. A worked example, based on simulated data, illustrates geometric relationships among model choices, estimated recruitment curves, and data interpretations.

For computational purposes, we compile most analytical results into tables that can readily be converted to computer code. Our numbering scheme reflects this organization; for example, equation (T3.5) denotes the fifth equation in Table 3.

Model formulation

From a deterministic perspective, the recruitment function (1) implies a long-term yield associated with a constant harvest rate h. More precisely, the three equations

(6) $R = f(S;\theta),\ C = hR,\ S = R - C,$

define equilibrium levels of recruitment $R(h)$, catch $C(h)$, and spawning stock $S(h)$ for a given h. In particular, the catch C represents a fraction h of the recruitment R, and the stock S consists of all fish that remain after the catch is removed. When $h = 0$, (6) defines the pristine stock size $S' = R'$, where $S' = f(S';\theta)$. As h increases, the catch $C(h)$ increases to a maximum value C^*, which is achieved at a harvest rate h^*. A further increase of h beyond h^* causes a reduction in catch $C(h)$, due to stock depletion. A sufficiently high harvest rate

©2002 NRC Canada

$h^\dagger$ drives the stock to extinction. Throughout this paper, we use the accents mentioned here to denote reference values for three conditions: pristine (prime accent), maximum sustainable yield (MSY, asterisk), and extinction (dagger).

Tables 1 and 2 summarize the results of such an analysis (Appendix A). We begin with the function (T1.2), suggested by Deriso (1980) and Schnute (1985). This curve, with parameter vector $\phi = (\alpha, \beta, \gamma)$, reduces to the Ricker case (2) when $\gamma = 0$. The cases $\gamma = -1$ and $\gamma = 1$ also have historical interest, corresponding to proposals by Beverton and Holt (1957) and Schaefer (1954), respectively. Schnute and Kronlund (1996) expressed the parameters (α, β) in (T1.2) analytically in terms of MSY parameters. For example, $\alpha = e^{h^*}/(1 - h^*)$ in the Ricker model (2), even though h^* cannot be represented analytically as a function of α.

In this paper, we follow Schnute et al. (2000) by adopting the parameter vector $\theta = (h^*, S^*, \gamma)$ in (T1.1). These parameters determine (α, β) by the relationships (T1.6)–(T1.7). Furthermore, the recruitment function itself can be written analytically in terms of θ, as shown in (T1.3). When $\gamma > 0$, the function $f(S)$ increases to a maximum value and then decreases to 0 at the critical value

$$S = \frac{1}{\beta\gamma} = S^*\left(1 + \frac{1}{\gamma h^*}\right).$$

This explains why $f(S) = 0$ for sufficiently large values S in (T1.2)–(T1.3) when $\gamma > 0$. Similar technical reasons imply the parameter constraints (T1.4)–(T1.5). For example, the number of recruits per spawner $R/S = \alpha(1 - \beta\gamma S)^{1/\gamma}$ increases steadily as S decreases and approaches a maximum value α as $S \to 0$. A finite stock $S > 0$ cannot replace itself unless $\alpha > 1$, as indicated in (T1.4).

Table 2 shows the solution (T2.1)–(T2.3) to the equilibrium equations (6) for the recruitment function (T1.3), where $R(h)$ and $C(h)$ are expressed in terms of $S(h)$. The reader can confirm that $S(h^*) = S^*$ in (T2.1). Equations (T2.4)–(T2.5) define corresponding equilibrium levels of recruitment R^* and catch C^* achieved at the MSY harvest rate h^*. Furthermore, the values $R(0) = S(0)$, obtained from (T2.1)–(T2.2) when $h = 0$, give the pristine stock values (T2.6). The harvest rate $h^\dagger$ in (T2.7) produces extinction because the fishery removes all but one of the maximum number α of recruits per spawner. Thus, a finite stock $S > 0$ with productivity less than α cannot sustain itself when impacted by a harvest rate $h \geq h^\dagger$.

Table 3 extends the recruitment function (T1.3) to a full simulation model with measurement and process error. The complete parameter vector Θ_S in (T3.1) includes parameters of four types: recruitment (h^*, S^*, γ), random error (σ, τ), harvest rate (h_1, h, k), and duration (m, n). The control policy (T3.2) determines a sequence of harvest rates h_t that oscillate sinusoidally between an initial rate h_1 and another rate h, where k oscillations occur during a period of n years. A simulation begins with a pristine stock (T3.3) in some historical year $t = -m$. A constant harvest rate $h_t = h_1$ is then maintained until year $t = 1$, so that the initial stock R_1 reflects this historical level of fishing. Output data $\{C_t, E_t\}_{t=1}^n$ come from the years $t = 1, \ldots, n$ with an oscillatory harvest policy. Four dynamic equations (T3.4)–(T3.7) describe the removal of catch C_t, survival of spawners S_t, enumeration of escapement E_t, and production of new recruits R_{t+1}. In particular, (T3.6) includes lognormal measurement error with standard deviation σ, and (T3.7) includes lognormal process error with standard deviation τ. We assume that the standard normal variates δ_t and ϵ_t are independent for all time. Equations (T3.6)–(T3.7) give analytical form to the transitions (3)–(4), respectively.

Table 2. Equilibrium states corresponding to a constant harvest rate h and additional reference points for the stock–recruitment model in Table 1.

Equilibrium states

(T2.1) $$S(h) = \begin{cases} \dfrac{\gamma h^* + 1 - \left(\dfrac{1-h^*}{1-h}\right)^\gamma}{\gamma h^*} S^*; & \gamma > 0 \\ \dfrac{h^* - \log\left(\dfrac{1-h^*}{1-h}\right)}{h^*} S^*; & \gamma = 0 \end{cases}$$

(T2.2) $$R(h) = \frac{S(h)}{1-h}$$

(T2.3) $$C(h) = \frac{hS(h)}{1-h}$$

Reference points

(T2.4) $$R^* = \frac{S^*}{1-h^*}$$

(T2.5) $$C^* = \frac{h^* S^*}{1-h^*}$$

(T2.6) $$R' = S' = \begin{cases} \dfrac{\gamma h^* + 1 - (1-h^*)^\gamma}{\gamma h^*} S^*; & \gamma \neq 0 \\ \dfrac{h^* - \log(1-h^*)}{h^*} S^*; & \gamma = 0 \end{cases}$$

(T2.7) $$h^\dagger = \frac{\alpha - 1}{\alpha}$$

Conceptually, the model in Table 3 describes a system in which a given control policy generates a data set:

(7) $$\{h_t\}_{t=1}^n \mapsto \{C_t, E_t\}_{t=1}^n.$$

Our analysis deals with the case in which only the output data are available for parameter estimation. The controls (h_t) and internal states (S_t, R_t) are not observed directly and must be estimated along with model parameters $(h^*, S^*, \gamma, \sigma, \tau)$. We consider an oscillatory control policy that produces contrast in the output data with improved prospects for reasonable system identification.

Parameter estimation

Algorithms for parameter estimation depend on the two stochastic equations (T3.6)–(T3.7). Table 4 summarizes their role in a model for developing a likelihood function or Bayes posterior. In terms of unknown states S_t and observed data (C_t, E_t), the original model takes the form (T4.9)–(T4.10). To capture the normal error in (T4.9), we use the unknown states

©2002 NRC Canada

Table 3. A stochastic simulation model to generate catch and escapement data $\{C_t, E_t\}_{t=1}^n$ from the parameter vector Θ_S.

Simulation parameters

(T3.1) $\Theta_S = (h^*, S^*, \gamma; \sigma, \tau; h_1, h, k; m, n)$

Control policy

(T3.2) $$h_t = \begin{cases} h_1; & t = -m, \ldots, 0 \\ h_1 + (h - h_1)\sin^2\left(\dfrac{t-1}{n-1}k\pi\right); & t = 1, \ldots, n \end{cases}$$

Initial condition

(T3.3) $R_{-m} = S'(h^*, S^*, \gamma)$

Simulation $(t = -m, \ldots, n)$

(T3.4) $C_t = h_t R_t$

(T3.5) $S_t = R_t - C_t$

(T3.6) $E_t = S_t e^{\sigma\delta_t}$

(T3.7) $R_{t+1} = f(S_t; h^*, S^*, \gamma)e^{\tau\epsilon_t}$

Table 4. Conceptual model for estimating parameters from the data $\{C_t, E_t\}_{t=1}^n$.

States and observations

(T4.1) $X_t = \log S_t$

(T4.2) $Y_t = \log E_t$

Parameters

(T4.3) $\Theta = (h^*, S^*, \gamma, \sigma, \tau, X_1)$

(T4.4) $\Phi = (h^*, S^*, \gamma, \sigma, \tau, X_1, \ldots, X_n)$

Variance transformations

(T4.5) $\kappa^2 = \sigma^2 + \tau^2, \quad \rho = \dfrac{\sigma^2}{\sigma^2 + \tau^2}$

(T4.6) $\sigma^2 = \rho\kappa^2, \quad \tau^2 = (1 - \rho)\kappa^2$

(T4.7) $\dfrac{\sigma^2}{\tau^2} = \dfrac{\rho}{1 - \rho}$

(T4.8) $\dfrac{\partial(\sigma, \tau)}{\partial(\rho, \kappa)} = \dfrac{\kappa}{2\sqrt{\rho(1 - \rho)}}$

Original model

(T4.9) $E_t = S_t e^{\sigma\delta_t}$

(T4.10) $S_{t+1} + C_{t+1} = f(S_t; h^*, S^*, \gamma)e^{\tau\epsilon_t}$

Alternative model

(T4.11) $Y_t = X_t + \sigma\delta_t$

(T4.12) $\log\left(e^{X_{t+1}} + C_{t+1}\right) = \log f\left(e^{X_t}; h^*, S^*, \gamma\right) + \tau\epsilon_t$

X_t and observations Y_t as surrogates for S_t and E_t, as defined in (T4.1)–(T4.2). The model then takes the alternative form (T4.11)–(T4.12). Unknown quantities consist of the recruitment parameters (h^*, S^*, γ), standard errors (σ, τ), and states (X_t), which must all be estimated from the data $\{C_t, E_t\}_{t=1}^n$.

Schnute (1994) describes two paradigms for estimating parameters in a state space model, and we summarize these briefly here. The Kalman filter (KF) approach, which is consistent with a frequentist viewpoint, treats the unknown states as random variables. The likelihood function involves an integral across all possible values of these states, and the extended KF algorithm gives an approximate value for this integral. Only the initial state X_1 appears in the parameter vector Θ, as in (T4.3). The errors-in-variables (EV) approach, which requires a Bayes perspective, treats all unknown states as parameters in the vector Φ defined by (T4.4). The model equation (T4.12) describes the state parameters as random variables, with the distribution of X_{t+1} conditional on X_t. A Bayesian can adopt this distribution as a prior on the parameters X_t $(t = 2, \ldots, n)$, where the likelihood comes from the observations (T4.11).

The parameter vector Θ has fixed length for any number n of observed data points (C_t, E_t). By contrast, the vector Φ becomes longer as n increases, similar to the parameters in a classical functional relationship (Kendall and Stuart 1979, chapter 29). A strict frequentist interpretation requires that all unknown parameters be constants, which by definition cannot follow a probability distribution, like (T4.12). A Bayesian resolves this logical issue by treating (T4.12) as a prior on Φ, where in a hierarchical sense the parameters Θ govern the distribution of $X_2, \ldots, X_n$. In this way, the Bayes approach easily adapts to functional or structural relationships in which parameters act as constants or random variables, respectively. Our worked example highlights a similarity between the Bayes posterior mode and the likelihood mode for a classical functional relationship.

The extended Kalman filter uses a linear approximation that depends on the designated state and observation variables (X_t, Y_t). Our choices (T4.1)–(T4.2) linearize the observation equation (T4.11) but give a rather complex nonlinear form to the process equation (T4.12). We considered other choices but

©2002 NRC Canada

Table 5. Approximate likelihood function, computed via an extended Kalman filter from the parameter vector Θ in (T4.3) and the data $\{C_t, E_t\}_{t=1}^n$.

Initialize

(T5.1) $\widetilde{X}_1 = X_1$

(T5.2) $\widetilde{U}_1 = 0$

Kalman recursions ($t = 1, \ldots, n$)

(T5.3) $\widetilde{Y}_t = \widetilde{X}_t$

(T5.4) $\widetilde{V}_t = \widetilde{U}_t + \sigma^2$

(T5.5) $\widehat{X}_t = \widetilde{X}_t + \dfrac{\widetilde{U}_t}{\widetilde{V}_t}(\log E_t - \widetilde{Y}_t)$

(T5.6) $\widehat{U}_t = \dfrac{\widetilde{U}_t}{\widetilde{V}_t}\sigma^2$

(T5.7) $\widetilde{X}_{t+1} = \log[f(e^{\widehat{X}_t}; h^*, S^*, \gamma) - C_{t+1}]; \quad t \le n-1$

(T5.8) $\widetilde{U}_{t+1} = \left[\left(\dfrac{1-\beta(1+\gamma)e^{\widehat{X}_t}}{1-\beta\gamma e^{\widehat{X}_t}}\right)^2 \widehat{U}_t + \tau^2\right]\left(1 + C_{t+1}e^{-\widehat{X}_{t+1}}\right)^2; \quad t \le n-1$

Approximate likelihood function

(T5.9) $F(\Theta) = \dfrac{1}{2}\sum_{t=1}^{n}\left[\log \widetilde{V}_t + \dfrac{(\log E_t - \widetilde{Y}_t)^2}{\widetilde{V}_t}\right]$

(T5.10) $L(\Theta) \propto e^{-F(\Theta)}$

Table 6. Bayes posterior distribution, computed from the parameter vector Φ in (T4.4) and the data $\{C_t, E_t\}_{t=1}^n$.

Residuals ($t = 1, \ldots, n$) **and sums**

(T6.1) $S_t = e^{X_t}$

(T6.2) $h_t = \dfrac{C_t}{S_t + C_t}$

(T6.3) $\xi_t = \log\left[\dfrac{E_t}{S_t}\right]$

(T6.4) $\eta_t = \log\left[\dfrac{S_{t+1} + C_{t+1}}{f(S_t; h^*, S^*, \gamma)}\right]; \quad t \le n-1$

(T6.5) $T_1 = \sum_{t=1}^{n}\xi_t^2$

(T6.6) $T_2 = \sum_{t=1}^{n-1}\eta_t^2$

(T6.7) $T_3 = -\sum_{t=2}^{n}\log(1-h_t)$

Prior distributions

(T6.8) $P_0(X_1) \propto 1$

(T6.9) $P_0(\sigma, \tau) \propto \dfrac{1}{\sigma\tau}$

(T6.10) $P_0(\rho, \kappa) \propto \dfrac{1}{\rho(1-\rho)\kappa}$

(T6.11) $P_0(h^*, S^*, \gamma) \propto P_0(h^*|\gamma)P_0(S^*)P_0(\gamma)$

Posterior distribution

(T6.12) $G(\Phi) = (2n-1)\log\kappa + \dfrac{n}{2}\log\rho + \dfrac{n-1}{2}\log(1-\rho) + T_3 + \dfrac{1}{2\kappa^2}\left[\dfrac{T_1}{\rho} + \dfrac{T_2}{1-\rho}\right]$

(T6.13) $P(\Phi) \propto e^{-G(\Phi)}\, P_0(\rho, \kappa)\, P_0(h^*, S^*, \gamma)$

©2002 NRC Canada

Table 7. Exact likelihood function in the case $\rho = 0$ with no measurement error ($\sigma = 0$).

Parameters

(T7.1) $\Theta_0 = (h^*, S^*, \gamma, \tau)$

Residuals ($t = 1, \ldots, n-1$)

(T7.2) $\eta_t = \log\left[\dfrac{E_{t+1} + C_{t+1}}{f(E_t; h^*, S^*, \gamma)}\right]$

Likelihood function

(T7.3) $F(\Theta_0) = (n-1)\log\tau + \dfrac{1}{2\tau^2}\sum_{t=1}^{n-1}\eta_t^2$

(T7.4) $L(\Theta_0) \propto e^{-F(\Theta_0)}$

Table 8. Exact likelihood function in the case $\rho = 1$ with no process error ($\tau = 0$).

Parameters

(T8.1) $\Theta_1 = (h^*, S^*, \gamma, \sigma, X_1)$

Residuals ($t = 1, \ldots, n$)

(T8.2) $S_1 = e^{X_1}$

(T8.3) $S_{t+1} = f(S_t; h^*, S^*, \gamma) - C_{t+1}; \quad t \le n-1$

(T8.4) $\xi_t = \log\left[\dfrac{E_t}{S_t}\right]$

Likelihood function

(T8.5) $F(\Theta_1) = n\log\sigma + \dfrac{1}{2\sigma^2}\sum_{t=1}^{n}\xi_t^2$

(T8.6) $L(\Theta_1) \propto e^{-F(\Theta_1)}$

adopted those in Table 4 to obtain a relatively easy derivation of the extended filter. Incidentally, the KF paradigm also has a Bayesian interpretation, where integrals across the unknown states eliminate them as nuisance parameters.

Estimated parameters and states depend on the relative magnitudes of measurement and process error. In the present context, σ and τ have the same dimensional units associated with error in logarithmic numbers of fish. Thus, it makes sense to define the total variance κ^2 and the proportion ρ of measurement error variance, as in (T4.5). Effectively, the parameters (ρ, κ) can replace (σ, τ) in the model, where (T4.5)–(T4.6) give the transformations needed to switch between the two pairs. For $0 < \rho < 1$, the transformation has a positive Jacobian (T4.8). Also, as shown in (T4.7), the proportion ρ determines the ratio σ^2/τ^2 between measurement and process error variances.

For models with normal error and linear relationships among the states and observations, the KF algorithm gives an exact calculation of the likelihood function (Schnute 1994). The model here has normal error and the observation equation (T4.11) is linear, but the process equation (T4.12) is not. Table 5 lists sequential steps in an extended KF calculation that gives an approximate likelihood value (Appendix B). Intuitively, the algorithm assumes that X_t and Y_t have normal distributions. Based only on the observations up to time $t-1$, the formulas

(8) $X_t \sim N(\widetilde{X}_t, \widetilde{U}_t)$ and $Y_t \sim N(\widetilde{Y}_t, \widetilde{V}_t)$

define notation for the respective means and variances. After the observation $Y_t = \log E_t$ at time t, the distribution of X_t is updated to give

(9) $X_t \sim N(\widehat{X}_t, \widehat{U}_t)$.

In particular, (T5.5) expresses the correction $\widehat{X}_t - \widetilde{X}_t$ in the mean of X_t as a multiple of the observed residual $\log E_t - \widetilde{Y}_t$. The transition equations (T5.7)–(T5.8) from time t to $t+1$ are approximate, based on linear expansions of terms in (T4.12).

The calculation in Table 5 defines a function F in (T5.9) that depends only on the parameter vector Θ and the data $\{C_t, E_t\}_{t=1}^n$. Except for an additive constant, F represents the negative log likelihood, as indicated in (T5.10). Each term in F corresponds to a normal distribution of the observation $\log E_t$, conditional on the mean $\widetilde{Y}_t$ and variance $\widetilde{V}_t$.

Table 9. Recruitment parameters θ, reference points, variances, controls, and durations for the simulation presented here.

Category	Quantity	Value
Parameters	h^*	0.60
	S^*	1.00
	γ	0.00
	α	4.56
	β	0.60
Reference points	C^*	1.50
	R^*	2.50
	R'	2.53
	$R_{\max}$	2.79
	$h^\dagger$	0.78
Variances	σ	0.28
	τ	0.28
	κ	0.40
	ρ	0.50
Controls	h_1	0.10
	h	0.70
	k	1.00
Durations	m	100
	n	25

Table 6 similarly gives a sequential calculation for implementing the EV paradigm (Appendix C). Equations (T6.1)–(T6.2) recover the internal state variables S_t and h_t from the parameters X_t and data C_t. The model equations (T4.9)–(T4.10) imply corresponding residuals (T6.3)–(T6.4) and sums of squares (T6.5)–(T6.6). A third sum (T6.7) collects Jacobians associated with the parameter transformations

(10) $X_{t+1} \mapsto S_{t+1} \mapsto \eta_t$

in (T6.1) and (T6.4). All three sums (T6.5)–(T6.7) have positive values. In particular, $T_3 > 0$ because $0 \le h_t < 1$ and $\log(1 - h_t) \le 0$.

The calculation in Table 6 gives a function G that depends

©2002 NRC Canada

Fig. 1. Stock–recruitment simulation corresponding to parameter values listed in Table 9. (*a*) Simulated points (S_t, R_{t+1}) and the theoretical stock–recruitment curve. A vertical solid line joins $(S^*, 0)$ to (S^*, S^*), and a vertical dotted line joins (S^*, S^*) to (S^*, R^*). A broken line indicates the replacement condition $R = S$. (*b*) Circles representing observed data $(E_t, C_{t+1} + E_{t+1})$ in relation to the stock–recruitment curve. A line attached to each observed point indicates the shift from the true state (S_t, R_{t+1}), owing to measurement error. The symbol "+" emphasizes years $(t = 3, 4, 20, 21, 24)$ with particularly large displacements. (*c*) Scatter plot (S_t, E_t) in relation to the line $E = S$, where three years $(t = 4, 21, 25)$ exhibit large positive measurement error. (*d*, *e*, *f*) Time series h_t, S_t (solid line), E_t (broken line), and C_t. The dotted horizontal line in (*d*) indicates the maximum sustainable yield level $h = h^*$.

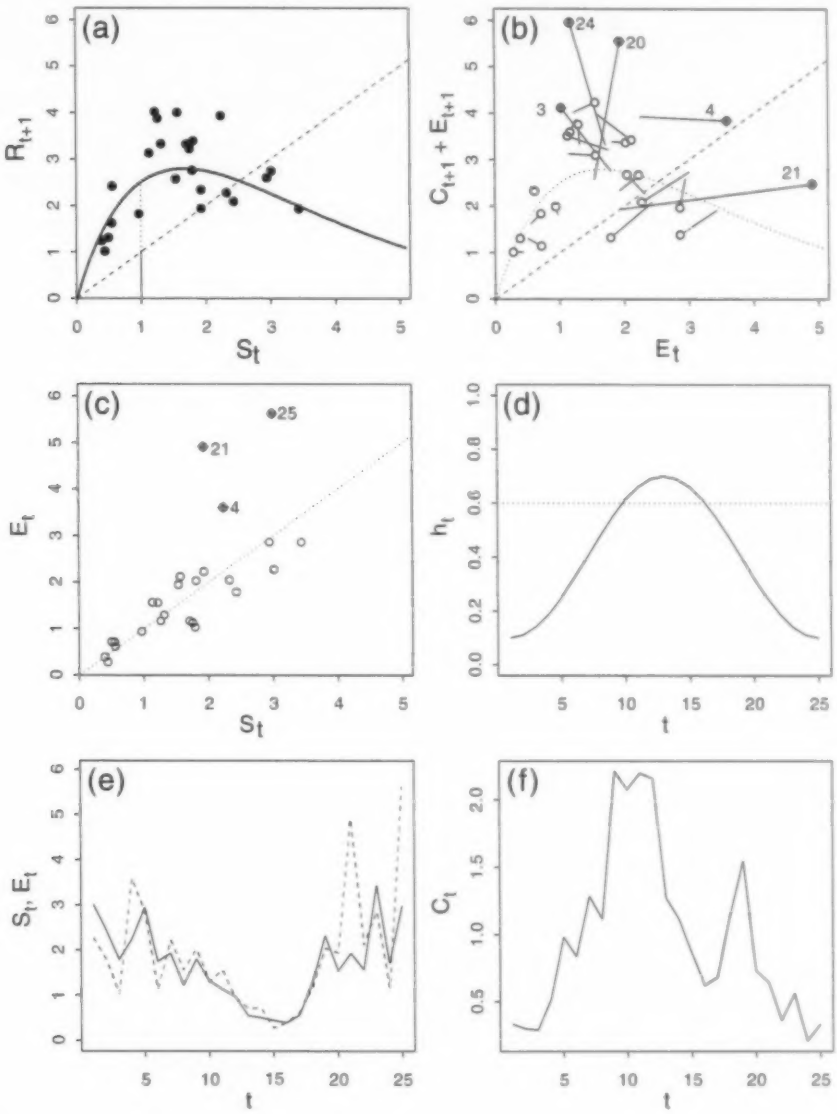

only on the parameter vector Φ and the data. Essentially, G is the negative log posterior, except for an additive constant and terms associated with prior distributions for (ρ, κ) and (h^*, S^*, γ). We adopt the usual noninformative prior $P_0(\sigma, \tau)$ in (T6.9). This implies the prior $P_0(\rho, \kappa)$ in (T6.10), given the Jacobian (T4.8). Following Schnute et al. (2000), we adopt uniform priors on the recruitment parameters (h^*, S^*, γ) to facilitate the interpretation of our results. Thus, we bound S^* in an interval $0 < S^* \leq S_{\max}$ with a specified upper limit $S_{\max}$. Similarly, we confine γ to a fixed interval $\gamma_{\min} \leq \gamma \leq \gamma_{\max}$ and impose the constraint (T1.5) on h^*. These priors and the function G define a function proportional to the posterior $P(\Phi)$, as in (T6.13).

Estimation becomes particularly simple in the extreme cases with no measurement error ($\sigma = 0$) or no process error ($\tau = 0$),

©2002 NRC Canada

Fig. 2. Estimated stock–recruitment curves, based on observed data (C_t, E_t) from the simulation in Fig. 1. Open and solid circles represent observed data $(E_t, C_{t+1} + E_{t+1})$ and estimated points $(\widehat{S}_t, \widehat{R}_{t+1})$ points. (*a–l*) The 12 cases A–L listed in Table 10. In particular, panels in the left, middle, and right columns correspond to three choices of curve type, $\gamma = -1, 0, 1$, respectively. The rows from top to bottom represent four alternatives to estimating measurement error: $\rho = 0$, the EV paradigm with $\rho = 0.5$, the KF paradigm with $\rho = 0.5$, and the EV paradigm with $\rho = 0.95$.

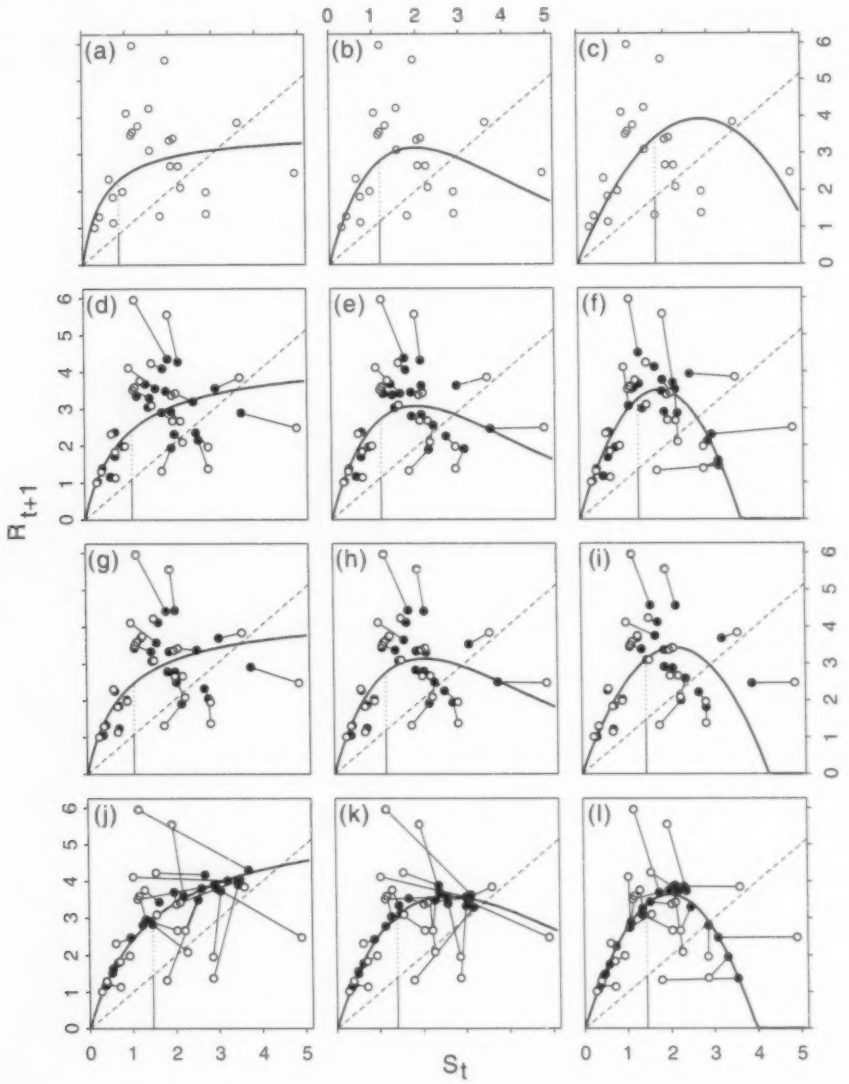

for which $\rho = 0$ and $\rho = 1$, respectively. Tables 7 and 8 show the exact likelihood function for each case. Under the assumption that the escapement count E_t exactly measures the spawning stock S_t, the likelihood comes from the normal distribution of recruitment residuals (T7.2). On the other hand, a deterministic recruitment scenario (T8.3) implies a likelihood associated with normal observation residuals (T8.4). Most historical analyses of stock and recruitment data use the calculation in Table 7. The deterministic scenario in Table 8 has theoretical value, but natural stocks are never as predictable as (T8.3).

Ideally, one might hope to estimate ρ via the KF or EV paradigm. However, it can be shown in Table 5 that $\max L(\Theta) \to \infty$ as $\rho \to 0$ (Appendix B). Consequently, a global maximum likelihood occurs when $\rho = 0$, regardless of the data. Similarly, in Table 6, $\max P(\Phi) \to \infty$ as $\rho \to 0$ or $\rho \to 1$ (Appendix C). Thus, the posterior has at least two global modes, corresponding to the extreme values of ρ. In the examples that follow, we estimate parameters with ρ fixed and investigate how the choice of ρ influences the results.

We have formulated Tables 5, 7, and 8 as likelihood cal-

©2002 NRC Canada

Table 10. Estimates obtained from a data set simulated with the parameters in Table 9, where 12 cases A–L are defined by choices of algorithm (EV, KF), ρ (0, 0.5, 0.95), and γ (−1, 0, 1). A hat symbol ($\widehat{\ }$) denotes modal parameter estimates. A bar symbol ($\bar{\ }$) and the notation SE denote means and standard errors calculated from systematic subsamples of size 2000 drawn from MCMC samples of length 500 000.

	$\rho = 0$			EV: $\rho = 0.5$			KF: $\rho = 0.5$			EV: $\rho = 0.95$		
Case	A	B	C	D	E	F	G	H	I	J	K	L
ρ	0.00	0.00	0.00	0.50	0.50	0.50	0.50	0.50	0.50	0.95	0.95	0.95
γ	−1.00	0.00	1.00	−1.00	0.00	1.00	−1.00	0.00	1.00	−1.00	0.00	1.00
$\widehat{h^*}$	0.63	0.58	0.47	0.55	0.58	0.58	0.56	0.57	0.52	0.51	0.54	0.57
$\overline{h^*}$	0.61	0.56	0.45	0.57	0.56	0.52	0.56	0.56	0.51	0.51	0.53	0.54
SE[h^*]	0.09	0.06	0.06	0.08	0.05	0.04	0.06	0.04	0.03	0.06	0.04	0.03
$\widehat{S^*}$	0.84	1.16	1.81	1.10	1.14	1.36	1.08	1.19	1.48	1.46	1.40	1.44
$\overline{S^*}$	0.96	1.23	1.98	1.10	1.26	1.54	1.21	1.27	1.63	1.47	1.48	1.53
SE[S^*]	0.36	0.20	0.39	0.34	0.19	0.17	0.30	0.17	0.19	0.30	0.20	0.14
$\widehat{\kappa}$	0.43	0.41	0.48	0.32	0.29	0.26	0.45	0.43	0.40	0.39	0.35	0.28
$\overline{\kappa}$	0.48	0.46	0.54	0.50	0.46	0.43	0.51	0.48	0.46	0.61	0.56	0.47
SE[κ]	0.08	0.08	0.10	0.08	0.08	0.07	0.09	0.08	0.08	0.11	0.09	0.08
$\widehat{C^*}$	1.44	1.63	1.60	1.33	1.57	1.89	1.39	1.56	1.62	1.50	1.67	1.93
$\widehat{R^*}$	3.12	2.91	3.62	3.52	2.85	2.73	3.56	2.94	2.96	4.42	3.43	2.89
$\widehat{h^*}$	0.86	0.77	0.64	0.80	0.76	0.74	0.81	0.75	0.69	0.76	0.73	0.73

culations, in contrast with the Bayesian formulation in Table 6. Incorporating the priors in Table 6 into the likelihood tables gives a Bayes perspective throughout. Thus, if $F(\Theta)$ and $P_0(\Theta)$ denote a negative log likelihood function and prior distribution for the parameter vector Θ, then

$$P(\Theta) \propto e^{-F(\Theta)} P_0(\Theta)$$

defines the posterior. We use this formulation in our worked examples, where the prior (T6.10) is replaced by $1/\tau$ and $1/\sigma$, respectively, when $\rho = 0$ and $\rho = 1$.

Results

We illustrate our analysis with a simulation based on the parameters listed in Table 9. In particular, we generate $n = 25$ years of data associated with a Ricker curve ($\gamma = 0$). The total error variance is split evenly between measurement and process components ($\rho = 0.5$). Figure 1*a* shows simulated states (S_t, R_{t+1}), $t = 1, \ldots, 24$, which exhibit scatter about the underlying recruitment curve due to process error. Measurement error displaces these true states to the observed points $(E_t, C_{t+1} + E_{t+1})$ shown in Fig. 1*b*. The points corresponding to $t = 20$ and $t = 21$ have particularly large vertical and horizontal displacements, respectively, owing to a large positive measurement error in the escapement E_{21}. Thus, the recruitment from the stock in year 20 and the spawning stock in year 21 both appear larger than the actual states R_{21} and S_{21}. Similarly, a positive measurement error in E_4 produces notable displacements in the points corresponding to $t = 3, 4$, and a notable positive error in the final measurement E_{25} causes the point with $t = 24$ to be displaced vertically upward.

Figure 1*c* shows the explicit relationship between E_t and S_t. With no measurement error, all points would lie on the line $E = S$. Vertical displacement from this line corresponds to measurement error, just as vertical displacement from the Ricker curve indicates process error in Fig. 1*a*. Because of the assumed lognormal distribution, positive errors tend to have higher magnitude than negative errors in Figs. 1*a* and 1*c*. Our simulation uses a high contrast control policy (Fig. 1*d*), with a harvest rate h_t that increases from $h_1 = 0.1$ to a maximum $h = 0.7$ and then declines back to $h_{25} = 0.1$ (Table 9, control parameters). This produces the pattern of spawners S_t and catches C_t in Figs. 1*e*–1*f*. Figures 1*c* and 1*e* show clearly the large positive measurement errors in E_t when $t = 4, 21, 25$.

Geometrically, an estimation algorithm attempts to recover the solid circles and recruitment curve in Fig. 1*a* from the data portrayed as open circles in Fig. 1*b*. Two key parameters (γ, ρ) govern this attempt, where γ determines the curve type and ρ specifies the relative amount of measurement error. In slightly more general terms, these parameters correspond to choices of recruitment model and error structure. Furthermore, when $0 < \rho < 1$, the algorithm can follow either the EV or KF paradigm.

Figure 2 illustrates 12 such estimation choices applied to our simulated data, where panels *a*–*l* correspond to cases A–L in Table 10. The three columns in Fig. 2 use the fixed choices $\gamma = -1, 0, 1$. The four rows use fixed error structures ($\rho = 0$, EV with $\rho = 0.5$, KF with $\rho = 0.5$, EV with $\rho = 0.95$). Curves shown in Fig. 2 correspond to modal parameter estimates $(\widehat{h^*}, \widehat{S^*})$ (Table 10). Solid circles show modal estimates $(\widehat{S}_t, \widehat{R}_{t+1})$, in contrast with open circles that portray the observed data $(E_t, C_{t+1} + E_{t+1})$. In the KF case, $\widehat{S}_t = e^{\widehat{X}_t}$ from (T5.5). No solid circles appear in the first row, because cases A–C assume no measurement error ($\rho = 0$).

Recruitment curves in the three columns of Fig. 2 have shapes familiar from the fishery literature. The Beverton–Holt curve (column 1, $\gamma = -1$) rises toward an asymptote. The Ricker curve (column 2, $\gamma = 0$) reaches a peak and descends asymptotically toward $R = 0$. The parabolic Schaefer curve (column 3, $\gamma = 1$) is symmetric about the peak. As ρ increases (rows 1,

©2002 NRC Canada

Fig. 3. Plots of 2000 parameter values (S^*, h^*) taken systematically from an MCMC sample of size 500 000. (*a–l*) The 12 cases A–L listed in Table 10 and portrayed in Fig. 2. A square (□) in each panel represents the true parameter values $(S^*, h^*) = (1.0, 0.6)$ from Table 9 used to generate simulated data (Fig. 1). An open circle (○) indicates the mean $(\overline{S^*}, \overline{h^*})$ of the MCMC subsample. An oplus symbol (⊕) designates the modal estimate $(\widehat{S^*}, \widehat{h^*})$.

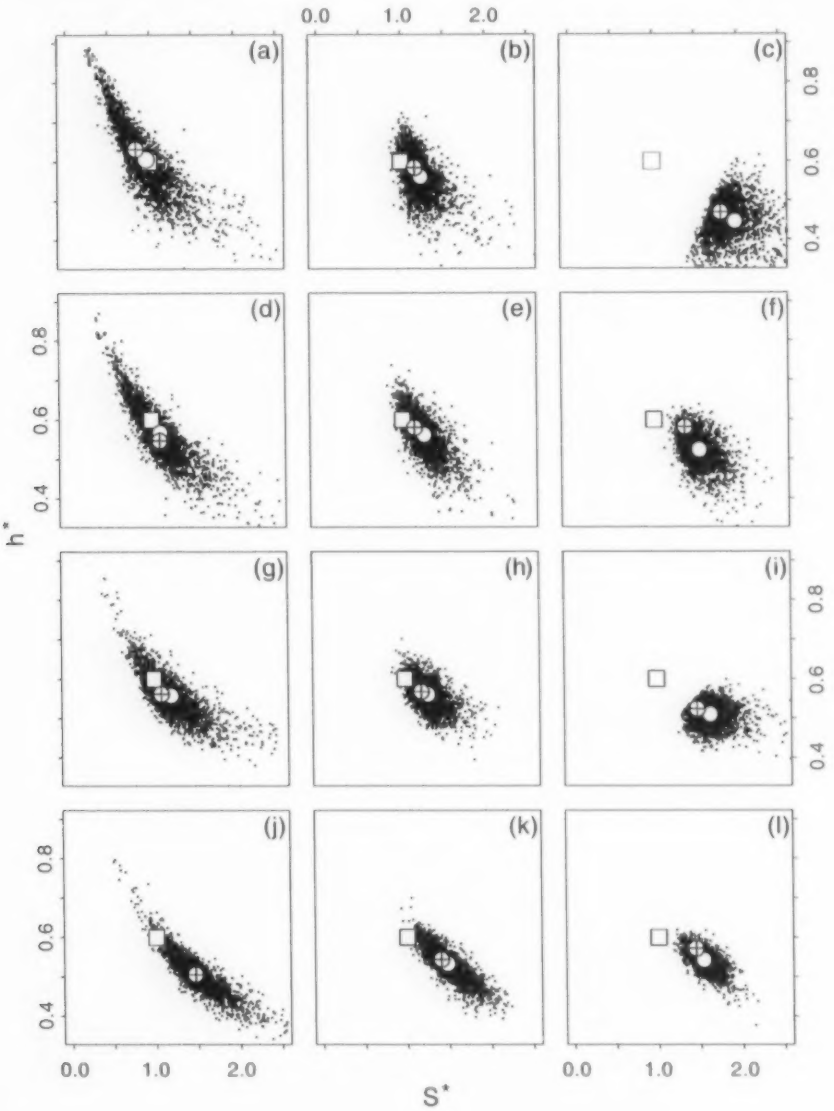

2, 4), the estimated points shift greater distances to lie near the fitted curve. The EV and KF paradigms (rows 2 and 3) produce similar results. In the two cases with correct parameter choices $\gamma = 0$ and $\rho = 0.5$ (Figs. 2*e*, 2*h*), the recruitment curves look similar to the correct curve in Fig. 1*a*. The open circles with greatest displacement in Fig. 1*b* typically move in the correct direction back toward a solid circle, as the model attempts to recover the underlying states (S_t, R_{t+1}).

Figure 3 extends the analysis in Fig. 2 by using a Markov chain Monte Carlo (MCMC; Gilks et al. 1996) sample to assess uncertainty in the parameter estimates. For this and all subsequent analyses, we use a systematic subsample of 2000 points drawn from an MCMC sample of size 500 000. Table 10 summarizes the results numerically by showing MCMC means $(\overline{h^*}, \overline{S^*})$ and standard errors (SE). The choices $\gamma = -1$ and $\gamma = 0$ produce similar patterns (Fig. 3, columns 1 and 2), but the estimated error is reduced by choosing the correct model $\gamma = 0$. The choice $\gamma = 1$ gives means and posterior sample regions that distinctly exclude the true values $(h^*, S^*) = (0.6, 1)$ (Fig. 3, column 3). For this example, Fig. 3 suggests broadly

©2002 NRC Canada

Fig. 4. Pairs plot of 2000 parameter values $(h^*, S^*, \gamma, \kappa)$ taken systematically from an MCMC sample of length 500 000, based on a classical stock–recruitment model with no measurement error ($\rho = 0$). For instance, sample points (γ, h^*) appear in the third column of the first row along with their mirror images (h^*, γ) in the third row of the first column. A square (□) in each panel represents true parameter values from Table 9 used to generate simulated data (Fig. 1). An open circle (○) indicates mean parameter estimates from the MCMC subsample. An oplus symbol (⊕) designates modal estimates.

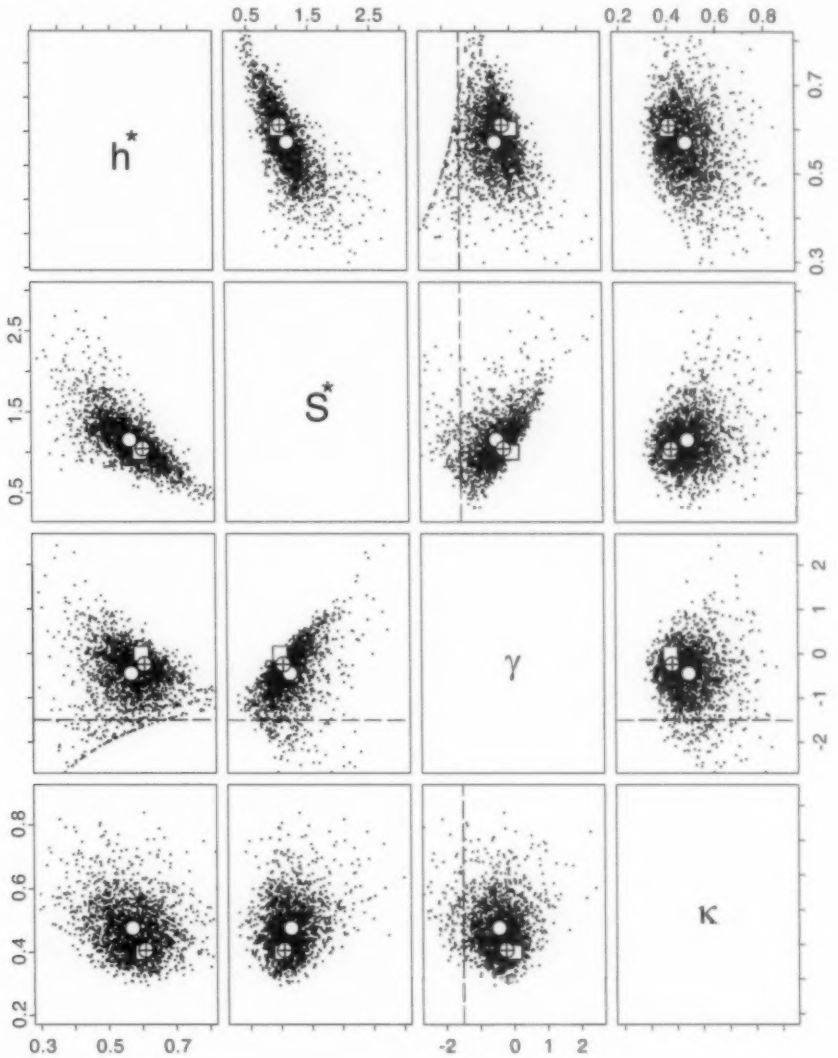

that the choice γ of recruitment model has greater influence on the statistical analysis than the choice ρ of error structure.

Panels in Fig. 3 have fixed scales that make cases A–L comparable. Some points in each scatter plot, particularly Fig. 3*c*, may lie outside the chosen scale. We constrain S^* to lie below the maximum $S_{\max} = 5$, nearly the highest observed escapement (Fig. 1*e*), although this constraint has almost no practical influence on the results in Fig. 3. Estimated points h^* in the MCMC sample lie well within the allowable range between 0 and 1.

We next examine the possibility of estimating the shape parameter γ ($\gamma_{\min} \le \gamma \le \gamma_{\max}$), rather than specifying fixed values. For these analyses, the upper bound $\gamma_{\max} = 3$ allows adequate scope for the MCMC sample, but the lower bound $\gamma_{\min}$ has to be chosen with some care. When $\gamma_{\min} < -1$, the additional constraint

$$(11) \qquad h^* < -\frac{1}{\gamma}$$

from (T1.5) adds a depression to the posterior surface that can trap the MCMC sample in regions of low probability. In general, we choose $\gamma_{\min} = -3$, but we adopt a more restrictive value

©2002 NRC Canada

Fig. 5. Pairs plot of 2000 parameter values $(h^*, S^*, \gamma, \kappa)$ taken systematically from an MCMC sample of length 500 000, based the EV paradigm with $\rho = 0.5$. The symbols □, ○, and ⊕ have interpretations defined in Fig. 4.

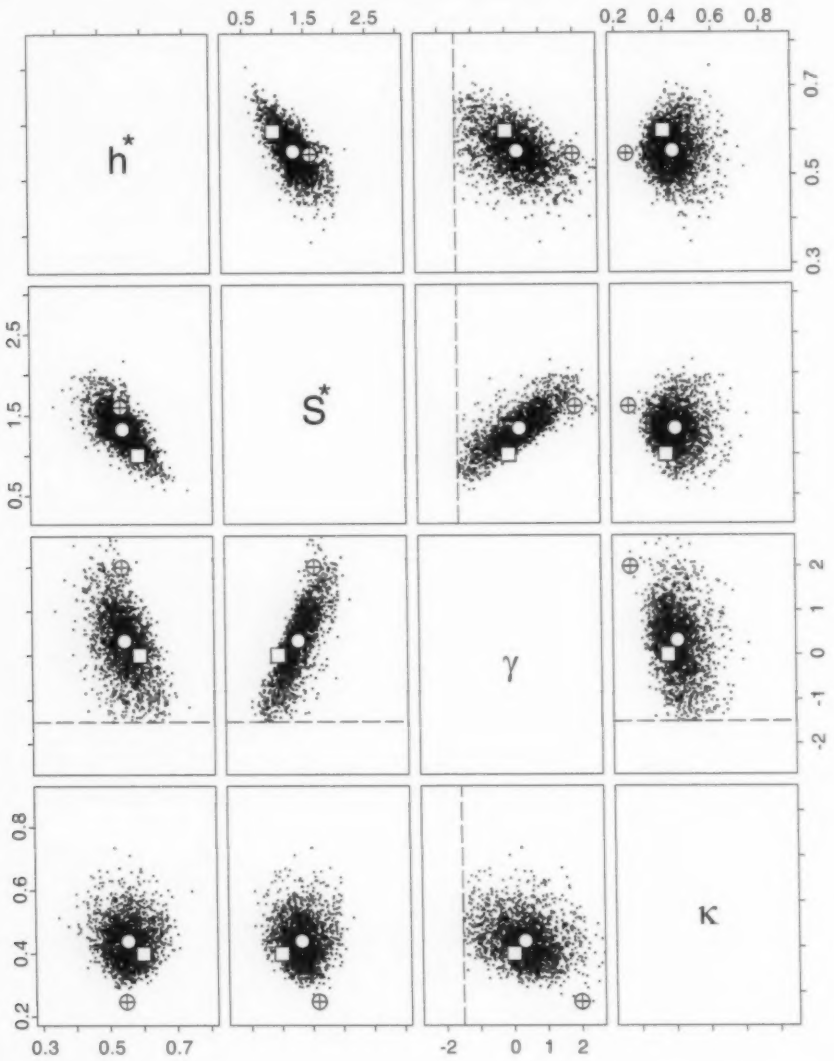

$\gamma_{min} = -1.5$ for the EV paradigm.

Figures 4–6 correspond to the error structure choices in the first three rows of Fig. 2, and Table 11 summarizes numerical results. The case with no measurement error ($\rho = 0$, Fig. 4) shows broader scatter plots, i.e. higher variances, for h^* and S^* than cases with the true value $\rho = 0.5$ (Fig. 5, EV; Fig. 6, KF). The plots of h^* vs. γ in Figs. 4 and 6 show some evidence of the constraint (11); in particular, points accumulate along the left margin of the scatter plot, which corresponds to the constraint boundary. The EV posterior surface, with n free state parameters X_t, offers many routes toward this boundary. The MCMC algorithm for this case can become trapped there, just as a wandering mountain climber who generally aims for the summit might fall into a crevasse. The lower bound $\gamma_{min} = -1.5$, illustrated by a broken line in Figs. 4–6, fences off this potential climbing hazard in Fig. 5.

The behaviour of the MCMC sample for large negative values γ has a simple geometric interpretation. As $\gamma \to -\infty$, the recruitment curve (T1.2) becomes a straight line with slope α. The constraint (11) forces $h^* \to 0$. Consequently, $S^* \to \infty$ to maintain a reasonable MSY harvest level C^* in (T2.5). In summary, the model contains possible scenarios in which the stock becomes very large and the catch C^* is achieved at a low harvest rate. Although the observed data in Fig. 2 suggest a limited carrying capacity, such scenarios can't entirely be ruled out. The EV paradigm, with many flexible state variables X_t, has MCMC samples that become locked into these scenarios without moving back into regions of much higher probability,

©2002 NRC Canada

Fig. 6. Pairs plot of 2000 parameter values $(h^*, S^*, \gamma, \kappa)$ taken systematically from an MCMC sample of length 500 000, based the KF paradigm with $\rho = 0.5$. The symbols □, ○, and ⊕ have interpretations defined in Fig. 4.

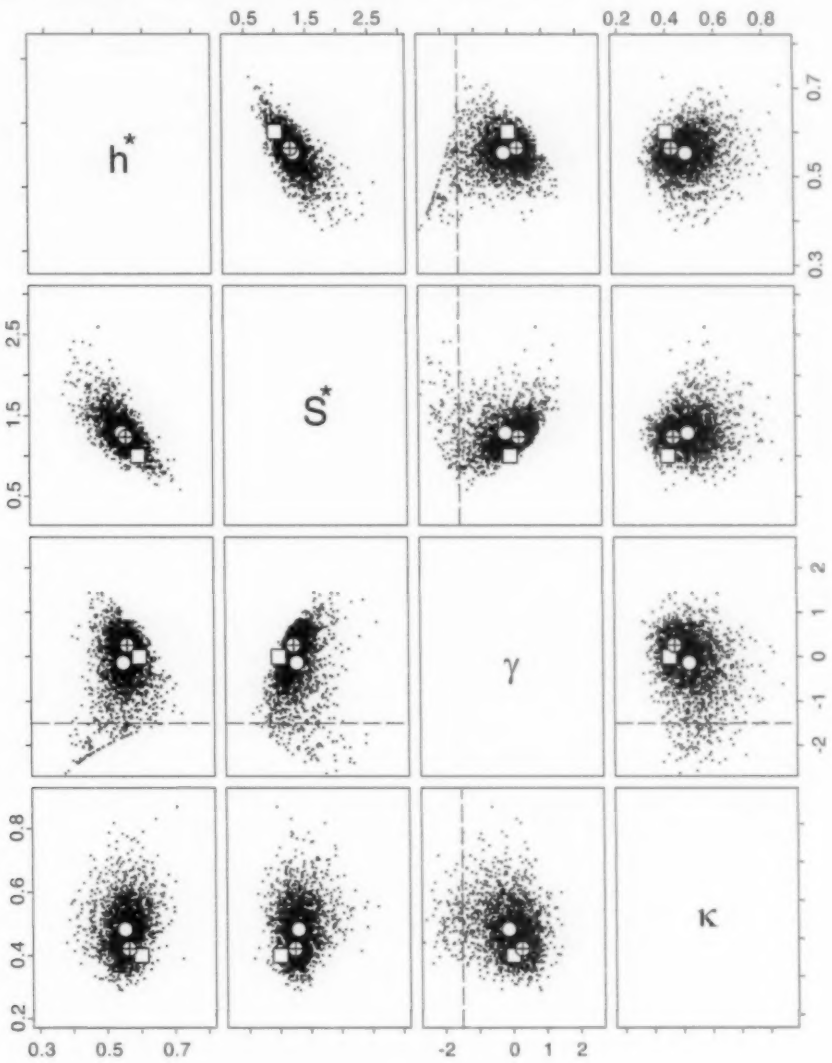

where the recruitment curve indicates a finite carrying capacity.

The EV and KF paradigms produce similar patterns (Figs. 5–6). Figure 5 does not portray the state parameter estimates $(X_1, \ldots, X_n)$ in the vector Φ, although these are generated in the MCMC samples. Similarly, Fig. 6 does not show the component X_1 of Θ. The figures do, however, include MCMC estimates of κ. Theoretical results suggest that $\hat{\kappa}$ should underestimate κ. For the classical linear EV functional regression model, it can be proved that $\hat{\kappa}^2 \to \kappa^2/2$ in probability as $n \to \infty$ (Kendall and Stuart 1979, section 29.19, p. 411). Thus, in this case, the maximum likelihood variance estimate $\hat{\kappa}^2$ is inconsistent by a factor of 1/2. Intuitively, this difficulty stems from the degrees of freedom associated with the nuisance parameters X_t, whose number increases with the sample size n.

The nonlinear EV analyses here produce similar low modal estimates $\hat{\kappa}$, although the MCMC means $\bar{\kappa}$ appear more reasonable. All applications of the EV paradigm in Tables 10 and 11 have modal estimates $\hat{\kappa}$ markedly smaller that the corresponding MCMC means $\bar{\kappa}$, which lie closer to the true value $\kappa = 0.4$ in Table 9. A correction to the bias in $\hat{\kappa}$ can also be seen in trace plots (Fig. 7) of the MCMC runs in Figs. 4–6. Each run begins at the mode for all parameters. The EV case in Fig. 7*c* exhibits the most obvious initial burn-in, consistent with the outlying mode shown in Fig. 5. This effect is less pronounced for the KF paradigm (Fig. 1*e*), where the algorithm eliminates most nuisance parameters X_t by integrating them from the likelihood function.

©2002 NRC Canada

Fig. 7. Trace plots (a, c, e) and kernel density plots (b, d, f) for κ, drawn from the MCMC samples of size 500 000 used to produce Figs. 4–6. Trace plots show 500 points taken systematically from the full MCMC sample, where the symbol $\oplus$ denotes the initial point at the posterior mode. Kernel density plots use larger subsamples of size 2000, with jittered values κ near the bottom of each panel. Density curves come from a Gaussian kernel with band width computed using biased cross-validation (Venables and Ripley 1999, section 5.6). (a, b), (c, d), and (e, f) correspond, respectively, to the samples in Fig. 4 ($\rho = 0$), Fig. 5 (EV paradigm with $\rho = 0.5$), and Fig. 6 (KF paradigm with $\rho = 0.5$).

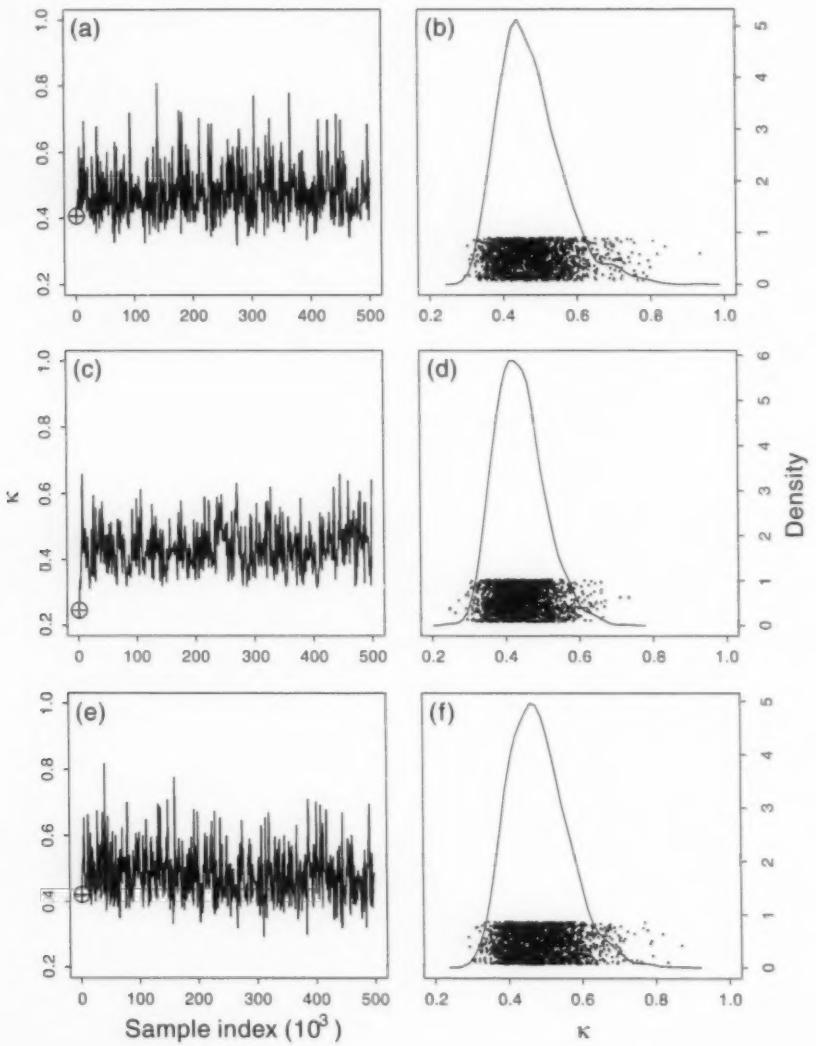

Discussion

To give our analysis perspective, we examine its position in the broader context of stochastic fishery models. Conceptually, the two equations $S_t = R_t - C_t$ and $R_{t+1} = f(S_t; \theta)$ could apply to any fish population from which catch is removed prior to regeneration in the next cycle. From this point of view, the second equation encapsulates the combined effects of survival and recruitment. It could even include growth if the population is measured in biomass units. Adding statistical error to this equation, as in (T3.7), defines a general nonlinear stochastic process for the states (R_t, S_t).

We make two assumptions about the observed data: the catch C_t is known, and the escapement E_t represents a noisy measurement of the spawning stock S_t, as in (T3.6). A revised analysis could accommodate changes in both assumptions. For example, the observation equation assumes that E_t is strictly proportional to S_t, with proportionality constant 1. A more general model could consider a stochastic escapement index $E_t = qS_t$ with unknown parameter q, or even an index E_t that depends nonlinearly on S_t. Such changes could be incorporated fairly easily into the EV algorithm by altering the residual definition (T6.3).

©2002 NRC Canada

Table 11. Estimates with free shape parameter γ ($\gamma_{\min} \le \gamma \le \gamma_{\max}$) obtained from the simulated data set, where the three cases portrayed in Figs. 4–6 are defined by the choice of algorithm (EV, KF) and ρ (0, 0.5). MCMC means and standard errors come from systematic subsamples of 2000 points drawn from samples of size 500 000.

	Figure 4	Figure 5: EV	Figure 6: KF
ρ	0.00	0.50	0.50
$\gamma_{\min}$	−3.00	−1.50	−3.00
$\gamma_{\max}$	3.00	3.00	3.00
$\widehat{h^*}$	0.61	0.55	0.56
$\overline{h^*}$	0.57	0.55	0.55
SE[h^*]	0.08	0.05	0.05
$\widehat{S^*}$	1.04	1.60	1.24
$\overline{S^*}$	1.16	1.33	1.29
SE[S^*]	0.35	0.24	0.23
$\widehat{\gamma}$	−0.24	2.00	0.26
$\overline{\gamma}$	−0.45	0.33	−0.13
SE[γ]	0.62	0.73	0.66
$\widehat{\kappa}$	0.41	0.25	0.42
$\overline{\kappa}$	0.48	0.44	0.48
SE[κ]	0.09	0.07	0.08
$\widehat{C^*}$	1.63	1.93	1.60
$\widehat{R'}$	2.85	2.76	2.88
$\widehat{h^\dagger}$	0.80	0.69	0.74

The KF algorithm, however, would require a second approximation if the observation equation (T4.11) becomes nonlinear. In our analysis, (T4.11) implies exact update equations (T5.3)–(T5.4), whereas the nonlinear process equation (T4.12) gives approximate updates (T5.7)–(T5.8). A similar approximation would be required to incorporate a nonlinear observation equation.

We have confined our analysis to one simulation, based on the particular choice of parameters in Table 9. Our graphical and numerical results illustrate techniques that can be applied to real data sets. The MCMC runs capture uncertainty about important system parameters, such as MSY levels of harvest rate h^* and spawning stock S^*. Each point $(h^*, S^*, \gamma, \kappa)$ in Fig. 5, for example, represents a potential system configuration consistent with the known data. A proposed policy has a range of outcomes that depend on the set of possible system configurations. Thus, as demonstrated by Schnute et al. (2000), the results in Fig. 5 can be used as input for policy analysis and risk evaluation.

Our example uses $n = 25$ years data with harvest rates h_t that undergo large fluctuations between low and high values. We obtain simulated data that reflect both the ascending and descending limbs of the dome-shaped Ricker curve. These highly contrasting data give fairly reasonable estimates of various reference points. Modal estimates $\widehat{h^*}$, $\widehat{S^*}$, $\widehat{C^*}$, $\widehat{R'}$, and $\widehat{h^\dagger}$ in Table 10 appear somewhat robust to assumptions about curve type γ and error structure ρ. The scatter plots in Fig. 3 suggest that the choice of γ counts more heavily than ρ. The MCMC means $\overline{\gamma}$ provide reasonable estimates of the true value $\gamma = 0$ (Figs. 4–6).

Real data sets may have fewer points and less contrast than ours. We find it helpful to start with a set of fixed choices (γ, ρ), as illustrated by prototypes in Fig. 2 and Table 10. These may suggest alternative interpretations of the data, particularly if different assumptions produce extremely different estimates of the key parameters (h^*, S^*). Geometric patterns can guide the interpretation. Our example demonstrates that a large measurement error in one year generally produces two large displacements in the stock–recruitment scatter plot. (The large error in year 25 is an exception here, because the time series doesn't include recruitment in year 26.) The estimation algorithms seem to correct for the largest errors, a feature lacking in historical analyses with $\rho = 0$. Knowledge of the data collection processes may help clarify whether or not large measurement errors in particular years make sense.

For the example here, the KF algorithm seems to work fairly well. Although only an approximation, it has a strict frequentist interpretation for non-Bayesians. Also, it involves the small parameter vector Θ in (T4.3), rather than the longer vector Φ in (T4.4). With the correct error model $\rho = 0.5$, both the EV and KF paradigms perform similarly, and the true simulation parameter values lie reasonably inside most scatter plots generated by the MCMC runs. Despite these results, we suggest caution in applying an extended Kalman filter, which is at best an approximation to the true likelihood (Schnute 1994). Quinn and Deriso (1999, pp. 236–238) discuss another filter that appears to give superior performance on highly nonlinear systems.

An MCMC sample with sufficiently large size should theoretically reflect the true shape of the posterior distribution. Our example illustrates that the mode sometimes lies on the periphery of the posterior. We show this particularly for the parameter κ, which has a known bias in classical linear EV models. Remarkably, the MCMC mean $\overline{\kappa}$ seems to correct the bias present in the mode $\hat{\kappa}$. Because the EV paradigm allows states X_t to be assigned with great flexibility, residuals at the mode may be unrealistically small. In a sense, the modal fit can be too good. For example, the mode in Fig. 5 corresponds to a high posterior probability density, but the bulk of the posterior distribution lies elsewhere.

Intuition must always play an important role in stock–recruitment analyses. For example, cases J, K, and L (Table 10, Fig. 2) include almost no process error, a highly unlikely scenario for any natural system. We present these examples only to bound the analysis by investigating results for a high value $\rho = 0.95$. Model assumptions can produce varying geometries of data points, unknown states, and recruitment curves. The location of a key parameter, such as S^*, may or may not be robust to model choices. The techniques described here provide a convenient framework for exploring the alternatives.

Acknowledgements

We thanks reviewers R. Deriso and G. Thompson for helpful comments leading to an improved final draft.

References

Beverton, R.J.H., and Holt, S.J. 1957. On the dynamics of exploited fish populations. U.K. Minist. Agric. Fish. Food Fish. Invest. Ser. 2, No. 19.

©2002 NRC Canada

Deriso, R.B. 1980. Harvesting strategies and parameter estimation for an age-structured model. Can. J. Fish. Aquat. Sci. **37**: 268–282.

Gilks, W.R., Richardson, S., and Spiegelhalter, D.L. 1996. Markov chain Monte Carlo in practice. Chapman and Hall, London, U.K.

Harvey, A.C. 1989. Forecasting, structural time series models and the Kalman filter. Cambridge University Press, Cambridge, U.K.

Kendall, M., and Stuart, A. 1979. The advanced theory of statistics. Vol. 2. Inference and relationship. 4th ed. MacMillan Publishing Company, Inc., New York.

Ludwig, D., and Walters, C.J. 1981. Measurement error and uncertainty in parameter estimates for stock and recruitment. Can. J. Fish. Aquat. Sci. **38**: 711–720.

Quinn, T.J., and Deriso, R.B. 1999. Quantitative fish stock dynamics. Oxford University Press, Oxford, U.K.

Ricker, W.E. 1954. Stock and recruitment. J. Fish. Res. Board Can. **11**: 559–623.

Ricker, W.E. 1958. Handbook of computations for biological statistics of fish populations. Bull. Fish. Res. Board Can. **119**.

Schaefer, M.B. 1954. Some aspects of the dynamics of populations important to the management of the commercial marine fisheries. Int.-Am. Trop. Tuna Comm. Bull. **1**: 26–56.

Schnute, J. 1985. A general theory for the analysis of catch and effort data. Can. J. Fish. Aquat. Sci. **42**: 414–429.

Schnute, J.T. 1993. Ambiguous inferences from fisheries data. *In* Statistics for the environment. *Edited by* V. Barnett and K.F. Turkman. John Wiley & Sons, London. pp. 293–309.

Schnute, J.T. 1994. A general framework for developing sequential fisheries models. Can. J. Fish. Aquat. Sci. **51**: 1676–1688.

Schnute, J.T., and Kronlund, A.R. 1996. A management oriented approach to stock recruitment analysis. Can. J. Fish. Aquat. Sci. **53**: 1281–1293.

Schnute, J.T., Cass, A., and Richards, L.J. 2000. A Bayesian decision analysis for Fraser River sockeye salmon (*Oncorhynchus nerka*). Can. J. Fish. Aquat. Sci. **57**: 962–979.

Venables, W.N., and Ripley, B.D. 1999. Modern applied statistics with S-Plus. 3rd ed. Springer-Verlag, New York.

Walters, C.J., and Ludwig, D. 1981. Effects of measurement error on the assessment of stock–recruitment relationships. Can. J. Fish. Aquat. Sci. **38**: 704-710.

Appendix A: Proofs for Tables 1 and 2

The equilibrium equations (6) imply that

$$\text{(A.1)}\quad S(h) = \frac{1 - [\alpha(1-h)]^{-\gamma}}{\beta\gamma},$$

$$\text{(A.2)}\quad R(h) = \frac{S(h)}{1-h},$$

$$\text{(A.3)}\quad C(h) = \frac{hS(h)}{1-h}.$$

Consequently, the derivative of $\log C(h)$ is

$$\text{(A.4)}\quad \frac{1}{C}\frac{\partial C}{\partial h} = \frac{1}{h} + \frac{1}{1-h} + \frac{1}{S}\frac{\partial S}{\partial h} = \frac{1}{1-h}\left[\frac{1}{h} - \frac{\gamma[\alpha(1-h)]^{-\gamma}}{1-[\alpha(1-h)]^{-\gamma}}\right].$$

The equilibrium catch $C(h)$ takes its maximum value C^* when $h = h^*$ and $\partial C/\partial h = 0$. Equivalently, the expression (A.4) is 0 when $h = h^*$. Solving this equation for α, gives (T1.6). Furthermore, in (A.1) the equation $S^* = S(h^*)$ can be solved for β to prove (T1.7).

Substituting the expressions (T1.6)–(T1.7) for α and β into the equilibrium value $S(h)$ in (A.1) gives (T2.1). The results (T2.2)–(T2.5) follow from equilibrium values $R(h)$ and $C(h)$ in (A.2)–(A.3), and (T2.6) corresponds to the case $h = 0$ in (T2.1). Finally, $S(h) = 0$ in (A.1) when $h = (\alpha - 1)/\alpha$; this proves (T2.7).

Appendix B: Kalman filter derivation

The algorithm in Table 5 is recursive for the distributions (8)–(9). The parameter vector Θ, defined by (T4.3), includes the initial state X_1. Thus, although uncertainty in X_1 is captured through the uncertainty in Θ, this state is presumed known exactly in the KF algorithm with mean $\tilde{X}_1 = X_1$ and variance $\tilde{U}_1 = 0$. This logic explains the initial equations (T5.1)–(T5.2).

The model equation (T4.11) determines the distribution of Y_t from the distribution of X_t. The two means (T5.3) are the same, but measurement error increases the variance of Y_t by an additional term σ^2, as in (T5.4). Furthermore,

$$\begin{aligned}\mathrm{Cov}[X_t, Y_t] &= \mathrm{E}[(X_t - \widetilde{X}_t)(Y_t - \widetilde{Y}_t)] \\ &= \mathrm{E}[(X_t - \widetilde{X}_t)(\sigma\delta_t + X_t - \widetilde{X}_t)] \\ &= \sigma\mathrm{E}[(X_t - \widetilde{X}_t)\delta_t] + = \mathrm{E}[(X_t - \widetilde{X}_t)^2] \\ &= 0 + \widetilde{U}_t,\end{aligned}$$

where the final step uses the fact that the measurement residual δ_t is independent of the state X_t. Combining this result with (8) and (T5.3)–(T5.4) shows that X_t and Y_t are binormal:

$$\text{(B.1)}\quad \begin{pmatrix} X_t \\ Y_t \end{pmatrix} \sim N\left[\begin{pmatrix} \widetilde{X}_t \\ \widetilde{Y}_t \end{pmatrix}, \begin{pmatrix} \widetilde{U}_t & \widetilde{U}_t \\ \widetilde{U}_t & \widetilde{V}_t \end{pmatrix}\right].$$

Given an observed value Y_t, (B.1) implies the conditional regression (Harvey 1989, p. 165; Schnute 1994, equation A.1)

$$\text{(B.2)}\quad X_t|Y_t \sim N\left[\widetilde{X}_t + \frac{\widetilde{U}_t}{\widetilde{V}_t}(Y_t - \widetilde{Y}_t), \widetilde{U}_t - \frac{\widetilde{U}_t^2}{\widetilde{V}_t}\right].$$

After some algebra, the mean and variance of $X_t|Y_t$ reduce to the updates $\widehat{X}_t$ and $\widehat{U}_t$ in (T5.5)–(T5.6).

The calculation so far is exact, based on model equation (T4.11) and the normality assumptions (8)–(9). The transition from time t to $t+1$ involves an approximation to the nonlinear model equation (T4.12). Define residuals r_t and s_{t+1} such that $X_t = \widetilde{X}_t + r_t$ and $X_{t+1} = \widehat{X}_{t+1} + s_{t+1}$. With respect to these residuals, first-order Taylor expansions of the left and right sides of (T4.12) lead to the approximate result

©2002 NRC Canada

$$\text{(B.3)}\qquad \log\left(e^{\widetilde{X}_{t+1}} + C_{t+1}\right) + \frac{e^{\widetilde{X}_{t+1}}}{e^{\widetilde{X}_{t+1}} + C_{t+1}} s_{t+1}$$
$$\approx \log f(e^{\widehat{X}_t}) + \frac{1 - \beta(\gamma+1)e^{\widehat{X}_t}}{1 - \beta\gamma e^{\widehat{X}_t}} r_t + \tau\epsilon_t.$$

Equating constant and random terms in (B.3), i.e., terms with orders 0 and 1, gives the two equations

$$\text{(B.4)}\quad e^{\widetilde{X}_{t+1}} = f(e^{\widehat{X}_t}) - C_{t+1},$$

$$\text{(B.5)}\quad s_{t+1} = \left(1 + C_{t+1}e^{-\widetilde{X}_{t+1}}\right)\left[\frac{1 - \beta(\gamma+1)e^{\widehat{X}_t}}{1 - \beta\gamma e^{\widehat{X}_t}} r_t + \tau\epsilon_t\right].$$

The result (B.4) implies (T5.7). By assumption, the residuals s_{t+1}, r_t, and $\tau\epsilon_t$ have variances $\widetilde{U}_{t+1}$, $\widehat{U}_t$, and τ^2, respectively. Furthermore, the process residual $\tau\epsilon_t$ is independent of r_t, which depends only on variates computed prior to the transition from time t to $t+1$. Equating variances of both sides of (B.5) gives (T5.8) and completes the proof of the algorithm in Table 5.

The function $F(\Theta)$ has a singularity at $\sigma = 0$. To see this, fix $X_1 = \log E_1$ and allow σ to vary. Equations (T5.1)–(T5.4) then imply that $\widetilde{Y}_1 = \log E_1$ and $\widetilde{V}_1 = \sigma^2$, so that the first term in the summation (T5.9) reduces to $\log\sigma$. Consequently, $F \to -\infty$ and $L \to \infty$ as $\sigma \to 0$ in (T5.9)–(T5.10). This singularity shows that both σ and X_1 cannot be unrestricted if the algorithm in Table 5 is used to obtain maximum likelihood estimates. We have chosen to restrict σ by a fixed choice of ρ. Theoretically, X_1 might also be constrained to a value (such as X') dependent on the other model parameters, but we do not pursue that option here.

Appendix C: EV posterior derivation

Assumption (T4.11) implies a normal Bayes distribution for X_t, given data Y_t.

$$\text{(C.1)}\quad P(X_t|Y_t) = \frac{1}{\sqrt{2\pi}\,\sigma} e^{-\xi_t^2/(2\sigma^2)},$$

where (T6.3) defines $\xi_t = X_t - Y_t = \log(S_t/E_t)$. Similarly, (T4.12) implies that

$$\text{(C.2)}\quad P(X_{t+1}|X_t) = \frac{1}{\sqrt{2\pi}\,\tau} e^{-\eta_t^2/(2\tau^2)} \frac{\partial\eta_t}{\partial X_{t+1}},$$

where (T6.4) defines $\eta_t = \log(e^{X_{t+1}} + C_{t+1}) - \log f(e^{X_t}) = \log(S_{t+1} + C_{t+1}) - \log f(S_t)$. The Jacobian in (C.2) can be expressed analytically as

$$\text{(C.3)}\quad \frac{\partial\eta_t}{\partial X_{t+1}} = \frac{e^{X_{t+1}}}{e^{X_{t+1}} + C_{t+1}} = \frac{S_{t+1}}{S_{t+1} + C_{t+1}} = 1 - h_t.$$

The variance transformations (T4.6) and the results (C.1)–(C.3) show that

$$\text{(C.4)}\quad \prod_{t=1}^{n-1} P(X_{t+1}|X_t) \prod_{t=1}^{n} P(X_t|Y_t) \propto e^{G(\Phi)},$$

where (T6.12) defines the function $G(\Phi)$ of the parameter vector Φ in (T4.4). Multiplying (C.4) by the prior distributions for (ρ, κ) and (h^*, S^*, γ) gives the posterior (T6.13).

The function $G(\Phi)$ has singularities at $\rho = 0$ and $\rho = 1$. The first occurs when the state parameters are fixed at the values $X_t = \log E_t$ for $t = 1, \ldots, n$. It follows from (T6.1), T6.3), and (T6.5) that $T_1 = 0$ in this case. Consequently, due to the term $(n/2)\log\rho$ in (T6.12), $G \to -\infty$ and $P \to \infty$ as $\rho \to 0$. Similarly, suppose that X_1 is chosen arbitrarily and the remaining states are computed iteratively from a deterministic stock–recruitment relationship $X_t = \log[f(e^{X_{t-1}} - C_t]$ for $t = 2, \ldots, n$. In this case, it follows from (T6.1), (T6.4), and (T6.6) that $T_2 = 0$. Because of the term $[(n-1)/2]\log(1-\rho)$ in (T6.12), $G \to -\infty$ and $P \to \infty$ as $\rho \to 1$

©2002 NRC Canada

Bomb dating and age determination of large pelagic sharks

Steven E. Campana, Lisa J. Natanson, and Sigmund Myklevoll

Abstract: Despite their notoriety and role as apex predators, the longevity of large pelagic sharks such as the porbeagle (*Lamna nasus*) and shortfin mako (*Isurus oxyrinchus*) is unknown. Vertebral growth bands provide an accurate indicator of age in young porbeagle, but age validation has never been reported for any large shark species past the age of sexual maturity. Here, we report the first application of bomb radiocarbon as an age validation method for long-lived sharks based on date-specific incorporation of radiocarbon into vertebral growth bands. Our results indicate that porbeagle vertebrae recorded and preserved a bomb radiocarbon pulse in growth bands formed during the 1960s. Through comparison of radiocarbon assays in young, known-age porbeagle collected in the 1960s with the corresponding growth bands in old porbeagle collected later, we confirm the validity of porbeagle vertebral growth band counts as accurate annual age indicators to an age of at least 26 years. The radiocarbon signatures of porbeagle vertebral growth bands appear to be temporally and metabolically stable and derived mainly from the radiocarbon content of their prey. Preliminary radiocarbon assays of shortfin mako vertebrae suggest that current methods for determining shortfin mako age are incorrect.

Résumé : Malgré leur notoriété et leur rôle de prédateurs supérieurs, les grands requins pélagiques, tels que les requins taupes communs (*Lamna nasus*) et les requins taupes bleus (*Isurus oxyrinchus*), ont une durée de vie encore inconnue. Les bandes de croissance des vertèbres sont des indicateurs précis de l'âge chez de jeunes requins taupes communs, mais aucune validation de l'âge n'a été faite chez les grands requins au delà de l'âge de la maturité sexuelle. On trouvera ici une première utilisation du carbone radioactif produit par les essais nucléaires pour valider l'âge des requins à grande longévité, par l'analyse de l'incorporation du carbone radioactif dans les bandes de croissance de leurs vertèbres à des dates précises. Les vertèbres des requins taupes communs ont enregistré et conservé une signature de carbone radioactif provenant des essais nucléaires faits dans les années 1960. La comparaison des analyses de carbone radioactif faites chez de jeunes requins taupes communs d'âge connu et récoltés dans les années 1960 avec celles des bandes de croissance chez de vieux requins capturés plus tard confirme la validité de l'utilisation des bandes de croissance des vertèbres pour déterminer avec précision l'âge au moins jusqu'à 26 ans. Les signatures de carbone radioactif dans les bandes de croissance des vertèbres des requins taupes communs semblent être stables dans le temps et peu affectées par le métabolisme; elles sont dérivées en majeure partie du contenu en carbone radioactif de leurs proies. Les analyses préliminaires de carbone radioactif dans les vertèbres des requins taupes bleus semblent indiquer que les méthodes courantes de détermination de l'âge chez ce poisson sont erronées.

[Traduit par la Rédaction]

Introduction

Porbeagle (*Lamna nasus*) and shortfin mako (*Isurus oxyrinchus*) sharks have been reported to grow at very different rates and achieve very different longevities (Cailliet et al. 1983; Pratt and Casey 1983; Natanson et al. 2002), despite their common family membership (Lamnidae) and similar life history characteristics. The most likely explanation for such differences is errors in age determination associated with the interpretation of the vertebral growth bands, a process that is subjective and whose accuracy has seldom been confirmed (Cailliet 1990). Based on recaptures of known-age and oxytetracycline-tagged individuals, the vertebral bands have been demonstrated to form annually in sexually immature porbeagle up to an age of 11 years (Natanson et al. 2002). However, the interpretation of growth bands in sexually mature porbeagle has not been validated and is complicated by the extreme narrowness of the bands and the potential for resorption along the growing edge. Vertebrae are one of the few structures known to produce periodic growth bands in sharks, given that elasmobranchs lack the otoliths that form the basis for accurate age determinations in bony fishes (Secor et al. 1995). Therefore, vertebrae are usually the best structures upon which to base estimates of shark age, longevity, growth, and mortality rate.

Atmospheric testing of atomic bombs in the 1950s and 1960s resulted in a rapid and well-documented increase in radiocarbon (^{14}C) in the world's oceans (Druffel and Linick

Received 22 November 2001. Accepted 28 February 2002. Published on the NRC Research Press Web site at http://cjfas.nrc.ca on 4 April 2002.
J16625

S.E. Campana.[1] Department of Fisheries and Oceans, Bedford Institute of Oceanography, P.O. Box 1006, Dartmouth, NS B2Y 4A2, Canada.
L.J. Natanson. National Marine Fisheries Service, 28 Tarzwell Drive, Narragansett, RI 02882, U.S.A.
S. Myklevoll. Institute of Marine Research, P.O. Box 1870, Nordnes, N-5817 Bergen, Norway.

[1]Corresponding author (e-mail: campanas@mar.dfo-mpo.gc.ca).

 DOI: 10.1139/F02-027 © 2002 NRC Canada

1978). The period of radiocarbon increase was almost synchronous in marine carbonates such as corals, bivalves, and fish otoliths around the world (Kalish 1993; Weidman and Jones 1993; Campana 1997), allowing the period of increase to be used as a dated marker in calcified structures exhibiting growth bands. Here, we report the first radiocarbon assays of growth bands in pelagic shark vertebrae, demonstrating that they too recorded and preserved a bomb radiocarbon pulse in growth bands formed during the 1960s. Through comparison of radiocarbon assays in young, known-age porbeagle with growth bands of old porbeagle matched for year of formation, we confirm the validity of porbeagle vertebral growth band counts as accurate age indicators. Finally, we use the porbeagle radiocarbon chronology to question the validity of accepted methods for determining age in shortfin mako.

Methods

Cervical vertebrae were collected from 15 porbeagle caught in the northwest Atlantic between 1962 and 2000, ranging in length from 72 to 264 cm fork length. Ages were presumed to be 0–26 years based on band counts visible in transverse sections using the interpretation criteria of Natanson et al. (2002). Vertebrae were stored in 70% ethanol or frozen prior to sectioning; the samples collected in the 1960s were preserved in formalin.

Multiple samples from each of the 15 vertebral sections (N = 35 samples, 12–37 mg each) were extracted from individual growth bands visible in the corpus calcareum region while working at 16× magnification under a binocular microscope. In all cases, the first-formed growth band (corresponding to the first year of growth) was extracted from each vertebra; additional growth bands corresponding to later growth were extracted from some, but not all, vertebrae. Extracted samples were isolated as solid pieces using a Gesswein high-speed hand tool fitted with steel bits <1 mm in diameter. To minimize surface contamination, the external surface of each sample was removed and discarded using the hand tool, and then the remaining sample was sonified in Super Q water. After drying, the sample was weighed to the nearest 0.1 mg in preparation for assay with accelerator mass spectrometry. All samples were assayed for $\delta^{13}C$ (to determine the carbon source) and $\Delta^{14}C$ (measure of radiocarbon), with $\Delta^{14}C$ calculated as per Stuiver and Polach (1977).

The onset of nuclear testing in the late 1950s resulted in a marked and widespread increase in $\Delta^{14}C$ in marine dissolved inorganic carbon (DIC) that is easily detected in all marine carbonates growing in surface waters during the 1960s (Druffel 1989; Campana and Jones 1998). To assign dates of formation to an unknown sample, it is necessary that the $\Delta^{14}C$ of the unknown sample be compared with a $\Delta^{14}C$ chronology based on known-age material (a reference chronology). In the case of carbonates, the years corresponding to the onset of radiocarbon increase are synchronous in reference chronologies based on corals, bivalves, and otoliths and are thus interchangeable (Campana 1999). In the case of vertebral material, however, synchrony with carbonates could not be assumed. Therefore, we used vertebrae from young porbeagle (age ≤6 and fork length <188 cm) as our known-age, or reference, chronology (N = 5 sharks, 8 samples). Fork length and growth band numbers are accurate indicators of age in young porbeagle (Natanson et al. 2002), with a maximum ageing error of no more than ±2 years. Therefore, the age of the young porbeagle was known with enough certainty to be considered known age.

A single shortfin mako vertebra from a 328-cm female captured in the northwest Atlantic in 1977 was sectioned, aged, and microsampled using the same protocol described above for the porbeagle. A total of four growth bands, including the first and last formed, were removed from this vertebra for assay.

The reference $\Delta^{14}C$ carbonate chronology for the northwest Atlantic was derived from assays of known-age fish otoliths formed between 1949 and 1982. The collection and radiocarbon assay of 39 age 1–3 haddock (*Melanogrammus aeglefinus*) otoliths have been described elsewhere (Campana 1997); the chronology was supplemented by 17 age-1 redfish (*Sebastes* spp.) otoliths collected between 1957 and 1969 and prepared in a similar manner. There was no detectable difference between the haddock and redfish chronologies; therefore, they were pooled and used as the reference carbonate chronology. The $\Delta^{14}C$ chronology of aragonitic fish otoliths parallels that of North Atlantic corals and bivalves (Campana 1997) and thus is a good proxy for the $\Delta^{14}C$ DIC history of the porbeagle environment.

Results and discussion

Growth bands visible in porbeagle vertebral sections tended to be broad and diffuse in sharks <4 years old, increasing in clarity but decreasing in width with age (Fig. 1). In sharks >12–15 years of age, growth bands narrowed to the point where greater magnification and digital enhancement was required to resolve bands near the growing margin. Nevertheless, growth band counts were consistent and reproducible between independent age readers and sections, giving us confidence that we were not missing a portion of the vertebral growth history.

Porbeagle $\delta^{13}C$ was relatively constant across all samples, averaging –14.27 (SE = 0.09) (Table 1). Depleted values such as these are characteristic of metabolic and dietary carbon and are markedly different from the values of –1 to –3 typically found in otoliths (Fry 1988; Kalish 1993; Campana 1997). Although the $\delta^{13}C$ values did not vary with the date of formation, $\Delta^{14}C$ values increased sharply from about –100 in vertebral material formed before 1960 to about +50 after 1970, declining slowly thereafter to about +25 in the year 2000 (Fig. 2*a*). Although the period of increasing $\Delta^{14}C$ differed, the sigmoidal shape of the porbeagle $\Delta^{14}C$ curve was very similar to the bomb signal expected of $\Delta^{14}C$ in the marine environment (Druffel 1989).

The $\Delta^{14}C$ chronology prepared using only the young, known-age porbeagle is considered a reference chronology, since the year of formation of each micromilled sample is known with certainty. Since the date of growth band formation of an unknown sample can then be determined from its $\Delta^{14}C$ value (at least if the date falls in the critical period of rapid increase in the 1960s), this date can subsequently be compared with the date estimated from a count of the growth bands; congruence indicates age validation, since incorrectly interpreted annuli would result in an incorrect age

© 2002 NRC Canada

Fig. 1. Thin section of a vertebra from a 264-cm fork length porbeagle collected in 1999. White circles indicate growth bands presumed to be formed annually; the photographic inset indicates the very narrow growth bands seen near the growing edge. The age of the shark was 26 years based on the number of growth bands and no more than 31 years based on radiocarbon values. Scale bar = 1 mm.

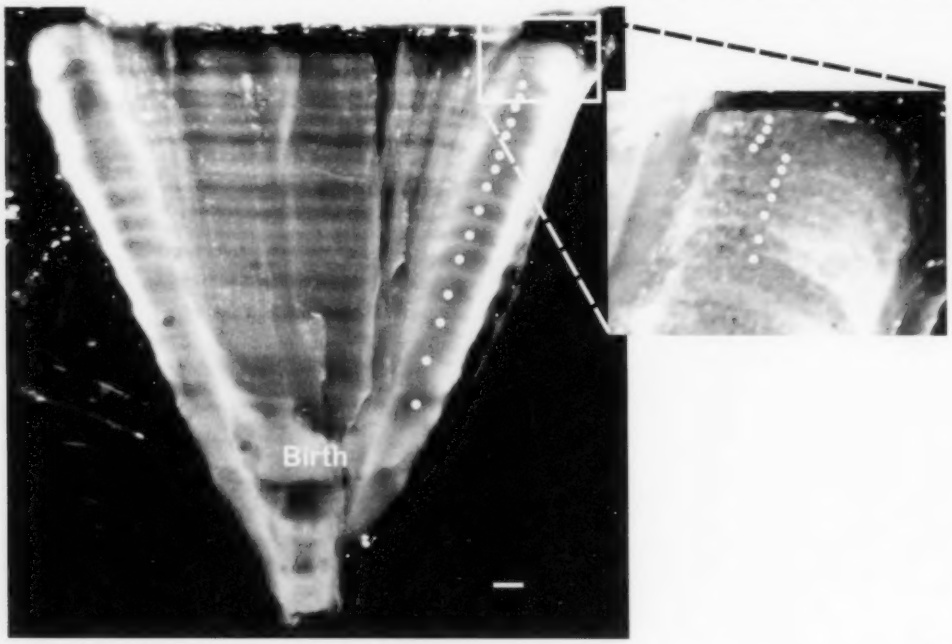

and hence an incorrect estimate of date of formation. In this study, the reference chronology of the known-age porbeagle was indistinguishable from that based on older porbeagle through the critical period of rapid increase in the 1960s (Fig. 2*a*). Since any errors in the age interpretation of the older sharks would have been evident in $\Delta^{14}C$ values that lay off the curve defined by the known-age sharks, the sharks aged 9–26 years must have been aged correctly (on average) based on the vertebral growth bands. In light of the relative stability in $\Delta^{14}C$ after 1970, it would have been very difficult to detect any underageing in sharks born after 1970. However, overageing would have been easily detected, since a $\Delta^{14}C$ value of more than 0 would have been completely incompatible with a date of formation before about 1963. Thus, the $\Delta^{14}C$ value of 55 in the first-formed growth band of a 26-year-old porbeagle collected in 2000 cannot have formed prior to 1970, indicating an age of no more than 31. Similarly, underageing of any sharks born between 1959 and 1962 would be easily detected based on depleted $\Delta^{14}C$ values. With the exception of a 24-year-old shark, which appears to have been underaged by about 3 years, vertebral band counts provided accurate ages for porbeagle up to age 26.

Shark vertebrae have been considered to be metabolically unstable ever since Welden et al. (1987) reported that Pb:Ra dating failed to produce the expected gradient between inner and outer growth zones. However, our results indicate that any metabolic reworking must be minimal. Of the nine sharks from which multiple growth bands were sampled, all showed the same within-shark bomb signal across year of formation as that demonstrated by the across-shark analysis (Fig. 2*b*). Ontogenetic effects were not evident, indicating that the bomb signal was not diluted by subsequent growth over a period of up to 23 years. Comparison of $\Delta^{14}C$ values in vertebral growth bands formed at different ages, matched by year of formation, showed no consistent differences, indicating that the bomb signal was not transported across growth bands through time. There was a visible but nonsignificant tendency for the recently formed growth bands in some of the older sharks to be slightly depleted in $\Delta^{14}C$ compared with younger sharks growing at the same time (median depletion <20). As discussed in the next paragraph, the most likely explanation for this minor depletion is that of diet switching to larger, and hence older (more depleted), prey by the larger sharks. Since the $\Delta^{14}C$ signal was incorporated into the noncalcified component of the vertebrae, and since the previously reported Pb:Ra assays were based on elemental analogs of calcium that were not clearly part of the growth band (Welden et al. 1987), it seems likely that the organic fraction of the shark vertebral growth band analyzed in our study was more stable physiologically than any calcified components. This finding has important implications for future bomb-dating studies of sharks, since it satisfies an important assumption of this age validation method: that the carbon in the vertebral material is metabolically and temporally stable.

The shark $\Delta^{14}C$ chronology was phase shifted about 3 years towards more recent dates compared with a reference carbonate $\Delta^{14}C$ chronology characteristic of bivalves, corals, and fish otoliths in the northwest Atlantic (Fig. 3). This phase shift appears to have been due to the source of carbon used for vertebral growth. No detectable CO_2 was generated by acid dissolution of the vertebral material sampled for ^{14}C assay, indicating that calcium carbonate was not present. Therefore, the ^{14}C must have been incorporated into pro-

© 2002 NRC Canada

Table 1. Summary of $\delta^{13}C$ and $\Delta^{14}C$ assay results for individual growth zones microsampled from shark vertebrae.

Species	Sample	Fork length (cm)	Year collected	Age (years)	Year of annulus formation	$\delta^{13}C$ of annulus	$\Delta^{14}C$ of annulus
Porbeagle	762-14	127	1962	2	1962	–15.0	–74.6
	762-31	187	1962	12	1961	–14.4	–91.7
					1960	–14.2	–105.2
	862-10	166	1962	9	1962	–14.3	–114.7
	862-1	145	1962	4	1960	–14.3	–83.3
					1962	–14.4	–75.8
					1959	–14.6	–97.4
	862-5	188	1962	6	1959	–14.5	–97.4
					1959	–14.4	–88.9
	862-6	181	1962	7	1962	–14.7	–84.4
	862-8	174	1962	9	1955	–14.6	–101.9
	LN19	227	1985	16	1985	–13.3	50.0
					1980	–14.0	52.6
					1975	–14.8	42.2
					1970	–14.9	55.2
	LN23	198	1985	15	1985	–13.9	46.1
					1980	–14.2	55.2
					1975	–14.7	63.1
					1971	–15.3	59.2
	LN3	72	1965	0	1965	–13.5	1.5
	LN37	236	1993	24	1993	–14.7	42.2
					1980	–14.2	42.2
					1970	–13.9	12.2
	LN4	70	1965	0	1965	–12.6	1.5
	LN6	146	1966	7	1966	–14.2	–4.8
					1962	–14.1	–54.3
					1960	–13.8	–59.0
	LN85	239	1993	21	1993	–14.0	51.3
					1980	–14.1	57.8
					1973	–14.9	59.2
	P99	264	2000	26	2000	–13.8	25.4
					1990	–13.9	46.1
					1980	–14.1	48.7
					1975	–14.9	55.2
Shortfin mako	M151	328	1977	11	1977	–12.7	52.6
					1974	–12.4	38.8
					1970	–12.3	–90.1
					1967	–13.9	–100.2

teinaceous or cartilaginous material rather than the calcium carbonate characteristic of other bomb-dated taxa (Kalish 1993). Since dietary sources are the primary source of carbon into noncalcified fish tissues (Fry 1988), the ^{14}C content of the porbeagle prey would be expected to have a major influence on the ^{14}C content of the porbeagle itself. Stomach content analyses of 533 porbeagle collected throughout the year demonstrated that the diet of porbeagle was dominated by fish (91% by weight), primarily alepisaurids, gadids, pleuronectids, and clupeids (S.E. Campana, unpublished data). On the basis of the length frequencies of the major prey taxa and published age–length keys, the mean weighted age of the prey was estimated to be 3.3 years. Reasonable errors in assigning ages to the prey taxa do not appreciably change this result. Since fish growth (in weight) is exponential, the weighted mean age of the prey tissue was 1.8 years, thus accounting for most of the phase differential between the porbeagle and reference $\Delta^{14}C$ chronology. The remaining phase discrepancy was presumably due to the >100 m depth occupied by porbeagle and its prey, a depth range at which the appearance of the bomb ^{14}C signal is delayed relative to shallower waters (Williams et al. 1987).

The prebomb vertebral $\Delta^{14}C$ was depleted by about 30 relative to otolith carbonate chronologies from the same waters (Fig. 3), presumably reflecting the reduced $\Delta^{14}C$ levels in DIC and prey at depths >100 m. Although the postbomb vertebral $\Delta^{14}C$ of 50 was similar to that of the otolith carbonate chronology, the correspondence may have been fortuitous; the absolute value of postbomb $\Delta^{14}C$ in the water column is highly variable and can vary between 0 and 200 across depths and locations depending on water mass mixing rates and residence times (Druffel 1989; Weidman and Jones 1993).

Radiocarbon assays of a single shortfin mako vertebra suggested that the shark was considerably older than first suspected. Samples of the first, last, and two intermediate growth bands from a large female caught in 1977 contained

© 2002 NRC Canada

Fig. 2. $\Delta^{14}C$ in individual growth bands of porbeagle vertebrae versus year of formation inferred from counts of the growth bands. (*a*) The period of bomb-induced increase apparent in growth bands of young, known-age porbeagle (open circles) was indistinguishable from that based on older porbeagle (solid circles), indicating that the growth bands were accurately interpreted in the older porbeagle. (*b*) The $\Delta^{14}C$ chronology within individual sharks (each line corresponds to a shark) was similar to the across-shark chronology, indicating that the bomb signal of a single growth band remained stable as the shark grew older.

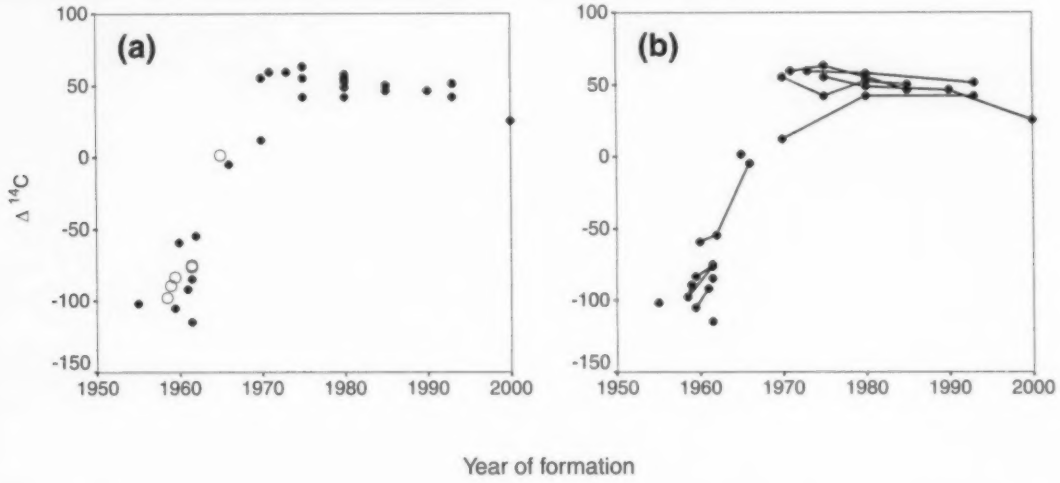

Fig. 3. $\Delta^{14}C$ in individual growth bands of porbeagle vertebrae versus year of formation inferred from counts of the growth bands. The $\Delta^{14}C$ chronology of porbeagle vertebrae (circles, fitted with a Loess curve) was similar to that of a reference carbonate chronology from the northwest Atlantic (solid line, smoothed with a Loess curve) but lagged because of the depleted $\Delta^{14}C$ of the diet. While not evident from the figure, the unsmoothed reference chronology is relatively constant prior to 1956.

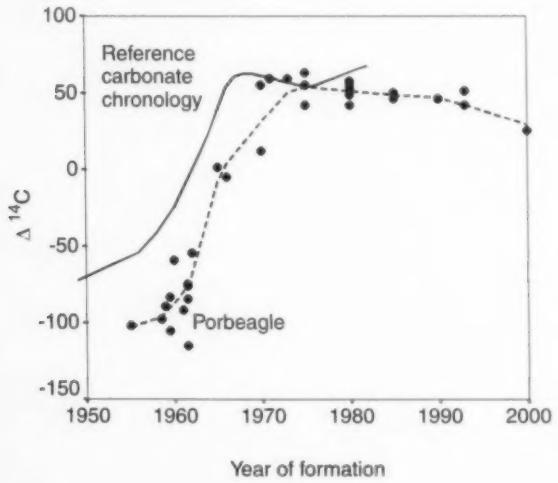

Fig. 4. $\Delta^{14}C$ in individual growth bands of a large shortfin mako vertebra versus year of formation inferred from two alternative interpretations of the growth bands. $\Delta^{14}C$ values would be expected to fall on the curve defined by the porbeagle (Loess fit shown by dashed line) if the age interpretation of the growth bands in the mako were correct. An age of 10 years (open circles) was based on published criteria (Pratt and Casey 1983), while an age of 21 years (solid circles) was based on criteria used to age porbeagle (Natanson et al. 2002).

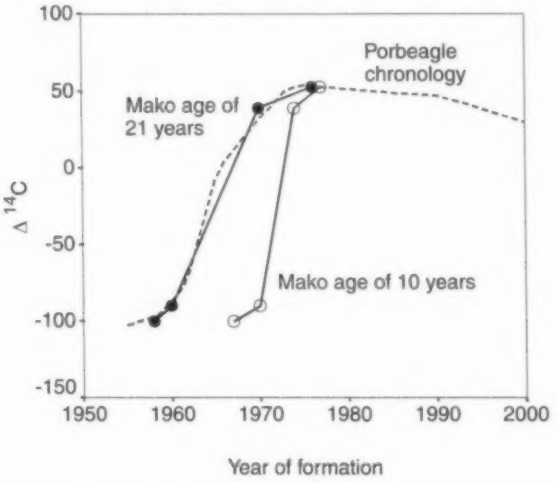

a $\Delta^{14}C$ signal that would be expected of a porbeagle between the ages of 19 and 23 years (Fig. 4). Interpretation of the vertebral growth bands using published criteria for shortfin mako (Pratt and Casey 1983) yielded an age of 10 years; the ageing protocol of Pratt and Casey (1983) assumed that two band pairs form each year. An age of 21–22 years was obtained by the authors using criteria used to age porbeagle (Natanson et al. 2002) and Pacific shortfin mako (Cailliet et al. 1983), which assumes a single band pair formed each year. Assuming that the porbeagle bomb signal is also applicable to the shortfin mako, the depleted $\Delta^{14}C$ values of the

© 2002 NRC Canada

first and fourth growth bands were completely inconsistent with an age of <19 years and most consistent with an age of 21 years. Furthermore, there is no obvious reason why the shortfin mako vertebra would fail to record the bomb $\Delta^{14}C$ signal in a manner similar to that of porbeagle; the differences in distributional range, diet, temperature, and preferred depth between the species (at young ages) are insufficient to produce anything other than minor differences in the vertebral bomb chronology. Clearly, a definitive growth rate cannot be based on a single shark. Nevertheless, these results clearly indicate that only the older of the two age interpretations is possible for the shortfin mako analyzed. Further radiocarbon assays of shortfin mako vertebrae should provide a definitive resolution of this age determination question.

The use of vertebral bomb radiocarbon to determine age and confirm the periodicity of growth bands should be appropriate for all shark species where at least some of the growth bands were formed prior to 1965. Whereas bomb signals in fish otoliths are limited by the small amounts of material available for assay (Campana 1999), sequential sampling of multiple growth bands from a single vertebra can be used to prepare a complete $\Delta^{14}C$ chronology and thus confirm the age of a single shark. Adjustments for phase shifting of the bomb signal in otoliths are sometimes required depending on location and depth; phase shifting due to diet would also be expected in the case of sharks.

Acknowledgements

We thank W. Joyce and L. Marks for technical assistance and C. Weidman for helpful comments. G. Cailliet provided constructive suggestions on the manuscript.

References

Cailliet, G.M. 1990. Elasmobranch age determination and verification: an updated review. NOAA Tech. Rep. NMFS, **90**: 157–165.

Cailliet, G.M., Martin, L.K., Kusher, D., Wolf, P., and Welden, B.A. 1983. Preliminary studies on the age and growth of the blue, *Prionace glauca*, common thresher, *Alopias vulpinus*, and shortfin mako, *Isurus oxyrinchus*, sharks from California waters. NOAA Tech. Rep. NMFS, **8**: 179–188.

Campana, S.E. 1997. Use of radiocarbon from nuclear fallout as a dated marker in the otoliths of haddock, *Melanogrammus aeglefinus*. Mar. Ecol. Prog. Ser. **150**: 49–56.

Campana, S.E. 1999. Chemistry and composition of fish otoliths: pathways, mechanisms and applications. Mar. Ecol. Prog. Ser. **188**: 263–297.

Campana, S.E., and Jones, C.M. 1998. Radiocarbon from nuclear testing applied to age validation of black drum, *Pogonias cromis*. Fish. Bull. U.S. **96**: 185–192.

Druffel, E.M. 1989. Decadal time scale variability of ventilation in the North Atlantic: high-precision measurements of bomb radiocarbon in banded corals. J. Geophys. Res. **94**: 3271–3285.

Druffel, E.M., and Linick, T.W. 1978. Radiocarbon in annual coral rings of Florida. Geophys. Res. Lett. **5**: 913–916.

Fry, B. 1988. Food web structure on Georges Bank from stable C, N and S isotopic compositions. Limnol. Oceanogr. **33**: 1182–1190.

Kalish, J.M. 1993. Pre- and post-bomb radiocarbon in fish otoliths. Earth Planet. Sci. Lett. **114**: 549–554.

Natanson, L.J., Mello, J.J., and Campana, S.E. 2002. Validated age and growth of the porbeagle shark, *Lamna nasus*, in the western North Atlantic Ocean. Fish. Bull. U.S. **100**: 266–278.

Pratt H.L., Jr., and Casey, J.G. 1983. Age and growth of the shortfin mako, *Isurus oxyrinchus*, using four methods. Can. J. Fish. Aquat. Sci. **40**: 1944–1957.

Secor, D.H., Dean, J.M., and Campana, S.E. (*Editors*). 1995. Recent developments in fish otolith research. University of South Carolina Press, Columbia, S.C.

Stuiver, M., and Polach, H.A. 1977. Reporting of C-14 data. Radiocarbon, **19**: 355–363.

Weidman, C.R., and Jones, G.A. 1993. A shell-derived time history of bomb C-14 on Georges Bank and its Labrador Sea implications. J. Geophys. Res. **98**: 14 577 – 14 588.

Welden, B.A., Cailliet, G.M., and Flegal, A.R. 1987. Comparison of radiometric with vertebral band age estimates in four California elasmobranchs. *In* Age and growth of fish. *Edited by* R.C. Summerfelt and G.E. Hall. Iowa State University Press, Ames, Iowa. pp. 301–315.

Williams, P.M., Druffel, E.R.M., and Smith, K.L., Jr. 1987. Dietary carbon sources for deep-sea organisms as inferred from their organic radiocarbon activities. Deep-Sea Res. **34**: 253–266.

© 2002 NRC Canada

Opposite effects of ocean temperature on survival rates of 120 stocks of Pacific salmon (*Oncorhynchus* spp.) in northern and southern areas

Franz J. Mueter, Randall M. Peterman, and Brian J. Pyper

Abstract: To improve the understanding of linkages between ocean conditions and salmon productivity, we estimated effects of ocean temperature on survival rates of three species of Pacific salmon (*Oncorhynchus* spp.) across 120 stocks. This multistock approach permitted more precise estimates of effects than standard single-stock analyses. The estimated effects were opposite in sign between northern and southern stocks and were quite consistent across stocks within species and areas. Warm anomalies in coastal temperatures were associated with increased survival rates for stocks in Alaska and decreased survival rates in Washington and British Columbia, suggesting that different mechanisms determine survival rates in the two areas. Regional-scale sea surface temperatures (SST, within several hundred kilometres of a stock's ocean entry point) were a much better predictor of survival rates than large-scale climate anomalies associated with the Pacific Decadal Oscillation (PDO), suggesting that survival rates are primarily linked to environmental conditions at regional spatial scales. With appropriate cautions, these results may be used to predict the potential effects of climatic changes on salmon productivity in different areas of the Northeast Pacific.

Résumé : Dans le but d'améliorer notre compréhension des liens entre les conditions océaniques et la productivité du saumon, nous avons estimé les effets de la température de l'océan et les taux de survie chez 120 stocks de 3 espèces de saumons du Pacifique (*Oncorhynchus* spp.). Cette approche impliquant de nombreux stocks a fourni des estimations plus précises que l'analyse habituelle de stocks individuels. Les effets estimés sont de signe contraire dans les stocks du nord et du sud et sont uniformes d'un stock à l'autre pour une même espèce dans une même région. Des réchauffements anormaux des températures côtières sont associés à des augmentations des taux de survie des stocks d'Alaska et des diminutions des taux de survie au Washington et en Colombie-Britannique, ce qui laisse croire que des mécanismes différents régissent la survie dans ces deux régions. Les températures de surface de la mer (SST) à l'échelle régionale (sur une distance de plusieurs centaines de km du point d'entrée d'un stock dans l'océan) sont de meilleures variables prédictives du taux de survie que les anomalies climatiques à grande échelle associées à l'Oscillation décennale du Pacifique (PDO), ce qui indique que les taux de survie sont liés principalement aux conditions environnementales à l'échelle spatiale régionale. Avec les précautions appropriées, ces résultats pourraient servir à prédire les effets potentiels des changements climatiques sur la productivité des saumons de différentes régions du nord-est du Pacifique.

[Traduit par la Rédaction]

Introduction

Although fishing has been an important factor in the decline of many fish stocks (Botsford et al. 1997; Pauly et al. 1998), climatic and oceanographic conditions also affect their productivity (Beamish 1995). For example, environmental conditions are believed to cause large year-to-year variations in productivity (rate of change in abundance) of Northeast Pacific salmon (*Oncorhynchus* spp.), as well as decade-long persistent changes in their mean productivity (e.g., Adkison et al. 1996). Uncertainties about such environmentally driven changes limit the accuracy of annual forecasts of abundance used to plan fishing seasons and the ability to predict effects of climatic change on future productivity, thereby creating risks to the long-term sustainability of these salmon stocks.

To conserve salmon stocks, fisheries scientists and manag-

Received 19 October 2001. Accepted 8 February 2002. Published on the NRC Research Press Web site at http://cjfas.nrc.ca on 4 April 2002.
J16577

F.J. Mueter,[1,2] R.M. Peterman, and B.J. Pyper.[3] School of Resource and Environmental Management, Simon Fraser University, 8888 University Drive, Burnaby, BC V5A 1S6, Canada.

[1]Corresponding author (e-mail: fmueter@mosquitonet.com).
[2]Present address: 697 Fordham Drive, Fairbanks, AK 99709, U.S.A.
[3]Present address: Juneau Center, School of Fisheries and Ocean Sciences, University of Alaska Fairbanks, 1120 Glacier Highway, Juneau, AK 99801, U.S.A.

 DOI: 10.1139/F02-020 © 2002 NRC Canada

ers need a better quantitative understanding of linkages between environmental conditions and salmon productivity. To estimate effects of ocean conditions on salmon populations, we used a statistical modelling approach that improves on previous research in three important ways. First, we measured biological productivity for individual stocks as $\log(R/S)$, or "survival rate" from eggs to adult recruits (R) after accounting for density-dependent effects of spawner abundance (S) (eq. 1 below). This index provides a more rigorous measure for identifying environmental effects on productivity than catch data, which have been linked with large-scale climate indicators like ocean temperature (Mantua et al. 1997; Downton and Miller 1998; Hare et al. 1999). Catch data are potentially confounded by changes in fishing effort, spawner abundance, and hatchery production, and, if aggregated across stocks, may reflect changes in productivity of only the most abundant stocks in a given area.

Second, we defined spatial scales for appropriate climate indices based on recent analyses of spatial covariation among salmon stocks and among coastal oceanographic variables (Peterman et al. 1998; Pyper et al. 2001; Mueter et al. 2002). Previous studies have related indices of salmon productivity to a variety of environmental variables without first determining whether the biological and physical indices had similar spatial characteristics (e.g., spatial autocorrelation scales). For example, aggregate catch data have been related to large-scale indicators of ocean climate in the Northeast Pacific such as the Pacific Decadal Oscillation (PDO), a measure of ocean temperature across thousands of kilometres (Mantua et al. 1997; Hare et al. 1999). However, recent analyses of survival rate anomalies (residuals in $\log(R/S)$ from stock–recruitment curves) show significant positive covariation among stocks across local or regional scales of several hundred kilometres, but not at larger scales (Myers et al. 1997; Peterman et al. 1998; Pyper et al. 2001). Results of these studies suggest that this shared variation in survival rates is due to environmental processes operating primarily at regional spatial scales during early ocean life. Mueter et al. (2002) found that, unlike upwelling and salinity measures, coastal sea surface temperature (SST) during the summer when juvenile salmon first enter coastal waters shows a similar regional scale of covariation to that of survival rates. We therefore hypothesized that SST in regions corresponding to the distribution of juvenile salmon during early ocean life would be more useful in predicting survival rates of a given stock than a large-scale climate index like the PDO.

A third and major improvement was the use of numerous salmon stocks as statistical replicates to identify the underlying "signal" of environmental effects more clearly than is possible with single-stock analyses. While environment–recruitment relationships have been identified for some stocks, they often fail to hold after more recent data are added (Walters and Collie 1988; Myers 1998). A multistock approach can reduce the chance of finding spurious relationships (Myers and Mertz 1998). The objectives of our analysis were to quantify temperature effects on survival rates of pink salmon (*Oncorhynchus gorbuscha*), chum salmon (*Oncorhynchus keta*), and sockeye salmon (*Oncorhynchus nerka*) across multiple stocks, to examine differences in these effects among stocks from different areas, and to determine the relative importance of regional and large-scale measures of ocean temperature for explaining variability in survival rates.

Methods

Data

To quantify productivity of Northeast Pacific salmon stocks, we used time-series of abundance for spawners and recruits (catch plus escapement) to compute survival rates ($\log(R/S)$) for 120 wild stocks of pink (43 stocks), chum (40), and sockeye (37) salmon (Fig. 1). For a detailed description of the data, see Peterman et al. (1998), Pyper et al. (2001), and Pyper et al. (2002). Data series ranged in length from 15 to 47 years (brood years 1948–1996) with an average length of 31 years. Because adult returns of sockeye and chum salmon typically consist of a mixture of age classes, we used age-composition data for adult returns, where available, to allocate recruits to the appropriate brood year in which their parents spawned. Complete age data for adult returns were available for all sockeye stocks and for some chum stocks. For chum stocks with incomplete time-series of age-specific recruits, but with age data in more than half of the brood years, we used each stock's average age structure across return years to allocate recruits in years with missing data. For 18 chum stocks with no age data in more than half of the brood years, we allocated recruits from return years to brood years under the assumption that all recruits were age 4. This approach provided measures of survival rate that minimized the potential to induce spurious autocorrelation and cross-correlations in time-series of survival rate, as indicated by simulations and empirical analyses (Pyper et al. 2002).

As regional measures of ocean temperature, we computed spatial and temporal averages of SST experienced by juveniles of each salmon stock during early ocean life. Using SST data from the Comprehensive Ocean–Atmosphere Data Set (COADS, http://www.cdc.noaa.gov/coads/), we selected coastal COADS grid cells (2° latitude by 2° longitude), whose centres were located within 400 km of the ocean-entry point of a given salmon stock included in our analysis. We then computed monthly SST anomalies (deviations from the long-term mean for a given month) at each location (Appendix A). Based on information about the timing of outmigration and early ocean residence compiled from literature, SST anomalies were averaged across those COADS grid cells and months that encompassed the coastal areas judged to be occupied by juveniles of a given stock during early ocean residence (April–July for stocks in Washington, British Columbia (B.C.), and southeast Alaska; May–August for most Alaska stocks; June–September for stocks in western Alaska).

To determine the relative importance of regional-scale SST effects and large-scale climate effects, we also included a winter average of the PDO (November–March, Mantua et al. 1997) as a potential covariate in modelling survival rates. The PDO was only moderately correlated with our regional averages of coastal SST (r from 0.07 to 0.61 for 1961–1996, average $r = 0.32$) and thus largely reflects different processes.

© 2002 NRC Canada

Fig. 1. Map of ocean entry points for all stocks used in the analysis. Stocks of each species are numbered consecutively along the coast from south to north for identification of stocks in Fig. 2. These stocks represent the majority of wild (*a*) pink salmon (*Oncorhynchus gorbuscha*), (*b*) chum salmon (*Oncorhynchus keta*), and (*c*) sockeye salmon (*Oncorhynchus nerka*) entering the Northeast Pacific each year. Heavy lines, whose locations were estimated by intervention models (see text), separate distinct northern and southern groups of stocks for each species based on their sea surface temperature (SST) coefficients, as estimated from single-stock models.

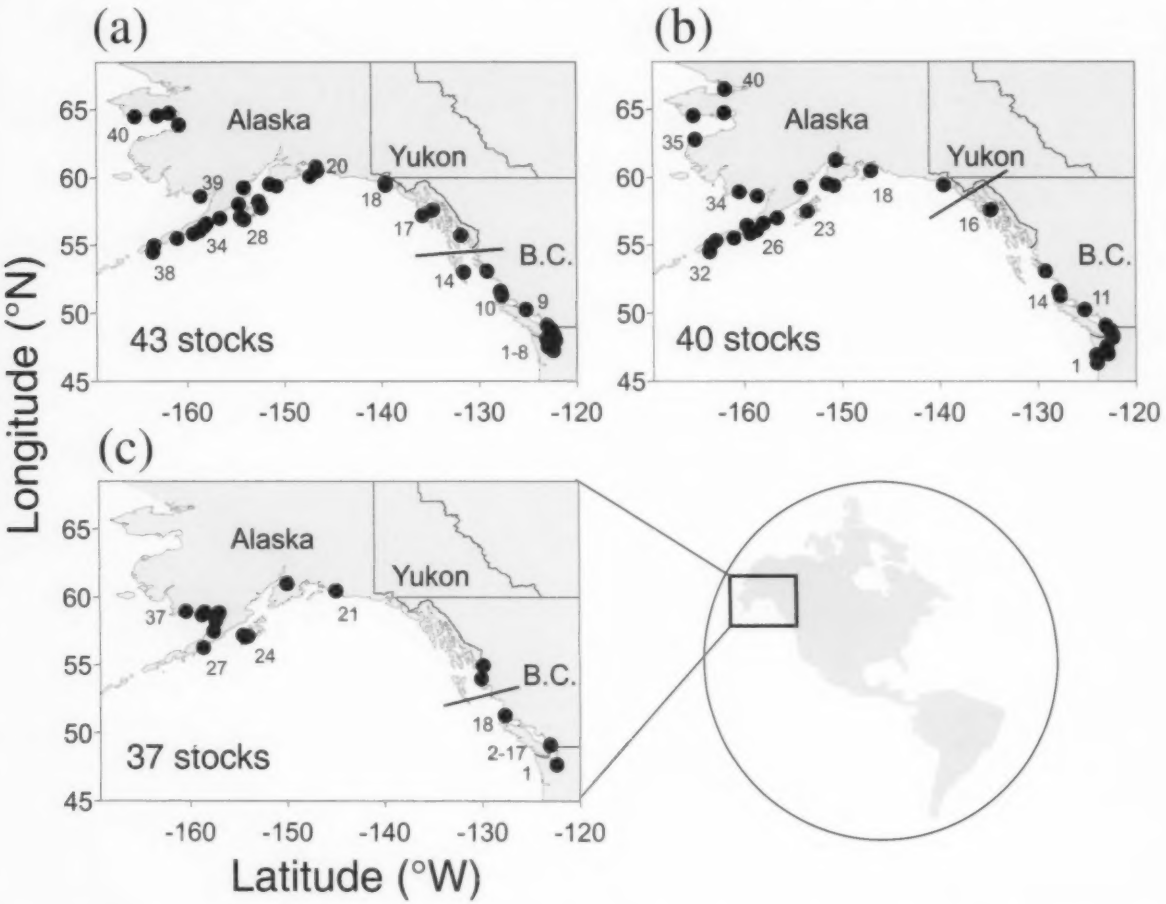

Statistical analyses

To help formulate appropriate multistock models (eq. 2 below), we initially estimated temperature effects for each stock i separately using a generalized Ricker model

$$(1) \qquad \log(R_{it}/S_{it}) = \alpha_i - \beta_i S_{it} + \gamma_i X_{i,t+k} + \varepsilon_{it},$$

where S_{it} is spawner abundance for the ith stock of a given species in the year of spawning (t), R_{it} is the resulting recruitment, and X is either a stock-specific measure of coastal SST ($SST_{i,t+k}$) or the PDO index (PDO_{t+k}). Parameters reflect productivity at low spawner abundance (α_i), the magnitude of density dependence (β_i), and SST or PDO effects (γ_i). Both SST and PDO were lagged to correspond to conditions during the year of ocean entry, k years after spawning. Pink and chum salmon enter the ocean one winter after spawning ($k = 1$), whereas sockeye salmon spend two or three winters in fresh water prior to outmigration. For each sockeye salmon stock, we therefore used a weighted average of environmental conditions two and three winters after spawning, with weights equal to the average proportions of juveniles entering the ocean at lags 2 and 3. Because survival rates are often autocorrelated over time, we allowed for first-order autocorrelation in the errors by estimating stock-specific first-order autoregressive coefficients ϕ_i (i.e., $\varepsilon_{it} = \phi_i \varepsilon_{i,t-1} + \nu_{it}$, where $\nu_{it} \sim N(0, \sigma_i^2)$). We then examined the distributions of parameters from the single-stock models to identify geographical differences across stocks and to determine whether parameters were approximately normally distributed, which is a necessary assumption for our multistock models (eq. 2 below).

Results from the single-stock models were used to identify appropriate models for estimating SST and PDO effects across a large number of stocks simultaneously. We extended the multistock mixed-effects model used by Myers et al. (1999) to include a temperature covariate (X) and autocorrelated errors

© 2002 NRC Canada

$$(2)\quad \log(R_{it}/S_{it}) = \alpha + a_i - \beta_i S_{it} + \gamma X_{i,t+k} + g_i X_{i,t+k} + \varepsilon_{it},$$

where stock productivity is estimated by a fixed intercept α, common to all stocks of a species and area, and a random, stock-specific deviation that reflects the relative productivity of stock i (a_i). Similarly, the environmental effect consists of an overall effect γ, and a random, stock-specific effect (g_i). The random effects a_i and g_i are assumed to follow a joint normal distribution with means zero, variances σ_a^2 and σ_g^2, and covariance σ_{ag}. Because the magnitude of density dependence varied greatly among stocks and was not normally distributed, parameter β was estimated as a separate fixed effect for each stock. Errors were assumed to be first-order autocorrelated (i.e., $\varepsilon_{it} = \phi\,\varepsilon_{i,t-1} + \nu_t$, where $\nu_t \sim N(0, \sigma^2)$). We fit the model separately to stocks of each species because of their different life histories. As suggested by single-stock analyses (see Results section), we also fit models separately to stocks from northern and southern areas (Fig. 1) to allow for differences between these geographical areas in average stock productivity (α), environmental effects (γ), and first-order autocorrelation (ϕ). All parameters in eq. 2 were estimated via restricted maximum likelihood (Pinheiro and Bates 2000) and model fits were compared using the small-sample Akaike Information Criterion (AIC_c), or, in the case of nested models, likelihood ratio tests. All AIC_c values were computed as the difference between the AIC_c of the model with the lowest AIC_c value and that of other models. Small differences in AIC_c ($\triangle AIC_c < 3$) indicate that two models fit almost equally well, whereas larger differences indicate that the model with the smaller AIC_c value is preferable (Burnham and Anderson 1998). Model comparisons were based on models fit via maximum likelihood because models fit by restricted maximum likelihood (REML) cannot be compared using the AIC_c. However, all final parameter values are REML estimates, which are less biased (Pinheiro and Bates 2000).

Sensitivity analysis

We examined the sensitivity of our results to model assumptions, to the presence of outliers, and to strong trends in SST associated with the 1976–1977 regime shift in the Northeast Pacific. First, the assumption that errors were first-order autocorrelated was tested by comparing models with and without autocorrelated errors using likelihood ratio tests. In addition, we refit the models for each species and area using different error structures with higher-order autoregressive and moving average terms (ARMA(p,q)), where p and q refer to the order of the autoregressive and moving average terms, respectively. Second, we examined our assumption for the multistock model that geographical differences in the temperature effect consist of different mean effects between areas and a common mean effect across stocks within each area. As an alternative, we modeled geographical differences as a linear gradient in the mean temperature effect along the coast (indexed by "alongshore distance", D, which we defined as the distance along the outer coast from the southernmost stock included in our analysis (km 0) to a given stock's ocean entry point). A linear gradient was modeled by allowing γ in eq. 2 to vary as a function of D ($\gamma = m + bD$). This linear-gradient model was compared with the two-area model using the AIC_c model selection criterion. Finally, we examined the influence of several years with extremely cold temperatures in the early 1970s and the effect of the regime shift in 1976–1977 on our results by repeating the analysis using only data after the regime shift.

Results

Estimated SST coefficients, γ_i, from single-stock models (eq. 1) were bimodally distributed across stocks for all species (histograms in Fig. 2) because of different effects of SST on the survival rates of stocks from two broad areas. SST coefficients for these single-stock models (open circles in Figs. 2*a*–2*c*) were generally negative for southern pink and sockeye stocks and positive for northern stocks of all three species, although coefficients were highly variable among stocks and rarely differed significantly from zero. Patterns for PDO coefficients were similar but less pronounced. For each species, significant discontinuities in the SST coefficients were confirmed by ordering stocks along the coast from Washington to Western Alaska and fitting a one-step intervention model (two separate means) to SST coefficients with a location for the break point chosen to minimize the residual sum of squares. For all species, significant steps (t tests, $P < 0.05$) occurred in either northern B.C. or Southeast Alaska (Fig. 1). Productivity, α_i of sockeye salmon exhibited a similar step between stocks in central and northern B.C. ($P < 0.001$). Furthermore, errors from single-stock models (eq. 1) were moderately autocorrelated for northern stocks of all species, indicating slowly changing trends in survival rates, but showed little autocorrelation for southern stocks. Thus, the magnitudes of SST coefficients, productivity of sockeye salmon, and autocorrelation in survival rates all differed markedly between southern and northern stocks. Parameters within each area were close to normally distributed, as required for the multistock models.

Results from the multistock models (eq. 2) suggest that, for all species, SST had a strong and significant effect on survival rates. Models that included the SST terms in eq. 2 ($\gamma X + g_i X$) fit the data significantly better than models without these terms for all species–area combinations (likelihood ratio tests: $L = 25.2$, $p < 0.001$ for southern pink salmon; $L = 104.9$, $P < 0.001$ for northern pink salmon; $L = 37.6$, $P < 0.001$ for northern chum salmon; $L = 15.7$, $P = 0.001$ for southern sockeye salmon; $L = 32.0$, $P < 0.001$ for northern sockeye salmon). The only exception was southern chum salmon ($L = 3.1$, $P = 0.309$).

The estimated SST effects differed significantly between areas, but the magnitudes of effects were remarkably consistent across stocks within each area (solid triangles in Figs. 2*a*–2*c*; Table 1). All northern stocks had positive SST coefficients, suggesting that survival rates in Alaska increased for salmon that experienced above-average coastal temperatures during early ocean residence. In contrast, survival rates of southern pink and sockeye salmon stocks were poor during years with warm SST anomalies. The magnitudes of the estimated effects imply that variations in coastal

© 2002 NRC Canada

Fig. 2. Estimated coefficients for effects of sea surface temperature (SST) on log(*R*/*S*) for 120 stocks of pink salmon (*Oncorhynchus gorbuscha*), chum salmon (*Oncorhynchus keta*), and sockeye salmon (*Oncorhynchus nerka*). Estimates based on single-stock models (γ_i in eq. 1, open circles in *a–c*) are compared with estimates based on mixed-effects models, which consist of a mean SST effect by area (γ in eq. 2, vertical solid lines) and stock-specific random effects (g_i in eq. 2, solid triangles show $\gamma + g_i$). Stocks in *a–c* are arranged along the *y* axis from south to north with stock numbers corresponding to those in Fig. 1. Northern and southern areas are defined for each species in Fig. 1 and stocks from the two areas are separated here by a horizontal line. Bottom panels (*d–f*) show histograms of the fixed SST effects based on single-stock models (eq. 1) and estimated probability density functions (smooth curves) for the estimated random SST effects based on multistock mixed-effects models (eq. 2).

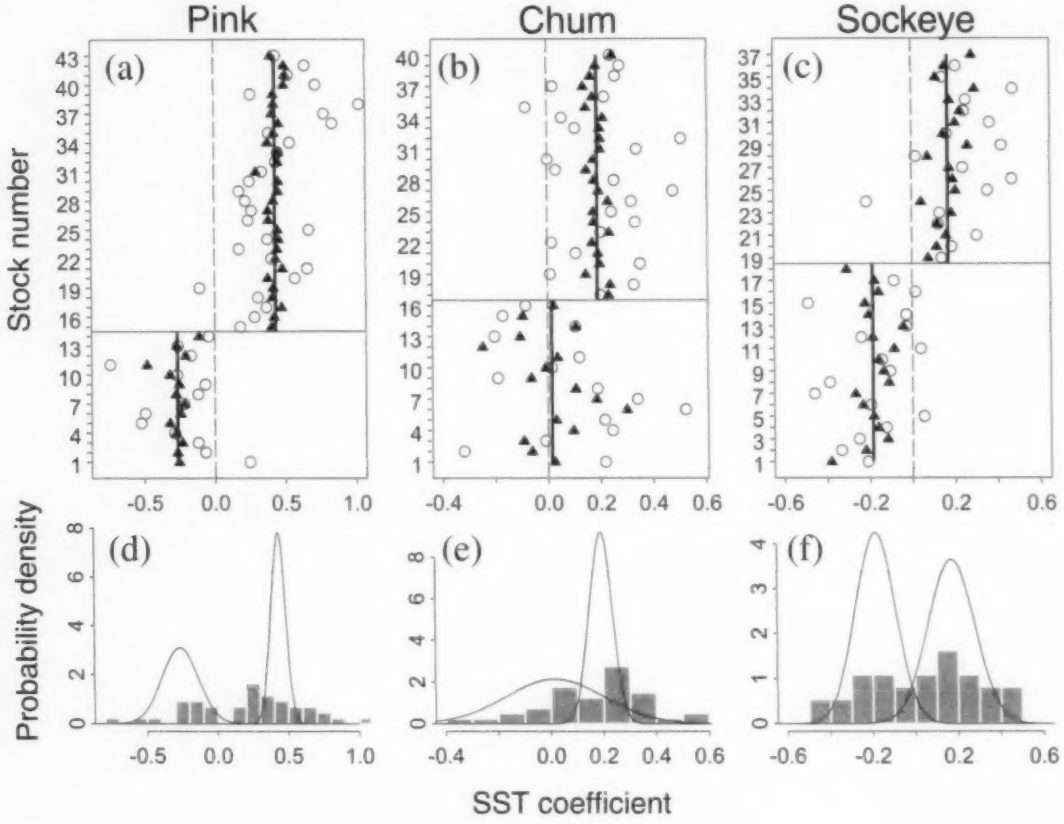

Table 1. Summary of temperature effects on survival rates of salmon.

						Regional SST effects			Large-scale PDO effect		
Salmon species	Area	Stocks[a]	N^a	α	ϕ	γ (°C^{-1})	SE_γ	ΔR (%)	γ (°C^{-1})	SE_γ	ΔR
Pink	North	29	808	1.13	0.217	0.431**	0.042	45	0.206**	0.047	20
	South	14	406	1.25	–0.090	–0.266**	0.068	–20	–0.046	0.052	n.s.
Chum	North	24	647	1.32	0.438	0.191**	0.031	18	0.073*	0.035	7
	South	16	448	1.39	0.131	0.015	0.071	n.s.	0.094	0.038	n.s.
Sockeye	North	19	641	1.44	0.341	0.169**	0.044	19	0.004	0.039	n.s.
	South	18	753	2.53	0.189	–0.186**	0.054	–14	–0.108**	0.036	–9

Note: Estimated mean productivity (α), first-order autocorrelation (ϕ), and effects of regional sea-surface temperature (SST) or Pacific Decadal Oscillation (PDO) on survival rates (log(recruits-per-spawner)) of three species of salmon by area. Areas are defined in Fig. 1. Mean effects (γ) and standard errors (SE_γ) were estimated by including either SST or PDO as an explanatory variable in a multistock mixed-effects model (eq. 2). To illustrate temperature effects, we computed the estimated percent change in recruitment, ΔR, at a given spawner abundance that would result from an increase in SST or PDO corresponding to one standard deviation above the long-term (1950–1999) mean. No estimate is given if an effect was not significant at the 5% level (n.s.). *Significantly different from zero at $P < 0.05$; **significant at $P < 0.001$.

[a]Number of stocks and total number of observations (N = stocks times average number of years) included in analysis.

© 2002 NRC Canada

SST are associated with substantial variations in recruitment and therefore in the abundance of fish available to be harvested (Table 1).

For each species, models with SST (X = SST in eq. 2) fit much better than the same model using PDO instead of SST ($\triangle AIC_c > 20$ for all species in both areas, except southern chum stocks). Model fits did not improve significantly by including both PDO and SST as explanatory variables, except for northern pink salmon (likelihood ratio test: $L = 9.97$, $P = 0.041$).

Our results were robust to the underlying assumptions and to the exclusion of data prior to the 1976–1977 regime shift. First, comparing different error structures suggests that assuming first-order autocorrelated errors was reasonable. The first-order autoregressive parameter (Table 1) was highly significant ($P < 0.01$) for all three species in the northern area and for sockeye salmon in the southern area, but not for pink ($L = 2.35$, $P = 0.125$) or chum salmon ($L = 2.41$, $P = 0.121$) in the southern area. Higher-order autocorrelation was evident for northern chum (positive at lag 2) and northern sockeye stocks (negative at lag 5), but including higher-order autoregressive terms for the error in eq. 2 did not change estimated effects appreciably. Second, compared to the base-case analysis with different mean effects by area, a linear-gradient model fit the data almost equally well ($\triangle AIC_c < 1$ for pink and sockeye salmon, $\triangle AIC_c = 6.3$ for chum salmon), suggesting that the gradient in SST coefficients may be more gradual than is indicated by the statistically best model. Regardless, both models indicated strong north–south differences and very similar SST effects (fixed mean effect + random effect) for a given stock. Finally, our results were not strongly influenced by unusual temperature conditions in the early 1970s or the regime shift of 1976–1977. Excluding data prior to the regime shift resulted in the same geographical differences and very similar estimated effects of SST on survival rates for all three species.

Discussion

Our results suggest that (*i*) survival rates of pink, sockeye, and northern chum salmon are strongly affected by coastal processes related to variations in regional-scale SST during early ocean life; (*ii*) effects of temperature on survival rates are remarkably consistent across stocks within areas; and (*iii*) northern and southern stocks of Northeast Pacific salmon respond in opposite ways to variations in coastal SST. Furthermore, regional SST anomalies specific to each stock were a much better predictor of survival rate than the PDO, suggesting that coastal conditions during the first few months at sea have a larger effect on the survival rate and subsequent recruitment of salmon than large-scale variability related to the PDO index.

We suggest two possible explanations for the strong north–south difference in the effects of temperature on survival rates. First, a latitudinal gradient could result if juvenile salmon from northern and southern stocks, on average, encounter temperatures at the lower and upper end of their optimum temperature range, respectively. During periods of positive SST anomalies, northern stocks may experience more favorable conditions for growth and subsequent survival (Mortensen et al. 2000), whereas southern stocks may experience less favorable temperatures. However, this mechanism seems unlikely, except at the extremes of the range, because interannual temperature differences are typically small relative to the physiological limits of salmon and fish from different stocks have presumably adapted to average local conditions.

More likely, SST is a proxy for other, indirect effects on survival related to oceanographic differences between the two areas. The observed break points for SST effects are located within the transition zone between two oceanographic domains: the "downwelling domain" to the north, and the "upwelling domain" to the south (Ware and McFarlane 1989). Mechanisms determining the distribution and abundance of prey and predators of juvenile salmon differ between these domains and are likely associated with variations in coastal SST. In the upwelling domain, increased SST is associated with reduced prey availability for juvenile salmon due to decreased upwelling, increased stratification, and decreased primary and secondary production (Ware and Thomson 1991; Gargett et al. 2001). Warm ocean temperatures are also associated with increased abundances of predators of juvenile salmon, such as Pacific hake (*Merluccius productus*), off the coast of southern B.C. (Ware and McFarlane 1995). Both processes are consistent with a negative effect of increasing SST on pink and sockeye salmon survival in the southern area. In contrast, a positive effect of higher SST on survival rates of all three salmon species in Alaska may result from increased zooplankton abundances during periods of intensified cyclonic winds and downwelling along the coast, which are associated with warmer coastal temperatures and increased advection of oceanic plankton into nearshore areas (Cooney 1984; Brodeur and Ware 1992).

Regardless of the underlying mechanisms, regional measures of SST are potentially powerful and readily available predictors of salmon survival rates. The effects of SST on survival rates estimated from multistock models provide useful prior distributions for SST effects on other stocks not included in our analysis. SST coefficients estimated from single-stock models may be misleading and may result in poor management decisions. Results from our multistock, mixed-effects models show that temperature effects are much more consistent across adjacent stocks than indicated by single-stock analyses, and the mixed-effects models provide precise estimates of mean effects within each area.

Our finding that SST effects are opposite in the north and south suggests that survival rates between these areas will vary out-of-phase if both areas show synchronous variations in coastal SST. This finding is relevant to other recent research. For instance, Hare et al. (1999) hypothesized such inverse patterns in productivity based on observations that salmon catches (in particular, catches of chinook and coho) are inversely related between Alaska and more southern areas (i.e., California through B.C.). This inverse (north–south) pattern in catches is coherent with variations in large-scale climate indices such as the PDO (Hare et al. 1999). Our results can help explain the "inverse production regime" hypothesis of Hare et al. (1999) if variations in coastal ocean temperatures (and (or) the changes in coastal habitat for which they are a proxy) along the entire coast are correlated with large-scale indices like the PDO. However, coastal

© 2002 NRC Canada

SSTs during summer, when juvenile salmon are in the coastal ocean, tend to be only weakly correlated between the two areas (Mueter et al. 2002) and with the PDO (F. Mueter, unpublished data). Consequently, the pink, chum, and sockeye salmon stocks analyzed here show little evidence of inverse patterns in survival rates between northern and southern areas (e.g., Pyper et al. 2001). Similarly, for these species, there is little evidence for an inverse pattern in catches (Hare et al. 1999). It should be noted that inverse patterns in survival rates could alternatively arise from inverse trends in spawner abundances between stocks in the northern and southern areas (because log(R/S) depends on both S and SST; see eq. 1). However, there is no evidence for such inverse trends in spawner abundances between stocks in the two areas (F. Mueter, unpublished data).

Differences in species and geographical areas covered and previously noted difficulties in interpreting aggregate catch data make it difficult to compare our results directly with those of Hare et al. (1999). Nevertheless, if our results generalize to chinook and coho salmon, they may help explain inverse patterns in catch trends of these species between Alaska and more southern areas. Marine survival of coho salmon off the coast of Oregon is negatively correlated with SSTs during the winter (rather than summer) following smolt migration (e.g., Cole 2000), whereas survival rates of northern hatchery coho tend to increase with SSTs at the time of release (Hobday and Boehlert 2001). Unlike in the summer, SSTs in winter tend to be coherent along the entire west coast (Mueter et al. 2002). Thus, to the extent that SST at the time of release and winter SSTs in the northern area are correlated, large-scale changes in winter SST could contribute to opposite trends in survival rate and recruitment of coho salmon between northern and southern areas. Indeed, patterns in marine survival differ between hatchery coho originating north of Vancouver Island and hatchery coho originating further south (Hobday and Boehlert 2001), and catch trends in the two areas are inversely related (Hare et al. 1999).

We caution that our results should be used to estimate effects of future climatic changes on recruitment of Pacific salmon only if such changes do not alter processes underlying the relationships that we found between SST and salmon survival rates. Because SST is likely an indirect measure of these processes, the observed relationships may be disrupted if unprecedented climatic changes modify the structure and dynamics of the Northeast Pacific ecosystem. For instance, climatic changes are likely to affect average wind speeds and associated patterns of upwelling and coastal ocean circulation (Bakun 1990), which may affect food availability for salmon independently of changes in coastal temperatures. Regardless of how future climatic change affects the Northeast Pacific, our findings improve the understanding of processes currently affecting survival rates of Pacific salmon.

Acknowledgments

We thank Milo Adkison, Jim Anderson, Judith Anderson, Mary Downton, Marie-Josée Fortin, Steven Hare, Jeff Hutchings, Brice MacGregor, Nathan Mantua, Ashley Steel, Dan Ware, and Chris Wood for reviewing earlier drafts of the manuscript and Mike Bradford, Dan Ware, and Chris Wood for helpful discussions. Thanks to the many biologists and technicians in various management agencies for gathering and processing lengthy time-series of data and providing them. Supported by a Strategic Grant from the Natural Sciences and Engineering Research Council of Canada. This paper is dedicated to the memory of W.E. Ricker (1908–2001) whose work so greatly influenced fisheries science.

References

Adkison, M.D., Peterman, R.M., Lapointe, M.F., Gillis, D.M., and Korman, J. 1996. Alternative models of climatic effects of sockeye salmon, *Oncorhynchus nerka*, productivity in Bristol Bay, Alaska, and the Fraser River, British Columbia. Fish. Oceanogr. **5**: 137–152.

Bakun, A. 1990. Global climate change and intensification of coastal ocean upwelling. Science, **247**: 198–201.

Beamish, R.J. (*Editor*). 1995. Climate change and northern fish populations. Can. Spec. Publ. Fish. Aquat. Sci. No. 121. National Research Council of Canada, Ottawa.

Botsford, L.W., Castilla, J.C., and Peterson, C.H. 1997. The management of fisheries and marine ecosystems. Science, **277**: 509–515.

Brodeur, R.D., and Ware, D.M. 1992. Long-term variability in zooplankton biomass in the Subarctic Pacific Ocean. Fish. Oceanogr. **1**: 32–38.

Burnham, K.P., and Anderson, D.R. 1998. Model selection and inference: a practical information–theoretic approach. Springer-Verlag, New York.

Cole, J. 2000. Coastal sea surface temperature and coho salmon production off the north-west United States. Fish. Oceanogr. **9**: 1–16.

Cooney, R.T. 1984. Some thoughts on the Alaska Coastal Current as a feeding habitat for juvenile salmonids. *In* The influence of ocean conditions on the production of salmonids in the North Pacific Ocean. *Edited by* W.G. Pearcy. Oregon State University Press, Corvallis. pp. 256–268.

Downton, M.W., and Miller, K.A. 1998. Relationships between Alaska salmon catch and North Pacific climate on interannual and interdecadal time scales. Can. J. Fish. Aquat. Sci. **55**: 2255–2265.

Gargett, A.E., Li, M., and Brown, R. 2001. Testing mechanistic explanations of observed correlations between environmental factors and marine fisheries. Can. J. Fish. Aquat. Sci. **58**: 208–219.

Hare, S., Mantua, N., and Francis, R. 1999. Inverse production regimes: Alaska and West coast Pacific salmon. Fisheries, **24**: 6–14.

Hobday, A.J., and Boehlert, G.W. 2001. The role of coastal ocean variation in spatial and temporal patterns in survival and size of coho salmon (*Oncorhynchus kisutch*). Can. J. Fish. Aquat. Sci. **58**: 2021–2036.

Mantua, N., Hare, S., Zhang, Y., Wallace, J., and Francis, R. 1997. A Pacific interdecadal climate oscillation with impacts on salmon production. Bull. Am. Meteorol. Soc. **78**: 1069–1080.

Mortensen, D., Wertheimer, A., Taylor, S., and Landingham, J. 2000. The relation between early marine growth of pink salmon, *Oncorhynchus gorbuscha*, and marine water temperature, secondary production, and survival to adulthood. Fish. Bull. **98**: 319–335.

Mueter, F.J., Ware, D.M., and Peterman, R.M. 2002. Spatial correlation patterns in coastal environmental variables and survival rates of Pacific salmon in the Northeast Pacific Ocean. Fish. Oceanogr. **11**: In press.

Myers, R.A. 1998. When do environment–recruitment correlations work? Rev. Fish Biol. Fish. **8**: 285–305.

© 2002 NRC Canada

Myers, R.A., and Mertz, G. 1998. Reducing uncertainty in the biological basis of fisheries management by meta-analysis of data from many populations: a synthesis. Fish. Res. **37**: 51–60.

Myers, R.A., Mertz, G., and Bridson, J. 1997. Spatial scales of interannual recruitment variations of marine, anadromous, and freshwater fish. Can. J. Fish. Aquat. Sci. **54**: 1400–1407.

Myers, R.A., Bowen, K.G., and Barrowman, N.J. 1999. Maximum reproductive rate of fish at low population sizes. Can. J. Fish. Aquat. Sci. **56**: 2404–2419.

Pauly, D., Christensen, V., Dalsgaard, J., Froese, R., and Torres, F., Jr. 1998. Fishing down marine food webs. Science, **279**: 860–863.

Peterman, R.M., Pyper, B.J., Lapointe, M.F., Adkison, M.D., and Walters, C.J. 1998. Patterns of covariation in survival rates of British Columbian and Alaskan sockeye salmon (*Oncorhynchus nerka*) stocks. Can. J. Fish. Aquat. Sci. **55**: 2503–2517.

Pinheiro, J.C., and Bates, D.M. 2000. Mixed-effects models in S and S-Plus. Statistics and Computing. Springer Verlag, New York.

Pyper, B.J., Mueter, F.J., Peterman, R.M., Blackbourn, D.J., and Wood, C. 2001. Spatial covariation in survival rates of Northeast Pacific pink salmon (*Oncorhynchus gorbuscha*). Can. J. Fish. Aquat. Sci. **58**: 1501–1515.

Pyper, B.J., Mueter, F.J., Peterman, R.M., Blackbourn, D.J., and Wood, C. 2002. Spatial covariation in survival rates of Northeast Pacific chum salmon. Trans. Am. Fish. Soc. **131**: In press.

Schafer, J.L. 1997. Analysis of incomplete multivariate data. Monogr. Stat. Appl. Probab. 72. Chapman and Hall, London.

Walters, C.J., and Collie, J.S. 1988. Is research on environmental factors useful to fisheries management? Can. J. Fish. Aquat. Sci. **45**: 1848–1854.

Ware, D.M., and McFarlane, G.A. 1989. Fisheries production domains in the Northeast Pacific Ocean. *In* Effects of ocean variability on recruitment and an evaluation of parameters used in stock assessment models. Can. Spec. Publ. Fish. Aquat. Sci. No. 108. *Edited by* R.J. Beamish and G.A. McFarlane. National Research Council of Canada, Ottawa. pp. 359–379.

Ware, D.M., and McFarlane, G.A. 1995. Climate-induced changes in Pacific hake (*Merluccius productus*) abundance and pelagic community interactions in the Vancouver Island upwelling system. *In* Climate change and northern fish populations. Can. Spec. Publ. Fish. Aquat. Sci. No. 121. *Edited by* R.J. Beamish. National Research Council of Canada, Ottawa. pp. 509–521.

Ware, D.M., and Thomson, R.E. 1991. Link between long-term variability in upwelling and fish production in the Northeast Pacific Ocean. Can. J. Fish. Aquat. Sci. **48**: 2296–2306.

Appendix A

The COADS data set used in our analysis contained missing values for many of the locations that we included. Missing monthly averages were replaced with predicted values from regressing SST at a given location x_i on the best linear combination of SST at all other locations x_j ($j = 1,\ldots, n, j \neq i$), where the "best" linear combination was the linear combination of SSTs at locations x_j that maximized the correlation with SST at location x_i. We used long-term means as starting values to regress SST at the first location and iteratively cycled through all locations until convergence (Schafer 1997).

© 2002 NRC Canada

The link between precipitation, river runoff, and blooms of the toxic dinoflagellate *Alexandrium tamarense* in the St. Lawrence

Andréa M. Weise, Maurice Levasseur, François J. Saucier, Simon Senneville, Esther Bonneau, Suzanne Roy, Gilbert Sauvé, Sonia Michaud, and Juliette Fauchot

Abstract: Blooms of the toxic dinoflagellate *Alexandrium tamarense*, which is responsible for paralytic shellfish poisoning, are annually recurrent events in the Estuary and Gulf of St. Lawrence, Québec, Canada. The analysis of abundance data for this algal species between 1989 and 1998 at Sept-Îles, a presumed initiation site in the northwestern Gulf of St. Lawrence, revealed yearly fluctuations in the onset, duration, and magnitude of toxic *A. tamarense* blooms. Hydrological and meteorological data for the region indicate that rainfall, Moisie River runoff, and wind are highly related to the pattern of bloom development each year. Results from the 10-year data set reveal that in this system: (*i*) high Moisie River runoff from a prolonged spring freshet or from heavy rainfall events in the summer and fall can initiate *A. tamarense* blooms; (*ii*) high Moisie River runoff combined with prolonged periods of weak winds (<4 $m \cdot s^{-1}$) favour the continued development of blooms; and (*iii*) winds >8 $m \cdot s^{-1}$ disrupt blooms. Salinity, which reflects the general state of the water column in terms of freshwater input and stability, had a strong negative correlation with the probability of observing *A. tamarense* cells at this station and could thus be used as a predictive tool for the presence of cells in this system.

Résumé : Les floraisons du dinoflagellé toxique *Alexandrium tamarense*, responsable de l'intoxication paralysante par les mollusques, sont des événements annuels récurrents dans l'estuaire et le golfe du Saint-Laurent, Québec, Canada. L'analyse des données d'abondances de *A. tamarense* entre 1989 et 1998 à Sept-Îles, un site présumé d'initiation des floraisons dans le nord-ouest du golfe du Saint-Laurent, montre que l'initiation, la durée et l'ampleur des floraisons toxiques de *A. tamarense* varient d'une année à l'autre. Les données hydrologiques et météorologiques indiquent que les précipitations, le débit de la rivière Moisie et le vent sont étroitement liés au patron annuel de floraisons. Les 10 années de résultats démontrent que dans ce système : (*i*) un débit élevé de la rivière Moisie dû à une importante crue printanière ou à de fortes précipitations durant l'été et l'automne peut déclencher des floraisons de *A. tamarense*, (*ii*) un débit élevé de la rivière Moisie combiné à une période de vents faibles (<4 $m \cdot s^{-1}$) favorise le développement continu des floraisons et (*iii*) des vents >8 $m \cdot s^{-1}$ dispersent et mettent fin aux floraisons. La salinité, qui reflète l'état général de la colonne d'eau en terme d'apport d'eau douce et de stabilité, démontre une forte corrélation négative avec la probabilité d'observer des cellules de *A. tamarense* à cette station. Ce paramètre pourrait donc être utilisé comme outil pour prédire la présence de *A. tamarense* dans ce système.

Introduction

Harmful algal blooms and the phycotoxins they produce represent a significant and increasing threat to human health, fishery resources, and marine ecosystems throughout the world. These blooms result from a combination of physical, chemical, and biological mechanisms and interactions that have not yet been well established. Several studies have shown that toxic blooms are often associated with freshwater plumes (Franks and Anderson 1992*a*; Taylor and Haigh 1993; Hallegraeff et al. 1995). For example, the timing and spread of shellfish toxicity in the waters of the Gulf of Maine was linked to the alongshore transport of *A. tamarense* in a buoyancy current originating from several rivers that empty into

Received 20 September 2001. Accepted 27 February 2002. Published on the NRC Research Press Web site at http://cjfas.nrc.ca on 4 April 2002.
J16538

A.M. Weise, M. Levasseur,[1] F.J. Saucier, S. Senneville, E. Bonneau, and S. Michaud. Fisheries and Oceans Canada, Maurice Lamontagne Institute, 850 route de la Mer, Mont-Joli, QC G5H 3Z4, Canada.
S. Roy and J. Fauchot. Institut des Sciences de la Mer, Université du Québec à Rimouski, 310 Allée des Ursulines, Rimouski, QC G5L 3A1, Canada.
G. Sauvé. Canadian Food Inspection Agency, Gare Maritime Champlain, 901 Cap Diamant, Québec, QC G1K 4K1, Canada.

[1]Corresponding author (e-mail: levasseurM@dfo-mpo.gc.ca).

 DOI: 10.1139/F02-024 © 2002 NRC Canada

the Gulf (Franks and Anderson 1992*a*, 1992*b*). Similarly, in the Strait of Georgia, British Columbia, the first appearance of substantial numbers of the marine raphidophyte *Heterosigma* coincides with maximum runoff from the Fraser river (Taylor and Haigh 1993). A number of studies have also indicated that toxic dinoflagellate blooms often coincide with enhanced rainfall and freshwater runoff, as well as with a stable water column (Ryther 1955 and references therein; Hallegraeff et al. 1995; Giacobbe et al. 1996). The association of toxic dinoflagellate blooms with freshwater runoff has not yet been elucidated but may be due to more favourable temperature and salinity conditions (Prakash 1967), the supply of humic substances (Granéli and Moreira 1990), increased water column stability (Margalef et al. 1979), or a combination of these factors that might be physiologically important for optimum cell growth.

In the St. Lawrence (Fig. 1), the species *Alexandrium tamarense* (Lebour) Balech, which is responsible for paralytic shellfish poisoning (PSP), produces extensive recurrent blooms during the summer months (Blasco et al. 1998). The factors controlling bloom dynamics are not yet fully understood, but previous studies in the lower St. Lawrence Estuary (LSLE) have emphasized the importance of freshwater runoff and water-column stability as the major factors controlling bloom dynamics (Therriault et al. 1985; Cembella et al. 1988; Larocque and Cembella 1990). Therriault et al. (1985) found that the pattern of PSP outbreaks and the spatial distribution of *A. tamarense* cells in the LSLE closely corresponded to the extent of the freshwater plume produced by the Manicouagan and Aux-Outardes rivers. However, the exact nature and the precise mechanisms underlying the freshwater *A. tamarense* relationship could not be clearly defined owing to the complex circulation pattern in the LSLE, which is characterized by eddies and transverse currents (Vezina et al. 1995; Savenkoff et al. 1997). We suspect that local populations of *A. tamarense* exist within the Estuary and Gulf, each with their own unique set of environmental and hydrological conditions that determine the timing and extent of bloom development. Until now, no study has examined in detail and over an extended period of time the association of *A. tamarense* blooms and river plumes in the St. Lawrence.

In this study, we examine the interannual variability of *A. tamarense* blooms over a 10-year period at Sept-Îles, in the Gulf of St. Lawrence (GSL). Sept-Îles, where significant *A. tamarense* concentrations are often observed, is an ideal site to examine the effects of freshwater runoff on bloom dynamics. First, Sept-Îles is located in an area where sources of freshwater are restricted to north shore rivers as a result of the general circulation pattern in the GSL with no direct influence from the St. Lawrence Estuary (Fig. 1). Second, the nearby Moisie River, the most important river in terms of discharge rate, is not regulated by hydroelectric dams. Thus, a more natural relationship is expected between variations in yearly snowmelt, precipitation, river runoff, and subsequent *A. tamarense* blooms. The objective of this study was to assess how variations in precipitation, river runoff, and wind affect the bloom dynamics of *A. tamarense* at Sept-Îles using the analysis of the biological, meteorological, and hydrological data between 1989 and 1998.

Materials and methods

Study area

The Sept-Îles monitoring station is located at the eastern entrance of the Sept-Îles Bay, in the northwestern GSL (Fig. 1). The GSL is a semi-enclosed sea and is forced at various temporal and spatial scales by tides from the Atlantic Ocean, local and large-scale meteorological seasonal and transient events, freshwater runoff and heat flux, and perturbations at the continental shelf (see review by Koutitonsky and Bugden 1991). The continuous supply of freshwater from the St. Lawrence River and other tributaries in the GSL watershed maintains a density-driven circulation with an outflow of lighter waters near the surface and a penetration of Atlantic waters in deeper layers (Koutitonsky and Bugden 1991). Figure 1 illustrates the main features of the summer surface circulation pattern in the St. Lawrence, which is characterized by the Gaspé current, a strong coastal jet flowing seaward along the Gaspé Peninsula, and by the presence of a quasi-permanent anti-clockwise gyre west of Anticosti Island (El-Sabh 1976, 1979). In the northwest sector of the Gulf, an offshore pressure gradient along the northern Québec shore created by lateral runoff induces a coastal current (5–10 $cm \cdot s^{-1}$) towards the west (Koutitonsky and Bugden 1991). The Moisie River, located approximately 20 km east of Sept-Îles, is the most important river near Sept-Îles in terms of discharge rate. The freshwater plume produced by this river is expected to influence our sampling station owing to the dominant westward surface currents created by the anticlockwise Anticosti gyre (refer to Fig. 1).

Oceanographic, hydrological, and meteorological data

Data presented in this paper were collected at Sept-Îles between 1989 and 1998 through the toxic algae monitoring program of the Department of Fisheries and Oceans Canada (Maurice Lamontagne Institute, Mont-Joli, Québec). Details of the field and laboratory analyses have already been fully described (Blasco et al. 1998). To summarize, surface water samples were collected at high tide from the Sept-Îles dock on a weekly basis between mid-May and the end of October of each year using a Niskin bottle (General Oceanics Inc., Miami, Fla.) or a bucket. In situ surface-water temperature was measured with a mercury thermometer. A subsample was fixed with acidic Lugol's iodine solution for later identification and enumeration of phytoplankton cells using the Utermöhl (Utermöhl 1931) technique with a Leitz phase contrast inverted microscope (Leica Microsystems (Canada) Inc., Richmond Hill, Ont.). Another subsample was taken for later analysis of salinity using a Guildline salinometer (model Autosal 8400T, Ocean Scientific International Ltd., Hampshire, U.K.). To test whether the presence of *A. tamarense* cells could be predicted from the surface salinity data at Sept-Îles, we tabulated the presence or absence of cells at the monitoring station between 1990 and 1998 for 13 salinity classes and converted this to the percent occurrence of cells per salinity class. The same analysis was carried out for Baie Comeau, located in the lower St. Lawrence Estuary (Fig. 1).

The daily Moisie River discharge, recorded about 35 km upstream from the mouth of the river, was supplied by Envi-

© 2002 NRC Canada

Fig. 1. Map of the Estuary and Gulf of St. Lawrence, Canada, showing the location of the Sept-Îles monitoring station, and the general summer surface circulation pattern (adapted from El-Sabh 1976, 1979).

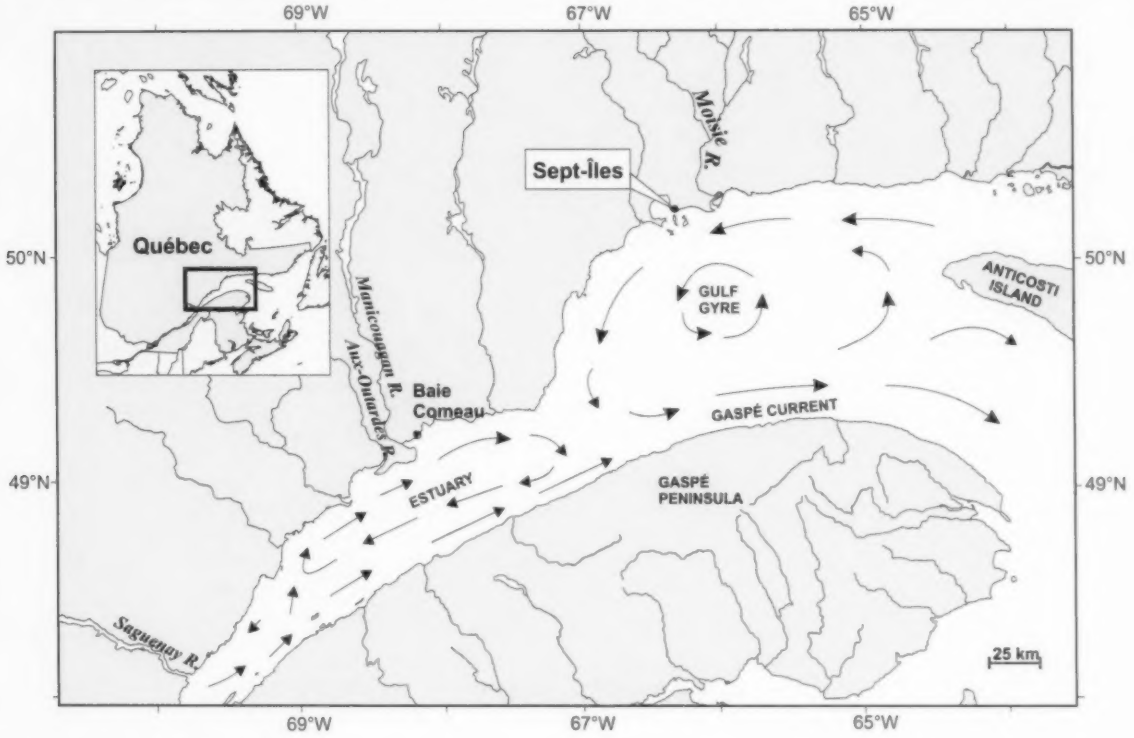

ronment Canada and the Ministère de l'Environnement et Faune Québec. We classified our 10-year data set into years of "low" and "high" summer Moisie River runoff relative to the 30-year average (1968–1997) to assess how variations in freshwater runoff affect the bloom dynamics of *A. tamarense* at Sept-Îles. Total daily rainfall and hourly winds (direction and speed) recorded at the weather station near Sept-Îles were supplied by Environment Canada.

Results

Oceanographic data

The analysis of the 10-year data set (i.e., weekly samples from mid-May to the end of October of each year between 1989 and 1998) revealed year-to-year variations in the timing and magnitude of *A. tamarense* blooms. Cells (≥20 cells·L^{-1}) were present as early as the week of 14 May and as late as the week of 22 October, but were recorded almost each year during a 3-week period between the week of 18 June and the week of 2 July (data not shown). This corresponds to a period when water temperatures are generally warm (12.0 ± 1.9°C) and salinity values relatively low (26.3 ± 2.6‰). Temperatures ranged from 2 to 18°C between mid-May and the end of October, 1989–1998, and followed the seasonal warming and cooling cycle each year (Fig. 2*a*). Salinity ranged between 20 and 31‰ during the same period, but exhibited significant interannual variability (Fig. 2*b*). Years during which low salinity values were recorded generally corresponded to years of high cell concentrations (Figs. 2*b* and 2*c*). Cells were detected each year, but exceeded 1000 cells·L^{-1} (the concentration at which shellfish generally become toxic in the St. Lawrence) during 1992, 1994, 1995, 1996, 1997, and 1998. The highest concentration was recorded in 1994, with 38 735 cells·L^{-1}, followed by 1996 and 1997, with 17 760 and 8480 cells·L^{-1}, respectively (Fig. 2*c*). Although *A. tamarense* cells were recorded in a wide range of temperature and salinity values, the highest cell concentrations were mainly associated with warm (≥12°C) and brackish (20–26‰) waters (Fig. 3).

Moisie River runoff, salinity, and *A. tamarense* blooms

The monthly Moisie River runoff and salinity values were averaged over each month between June and September, 1990–1998 (Fig. 4). We found a significant correlation (r^2 = 0.58, $P < 0.0001$) between Moisie River runoff and salinity recorded at Sept-Îles.

Years of low and high summer Moisie River runoff relative to the 30-year average (1968–1997) are presented in Fig. 5 along with associated salinity anomalies and *A. tamarense* cell concentrations. All six low-runoff years (1989, 1990, 1991, 1993, 1995, and 1998) were characterized by an earlier and (or) lower than average spring freshet, which translated into lower than average river runoff during June (Fig. 5*a*). These years, with the exception of 1993 and 1998, were also characterized by 5–32% less rainfall when compared with the average total rainfall recorded for the June to

© 2002 NRC Canada

Fig. 2. Interannual variability of (*a*) temperature (°C), (*b*) salinity (‰), and (*c*) *Alexandrium tamarense* cell abundance (cells·L^{-1}) at Sept-Îles between mid-May and the end of October, 1989–1998. Data were only available as of mid-June 1990 and mid-July 1989 and 1992. The dotted line at 1000 cells·L^{-1} represents the concentration at which shellfish generally become toxic in the St. Lawrence (80 µg STX eq·100 g meat^{-1}).

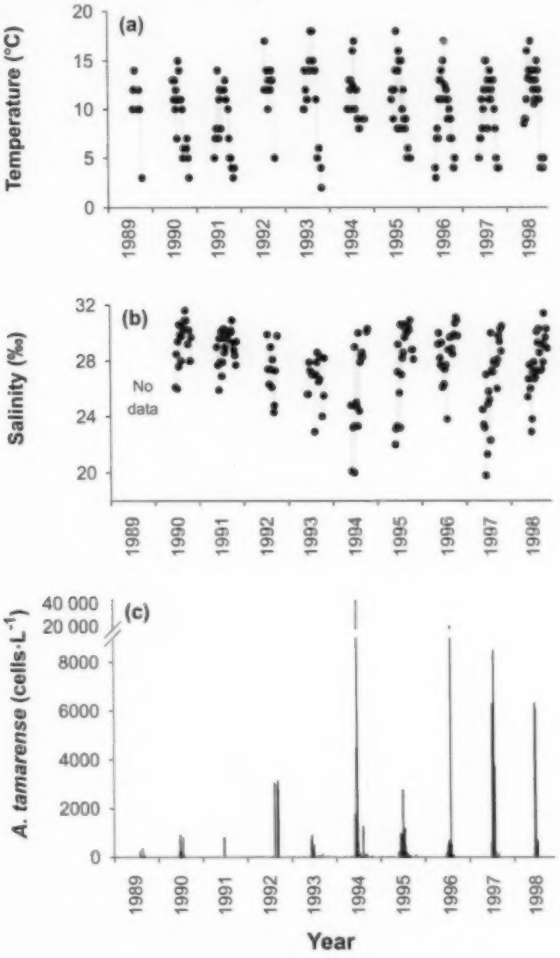

Fig. 3. Abundance ranking of *Alexandrium tamarense* vs. temperature (°C) and salinity (‰) at Sept-Îles between mid-May and the end of October, 1990–1998. No salinity data were available for 1989. The circle encompasses most of the highest cell concentrations.

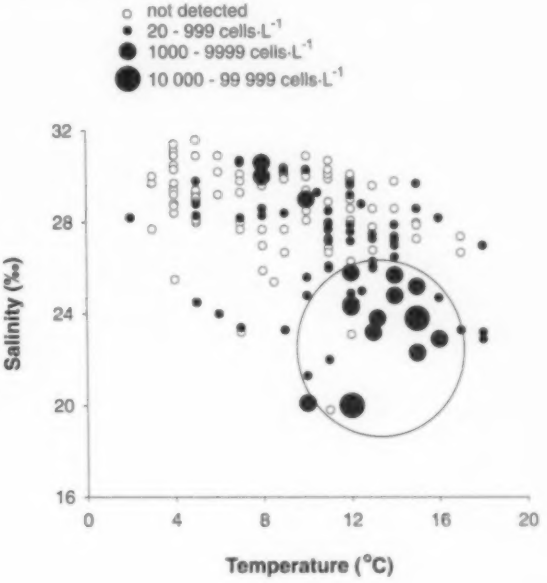

Fig. 4. Monthly salinity values (‰) recorded at Sept-Îles vs. the monthly Moisie River runoff (m^3·s^{-1}) from June to September, 1990–1998. No salinity data were available for 1989.

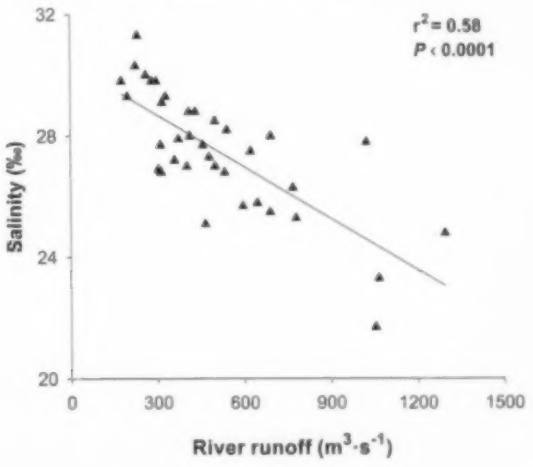

August, 1961–1990 period by Environment Canada (1993). Mainly above-average salinity values, relative to the 10-year average (Fig. 5*b*), and low *A. tamarense* cell concentrations (Fig. 5*c*) were associated with these six low-runoff years. When an exceptionally strong rainfall event occurred during an otherwise low runoff summer, substantial *A. tamarense* cell concentrations were recorded. For example during mid-June 1998, 91.8 mm of rain fell within seven days, which is almost the total average June rainfall (92.3 mm) recorded between 1961 and 1990 by Environment Canada (1993) (data not shown). This resulted in a negative salinity anomaly (Fig. 5*b*) and more than 6000 *A. tamarense* cells·L^{-1} (Fig. 5*c*). Years of high summer river runoff (i.e., 1992, 1994, 1996, and 1997) were characterized by a strong spring freshet occurring at approximately the same time as the 30-year average (Fig. 5*d*). Furthermore, during 1992 and 1994, 28–50% more rainfall was recorded for the June to August period than the average recorded by Environment Canada (1993). The four high-runoff years were characterized by mainly lower than average salinity values (Fig. 5*e*) and high *A. tamarense* cell concentrations (Fig. 5*f*). Thus, in general, years of low cell concentrations were associated with low

© 2002 NRC Canada

Fig. 5. The 10-year data set was classified into years of (*a*) low and (*d*) high summer Moisie River runoff relative to the 30-year average (1968–1997). The arrow indicates the timing of the 1968–1997 average spring freshet maximum ($m^3 \cdot s^{-1}$). The deviations (anomaly) with respect to the 1990–1998 mean weekly salinity (‰) in (*b*) and (*e*) for low and high runoff years, respectively. *Alexandrium tamarense* cell concentrations (cells·L^{-1}) in (*c*) and (*f*) for low and high runoff years, respectively. No salinity data were available for 1989. Salinity and cell abundance data were only available as of mid-June 1990 and mid-July 1989 and 1992.

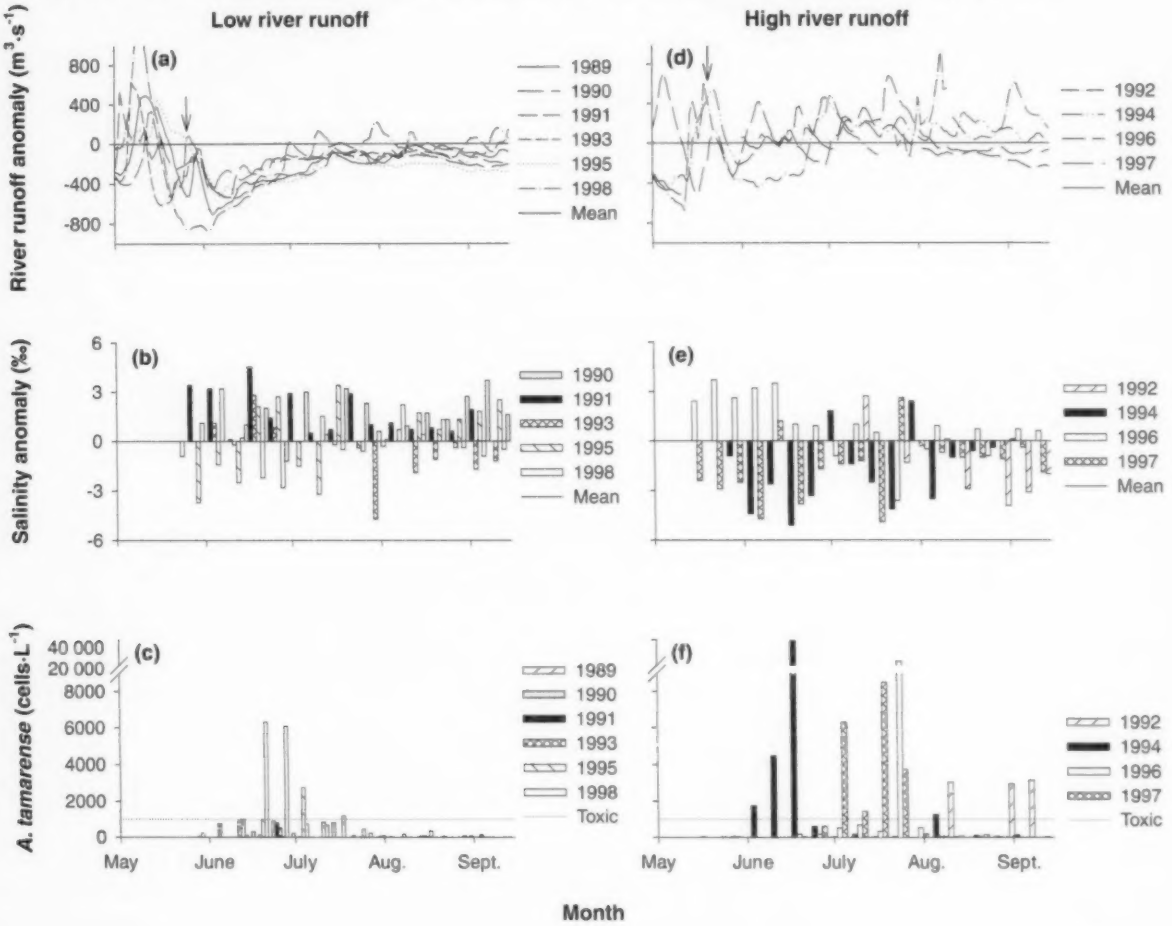

runoff, whereas high *A. tamarense* cell concentrations were associated with high runoff.

We illustrated the relationship between rainfall, Moisie River runoff, salinity, and *A. tamarense* blooms (Fig. 6). Both 1992 and 1996 were marked by exceptionally heavy rainfall during the summer months. Between 15 and 20 July 1996 a total of 95.2 mm of rain fell within only six days at Sept-Îles (Fig. 6*a*), which is more than the total monthly average of 90.8 mm recorded at this station during July (1961–1990) by Environment Canada (1993). This heavy rainfall event was followed by a sharp increase in Moisie River runoff by more than 400 $m^3 \cdot s^{-1}$, reaching a peak of 1150 $m^3 \cdot s^{-1}$ on 22 July. By 29 July, the salinity had decreased from 28‰ to 24‰ and more than 17 000 *A. tamarense* cells·L^{-1} were recorded (Figs. 6*b* and 6*c*). Similarly, high cell concentrations were recorded following two heavy rainfall events in 1992. The first event occurred during early August, when 54.0 mm fell within just three days (Fig. 6*d*). This is more than half the total rainfall usually recorded during the month of August by Environment Canada (Environment Canada 1993). The rainfall event was followed by a substantial increase in river runoff and the subsequent presence of more than 3000 *A. tamarense* cells·L^{-1} (Figs. 6*d* and 6*f*). The second event occurred during late August – early September (74 mm within 12 days) and resulted in increased Moisie River runoff by 600 $m^3 \cdot s^{-1}$, a drop in salinity by 4‰, and close to 3000 *A. tamarense* cells·L^{-1} the following week (Figs. 6*d*–6*f*). No cells were recorded above our level of detection at any other time during 1992.

An attempt was made to determine whether the first annual appearance of cells was triggered by a heavy rainfall event. The data from 1991, 1996, and 1998 suggest that the first appearance of cells is indeed preceded by strong rainfall and is followed by a period of weak winds, which is associated with a drop in salinity and a rise in temperature at the sampling station (Table 1). For example, *A. tamarense* cells

© 2002 NRC Canada

Fig. 6. Association between heavy rainfall, river runoff, salinity, and *Alexandrium tamarense* blooms at Sept-Îles during 1992 and 1996. Daily Moisie River runoff ($m^3 \cdot s^{-1}$; solid line) and rainfall (mm; bars) during (*a*) 1996 and (*d*) 1992; salinity (‰) during (*b*) 1996 and (*e*) 1992; *A. tamarense* cell concentrations ($cells \cdot L^{-1}$) during (*c*) 1996 and (*f*) 1992. Salinity and cell abundance data were only available as of mid-July 1992.

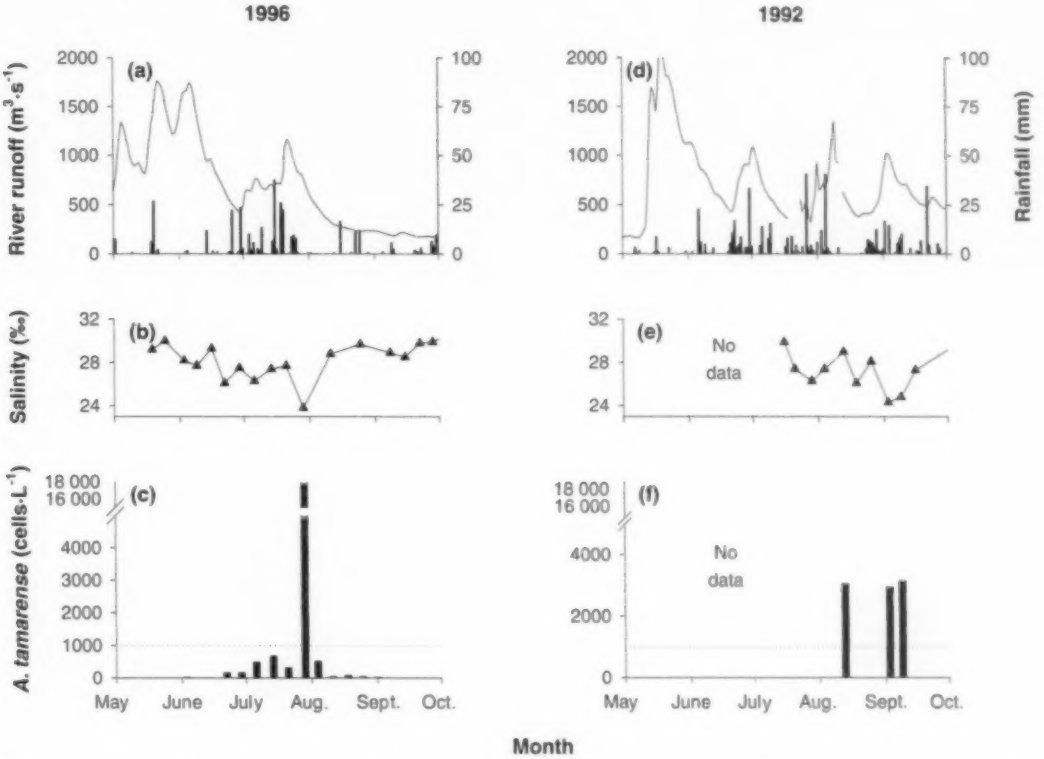

Table 1. Environmental conditions preceding the first appearance of *Alexandrium tamarense* cells in surface water samples in 1991, 1996, and 1998 at Sept-Îles.

Date of sample	*A. tamarense* concentration ($cells \cdot L^{-1}$)	Rainfall (mm)	Salinity (‰)	Temperature (°C)	Wind speed ($m \cdot s^{-1}$)
27 May 1991	0	0.8	29	5	5.0 ± 2.6
5 June 1991	0	5.6	28	7	4.7 ± 1.7
12 June 1991	0	18.4	26	8	4.8 ± 2.3
17 June 1991	0	16.8	30	8	6.0 ± 2.2
25 June 1991	785	13.1	28	14	3.8 ± 2.1
19 May 1996	0	0	29	4	4.9 ± 2.2
25 May 1996	0	35.6	30	3	5.1 ± 3.0
3 June 1996	20	0	28	7	4.0 ± 2.1
24 May 1998	0	32.4	25	9	3.0 ± 1.6
31 May 1998	0	16.0	27	9	3.6 ± 1.8
7 June 1998	0	51.4	28	9	4.1 ± 2.0
14 June 1998	100	8.0	26	11	2.7 ± 1.2

Note: For the first sampling day of each year, the total rainfall and average wind speed were calculated from the seven preceding days.

were first recorded on 25 June 1991 following a week of low wind speeds (3.8 ± 2.1 $m \cdot s^{-1}$) and 16.8 mm of rain. During this time, the salinity dropped from 30 to 28‰, the temperature rose from 8 to 14°C, and 785 $cells \cdot L^{-1}$ were recorded. Similar patterns were observed in 1996 and 1998. During 1993, 1994, 1995, and 1997, *A. tamarense* cells were already present as of the first sampling day (mid-May to early June) and were associated with low salinity values (22–25‰), and with the exception of 1997, warm temperatures (10–11°C). The years 1994 and 1995 were among the three years where average wind speeds during the month of May (4.0 ± 2.1 and 4.1 ± 2.2 $m \cdot s^{-1}$, respectively) were the

© 2002 NRC Canada

lowest in the 10-year period. Furthermore, the month of May in 1994 and 1997 received 20 and 65% more rain, respectively, than the 1961–1990 average recorded by Environment Canada (1993). As for 1989, 1990, and 1992, sampling data was only available later in the season (end of June or mid-July). Thus, the first appearance of cells appears to be preceded by strong rainfall and a period of weak winds, the timing varying from year to year.

Development and dissipation of blooms—the influence of wind

Although *A. tamarense* cells were often observed over several consecutive weeks during the summer months, high concentrations were generally only observed at Sept-Îles for a short period of time. In contrast, in 1994, the bloom period lasted several weeks and produced high cell concentrations that allowed us to investigate the hydrological and meteorological conditions responsible for the development, persistence, and dissipation of the bloom. We illustrated the combined influence of rainfall, river runoff, and wind on this *A. tamarense* bloom (Fig. 7). The runoff from the Moisie River remained high throughout the month of June following the spring freshet (Fig. 7*a*). An exceptionally long period of weak winds that averaged 3.3 ± 1.8 $m \cdot s^{-1}$ and lasted for three weeks was associated with low salinity values (20–23‰) in June (Figs. 7*b* and 7*c*). On 30 May the concentration of *A. tamarense* cells was 40 cells·L^{-1} and gradually increased to reach 38 735 cells·L^{-1} on 22 June (Fig. 7*d*), the highest concentration recorded throughout the 10-year period. The dissipation of the bloom coincided with strong wind events, that is: (*i*) speeds of 8–11 $m \cdot s^{-1}$ lasting for 15 h on 26 June and (*ii*) speeds of 9–13 $m \cdot s^{-1}$ lasting for 18 h on 28 June.

Salinity index

Because surface salinity reflects the general state of the water column in terms of freshwater input and water column stability, we examined the relationship between salinity and the occurrence of *A. tamarense* cells at Sept-Îles. We present the percent occurrence of *A. tamarense* cells in relation to salinity for the 1990–1998 period (Fig. 8). For example, for a salinity of 28‰, *A. tamarense* was present in 16 of 32 samples, i.e., 50% of the time; for a salinity of 23‰, cells were present in 8 of 10 samples, i.e., 80% of the time (Fig. 8). The regression of all data points results in $r^2 = 0.77$ ($y = -7.7x + 259.6$, $n = 175$) and when data points of three samples or less are omitted from the regression, we obtain $r^2 = 0.86$ ($y = -10x + 328.63$, $n = 168$) for the 23–31‰ salinity range, which comprises 96% of samples from the study period. One can clearly see that the probability of observing *A. tamarense* cells at Sept-Îles increases with decreasing salinity values. The same analysis carried out at Baie Comeau (refer to Fig. 1 for location) between 1990 and 1998 revealed a similar negative correlation ($r^2 = 0.72$, $y = -6.5x + 218.5$, $n = 175$) between salinity and the occurrence of *A. tamarense* cells for the 21–31‰ salinity range, comprising 94% of samples from the study period (Fig. 9).

Discussion

The strong correlation between salinity and the occurrence of *A. tamarense* cells at Sept-Îles highlights the importance of freshwater runoff for *A. tamarense* bloom dynamics in the St. Lawrence. Indeed, a previous study conducted in the St. Lawrence Estuary found that the spatial distribution of *A. tamarense* cells coincided with the brackish waters of the plume produced by the Manicouagan and Aux-Outardes rivers (Therriault et al. 1985). The present study, more in-depth and over a 10-year period (1989–1998), shows that this type of relationship also exists in the Gulf of St. Lawrence because *A. tamarense* blooms near Sept-Îles were mainly associated with low-salinity waters, essentially those of the plume produced by the Moisie River.

In general, few *A. tamarense* cells were recorded during years of low summer river runoff. Because there are no hydroelectric dams on the Moisie River, river runoff during the summer months is principally influenced by the timing and duration of the spring freshet and rainfall over the region. When the spring freshet occurred early, i.e., before mid-May, few *A. tamarense* cells were usually recorded. In con-

Fig. 7. Environmental conditions preceding the 1994 bloom at Sept-Îles. (*a*) Daily Moisie River runoff ($m^3 \cdot s^{-1}$) (solid line) and rainfall (mm) (bars), (*b*) salinity (‰), (*c*) wind speed ($m \cdot s^{-1}$), and (*d*) *A. tamarense* cell abundance (cells·L^{-1}).

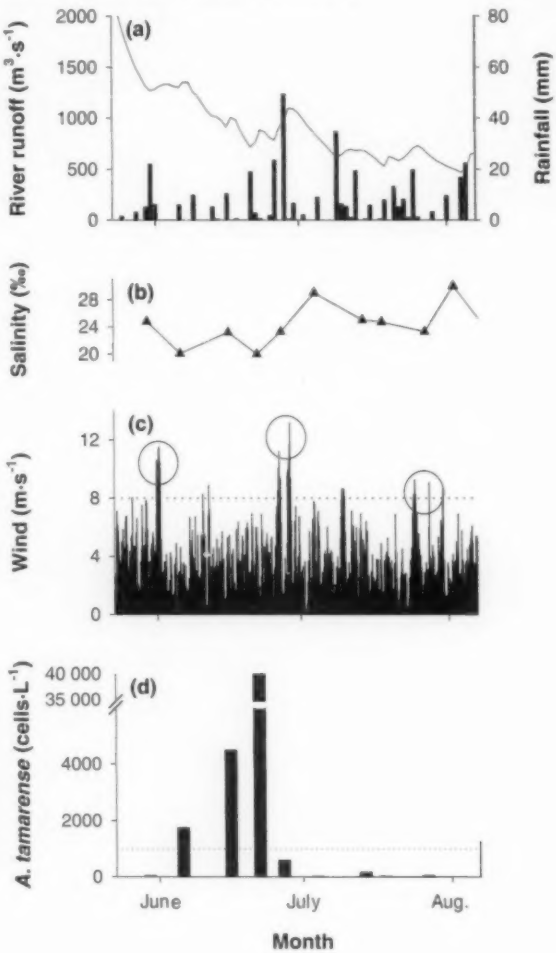

© 2002 NRC Canada

Fig. 8. The probability of observing *A. tamarense* cells at Sept-Îles vs. salinity. The percentage was calculated by tabulating when cells were present in samples for each salinity class, and converting this to a percent occurrence of cells. (○), Salinity classes consisting of three samples or less; (●), salinity classes consisting of between 5 and 36 samples. The linear regression of all data points is represented by the dotted line ($r^2 = 0.77$, $y = -7.7x + 259.6$, $n = 175$). The linear regression of points with four or more samples per salinity class (●) is represented by the solid line ($r^2 = 0.86$, $y = -10x + 328.63$, $n = 168$) and comprises 96% of samples from 1990 to 1998.

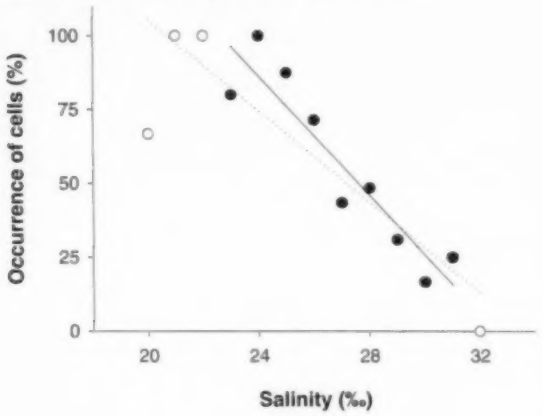

Fig. 9. The probability of observing *A. tamarense* cells at Baie Comeau vs. salinity. The percentage was calculated by tabulating when cells were present in samples for each salinity class, and converting this to a percent occurrence of cells. The linear regression of data points with four or more samples per salinity class is represented by the solid line ($r^2 = 0.72$, $y = -6.5x + 218.5$, $n = 175$) and comprises 94% of samples from 1990 to 1998.

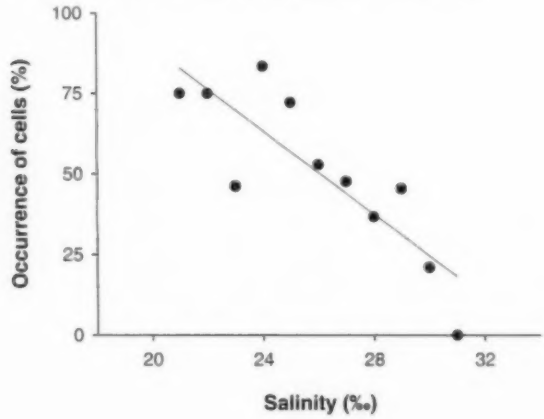

trast, an *A. tamarense* bloom developed in June 1994 when the spring freshet lasted for a long time, either because of more snow or slower melting. The June 1994 bloom was the earliest bloom recorded during the 10-year period, exceeding 1000 cells·L^{-1} as of the first week of June and reaching close to 40 000 cells·L^{-1} by mid-June. Although the timing and duration of the spring freshet may influence *A. tamarense* blooms early in the summer, day-to-day variations in precipitation appear to be more important in controlling *A. tamarense* bloom dynamics throughout the remainder of the summer.

Heavy rainfall events resulted in strong freshwater pulses from the Moisie River, a drop in salinity at Sept-Îles, and the subsequent presence of high *A. tamarense* cell concentrations. This is the first time that it is shown in the St. Lawrence that *A. tamarense* blooms can be initiated by heavy rainfall in the summer and fall. Previous studies have loosely associated rainfall events with phytoplankton blooms, such as that of an *Alexandrium minutum* bloom in a Mediterranean lagoon (Giacobbe et al. 1996) and a *Gyrodinium aureolum* bloom in a sea loch in Scotland (Jones et al. 1982). However, the timing and quantity of rainfall involved were not specified in these studies. Our results concord with those of Blanco et al. (1985) who reported that an *A. tamarense* red tide developed during a period of heavy precipitation, more than 2.75 times the average monthly rainfall, in the Ria de Ares and Betanzos, Spain.

The association between freshwater plumes and toxic phytoplankton blooms has been observed in several coastal areas of the world (Franks and Anderson 1992*a*; Taylor and Haigh 1993; Hallegraeff et al. 1995). However, it is unclear whether this association is principally caused by the direct effects of low salinity and high temperature on cellular growth rate, the supply of nutrients, dissolved organic matter, trace elements or other materials that might serve as growth stimulants, and (or) increased water column stability that favours the proliferation and retention of cells. Humic substances, which are supplied in freshwater runoff from heavily forested watersheds, such as those found on the Québec North Shore, may play a role in the bloom dynamics at Sept-Îles. Humic substances have been shown to have a positive effect on the growth rates and biomass production of several toxic dinoflagellates (Granéli and Moreira 1990; Carlsson et al. 1995; Doblin et al. 1999) and favour the growth of dinoflagellates over diatoms in culture (Granéli and Moreira 1990). Although no data on humic substances was available for this data set, recent laboratory studies carried out with *A. tamarense* cultures isolated from the St. Lawrence Estuary have shown that the addition of humic substances from three different sources (including a humic and a fulvic extract from the Manicouagan River) significantly enhanced overall cell density and growth rates relative to control treatments (R. Gagnon, Maurice Lamontagne Institute, Fisheries and Oceans Canada, Mont-Joli, Québec, personal communication).

Increased *A. tamarense* cell concentrations from one week to another at Sept-Îles are most likely the result of combined biological growth, vertical migration, and (or) advection of cells. If we assume only in situ biological growth, we obtain net population growth rates ranging between 0.1 day^{-1} and 0.5 day^{-1} throughout most of the sampling period (84%), which is within the 0.3–0.5 day^{-1} range of maximum growth observed in laboratory studies for this species (Levasseur et al. 1995; MacIntyre et al. 1997; Parkhill and Cembella 1999). However, the highest growth rate that we obtained was 0.7 day^{-1}, which is unrealistically high for this species. In addition to growth, increased cell concentrations could be

© 2002 NRC Canada

the result of high-density patches formed owing to the swimming behaviour of this species (Cullen and MacIntyre 1998 and references therein). Moreover, in frontal systems, vertical migration and convergent circulation can combine to accumulate cells (Franks 1992). In the Sept-Îles area, *A. tamarense* cells may be concentrated in convergence zones of the Moisie River plume front and advected to our coastal monitoring station. The increase in *A. tamarense* cell concentrations associated with high river runoff and low salinity may thus be the result of a combination of biological and physical processes.

Dinoflagellates are particularly well adapted for life in relatively calm, stratified conditions (Margalef 1978). They are active swimmers and are able to maintain themselves in the euphotic zone with comparative ease and access nutrients at depth if depleted in surface waters, whereas less-motile phytoplankton may sink out of the euphotic zone or become nutrient limited (Margalef 1978; Cullen and MacIntyre 1998). At our coastal monitoring station, prolonged periods of calm, stratified conditions favoured the continued development of *A. tamarense* blooms. For example, the June 1994 bloom was associated with high river runoff and an exceptionally long period of low wind speeds averaging 3.3 ± 1.8 $m \cdot s^{-1}$ over a 3-week period. Although 1996 and 1997 had a similar river runoff pattern during June, such a long and continuous period of low wind speeds was not observed and did not result in an *A. tamarense* bloom as in June 1994. These observations are in accordance with those of Hallegraeff et al. (1995) who noted that continuous periods of low wind speed (<5 $m \cdot s^{-1}$ for five days or more) were associated with PSP. Similarly, Blanco et al. (1985) reported that an *A. tamarense* bloom developed during a month of heavy precipitation and weak winds averaging 4 $m \cdot s^{-1}$ that was progressively destroyed following winds of 7 $m \cdot s^{-1}$. Although wind speeds greater than 8 $m \cdot s^{-1}$ accounted for only 5% of occurrences during the June–August period (1989–1998) at Sept-Îles, our results suggest that increased mixing of the water column, reflected in an increase in salinity and decrease in temperature, are associated with these winds. The wind-induced processes involved in the decline of blooms still remain uncertain. Mixing associated with turbulent conditions may discourage the formation of blooms because of the physical dispersion of cells. Dinoflagellate growth may also be negatively impacted by turbulence through the direct effects of fluid shear on cell physiology as demonstrated by several laboratory experiments (Thomas and Gibson 1990; Berdalet and Estrada 1993; review by Smayda 1997). Recently, Juhl et al. (2001) demonstrated that the net population growth of *A. fundyense* in cultures decreased with shear flow similar to levels expected in near-surface waters on a windy day for exposures greater than 1 $h \cdot day^{-1}$, and became negative with exposures greater than 12 $h \cdot day^{-1}$.

The analysis of this 10-year data set indicates that the timing of *A. tamarense* blooms at Sept-Îles is related to a combination of key environmental variables, notably temperature, salinity, rainfall, Moisie River runoff, and wind, whereas the magnitude of blooms is controlled by the duration of these favourable conditions promoting bloom development. The fact that significant interannual variability in both the timing and magnitude of *A. tamarense* blooms is observed over the 10-year period demonstrates that this proper combination of factors is not met every year. Our results reveal that there was a "window" when *A. tamarense* cells were present in the surface waters every year, i.e., the last two weeks of June and the first week of July. This is a period when the water column has warmed substantially and is more likely to be stratified. Nonetheless, our results indicate that other factors, such as high river runoff and low wind speeds that further intensify vertical stratification, are required for an *A. tamarense* bloom to fully develop at Sept-Îles. Year-to-year variations in the timing of the spring freshet, occurrence of heavy rainfall events, and periods of low wind speeds will thus influence *A. tamarense* bloom dynamics, as will climate changes that affect these forcing factors.

In summary, local oceanographic, hydrological, and meteorological conditions are important for the initiation, development, and maintenance of *A. tamarense* blooms at Sept-Îles. Salinity can be considered an indication of freshwater input and water column stability and the importance of both these factors is inferred by the strongly significant negative correlation between surface salinity and the occurrence of *A. tamarense* cells at Sept-Îles, as well as at Baie Comeau, during the study period. We suspect that a similar relationship exists between *A. tamarense* blooms and other rivers along the Québec North Shore. Finally, this simple index, whereby the presence of cells can be predicted from the surface salinity data, could be a very useful tool to predict toxic blooms.

Acknowledgements

The authors wish to thank A. Vezina, R. Gagnon, and J.-Y. Couture for helpful comments, G. Fortin for help with the map, and two anonymous reviewers for their critical review of the manuscript. This research was supported in part by the Government of Canada's Climate Change Action Fund and the Science Strategic Fund from Fisheries and Oceans Canada.

References

Berdalet, E., and Estrada, M. 1993. Effects of turbulence on several dinoflagellate species. *In* Toxic phytoplankton blooms in the sea. Developments in Marine Biology. Vol. 3. *Edited by* T.J. Smayda and Y. Shimizu. Elsevier, Amsterdam, The Netherlands. pp. 737–740.

Blanco, J., Marino, J., and Campos, M.J. 1985. The first toxic bloom of *Gonyaulax tamarensis* detected in Spain (1984). *In* Toxic dinoflagellates. *Edited by* D.M. Anderson, A.W. White, and D.G. Baden. Elsevier, New York. pp. 79–84.

Blasco, D., Levasseur, M., Gélinas, R., Larocque, R., Cembella, A.D., Huppertz, B., and Bonneau, E. 1998. Monitorage du phytoplancton toxique et des toxines de type IPM dans les mollusques du Saint-Laurent: 1989 à 1994. Rapp. Stat. Can. Hydrogr. Sci. Océan. No. 151.

Carlsson, P., Granéli, E., Tester, P., and Boni, L. 1995. Influences of riverine humic substances on bacteria, protozoa, phytoplankton, and copepods in a coastal plankton community. Mar. Ecol. Prog. Ser. **127**: 213–221.

Cembella, A.D., Turgeon, J., Therriault, J.-C., and Beland, P. 1988. Spatial distribution of *Protogonyaulax tamarensis* resting cysts in nearshore sediments along the north coast of the lower St. Lawrence Estuary. J. Shellfish Res. **7**: 597–609.

© 2002 NRC Canada

Cullen, J.J., and MacIntyre, J.G. 1998. Behavior, physiology, and the niche of depth-regulating phytoplankton. *In* Physiological ecology of harmful algal blooms. *Edited by* D.M. Anderson, A.D. Cembella, and G.M. Hallegraeff. NATO ASI Series. Vol. G41. Springer-Verlag, Berlin, Heidelberg. pp. 559–579.

Doblin, M.A., Blackburn, S.I., and Hallegraeff, G.M. 1999. Growth and biomass stimulation of the toxic dinoflagellate *Gymnodinium catenatum* (Graham) by dissolved organic substances. J. Exp. Mar. Biol. Ecol. **236**: 33–47.

El-Sabh, M.I. 1976. Surface circulation patterns in the Gulf of St. Lawrence. J. Fish. Res. Board Can. **33**: 124–138.

El-Sabh, M.I. 1979. The lower St. Lawrence Estuary as a physical oceanographic system. Nat. Can. **106**: 55–73.

Environment Canada. 1993. Canadian climate normals 1961–1990: Quebec. Atmospheric Environment Service, Environment Canada, Ottawa, Canada.

Franks, P.J.S. 1992. Sink or swim: accumulation of biomass at fronts. Mar. Ecol. Prog. Ser. **82**: 1–12.

Franks, P.J.S., and Anderson, D.M. 1992*a*. Alongshore transport of a toxic phytoplankton bloom in a buoyancy current: *Alexandrium tamarense* in the Gulf of Maine. Mar. Biol. **116**: 153–164.

Franks, P.J.S., and Anderson, D.M. 1992*b*. Toxic phytoplankton blooms in the southwestern Gulf of Maine: testing hypotheses of physical control using historical data. Mar. Biol. **112**: 165–174.

Giacobbe, M.G., Oliva, F.D., and Maimone, G. 1996. Environmental factors and seasonal occurrence of the dinoflagellate *Alexandrium minutum*, a PSP potential producer, in a Mediterranean lagoon. Est. Coast. Shelf Sci. **42**: 539–549.

Granéli, E., and Moreira, M.A. 1990. Effects of water of different origin on the growth of marine dinoflagellates and diatoms in laboratory cultures. J. Exp. Mar. Biol. Ecol. **136**: 89–106.

Hallegraeff, G.M., McCausland, M.A., and Brown, R.K. 1995. Early warning of toxic dinoflagellate blooms of *Gymnodinium catenatum* in southern Tasmanian waters. J. Plankton Res. **17**: 1163–1176.

Jones, K.J., Ayres, P., Bullock, A.M., Roberts, R.J., and Tett, P. 1982. A red tide of *Gyrodinium aureolum* in sea lochs of the Firth of Clyde and associated mortality of pond-reared salmon. J. Mar. Biol. Assoc. **62**:771–782.

Juhl, A.R., Trainer, V.L., and Latz, M.I. 2001. Effect of fluid shear and irradiance on population growth and cellular toxin content of the dinoflagellate *Alexandrium fundyense*. Limnol. Oceanogr. **46**: 758–764.

Koutitonsky, V.G., and Bugden, G.L. 1991. The physical oceanography of the Gulf of St. Lawrence: a review with emphasis on the synoptic variability of the motion. *In* The Gulf of St. Lawrence: small ocean or big estuary? *Edited by* J.-C. Therriault. Can. Spec. Publ. Fish. Aquat. Sci. No. 113. Fisheries and Oceans Canada, Ottawa. pp. 57–90.

Larocque, R., and Cembella, A.D. 1990. Ecological parameters associated with the seasonal occurrence of *Alexandrium* spp., and consequent shellfish toxicity in the lower St. Lawrence Estuary (eastern Canada). *In* Toxic marine phytoplankton. *Edited by* E. Granéli, B. Sundströem, L. Edler, and D.M. Anderson. Elsevier, New York. pp. 368–373.

Levasseur, M., Gamache, T., St.-Pierre, I., and Michaud, S. 1995. Does the cost of NO_3^- reduction affect the production of harmful compounds by *Alexandrium excavatum*? *In* Harmful marine algal blooms. *Edited by* P. Lassus, G. Arzul, E. Erard, P. Gentien, and C. Marcaillou. Lavoisier, Intercept Ltd., Paris. pp. 463–468.

MacIntyre, J.G., Cullen, J.J., and Cembella, A.D. 1997. Vertical migration, nutrition and toxicity in the dinoflagellate *Alexandrium tamarense*. Mar. Ecol. Prog. Ser. **148**: 201–216.

Margalef, R. 1978. Life-forms of phytoplankton as survival alternatives in an unstable environment. Oceanol. Acta, **1**: 493–509.

Margalef, R., Estrada, M., and Blasco, D. 1979. Functional morphology of organisms involved in red tides, as adapted to decaying turbulence. *In* Toxic dinoflagellate blooms. Proceedings of the 2nd International Conference. *Edited by* D.L. Taylor, H.H. Seliger, and C.M. Lewis. Elsevier North Holland, New York. pp. 89–94.

Parkhill, J.-P., and Cembella, A.D. 1999. Effects of salinity, light and inorganic nitrogen on growth and toxigenicity of the marine dinoflagellate *Alexandrium tamarense* from northeastern Canada. J. Plankton Res. **21**: 939–955.

Prakash, A. 1967. Growth and toxicity of a marine dinoflagellate, *Gonyaulax tamarensis*. J. Fish. Res. Board. Can. **24**: 1589–1606.

Ryther, J.H. 1955. Ecology of autotrophic marine dinoflagellates with reference to red water conditions. *In* The luminescence of biological systems. *Edited by* F.H. Johnson. American Association for the Advancement of Science, Washington, D.C. pp. 387–414.

Savenkoff, C., Vezina, A.F., and Gratton, Y. 1997. Effect of a freshwater pulse on mesoscale circulation and phytoplankton distribution in the lower St. Lawrence Estuary. J. Mar. Res. **55**: 353–381.

Smayda, T.J. 1997. Harmful algal blooms: their ecophysiology and general relevance to phytoplankton blooms in the sea. Limnol. Oceanogr. **42**: 1137–1153.

Taylor, F.J.R., and Haigh, R. 1993. The ecology of fish-killing blooms of the chloromonad flagellate *Heterosigma* in the Strait of Georgia and adjacent waters. *In* Toxic phytoplankton blooms in the sea. *Edited by* T.J. Smayda and Y. Shimizu. Elsevier Science Publishers B.V., Amsterdam, The Netherlands. pp. 705–710.

Therriault, J.-C., Painchaud, J., and Levasseur, M. 1985. Factors controlling the occurrence of *Protogonyaulax tamarensis* and shellfish toxicity in the St. Lawrence Estuary: freshwater runoff and the stability of the water column. *In* Toxic dinoflagellates. *Edited by* D.M. Anderson, A.W. White, and D.G. Baden. Elsevier, New York. pp. 141–146.

Thomas, W.H., and Gibson, C.H. 1990. Effects of small-scale turbulence on microalgae. J. Appl. Phycol. **2**: 71–77.

Utermöhl, N. 1931. Neue Wege in der quantitativen Erfassung des Planktons. Verh. Int. Verein. Theor. Angew. Limnol. **5**: 567–596.

Vezina, A.F., Gratton, Y., and Vinet, P. 1995. Mesoscale physical-biological variability during a summer phytoplankton bloom in the lower St Lawrence Estuary. Estuar. Coast. Shelf Sci. **41**: 393–411.

© 2002 NRC Canada

Avoidance of solar ultraviolet radiation by juvenile coho salmon (*Oncorhynchus kisutch*)

David J. Kelly and Max L. Bothwell

Abstract: Shade-seeking behavior and avoidance of solar ultraviolet radiation (UVR) by newly emerged coho salmon (*Oncorhynchus kisutch*) alevins and two-month-old coho juveniles was documented in experimental trials in the Little Qualicum River, British Columbia, using outdoor chambers that provided the fish with a binary choice of photo environments. Under high solar intensities (i.e., midsummer, cloudless skies) coho of both age classes strongly preferred 50% neutral density shaded conditions to unattenuated full-spectrum (280–700 nm) sunlight (t test, $p < 0.025$). In addition, coho alevins and juveniles showed a high selective avoidance of UVR (280–400 nm) (t test, $p < 0.05$). Within the UVR spectrum, coho responded significantly to UVA (320–400 nm) (t test, $p = 0.028$). Evidence of UVB (280–320 nm) avoidance was confounded by higher visible and UVA irradiance levels under screens exposing coho to UVB. Under lower solar intensities (i.e., cloudy skies) coho showed no spectral preference and did not seek neutral density shade. Behavioral avoidance of high intensity UVR, particularly UVA, suggests that shade-seeking behavior of juvenile coho may be linked to avoiding potentially harmful UVR exposure.

Résumé : Des chambres d'observation à l'extérieur qui offrent un choix binaire d'environnements lumineux nous ont permis d'étudier expérimentalement les comportements de recherche de l'ombre et d'évitement de la radiation solaire ultraviolette (UVR) chez des alevins nouvellement émergés et des jeunes saumons coho (*Oncorhynchus kisutch*) âgés de 2 mois dans la petite rivière Qualicum en Colombie-Britannique. Sous de fortes intensités de radiation solaire, (i.e., à la mi-été, sous un ciel découvert), les saumons des deux groupes préfèrent nettement des conditions d'ombrage de densité neutre de 50 % à la lumière solaire non-filtrée de plein spectre (280–700 nm) (test de t, $p < 0{,}025$). Les saumons réagissent de façon significative aux radiations UVA (320–400 nm) dans le spectre des UVR (test de t, $p = 0{,}028$). Les indications de l'existence d'un évitement des radiations UVB sont masquées par la présence de niveaux d'irradiance de lumière visible et UVA sous les filtres exposant les saumons à l'UVB. Dans des conditions d'intensité solaire réduites (i.e., sous un ciel nuageux), les saumons n'affichent pas de préférence pour une région particulière du spectre lumineux et ne recherchent pas l'ombre de densité neutre. L'évitement de l'UVR de haute intensité, particulièrement de l'UVA, par les jeunes saumons coho laisse croire que le comportement de recherche de l'ombre est relié à l'évitement d'une exposition potentiellement nocive à la radiation UVR.

[Traduit par la Rédaction]

Introduction

Ultraviolet radiation (UVR; 280–400 nm) is now recognized as a potentially important factor affecting organisms in fresh water (reviewed by Häder et al. 1998). Declines in coho salmon (*Oncorhynchus kisutch*) stocks throughout the Pacific Northwest have prompted speculation that increases in solar ultraviolet-B (UVB; 280–320 nm) radiation associated with global ozone depletion may be impacting salmonids during freshwater rearing, leading to reduced ocean survivorship (Walters and Ward 1998). Such a worrisome scenario would explain why declines in salmonid stocks have been observed over broad geographical areas (Beamish et al. 1997; Coronado and Hilborn 1998). Spring-time stratospheric ozone depletion has been worsening over northern regions in the past two decades (Hansen and Chipperfield 1998) and erythemal UVB reaching the earth's surface at mid-northerly latitudes has increased by between 4% (summer and fall) and 7% (winter–spring) since the 1970s (Madronich et al. 1998). Additionally, human activities such as deforestation and the effects of climate warming and acid deposition on dissolved organic matter (DOM) export (the principal attenuator of UVR in fresh water), synergistically act to increase the exposure of freshwater biota to UVR (Schindler et al. 1996; Williamson et al. 1996; Yan et al. 1996). Shallow freshwater systems used by coho during early life stages may therefore be exposed to biologically significant amounts of UVR.

UVR can have negative physiological effects on both fish and amphibians (Siebeck et al. 1994). Findings have included effects of UVB on egg survival (Williamson et al. 1997; Novales-Flamarique and Harrower 1999), larval development (Hunter et al. 1979; Blaustein et al. 1997), cataract formation (Allison 1963; Steuke et al. 1968), skin lesions (Little and Fabacher 1994; Bullock and Coutts 1985), respi-

Received 13 June 2001. Accepted 5 February 2002. Published on the NRC Research Press Web site at http://cjfas.nrc.ca on 4 April 2002.
J16402

D.J. Kelly.[1,2] Department of Biological Sciences, University of Alberta, Edmonton, AB T6G 2E9, Canada.
M.L. Bothwell. National Water Research Institute, Pacific Biological Station, Nanaimo, BC V9R 5K6, Canada.

[1]Corresponding author (e-mail: d.kelly@niwa.cri.nz).
[2]Present address: National Institute of Water and Atmospheric Research, P.O. Box 8602, Riccarton, Christchurch, New Zealand.

 DOI: 10.1139/F02-023 © 2002 NRC Canada

Fig. 1. Schematic of the in-stream binary choice experimental enclosures used for the juvenile coho salmon (*Oncorhynchus kisutch*) behavioral trials at the Little Qualicum Channels. Each side of a chamber was covered with a different solar exclusion panel to create a binary choice for the fish. Four chambers, each with a different filter combination, were routinely used on each day. Spectral transmissions of the solar exclusion treatments are shown in Fig. 2.

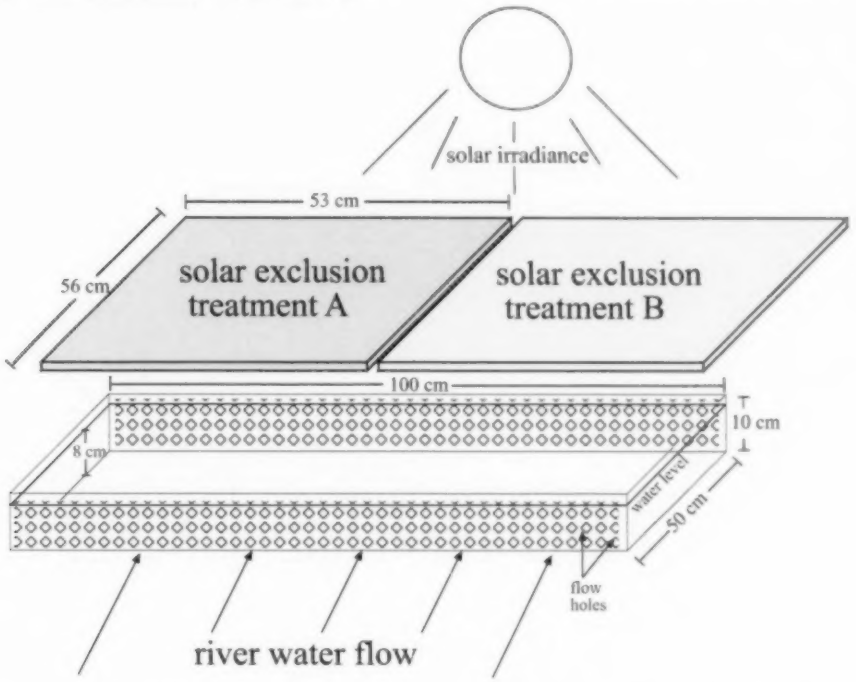

ratory control (Freitag et al. 1998), and immune system function (Salo et al. 1998). Early life history stages appear to be particularly susceptible to damage by UVR, most notably for species with pelagic nonpigmented larval forms (Hunter et al. 1979). In pigmented fish species, damage from UVB often occurs with the formation of epidermal lesions (Bullock and Coutts 1985), but recently has also been linked with sublethal impairment of immune system response (Salo et al. 1998). Although salmonid eggs incubate under gravel and alevins are pigmented upon emergence, juvenile coho potentially receive high exposure to UVR because of their extended rearing period (up to 2 years) in shallow freshwater environments.

Light is an important abiotic factor influencing habitat selection by salmonids (Fausch 1993). Juvenile salmonids are known to preferentially select habitat with overhead canopy cover and reduced light intensity (Lister and Genoe 1970; Heggenes et al. 1991). Use of in-stream cover to avoid high light levels is now recognized as an important feature of salmonid ecology in forested streams that have been subjected to clear-cutting (Shirvell 1990; Bugert et al. 1991). Traditionally, this shade-seeking behavior has been thought to be associated with predator avoidance. However, the known deleterious effects of UVR exposure on fish indicate another potential benefit of such behavior.

We conducted a series of binary choice experiments using in-stream enclosures to determine if juvenile coho selectively avoid UVR and to gauge the relative importance of UVA and UVB wavelengths in photo-avoidance behavior. Whereas previous studies have examined the behavioral response of juvenile coho to overall light intensity, none have specifically addressed the role of UVR. Trials were performed on both newly emerged coho alevins (13–18 May 1997) and juvenile coho, two months post emergence (19–27 July 1997), to determine if behavior changed during development and exposure to sunlight. Experiments conducted under different cloud-cover conditions allowed an assessment of behavioral response under varying ambient solar intensity.

Material and methods

Little Qualicum River Channel study site

Experiments were conducted in the Little Qualicum River Spawning Channel (49°17′N, 124°35′W), on the east coast of Vancouver Island, B.C. Although the channel primarily serves as a spawning habitat for chum salmon (*Oncorhynchus keta*), incidental wild populations of other salmon species including coho also spawn there. Coho juveniles rear for up to two years in the channel before emigrating to the river estuary. The channel is exposed to full sunlight and with a mean dissolved organic carbon (DOC) concentration of 1.3 $mg \cdot L^{-1}$, water transparency to UVR is high (Kelly 2001). Mean daily water temperatures were 9.6°C and 18.1°C during the 13–18 May 1997 and 19–27 July 1997 trials, respectively.

Behavioral experiment design

Photopreference by coho alevins and juveniles was determined by allowing fish to choose between two different sun-

© 2002 NRC Canada

Fig. 2. Transmittance of the four plastic light filters used in the experimental trials at the Little Qualicum Channel through the mid-ultraviolet radiation (UVB, 280–320 nm), near-ultraviolet radiation (UVA, 320–400 nm), and photosynthetically active radiation (PAR, 400–700 nm) spectral ranges. The filters used were UF-4 Plexiglas sheets (PAR+UVA+UVB), OP-4 acrylic sheets (PAR only), Mylar-D (PAR+UVA), and neutral density (ND) fine-mesh window screening on OP-4 acrylic sheets (50% PAR+UVA+UVB).

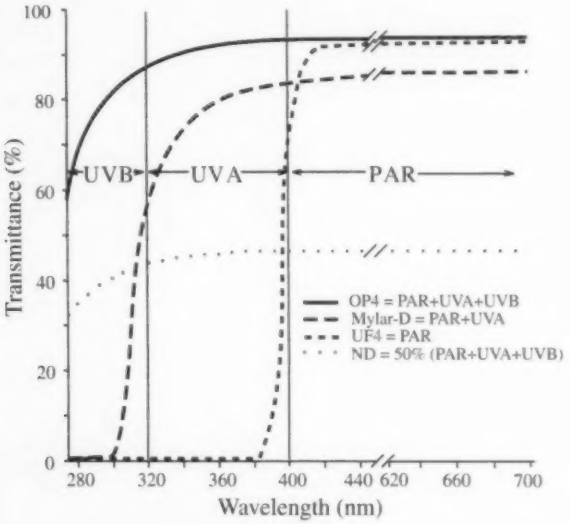

light filtering treatments in outdoor enclosures (Fig. 1). Four rectangular enclosures (100 cm × 50 cm × 10 cm) constructed from UVR transparent Plexiglas were positioned side by side (separated by ~10 cm) across the breadth of the channel on concrete blocks at a depth of 8 cm. Holes (0.5-cm diameter) in the front and rear sides of the enclosures allowed free exchange of water to prevent temperature or dissolved oxygen anomalies. The two halves of each enclosure were covered by different solar exclusion filters, creating a binary choice for the fish in each chamber (Fig. 1). The solar exclusion filters used were (*i*) UF-4 Plexiglas (Rohm and Hass, Philadelphia, Pa.; 6.4 mm thick; 50% transmission at 398 nm) for photosynthetically active radiation (PAR; 400–700 nm) only; (*ii*) Mylar-D (DuPont, Wilmington, Del.; 0.1 mm thick, 50% transmission at 318 nm) for PAR+UVA; (*iii*) OP-4 acrylic (CYRO, Rockaway, N.J., 4.7 mm thick, 70–90% transmittance throughout the UVB and UVA) for PAR+UVA+UVB; and (*iv*) a neutral-density window screening to reduce sunlight intensity by half in combination with OP-4 for 50% (PAR+UVA+UVB) (Fig. 2). A combination of four phototreatments were compared with both newly emerged alevins and 2-month-old juveniles as follows: PAR vs. PAR+UVA+UVB; PAR+UVA vs. PAR+UVA+UVB; 50% (PAR+UVA+UVB) vs. PAR+UVA+UVB; and PAR+UVA+UVB against itself as a control. Two additional comparisons were run with age-0 alevins as follows: PAR vs. PAR+UVA and PAR vs. 50% (PAR+UVA+UVB).

Experiments were initiated by introducing ~40 coho (36–41) into each chamber at 1900 hours to allow overnight acclimation. Coho were free to move within the enclosures and choose between the two light treatments of each chamber. The following day, the number of coho under each light treatment was enumerated hourly between 0900 and 1800 by photographing the chambers from a ~10-m distance using a Tamron 300- to 700-mm zoom telephoto lens (Commack, N.Y.). Light treatments were initially assigned at random to the four enclosures and then moved to the adjacent enclosure over the next three days so that each chamber was used for the four light treatment combinations for a single day and hourly observations of each binary phototreatment trial were replicated on four separate days. Fish were left in the chambers for the 4-day duration of the experiment (i.e., not replaced), and were exposed to each of the phototreatment combinations. The PAR vs. PAR+UVA and PAR vs. 50% (PAR+UVA+UVB) comparisons were run only on two successive days.

Experimental trials were conducted on recently emerged alevins at age 0 (13–18 May 1997) and juveniles at age 2 months (19–27 July 1997). Age-0 coho alevins were obtained from the Big Qualicum River Hatchery (Department of Fisheries and Oceans, Qualicum Beach, B.C.). Coho eggs had been incubated in shallow (2-cm) indoor flowing trays under dimly lit conditions. The alevins used in the experiment had just finished absorbing their yolk sac, which coincides with the time they normally emerge from the gravel to start feeding (Lister and Genoe 1970). Two-month-old coho juveniles (~60-mm fork length; ~2.5 g wet wt.) were collected from the Little Qualicum Channel using a beach seine and transferred to enclosures.

Light

During behavior trials, hourly scans of solar irradiance were measured over daylight hours with an Optronics OL-752 spectroradiometer (Optronic Instruments, Orlando, Fla.). Scans were made at 2-nm intervals between 280 and 700 nm recorded in $W \cdot m^{-2} \cdot nm^{-1}$, and converted to $mol \cdot m^{-2} \cdot h^{-1}$ of PAR, UVA, and UVB using Planck's equation. Diffuse attenuation coefficient (K_d) and light transmittance (%) to mid (4 cm) and bottom (8 cm) enclosure depths for the PAR, UVA, and UVB waveband regions were calculated from absorbance measurements of river water collected during each trial. Absorbance scans of river water were made at 0.5-nm intervals between 280 and 700 nm using a Cary 50 scanning spectrophotometer (Varian Instruments, Walnut Creek, Calif.) equipped with a 2-cm quartz cuvette. Spectral transmittance of the solar exclusion filters used in the experiment was also quantified spectrophotometrically over PAR and UVR wavelengths. Total mid-day (1300) PAR, UVA, and UVB irradiance at mid-enclosure depth (4 cm) was calculated by multiplying the transmission of the filters (%), water column transmittance (%), and above-surface irradiance ($mmol \cdot m^2 \cdot h^{-1} \cdot nm^{-1}$) between 290 and 700 nm at 2-nm intervals and integrating over the spectral region.

Statistical analyses

One-sample *t* tests were used to statistically test for preference between the photo-environments presented to the coho in each chamber with the assumption of a 1:1 ratio between paired light treatments indicating no preference. Mean daily proportions for a particular phototreatment (calculated from the average of all hourly counts in a day) were used in

© 2002 NRC Canada

Fig. 3. Mean hourly photo-flux densities (±1 SD) during daylight hours of (*a*) photosynthetically active radiation (PAR, 400–700 nm), (*b*) near-ultraviolet radiation (UVA, 320–400 nm), and (*c*) mid-ultraviolet radiation (UVB, 280–320 nm) during juvenile coho salmon (*Oncorhynchus kitsutch*) behavioral trials at the Little Qualicum Channels. Trials with age-0 coho alevins occurred under cloudless conditions 13–18 May 1997 (□); trials with 2-month-old coho juveniles occurred 21–27 July 1997 under both cloudless (■) and cloudy conditions (◆).

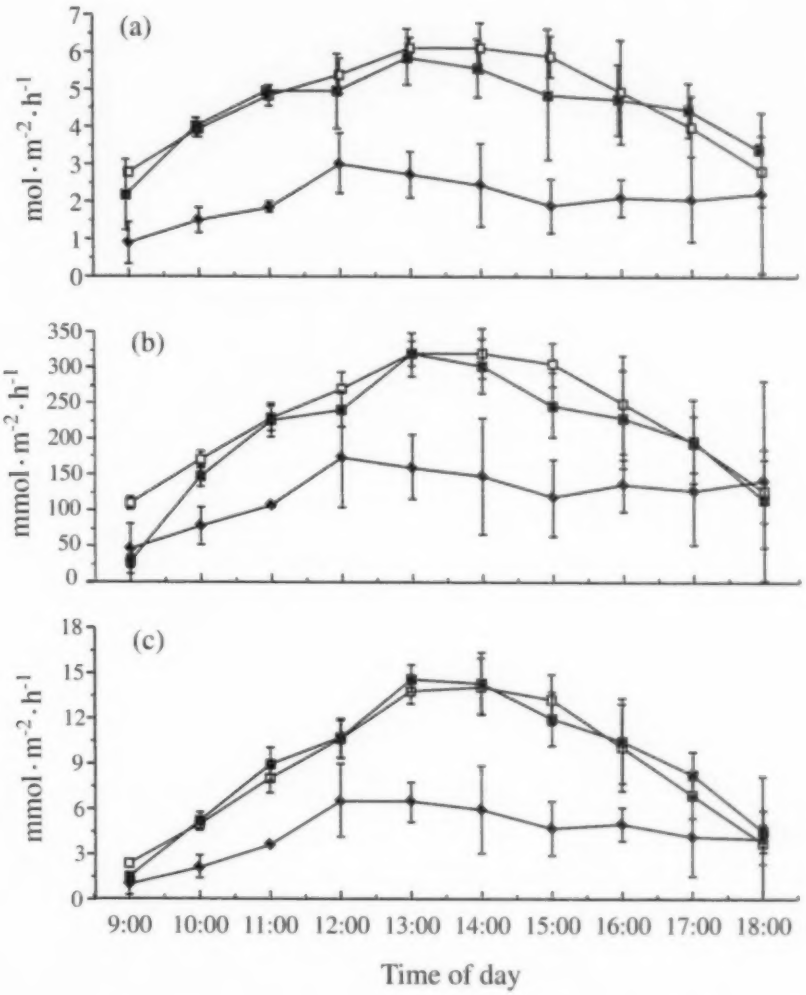

Table 1. Diffuse attenuation coefficients (K_d) and percent transmittance to mid (T_{4cm}) and bottom (T_{8cm}) enclosure depths for UVB (280–320 nm), UVA (320–400 nm), and PAR (400–700 nm) during May and July 1997 experimental trials at the Little Qualicum Channels.

	18 May 1997			26 July 1997		
Variable	UVB	UVA	PAR	UVB	UVA	PAR
K_d (m^{-1})	10.1	4.7	0.9	8.3	4.2	0.5
T_{4cm} (%)	66.7	83.0	96.5	71.8	84.4	98.2
T_{8cm} (%)	44.6	69.1	93.1	51.6	71.5	96.5

the *t* test, which was then compared against 50%, or no departure from random choice. All proportion data were arcsine transformed to normalize the data before conducting parametric analyses (Zar 1983), and all quoted probabilities are for two-tailed tests of significance. Separate analyses were conducted for both age classes of coho (i.e., age 0 and 2 months), and in the case of 2-month-old coho, for both cloudy and cloudless conditions. Although the power of our analyses was slightly diminished by repeating trials over time rather than conducting multiple replicates simultaneously, we feel this approach was statistically robust because trials were conducted under stable weather conditions (i.e., cloudless days) that minimized differences in hourly irradiance between successive trials.

A two-way analysis of variance (ANOVA; factors included trial and coho age class) was used to test for differences in hourly irradiance between cloudless-day trials conducted on coho alevins and 2-month-old coho. Similarly, a two-way ANOVA (factors included trial and cloud cover) was used to

© 2002 NRC Canada

Table 2. Mean mid-day (13:00) enclosure irradiance ($mmol \cdot m^{-2} \cdot h^{-1}$) at 4-cm depth under the four light treatments for UVB (280–320 nm), UVA (320–400 nm), PAR (400–700 nm), total irradiance (Total, 280–700 nm), and percent above surface photon-flux density (%PFD, 280–700 nm) during May and July 1997 experimental trials at the Little Qualicum Channels.

	13–18 May 1997 (Cloudless)					19–23 July 1997 (Cloudless)					24–27 July 1997 (Cloudy)				
Light treatment	UVB	UVA	PAR	Total	%PFD	UVB	UVA	PAR	Total	%PFD	UVB	UVA	PAR	Total	%PFD
PAR+UVA+UVB	6.9	228	5240	5500	90%	7.8	241	5640	5890	91%	1.4	123	2500	2630	91%
PAR+UVA	1.2	187	4830	5020	82%	1.4	200	5190	5400	84%	0.3	101	2310	2410	84%
PAR	0.0	12	5160	5170	85%	0.0	13	5540	5560	86%	0.0	6.5	2470	2470	86%
50% (PAR+UVA+UVB)	3.5	113	2620	2730	45%	3.9	122	2810	2940	46%	0.7	61	1250	1320	46%

Table 3. Mean percent reduction in solar UVB (280–320 nm), UVA (320–400 nm), and PAR (400–700 nm) under treatments used in the coho salmon (*Oncorhynchus kisutch*) behavioral experiments at the Little Qualicum Channels relative to the full-spectrum control treatment (OP-4; PAR+UVA+UVB).

Filter type	UVB	UVA	PAR	Total
OP4 (PAR + UVA + UVB)	0%	0%	0%	0%
Mylar-D (PAR + UVA)	82%	18%	7.8%	8.3%
UF4 (PAR only)	100%	94%	1%	5.4%

Note: Values were determined from the mean mid-day (1300) solar flux ($mmol \cdot m^{-2} \cdot h^{-1}$) at mid-depth (4 cm) of the enclosure during cloudless conditions in May and July 1997.

test for differences in hourly irradiance between cloudy and cloudless trials on 2-month-old coho.

Results

Light

Hourly flux of PAR, UVA, and UVB during cloudless days did not differ significantly between experiments on age-0 alevins during May and those conducted on 2-month-old juveniles in July (two-way ANOVA, $p > 0.41$) (Fig. 3). This was likely because of the equivalent timing of these trials on either side of the summer solstice. There were also no differences in the hourly flux of PAR, UVA, or UVB irradiance between individual days of each experimental trial (two-way ANOVA, $p > 0.33$). During cloudless days, hourly irradiance ranged from 2 to 7 $mol \cdot m^2 \cdot h^{-1}$ PAR, 40 to 350 $mmol \cdot m^2 \cdot h^{-1}$ UVA, and 1.6 to 17 $mmol \cdot m^2 \cdot h^{-1}$ UVB, with peak solar flux at 1300 hours. On cloud-covered days (24–27 July) mean hourly PAR, UVA, and UVB fluences were 57, 50, and 46% lower (two-way ANOVA, $p < 0.001$), respectively, than on cloudless days (Fig. 3).

Small decreases in DOC (from 1.75 to 1.16 $mg \cdot L^{-1}$) between May and July trials resulted in slightly more UVB penetrating to the bottom of the enclosure (44.6–51.6% surface irradiance) during July trials (Table 1). K_{dUVB} decreased from 10.1 m^{-1} on 18 May to 8.3 m^{-1} by 26 July, whereas K_{dUVA} and K_{dPAR} both only decreased by ~0.5 m^{-1} (Table 1).

Total photon flux densities (PFD) between 280 and 700 nm within the enclosures differed between photo-treatments with PAR+UVA+UVB > PAR > PAR+UVA > 50% (PAR+UVA+UVB) (Table 2). The higher total PFD under PAR compared with PAR+UVA (Tables 2 and 3) resulted from greater exclusion of PAR wavelengths by Mylar-D than UF-4 (Fig. 2; Table 3). Although Mylar-D was intended to block only UVB wavelengths, it also removed 18% of the UVA and nearly 8% of the PAR irradiance (Table 3). In contrast, the UF-4 filter provided a fairly clean separation between PAR and UVR by passing 99% of PAR while blocking virtually all of the UVB and 94% of the UVA.

Coho behavioral trials

Age-0 coho alevins showed significant preference for PAR ($t_{2,3} = 3.62$, $p = 0.036$) and 50% (PAR+UVA+UVB) ($t_{2,3} = 6.01$, $p = 0.009$) over full sunlight (PAR+UVA+UVB) (Figs. 4*a* and 4*b*). They also showed a significant preference for PAR over PAR+UVA ($t_{2,1} = 22.92$, $p = 0.028$) and for PAR+UVA over PAR+UVA+UVB ($t_{2,3} = 5.17$, $p = 0.014$) (Figs. 4*e* and 4*d*). In addition, they preferred a total reduction in solar intensity (50% PAR+UVA+UVB) over removal of just UVR (i.e., PAR); however, this difference was nonsignificant ($t_{2,1} = 5.77$, $p = 0.109$) (Fig. 4*f*). The control enclosure comparing PAR+UVA+UVB against itself confirmed the validity of our approach to determination of photopreference. No significant differences in coho alevin abundance were found between the two sides of the chamber ($t_{2,3} = 0.11$, $p = 0.922$) (Fig. 4*c*).

The response patterns of 2-month-old coho to light manipulations during cloudless conditions were the same as those of age-0 alevins (Figs. 5*a*–5*d*). Coho juveniles showed a significant preference for the absence of UVR ($t_{2,3} = 4.69$, $p = 0.018$) (Fig. 5*a*). Likewise, a strong preference for a total reduction in irradiance by 50% was also found ($t_{2,3} = 4.33$, $p = 0.023$) (Fig. 5*b*). A significant preference for PAR+UVA over PAR+UVA+UVB ($t_{2,3} = 4.51$, $p = 0.020$) was also seen among coho juveniles (Fig. 5*d*). Again, full-spectrum sunlight paired against itself showed no significant difference ($t_{2,3} = 0.33$, $p = 0.765$) (Fig. 5*c*).

Under reduced solar intensities (i.e., cloudy days) coho showed no preference for any spectral treatment (Figs. 6*a*–6*d*). No significant differences were found for coho frequenting any of the light manipulations (t tests, $p > 0.16$) during trials conducted on cloudy days when total photon flux densities were around half those found on sunny days (Fig. 3).

Discussion

Shade-seeking behavior of stream-dwelling salmonids is well known and has been thought to be principally a predator-avoidance mechanism (Lister and Genoe 1970; Shirvell 1990). We corroborate the preference for lower-light environments in juvenile coho when shading is neutral density and the spectral composition of the sunlight is unaltered. When ambient sunlight levels were high, we found significant avoidance of full-spectrum sunlight (PAR+UVA+UVB) compared with shading by 50% (PAR+UVA+UVB) in both

© 2002 NRC Canada

Fig. 4. Percent abundance of age-0 coho salmon (*Oncorhynchus kisutch*) alevins (mean ± SD) occupying paired light treatments over daylight hours and the daily mean during behavioral trials in the Little Qualicum Channels under cloudless conditions 13–18 May 1997. Paired photo-environment comparisons tested were as follows: (*a*) PAR vs. PAR+UVA+UVB, (*b*) 50% (PAR+UVA+UVB) vs. PAR+UVA+UVB, (*c*) PAR+UVA+UVB vs. itself (control), (*d*) PAR+UVA vs. PAR+UVA+UVB, (*e*) PAR vs. PAR+UVA, and (*f*) PAR vs. 50% (PAR+UVA+UVB). Each comparison was replicated on multiple days (2–4 days). The dashed lines represent equal distribution between the light treatments, i.e., no preference. *P* values for one-sample *t* tests comparing daily means are shown on each panel.

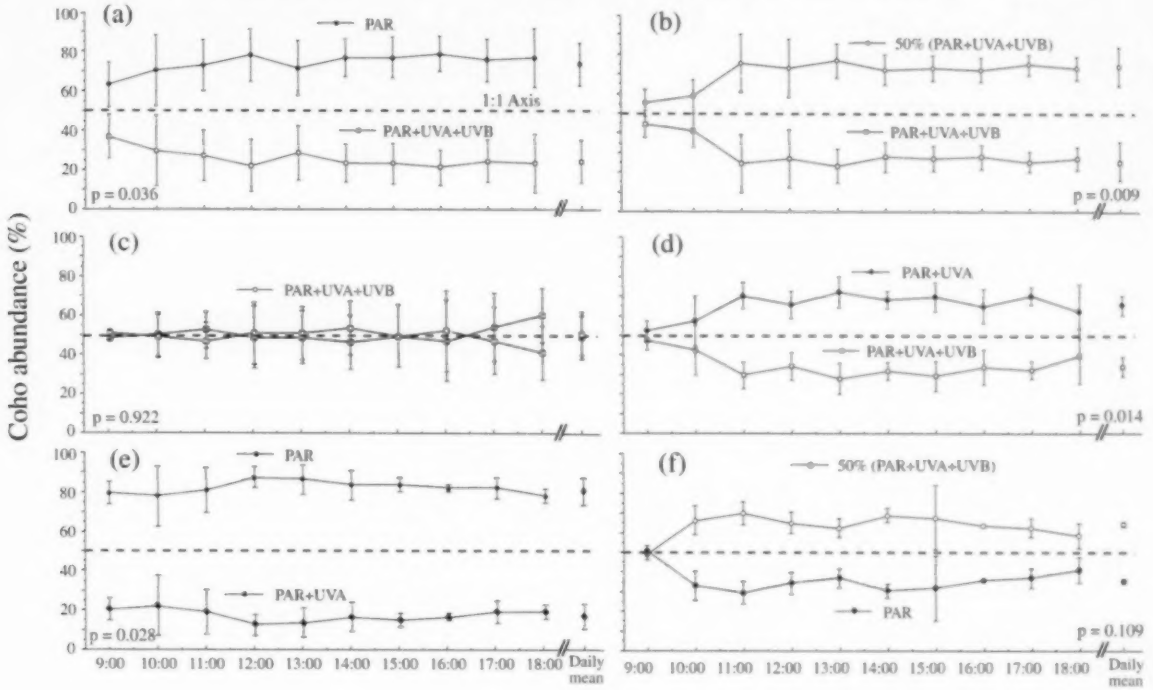

newly emerged alevins and 2-month-old juveniles. When ambient levels of sunlight were cut in half during extensive cloud cover, coho juveniles showed no tendency to avoid the higher of two light environments and numbers of individuals under 50% (PAR+UVA+UVB) and PAR+UVA+UVB were not significantly different. The amount of mid-day incident solar flux (PAR+UVA+UVB) at which coho no longer actively sought shade was ~2600 $mmol \cdot m^{-2} \cdot h^{-1}$.

Our most important finding was that juvenile coho also actively and selectively avoided environments with high levels of solar UVR. Significant preference was shown by both age groups of fish for photo-environments with both UVA and UVB removed. However, the total photon flux under the full UVR-filtered treatments was also reduced by about 5% compared with the full-spectrum sunlight treatment. Although it seemed unlikely that such a minor reduction in total photon flux would trigger the dramatic preference observed for the UVR-reduced environment, it is possible that this may have influenced behavioral responses. However, we also found that coho alevins showed a significant preference for PAR only compared with PAR+UVA, even though the total radiant flux under PAR (~94.6% transmission) was actually 3% greater than under PAR+UVA (~91.7% transmission), because Mylar-D is less transparent throughout the visible spectrum than UF-4 Plexiglas. Therefore, the coho were unequivocally avoiding higher levels of UVA irradiance in this comparison. Under cloudy skies when solar intensity was half of that under full summer sun, coho juveniles did not avoid UVA. The amount of mid-day incident solar UVA photon flux at which coho no longer actively avoided this radiation was ~150 $mmol \cdot m^{-2} \cdot h^{-1}$ or 42 $kJ \cdot m^{-2} \cdot h^{-1}$.

When PAR+UVA was compared with PAR+UVA+UVB, coho alevins and juveniles appeared to show a preference for the absence of UVB. Although this might indicate selective avoidance of UVB, the interpretation is confounded by the fact that the Mylar-D filter used to create the PAR+UVA environment also reduced the total solar flux by 8% compared with the full-spectrum sunlight treatment. More importantly, Mylar-D also reduced UVA irradiance by 18% and UVA was an important trigger for photo-avoidance. Therefore, it seems likely that coincidental reductions in UVA and PAR by Mylar-D would also influence to some degree the preference shown by the fish for this treatment relative to full-spectrum sunlight, thus our evidence for specific avoidance of UVB is compromised.

The retina of bony fishes possess light-sensitive cones specific for ultraviolet wavelengths (Douglas and Hawryshyn 1990). Although the sensitivity of ultraviolet cones varies

© 2002 NRC Canada

Fig. 5. Percent abundance of 2-month-old coho salmon (*Oncorhynchus kisutch*) juveniles (mean ± SD) occupying paired light treatments over daylight hours and the daily mean during behavioral trials in the Little Qualicum Channels under cloudless conditions 19–27 July 1997. Paired photo-environment comparisons tested were as follows: (*a*) PAR vs. PAR+UVA+UVB, (*b*) 50% (PAR+UVA+UVB) vs. PAR+UVA+UVB, (*c*) PAR+UVA+UVB vs. itself (control), and (*d*) PAR+UVA vs. PAR+UVA+UVB. Each comparison was replicated on four days. The dashed lines represent equal distribution between the light treatments, i.e., no preference. *P* values for one-sample *t* tests comparing daily means are shown on each panel.

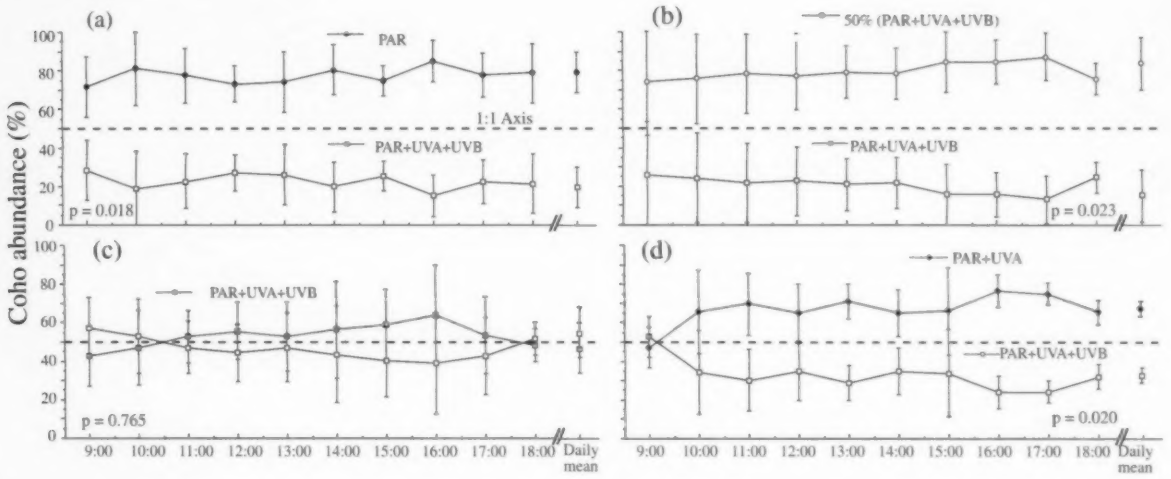

Fig. 6. Percent abundance of 2-month-old coho salmon (*Oncorhynchus kisutch*) (mean ± standard deviation) occupying paired light treatments over daylight hours and the daily mean during behavioral trials in the Little Qualicum Channels under cloudy skies 21–22 July 1997. Paired photo-environment comparisons tested were as follows: (*a*) PAR vs. PAR+UVA+UVB, (*b*) 50% (PAR+UVA+UVB) vs. PAR+UVA+UVB, (*c*) PAR+UVA+UVB vs. itself (control), and (*d*) PAR+UVA vs. PAR+UVA+UVB. Each comparison was replicated on two days. The dashed lines represent equal distribution between the light treatments, i.e., no preference. *P* values for one-sample *t* tests comparing daily means are shown on each panel.

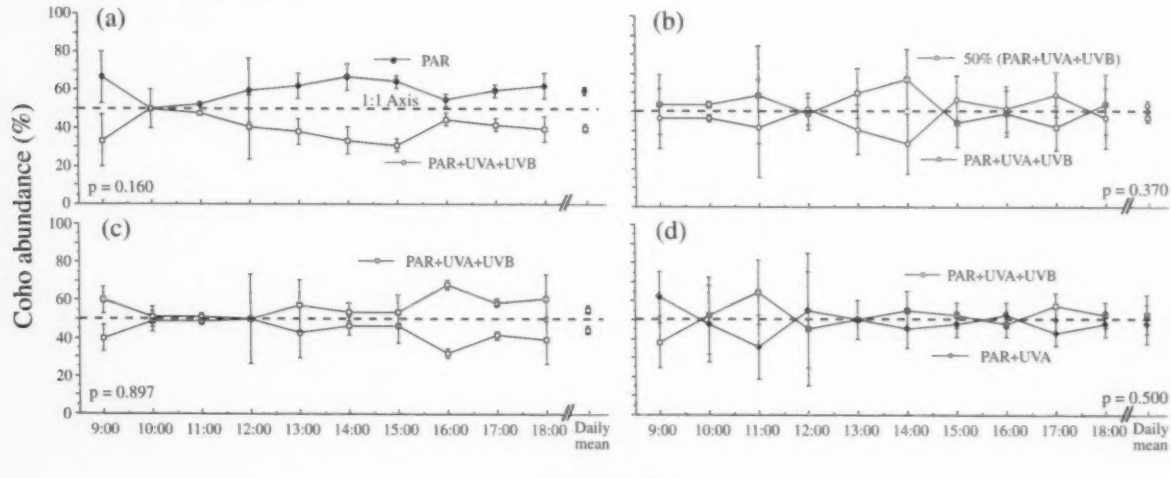

among species, for closely related rainbow trout (*Oncorhynchus mykiss*) the strongest response is in the middle of the UVA spectral band (λ_{max} = 360–370 nm) (Browman et al. 1994). UV cones in salmonids have been shown to contribute to prey detection during visually guided foraging behavior (Douglas and Hawryshyn 1990; Browman et al. 1994) and the ability of the UV photoreceptor cones to discriminate polarized light has also been implicated in the navigational ability of seagoing salmonids (Hawryshyn et al. 1990). Our observations that juvenile coho behaviorally avoid high levels of

© 2002 NRC Canada

UVA radiation suggest another potential benefit of UV visual sensitivity in these fish.

Avoidance of high light environments by salmonids has been thought to be principally a predator-avoidance mechanism with fish taking cover under bank ledges, logs, and rootwads (Lister and Genoe 1970; Shirvell 1990). In the absence of overhead cover, coho have been shown to select deeper water habitats (Gibson and Power 1975; Bugert et al. 1991), presumably for the same reason. However, we now know that the intensity of UVR dramatically declines with depth in fresh waters and that the rate of decline largely depends upon the DOM concentration (Scully and Lean 1994). In freshwater streams with very low DOM, UVB can penetrate at biologically significant doses (Kiffney et al. 1997; Kelly et al. 2001). Taking refuge in deeper water may serve many functions including shielding fish from excessive UVR. Williamson et al. (1997) have shown that the egg-laying behavior of yellow perch (*Perca flavescens*) can be influenced by UVR, with the fish selecting deeper egg-laying depths in lakes with higher UVR penetration. This behavior by yellow perch was shown to increase egg survivorship (Williamson et al. 1997). Likewise, the behavioral avoidance of UVR we document here for juvenile coho salmon in shallow streams may be beneficial to the fish, but in ways we do not yet fully understand.

Acknowledgements

This work was supported by a grant from Forestry Renewal British Columbia. We are grateful to Pat Slobodzian and Grant Ladoceur for use of the hatchery facilities at the Little Qualicum River (Department of Fisheries and Oceans Canada). We also wish to thank Blair Holtby and Bill MacLean for advice on coho biology, behavior, and life history. Brian Parker, David Schindler, and three anonymous reviewers provided very helpful comments on the manuscript. D.J. Kelly would like to acknowledge the support of NSERC and the Walter H. Johns Foundation for postgraduate support.

References

Allison, L.N. 1963. Cataract in hatchery lake trout. Trans. Am. Fish. Soc. **92**: 34–38.

Baltz, D.M., Vondracek, L.R., Brown, L.R., and Moyle, P.B. 1991. Seasonal changes in microhabitat selection by rainbow trout in a small stream. Trans. Am. Fish. Soc. **120**: 166–176.

Beamish, R.J., Neville, C.E.M., and Cass, A.J. 1997. Production of Fraser River sockeye salmon (*Oncorhynchus nerka*) in relation to decadal-scale changes in the climate and the ocean. Can. J. Fish. Aquat. Sci. **54**: 543–554.

Blaustein, A.R., Kiesecker, J.M., Chivers, D.P., and Anthony, R.G. 1997. Ambient UV-B radiation causes deformities in amphibian embryos. Proc. Natl. Acad. Sci. U.S.A. **94**: 13 735 – 13 737.

Browman, H.I., Novales-Flamarique, I., and Hawryshyn, C.W. 1994. Ultraviolet photoreception contributes to prey search behaviour in two species of zooplanktivorous fishes. J. Exp. Biol. **186**: 187–198.

Bugert, R.M., Bjorn, T.C., and Meehan, W.R. 1991. Summer habitat use by young salmonids and their response to cover and predators in a small southeast Alaska stream. Trans. Am. Fish. Soc. **120**: 474–485.

Bullock, A.M., and Coutts, R.R. 1985. The impact of solar ultraviolet radiation upon the skin of rainbow trout, *Salmo gairdneri* Richardson, farmed at high altitude in Bolivia. J. Fish Dis. **8**: 263–272.

Coronado, C., and Hilborn, R. 1998. Spatial and temporal factors affecting survival in coho salmon (*Oncorhychus kisutch*) in the Pacific Northwest. Can. J. Fish. Aquat. Sci. **55**: 2067–2077.

Douglas, R.H., and Hawryshyn, S.W. 1990. Behavioral studies of fish vision: an analysis of visual capabilities. *In* The visual system of fish. *Edited by* R.H. Douglas and M.B.A. Djamgoz. Chapman and Hall, London. pp. 373–418.

Fausch, K.D. 1993. Experimental analysis of microhabitat selection by juvenile steelhead (*Oncorhychus mykiss*) and coho salmon (*O. kisutch*) in a British Columbia stream. Can. J. Fish. Aquat. Sci. **50**: 1198–1207.

Freitag, J.F., Steeger, H.-U., Storz, U.C., and Paul, R.J. 1998. Sublethal impairment of respiratory control in plaice (*Plueonectes platessa*) larvae induced by UV-B radiation, determined using a novel biocybernetical approach. Mar. Biol. **132**: 1–8.

Gibson, R.J., and Power, G. 1975. Selection by brook trout (*Salvelinus fontinalis*) and juvenile atlantic salmon (*Salmo salar*) of shade related to water depth. J. Fish. Res. Board Can. **32**: 1652–1656.

Häder, D.-P., Kumar, H.D., Smith, R.C., and Worrest, R.C. 1998. Effects on aquatic ecosystems. Photochem. Photobiol. B Biol. **46**: 53–68.

Hansen, G., and Chipperfield, M.P. 1998. Ozone depletion at the edge of the arctic polar vortex 1996/1997. J. Geophys. Res. **104**: 1837–1845.

Hawryshyn, C.W., Arnold, M.G., Bowering, E., and Cole, R.L. 1990. Spatial orientation of rainbow trout to plane-polarized light: the ontogeny of E-vector discrimination and spectral sensitivity characteristics. J. Comp. Physiol. A, **166**: 565–574.

Heggenes, J., Northcote, T.G., and Peter, A. 1991. Seasonal habitat selection and preferences by cutthroat trout (*Oncorhynchus clarki*) in a small, coastal stream. Can. J. Fish. Aquat. Sci. **48**: 1364–1370.

Hunter, J.R., Taylor, J.H., and Moser, H.G. 1979. Effect of ultraviolet irradiation on eggs and larvae of the northern anchovy, *Engraulis mordax*, and the Pacific mackeral, *Scomber japonicus*, during the embryonic stage. Photochem. Photobiol. **29**: 325–338.

Kelly, D.J. 2001. Effects of solar ultraviolet radiation on stream ecosystems and their application to forestry practices in British Columbia. Ph.D. Dissertation. University of Alberta, Edmonton, Canada.

Kelly, D.J., Clare, J.J.,and Bothwell, M.L. 2001. Attenuation of ultraviolet radiation by dissolved organic matter alters benthic colonization patters in streams. J. North Am. Benthol. Soc. **20**: 96–108.

Kiffney, P.M., Clements, W.H., and Cady, T.A. 1997. Influence of ultraviolet radiation on the colonization dynamics of a Rocky Mountain stream benthic community. J. North Am. Benthol. Soc. **16**: 520–530.

Lister, D.B., and Genoe, H.S. 1970. Stream habitat utilization by cohabiting underyearlings of chinook (*Oncorhynchus tshawytscha*) and coho (*O. kisutch*) salmon in the Big Qualicum River, British Columbia. J. Fish. Res. Board Can. **27**: 1215–1224.

Little, E.E., and Fabacher, D.L. 1994. Comparative sensitivity of rainbow trout and two threatened salmonids, Apache trout and Lahontan cutthroat trout, to ultraviolet-B radiation. Arch. Hydrobiol. **43**: 217–226.

Madronich, S., McKenzie, R.L., Bjorn, L.O., and Caldwell, M.M. 1998. Changes in biologically active ultraviolet radiation reaching the earth's surface. Photochem. Photobiol. B Biol. **46**: 5–19.

Novales-Flamarique, I., and Harrower, W.L. 1999. Mortality of sockeye salmon raised under light backgrounds of different spectral composition. Environ. Biol. Fishes, **55**: 279–293.

© 2002 NRC Canada

Salo, H.M., Aaltonen, T.E., Markkula, S.E., and Jokinen, E.I. 1998. Ultraviolet B irradiation modulates the immune system of fish (*Rutilus rutilus*, Cyprinidae). I. Phagocytes. Photochem. Photobiol. **67**: 433–437.

Schindler, D.W., Curtis, P.J., Parker, B.R., and Stainton, M.P. 1996. Consequences of climatic warming and lake acidification for UV-B penetration in North American boreal lakes. Nature (London), **379**: 705–708.

Scully, N.M., and Lean D.R.S. 1994. The attenuation of ultraviolet radiation in temperate lakes. Arch. Hydrobiol. **43**: 135–144.

Shirvell, C.S. 1990. Role of instream rootwads as juvenile coho (*Oncorhynchus kisutch*) and steelhead trout (*O. mykiss*) cover habitat under varying streamflows. Can. J. Fish. Aquat. Sci. **47**: 852–861.

Siebeck, O., Vail, T.L., Williamson, C.E., Vetter, R., Hessen, D., Zagarese, H., Little, E., Balseiro, E., Modenutti, B., Seva, J., and Shumate, A. 1994. Impact of UV-B radiation on zooplankton and fish in pelagic freshwater ecosystems. Arch. Hydrobiol. **43**: 101–114.

Steuke, E.W., Jr., Allison, L.N., Piper, R.G., Robertson, R., and Bowen, J.T. 1968. Effects of light and diet on the incidence of cataract in hatchery-reared lake trout. Prog. Fish-Cult. **30**: 220–226.

Walters, C., and Ward, B. 1998. Is solar ultraviolet radiation responsible for declines in marine survival rates of anadromous salmonids that rear in small streams? Can. J. Fish. Aquat. Sci. **55**: 2533–2538.

Williamson, C.E., Stemberger, R.S., Morris, D.P., Frost, T.M., and Paulsen, S.G. 1996. Ultraviolet radiation in North American lakes: attenuation estimates from DOC measurements and implications for plankton communities. Limnol. Oceanogr. **41**: 1024–1034.

Williamson, C.E., Metzgar, S.L., Lovera, P.A., and Moeller, R.E. 1997. Solar ultraviolet radiation and the spawning habitat of yellow perch, *Perca flavescens*. Ecol. Appl. **7**: 1017–1023.

Yan, N.D., Keller, W., Scully, N.M., Lean, D.R.S., and Dillon, P.J. 1996. Increased UV-B penetration in a lake owing to drought-induced acidification. Nature (London), **381**: 141–143.

Zar, J.H. 1983. Biostatistical Analysis. 2nd ed. Prentice-Hall, Englewood Cliffs, N.J.

© 2002 NRC Canada

Whole-lake algal responses to a century of acidic industrial deposition on the Canadian Shield

Rolf D. Vinebrooke, Sushil S. Dixit, Mark D. Graham, John M. Gunn, Yu-Wei Chen, and Nelson Belzile

Abstract: A century of cultural acidification is hypothesized to have altered algal community structure in boreal lakes. To date, this hypothesis has remained untested because of both the lack of data predating the onset of industrial pollution and incomplete estimates of whole-lake algal community structure. High-pressure liquid chromatography (HPLC) of sedimentary pigments was used to quantify whole-lake algal responses to acid deposition in six boreal lakes located in Killarney Park, Ontario, Canada. Concomitant significant increases in chlorophyll and carotenoid concentrations, diatom-inferred lake acidity, and metal levels since 1900 suggested that algal abundances in four acidified lakes and one small, circumneutral lake were enhanced by aerial pollution. An alternate explanation is that increased acidity and underwater light availability in the acidified lakes shifted algal abundance towards phytobenthos and deepwater phytoplankton, whose pigment signatures were better preserved in the sediments. Taxonomically diagnostic pigment stratigraphies were consistent with shifts in algal community structure towards filamentous green phytobenthos and deepwater phytoflagellates in the acidified lakes. Our findings suggest that decades of aerial pollution have altered the base of foodwebs in boreal lakes, potentially rendering them less resilient to other environmental stressors.

Résumé : L'acidification causée par l'activité humaine depuis un siècle a, croit-on, modifié la structure des communautés d'algues dans les lacs boréaux. Cette hypothèse n'a pas encore été éprouvée, tant à cause du manque de données qui datent d'avant la pollution industrielle qu'à cause des estimations incomplètes de la structure de la communauté d'algues à l'échelle de lacs entiers. La chromatographie liquide à haute pression (HPLC) des pigments des sédiments nous a permis d'évaluer quantitativement la réponse des algues à l'échelle lacustre aux retombées acides dans 6 lacs boréaux du parc de Killarney en Ontario, Canada. Des accroissements significatifs et concomitants des concentrations de chlorophylle et de caroténoïdes, de l'acidité du lac déterminée d'après les diatomées et des concentrations de métaux depuis 1900 laissent croire qu'une augmentation de l'abondance des algues a été favorisée par la pollution aérienne dans 4 lacs acidifiés et un petit lac à eau à peu près neutre. Une explication de rechange serait que la hausse de l'acidité et la disponibilité accrue de la lumière dans l'eau des lacs acides aient plutôt avantagé le phytobenthos et le phytoplancton profond, dont les signatures pigmentaires se sont mieux conservées dans les sédiments. La stratigraphie des pigments d'intérêt taxonomique dans les lacs acidifiés est compatible avec un changement de dominance dans la structure de la communauté d'algues qui privilégie les algues vertes filamenteuses benthiques et les phytoflagellés d'eau profonde. Des décennies de pollution aérienne ont sans doute modifié la base des réseaux alimentaires dans les lacs boréaux, ce qui les rend potentiellement moins résilients aux autres sources environnementales de stress.

[Traduit par la Rédaction]

Introduction

There is increasing concern over the consequences of anthropogenic stresses and loss of biodiversity on the productivity and stability of boreal lakes (Schindler 1998). Acid rain, climate warming, and increased ultraviolet-B (UVB; 280–320 nm wavelength) irradiance impact biodiversity of naturally species-poor communities in boreal lakes, which may reduce or destabilize vital ecosystem functions, such as primary production (Schindler 1995). For example, experimental acidification of boreal lakes caused significant loss of algal species, resulting in increased temporal variability of primary production (Turner et al. 1995; Findlay et al. 1999). However, primary production is not suppressed by

Received 20 June 2001. Accepted 27 February 2002. Published on the NRC Research Press Web site at http://cjfas.nrc.ca on 6 April 2002.
J16416

R.D. Vinebrooke[1] **and M.D. Graham.** Department of Biology, University of Regina, Regina, SK S4S 0A2, Canada.
S.S. Dixit. Paleoecological Environmental Assessment and Research Laboratory, Department of Biology, Queen's University, Kingston, ON K7L 3N6, Canada.
J.M. Gunn. Ontario Ministry of Natural Resources, Cooperative Freshwater Ecology Unit, Laurentian University, Sudbury, ON P3E 2C6, Canada.
Y.-W. Chen and N. Belzile. Department of Chemistry and Biochemistry, Laurentian University, Sudbury, ON P3E 2C6, Canada.

[1]Corresponding author (e-mail: rolf.vinebrooke@uregina.ca).

 DOI: 10.1139/F02-025 © 2002 NRC Canada

experimental acidification because acid-tolerant species compensate for the extirpation of acid-sensitive competitors (Findlay et al. 1999; Klug et al. 2000). Nevertheless, algal abundance in boreal lakes may have been adversely affected by chronic exposure to several decades of cultural acidification and biological impoverishment, but such impacts have not been verified.

Boreal lakes show consistent changes in algal community structure during cultural and experimental acidification (Schindler et al. 1991). In general, phytoplankton assemblages shift from chrysophytes, diatoms, and cyanobacteria towards large dinoflagellates (Findlay et al. 1999). In addition, deepwater blooms of hypolimnetic phytoflagellates can flourish in acidified lakes (Findlay and Kasian 1990), possibly as a result of loss of light-attenuating dissolved organic carbon (DOC) from the water column (Schindler et al. 1996; Yan et al. 1996). Whole-lake experiments (Findlay et al. 1999) and lake surveys (Vinebrooke 1996; Vinebrooke and Graham 1997) show that phytobenthos assemblages shift from cyanobacteria to filamentous green algae and diatoms with increasing water acidity. Benthic mats of filamentous green algae often proliferate and detach to form floating clouds, termed metaphyton, that shift primary production in the littoral zone from the phytobenthos to the overlying water column during late summer (Turner et al. 1995; Vinebrooke et al. 2001). Thus, anthropogenic acidification can cause long-term alteration of algal communities by changing their abundance, taxonomic composition, and spatial distribution in boreal lakes.

Paleolimnological techniques are being increasingly used to reconstruct the chemical and biological histories of experimentally and culturally acidified lakes. In the Sudbury area, sedimentary stratigraphies of diatom valves and chrysophyte scales have been used to infer long-term changes in lake water chemistry in response to changes in industrial acid deposition (Dixit et al. 1992*a*, 1992*b*, 2001). Similarly, analysis of sedimentary pigments showed that algal responses to experimental acidification were associated with complex changes in pH, DOC, and light in experimentally acidified Lake 302 (Leavitt et al. 1999). Calibration studies using long-term phytoplankton records have shown that sedimentary pigment concentrations are significantly related to phytoplankton abundance, and function as reliable indicators of whole-lake algal abundance and gross community composition (Leavitt et al. 1997, 1999). Therefore, in the absence of long-term environmental data, sedimentary pigment stratigraphies provide the only means of documenting the responses of primary producers in Canadian Shield lakes to decades of acid deposition.

Here we report on evidence from sedimentary pigment stratigraphies indicating that nearly a century of industrial activity has altered whole-lake algal-community structure in five of six boreal lakes located in a region of high acid deposition. Pigment stratigraphies were used to determine if long-term cultural acidification of boreal lakes reduced or destabilized whole-lake algal abundance and taxonomic composition. This expectation was based on the well-documented negative effects of anthropogenic acidification on algal diversity (Turner et al. 1995; Vinebrooke and Graham 1997; Findlay et al. 1999), and consequently, how a major loss of species can impair a community's ability to acquire resources and tolerate environmental stress and variability (Schindler 1995).

Material and methods

Study area

Killarney Provincial Park is a wilderness area impacted by industrial emissions from nearby (~50 km northwest) Sudbury, Ont. (Fig. 1). Industrial activities began in the Sudbury area at the turn of the 20th century and accelerated thereafter with the construction of mining smelters nearby following World War I (Howard-White 1963). Industrial emission of sulphur dioxide increased to over 2.5 million tonnes per year by the 1960s. As a consequence, several lines of evidence show that lakes in central Ontario, including Killarney lakes, experienced substantial chemical and biological damage during this period (Jeffries 1997). Subsequently, 50–90% reductions of regional SO_2 and trace metal emissions over the last two decades have resulted in chemical recovery in many lakes, but biological recovery in only a few lakes (Keller et al. 1992; Snucins et al. 2001). Currently, pollutant levels over Killarney lakes are mainly attributable to continent-wide (Canada–U.S.A.) industrial activities and combustion of fossil fuels (Jeffries 1997).

The study lakes are situated along the La Cloche Mountain Range, which is characterized by a series of geological formations (Fig. 1). Poor acid-neutralizing capacities (ANC) and low concentrations of DOC characterize the high-elevation lakes, because their catchments consist of coniferous forests, thin podzolic soils, and orthoquartzite bedrock. At lower elevations, lakes have higher ANC and DOC levels because of higher bedrock mineralization rates and mixed forests and wetlands in their catchments. Well-buffered, mesotrophic lakes occur on predominantly calcareous bedrock located in the northwestern region of the park. Regional differences in geology and other catchment characteristics influence the water chemistries of the six study lakes (Snucins and Gunn 1998).

Six study lakes were selected to span gradients of lake acidity and recovery rates (Fig. 1; Table 1). Acid Lake and OSA Lake were included as highly acidified (>1 diatom-inferred pH unit decline since 1880; Dixit et al. 1992*a*) clearwater lakes that have shown slow recovery trajectories (~0.1 pH unit·10 $year^{-1}$ since 1980; Snucins et al. 2001). Acid Lake is located on a quartzite ridge with a catchment consisting of mixed forest (~300 ha), exposed bedrock (~100 ha), and upstream lakes, ponds, and wetlands (~40 ha). OSA Lake is situated in a lowland underlain by bedrock consisting of siltstone and sandstone, and surrounded by quartzite ridges covered ~50% by coniferous forests. Bell Lake and George Lake were less acidified (<1 diatom-inferred pH unit decline since 1880; Dixit et al. 1992*a*, 1992*b*, 2001), and have exhibited relatively fast recovery rates (~0.5 pH unit·10 $year^{-1}$ since 1980; Snucins et al. 2001). Bell Lake is situated between high outcrops of white orthoquartzite on the northwestern shore and bedrock consisting of metamorphosed sedimentary rock and granite on the southeastern shore. The catchment of Bell Lake consists primarily of mixed forest (~75%) and upstream lakes

© 2002 NRC Canada

Fig. 1. Location of the paleolimnological study lakes in Killarney Park, Ont. Other major water bodies, waterways, and watershed boundaries (solid black lines) are also shown.

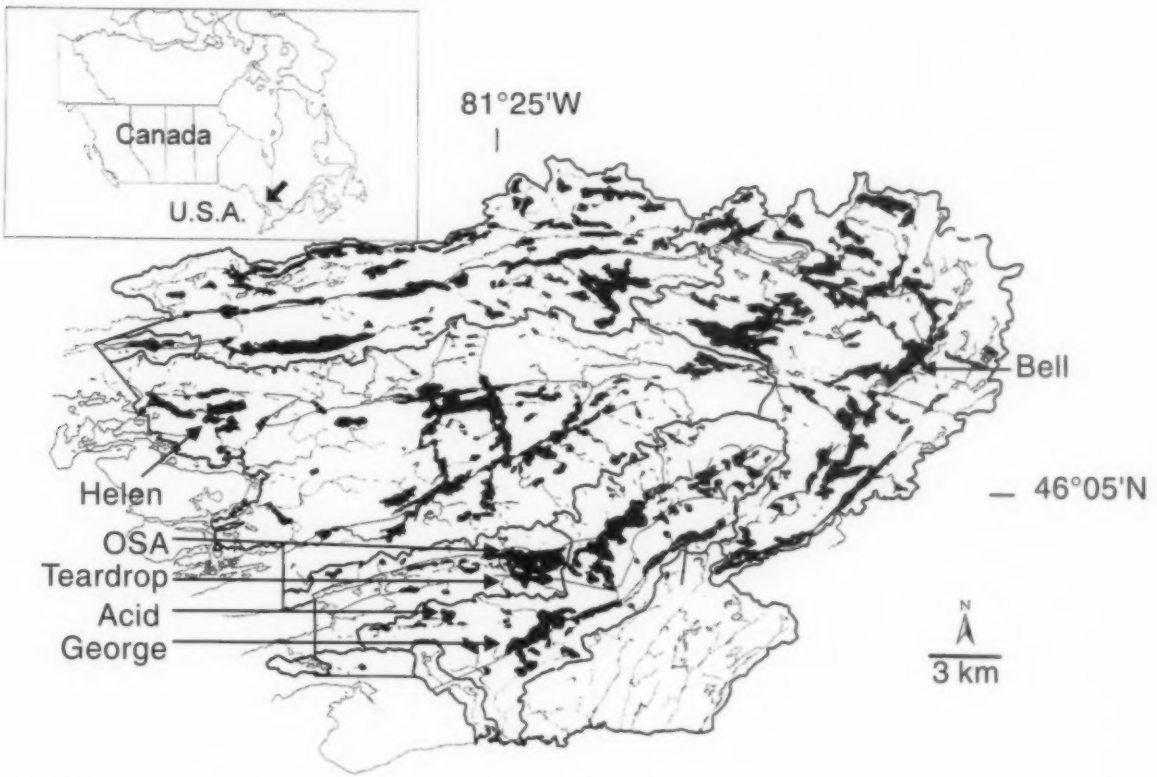

Table 1. Select chemical and physical characteristics of the six Killarney study lakes.

Lake	Elevation (m)	Lake surface area (ha)	Volume (10^4 m^3)	Maximum depth (m)	Total catchment (ha)	pH	Pre-1880 diatom-inferred pH	DOC* ($mg \cdot L^{-1}$)	Total nitrogen ($\mu g \cdot L^{-1}$)	Total phosphorus ($\mu g \cdot L^{-1}$)
Acid	275	19.6	213	29.0	463.8	5.1	5.6	0.4	160	5.6
OSA	205	279	3341	39.7	879.0	4.9	6.9	0.3	80	3.4
George	189	189	3086	36.6	5716.7	6.2	6.1	1.4	160	12.2
Bell	221	347	2827	26.8	8596.3	6.1	6.0	3.9	320	17.6
Teardrop	325	3.4	33	16.6	12.8	6.8	7.1	0.8	120	5.6
Helen	187	83	1692	41.2	883.5	6.9	6.7	3.1	240	14.0

Note: Lakes were sampled using a 5-m integrating tube on 2–3 November 1998.
*DOC = dissolved organic carbon.

and wetlands. Similarly, George Lake is surrounded mainly by mixed forest (~60%) and overlies the contact between high northern outcrops of orthoquartzite and siltstone and southern outcrops of granite and sedimentary rock. Helen Lake and Teardrop Lake were included as circumneutral reference sites that currently have pH readings that are comparable to diatom-inferred pre-1880 values (Table 1). Helen Lake has a relatively small catchment underlain by conglomerate bedrock consisting of limestone, diabase, and sandstone, along with glacial deposits and ~60% vegetation cover. Teardrop Lake is perched on an orthoquartzite ridge, but is well buffered because of an intrusion of calcium-bearing diabase within its catchment. The very small catchment of Teardrop Lake is composed of ~50% mixed forest and ~25% exposed rock.

Sediment analyses

Sediment cores were recovered from the deepest central portion of each lake during February 1999 using a Glew Maxi gravity corer and extrusion device (Glew 1989). The cores were sectioned at close intervals (0.5-cm intervals for top 5 cm; 1.0-cm intervals for bottom 30 cm). The cores were dated by measuring the ^{210}Pb activity in the sediment samples using a low-background Gamma detector at the

© 2002 NRC Canada

Paleoecological Environmental Assessment and Research Laboratory (PEARL) of Queen's University (Kingston, Ont.). Subsamples of sediment for pigment analysis were frozen and stored in the dark until pigment extraction. Although we analyzed only one core from each lake, quality assurance studies have shown that single cores collected from the middle of deep-basin lakes can provide representative samples for paleolimnological analyses (e.g., Renberg and Battarbee 1990).

Sedimentary pigment concentrations were quantified using a standard reversed-phase, high-pressure, liquid chromatography (HPLC) procedure (Vinebrooke and Leavitt 1998). Pigments were extracted by soaking freeze-dried sediments in acetone, methanol, and water (80:15:5 v/v) for 24 h in darkness at 10°C. Extracts were filtered through 0.2-μm pore nylon filters, dried, and stored under nitrogen gas in the dark at –20°C. Dried extracts were reconstituted using injection solution (70% acetone: 25% ion-pairing reagent: 5% methanol) containing Sudan II (3.2 $mg \cdot L^{-1}$) as an internal reference. Ion-pairing reagent consisted of 0.75 g tetrabutylammonium acetate and 8 g ammonium acetate in 100 mL deionized water. Pigments were separated on a Hewlett-Packard (Hewlett-Packard Canada Ltd., Mississauga, Ont.) model 1100 system with a Rainin Model 200 C-18 column (10-cm length, 5-μm particle size). Pigments were detected with an inline HP Series 1100 diode array detector (435-nm detection wavelength) and a fluorescence detector (435-nm excitation wavelength, 667-nm detection wavelength). Analytical separation involved isocratic delivery (1.0 $mL \cdot min^{-1}$) of a mobile phase A (10% IPR in methanol) for 1.5 min, a linear succession to 100% solution B (27% acetone in methanol) over 7 min, and isocratic hold for 12.5 min. The column was re-equilibrated by continued isocratic delivery for 3 min, a linear return to 100% solution A over 3 min, and isocratic delivery for a final 4 min. Pigment concentrations were quantified using equations derived from dilution series of authentic standards supplied by the United States Environmental Protection Agency (USEPA, National Exposure Research Laboratory, Cincinnati, Ohio), or commercial standards (Sigma Chemicals, St Louis, Mo.). All pigment concentrations were expressed per gram organic matter, which was determined by weight lost on ignition (500°C for 2 h).

Whole-lake algal abundance and gross community composition were inferred from concentrations of undegraded chlorophylls (chl *a*, *b*, and *c* and total chl) and taxonomically diagnostic carotenoids (Jeffrey and Vesk 1997). Major algal groups identified included chlorophytes (chl *b*, pheophytin *b*, lutein), chl *c* producing chromophytes (chrysophytes, diatoms, and dinoflagellates such as diadinoxanthin, diatoxanthin, and fucoxanthin), cryptophytes (alloxanthin), and cyanobacteria (zeaxanthin), including select filamentous forms (canthaxanthin). Lutein could not be separated from zeaxanthin, so HPLC analyses of *b*-phorbins were used to determine the relative abundance of chlorophytes. Pigments were identified by comparison of profiles of spectral absorbance and chromatographic mobility with USEPA authentic standards and extracts of known pigment composition. Sedimentary pigments were not used to infer whole-lake algal productivity or production because cellular pigment concentrations and photosynthetic rates can be decoupled by various factors (e.g., cell cycle, nutrient status, and irradiance).

Statistical analyses

For each lake core, differences between pre- and post-industrial total chlorophyll and carotenoid concentrations and their variances were tested for using *t* tests and *Z* tests of coefficients of variation, respectively. Smelter activities in nearby Sudbury had become very active by 1900 (Howard-White 1963); therefore, this year was used to differentiate ^{210}Pb-dated lake cores into pre- and post-industrial sediment intervals. Surface-sediment samples and samples associated with transition years (1890–1910) were excluded from statistical analyses to minimize the confounding effect of pigment diagenesis and establish clear temporal separation between pre- and post-industrial eras. Pigment data were inspected for normal distributions prior to statistical analysis, and logarithmic transformations performed when necessary. Coefficient of variation (CV) was used as a measure of temporal variability because, unlike other measures of variability (e.g., variance, standard deviation), it was independent of the mean. To avoid temporal pseudoreplication (Hurlbert 1984) and violation of the statistical assumption of sample independence when analyzing each core, significance of actual *t* test and *Z* test values was determined using randomization testing (Manly 1997). Stratigraphic pigment concentrations were randomly assigned (999 permutations) to either before or after the year 1900, and the approximate *P* value was determined by the number of times the randomly generated test statistics exceeded the observed values based on analyses of the original data.

Correspondence analysis (CA) was used to ordinate concentrations of major taxonomically diagnostic chlorophylls and carotenoids and ^{210}Pb-dated samples from each lake sediment core. CA summarized the maximum amount of variation in the pigment data and constructed primary (*x* axis) and secondary (*y* axis) environmental and temporal gradients along which pigments and sediment samples were ordered. Specifically, ^{210}Pb-dated samples that contained similar pigment concentrations appeared closer together in ordinate space than did samples with very different pigment compositions. Also, the proximity of pigments to ^{210}Pb-dated samples in ordinate space represented how closely they are associated. For example, a post-industrial sediment sample that occurred close to chl *b* in a CA plot would have contained a high concentration of that pigment. All pigment data were $\ln(x + 1)$ transformed, but not weighted prior to CA. Pigment scores were weighted by mean sample scores to scale ordination scores. Ordinations were performed using the computer program CANOCO version 3.12 (ter Braak 1990).

Results

Whole-lake algal abundance

Post-industrial (ca. 1900) sedimentary pigment concentrations increased significantly by 50–300% in five of the six study lakes (Fig. 2; Table 2). The most significant increases in total chlorophyll and carotenoid concentrations occurred after 1940 in the cores retrieved from the heavily acidified clearwater lakes (Acid and OSA). Similarly, post-industrial

© 2002 NRC Canada

Fig. 2. Temporal patterns of total sedimentary carotenoid (●) and chlorophyll (○) concentrations in (*a*) Acid Lake, (*b*) OSA Lake, (*c*) George Lake, (*d*) Bell Lake, (*e*) Teardrop Lake, and (*f*) Helen Lake of Killarney Provincial Park, Ont. The onset of industrial deposition over the lakes (ca. 1900) is indicated by dashed vertical lines.

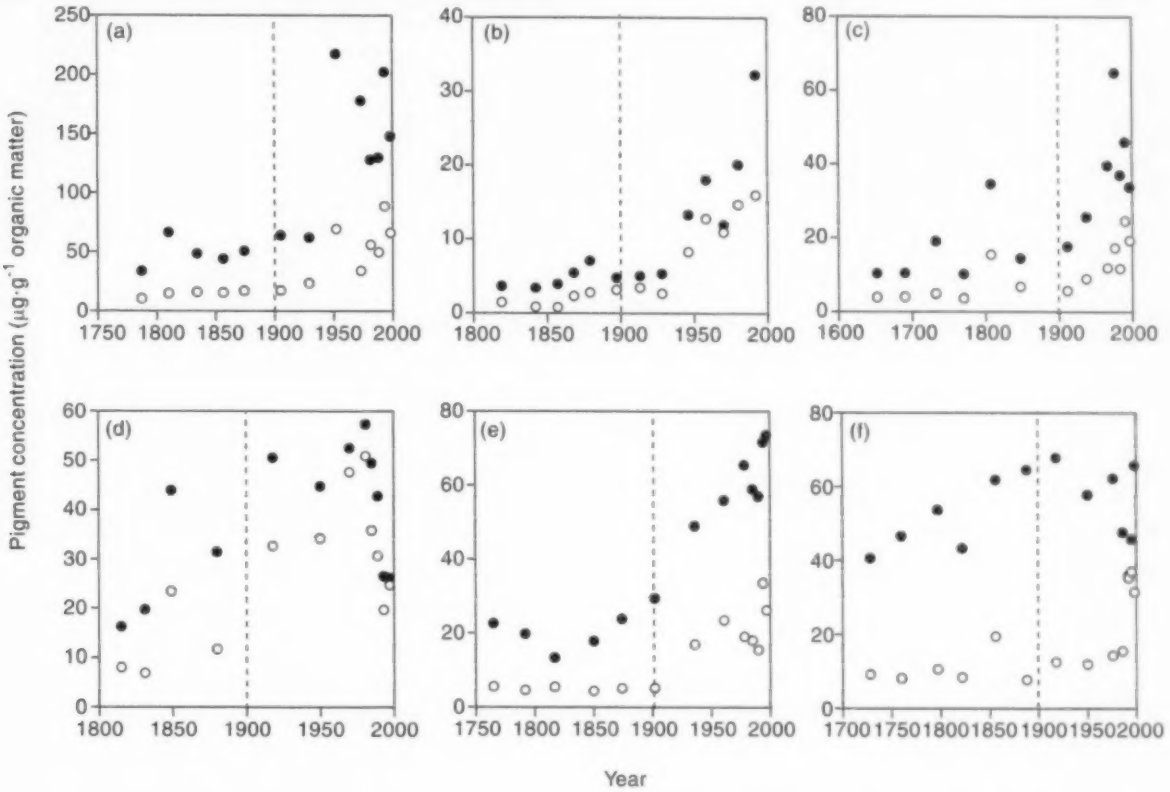

Table 2. Comparisons of pre- and post-industrial mean total chlorophyll and carotenoid concentrations in sediment cores from six Canadian lakes located in a region of high acid deposition.

Lake	Chlorophylls	Carotenoids
Acid	17.12***	28.94***
OSA	7.13***	6.81***
George	6.28**	9.45***
Bell	13.67***	7.07***
Teardrop	22.98***	54.96***
Helen	1.61	0.18

Note: Significance of difference between two means was determined using randomization testing (999 permutations) of *t* values. **, $P < 0.01$; ***, $P < 0.001$.

pigment concentrations were significantly higher in the recovering acidified lakes (George, Bell), and in a circumneutral reference site (Teardrop Lake). Chlorophyll *b* concentrations were also higher in post-industrial sediments in Acid Lake, OSA Lake, George Lake, and Bell Lake (Fig. 3*a*). In contrast, pre- and post-industrial sedimentary pigment concentrations were not significantly different in the other reference site, namely Helen Lake (Figs. 2 and 3*a*). Concentration ratios of total undegraded chlorophylls to chlorophyll derivatives (pheophytins *a*, *b*) were not related significantly to Pb^{210}-inferred sediment age, which confirmed that lower pre-industrial pigment concentrations were not attributable to pigment diagenesis (Fig. 3*b*). Relative temporal variability of pigment-inferred whole-lake algal abundance in the six study lakes did not change significantly after 1900 (Figs. 2 and 4). Sediments from all study lakes lacked visible laminae, which prevented finer inter-annual resolution of the pigment stratigraphies.

Whole-lake algal community structure

Sedimentary pigment signatures of five of the six lakes changed following the onset of industrial deposition (ca. 1900 AD) over the study area (Figs. 4 and 5). In general, higher post-industrial concentrations of sedimentary chlorophylls and carotenoids in the Killarney lakes were primarily attributable to increases in chl *b*, alloxanthin, and fucoxanthin. Chlorophyll *b* and alloxanthin represented reliable taxonomic signatures because they are major specific pigments (>10% of total cellular chlorophylls or carotenoids) of chlorophytes and cryptophytes, respectively (Jeffrey and Vesk 1997). However, the taxonomic resolution of fucoxanthin, diadinoxanthin, and diatoxanthin were rela-

© 2002 NRC Canada

Fig. 3. Temporal patterns of (*a*) sedimentary chlorophyll *b* concentrations, and (*b*) total undegraded chlorophyll to pigmented derivative (pheophytin *a* and *b*) concentration ratios in six Killarney lakes. Onset of industrial deposition over the lakes (ca. 1900) is indicated by dashed vertical lines.

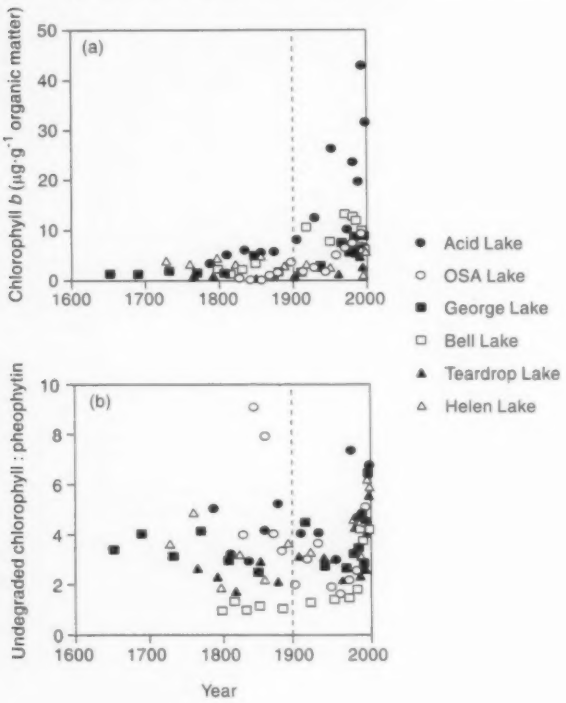

tively poor because these pigments are produced by most chl *c* containing chromophytes, such as chrysophytes, diatoms, and certain dinoflagellates (Jeffrey and Vesk 1997).

In Acid Lake, increased post-industrial total carotenoid concentrations were primarily attributable to higher alloxanthin levels starting around 1929 (Fig. 4). CA of the sedimentary data accounted for 84% of the variance in the pigment concentrations with its first two axes, and separated pre- and post-industrial pigment signatures (Fig. 5). After 1929, the pigment signal became more variable in Acid Lake and shifted towards the upper right quadrant of the ordinate axes, which was associated with higher concentrations of pigments, such as cryptophycean alloxanthin and chlorophycean chl *b* (Fig. 5).

In OSA Lake, increased fucoxanthin, diatoxanthin, and lutein–zeaxanthin concentrations mainly accounted for a significant increase in total carotenoid levels after 1900 (Fig. 4). The first two CA axes captured 82% of the variance contained within the pigment data, and showed that pigment signatures began to shift towards higher concentrations of chl *b* and fucoxanthin between 1913 and 1946 (Fig. 5). The trajectory of ^{210}Pb-dated sediment scores for OSA Lake also showed greater relative variability and no reversal back to pre-industrial scores since 1913 (Fig. 5).

In George Lake, higher post-industrial total carotenoid concentrations consisted primarily of alloxanthin and fucoxanthin (Fig. 4). CA axes 1 and 2 extracted 75% of the total variance in the sedimentary pigment data, and contrasted pre- and post-industrial sediments on the basis of disproportionate increases in alloxanthin, fucoxanthin, and chl *b* concentrations since 1911 (Fig. 5). Although total sedimentary carotenoid concentrations in George Lake have declined over the past decade (Fig. 4), pigment signatures have continued to move from left to right in ordinate space (Fig. 5).

In Bell Lake, higher post-industrial total carotenoid concentrations resulted mainly from increases in alloxanthin and fucoxanthin (Fig. 4). CA axes 1 and 2 accounted for 81% of the total variance contained within the pigment data set, and contrasted pre- and post-industrial pigment signatures (Fig. 5). In general, pigment signatures have moved downward into the lower left-hand quadrant of ordinate space from 1880 to 1970, with a slight return to the right since 1985 owing to recent declines in alloxanthin and fucoxanthin concentrations to pre-industrial levels (Fig. 5).

In Teardrop Lake, post-industrial total carotenoid concentrations increased owing to higher concentrations of alloxanthin, diatoxanthin, lutein–zeaxanthin, and fucoxanthin (Fig. 4). The first two CA axes captured 89% of the total variance of the pigment data, and separated pre- and post-industrial pigment signatures based on higher concentrations of most pigments, except canthaxanthin, in sediments after 1902 (Fig. 5). Lake scores moved right in ordinate space from 1902 to 1994, and remained displaced from the pre-industrial scores that occur in the left side of the plot (Fig. 5). Trace-metal concentrations also increased in post-industrial sediments, whereas diatom-inferred pH remained relatively stable in Teardrop Lake (Fig. 6).

In Helen Lake, pigment signatures have remained relatively unchanged over the past 300 years, except for a recent, but temporary, decline in alloxanthin in near-surface pigments (Fig. 4). Before 1976, lake scores showed little variation in ordination space (Fig. 5). Recent variation of lake scores occurred because of higher concentrations of undegraded chl *b* and recent declines in alloxanthin since 1976 (Figs. 4 and 5).

Discussion

Our study provides paleolimnological evidence of increased pigment-inferred algal abundance in five of six Killarney lakes following the onset of acidic industrial deposition over central Ontario. Specifically, higher post-industrial sedimentary pigment concentrations in the four acidified lakes (Acid, OSA, George, Bell) suggested that whole-lake algal abundance increased as a result of anthropogenic acidification. In addition, pigment concentrations also increased significantly in a small, circumneutral reference site (Teardrop Lake) over the last century. In contrast, our findings suggested that whole-lake algal abundance had remained relatively unchanged in a larger, circumneutral site (Helen Lake) over the past 300 years. Sedimentary pigment stratigraphies in the six lakes could not have involved temporal changes in macrophyte or terrestrial vegetation because both are relatively sparse in the study area (R. Vinebrooke, personal observation). Instead, changes in sedimentary pigment signatures in the five Killarney lakes can be linked to temporal and spatial shifts in whole-lake algal community structure.

© 2002 NRC Canada

Fig. 4. Temporal patterns of taxonomically diagnostic sedimentary carotenoid concentrations in (*a*) Acid Lake, (*b*) OSA Lake, (*c*) George Lake, (*d*) Bell Lake, (*e*) Teardrop Lake, and (*f*) Helen Lake of Killarney Provincial Park, Ont. The onset of industrial deposition over the lakes (ca. 1900) is indicated by dashed vertical lines. Characteristic algal groups associated with each carotenoid are identified in the legend.

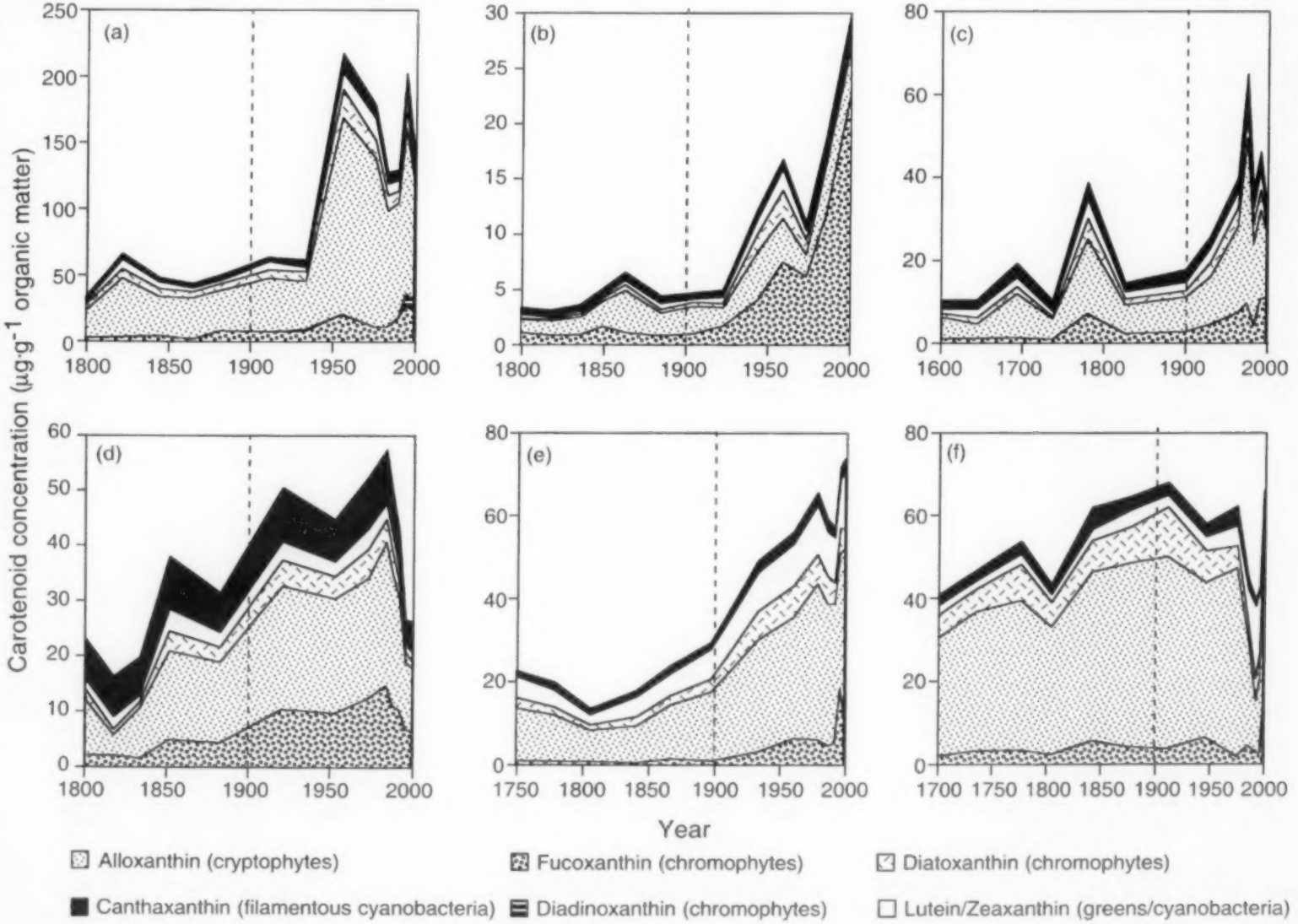

© 2002 NRC Canada

Fig. 5. Ordination diagrams based on correspondence analysis (CA) of taxonomically diagnostic pigment concentrations (●) in ^{210}Pb-aged lake sediment cores (■, pre-industrial sediment intervals; □, post-industrial sediment intervals) showing temporal trajectories of (*a*) Acid Lake, (*b*) OSA Lake, (*c*) George Lake, (*d*) Bell Lake, (*e*) Teardrop Lake, and (*f*) Helen Lake. Abbreviations: Allo, alloxanthin; Canth, canthaxanthin; Chl *b*, chlorophyll *b*; Diato, diatoxanthin; Fuco, fucoxanthin; Lut/Zea, lutein/zeaxanthin.

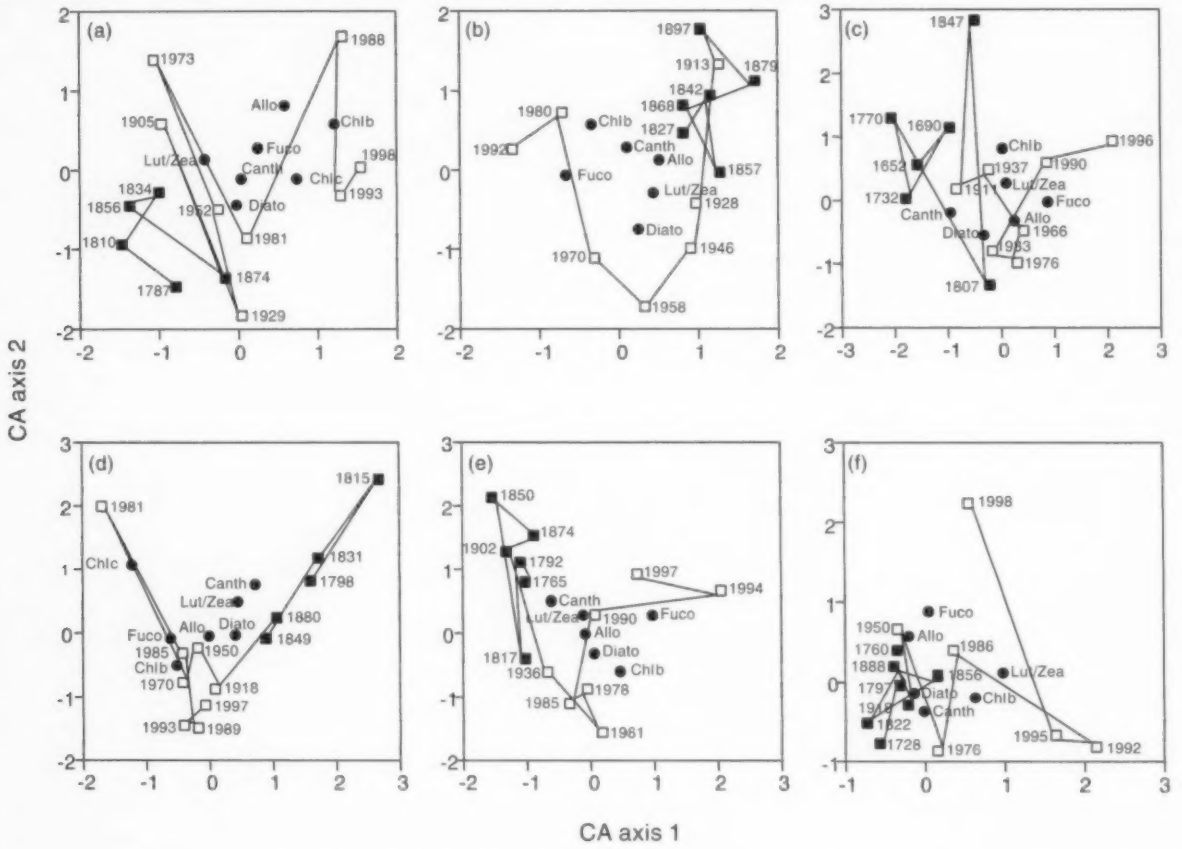

Sedimentary pigment-inferred increases in post-industrial algal abundance in the acidified Killarney lakes possibly resulted from enhanced blooms of deepwater phytoplankton. The rationale for this explanation is based on evidence of increased metalimnetic and hypolimnetic phytoplankton abundances, but not primary productivity, in three experimentally acidified lakes (Schindler et al. 1991). Similarly, post-industrial increases in sedimentary alloxanthin and fucoxanthin concentrations in Acid Lake, OSA Lake, George Lake, and Bell Lake are consistent with increased abundances of deepwater phytoflagellates, namely cryptophytes, chrysophytes, and some dinoflagellates. Deepwater phytoplankton consists of facultative photoautotrophic species that must cope with light limitation, and therefore, contain relatively high concentrations of chlorophylls and accessory pigments (St. Amand and Carpenter 1993). Therefore, leaching of light-attenuating DOC by acid deposition in boreal lakes (Schindler et al. 1996; Yan et al. 1996) could have increased light availability and the abundance of deepwater algae in the Killarney lakes. For example, diatom-inferred DOC concentrations declined from 2.5 mg·L^{-1} to 1.2 mg·L^{-1} during the acidification of George Lake from 1920 to 1970 (Dixit et al. 2001), which would have substantially increased underwater light penetration. Motile phytoflagellates, such as chrysophytes, cryptophytes, and dinoflagellates, can also avoid increased penetration of damaging UVB radiation (Schindler et al. 1996; Yan et al. 1996) and seek refuge in the less-acidic, nutrient-rich hypolimnion of acidified boreal lakes (Findlay et al. 1999). Similar increases in sedimentary chlorophyll and fucoxanthin concentrations also accurately recorded enhanced blooms of deepwater chrysophytes in Lake 302S during experimental acidification from pH 6.8 to 4.7 (Leavitt et al. 1999).

Another potential explanation for pigment-inferred increases in whole-lake algal abundances in the severely acidified lakes (Acid, OSA) involves release from grazing pressure. Specifically, herbivorous copepods and cladocerans are suppressed significantly by anthropogenic acidification below pH 5, whereas algal biomass is more resilient to increased acidity (Findlay et al. 1999; Klug et al. 2000). However, pigment-inferred increases in post-industrial phytoplankton biomass in the acidified Killarney lakes were likely not attributable to epilimnetic algae because epilimnetic chlorophyll concentrations are unaffected by lake acidity (Schindler et al. 1991).

© 2002 NRC Canada

Fig. 6. Sedimentary stratigraphies of lead (■), nickel (○), and zinc (□) concentrations and diatom-inferred pH values (solid line) in Teardrop Lake, Killarney Park, Ont. The onset of industrial deposition over the lakes (ca. 1900) is indicated by dashed vertical lines. Details of field and laboratory methods are presented in Dixit et al. (2001).

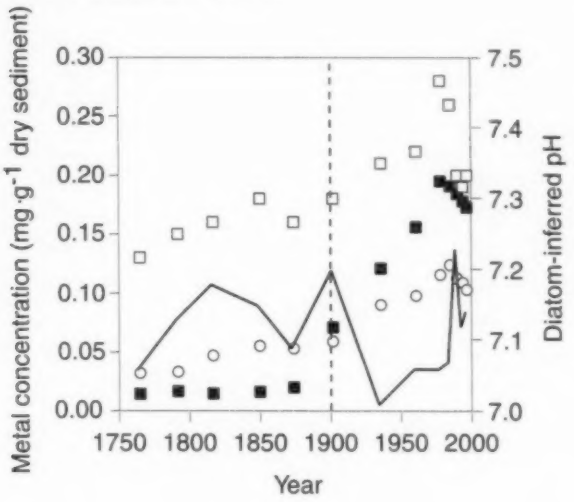

Nevertheless, epilimnetic algal biovolume did increase significantly in experimentally acidified Lake 302S owing to a size shift towards large-celled dinoflagellates (Findlay et al. 1999). Unfortunately, our analyses could not accurately detect dinoflagellate responses to biotic and abiotic changes in the acidified Killarney lakes because their taxonomically diagnostic pigment (peridinin) is highly labile and poorly preserved in lake sediments (Hurley and Garrison 1993).

The characteristic proliferation of filamentous green algae in the littoral zones of anthropogenically acidified lakes (Turner et al. 1995; Vinebrooke et al. 2001) also likely contributed to pigment-inferred increases in post-industrial algal abundance in the acidified Killarney lakes. In particular, increased sedimentary chl *b* concentrations in Acid Lake, OSA Lake, George Lake, and Bell Lake after 1900 suggested that green algae became more abundant in these lakes following the onset of acid deposition. Diatom-inferred pH reconstructions for Acid Lake and George Lake show that pH values fell below 6 between 1900 and 1920 (Dixit et al. 1992*a*, 2001), which corresponds with pigment-inferred increases in acidophilic green algae in both lakes. Filamentous zygnematacean algae (*Mougeotia*, *Spirogyra*, *Zygogonium*) flourish in the absence of benthic grazers in the littoral zone of acidified lakes, as they are superior competitors (Vinebrooke 1996; Graham and Vinebrooke 1998) for dissolved inorganic carbon (DIC), which increasingly limits phytobenthic production in lakes below pH 6 (Turner et al. 1991). Post-industrial increases in filamentous green algae in the acidified lakes possibly also resulted from the extirpation of acid-sensitive zoobenthos such as snails and tadpoles, which are effective grazers of the early developmental stages of these algae in circumneutral Killarney lakes (Vinebrooke 1996; Graham and Vinebrooke 1998). Pigment-inferred post-industrial increases in green algal abundance in the acidified Killarney lakes could not result from increases in phytoplankton biomass because it is mainly composed of chrysophytes, cryptophytes, and dinoflagellates in boreal lakes. Increases in filamentous green algae in the Killarney lakes and in the experimentally acidified Lake 302S (Leavitt et al. 1999) were better recorded by chl *b* than by lutein–zeaxanthin, possibly because increases in chlorophycean lutein were offset by declines in cyanobacterial zeaxanthin.

Diatom-inferred declines in UVB-attenuating DOC in the acidified Killarney lakes (Dixit et al. 2001) were not recorded by increases in UV-absorbing pigment concentrations in the sediment cores. In contrast, sediment-dwelling cyanobacteria produced UV-absorbing pigments (e.g., scytonemin) in response to an 8-fold increase in the penetration of UVB radiation in Lake 302S as it was acidified from pH 6.8 to 5.1 (Leavitt et al. 1997). The absence of UV-absorbing pigments in acidified Killarney lakes might be attributed to the inability of these sediment-dwelling, filamentous cyanobacteria to tolerate high acidity and inhabit the shallow littoral habitats of the heavily acidified Killarney lakes, which are composed mainly of rocky substrate (Vinebrooke 1996; Vinebrooke and Graham 1997). The expected lack of cyanobacteria in the highly acidified Killarney lakes (Acid Lake, OSA Lake, and George Lake) was supported by low concentrations of canthaxanthin, which is an indicator of filamentous cyanobacteria (Jeffrey and Vesk 1997). Interestingly, UV-absorbing pigment concentrations in Lake 302S also declined as the lake was acidified below pH 5 despite further increases in underwater UVB irradiance (Leavitt et al. 1999).

Pigment-inferred increases in post-industrial total algal abundance in circumneutral Teardrop Lake might be attributed to aeolian (windblown) nutrient inputs, but not anthropogenic acidification. Paleolimnological reconstruction of the water chemistry of Teardrop Lake using diatoms showed that pH varied between 7.0 and 7.3 over the last 400 years. However, 3-fold increases in sedimentary trace element concentrations in Teardrop Lake since 1875 revealed that this small headwater lake was strongly influenced by aeolian dust associated with smelting activities. Aeolian dust arising from human disturbance of land surfaces and fly ash can represent a substantial source of trace elements, including phosphorus, to small waterbodies at high elevations (Reynolds et al. 2001). Because many circumneutral boreal lakes are likely phosphorus limited, and because Teardrop Lake receives only limited allochthonous inputs of phosphorus given its small catchment, this little lake is likely very responsive to aerial deposition. Interestingly, there has also been a taxonomic shift by the diatom assemblage in Teardrop Lake, which shows an onset of more productive conditions since 1930 (S.S. Dixit, unpublished data). In contrast, the fertilizing effects of long-range aeolian inputs on the other Killarney lakes (Acid, Bell, George, Helen, OSA) were likely diluted by their larger water volumes and outweighed by allochthonous nutrient inputs from relative vast watersheds. In addition, other regional processes (e.g., climate change) over the past century may also have contributed to synchronous changes in whole-lake algal community structure in Teardrop Lake and the acidified Killarney lakes. For instance, climate change has resulted in phytoplankton showing temporally coherent taxonomic patterns in other boreal lakes over the past 30 years (Findlay et al. 2001).

© 2002 NRC Canada

Recent declines in total sedimentary pigment concentrations and shifts in pigment signatures in acidified George Lake and Bell Lake may be indicative of chemical and biological recovery since the mid-1980s. In both lakes, chemical recovery over the last two decades has enabled them to almost re-establish their historical (diatom-inferred) pH of 6 (Dixit et al. 2001), which also represents the threshold for the proliferation of filamentous green algae in the littoral zone of acid-sensitive boreal lakes (Turner et al. 1991). Therefore, lower carotenoid and chl *b* levels in surface sediments of Bell Lake and George Lake may be partly attributed to the decline of acidophilic filamentous green algae. In addition, DOC levels in George Lake have increased since the 1980s to pre-1920 inferred values (Dixit et al. 2001), which would decrease the availability of light and dampen deepwater phytoplankton blooms. Chemical recovery has also allowed many acidified Killarney lakes to be recolonized by extirpated herbivores, which can further suppress algal blooms (Vinebrooke 1996). Similar transient declines in near-surface sedimentary carotenoid concentrations in circumneutral Helen Lake suggest that other regional factors, such as climate (Findlay et al. 2001), are also affecting algal community structure in the Killarney lakes in addition to chemical recovery from cultural acidification.

Inferences of changes in whole-lake algal community structure in the Killarney lakes based on sedimentary pigment stratigraphies are potentially complicated by several factors of pigment deposition. For example, phytoplankton depth can have a positive effect on pigment deposition in lakes because of a reduction in pigment loss associated with abiotic and biotic processes (Hurley and Garrison 1993). Downward shifts in algal distribution from the epilimnion to the metalimnion may result in several-fold increases in pigment deposition (Cuddington and Leavitt 1999), which confound inferences of increased whole-lake algal abundance based on higher sedimentary pigment concentrations. Therefore, concomitant increases in total pigment concentrations and in pigment signatures of deepwater phytoplankton in the acidified Killarney lakes may reflect both enhanced whole-lake algal abundance and better preservation of pigments. Herbivory can also have a positive effect on pigment deposition if digestive loss of pigments is low, and compaction of pigments into fecal material reduces the oxidative losses that mainly occur in the epilimnion (Cuddington and Leavitt 1999). However, herbivore biomass declines significantly during lake acidification (R.D. Vinebrooke and M. Paterson, Freshwater Institute, Winnipeg, Man., unpublished data), and therefore, cannot account for increased pigment deposition in the four acidified study lakes. Otherwise, we restricted our interpretation of sedimentary pigment signatures to individual Killarney lakes to avoid variation in other environmental variables, such as lake morphometry and chemical stratification, which affect pigment preservation and confound between-lake comparisons of pigment stratigraphies (Cuddington and Leavitt 1999).

In summary, our findings suggest that decades of acidic industrial deposition have altered algal community structure in boreal lakes. Although it is difficult to clearly separate the relative importance of pigment-inferred changes in whole-lake algal abundance from spatial shifts in algal community structure, smelter activities appeared to enhance total algal abundance by increasing representation of deepwater and benthic algae in four acidified lakes and a small circumneutral lake. As a consequence, alteration of the base of aquatic foodwebs has likely contributed to the adverse effects of industrial emissions on higher trophic levels in the Killarney lakes.

Acknowledgements

This study was supported by a Canada Foundation for Innovation New Opportunities Grant (R.D.V.), a Natural Sciences and Engineering Council of Canada (NSERC) operating grant (R.D.V.), an NSERC Collaborative Research and Development Grant (S.S.D. and J.M.G.), and the Canada–Norway Northern Lakes Recovery Study Program at Laurentian University, Sudbury, Ont.

References

Cuddington, K., and Leavitt, P.R. 1999. An individual-based model of pigment flux in lakes: implications for organic biogeochemistry and paleoecology. Can. J. Fish. Aquat. Sci. **56**: 1964–1977.

Dixit, A.S., Dixit, S.S., and Smol, J.P. 1992*a*. Long-term trends in lake water pH and metal concentrations inferred from diatoms and chrysophytes in three lakes near Sudbury, Ontario. Can. J. Fish. Aquat. Sci. **49**(Suppl. 1): 17–24.

Dixit, S.S., Dixit, A.S., and Smol, J.P. 1992*b*. Assessment of changes in lake water chemistry in Sudbury area lakes since preindustrial times. Can. J. Fish. Aquat. Sci. **49**(Suppl. 1): 8–16.

Dixit, S.S., Keller, W., Dixit, A.S., and Smol, J.P. 2001. Diatom-inferred dissolved organic carbon reconstructions provide assessments of past UV-B penetration in Canadian Shield lakes. Can. J. Fish. Aquat. Sci. **58**: 543–550.

Findlay, D.L., and Kasian, S.E.M. 1990. Phytoplankton communities of lakes experimentally acidified with sulfuric and nitric acids. Can. J. Fish. Aquat. Sci. **47**: 1378–1386.

Findlay, D.L., Kasian, S.E.M., Turner, M.A., and Stainton, M.P. 1999. Responses of phytoplankton and epilithon during acidification and recovery of a lake. Freshwater Biol. **42**: 159–175.

Findlay, D.L., Kasian, S.E.M., Stainton, M.P., Beaty, K., and Lyng, M. 2001. Climatic influences on algal populations of boreal forest lakes in the Experimental Lakes Area. Limnol. Oceanogr. **46**: 1784–1793.

Glew, J.R. 1989. A new trigger mechanism for sediment samplers. J. Paleolimnol. **2**: 241–243.

Graham, M.D., and Vinebrooke, R.D. 1998. Trade-offs between herbivore-resistance and competitiveness in periphyton of acidified lakes. Can. J. Fish. Aquat. Sci. **55**: 806–814.

Howard-White, F.B. 1963. Nickel, an historical review. Longmans, Toronto.

Hurlbert, S.H. 1984. Pseudoreplication and the design of ecological field experiments. Ecol. Appl. **54**: 187–211.

Hurley, J.P., and Garrison, P.J. 1993. Composition and sedimentation of aquatic pigments associated with deep plankton in lakes. Can. J. Fish. Aquat. Sci. **50**: 2713–2722.

Jeffrey, S.W., and Vesk, M. 1997. Introduction to marine phytoplankton and their pigment signatures. *In* Phytoplankton pigments in oceanography. *Edited by* S.W. Jeffrey, R.F.C. Mantoura, and S.W. Wright. UNESCO publishing, Paris. pp. 37–84.

Jeffries, D.S. 1997. Canadian acid rain assessment. Vol. 3. The effects on Canada's lakes, rivers, and wetlands. Environment Canada, Burlington, Ont.

© 2002 NRC Canada

Keller, W., Gunn, J.M., and Yan, N.D. 1992. Evidence of biological recovery in acid-stressed lakes near Sudbury, Canada. Environ. Pollut. **78**: 79–85.

Klug, J.L., Fischer, J.M., Ives, A.R., and Dennis, B. 2000. Compensatory dynamics in planktonic community responses to pH perturbations. Ecology, **81**: 387–398.

Leavitt, P.R., Vinebrooke, R.D., Donald, D.B., Smol, J.P., and Schindler, D.W. 1997. Past ultraviolet radiation environments in lakes derived from fossil pigments. Nature (London), **388**: 457–459.

Leavitt, P.R., Findlay, D.L., Hall, R.I., and Smol, J.P. 1999. Algal responses to dissolved organic carbon loss and pH decline during whole-lake acidification: evidence from paleolimnology. Limnol. Oceanogr. **44**: 757–773.

Manly, B.J.F. 1997. Randomization, bootstrap and Monte Carlo methods in biology. Chapman and Hall, London.

Renberg, I., and Battarbee, R.W. 1990. The SWAP paleolimnology programme: a synthesis. Phil. Trans. R. Soc. Lond. B, **327**: 227–232.

Reynolds, R., Belnap, J., Reheis, M., Lamothe, P., and Luiszer, F. 2001. Aeolian dust in Colorado plateau soils: nutrient inputs and recent change in source. Proc. Natl. Acad. Sci. U.S.A. **98**: 7123–7127.

Schindler, D.W. 1995. Linking species and communities to ecosystem management: a perspective from the experimental lakes experience. *In* Linking species and ecosystems. *Edited by* C.G. Jones and J.H. Lawton. Chapman & Hall, New York. pp. 313–325.

Schindler, D.W. 1998. A dim future for boreal waters and landscapes. BioScience, **48**: 157–164.

Schindler, D.W., Frost, T.M., Mills, K.H., Chang, P.S.S., Davies, I.J., Findlay, D.L., Malley, D.F., Shearer, J.A.,Turner, M.A., Garrison, P.J., Watras, C.J., Webster, K., Gunn, J.M., Brezonik, P.L., and Swenson, W.A. 1991. Comparisons between experimentally and atmospherically acidified lakes during stress and recovery. Proc. R. Soc. Edinb. Sect. B, **97**: 193–226.

Schindler, D.W., Curtis, P.J., Parker, B.R., and Stainton, M.P. 1996. Consequences of climate warming and lake acidification for UV-B penetration in North American boreal lakes. Nature (London), **379**: 705–706.

Snucins, E., and Gunn, J.M. 1998. Chemical and biological status of Killarney Park lakes (1995–1997). A study of lakes in the early stages of recovery from acidification. Ontario Ministry of Natural Resources Cooperative Freshwater Ecology Unit, Sudbury, Ont.

Snucins, E., Gunn, J.M., Keller, W., Dixit, S., Hindar, A., and Henriksen, A. 2001. Effects of regional reductions in sulphur deposition on the chemical and biological recovery of lakes within Killarney Park, Ontario, Canada. Environ. Monit. Assess. **67**: 179–194.

St. Amand, A., and Carpenter, S.R. 1993. Metalimnetic phytoplankton dynamics. *In* The trophic cascade in lakes. *Edited by* S.R. Carpenter and J.F. Kitchell. Cambridge University Press, Cambridge, U.K. pp. 210–224.

ter Braak, C.J.F. 1990. CANOCO: a FORTRAN program for canonical community ordination. Microcomputer Power, Ithaca, New York.

Turner, M.A., Howell, E.T., Summerby, M., Hesslein, R.H., Findlay, D.L., and Jackson, M.B. 1991. Changes in epilithon and epiphyton associated with experimental acidification of a lake to pH 5. Limnol. Oceanogr. **36**: 1390–1405.

Turner, M.A., Robinson, G.G.C., Townsend, B.E., Hann, B.J., and Amaral, J.A. 1995. Ecological effects of blooms of filamentous green algae in the littoral zone of an acid lake. Can. J. Fish. Aquat. Sci. **52**: 2264–2275.

Vinebrooke, R.D. 1996. Abiotic and biotic regulation of periphyton in recovering acidified lakes. J. North Am. Benthol. Soc. **15**: 318–331.

Vinebrooke, R.D., and Graham, M.D. 1997. Periphyton assemblages as indicators of recovery in acidified Canadian Shield lakes. Can. J. Fish. Aquat. Sci. **54**: 1557–1568.

Vinebrooke, R.D., and P.R. Leavitt. 1998. Direct and interactive effects of allochthonous dissolved organic matter, inorganic nutrients, and ultraviolet radiation on an alpine littoral food web. Limnol. Oceanogr. **43**: 1065–1081.

Vinebrooke, R.D., Turner, M.A., Kidd, K., Hann, B., and Schindler, D.W. 2001. Truncated foodweb effects of omnivorous minnows in a recovering acidified lake. J. North Am. Benthol. Soc. **20**: 697–710.

Yan, N.D., Keller, W., Scully, N.M., Lean, D.R.S., and Dillon, P. 1996. Increased UV-B penetration in a lake owing to drought-induced acidification. Nature (London), **381**: 141–143.

© 2002 NRC Canada

The food-unlimited growth rate of Atlantic cod (*Gadus morhua*)

Björn Björnsson and Agnar Steinarsson

Abstract: Results from laboratory experiments showed that food-unlimited growth rate (G) of Atlantic cod (*Gadus morhua*) declined linearly with fish weight (W) on a log–log scale at six different temperatures: 2, 4, 7, 10, 13, and 16°C. The intercept (α_i) and slope (β_i) of these regressions increased linearly with temperature (T), implying that $G = \alpha_i W^{\beta_i}$, where $\alpha_i = \gamma_1 + \delta_1 T$ and $\beta_i = \gamma_2 + \delta_2 T$. Nonlinear fit of the four-parameter model showed that γ_1 was not significantly different from 0, and thus the following three-parameter model is suggested for the food-unlimited growth rate of cod ranging in size from 2 to 5000 g at any temperature from 2 to 16°C: $G = (0.5735T)W^{(-0.1934-0.020017T)}$. The results indicate that temperature in this size range has a much greater effect on the growth rate of small juvenile cod than on that of larger cod. The model predicts that the optimal temperature for growth of cod decreases with increased size of fish, from 14.3°C for 50-g fish to 5.9°C for 5000-g fish. Growth curves were derived for cod at constant and seasonally variable temperatures. Weight-at-age was calculated for different temperatures.

Résumé : Des expériences en laboratoire démontrent que le taux de croissance de la morue en présence de nourriture illimitée (G) décroît de façon linéaire sur une double échelle logarithmique en fonction de la masse du poisson à 6 températures différentes, 2, 4, 7, 10, 13 et 16°C. Les points d'intersection (α_i) et les pentes (β_i) de ces droites augmentent de façon linéaire en fonction de la température (T), si bien que $G = \alpha_i W^{\beta_i}$, où $\alpha_i = \gamma_1 + \delta_1 T$ et $\beta_i = \gamma_2 + \delta_2 T$. Puisque l'ajustement non-linéaire du modèle à quatre paramètres indique que γ_1 n'est pas significativement différent de 0, le modèle suivant à trois paramètres permet de décrire la croissance avec nourriture illimitée chez des morues de 2–5000 g à toute température comprise entre 2 et 16°C: $G = (0{,}5735T)W^{(-0{,}1934 + 0{,}020017T)}$. La température a un effet plus important sur le taux de croissance des petites morues que sur celui des plus grandes dans cet intervalle de tailles. Le modèle prédit que la température optimale pour la croissance de la morue diminue en fonction de la taille, de 14,3°C chez les poissons de 50 g à 5,9°C chez ceux de 5000 g. Nous avons tracé des courbes de croissance pour les morues à températures constantes et à des températures qui varient d'après la saison. Nous avons aussi calculé la masse des morues des différents âges pour chacune des températures.

[Traduit par la Rédaction]

Introduction

In the North Atlantic, there are several Atlantic cod stocks (*Gadus morhua*) that occupy different geographic areas with mean yearly temperatures ranging between 2 and 11°C (Brander 1994). The growth rates are affected by temperature, food availability, and other factors, but it has been difficult to quantify their effects in population studies (Brander 1995). Weight-at-age data from commercial catches are available for all major cod stocks, providing some indications about the year-to-year changes in growth rates, but it is difficult to estimate the mean ambient temperatures of each stock (Heessen and Daan 1994; Michalsen et al. 1998; Ottersen et al. 1998). The year-to-year changes in mean ambient temperature of a given cod stock are small compared with the total range in temperature experienced by the different cod stocks; thus, a comparison between stocks may be useful in determining the effects of temperature on growth rate of cod (Brander 1994, 1995). However, the effects of food availability, genetic differences, and other factors are difficult to assess across stocks.

An alternative approach to studying the environmental effects on growth is to carry out laboratory experiments. Jones and Hislop (1978), Braaten (1984), and Hawkins et al. (1985) studied the growth rate of cod in relation to fish size and ration, and Björnsson et al. (2001) studied the effects of size on optimal temperature for growth and feed conversion of cod. In the present study, data from several laboratory experiments were analysed with the aim of developing an empirical relationship for estimating the food-unlimited growth rate of cod over a wide range of temperatures and fish size. Such a relationship may be useful when interpreting growth rate measurements in wild fish stocks. It may also be useful when assessing the feasibility of cod farming, which is currently under consideration in Norway, Scotland, Iceland, and Canada.

Received 16 May 2001. Accepted 28 February 2002. Published on the NRC Research Press Web site at http://cjfas.nrc.ca on 6 April 2002.
J16352

B. Björnsson[1] **and A. Steinarsson.** Marine Research Institute, Skúlagata 4, P.O. Box 1390, 121 Reykjavík, Iceland.

[1]Corresponding author (e-mail: bjornb@hafro.is).

Materials and methods

Experiments

The experiments were carried out at the Mariculture Laboratory of the Marine Research Institute at Grindavík in southwest Iceland. The seawater supply of the laboratory, obtained from a 50-m-deep well, has a constant temperature (7°C) and salinity (32‰).

 DOI: 10.1139/F02-028 © 2002 NRC Canada

The cod were reared in groups of 31–155 fish per tank; 82% of the groups contained at least 90 fish per group (Appendix A). A total of 126 growth rate measurements were made at six different mean temperatures: 2.1 (range 1.9–2.2), 4.1 (3.2–5.1), 7.3 (6.8–7.6), 10.0 (9.0–11.2), 13.0 (12.8–13.4), and 15.7°C (15.0–16.0°C). Of these, 104 measurements were made with cod hatched in the laboratory (geometric mean weight (W) = 1–134 g) and 22 with wild cod brought to the laboratory some months prior to the experiments (W = 0.6–6.6 kg). The experiments were carried out during the periods 1993–1994 and 1995–2000 with the wild and hatchery-reared fish, respectively. The broodstock and the wild fish used in the experiments were collected near the southwest coast of Iceland in the autumns of 1992 and 1993. The hatchery-reared fish were hatched in April 1995, 1996, and 2000, mainly from eggs collected from the broodstock tank, but some of the eggs and milt were obtained at sea near the southwest coast. The experimental fish were weighed individually without anaesthesia at the start and termination of each experiment.

Rearing conditions

The smallest fish (W = 1–16 g) were reared in rectangular fibreglass tanks (90 × 90 × 30 cm), fish of intermediate size (W = 7–2300 g) in circular fibreglass tanks (2.9 m in diameter and 0.8 m deep), and the largest fish (W = 1.2–6.6 kg) in circular fibreglass tanks (8.0 m in diameter and 1.0 m deep). The rearing temperatures were measured daily and the oxygen concentration once a week. Water exchange was regulated so that the oxygen concentration in the outlet of each tank was always above 6 mg·L^{-1}. All of the oxygen measurements were above 60% saturation and more than 95% of them above 65% saturation level. The maximum stocking density was always below 20 kg·m^{-3}. The fish subject to the highest and lowest temperatures were gradually acclimated to the experimental temperatures over a 2-day period. A natural photoperiod (64°N) was maintained, except in the experiments carried out in the smallest tanks, where a fixed photoperiod was maintained (12 h light : 12 h dark) (Appendix A). In all of the experiments, the light intensity at the surface was about 25 lx during the daytime.

Feeding

In all of the experiments, the fish were handfed to satiation. The hatchery-reared fish were fed three to five times a day using a commercial dry feed for salmonids made by Ewos (Reykjavík) and Laxá (Akureyri). The protein, fat, carbohydrate, water, and ash contents of the dry feed ranged between 42 and 54, 18 and 26, 8 and 16, 7 and 9, and 8 and 11%, respectively. The feed for the smallest fish had the highest protein content and lowest fat content (Björnsson et al. 2001).

As it is difficult to wean wild cod onto dry feed, they were fed on a more natural wet feed, whole capelin (*Mallotus villosus*) and shrimp (*Pandalus borealis*), usually six times a week in a 5:2 ratio (Björnsson et al. 2001). The protein, fat, carbohydrate, water, and ash contents of the wet feed were 15, 10–17, 0, 67–72, and 2–3%, respectively. Periodically, the wet feed was supplemented with vitamins according to Björnsson et al. (1992). Feeding studies do not indicate that energy density of the diet affects growth rate of cod significantly (Jobling et al. 1991; Dos Santos et al. 1993; Morais et al. 2001).

Data analysis

Specific growth rate (G) was calculated as percent per day according to the formula $G = 100(\ln W_2 - \ln W_1)/(t_2 - t_1)$, where W_1 and W_2 are the weights of the fish at times t_1 and t_2. The growth rate was calculated over a period of at least 3 weeks for fish 1–10 g, at least 6 weeks for fish 10–250 g, and 36–53 weeks for fish 0.6–6.6 kg. Most of the cod of wild origin became sexually mature during the experiments. Their growth rates were calculated over a long period of time, a year when possible, to minimize the effects of sexual maturity on growth.

Specific growth rate was found to change linearly with geometric mean weight, $W = (W_1W_2)^{1/2}$, on a log–log scale, and thus the relationship could be described with the following formula: $G = \alpha_i W^{\beta_i}$. The intercept (α_i) and slope (β_i) of the relationship were found to change linearly with temperature (T) in the experimental tanks, $\alpha_i = \gamma_1 + \delta_1 T$ and $\beta_i = \gamma_2 + \delta_2 T$, resulting in the following model: $G = (\gamma_1 + \delta_1 T)W^{(\gamma_2 + \delta_2 T)}$. The model was parametrized by three different methods.

In Method 1, first, linear least square regressions were found for ln$G$ vs. ln$W$ for the six different temperatures. Then the intercepts and slopes of these regressions were fitted linearly against T to find the four parameters in the model (Table 1). In Method 2, nonlinear fit of the model in one step for the whole data set using AD-Model Builder version 4 (Otter Research Ltd., Sidney, B.C.) gave somewhat different parameters (Table 1). In Method 3, nonlinear fit of the model using AD-Model Builder was done as before but now assuming that $\gamma_1 = 0$, since this parameter was not found to be significantly different from 0. The model results are only shown for this three-parameter model. However, the model results were similar for all three sets of parameters. Growth curves from the initial weight of 1 g were also calculated from the three-parameter model using the following recursion formula: $W_2 = W_1 e^k$ where $k = (\alpha_i / 100)W_1^{\beta_i}$ and W_1 is the fish weight at day d and W_2 is the fish weight at day $d + 1$ (Björnsson et al. 2001).

Seasonal changes in temperature (T_s) were calculated with the following equation: $T_s = T_m + T_a \cos((2\pi/365)t)$, where T_m is the mean temperature, T_a is the amplitude, and t is time in days. An amplitude of 2°C was used in all calculations. The simulation begins when cod reach 1 g near the highest seasonal temperature. Wild cod juveniles in Iceland and Norway normally reach this size in August (Loeng and Gjøseter 1990; Astthorsson et al. 1994).

Results

On a log–log scale, growth rate decreased linearly with fish weight at all temperatures (Fig. 1). Between 85 and 98% of the variation in growth rate could be explained by variation in fish size at a given temperature (Table 2). ANOVA assuming equal variances for the different temperatures shows that the H_0 hypothesis, that there is no difference between the six different slopes in Fig. 1, can be rejected (F = 15.67, df = 5 and 114, $p < 0.0001$).

The intercepts of the regressions in Fig. 1 increased linearly with temperature, with almost 100% of the variation

© 2002 NRC Canada

Table 1. The three sets of parameters found for the food-unlimited growth model for cod, $G = \alpha_i W^{\beta_i}$, where $\alpha_i = \gamma_1 + \delta_1 T$ and $\beta_i = \gamma_2 + \delta_2 T$, using three different methods of parameterization (see text).

Parameter	Method 1	Method 2	Method 3
γ_1	–0.6064	–0.1390	0
δ_1	0.6706	0.5952	0.5735
γ_2	–0.1481	–0.1851	–0.1934
δ_2	–0.0254	–0.02105	–0.02001

Note: G, specific growth rate; W, geometric mean weight of the fish; T, experimental temperature.

being explained by variation in temperature (Fig. 2*a*). Also, the slopes of the regressions in Fig. 1 increased linearly with temperature, with 97% of the variation being explained by variation in temperature (Fig. 2*b*). These findings suggested a four-parameter growth model of the form $G = (\gamma_1 + \delta_1 T)W^{(\gamma_2 + \delta_2 T)}$. However, a more sophisticated fit to the data (see Materials and methods) indicated that a three-parameter growth model of the form $G = (\delta_1 T)W^{(\gamma_2 + \delta_2 T)}$ seems to be adequate for cod, implying that $G = 0$ at $T = 0$°C. The model appears to be applicable in the size range 2–5000 g and in the temperature range 2–16°C. There is some indication that the model overestimates the growth rate of smaller (<2 g) and larger (>5000 g) fish.

The food-unlimited growth model indicates that temperature has a relatively greater effect on the growth rate of small juvenile cod (2–10 g) than on that of larger cod, e.g., an increase in temperature from 2 to 7°C increased the growth rate 3.3, 2.2, and 1.5 times for the 2-, 100-, and 5000-g cod, respectively (Fig. 3; Table 3). The optimal temperature for growth was found to decline with weight of cod in the weight range studied (Fig. 3; Table 3).

The model calculation from an initial weight of 1 g for six selected temperatures shows that after 3 years, cod at 7°C catch up with cod reared at 10°C at a weight of 3.8 kg (Fig. 4). However, cod at 2°C only reach 353 g by the end of the 3-year period. Cod reared at 4°C grow initially more slowly than cod at 16°C, but after 3 years, they have almost caught up with the cod reared at 16°C (Fig. 4).

A regular seasonal variation in temperature of ±2°C resulted in significant seasonal variations in growth rate at low temperatures (<5°C), with the fastest growth rates during summer (Fig. 5). No seasonal variation in growth rate was, however, apparent at a mean temperature of 7°C, and at higher temperatures the fastest growth rates were found during winter.

The food-unlimited growth model indicates that weight-at-age (from an initial weight of 1 g) increases rapidly with temperature, reaching a maximum at intermediate temperatures before declining with a further increase in temperature (Fig. 6). The weights calculated at 3 years of age were 1.0, 2.8, 3.8, 4.0, and 3.6 kg at 3, 5, 7, 9, and 11°C, respectively.

Discussion

The results indicate that the food-unlimited growth rate of cod reared at a given temperature decreases linearly with fish weight from 2 to 5000 g on a log–log scale. A similar relationship has been found for salmonids (Brett and Shelbourn 1975; Brett 1979), cod (Braaten 1984), turbot (Nijhof 1994), and several other species (Jobling 1983), and generally, the slopes of these relationships tend to be around –0.4 for most species of fish. Braaten (1984) found a slope of –0.45 for 100- to 4000-g cod reared at 8.5°C and Björnsson et al. (2001) a slope of –0.40 for 2- to 2000-g cod reared at optimal temperatures for growth. Brett and Shelbourn (1975) found no variation in the slope of the above relationship with temperature for salmonids and concluded that environmental and genetic differences would have the greatest effect on the intercept. No change in the slope with temperature implies no change in optimal temperature with fish size. The present study indicates, however, that for cod, both the intercept and the slope of the log G – log W relationship increase linearly with temperature.

The model shows that optimal temperature for growth (T_{optG}) decreases with the weight of cod in the size range studied. In the size range 50–5000 g, T_{optG} was usually slightly lower in the model than in the study by Björnsson et al. (2001), where a parabola was used to correlate growth rate and temperature for different size groups. However, the G versus T curves derived from the model are asymmetrical with steeper slopes on the left side. The maximum difference in T_{optG} between the two studies was only 1.4°C for cod in this size range, which is not much when considering the flatness of the G versus T curves near the top.

For the smallest fish (2–20 g), the optimal temperatures were clearly overestimated ($T_{optG} > 16$°C), indicating that the model is not applicable for temperatures above 16°C. Furthermore, the model does not apply to cod larvae and juveniles <1 g. Indeed, Steinarsson and Björnsson (1999) have demonstrated that both T_{optG} and the growth rates of larval cod increase with weight.

The growth rate of mature cod varies greatly throughout the year from the negative growth during the spawning period to the fast postspawning compensatory growth (Pedersen and Jobling 1989). The model does not account for this seasonal variation in growth rate. The model may underestimate the food-unlimited growth rate of large immature cod. For example, in one of the experiments included in the regression analysis, wild immature cod grew from 1.2 to 5.0 kg in 1 year at 7°C but should only have grown to 3.7 kg according to the model. In the year after, the same cod, when becoming sexually mature, grew from 5.0 to 8.2 kg instead of to 10.6 kg as predicted by the model, showing that the model may overestimate the growth rate of sexually mature cod. Cod hatched in the laboratory tend to mature at a much smaller size than wild cod, and the model may overestimate the growth rate of these cod. If, however, the maturity of these cod could be delayed or prevented, the scope of the model would be increased.

According to Braaten (1984), the specific growth rates of 200-, 500-, and 2000-g cod reared at 8.5°C were 0.89, 0.59, and 0.32%·day^{-1}, respectively, compared with 0.71, 0.51, and 0.31%·day^{-1}, respectively, in the present study. Thus, the agreement is good for 500- and 2000-g cod, but Braaten's (1984) estimate for 200-g cod is 25% higher than in the present study. The agreement between the model of Jobling (1988) and our model is much less. For example, his model

© 2002 NRC Canada

Fig. 1. Food-unlimited growth rate of cod as a function of fish weight; linear regression on a log–log scale for six different temperatures as follows: (*a*) 2, (*b*) 4, (*c*) 7, (*d*) 10, (*e*) 13, and (*f*) 16°C.

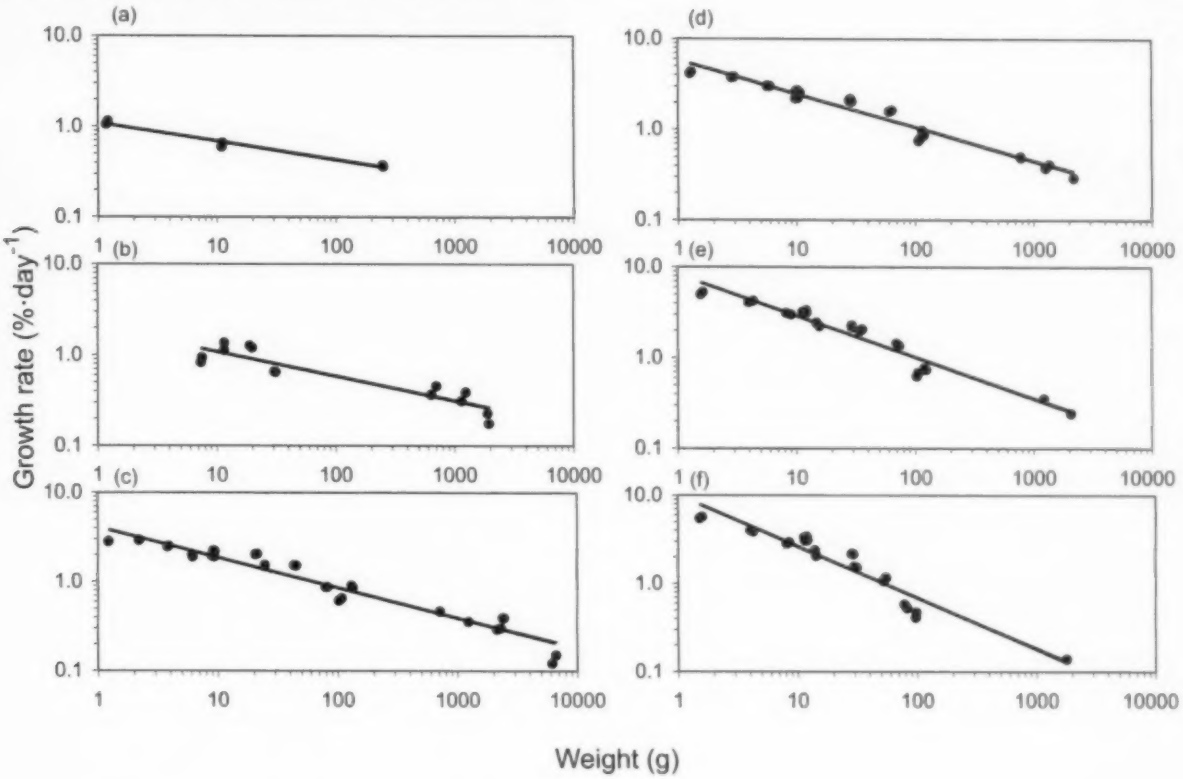

Table 2. Parameters from the regression analysis in Fig. 1.

T (°C)	α_i	β_i	r^2	n
2.1	1.0928	–0.2017	0.978	6
4.1	2.0215	–0.2694	0.852	14
7.3	4.0959	–0.3387	0.942	32
10.0	5.7903	–0.3686	0.959	27
13.0	8.2806	–0.4558	0.939	24
15.7	10.0580	–0.5810	0.913	23

Note: T, mean temperature; α_i, intercept; β_i, slope; r^2, coefficient of determination; n, number of measurements.

predicts that 2000-g cod at 4, 8, 12, and 16°C grow 0.14, 0.36, 0.61, and 0.56%·day^{-1}, respectively, compared with 0.29, 0.31, 0.26, and 0.18%·day^{-1} according to our model. This large discrepancy may partly be due to the limited data available to the author and partly because the optimal temperature of cod was not considered to vary with fish weight. There is very good agreement between our model and the growth rate of cod in a sea pen in Iceland at a mean yearly temperature of 3.7°C (Björnsson 1999). The mean weight of 90 tagged cod increased from 0.91 to 2.57 kg in 347 days, but they should have grown to 2.62 kg according to the model.

It is well known that during the first few years, cod grow much faster in warmer areas such as the North Sea or the Gulf of Maine than in colder areas such as the Barents Sea and the Newfoundland region (Brander 1994; Nakken 1994; Serchuk et al. 1994), which is in agreement with the model. However, there is some evidence that the maximum attainable size of cod decreases with increased ambient temperature (Taylor 1958; Pauly 1984), and apparently, most of the largest cod on the world market originate from the cold areas. This may partly be explained by the decrease in optimal temperature with size of cod (Björnsson et al. 2001; this paper) and partly by changes in natural mortality, which at high temperatures tends to increase with the size of cod (Björnsson et al. 2001).

The model can be used for predicting the food-unlimited growth of cod up to 3 years of age (from the initial weight of 1 g). As wild juvenile cod in many stocks reach 1 g in August, the mean weights-at-age in the summer and autumn groundfish surveys are comparable with the model results. In the Icelandic groundfish surveys in October 1995–1998, the mean weight of 3-year-old cod was 1.0 kg at a mean annual temperature of approximately 4°C (Dr. Einar Hjörleifsson, Marine Research Institute data bank, Reykjavík, Iceland; Sigurdsson et al. 1997) compared with 1.9 kg as predicted by the model. The mean weight of 3-year-old North Sea cod

© 2002 NRC Canada

Fig. 2. Linear regression of the (*a*) intercept and temperature and (*b*) slope and temperature of the relationships in Fig. 1.

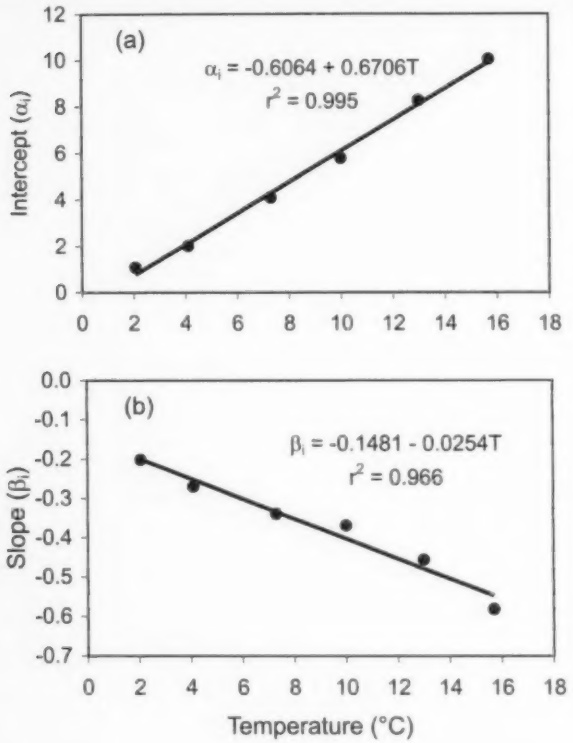

Fig. 3. Model calculation of food-unlimited growth rate (*G*) of cod as a function of temperature (*T*) for (*a*) fish weight (*W*) from 2 to 100 g and (*b*) from 200 to 5000 g. $G = (0.5735T)W^{(-0.1934-0.020017)}$.

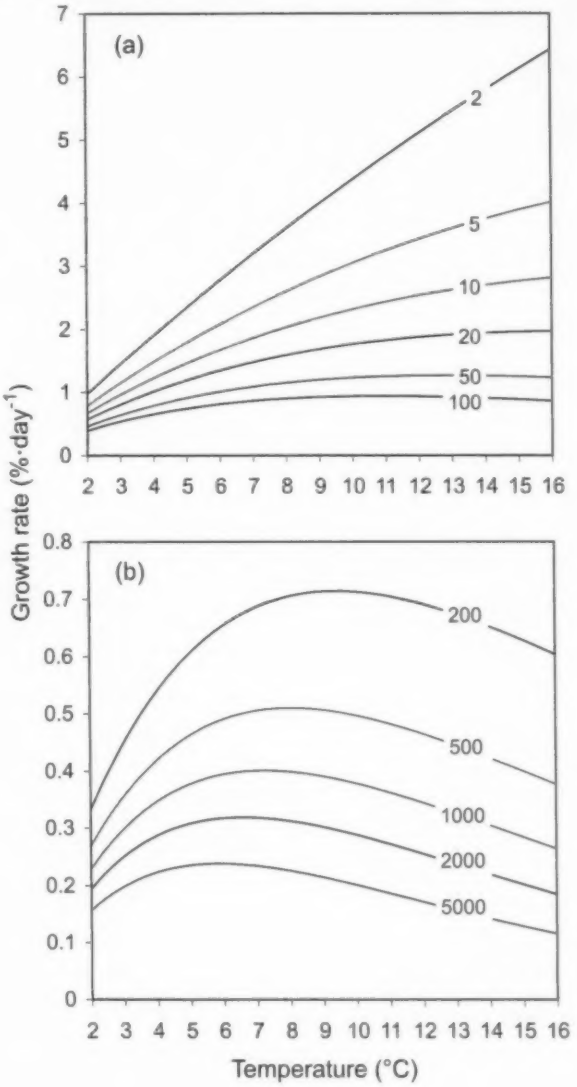

(8.6°C) was 1.9 kg (Brander 1995) compared with 4.0 kg as predicted by the model. The generally lower growth rates of wild cod compared with cod reared in laboratory experiments may indicate that the growth of wild cod is frequently food limited, as suggested earlier (Braaten 1984; Björnsson 1999).

The model predicts that the maximum attainable weight of 3-year-old cod increases almost linearly with temperature from 3–6°C before leveling off and reaching a maximum of 4.0 kg at 8.5°C. A further increase in temperature results in a decrease in maximum weight. In contrast, Brander (1995) compared several cod stocks and found that the mean weight of 3-year-old cod in commercial catches increased exponentially with mean annual temperature from 0.53 kg at 2°C to 3.4 kg at 11°C. At intermediate temperatures, 4–10°C, our model predicts a much larger weight of 3-year-old cod than that found by Brander (1995), whereas the difference is less at low and high temperatures. The field data are based on averages for whole year-classes of cod experiencing temperatures varying greatly in time and space, whereas the food-unlimited growth model is based on growth rate measurements of fish reared at constant temperatures. Data for individual fish in the wild, e.g., those collected by data storage tags, may be more suitable for comparison with the model than averages for whole year-classes.

A seasonal variation in temperature affects the model differently depending on the temperature range. In cold areas, slow growth rates are predicted during winter, whereas in warmer areas, slow growth rates are predicted during summer. A seasonal sampling of 0-, 1-, and 2-year-old cod north of Iceland, where bottom temperatures normally vary between 2 and 6°C, showed that the growth was much faster in summer and autumn than in winter and spring (Pálsson 1980) as predicted by the model.

Although the model is based on laboratory experiments with fish from the Icelandic cod stock only, it is likely that similar relationships exist for other cod stocks, even though the food-unlimited growth rate may differ to some extent between stocks. Only a minor difference in growth rate was found between Arcto-Norwegian and Norwegian coastal ju-

© 2002 NRC Canada

Table 3. Optimal temperature for growth (T_{optG}) at selected fish weights (W) according to the three-parameter model and the study by Björnsson et al. (2001).

	T_{optG} (°C)		
W (g)	Model	Björnsson et al. (2001)	$(G_{T=7})/(G_{T=2})$*
2	>16.0	17.3	3.3
5	>16.0	16.0	3.0
10	>16.0	15.0	2.8
20	>16.0	14.0	2.6
50	12.8	12.7	2.4
100	10.9	11.7	2.2
200	9.4	10.7	2.1
500	8.0	9.4	1.9
1000	7.2	8.4	1.8
2000	6.6	7.4	1.6
5000	5.9	6.1	1.5

*Ratio of growth rate at 7°C ($G_{T=7}$) and 2°C ($G_{T=2}$) at different weights according to the model.

Fig. 4. Growth curves for cod at six different constant temperatures: 2, 4, 7, 10, 13, and 16°C (model calculation from an initial weight of 1 g).

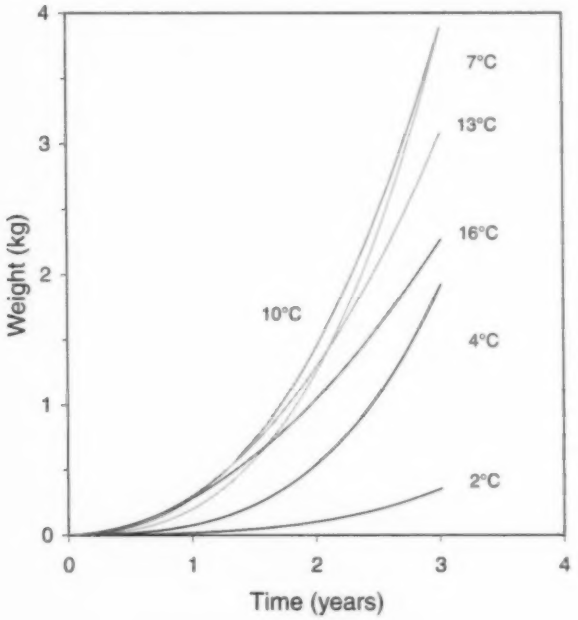

venile cod reared under similar conditions (Svåsand et al. 1994), and no differences were found between the growth rates of juvenile cod from the Grand Banks and the Gulf of Maine (Purchase and Brown 2000) or between the growth rates of juvenile cod from the Bonavista Bay and Fortune Bay (Purchase and Brown 2001). Therefore, it seems likely that the growth rate of cod may be more affected by environmental than genetic factors and that the model may have use in predicting the food-unlimited growth rate of cod from different stocks. It is hoped that the model may be useful in interpreting growth rate measurements of wild cod as well

Fig. 5. Growth curves for cod at five different mean temperatures, 2, 3, 4, 5, and 7°C, fluctuating seasonally by ±2°C (model calculation from an initial weight of 1 g).

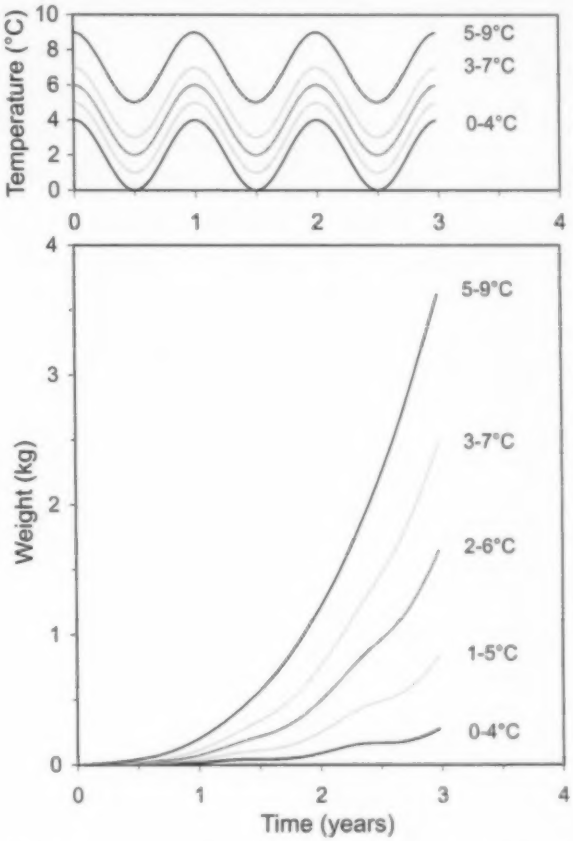

Fig. 6. Weight-at-age as a function of temperature for 1-, 2-, and 3-year-old cod (model calculation from an initial weight of 1 g).

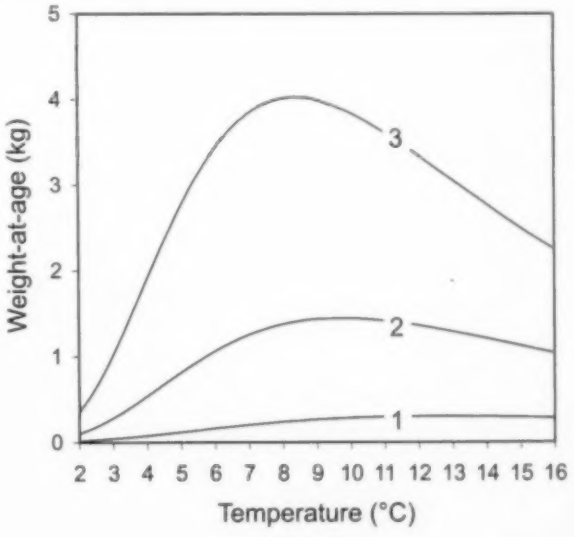

© 2002 NRC Canada

as in assessing the feasibility of cod farming in different geographic areas.

Acknowledgements

We thank Mr. Ellert Gudmundsson, Mr. Njáll Jónsson, Mr. Matthías Oddgeirsson, and Mr. Sverrir Valdemarsson for taking good care of the fish during the experiments. Dr. Birgir Hrafnkelsson, Dr. Einar Hjörleifsson, Dr. Gunnar Stefánsson, and Mr. Höskuldur Björnsson, Marine Research Institute, assisted with the statistical analysis of the data, and three anonymous referees provided valuable help with the manuscript.

References

Astthorsson, O.S., Gislason, A., and Gudmundsdottir, A. 1994. Distribution, abundance, and length of pelagic juvenile cod in Icelandic waters in relation to environmental conditions. ICES Mar. Sci. Symp. **198**: 529–541.

Björnsson, B. 1999. Is the growth rate of Icelandic cod (*Gadus morhua* L.) food-limited? A comparison between pen-reared cod and wild cod living under similar thermal conditions. Rit Fiskideildar, **16**: 271–279.

Björnsson, B., Sigurthorsson, G., Hemre, G.-I., and Lie, Ø. 1992. Growth rate and feed conversion factor of young halibut (*Hippoglossus hippoglossus* L.) fed six different diets. Fiskeridir. Skr. Ser. Ernaer. **5**: 25–35.

Björnsson, B., Steinarsson, A., and Oddgeirsson, M. 2001. Effects of size on optimal temperature for growth and feed conversion of immature cod (*Gadus morhua* L.). ICES J. Mar. Sci. **58**: 29–38.

Braaten, B. 1984. Growth of cod in relation to fish size and ration level. *In* The propagation of cod *Gadus morhua* L. Vol. 1. Flødev. rapports. *Edited by* E. Dahl, D.S. Danielssen, E. Moksness, and P. Solemdal. Institute of Marine Research, Arendal, Norway. pp. 677–710.

Brander, K.M. 1994. Patterns of distribution, spawning, and growth in North Atlantic cod: the utility of inter-regional comparisons. ICES Mar. Sci. Symp. **198**: 406–413.

Brander, K.M. 1995. The effects of temperature on growth of Atlantic cod (*Gadus morhua* L.). ICES J. Mar. Sci. **52**: 1–10.

Brett, J.R. 1979. Environmental factors and growth. *In* Fish physiology. Vol. VIII. Bioenergetics and growth. *Edited by* W.S. Hoar, D.J. Randall, and J.R. Brett. Academic Press, New York. pp. 599–675.

Brett, J.R., and Shelbourn, J.E. 1975. Growth rate of young sockeye salmon, *Oncorhynchus nerka*, in relation to fish size and ration level. J. Fish. Res. Board Can. **32**: 2103–2110.

Dos Santos, J., Burkow, I.C., and Jobling, M. 1993. Patterns of growth and lipid deposition in cod (*Gadus morhua* L.) fed natural prey and fish-based feeds. Aquaculture, **110**: 173–189.

Hawkins, A.D., Soofiani, N.M., and Smith, G.W. 1985. Growth and feeding of juvenile cod (*Gadus morhua* L.). J. Cons. Int. Explor. Mer, **42**: 11–32.

Heessen, H.J.L., and Daan, N. 1994. Cod distribution and temperature in the North Sea. ICES Mar. Sci. Symp. **198**: 244–253.

Jobling, M. 1983. Growth studies with fish-overcoming the problems of size variation. J. Fish Biol. **22**: 153–157.

Jobling, M. 1988. A review of the physiological and nutritional energetics of cod, *Gadus morhua* L., with particular reference to growth under farmed conditions. Aquaculture, **70**: 1–19.

Jobling, M., Knudsen, R., Pedersen, P.S., and Dos Santos, J. 1991. Effects of dietary composition and energy content on the nutritional energetics of cod, *Gadus morhua*. Aquaculture, **92**: 243–257.

Jones, R., and Hislop, J.R.G. 1978. Further observations on the relation between food intake and growth of gadoids in captivity. J. Cons. Int. Explor. Mer, **38**: 244–251.

Loeng, H., and Gjøseter, H. 1990. Growth of 0-group fish in relation to temperature conditions in the Barents Sea during the period 1965–1989. ICES CM 1990/G:49.

Michalsen, K., Ottersen, G., and Nakken, O. 1998. Growth of North-east Arctic cod (*Gadus morhua* L.) in relation to ambient temperature. ICES J. Mar. Sci. **55**: 863–877.

Morais, S., Bell, J.G., Robertson, D.A., Roy, W.J., and Morris, P.C. 2001. Protein/lipid ratios in extruded diets for Atlantic cod (*Gadus morhua* L.): effects on growth, feed utilisation, muscle composition and liver histology. Aquaculture, **203**: 101–119.

Nakken, O. 1994. Causes of trends and fluctuations in the Arcto-Norwegian cod stock. ICES Mar. Sci. Symp. **198**: 212–228.

Nijhof, M. 1994. Research on nutrition and growth in the culture of post larval turbot (*Scophthalmus maximus* L.). *In* Turbot culture: problems and prospects. *Edited by* P. Lavens and R.A.M. Remmerswaal. Spec. Publ. 22. European Aquaculture Society, Gent, Belgium. pp. 137–165.

Ottersen, G., Michalsen, K., and Nakken, O. 1998. Ambient temperature and distribution of north-east Arctic cod. ICES J. Mar. Sci. **55**: 67–85.

Pálsson, Ó.K. 1980. Über die Biologie junger Gadiden der Altersgruppen 0, I und II in isländischen Gewässern. Meeresforschung, **28**: 101–145.

Pauly, D. 1984. A mechanism for the juvenile-to-adult transition in fishes. J. Cons. Int. Explor. Mer, **41**: 280–284.

Pedersen, T., and Jobling, M. 1989. Growth rates of large, sexually mature cod, *Gadus morhua*, in relation to condition and temperature during an annual cycle. Aquaculture, **81**: 161–168.

Purchase, C.F., and Brown, J.A. 2000. Interpopulation differences in growth rates and food conversion efficiencies of young Grand Banks and Gulf of Maine Atlantic cod (*Gadus morhua*). Can. J. Fish. Aquat. Sci. **57**: 2223–2229.

Purchase, C.F., and Brown, J.A. 2001. Stock-specific changes in growth rates, food conversion efficiencies, and energy allocation in response to temperature change in juvenile Atlantic cod. J. Fish Biol. **58**: 36–52.

Serchuk, F.M., Grosslein, M.D., Lough, R.G., Mountain, D.G., and O'Brien, L. 1994. Fishery and environmental factors affecting trends and fluctuations in the Georges Bank and Gulf of Maine Atlantic cod stocks: an overview. ICES Mar. Sci. Symp. **198**: 77–109.

Sigurdsson, Th., Hjörleifsson, E., Björnsson, H., and Pálsson, Ó.K. 1997. Icelandic groundfish survey, autumn 1996. Rep. No. 61. Marine Research Institute, Reykjavík, Iceland. [In Icelandic.]

Steinarsson, A., and Björnsson, B. 1999. The effects of size and temperature on growth and mortality of cod larvae. J. Fish Biol. **55**(Suppl. A): 100–109.

Svåsand, T., Jørstad, K.E., and Otterå, H. 1994. Growth of juvenile Arcto-Norwegian and Norwegian coastal cod reared under similar conditions. ICES Mar. Sci. Symp. **198**: 624–625. (Abstr.)

Taylor, C.C. 1958. Cod growth and temperature. J. Cons. Int. Explor. Mer, **23**: 366–370.

© 2002 NRC Canada

Appendix A

Table A1. Growth data of cod used to develop the model: starting date, temperature (T), initial number of fish (n_1), initial mean weight (W_1), final mean weight (W_2), number of days (d).

Date	T (°C)	n_1	W_1	W_2	d	Date	T (°C)	n_1	W_1	W_2	d
4 Aug. 2000	1.9	90*	0.9	1.5	53	4 Aug. 2000	2.0	90*	0.9	1.6	53
26 Sept. 2000	2.2	70*	8.5	14.1	86	26 Sept. 2000	2.2	70*	8.4	14.8	86
30 May 2000	2.1	100	179.3	348.2	182	30 May 2000	2.0	100	175.9	348.7	182
28 July 1995	4.2	143	6.2	9.1	41	7 Sept. 1995	4.0	132	9.1	14.6	42
19 Oct. 1995	4.0	131	14.6	24.8	42	30 Nov. 1995	4.1	131	24.8	37.5	63
28 July 1995	4.2	143	6.2	8.7	41	7 Sept. 1995	4.0	142	8.7	15.4	42
19 Oct. 1995	4.1	138	15.4	25.5	42	30 Nov. 1995	4.1	137	25.5	38.4	63
16 Feb. 1994	3.2	47	325.0	1235.0	365	17 Feb. 1994	3.2	33	639.0	2038.0	371
16 Feb. 1994	5.1	47	306.0	1603.0	364	17 Feb. 1994	5.1	33	602.0	2552.0	371
3 May 1993	3.2	31	1412.0	2524.0	254	3 May 1993	5.1	32	1550.0	2421.0	254
6 Aug. 1996	7.5	100*	0.9	1.6	21	27 Aug. 1996	7.4	97*	1.6	2.9	20
16 Sept. 1996	7.4	96*	2.9	4.9	21	7 Oct. 1996	7.3	93*	4.9	7.6	21
6 Aug. 1996	7.5	100*	0.9	1.7	21	27 Aug. 1996	7.4	96*	1.7	3.0	20
16 Sept. 1996	7.4	95*	3.0	5.1	21	7 Oct. 1996	7.3	95*	5.1	7.5	21
28 July 1995	7.5	143	6.0	13.4	41	7 Sept. 1995	7.6	143	13.4	31.5	42
19 Oct. 1995	7.5	142	31.5	60.2	42	30 Nov. 1995	7.3	142	60.2	104.5	63
31 Jan. 1996	7.2	142	104.5	162.9	49	28 July 1995	7.5	143	6.3	13.8	41
7 Sept. 1995	7.6	143	13.8	32.8	42	19 Oct. 1995	7.5	143	32.8	62.2	42
30 Nov. 1995	7.3	143	62.2	108.2	63	31 Jan. 1996	7.2	143	108.2	165.4	49
24 Sept. 1996	7.6	100	6.2	13.5	35	24 Sept. 1996	7.6	100	6.4	13.9	35
1 Nov. 1996	7.3	100	17.1	35.6	49	1 Nov. 1996	7.3	100	16.9	36.1	49
16 Jan. 1997	7.0	100	90.4	129.6	55	16 Jan. 1997	7.0	100	86.4	121.3	55
16 Feb. 1994	6.8	47	304.0	1671.0	364	17 Feb. 1994	6.8	33	637.0	2409.0	371
3 May 1993	7.2	32	1554.0	3435.0	261	3 May 1993	7.2	32	1469.0	3154.0	261
9 Feb. 1994	7.0	155	1162.0	4926.0	366	10 Feb. 1995	7.0	126	4926.0	7691.0	364
9 Feb. 1994	7.0	153	1188.0	5033.0	366	10 Feb. 1995	7.0	127	5033.0	8728.0	364
6 Aug. 1996	10.0	100*	0.8	1.9	21	27 Aug. 1996	10.0	99*	1.9	4.1	20
16 Sept. 1996	10.1	97*	4.1	7.7	21	7 Oct. 1996	9.9	96*	7.7	12.4	21
6 Aug. 1996	10.2	100*	0.8	2.0	21	27 Aug. 1996	10.0	93*	2.0	4.3	20
16 Sept. 1996	10.1	93*	4.3	8.1	21	7 Oct. 1996	10.0	92*	8.1	13.0	21
28 July 1995	10.0	143	6.1	17.9	41	7 Sept. 1995	9.9	141	17.9	43.5	42
19 Oct. 1995	10.0	139	43.5	84.8	42	30 Nov. 1995	9.9	138	84.8	156.4	63
28 July 1995	10.1	143	6.3	18.1	41	7 Sept. 1995	10.0	143	18.1	45.3	42
19 Oct. 1995	10.1	141	45.3	90.1	42	30 Nov. 1995	9.8	141	90.1	155.2	63
24 Sept. 1996	10.0	100	6.2	15.9	35	24 Sept. 1996	10.1	100	6.3	16.3	35
1 Nov. 1996	10.0	100	17.5	47.6	49	1 Nov. 1996	10.1	100	17.7	48.4	49
16 Jan. 1997	10.0	100	88.8	138.3	55	16 Jan. 1997	10.1	100	86.6	131.3	55
16 Feb. 1994	9.0	47	309.0	1957.0	365	17 Feb. 1994	9.0	33	628.0	2542.0	370
16 Feb. 1994	11.2	48	318.0	1945.0	365	17 Feb. 1994	11.2	33	634.0	2930.0	370
3 May 1993	9.9	31	1503.0	3154.0	254						
6 Aug. 1996	13.0	100*	0.9	2.8	21	27 Aug. 1996	12.9	86*	2.8	6.6	20
16 Sept. 1996	12.9	83*	6.6	12.4	21	7 Oct. 1996	12.8	81*	12.4	19.7	21
6 Aug. 1996	13.0	100*	0.9	2.6	21	27 Aug. 1996	13.0	100*	2.6	5.9	20
16 Sept. 1996	12.9	98*	5.9	11.4	21	7 Oct. 1996	12.8	98*	11.4	19.0	21
28 July 1995	13.0	143	6.1	22.6	41	7 Sept. 1995	13.0	140	22.6	51.5	42
19 Oct. 1995	13.0	135	51.5	94.3	42	30 Nov. 1995	12.8	133	94.3	153.6	63
28 July 1995	13.0	143	6.4	23.3	41	7 Sept. 1995	12.9	138	23.3	55.3	42
19 Oct. 1995	13.1	133	55.3	97.7	42	30 Nov. 1995	12.9	133	97.7	155.8	63
24 Sept. 1996	13.0	100	6.8	21.7	35	24 Sept. 1996	13.0	100	6.4	19.7	35
1 Nov. 1996	13.1	100	16.8	51.3	49	1 Nov. 1996	13.0	100	17.3	50.2	49

© 2002 NRC Canada

Table A1 (*concluded*).

Date	T (°C)	n_1	W_1	W_2	d	Date	T (°C)	n_1	W_1	W_2	d
16 Jan. 1997	12.8	100	86.8	122.7	55	16 Jan. 1997	12.8	100	87.6	127.5	55
17 Feb. 1994	13.4	33	633.0	2354.0	371	3 May 1993	12.8	31	1517.0	2810.0	254
6 Aug. 1996	15.9	100*	0.9	2.9	21	27 Aug. 1996	15.9	99*	2.9	6.2	20
16 Sept. 1996	15.8	99*	6.2	11.5	21	7 Oct. 1996	15.7	99*	11.5	17.8	21
6 Aug. 1996	15.9	100*	0.9	2.7	21	27 Aug. 1996	15.9	99*	2.7	6.0	20
16 Sept. 1996	15.8	99*	6.0	10.9	21	7 Oct. 1996	15.7	99*	10.9	17.9	21
28 July 1995	16.0	143	6.1	21.6	41	7 Sept. 1995	15.8	135	21.6	41.7	42
19 Oct. 1995	16.0	130	41.7	65.3	42	30 Nov. 1995	15.7	126	65.3	94.2	63
28 July 1995	16.0	143	6.4	22.7	41	7 Sept. 1995	15.8	135	22.7	43.0	42
19 Oct. 1995	15.9	132	43.0	70.0	42	30 Nov. 1995	15.7	129	70.0	97.6	63
24 Sept. 1996	15.7	100	6.6	21.6	35	24 Sept. 1996	15.7	100	6.3	20.2	35
1 Nov. 1996	15.2	100	17.3	49.6	49	1 Nov. 1996	15.2	100	16.7	48.6	49
16 Jan. 1997	15.1	100	86.6	112.4	55	16 Jan. 1997	15.0	100	87.0	109.2	55
3 May 1993	15.6	33	1500.0	2137.0	254						

Note: Horizontal breaks signify six different temperature groups: 2, 4, 7, 10, 13, and 16°C, as addressed in the text.
*The smallest tanks with a photoperiod of 12 h light : 12 h dark.

© 2002 NRC Canada

Does red alder (*Alnus rubra*) in upland riparian forests elevate macroinvertebrate and detritus export from headwater streams to downstream habitats in southeastern Alaska?

Jack J. Piccolo and Mark S. Wipfli

Abstract: We assessed the influence of riparian forest canopy type on macroinvertebrate and detritus export from headwater streams to downstream habitats in the Tongass National Forest, southeastern Alaska. Twenty-four fishless headwater streams were sampled monthly, from April to August 1998, across four riparian canopy types: old growth, clearcut, young-growth alder, and young-growth conifer. Young-growth alder sites exported significantly greater count (mean = 9.4 individuals·m^{-3} water, standard error (SE) = 3.7) and biomass (mean = 3.1 mg dry mass·m^{-3} water, SE = 1.2) densities of macroinvertebrates than did young-growth conifer sites (mean = 2.7 individuals·m^{-3} water, SE = 0.4, and mean = 1.0 mg dry mass·m^{-3} water, SE = 0.2), enough prey to support up to four times more fish biomass if downstream habitat is suitable. We detected no significant differences in macroinvertebrate export between other canopy types or in detritus export among different canopy types. Roughly 70% of the invertebrates were aquatic; the rest were terrestrial or could not be identified. Although we do not recommend clearcutting as a means of generating red alder, maintaining an alder component in previously harvested stands may offset other potentially negative effects of timber harvest (such as sedimentation and loss of coarse woody debris) on downstream, salmonid-bearing food webs.

Résumé : Nous avons évalué l'influence du type de couverture forestière de la rive sur l'exportation de macroinvertébrés et de détritus depuis des ruisseaux d'amont vers les habitats d'aval dans la forêt nationale de Tongass dans le sud-est de l'Alaska. Vingt-quatre ruisseaux d'amont dépourvus de poissons ont été échantillonnés tous les mois, d'avril à août 1998, dans quatre types de couverture végétale riparienne: forêt mature, surface coupée à blanc, jeune forêt d'aulnes et jeune forêt de conifères. Les sites de forêt jeune à aulnes exportent significativement plus de macroinvertébrés, en nombre (moyenne = 9,4 individus·m^{-3} d'eau, erreur type (SE) = 3,7) et en biomasse (moyenne = 3,1 mg de masse sèche·m^{-3} d'eau, SE = 1,2) que les sites de forêt jeune à conifères (moyenne = 2,7 individus·m^{-3} d'eau, SE = 0,4; moyenne = 1,0 mg de masse sèche·m^{-3} d'eau, SE = 0,2), soit assez de proies pour subvenir à des biomasses de poissons quatre fois plus grandes, à condition que les habitats d'aval soient convenables. Il n'y a pas de différences significatives décelables d'exportation de macroinvertébrés entre les autres types forestiers, ni de différences d'exportation de détritus entre les quatre types de couverture forestière. En gros, 70 % des invertébrés sont aquatiques; les autres sont terrestres ou impossibles à identifier. Bien que nous ne recommandions pas la coupe à blanc comme moyen de favoriser l'aulne rouge, le maintien d'une composante d'aulnes dans les secteurs déjà coupés pourrait contrebalancer les effets potentiellement négatifs de la coupe du bois, tels que la sédimentation et la perte de débris ligneux grossiers, sur les réseaux alimentaires d'aval qui contiennent des salmonidés.

[Traduit par la Rédaction]

Introduction

Headwater habitats play a critical role in the structure and function of downstream ecosystems (Haigh et al. 1998). The headwater streams that drain these habitats transport water, sediment, debris, and invertebrates (Cuffney and Wallace 1988; Naiman et al. 1992; Wipfli and Gregovich 2002), influencing downstream habitats and food webs. Physical and biological attributes that may influence the productivity of headwater streams and the material available for export in-

Received 5 July 2001. Accepted 12 February 2002. Published on the NRC Research Press Web site at http://cjfas.nrc.ca on 6 April 2002.
J16435

J.J. Piccolo[1,2] and M.S. Wipfli.[1,3] Pacific Northwest Research Station, U.S. Department of Agriculture Forest Service, 2770 Sherwood Lane, Suite 2A, Juneau, AK 99801-8545, U.S.A.

[1]Corresponding authors (e-mail: ftjjp1@uaf.edu, mwipfli@fs.fed.us).
[2]Present address: University of Alaska Fairbanks, School of Fisheries and Ocean Sciences, Juneau Fisheries Center, 11120 Glacier Highway, Juneau AK 99801, U.S.A.
[3]Present address: Pacific Northwest Research Station, U.S. Department of Agriculture Forest Service, 1133 N. Western Avenue, Wenatchee, WA 98801, U.S.A.

 DOI: 10.1139/F02-019 © 2002 NRC Canada

clude catchment size, geology, soil type, aspect, gradient, temperature, precipitation, and plant and animal communities (Naiman et al. 1992). Natural or human-induced disturbances can alter these attributes (Resh et al. 1988), thereby altering productivity in both headwater streams and downstream habitats.

Stone and Wallace (1998) identify clearcut logging as a long-term disturbance that alters stream ecosystems. Their literature review identifies the following effects of clearcutting on stream macroinvertebrate communities: changes in stream temperature, stream flow, primary production, and community structure. The short-term effects of clearcutting may include reduced allochthonous input and increased autochthonous production, which alter macroinvertebrate communities and, consequently, detritus export. The long-term effects of clearcutting on macroinvertebrate export from headwater streams to downstream food webs, however, have not been addressed.

In the temperate rainforest of southeastern Alaska, clearcutting changes terrestrial and aquatic productivity (Alaback 1982; Duncan and Brusven 1985) and the energy flow from terrestrial to aquatic habitats (Wipfli 1997). Canopy removal increases the amount of light reaching the forest floor, increasing the productivity of understory plants (Alaback 1982) and streams (Duncan and Brusven 1985; Hetrick et al. 1998). Following clearcutting, forest succession often includes the development of red alder (*Alnus rubra*) stands in those places where there has been enough surface disturbance to expose mineral soils (Newton and Cole 1994). The establishment of alder may increase understory plant diversity (Deal 1997) and abundance (Hanley and Barnard 1998), and alder-dominated riparian canopies may also provide more terrestrial invertebrates as prey for juvenile salmonids than do conifer-dominated canopies (Wipfli 1997). Although the productivity of terrestrial habitat declines as a dense coniferous canopy develops in later successional stages (Alaback 1982), little information exists on the influence of riparian forest succession on headwater streams and associated export of material.

Forest management plans for southeastern Alaska include timber harvesting in forested headwaters (U.S. Department of Agriculture (USDA) Forest Service 1997). These headwaters contain many small, fishless streams (Swanston 1967), classified by the USDA Forest Service as classes III and IV. Riparian buffer protection during logging operations varies along these streams; most class III streams receive some buffer protection, but few class VI streams do (USDA Forest Service 1997). Many of these streams drain into salmonid-rearing habitats, and it is important to understand how timber harvest and forest regeneration in upland forests influence downstream food webs, including the flow of energy (invertebrates and detritus) to these habitats.

Our objective was to measure the effects of different riparian forest canopy types on macroinvertebrate (aquatic and terrestrial) and organic detritus export from headwater streams to downstream habitats. We tested the null hypothesis that during the salmonid growing season (April–August), headwater streams with old growth, clearcut, young-growth alder, and young-growth conifer riparian canopies do not differ in the amount (number and mass) of macroinvertebrates and detritus they export.

Methods

Study site

Research was conducted in small (mean discharge <3.1 $L \cdot s^{-1}$), fishless headwater streams (classified as class III and class IV streams, USDA Forest Service 1997) on Prince of Wales Island in the Tongass National Forest, southeastern Alaska. The climate there is maritime and precipitation can exceed 500 $cm \cdot year^{-1}$ (Harris et al. 1974). We sampled macroinvertebrate and coarse detritus (>250 μm) export monthly, from April to August 1998, in 24 streams characterized by four distinct riparian canopy types: old growth (OG); clearcut (CC), <5 years post-cut; young-growth alder (YA), 35–40 years post-cut; and young-growth conifer (YC), 35–40 years post-cut. Six replicate streams of similar size and gradient were selected for each canopy type. All streams were within the Harris and Maybeso watersheds (Fig. 1), an area clearcut extensively during the 1950s and 1960s as part of the first large-scale, commercial timber harvest in southeastern Alaska (Swanston 1967). Eighteen sites were selected within the Harris River watershed (3 YA, 3 YC, 6 CC, 6 OG); and six were selected within the Maybeso Creek watershed (3 YA and 3 YC) (Table 1). Because of unusually low precipitation during the sampling season, surface flow became intermittent in nine streams, for which we substituted nearby streams with continuous surface flow to maintain an adequate number of replicates. Because of a scarcity of suitable old-growth headwater streams within these two basins, one OG stream substantially larger than the other study streams (mean discharge 58.2 $L \cdot s^{-1}$) was substituted in June–August. Stream temperature for one of each group of three streams (clustered by canopy type and watershed) was monitored continuously with Onset® temperature meters (Onset Computer Corp., Pocasset, Mass.), and stream temperature was taken with a hand-held thermometer on each stream at 0, 48, and 96 h during the sampling period.

Macroinvertebrate and detritus export

The density of macroinvertebrate and detritus export from the 24 streams was sampled continuously for 96 h once each month from April through August. Remote location and difficult terrain prevented quick access to sampling sites, so they were divided into two groups of 12 streams each, and sampling start and stop dates were staggered by one day for each group, i.e., 12 streams were sampled on days 0–4 and 12 were sampled on days 1–5. Streams were sampled systematically, based upon their proximity to each other, in the same order each month. Export was sampled by constructing a sandbag dam to divert the entire surface flow of each stream (with the exception of the one larger, old-growth stream) through a polyvinyl chloride (PVC) pipe (1-m long, 10-cm inside diameter), and drift nets (10-cm-diameter mouth, 1–2 m long, 250-μm mesh) were attached to the outflow end of each pipe (Wipfli and Gregovich 2002). Observations from previous studies in streams of this size showed that nets left on for more than 48 h without being emptied can result in occasional overflow (Wipfli and Gregovich 2002), therefore, nets were changed at 48-h intervals to ensure that they did not become clogged. Detritus and macroinvertebrates were washed into a 250-μm sieve and preserved in 95% ethanol, and the two 48-h samples were combined

© 2002 NRC Canada

Fig. 1. Map of Alaska, U.S.A., with inset showing the Harris and Maybeso drainages (132°67′W, 55°49′N) on eastern Prince of Wales Island. The drainage basin boundaries are represented by the dotted line. Both drainages empty into salt water in Twelvemile Arm (shaded area). Study streams are identified by canopy type: old growth (OG), clearcut (CC), young-growth alder (YA), and young-growth conifer (YC).

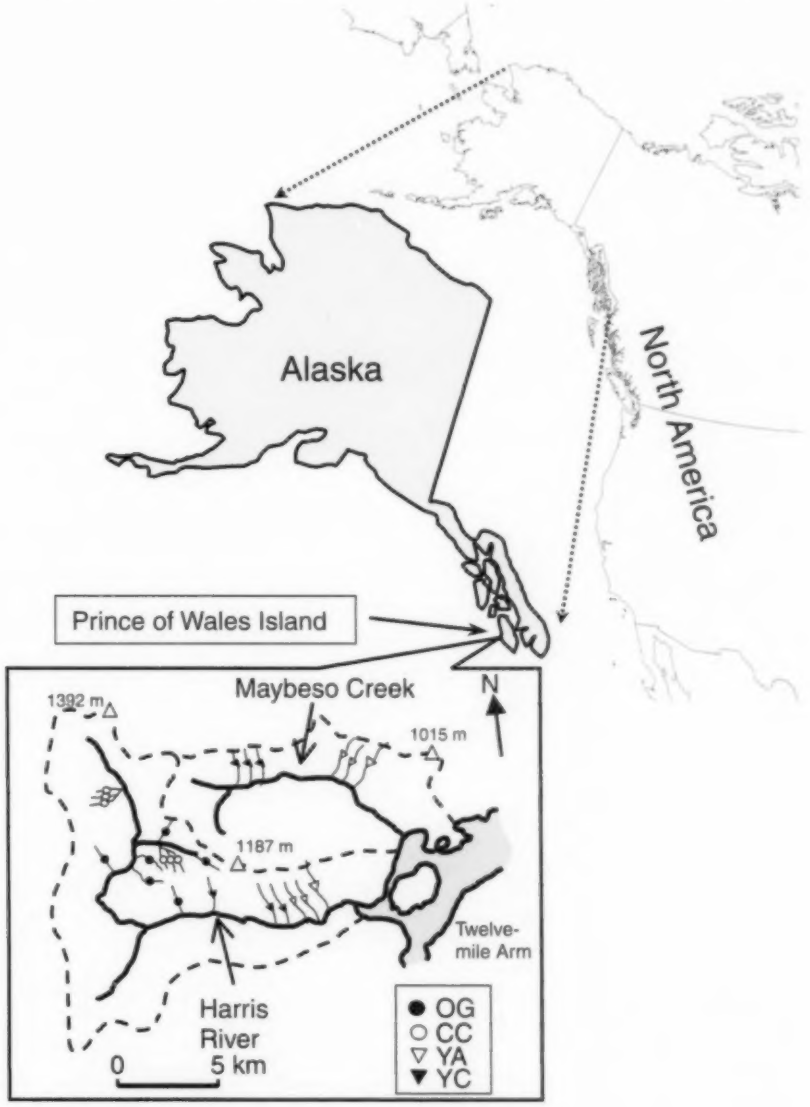

for data analysis. Discharge was measured by using a stopwatch to count the number of seconds it took for water from the dam outflow pipe to fill a known-volume container. Mean discharge for each stream during each sampling period was calculated by averaging measurements taken at 0, 48, and 96 h (3 replicates at each time). During occasional high flows, discharge sometimes exceeded pipe capacity and we were able to sample only a portion of the stream flow. In these instances, discharge through the pipe was measured as described above, the percentage of total streamflow flowing through the pipe (typically 90% or greater) was visually estimated, and total discharge was calculated using this correction factor.

Samples were sorted under a 7× dissecting microscope. Macroinvertebrates were identified to lowest reliable taxon, measured to the nearest millimetre (total length excluding antennae and cerci), and enumerated. Unusually large samples were subsampled. We used a subsampler that had a large, funnel-shaped container to which we added 16 L of water containing the sample and through which a continuous, vigorous stream of air was injected from the bottom to ensure uniform mixing and distribution of the sample. Part

© 2002 NRC Canada

Table 1. Physical and biological habitat characteristics of headwater study streams on Prince of Wales Island, Alaska, 1998, in old growth (OG), clearcut (CC), young-growth alder (YA), and young-growth conifer (YC) riparian forests.

	Canopy type			
Parameter	OG[a]	CC	YA	YC
Mean				
Stream reach length (m)	250 (260)	237	273	204
Channel width (m)	1.8 (2.7)	1.2	1.9	1.4
Gradient (%)	21.0 (20.4)	22.9	21.7	22.2
Discharge ($L \cdot s^{-1}$)	0.4 (3.5)	0.7	1.2	0.9
Stream temperature (°C)	7.7 (7.5)	8.5	9.0	8.2
% open canopy	32 (36)	100	14	26
% alder canopy	<1 (<1)	0	74	20
% conifer canopy	68 (64)	0	12	54
Predominant understory	*Vaccinium* sp.	*Rubus* sp.	*Rubus* sp.	*Rubus* sp.
Understory density	Moderate	Moderate	Sparse	Low
Sample size (n)	6	6	6	6

[a]Numbers in parenthesis include one old-growth stream that was uncharacteristically larger than all other study streams (see Methods, Study site).

of the sample (either 8 L or 4 L) was taken with a smaller known-volume container, and this portion was analyzed. Results were then multiplied by two or four to obtain a full-sample estimate. Macroinvertebrate biomass (mg dry mass) was estimated for individual invertebrates by using either published taxa-specific length–weight regression equations (e.g., Rogers et al. 1977; Sample et al. 1993; Burgherr and Meyer 1997) or our own equations. This was done for a previous study (Wipfli and Gregovich 2002) by drying a sample of known-length invertebrates of a given taxa (at 60°C for 24 h), weighing individuals (nearest 0.1 mg), and developing a length–weight regression (Smock 1980). Detritus was dried (at 60°C for 48 h), weighed, burned to ash (at 500°C for 5 h), and reweighed to determine ash-free dry mass (AFDM), the amount of organic, nonmineral material in the sample.

Physical habitat and riparian canopy measurements

Stream channel gradient, active channel width, canopy coverage, and understory vegetation type and density were surveyed along a 300-m reach of each stream directly upstream from the sample stations. Gradient was measured with a hand-held clinometer and canopy coverage was estimated every 20 m along the stream using a circular viewing tube (10-cm inside-diameter × 30-cm long). To estimate canopy coverage and composition, the observer stood in the center of the stream channel, looked through the vertically held tube, and recorded the percentage of alder, conifer, and open canopy. Foliage density (scale: 0 = none, 1 = sparse, 2 = low, 3 = moderate, 5 = high) and relative abundance (top five plant species in order of abundance) of understory shrubs were estimated visually for a 2-m-wide band along each stream bank (Table 1).

Statistical analysis

A completely randomized design was used incorporating canopy type (OG, YA, YC, CC) as the main factor, and 24 streams were sampled each month (April–August). We used a split-plot analysis of variance (ANOVA) (SAS 1990) to test for significant effects of canopy type, month, and canopy type × month interaction ($\alpha < 0.1$). We used a split-plot analysis because we were interested in the main effect of canopy type over the entire growing season (five months combined) and because we did not expect any carry-over effects between months (Winer et al. 1991). To further identify what differences might be driving the results of the main effects test, statistical comparisons between individual canopy types were tested using four a priori contrasts: OG vs. CC, OG vs. YA, OG vs. YC, and YA vs. YC. These contrasts were chosen so that we could detect differences between logged and unlogged areas (OG vs. CC, OG vs. YA, OG vs. YC) and differences between canopy types that commonly regenerate after logging (YA vs. YC). Alpha for the contrasts was set-wise at 0.025 (the comparison-wise error divided by a Bonferroni correction factor of four) because the four contrasts were not orthogonal (we did not perform all possible contrasts with the four canopy types) (SAS 1990). We did not contrast individual months, because we were interested in the effects of riparian canopy across the entire 5-month period. Response variables were total count density (number of macroinvertebrates·m^{-3} water), total biomass density (mg dry mass of macroinvertebrates·m^{-3} water), and detritus density (mg AFDM·m^{-3} water). All response variables were logarithmic transformed ($\ln(x + 0.1)$) to meet ANOVA assumptions of normally distributed residuals and equal variances among groups.

Results

Total count density differed significantly by canopy type ($p < 0.1$; Table 2), and YA sites exported significantly more macroinvertebrates than did YC sites ($p < 0.025$; Fig. 2*a*, Table 2). There were no significant differences between other contrasted canopy types (OG vs. CC, YA, YC). Total biomass density did not differ significantly among canopy types in the overall test ($p > 0.1$; Table 2), but YA sites exported significantly more total biomass density than did YC sites ($p < 0.025$; Fig. 2*b*, Table 2). There were no significant differences between other canopy types contrasted (OG vs. CC, YA, YC).

© 2002 NRC Canada

Table 2. Analysis of variance output for comparisons of natural log ($\ln(x + 0.1)$) macroinvertebrate count (individuals·m^{-3} water) and biomass (mg dry mass·m^{-3} water) and detritus densities (mg AFDM·m^{-3} water).

	p values for main effects tests			*p* values for a priori contrasts of riparian canopy type			
	Canopy effect	Month effect	Canopy × month	OG vs. CC	OG vs. YA	OG vs. YC	YA vs. YC
Count density	**0.0601**	**<0.0001**	**0.0026**	0.4142	0.2939	0.1200	**0.0166**
Biomass density	0.1419	**<0.0001**	**0.0398**	0.9810	0.1661	0.2892	**0.0228**
Detritus	0.1307	**<0.0001**	0.1445	0.4261	0.5227	0.0874	0.0292

Note: Output is *p* values for the main effects tests of canopy type, month, and canopy type × month interaction ($p < 0.10$), and the a priori contrasts between canopy types ($p < 0.025$). Riparian forest canopy types are old growth (OG), clearcut (CC), young-growth alder (YA), and young-growth conifer (YC). Significant test results are shown in bold type.

Fig. 2. Mean macroinvertebrate (*a*) count and (*b*) biomass densities by riparian forest canopy type, exported from headwater streams on Prince of Wales Island, Alaska. Each bar represents the mean with standard error of six replicate streams over five monthly sampling periods ($n = 6$) in old growth, clearcut, young-growth alder, and young-growth conifer streams. Treatment marked 1 differs significantly from treatment marked 2 ($p < 0.025$).

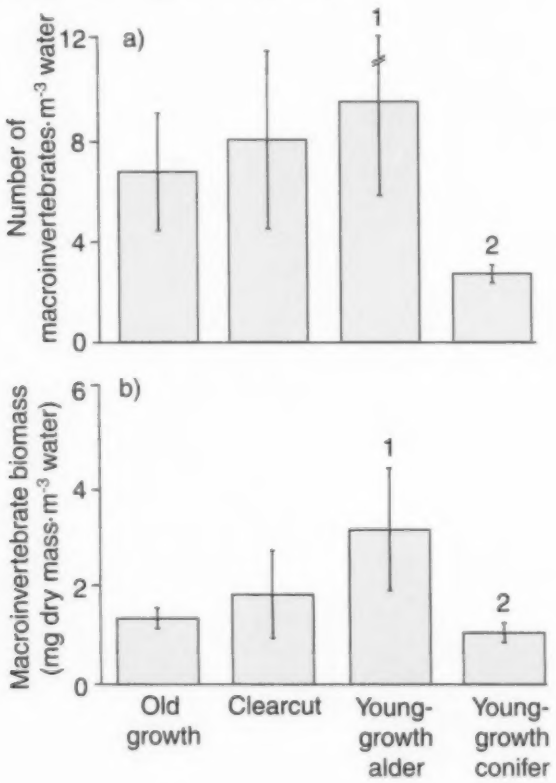

Fig. 3. Mean macroinvertebrate (*a*) count and (*b*) biomass densities by riparian forest canopy type and month, exported from headwater streams on Prince of Wales Island, Alaska. Each bar represents the mean with standard error of six replicate streams ($n = 6$) in old growth (open), clearcut (light shading), young-growth alder (dark shading), and young-growth conifer (solid).

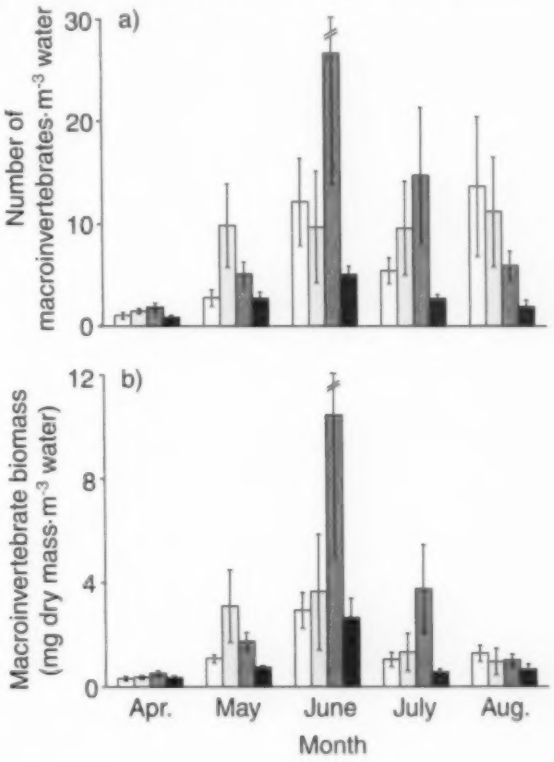

Both total count and biomass density differed significantly by month, and both displayed a significant canopy type × month interaction ($p < 0.1$; Table 2). Total count density peaked in June and dropped off in July and August, although temporal patterns varied among canopy types (Fig. 3*a*). Total biomass density peaked in June as well and dropped off sharply by August (Fig. 3*b*).

Detritus export did not vary significantly by treatment ($p > 0.1$; Table 2), and no significant differences were found between the canopy types contrasted ($p > 0.025$; Fig. 4*a*, Table 2). Young-growth alder streams exported more AFDM of detritus (mean = 17.2 mg AFDM·m^{-3} water, standard error (SE) = 7.3) than did YC streams (mean 2.9 mg AFDM·m^{-3} water, SE = 0.5), although this difference was not statistically significant ($p = 0.0292$; Table 2). Detritus export did vary significantly by month ($p < 0.1$; Table 2), peaking in August (Fig. 4*b*). This peak was probably due to a freshet during the sampling period.

All riparian canopy types exported greater count and biomass densities of aquatic versus terrestrial macroinvertebrates

© 2002 NRC Canada

Fig 4. (*a*) Detritus density by riparian forest canopy type and (*b*) canopy type by month, exported from headwater streams on Prince of Wales Island, Alaska. In (*a*), each bar represents the mean with standard error of six replicate streams over five monthly sampling periods ($n = 6$) in old growth, clearcut, young-growth alder, and young-growth conifer streams; there are no significant differences among canopy types contrasted ($p > 0.025$). In (*b*), each bar represents the mean with standard error of six replicate streams ($n = 6$) in old growth (open), clearcut (light shading), young-growth alder (dark shading), and young-growth conifer (solid).

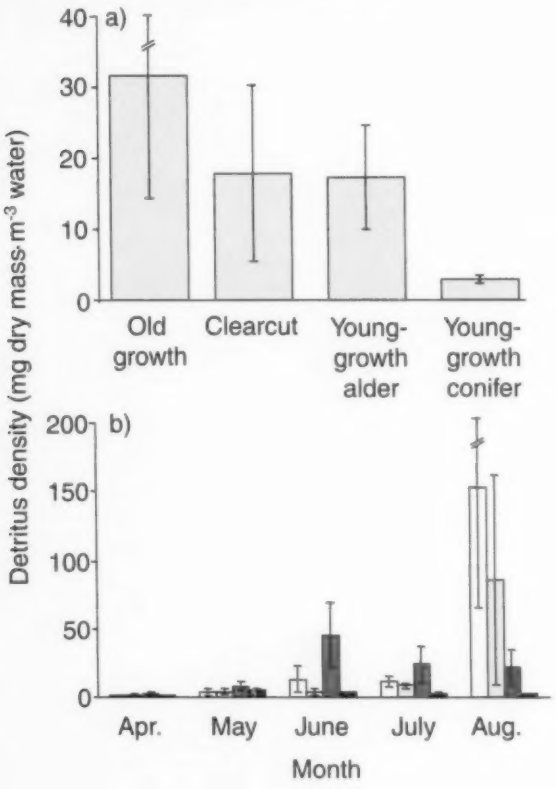

Fig. 5. Mean (*a*) count and (*b*) biomass densities of aquatic (light shading) and terrestrial (solid) macroinvertebrates by riparian forest canopy type, exported from headwater streams on Prince of Wales Island, Alaska. Each bar represents the mean with standard error of six replicate streams over five monthly sampling periods ($n = 6$).

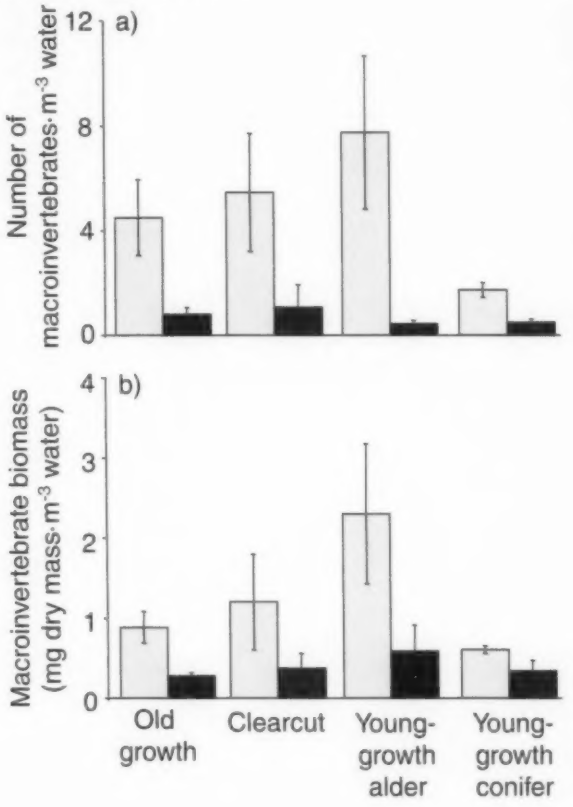

(Figs. 5*a*, 5*b*). Export of aquatic macroinvertebrates was greatest in YA streams and lowest in YC streams; terrestrial macroinvertebrate export was similar across all canopy types. Therefore, in YC streams, terrestrial macroinvertebrates made up a considerably larger proportion of total export than they did in YA streams.

More than 50 000 individual macroinvertebrates in at least 55 different taxa were identified and measured. A relatively small number of taxa comprised a large proportion of the total count (Fig. 6) and biomass (Fig. 7) densities. All of the macroinvertebrates exported, with the exception of the Nematophora, would be suitably sized prey (<10 mm long) for juvenile salmonids (Table 3).

Discussion

Headwater streams influence the structure and function of downstream habitats through export of organic and inorganic materials (Wallace et al. 1991; Naiman et al. 1992; Wipfli and Gregovich 2002). Because headwater streams can comprise more than 75% of total stream channel length in southeastern Alaska watersheds (Swanston 1967), their contribution to the energy budgets of downstream habitats may be substantial. To illustrate the potential influence of headwater export on fish-bearing foodwebs, Wipfli and Gregovich (2002) presented a trophic model of macroinvertebrate and detritus contribution from headwater streams to downstream, salmonid-producing habitats in southeastern Alaska. The model incorporates the amount of invertebrate biomass and detritus exported from fishless headwater streams that drain into a given length of downstream fish-bearing habitat. It uses these values to predict the number of juvenile salmonids that could be supported by this headwater export. Applying the model, they estimated that each kilometre of fish-bearing habitat receives enough invertebrates (mean = 1210 mg dry mass·day^{-1}) and detritus (mean = 78 g dry mass·day^{-1}) from fishless headwater streams to support 100–2000 young-of-the-year salmonids (equivilent to 0.1–2 fish per metre of fish-bearing stream). Timber harvest in these headwaters is likely to alter allochthonous inputs and is predicted to alter the energy flow and trophic linkages between upland forests and downstream

© 2002 NRC Canada

Fig. 6. Mean count densities of the six most abundant macroinvertebrate taxa by riparian forest canopy type and month, exported from headwater streams on Prince of Wales Island, Alaska. Each bar represents the mean with standard error of six replicate streams (n = 6) in old growth (open), clearcut (light shading), young-growth alder (dark shading), and young-growth conifer (solid). Taxa and percent relative abundance (for all canopy types and treatments combined) are as follows: (*a*) Baetidae, 20.5%; (*b*) Ostracoda, 19.1%; (*c*) Acarina, 11.7%; (*d*) Chironomidae, 9.8%; (*e*) Collembola, 8.4%; (*f*) Leuctridae, 5.5%.

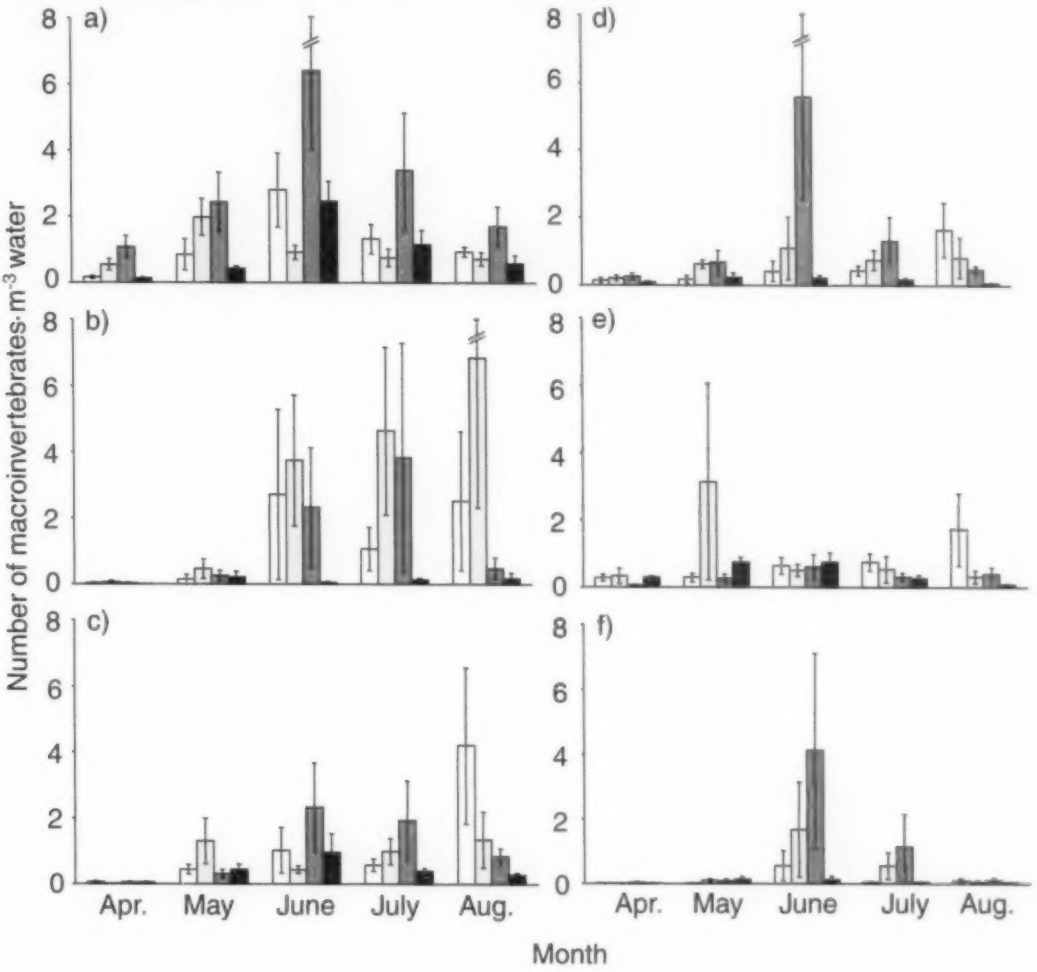

food webs (Wipfli and Gregovich 2002). To determine the long-term effects of timber harvest on the link between headwaters and downstream habitats, we sampled streams with different forest canopy types that commonly develop after clearcutting. Our results indicated that canopy type significantly affected the quantity and biomass of macroinvertebrates exported from headwaters to downstream habitats.

Timber management in the Tongass National Forest includes clearcutting and selective cutting, with stand rotations of 100–200 years between harvests (USDA Forest Service 1997, 1999). Although clearcuts may influence terrestrial and aquatic productivity (Newbold et al. 1980; Alaback 1982), they are a transient stage in forest succession. Greater long-term effects might be expected to result from forest succession following regrowth, which may last for more than 100 years. In southeastern Alaska, forest understory productivity increases immediately after clearcutting and then decreases below old-growth levels as second-growth conifer stands grow dense and the canopy closes (Alaback 1982). Mixed alder–conifer stands, however, may have greater understory plant diversity (Deal 1997) and abundance (Hanley and Barnard 1998) than do conifer-dominated stands. Further, studies from the Pacific Northwest have shown that alder benefits disturbed riparian ecosystems by fixing nitrogen (Binkley et al. 1994) and adding organic matter (Newton and Cole 1994). Our results indicated that alder and conifer in riparian canopies might have similar respective effects on productivity and on the link between terrestrial and aquatic habitats in upland forests of southeastern Alaska.

We found that in 35- to 40-year-old stands, macroinvertebrate export from streams with young-growth alder

© 2002 NRC Canada

Fig. 7. Mean biomass density of the six most abundant macroinvertebrate taxa by riparian forest canopy type and month, exported from headwater streams on Prince of Wales Island, Alaska. Each bar represents the mean with standard error of six replicate streams in (n = 6) old growth (open), clearcut (light shading), young-growth alder (dark shading), and young-growth conifer (solid). Taxa and percent relative abundance (for all canopy types and treatments combined) are as follows: (*a*) Terrestrial Coleoptera, 13.4%; (*b*) Heptageiidae, 10.2%; (*c*) Leuctridae, 9.6%; (*d*) Baetidae, 9.0%; (*e*) Rhyacophilidae, 7.5%; (*f*) Amphizoidae, 7.5%.

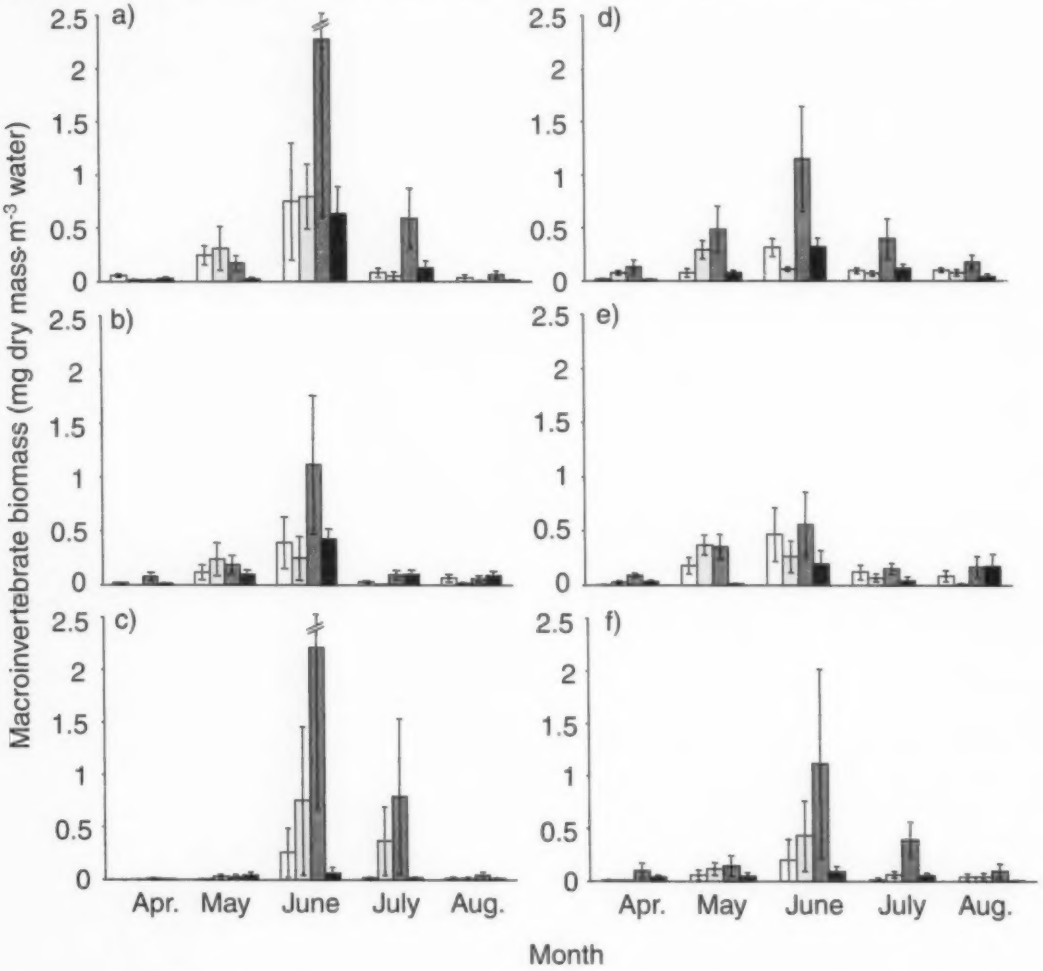

canopies was significantly greater than the export from streams with young-growth conifer canopies. By applying the trophic model of Wipfli and Gregovich (2002), we predict that YA streams may export enough invertebrate biomass and detritus to downstream habitats to support approximately four times more juvenile salmonids than will YC streams (0.8–11.5 fish·m^{-1} of fish-bearing stream vs. 0.2–2.4 fish·m^{-1} of fish-bearing stream). We apply this model to the data from this study to illustrate the potential influence of headwater canopy type on downstream food webs. Juvenile salmonids typically occupy small streams immediately downstream from headwater habitats and may reside in freshwater for up to 4 years (Groot and Margolis 1991). Headwater streams export prey and detritus to these fish-bearing habitats, potentially subsidizing these downstream food webs. We found that streams that developed alder canopies following clearcutting exported more prey to downstream food webs than did streams that developed conifer canopies.

The abundance of invertebrate prey may be important in limiting stream salmonid productivity (Hayes et al. 2000). We found that macroinvertebrate export from headwater streams to downstream habitats varied significantly seasonally and that there was a significant canopy type × month interaction. This indicates that the relative influence of each canopy type on downstream habitats may change throughout the year. Juvenile salmonids in southeastern Alaska make seasonal upstream migrations into small tributaries to overwinter (Bramblett et al. 2002), and they may be particularly dependent on prey from headwaters during these periods. Our results show that headwater invertebrate export varies seasonally and under different riparian forest canopy types;

© 2002 NRC Canada

Table 3. Macroinvertebrate taxa collected in drift nets on Prince of Wales Island, Alaska, 1998, and their percent relative abundance by count (number·m^{-3} water) and biomass (mg dry mass·m^{-3} water).

Taxon[a]	Percent relative abundance	
	Count	Biomass
Annelida		
Oligochaeta	0.3	0.9
Arthropoda		
Arachnida		
Acari	11.7	0.4
Araneae	0.5	4.5
Pseudoscorpiones	<0.1	<0.1
Amphipoda	<0.1	<0.1
Copepoda	<0.1	<0.1
Isopoda	<0.1	<0.1
Ostracoda	19.1	0.6
Chilopoda	<0.1	0.5
Diplopoda	<0.1	0.4
Insecta	<0.1	<0.1
Collembola	8.4	2.9
Ephemeroptera	0.2	0.3
Ameletidae	<0.1	0.1
Baetidae	20.5	9.0
Ephemerellidae	<0.1	0.1
Drunella	0.2	1.0
Leptophlebiidae	0.4	0.4
Paraleptophlebia	3.1	1.8
Heptageniidae	3.4	10.2
Plecoptera	0.5	0.6
Chloroperlidae	<0.1	0.1
Sweltsa	1.2	1.8
Leuctridae	5.5	9.6
Nemouridae	0.3	0.3
Zapada	0.5	0.4
Perlidae	<0.1	<0.1
Perlodidae	<0.1	<0.1
Psocoptera	<0.1	<0.1
Hemiptera	0.4	0.5
Aphididae	0.2	0.1
Tricoptera	0.6	0.3
Brachycentridae	<0.1	<0.1
Micrasema	0.3	0.2
Glossosomatidae	<0.1	<0.1
Glossosoma	<0.1	<0.1
Hydropsychidae	0.3	0.5
Lepidostomatidae	<0.1	<0.1
Limnephilidae	0.3	1.2
Chyranda	<0.1	0.1
Cryptochia	<0.1	<0.1
Homophylax	<0.1	<0.1
Onocosmoecus	<0.1	<0.1
Philopotamidae	<0.1	0.1
Polycentropodidae	<0.1	<0.1
Rhyacophilidae	0.8	7.5
Lepidoptera	<0.1	<0.1
Coleoptera	0.8	3.0
Misc. terrestrial	0.7	13.4
Amphizoidae	0.4	6.5
Elmidae	<0.1	0.5
Dytiscidae	0.2	5.4
Hydroporus	0.2	0.5
Hydrophilidae	<0.1	0.2
Diptera	3.8	4.5
Ceratopogonidae	<0.1	<0.1
Chironomidae	9.8	3.3
Culicidae	<0.1	<0.1
Dixidae	1.3	0.4
Empididae	<0.1	<0.1
Simulidae	0.5	0.4
Tipulidae	0.2	0.8
Hymenoptera	0.2	0.2
Formicidae	<0.1	<0.1
Mollusca		
Gastropoda	0.3	1.0
Nematomorpha	0.3	1.0
Platyhelminthes		
Turbellaria	1.2	1.5
Unidentified	<0.1	<0.1

[a]We identified macroinvertebrates to lowest reliable taxa (i.e., individuals that could not be positively identified to a certain taxonomic lever were assigned to the next higher category). Therefore, percent relative abundance by count or biomass of a higher taxon (i.e., family) does not include those from the taxon or taxa below them (i.e., genus).

the question of how this influences salmonid productivity in downstream habitats remains unanswered.

Terrestrial invertebrates are important prey for stream salmonids and may be particularly so for juvenile salmonids in southeastern Alaska (Wipfli 1997). We found a trend toward greater count and biomass densities of aquatic macroinvertebrates in YA vs. YC streams, whereas export of terrestrial macroinvertebrates was similar across all canopy types. In our YC streams, therefore, terrestrial macroinvertebrates comprised a greater percent of total export (40% by number and 47% by mass) than they did in YA streams (17% by number and 25% by mass). Thus, terrestrial macroinvertebrates may play a greater role in food webs supported by YC streams, where they make up a much greater percentage of total export if aquatic macroinvertebrates are less abundant.

Allochthonous input from alder probably was partly responsible for elevated export of macroinvertebrates and detritus from the young-growth alder streams in this study. We observed accumulations of leaf material from previous years along the banks of YA streams and frequently collected decaying leaves in our samples. Young-growth alder streams exported over five times more detritus than did YC streams, although this difference was not statistically significant. Also, macroinvertebrate shredders prefer alder leaves to birch, willow, or poplar leaves (Irons et al. 1988), and we found that YA streams exported more Leuctridae, the most abundant shredder in our study streams. Processed leaf material may be responsible for the increased count and biomass, as has been shown in other studies (Short and Maslin

© 2002 NRC Canada

1977). We also found a trend towards greater biomass of the most common invertebrate predators, Rhyacophilidae, in YA streams, which suggests that increased production from alder inputs may be influencing upper trophic levels (Wallace et al. 1997, 1999).

Many physical and biological factors may influence the productivity of headwater streams and the invertebrates and detritus available for export (Cuffney and Wallace 1988; Naiman et al. 1992). Our research focused on measuring the effects of riparian forest canopy type on this export. We selected streams similar in size and gradient and located near one another (within an area of 150 km^2) to minimize differences in geology, temperature, and precipitation. We sampled the maximum number of replicates that was practical in order to achieve suitable statistical power, although high natural variation greatly reduced statistical power. The high level of significance for the contrast between YA and YC sites, however, indicates that despite the variation added by other factors, these results were robust. Attributes for which we could not control included aspect, soil type, stream substrate, and others; these may have masked treatment effects.

Canopy removal has been reported to increase primary and secondary productivity in fish-bearing streams in southeastern Alaska (Duncan and Brusven 1985; Hetrick et al. 1998) and elsewhere in the Pacific Northwest (Bilby and Bisson 1992). Young et al. (1999) suggested a general model for Pacific Northwest streams of salmonid production initially increasing after clearcutting and subsequently decreasing below old-growth levels as forest canopy closes. Although this may be true for floodplain habitats, productivity in southeastern Alaska headwater streams may be influenced more by allochthonous input than by autochthonous production, as in other systems (Fisher and Likens 1973). Although we did not measure in-stream production, we measured macroinvertebrate and detritus export to assess how headwater streams might influence prey abundance and potentially salmonid production in downstream habitats. We found that clearcut sites did not export significantly more macroinvertebrate numbers or biomass than did old-growth sites, which may be due to low levels of allochthonous input. Also, we observed a trend toward alder-dominated sites exporting more macroinvertebrates than did clearcut sites, although we did not plan an a priori contrast for this pair. Because most nutrients are rapidly transported out of high-gradient streams (Fisher and Likens 1973), headwater productivity may not respond to increased light availability as readily as do lower-gradient streams. Thus, management activities that remove forest canopy along streams should take into account the differences in energy processes in headwater vs. floodplain channels.

Forests in southeastern Alaska are managed for multiple objectives, including sustainable timber harvest, maintenance of biodiversity, conservation of fish and wildlife resources, recreation, and aesthetic values (USDA Forest Service 1997). Successful land management for sustained yield of all of these forest resources depends upon sound knowledge of ecosystem processes for entire watersheds, of which headwaters are an integral part. We found that in areas clearcut 35–40 years ago, alder-dominated sites exported significantly greater numbers and biomass of macroinvertebrates than did conifer-dominated sites. The forest ecosystem of southeastern Alaska contains an alder component as a consequence of both natural and human-induced disturbance (Deal 1997; Hanley and Barnard 1998). Because present policy extends little or no riparian buffer protection to class IV streams during timber harvest, headwater ecosystems will likely continue to contain an alder component. Although we do not advocate timber harvesting as a means of generating alder to increase productivity in headwater streams, maintaining some alder in existing young-growth stands may help to offset other potentially negative effects of past timber harvest.

Because headwaters are an important component of stream ecosystems, understanding their contribution to downstream habitats holds important management implications. Alder appears to influence the link between terrestrial and aquatic systems in headwaters and between upland forests and downstream habitats. Maintaining an alder component during young-growth forest succession following timber harvest may be beneficial if salmonid productivity is a concern, and we recommend that forest managers consider the potential benefits of alder in stream riparian ecosystems.

Acknowledgments

We thank the U.S. Department of Agriculture Forest Service Craig Ranger District for technical support. Shully Millstein was indispensable as both field and laboratory assistant crew leader, as was John Caouette for statistical analysis. We thank Derek Busch, Brian Davies, Brittany Graham, Dave Gregovich, Heather Hodgins, Maria Lang, Steve McCurdy, Ozzie Hernandez, and Ewa Orlikowska for technical support and Takashi Gomi and Dustin T. Wittmer for providing Fig. 1. Peter A. Bisson, William R. Lorenz, Richard W. Merritt, John S. Richardson, Deanna J. Stouder, Robert L. Deal, and two anonymous reviewers provided constructive comments on earlier drafts of this manuscript. We also thank Linda Daniel for providing technical editing. This research was funded by the Wood Compatibility Initiative (WCI), U.S. Department of Agriculture Pacific Northwest Research Station, Portland, Oregon.

References

Alaback, P.B. 1982. Dynamics of understory biomass in Sitka spruce – western hemlock forests of Southeast Alaska. Ecology, **63**: 1932–1948.

Bilby, R.E., and Bisson, P.A. 1992. Allochthonous versus autochthonous organic matter contributions to the trophic support of fish populations in clear-cut and old-growth forested streams. Can. J. Fish. Aquat. Sci. **49**: 540–551.

Binkley, D., Cromack, K., Jr., and Baker, D.D. 1994. Nitrogen fixation by red alder: biology, rates, and controls. *In* The biology and management of red alder. *Edited by* D.E. Hibbs, D.S. DeBell, and R.F. Tarrant. Oregon State University Press, Corvallis, Oreg. pp. 57–72.

Bramblett, R.G., Bryant, M.D., and Wright, B.E. 2002. Seasonal movements and habitat use by juvenile steelhead in Southeast Alaska. Trans. Am. Fish. Soc. **131**: 498–506.

Burgherr, P., and Meyer, E.I. 1997. Regression analysis of linear body dimensions vs. dry mass in stream macroinvertebrates. Arch. Hydrobiol. **139**: 101–112.

© 2002 NRC Canada

Cuffney, T.F., and Wallace, J.B. 1988. Particulate organic matter export from three headwater streams: discrete versus continuous measurements. Can. J. Fish. Aquat. Sci. **45**: 2010–2016.

Deal, R.L. 1997. Understory plant diversity in riparian alder–conifer stands after logging in Southeast Alaska. U.S. Department of Agriculture Forest Service Research Note PNW-RN-523. (http://www.fs.fed.us/pnw/pubs/rn_523.pdf)

Duncan, W.F., and Brusven, M.A. 1985. Benthic macroinvertebrates in logged and unlogged low-order Southeast Alaskan streams. Freshwater Invertebr. Biol. **4**: 125–132.

Fisher, S.G., and Likens, G.E. 1973. Energy flow in Bear Brook, New Hampshire: an integrative approach to stream ecosystem metabolism. Ecol. Monogr. **43**: 421–439.

Groot, C., and Margolis, L. (*Editors*). 1991. Pacific salmon life histories. University of British Columbia Press, Vancouver, B.C.

Haigh, M.J., Singh, R.B., and Krecek, J. 1998. Headwater control: matters arising. *In* Headwaters: water resources and soil conservation. *Edited by* M.J. Haigh, J. Krecek, G.S. Rajwar, and M.P. Kilmartin. A.A. Balkema, Rotterdam, Netherlands. pp. 3–24.

Hanley, T.A., and Barnard, J.C. 1998. Red alder, *Alnus rubra*, as a potential mitigating factor for wildlife habitat following clearcut logging in southeastern Alaska. Can. Field-Nat. **112**: 647–652.

Harris, A.S., Hutchison, O.K., Meehan, W.R., Swanston, D.N., Helmers, A.E., Hendee, J.C., and Collins, T.M. 1974. The forest ecosystem of southeast Alaska. 1. The setting. U.S. Department of Agriculture Forest Service Gen. Tech. Rep. PNW-12. *Available from* Juneau Forestry Sciences Laboratory, 2770 Sherwood Lane Suite 2A, Juneau, AK 99801, U.S.A.

Hayes, J.W., Stark, J.D., and Shearer, K.A. 2000. Development and test of a whole-lifetime foraging and bioenergetics growth model for drift-feeding brown trout. Trans. Am. Fish. Soc. **129**: 315–332.

Hetrick, N.J., Brusven, M.A., Meehan, W.R., and Bjornn, T.C. 1998. Changes in solar input, water temperature, periphyton accumulation, and allochthonous input and storage after canopy removal along two small salmon streams in Southeast Alaska. Trans. Am. Fish. Soc. **127**: 859–875.

Irons, J.G., Oswood, M.W., and Bryant, J.P. 1988. Consumption of leaf detritus by a stream shredder: influence of tree species and nutrient status. Hydrobiologia, **160**: 53–61.

Naiman, R.J., Beechie, T.J., Benda, L.E., Berg, D.R., Bisson P.A., MacDonald, L.H., O'Connor, M.D., Olson, P.L., and Steel, E.A. 1992. Fundamental elements of ecologically healthy watersheds in the Pacific Northwest coastal ecoregion. *In* Watershed management: balancing sustainability and change. *Edited by* R.J. Naiman. Springer-Verlag, New York. pp. 127–188.

Newbold, J.D., Erman, D.C., and Roby, K.B. 1980. Effects of logging on macroinvertebrates in streams with and without buffer strips. Can. J. Fish. Aquat. Sci. **37**: 1076–1085.

Newton, M., and Cole, E.C. 1994. Stand development and successional implications: pure and mixed stands. *In* The biology and management of red alder. *Edited by* D.E. Hibbs, D.S. DeBell, and R.F. Tarrant. Oregon State University Press, Corvallis, Oreg. pp. 106–115.

Resh, V.H., Brown A.V., Covich, A.P., Gurtz, M.E., Li, H.W., Minshall, G.W., Reice, S.R., Sheldon, A.L., Wallace, J.B., and Wissmar, R.C. 1988. The role of disturbance in stream ecology. J. North Am. Benthol. Soc. **7**: 433–455.

Rogers, L.E., Buschbom, R.L., and Watson, C.R. 1977. Length–weight relationships of shrub–steppe invertebrates. Ann. Entomol. Soc. Am. **70**: 51–53.

Sample, B.E., Cooper, R.J., Greer, R.D., and Whitmore, R.C. 1993. Estimation of insect biomass by length and width. Am. Midl. Nat. **129**: 234–240.

SAS Institute, Inc. 1990. SAS/STST user's guide. SAS institute, Inc., Cary, N.C.

Short, R.A., and Maslin, P.E. 1977. Processing of leaf litter by a stream detritivore: effect on nutrient availability to collectors. Ecology, **58**: 935–938.

Smock, L.A. 1980. Relationships between body size and biomass of aquatic insects. Freshwater Biol. **10**: 375–383.

Stone, M.K., and Wallace, J.B. 1998. Long-term recovery of a mountain stream from clearcut logging: the effects of forest succession on benthic invertebrate community structure. Freshwater Biol. **39**: 151–169.

Swanston, D.N. 1967. Geology and slope failure in the Maybeso Valley, Prince of Wales Island, Alaska. PhD thesis, Michigan State University, East Lansing, Mich.

U.S. Department of Agriculture (USDA) Forest Service. 1997. Tongass land management plan revision: final environmental impact statement. Appendix, Vol. 1. U.S. Department of Agriculture Forest Service R10-MB-388e. (http://www.fs.fed.us/r10/TLMP/FEIS/FEIS_COV.PDF)

U.S. Department of Agriculture Forest Service. 1999. Record of decision. Tongass National Forest land and resource management plan. U.S. Department of Agriculture Forest Service FS-639. (http://www.fs.fed.us/r10/tongass/management%20news/decisions/tlmp_rod_summary_41999.html)

Wallace, J.B., Cuffney, T.F., Goldowitz, B.S., Chung, K., and Lugthart, G.J. 1991. Long-term studies of the influence of invertebrate manipulations and drought on particulate organic matter export from headwater streams. Verh. Int. Verein. Limnol. **24**: 1676–1680.

Wallace, J.B., Eggert, S.L. Meyer, J.L., and Webster, J.R. 1997. Multiple trophic levels of a forest stream linked to terrestrial litter inputs. Science (Washington, D.C.), **277**: 102–104.

Wallace, J.B., Eggert, S.L., Meyer, J.L., and Webster, J.R. 1999. Effects of resource limitation on a detrital-based ecosystem. Ecol. Monogr. **69**: 409–442.

Winer, B.J., Brown, D.R., and Michels, K.M. 1991. Statistical principles in experimental design. McGraw-Hill, New York.

Wipfli, M.S. 1997. Terrestrial invertebrates as salmonid prey and nitrogen sources in streams: contrasting old-growth and young-growth riparian forests in southeastern Alaska, U.S.A. Can. J. Fish. Aquat. Sci. **54**: 1259–1269.

Wipfli, M.S., and Gregovich, D.P. 2002. Export of invertebrates and detritus from fishless headwater streams in southeastern Alaska: implications for downstream salmonid production. Freshwater Biol. **47**: 957–969.

Young, K.A., Hinch, S.G., and Northcote, T.G. 1999. Status of resident coastal cutthroat trout and their habitat twenty five years after riparian logging. N. Am. J. Fish. Manag. **19**: 901–911.

© 2002 NRC Canada

A trophic study of a marine ecosystem off southeastern Australia using stable isotopes of carbon and nitrogen

Stephanie R. Davenport and Nicholas J. Bax

Abstract: The stable isotopes of carbon and nitrogen were used to investigate trophic relationships of fish and invertebrates on the continental shelf of southeastern Australia. We examined 87 fish species, marine mammals, penguins, invertebrates, algal samples, suspended particulate organic matter (POM), and sediments. The main source of primary production is oceanic phytoplankton, although there is evidence of a seagrass contribution to the benthos. Marine mammals, penguins, some benthic invertebrates, and some benthic fish filled the highest trophic positions. Sources of variability in isotope results included temporal (POM, some fish) and spatial (POM, sediments) elements, bottom depth (some fish), and size (some fish). Fish had muscle $\delta^{15}N$ values of 9.6‰ to 14.7‰ and $\delta^{13}C$ values of –20.6‰ to –14.6‰. Cluster analysis on fish stable isotope results produced fish groups that could be interpreted with trophic and habitat information. Trophic relationships in fish, suggested by stable isotope results, were supported by stomach contents analysis. Stable isotope results may indicate more representative trophic relationships, as stomach contents analyses tend to group prey by taxon rather than by trophodynamic position. In fish and invertebrates, stable isotope results related more to functional patterns of feeding than to taxonomic relationships.

Résumé : L'utilisation des isotopes stables de carbone et d'azote nous a permis d'étudier les relations trophiques des poissons et des invertébrés sur le plateau continental au large de la côte sud-est de l'Australie. Nous avons analysé 87 espèces de poissons, des mammifères marins, des manchots, des invertébrés, des échantillons d'algues, de la matière organique particulaire (POM) en suspension et des sédiments. La source principale de production primaire est le phytoplancton océanique, bien qu'il y ait des indices d'une contribution des herbes marines au benthos. Les mammifères marins, les manchots et quelques invertébrés et poissons benthiques représentent les échelons trophiques supérieurs. La variabilité des résultats obtenus à l'aide des isotopes est attribuable, entre autres, à des facteurs temporels (POM, certains poissons), à des facteurs spatiaux (POM, sédiments), à la profondeur du fond (quelques poissons) et la taille (quelques poissons). Chez les poissons, les valeurs de $\delta^{15}N$ varient de 9,6 ‰ à 14,7 ‰ et celles de $\delta^{13}C$ de –20,6 ‰ à –14,6 ‰. Des analyses de groupement des résultats obtenus génèrent des groupes de poissons qui peuvent s'interpréter à l'aide de données sur le régime alimentaire et l'habitat. Les relations trophiques des poissons révélées par l'étude des isotopes stables correspondent à celles obtenues par l'analyse des contenus stomacaux. L'étude des isotopes stables peut fournir des informations plus précises sur les relations trophiques, car l'analyse des contenus stomacaux a tendance à regrouper les proies par catégorie taxonomique plutôt que par position trophodynamique. Chez les poissons et les invertébrés, les résultats obtenus à l'aide des isotopes stables correspondent plus aux patterns alimentaires fonctionnels qu'aux relations taxonomiques.

[Traduit par la Rédaction]

Introduction

Australia's southeastern continental shelf has been fished for nearly 100 years. Over that time, there have been large changes in the fish community (Klaer 2001) with unknown consequences for species interactions between fish and between fish and other organisms. Predation can be a major force in structuring marine fish communities (reviewed by Bax 1998), and in this study we set out to describe the major trophic categories and links in the marine ecosystem on the continental shelf of southeastern Australia.

Stable isotopes can provide useful information about sources and processes within an ecosystem. The analysis of stable carbon isotopes ($\delta^{13}C$) in suspended particulate organic matter (POM) and sediments can indicate the origins of plant source materials (e.g., Fry and Sherr 1984). In a marine or coastal ecosystem, there are several potential sources of carbon with different $\delta^{13}C$ signatures; e.g., macroalgae (–27‰ to –8‰), seagrasses (–15‰ to –3‰), marine phytoplankton (–24‰ to –18‰), and terrestrial outflow (–30‰ to –10‰) (Fry and Sherr 1984). Analyses of stable nitrogen isotopes ($\delta^{15}N$) are frequently used to determine trophic relationships in an ecosystem (e.g., Schoeninger and DeNiro 1984; Sholto-Douglas et al. 1991) and also to provide information on source materials (e.g., France 1994).

For carbon, animals have an isotopic composition similar to their diets: typically they are enriched by only 1‰ or less

Received 4 January 2001. Accepted 27 February 2002. Published on the NRC Research Press Web site at http://cjfas.nrc.ca on 12 April 2002.
J16166

S.R. Davenport[1] **and N.J. Bax.** CSIRO Marine Research, G.P.O. Box 1538, Hobart, Tasmania 7001 Australia.

[1]Corresponding author (e-mail: stevie.davenport@marine.csiro.au).

 DOI: 10.1139/F02-031 © 2002 NRC Canada

(e.g., DeNiro and Epstein 1978; Fry and Sherr 1984). The enrichment of ^{13}C in aquatic systems varies from 0.2‰ for freshwater systems to 1.1‰ for oceanic systems, with estuarine and coastal systems somewhere in between (France and Peters 1997). Because the difference in $\delta^{13}C$ between an animal and its diet is small, animal $\delta^{13}C$ is indicative of the $\delta^{13}C$ of its diet, though less indicative of its trophic level. For $\delta^{15}N$, animals are usually enriched by 1–5‰ (average 3.4‰) compared with their diet, apparently due to the loss of the light ^{14}N isotope in excretory products (Minagawa and Wada 1984; Owens 1987; Peterson and Fry 1987). This relatively large difference in $\delta^{15}N$ between an animal and its diet allows trophic relationships within an ecosystem to be estimated. Each trophic level above the base source of nitrogen leads to an additional (average) increase in the ratio of about 3‰ (e.g., Minagawa and Wada 1984; Schoeninger and DeNiro 1984). Comparing between ecosystems requires knowing the base isotope ratios in each system (France 1995).

Because of the variability in isotope ratios due to ecosystem, taxa, tissue composition and trophic level, stable isotope analysis complements, rather than replaces, other methods for determining trophic relationships. The examination of stomach contents provides information on what an animal has recently eaten; the isotopic composition of an animal reflects its assimilated diet (not just what has been eaten) over a period determined by the turnover rate of the tissues. Apart from providing a "snapshot" of diet, stomach contents information is vulnerable to biases related to what material is identifiable in the stomach. Different prey types are digested and evacuated at different rates, and the importance of rapidly digested prey may be underestimated (e.g., MacDonald et al. 1982). Stable isotope information may provide a more representative description of fish trophodynamics than that provided by stomach contents analyses. Stomach contents analyses tend to aggregate prey species with different habitats and feeding specialisations (e.g., polychaetes, gastropods) that can represent very different trophic positions.

In this study we examined the stable isotope ratios of carbon and nitrogen in tissues of organisms that live on, or visit, the continental shelf of southeastern Australia. The main objective was to identify important trophic relationships and assess the usefulness of stable isotope results in elucidating feeding patterns within the ecosystem. Stable isotope results for fish were compared with information derived from stomach contents analysis. We also looked for temporal, spatial, and size changes in fish being reflected in their stable isotope signatures.

Methods

As part of a broad ecosystem study (Bax et al. 1999), the Commonwealth Scientific and Industrial Research Organisation (CSIRO) research vessel *Southern Surveyor* made four month-long surveys on the southeast Australian continental shelf, in depths of 20–250 m in 1993 to 1996. Each survey took place at a different time: July 1993 (early winter), August 1994 (late winter), April 1996 (autumn), and November 1996 (spring). Seven transects were sampled on each survey (Fig. 1).

Samples for stable isotope analysis included >1200 fish (teleosts and elasmobranchs) representing 87 species, 153 benthic and pelagic invertebrates from eight phyla, 10 species of marine mammals, one seabird species, nine algal species, 91 samples of POM from the water column, and 103 sediment samples (Appendix A). Pelagic samples (water column and plankton) were taken at stations at 40 and 200 m in bottom depth; benthic samples (invertebrates and sediments) were taken from stations at 25, 40, 80, 120, and 200 m in bottom depth along each transect. Stomach contents information was available for 57 of the 87 fish species examined. Most fish were caught by CSIRO's FRV *Southern Surveyor* using a commercial demersal trawl; some were caught by chartered commercial vessels using gillnets and traps. A few species (e.g., the inshore and offshore pelagics, *Sardinops neopilchardus* and *Gasterochisma melampus*, respectively) were collected by staff of the Marine and Freshwater Research Institute, Victoria, and CSIRO observers aboard commercial vessels. Penguins from the study region were collected opportunistically. They were birds that had died of natural causes (Phillip Island, west of Wilsons Promontory) or following an oil spill in the Bass Strait region. Cetacean samples were collected from animals that had died after stranding around the coast of Tasmania.

After sorting of the catch, fish for stable isotope analysis were placed on ice until they could be processed. Individual fish lengths and weights were recorded and a section of white muscle from the caudal region taken from each fish for stable isotope analysis. Vertebrate muscle tissue was frozen at –20°C until it could be prepared for stable isotope analysis. Muscle samples were then thawed, surfaces trimmed of tissue to reduce possible contamination, and the remaining clean tissue cut into small pieces and dehydrated in an oven at 60°C for at least two days. The dried tissue was ground into a fine powder using a mortar and pestle. This powder was used for stable carbon and nitrogen analyses. Muscle was chosen as the tissue for stable isotope analysis because the turnover of muscle tissue is short enough to allow examination for seasonal differences in isotope signature if they exist (Tieszen et al. 1983; Hesslein et al. 1993).

Invertebrates were collected with a benthic sled. Whole animals were frozen until they could be prepared for analysis. Small animals were prepared whole; large animals or animals with a hard shell or test were dissected and a sample of muscle tissue was taken for stable isotope analysis. Tissues were prepared as for vertebrate samples.

Although it is common to remove lipids from samples prior to stable isotope analysis or to adjust data for lipids (e.g., using the formulae of McConnaughey and McRoy 1979), lipid adjustment of these data was not warranted. Most Australian fish and crustaceans have low oil content, averaging about 1% in fish (Nichols et al. 1998), reflecting the generally oligotrophic waters surrounding the continent.

Analyses of stable carbon and stable nitrogen isotopes were performed by Dr. S. Bunn and staff at the Faculty of Environmental Sciences at Griffith University (Queensland) and Dr. A. Revill at CSIRO Marine Research (Tasmania). Powdered samples were weighed into tin capsules. The samples analysed at Griffith University were oxidized by a Roboprep–CN Biological Sample Converter. The resultant CO_2 and N_2 were analysed with a continuous flow isotope

© 2002 NRC Canada

Fig. 1. Study site and primary sampling transects off southeastern Australia. NSW, New South Wales.

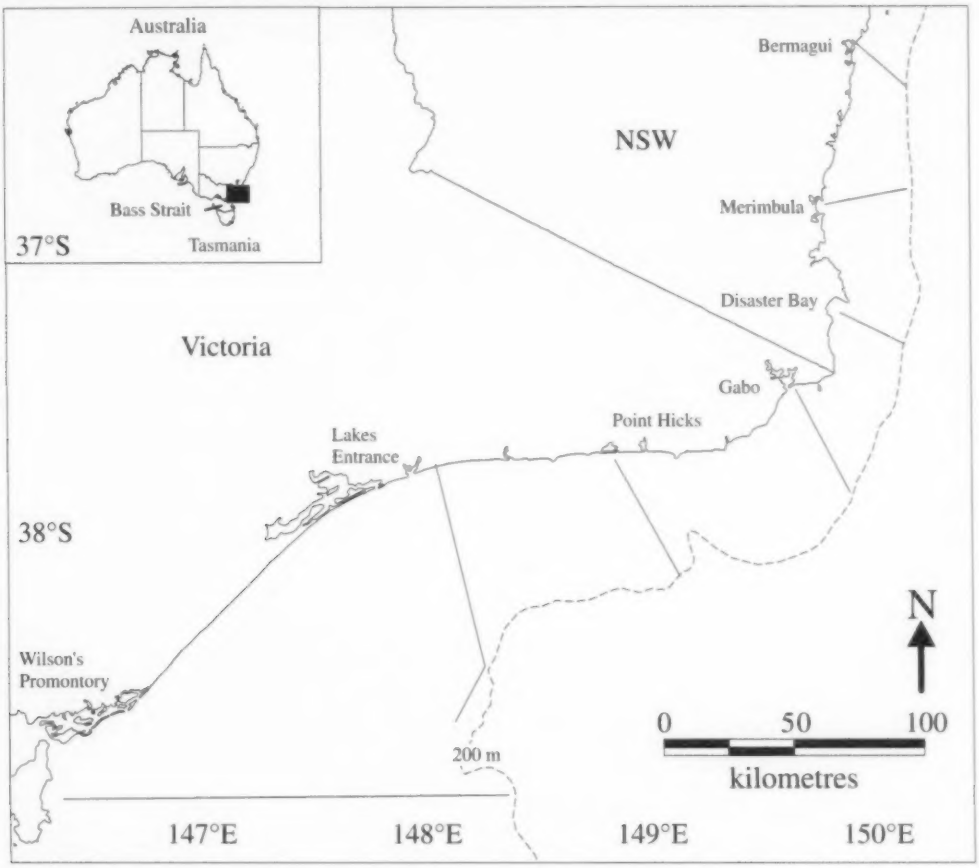

ratio mass spectrometer (CF–IRMS, Europa Tracermass, Crewe, U.K.). At CSIRO Marine Research, samples were analysed using a Carlo Erba NA 1500 CNS analyser interfaced via a Conflo II to a Finnigan Mat Delta S isotope ratio mass spectrometer operating in the continuous flow mode. Combustion and oxidation were achieved at 1090°C and reduction at 650°C. Where necessary the carbon signal was diluted using helium. ^{13}C:^{12}C and ^{15}N:^{14}N were expressed as the relative per mil (‰) difference between the sample and conventional standards (the primary standards are for carbon, Pee Dee Belemnite, a marine limestone fossil; and for nitrogen, N_2 in air). The formula used to express these standards is

$$\Delta X = [(R(\text{sample}))/(R(\text{standard})) - 1] \times 1000‰$$

where $X = {}^{13}C$ or ^{15}N, and $R = {}^{13}C/{}^{12}C$ or $^{15}N/{}^{14}N$. Data were analysed in four steps. First, stable isotope results were placed into broad taxonomic groups to give an overview of the trophic structure of the ecosystem (Fig. 2). Second, data were analysed for temporal and spatial variability by analysis of variance (ANOVA). Third, the 87 fish species were analysed further using cluster analysis of the mean $\delta^{13}C$ and $\delta^{15}N$ values for each fish species (Ward's minimum variance method, SAS JMP Version 3.1, SAS Institute Inc. 1995) to determine trophic relationships within the fish community. Fourth, we looked for changes in isotope signature that might be related to dietary changes with size (length in cm) in fish species where there were ≥25 samples.

Stomach contents of fish were analysed separately as part of the South East Fishery Ecosystem Study and reported in Bulman et al. (2001).

Results and discussion

Broad taxonomic groups had distinct combinations of $\delta^{13}C$ and $\delta^{15}N$ (Fig. 2). Red and brown macroalgae collected from coastal areas had the lowest values of $\delta^{13}C$ and $\delta^{15}N$, indicating their role as primary producers. However, their $\delta^{13}C$ values were ~5–7‰ less than that of oceanic zooplankton, indicating that they contributed little to secondary production in the shelf ecosystem. The two other sources of primary production, POM and seagrasses, had similarly low $\delta^{15}N$ but much higher $\delta^{13}C$. Seagrass $\delta^{13}C$ was higher than $\delta^{13}C$ for any other broad taxonomic group. Benthic invertebrates had $\delta^{13}C$ values intermediate between POM and seagrasses, suggesting some seagrass contribution to benthic food chains. Analysis of photosensitive pigments and stable isotopes in seawater and sediment samples from this area indicated a low contribution from terrestrial and nearshore production to this continental shelf ecosystem (Bax et al.

© 2002 NRC Canada

Fig. 2. Overall trophic structure based on mean stable isotope values (±1 standard deviation) for organisms from the southeast Australian continental shelf. BA, brown alga; MW, Minke whale; PC, pelagic cephalopods; POM, particulate organic matter; TW, toothed whales. Cetaceans were stranded in this region; some live and feed in this ecosystem (e.g., common and bottlenose dolphins, killer whales) but others (e.g., beaked whales and spectacled porpoise) may feed in other ecosystems (lighter shading for whales is used to indicate this). Mobile benthos includes asteroids, bivalves, crustaceans, echinoids, gastropods, octopus, and ophiuroids. Sessile benthos includes anemones, ascidians, bryozoans, crinoids, soft corals, and sponges.

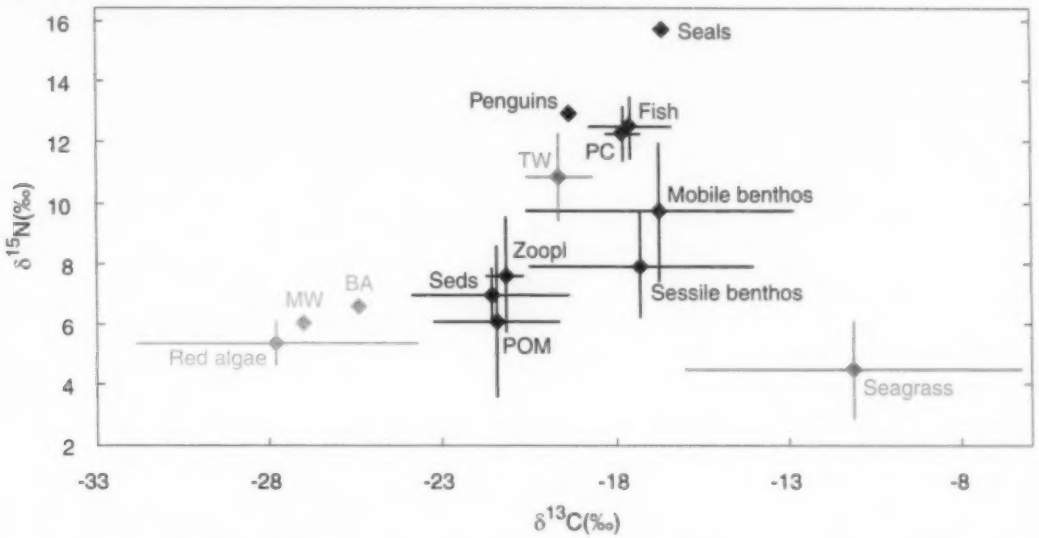

2001). This was not a surprising finding as the survey area lies off a dry corner of a dry continent, and river discharge is low owing to impoundments and diversions of river water for agricultural and power generation purposes. The $\delta^{13}C$ of POM, sediments, and zooplankton were similar (Fig. 2), indicating a major role for oceanic primary production in this system, particularly for pelagic organisms.

At the base of the food chain, organic matter in the water column (POM) varied little across the study area: mean $\delta^{13}C$ –21.5‰, standard deviation (SD) 0.2‰, n = 91; mean $\delta^{15}N$ 6.1‰, SD 2.5‰, n = 81. Most sample $\delta^{13}C$ values were typical of temperate marine phytoplankton: –24‰ to –18‰ (review by Fry and Sherr 1984), –25.3‰ to –19.8‰ (Rau et al. 1990), –22‰ (Boutton 1991). The only POM $\delta^{13}C$ outside these ranges came from a shallow site off Lakes Entrance in 1996. The enriched $\delta^{13}C$ result here was possibly due to outflow of Lakes Entrance water carrying a seagrass contribution. Nichols et al. (1985) found relatively high $\delta^{13}C$ (–12.9‰) in suspended matter from nearby Corner Inlet, near Wilsons Promontory. They attributed this signal to a seagrass contribution, a conclusion supported by seagrass-specific lipid marker compounds in their samples.

Whereas the range for POM $\delta^{15}N$ (2.3–18.2‰) suggests high variability, there were four outlying data points (>2 SD from the mean) responsible for the large range. These samples ($\delta^{15}N$ > 8.6‰) were collected during the 1994 winter voyage, all from shallow water (<45 m), the inshore sites of the three southernmost transects. These were the only sites where the influence of seagrasses, benthic macroalgae, or C4 plants was detected (Bax et al. 2001). When these outlying samples were removed from the data set, the $\delta^{15}N$ values for POM across the rest of the study area were as follows: mean 5.7‰, SD 1.4‰, range 2.3–8.4‰, n = 77.

Distinct pelagic and benthic trophic pathways were indicated by the data (Fig. 2; Table 1), although some caution is needed in interpretation, as vertebrate samples came from muscle tissue, whereas invertebrate samples typically comprised the whole organism. Demersal invertebrates (mobile and sessile benthos) had lower $\delta^{15}N$ and higher $\delta^{13}C$ values overall than pelagic and demersal vertebrates (fish, penguins, seals, toothed whales, and pelagic cephalopods).

Pooled isotope values for taxonomic groups obscure some of the individual variation within those groups. This is especially the case for invertebrates. The highest trophic levels ($\delta^{15}N$ > 14‰) in animals within this ecosystem are filled by a mixture of pelagic and benthic organisms: fur seals, polychaete worms, killer whale, bottlenose dolphin, hammerhead shark, and a few highly predatory fish, e.g., largetooth beardie, green moray, longfin pike, and speckled stargazer; the lowest trophic positions were filled by pelagic and benthic invertebrates (Appendix A). Apart from birds, mammals, and pelagic sharks, the top predators are mainly benthic organisms: fish and invertebrates.

Functional patterns of feeding rather than taxonomic links were important elements in the complex relationships that emerged from stable isotope analyses. Within a single taxonomic group (especially in benthic invertebrates in this study) there was a wide range of isotopic signatures and feeding mechanisms (Fig. 2; Tables 2 and 3).

Variability

Sources of variability in stable isotope results included temporal variability for POM, cross-shelf variability for sediments, size, depth, and perhaps temporal and spatial variability for some fish species, and probably dietary opportunism in most animals.

© 2002 NRC Canada

Table 1. Differences in stable isotope enrichment patterns in a simplified (*a*) pelagic and (*b*) benthic food chain from the southeast Australian continental shelf.

(*a*) Simplified pelagic food chain.				
	Organism	*n*	$\delta^{15}N$ (‰)	$\delta^{13}C$ (‰)
Quaternary consumers (e.g., secondary piscivores)	Australian fur seal (*Arctocephalus pusillus doriferus*)	2	15.8	–16.7
Tertiary consumers (e.g., primary piscivores)	Little penguin (*Eudyptula minor*)	19	13.0	–19.4
	Redbait (*Emmelichthys nitidis*)	25	11.6	–18.1
	Jack mackerel (*Trachurus declivis*)	52	12.5	–18.4
	Gould's squid (*Nototodarus gouldi*)	8	12.9	–17.8
Secondary consumers (e.g., zooplanktivorous fish)	Barber perch (*Caesioperca rasor*)	8	10.7	–18.3
	Hector's lanternfish (*Lampanyctodes hectoris*)	10	10.6	–19.8
	Pennant lightfish (*Maurolicus muelleri*)	5	10.2	–20.6
	Blue warehou (*Seriolella brama*)	28	12.6	–18.7
	Silver warehou (*Seriolella punctata*)	40	12.2	–19.2
Primary consumers	Zooplankton from surface tows	6	7.7	–21.3
Primary producers	Phytoplankton (1994 spring bloom)	4	6.2	–20.5
	POM (n = 77 for $\delta^{15}N$; 91 for $\delta^{13}C$)	77/91	6.1	–21.5
(*b*) Simplified benthic food chain.				
	Organism	*n*	$\delta^{15}N$ (‰)	$\delta^{13}C$ (‰)
Tertiary consumers (e.g., primary piscivores, benthic invertebrate feeders)	Pink ling (*Genypterus blacodes*)	18	13.1	–17.2
	Sand flathead (*Platycephalus bassensis*)	23	12.2	–16.9
	Tasmanian numbfish (*Narcine tasmaniensis*)	15	13.8	–14.6
Secondary consumers (e.g., feed on benthic invertebrates)	Morwong (*Nemadactylus macropterus*)	43	13.1	–17.9
	Elephant fish (*Callorhynchus milii*)	2	10.3	–16.8
	Hermit crab (*Strigopagrus strigimanus*)	3	10.4	–18.3
	Predatory polychaetes	13	8.7–15.5	–19.1 to –14.5
	Port Jackson shark (*Heterodontus portusjacksoni*)	6	12.0	–15.2
Primary consumers (e.g., detritus feeders)	Sea biscuit (Clypeaster)	1	8.3	–10.2
	Holothurian	1	7.2	–17.6
	Sea mouse (Aphrodite)	2	8.4	–16.7
	Ophiuroids	3	9.4	–9.8
(e.g., filter feeders)	Bivalve (*Glycymeris striatularis*)	4	6.8	–18.0
	Sabellid polychaetes	2	6.6	–18.1
	New Zealand screw shell (*Maoricolpus roseus*)	4	5.3	–18.1
	Sediment	103	7.0	–21.8
Primary producers	POM (n = 77 for $\delta^{15}N$; 91 for $\delta^{13}C$)	77/91	6.1	–21.5
	Seagrass sp. 1	1	3.5	–7.8
	Seagrass sp. 2	1	5.7	–14.6
	Macroalgae	1	6.6	–25.5

Note: POM, particulate organic matter.

Temporal and spatial variability

We could not separate seasonal and (or) annual factors, as ship availability mostly restricted our sampling to a different season in each year. Three surveys (August 1994, April 1996, and November 1996) provided sufficient data for us to look for temporal and spatial differences in the POM and sediment data.

There was a significant difference between years and (or) seasons in $\delta^{13}C$ and $\delta^{15}N$ for POM, but not for sediments. For POM $\delta^{13}C$, there was a significant difference (1.4‰ between means) between the August 1994 (winter) and November 1996 (spring) voyages ($p < 0.01$, $n = 91$). For POM $\delta^{15}N$, there was a significant difference between the August 1994 and April 1996 (autumn) voyages ($p < 0.05$, $n = 81$), although when the four enriched, southern inshore values from 1994 are removed, this difference disappears.

Spatial variability within the study area was examined by analysing POM and sediment isotope data between and across transects. There were no between-transect trends detected in either the POM or sediment isotope data. Cross-shelf enrichment in sediment $\delta^{15}N$ and $\delta^{13}C$ ($p < 0.001$, $n = 79$) was detected with a mean enrichment of 1.5‰ in $\delta^{15}N$ and 2‰ in $\delta^{13}C$ between the 25-m and 200-m sites. There were no cross-shelf trends in enrichment detected for POM $\delta^{13}C$ or $\delta^{15}N$ (although only two sites per transect were sampled for POM). There was greater variability in POM $\delta^{15}N$ at

© 2002 NRC Canada

Table 2. Stable nitrogen values and feeding behaviour in polychaete worms sampled on the southeastern continental shelf.

Polychaete family	$\delta^{15}N$ (‰) (*n*)	Feeding behaviour and structures
Lumbrinereidae	15.5 (1)	Carnivorous: eversible armed pharynx; well-developed mandibles and maxillae
Lysaretidae	13.7 (4)	Carnivorous: well-developed mandibles
Polynoidae	12.4 (1)	Predator: captures food using eversible armed pharynx
Eunicidae	11.9 (4)	A diverse group: eversible armed pharynx with 4 or more pairs of jaws
Ophelidae	11.7 (1)	Deposit feeder
Onuphidae	10.3 (1)	Tube-dwelling scavenger with eversible armed pharynx and well-developed mandibles
Sigalionidae	8.7 (2)	Burrowing predator with eversible armed pharynx
Aphrodite (sea mouse)	8.4 (2)	Detritus feeder
Sabellidae	6.6 (2)	Tube-dwelling filter feeder

Note: Information on diet from K. Gowlett-Holmes, CSIRO Marine Research, G.P.O. Box 1538, Hobart, Tasmania 7001, Australia, personal communication, and Hutchings (1982).

Table 3. Stable nitrogen values and feeding behaviour in gastropods sampled on the southeastern continental shelf.

Gastropod	$\delta^{15}N$ (‰) (*n*)	Feeding behaviour
Ericusa sowerbyi (Sowerby's volute)	13.7 (1)	Active carnivore
Fusinus novaehollandiae (spindle shell)	10.6 (1)	Detrital feeder, occasional carnivore
Amoria undulata (wavy volute)	10.2 (1)	Predator, especially on bivalves
Sinum zonale (ear snail)	9.0 (1)	Predator on bivalves
Philine (sea slug)	8.1 (1)	Burrowing predator on amphipods, bivalves
Maoricolpus roseus (New Zealand screw shell)	5.3 (4)	Suspension or detritus feeder

Note: Information on diet from K. Gowlett-Holmes, CSIRO Marine Research, G.P.O. Box 1538, Hobart, Tasmania 7001, Australia, personal communication, and Hutchings (1982).

inshore compared with offshore sites due to the four enriched southern inshore sites in winter 1994.

Fish

Fish with a high $\delta^{15}N$ signal generally had a high proportion of fish in their diet or they ate other species (e.g., polychaetes) with a high $\delta^{15}N$ signal (Bulman et al. 2001). Large fish, within and between species, generally had a higher $\delta^{15}N$ signal than small fish. Larger size provides more opportunity for feeding on large prey and selecting from a greater variety of prey species.

Fish $\delta^{13}C$ separated them according to primarily benthic or pelagic feeding modes. There were diet data for 41 of the 63 species where $\delta^{13}C \geq -18.0$‰. These 41 species are classified by the trophic guilds of Bulman et al. (2001) as follows: 12 benthopelagic omnivores and epibenthic invertebrate feeders specialising on megabenthos and small crustaceans, 11 benthopelagic piscivores, six benthic piscivores, four benthic invertebrate feeders and omnivores specialising on polychaetes, four epibenthic invertebrate feeders and omnivores specialising on small noncrustaceans, three invertebrate feeders with high levels of unknown prey, and one pelagic crustacean feeder or omnivore. There were diet data for 16 species of the 24 where $\delta^{13}C < 18.0$‰. The trophic guilds of Bulman et al. (2001) classify these as follows: three invertebrate feeders with high levels of unknown prey, three benthopelagic piscivores, three pelagic piscivores, three pelagic crustacean feeders and omnivores, two pyrosome feeders, one epibenthic invertebrate feeder, and one benthic piscivore. Five of the remaining eight fish in this category are lanternfish (typically zooplankton feeders). Thomas and Cahoon (1993) and McConnaughey and McRoy (1979) similarly found that benthic-feeding fish had more-enriched $\delta^{13}C$ (and lower $\delta^{34}S$) values than pelagic feeders. The $\delta^{15}N$ values (means for each species) for each of the 87 species of marine fish in this study were 9.6–14.7‰; for $\delta^{13}C$, the values were –20.6‰ to –14.6‰ (Appendix A).

Trends in stable isotope results and in benthic and pelagic feeding patterns with the diet classifications of Bulman et al. (2001) may be seen (Table 4). Most to least enriched $\delta^{15}N$ categories run down the table. Within the four $\delta^{15}N$ categories are three $\delta^{13}C$ categories, again most to least enriched down the table. Overlaps in feeding behaviour are obvious and there are no fixed cut-off points. Diet switching (apart from trends related to fish growth) is known to occur for at least some species, e.g., jack mackerel (Bulman et al. 2001).

For fish generally, and piscivores especially, there is a trend with the larger species at the top of the table (enriched $\delta^{15}N$), smaller species towards the bottom. For piscivores with enriched $\delta^{15}N$ (≥13‰) and where there was <90% fish in the stomachs, the rest of the stomach contents mostly comprised benthic organisms (e.g., megabenthos, benthic invertebrates). For piscivores with $\delta^{15}N < 13$‰, where there was <90% fish in the stomach contents, much of the remainder comprised pelagic crustaceans and other pelagic invertebrates (Bulman et al. 2001).

Cluster analysis of stable isotope values for carbon and nitrogen in muscle tissues of the 87 teleost and elasmobranch species was used to look for patterns in the data (Fig. 3; Table 4). The choice of cut-off point that defines the clusters is somewhat arbitrary, but comparison between the cluster results and the biological and ecological information available enabled a useful basis for a description of the different feeding patterns observed. A cut-off point was chosen that separated the data into five groups (Fig. 4). More or fewer groups could have been chosen; e.g., if four groups had been chosen, Groups 3 and 4 (Fig. 4) would have been combined.

© 2002 NRC Canada

Table 4. Comparison between stable isotope groups suggested by cluster analysis and diet information from Bulman et al. (2001).

$\delta^{15}N$ (‰) (*N*, *n*)	$\delta^{13}C$ (‰)	Number of fish species in stable isotope cluster groups					Feeding habits (% fish in gut for piscivores)
		1	2	3	4	5	
≥13.0 (30, 16)	≥ –16.5	6	2				1 Benthopelagic piscivore (59%)
							1 Benthic piscivore (69%)
							1 Benthic invertebrate feeder / omnivore specialising on polychaetes
	–18.0 to –16.4	18		3			5 Benthopelagic piscivores (≥93%)
							2 Benthic piscivores (59%, 80%)
							1 Epibenthic invertebrate feeder / omnivore specialising on small noncrustaceans
							1 Benthic invertebrate feeder / omnivore specialising on polychaetes
							2 Benthopelagic omnivores / epibenthic invertebrate feeders specialising on megabenthos and small crustaceans
							1 Invertebrate feeder: high levels of unknown prey
	< –18.0			1			1 Benthopelagic piscivore (99%)
12.0–12.9 (34, 30)	≥ –16.5		5				1 Benthic piscivore (97%)
							1 Benthopelagic omnivore / epibenthic invertebrate feeder specialising on megabenthos and small crustaceans
	–18.0 to –16.4		1	19			1 Pelagic crustacean feeder / omnivore
							4 Benthopelagic piscivores (96%, 99%, 99%, 60%)
							2 Benthic piscivores (83%, 91%)
							1 Epibenthic invertebrate feeder / omnivore specialising on small noncrustaceans
							1 Benthic invertebrate feeder / omnivore specialising on polychaetes
							8 Benthopelagic omnivores / epibenthic invertebrate feeders specialising on megabenthos and small crustaceans
							2 Invertebrate feeders: high levels of unknown prey
	< –18.0			1	8		3 Pelagic crustacean feeders and omnivores
							1 Pelagic piscivore (38%)
							2 Benthopelagic piscivores (93%, 98%)
							1 Invertebrate feeder: high levels of unknown prey
							2 Pyrosome feeders
11.0–11.9 (13, 10)	≥ –16.5		2				1 Benthopelagic piscivore (96%)
							1 Benthic invertebrate feeder / omnivore specialising on polychaetes
	–18.0 to –16.4		2	3			2 Epibenthic invertebrate feeders / omnivores specialising on small noncrustaceans
							1 Benthopelagic omnivore / epibenthic invertebrate feeder specialising on megabenthos and small crustaceans
	< –18.0				6		2 Pelagic piscivores (83%, 80%)
							1 Epibenthic invertebrate feeder / omnivore specialising on small noncrustaceans
							2 Invertebrate feeders: high levels of unknown prey
<11.0 (10, 1)	≥ –16.5						
	–18.0 to –16.4		2				
	< –18.0					8	1 Benthic piscivore (70%)

Note: *N*, number of fish species in stable nitrogen category; *n*, number of fish species with diet data.

© 2002 NRC Canada

Fig. 3. Hierarchical clustering (Ward's minimum variance method) of stable nitrogen and stable carbon results for 87 fish species from the continental shelf of southeast Australia.

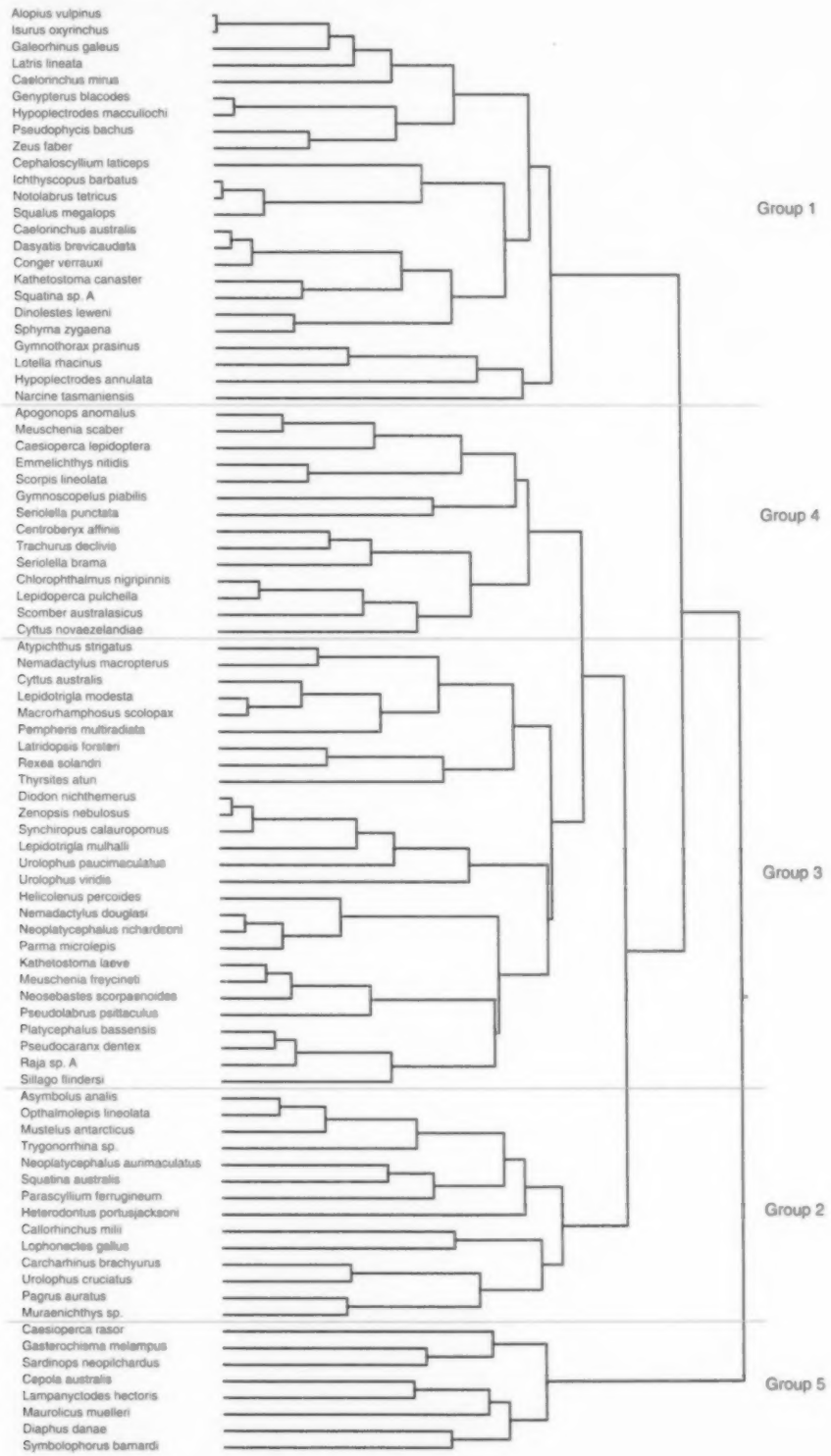

© 2002 NRC Canada

Whereas there are overlaps between the five groups, differences emerge between species feeding in predominantly benthic or pelagic systems (largely differentiated on $\delta^{13}C$ values).

Group 1 includes several large sharks and rays, eels, whiptails, pike, ling, seaperches, stargazers, striped trumpeter, cods, and John dory. Species in this group are highly piscivorous and have enriched $\delta^{15}N$ and $\delta^{13}C$ values, indicating a diet of prey with a high trophic position. The important diet components for Group-1 fish (fish, cephalopods, polychaetes) have high $\delta^{15}N$ values. This is supported by data from stomach content analysis. For species where stomach content data were available (11 of 24 species), fish made up >50% of the diet (51–95%), except for the Tasmanian numbfish, whose diet was 84% polychaetes, bluethroat wrasse with 32% fish and 59% benthic invertebrates, and southern whiptail with 25% megabenthos, 24% polychaetes, and 22% fish (Bulman et al. 2001). The Tasmanian numbfish has the highest $\delta^{13}C$ value (–14.6‰) of any fish in this study, presumably reflecting a polychaete-rich diet (polychaetes in this study had $\delta^{13}C$ values of –4.3‰ to –11.5‰). The high $\delta^{15}N$ (13.8‰) indicates that the numbfish is feeding on benthic prey with a high trophic position (e.g., the predatory polychaetes in this study had $\delta^{15}N$ values of 11.9–15.5‰).

Most of the 14 Group-2 fish species (five sharks, three skates or rays, five teleosts, and one chimaerid) display a strong benthic habit. The five species for which there are stomach contents data have a benthic or benthopelagic diet: the Port Jackson shark eats mostly gastropods; Maori wrasse 87% fish (identifiable species were benthic), 18% benthic invertebrates (e.g., ophiuroids and gastropods), 6% megabenthos (e.g., crabs); banded stingaree 42% polychaetes, 21% benthic invertebrates, 15% megabenthos and 5% benthic crustaceans; and the snapper 89% benthopelagic fish, 7% benthic fish, 4% benthic invertebrates (Bulman et al. 2001). One species in this group that might be considered a Group-1 pelagic predator is the bronze whaler shark. Only one was caught in this study and there are no diet data from Australian waters. Last and Stevens (1994), Cliff and Dudley (1992), and Bass et al. (1973) suggest that they are largely fish eaters and many prey species are benthic.

Group 3 was the largest and middle group in the cluster, contained the greatest mix of feeding behaviours, and is probably the most difficult group to describe, perhaps also displaying the most opportunism in feeding. Group 3 comprises 24 teleost and three ray species. The diets of some species showed low diversity and might be expected to fall into other groups: for example, gemfish, barracouta, mirror dory, and tiger flathead all contained more than 94% fish (a mixture of benthic and pelagic species) in the stomach contents and would intuitively fall into Group 1. The stomachs of some Group-3 fish (e.g., common bullseye and mirror dory) contained large proportions of prey of pelagic origin; others (e.g., globefish, eastern school whiting, and sand flathead) contained mostly benthic prey (Bulman et al. 2001). The bullseye, with a high proportion (74%) of euphausids in the stomach, reflects a Group-4 pattern, except that they also contained about 20% polychaetes, a prey group with a potentially enriched $\delta^{15}N$ signal. Several fish in this group ate a mixture of benthic and pelagic prey; for example, tiger flathead had 96% fish in the stomach: a mixture of benthic, benthopelagic, and pelagic fish.

Overall, the stomach contents data (Bulman et al. 2001) suggest that four species in this group are mainly benthic feeders, three feed on epibenthic invertebrates, 16 are benthopelagic feeders (piscivores or omnivores), one eats mostly pelagic prey, and three species are invertebrate feeders where the stomachs contain large quantities of unknown prey.

Most Group-4 fish (eight of 14 species) have an elongate shape and pelagic habit. The group includes warehous, jack mackerel, blue mackerel, redfish, threespine cardinal fish, butterfly perch, Eastern orange perch, cucumber fish, New Zealand dory, a myctophid, velvet leatherjacket, and mado. Most species in this group feed largely on pelagic zooplankton or on small pelagic fish that feed on pelagic zooplankton, or a mixture of both. Most species had a high proportion (12–95%) of pelagic zooplankton (euphausids and (or) thalacians) in the stomachs. Fish, if present in the stomach contents, generally composed <50%. All identifiable prey fish were pelagic species like myctophids.

There were some exceptions to these generalisations: the velvet leatherjacket has a diverse, largely benthic diet, the main component of which was bryozoan. The threespine cardinal fish, silver sweep, and Eastern orange perch had a high proportion of fish (83%, 80%, and 98%, respectively) in the stomach contents.

Group-5 fish are small, with one exception (butterfly mackerel), mostly lanternfish, that feed either on zooplankton or on fish that feed on zooplankton (Collette and Nauen 1983; Young and Blaber 1986; Bulman et al. 2001). Stomach contents data were only available for one species in this group, barber perch. Fish made up 70% of the diet; the rest was zooplankton, most of which was pelagic (Bulman et al. 2001). The presence of butterfly mackerel here appears to be anomalous, because it is much larger than the other fish in the group. Little is known of its biology (Collette and Nauen 1983), but it is thought to feed on plankton. This hypothesis is supported by the stable isotope results (mean butterfly mackerel $\delta^{15}N$ 10.4‰, $\delta^{13}C$ –19‰; mean zooplankton $\delta^{15}N$ 7.7‰, $\delta^{13}C$ –21.3‰).

Temporal and spatial variability

In 14 fish species, sample sizes were large enough for analysis (≥25), although the number of samples per season was often small (as few as five per season) with unequal numbers of samples from each season, so caution is needed in assessing the biological significance of the results. The 14 fish species showed different responses across years and (or) seasons. In eight species there were no significant differences in $\delta^{13}C$ or $\delta^{15}N$, in three species there were significant differences in $\delta^{13}C$ but no similarities in the pattern of enrichment, in five species there were significant differences in $\delta^{15}N$, all with enrichment in winter. These results suggest that fish species in this ecosystem respond differently to seasonal and (or) yearly influences.

Spatial trends in fish isotope distribution are confounded by factors that affect fish community distribution in the southeast Australian shelf ecosystem. Williams and Bax (2001) showed that fish distribution was correlated with depth, latitude, and seabed type.

Changes in isotope signature with fish size

Nineteen fish species provided large enough sample sizes

© 2002 NRC Canada

Fig. 4. Stable isotope values for 87 species of fish from the southeast Australian continental shelf. Each data point represents the mean stable carbon and stable nitrogen value for a single species. Sample sizes vary from 1 to 68 fish; most are >5. From the cluster analysis, five groups were chosen based on $\delta^{15}N$ and $\delta^{13}C$ (see Fig. 3). Group 1. Piscivory common: includes benthic and pelagic predators that consume prey with a high trophic position. Group 2. Benthic feeders: most take benthic prey (invertebrates, fish, cephalopods). Group 3. Benthic and pelagic feeders: most take a mix of benthic and pelagic prey (invertebrates and fish); there are overlaps with other groups. Opportunism and diet switching likely. Group 4. Pelagic feeders: most eat pelagic zooplankton and fish. Group 5. Pelagic planktivores: most are small fish (including several lanternfish) that eat small pelagic zooplankton or fish that eat zooplankton.

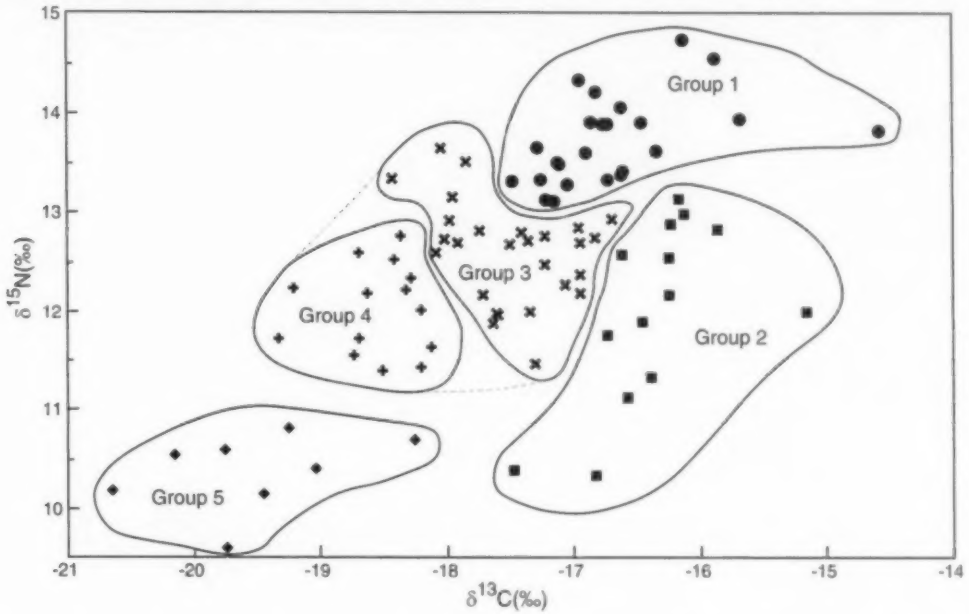

(≥20) to allow analysis of the data for changes in stable isotope values with fish length. Patterns were variable (Table 5), and included changes in both $\delta^{13}C$ and $\delta^{15}N$ (redfish, ocean perch, tiger flathead, silver dory, barracouta, and minor gurnard), change in $\delta^{13}C$ but not in $\delta^{15}N$ (jack mackerel, morwong, eastern school whiting, threespine cardinalfish, redbait, white trevally), change in $\delta^{15}N$ but not in $\delta^{13}C$ (John dory, draughtboard shark, blue warehou, sand flathead, sparsely spotted stingaree), and no change in either $\delta^{13}C$ or $\delta^{15}N$ (silver warehou and common stinkfish). All changes in stable isotope value with fish length were in the same direction, i.e., bigger fish had more enriched stable isotope values.

Based on changes in $\delta^{15}N$ values, bigger fish of many species from the South East Fishery (11 of 19 species examined) feed higher in the food chain. Some species move further offshore and into deeper water as they get bigger (e.g., redfish, ling, ocean perch, morwong, tiger flathead, white trevally, blue and silver warehous, John dory, jack mackerel) (D. Furlani, CSIRO Marine Research, G.P.O. Box 1538, Hobart, Tasmania 7001, Australia, unpublished data). The shift to feeding at higher trophic levels in some species is related to the offshore migration with size that increases the availability of prey and opportunism that allows bigger fish a greater selection of prey.

Other vertebrates

The Australian fur seal *Arctocephalus pusillus doriferus* had the most enriched stable $\delta^{15}N$ signature (15.8‰) of any animal sampled in this study. The fur seal eats mainly pelagic fish (e.g., jack mackerel, redbait) and cephalopods (Gales and Pemberton 1994).

The little penguin, *Eudyptula minor*, also has a high $\delta^{15}N$ signature (13‰). Off Phillip Island, Victoria, little penguins eat mainly small fish such as anchovy (*Engraulis australis*) and pilchards (*Sardinops neopilchardus*), as well as Gould's squid (*Nototodarus gouldi*) (Montague and Cullen 1988); around Tasmania, they eat blue grenadier, Gould's squid, and krill (*Nyctiphanes australis*) (Gales and Pemberton 1990).

The toothed whales showed a range of $\delta^{15}N$ and $\delta^{13}C$ signatures (Table 6) that suggests that some species (e.g., beaked whales, spectacled porpoise) may have fed in other ecosystems. In a study of the diet of two pilot whales and three bottlenose dolphins stranded around Tasmania, Gales and Pemberton (1992) found that cephalopods (*Sepioteuthis australis*) were the main food item in pilot whales (35.7% by number in the diet). In the dolphin diet, the squid *S. australis* was also the most common food item by number (42.9%); other cephalopod species in the stomachs included *Nototodarus gouldi*, *Todarodes filippovae*, and two benthic octopods; fish included silverbelly (*Parequula melbournensis*), Australian salmon (*Arripis trutta*), jack mackerel (*Trachurus declivis*), and leatherjackets (Monocanthidae sp.).

The only baleen whale sampled, a minke, had much lower $\delta^{15}N$ (6.0‰) and $\delta^{13}C$ (–27.0‰) signatures than the other vertebrates, reflecting a diet predominantly consisting of Antarctic zooplankton, which in turn feed directly or indirectly on Antarctic phytoplankton. High latitude phytoplankton typically have $\delta^{13}C$ values around –27‰ (Boutton

© 2002 NRC Canada

Table 5. Trends in stable carbon and nitrogen isotope data with fish length on the southeast Australian continental shelf.

		Correlation coefficient	
Species	*n*	Length with $\delta^{13}C$ (‰)	Length with $\delta^{15}N$ (‰)
Redfish	65	0.70, **	0.40, **
Ocean perch	58	0.40, **	0.36, **
Tiger flathead	58	0.33, *	0.36, **
Jack mackerel	52	0.30, *	n.s.
Silver dory	43	0.76, **	0.58, **
Morwong	43	0.70, **	n.s.
Silver warehou	40	n.s.	n.s.
John dory	40	n.s.	0.64, **
Barracouta	36	0.65, **	0.46, **
Draughtboard shark	30	n.s.	0.73, **
Minor gurnard	29	0.42, *	0.41, *
Blue warehou	28	n.s.	0.48, **
Eastern school whiting	28	0.60, **	n.s.
Common stinkfish	28	n.s.	n.s.
Threespine cardinalfish	23	0.65, **	n.s.
Redbait	25	0.68, **	n.s.
Sand flathead	21	n.s.	0.53, *
Sparsely-spotted stingaree	20	n.s.	0.61, **
White trevally	21	0.48, *	n.s.

Note: Fork length used for teleosts except common stinkfish where standard length is used; total length for elasmobranchs. n.s. (not significant), $0.05 < p$; *$0.05 > p > 0.01$; **$p < 0.01$.

Table 6. Stable carbon and nitrogen values from the muscle tissue of marine mammals found stranded around Tasmania or caught over the southeast Australian continental shelf.

Species	*n*	$\delta^{13}C$ (‰)	$\delta^{15}N$ (‰)	Known prey
Arctocephalus pusillus doriferus, Australian fur seal	2	–16.7	15.8	Fish, squid
Balaenoptera acutorostrata, Minke whale	1	–27.0	6.0	Planktonic crustaceans, squid, fish
Delphinus delphis, Common dolphin	3	–19.3 ± 0.8	13.3 ± 2.1	Cephalopods, fish
Globicephala melas, Pilot whale	94	–19.6 ± 0.4	10.7 ± 0.9	Cephalopods, fish
Lissodelphis peronii, Southern right whale dolphin	1	–17.7	10.6	Fish, squid
Mesoplodon grayi, Gray's Scamperdown beaked whale	1	–19.0	12.9	Unknown
Mesoplodon sp. 1, Beaked whale	1	–22.6	9.4	Unknown
Orcinus orca, Killer whale	1	–18.7	15.2	Squid, fish, seals, sharks, seabirds
Phocoena dioptrica, Spectacled porpoise	1	–20.9	9.9	Fish, squid
Tursiops truncatus, Bottlenose dolphin	5	–20.1 ± 0.1	14.4 ± 0.5	Cephalopods, fish

Note: Information on diet from Gales and Pemberton (1992) and Watson (1981).

Table 7. Differences in filter-feeding vs. deposit-feeding scenarios (water column, POM vs. sediment, respectively) for stable (*a*) nitrogen and (*b*) carbon in tissues of three species of bivalve mollusc from the southeast Australian continental shelf.

(*a*) $\delta^{15}N$ enrichments.						
Bivalve	*n*	$\delta^{15}N$ (‰)	POM $\delta^{15}N$ (‰)	△POM $\delta^{15}N$ (‰)	Sediment $\delta^{15}N$ (‰)	△Sediment $\delta^{15}N$ (‰)
Glycymeris striatularis	4	6.8 ± 0.2	5.4	1.4	7.2	–0.4
Tucetona flabellata	1	6.2	5.4	0.8	7.2	–1.0
Venericardia amabilis	1	6.5	5.4	1.1	7.2	–0.7
(*b*) $\delta^{13}C$ enrichments.						
Bivalve	*n*	$\delta^{13}C$ (‰)	POM $\delta^{13}C$ (‰)	△POM $\delta^{13}C$ (‰)	Sediment $\delta^{13}C$ (‰)	△Sediment $\delta^{13}C$ (‰)
Glycymeris striatularis	4	–18.0 ± 0.4	–20.8	2.8	–22.5	4.5
Tucetona flabellata	1	–18.5	–20.8	2.3	–22.5	4.0
Venericardia amabilis	1	–18.9	–20.8	1.9	–22.5	3.6

Note: Local, rather than mean, particulate organic matter (POM) and sediment isotope values are used.

© 2002 NRC Canada

1991), about 5‰ less than POM in this study. Both $\delta^{13}C$ and $\delta^{15}N$ values in POM decrease markedly south of the Subtropical Convergence (Francois et al. 1993). The minke whale sample provides an obvious outlier to the other samples and highlights the differences in $\delta^{13}C$ between sources of primary organic matter from different ecosystems. Although the minke whale feeds in an ecosystem that is also supported mainly by phytoplankton, the ^{13}C-depleted Antarctic phytoplankton clearly distinguish it from the temperate phytoplankton-supported community on the southeast Australian continental shelf.

Invertebrates

Strong trends in the relationship between prey and stable isotope signatures were observed within invertebrate groups. Two groups of invertebrates (polychaetes and gastropods) were examined in detail and the stable nitrogen signature was compared to what is known of their feeding behaviour (Hutchings 1982; K. Gowlett-Holmes, CSIRO Marine Research, G.P.O. Box 1538, Hobart, Tasmania 7001, Australia, personal communication) (Tables 2 and 3). Within the Polychaeta, large, actively carnivorous species with big jaws had high $\delta^{15}N$ signatures, e.g., *Lumbrineris* had one of the highest $\delta^{15}N$ signatures (15.5‰) of any animal in this study. At the lower end of the $\delta^{15}N$ range, a tube-dwelling, filter-feeding sabellid worm had a $\delta^{15}N$ signature of only 6.6‰.

A similar range of feeding strategies and $\delta^{15}N$ signatures was seen in gastropods. A large active carnivore, *Ericusa sowerbyi*, had a $\delta^{15}N$ signature of 13.7‰, whereas the smaller *Maoricolpus roseus*, a ciliary suspension feeder (Scott 1997), had a $\delta^{15}N$ signature of only 5.3‰.

Trophic level

The difference in $\delta^{15}N$ values between adjacent trophic levels is variable, but a difference of 3–4‰ is often found for stable nitrogen (e.g., Wada et al. 1993). For stable carbon, a predator's stable carbon signature is usually much closer to that of its prey, often <1‰ difference (Fry and Sherr 1984). In the ecosystem on the continental shelf off southeastern Australia, we found variable levels of enrichment in vertebrates and invertebrates.

Differences between predator and prey $\delta^{15}N$ at higher positions in the food web were closer to generally accepted values than they were at lower trophic levels. At a high trophic position the Australian fur seal had $\delta^{15}N$ and $\delta^{13}C$ values of 15.8‰ and –16.7‰, respectively. The main prey of the fur seal are redbait, leatherjackets, jack mackerel, and Gould's squid. A rough estimate of prey stable isotope values was made by taking the mean of the four most abundant dietary items. This gave a difference of 3.6‰ for $\delta^{15}N$ and 1.6‰ for $\delta^{13}C$ between fur seal and prey: values close to the generally observed trophic level differences.

Three species of bivalve, either filter or deposit feeders (K. Gowlett-Holmes, CSIRO Marine Research, G.P.O. Box 1538, Hobart, Tasmania, 7001 Australia, personal communication), were examined to look for the difference in $\delta^{13}C$ and $\delta^{15}N$ values between trophic levels. We compared stable carbon and stable nitrogen values between the molluscs and suspended POM (in the case of filter feeding) and between the molluscs and sediments (in the case of detritus feeding) (Table 7). In each case the difference between the $\delta^{15}N$ of the mollusc tissue and sediment (0.4–1.0‰) was a little less (and in the opposite direction) than between mollusc tissue and POM (0.8–1.4‰), but both are less than the generally accepted value of 3–4‰ per trophic level. The differences in $\delta^{13}C$ between mollusc tissue and sediment (3.6–4.5‰) were greater than the difference between mollusc tissue and POM (1.9–2.8‰); both are greater than the generally accepted value of 1‰ per trophic level. While there are no feeding studies on these bivalve species, studies on other bivalves have shown that they selectively ingest particles from the water or sediment surface (Morton et al. 1998). Our data support this selective feeding scenario. There are many factors affecting the $\delta^{13}C$ of individual compounds (Schouten et al. 1998) as well as differences between phytoplankton species (e.g., Wong and Sackett 1978) and size classes (Rau et al. 1990) in suspended POM and sediments. Trophic level differences of 3–4‰ were common for organisms at high trophic positions in this region, but were not always observed for organisms lower in the food web, feeding on small particles where the diet may include sources that have been modified by benthic recycling or selective ingestion or assimilation of a food source.

Acknowledgements

We gratefully acknowledge members of the CSIRO South East Shelf Ecosystem Project who assisted in field and laboratory, particularly B. Barker, C. Bulman, D. Furlani, K. Gowlett-Holmes, S. Rainer, V. Wadley, A. Williams, and K. Woolley. Thanks also to Dr. S. Bunn and staff, Faculty of Environmental Sciences at Griffith University (Queensland) and Dr. A. Revill, CSIRO Marine Research, for stable isotope analyses and valuable discussions, Dr. D. Thiele and K. Evans for marine mammal samples, P. Dann and Dr. D. Obendorf for little penguin samples, staff of the Marine and Freshwater Institute (Victoria) for pilchards, and F. Scott of the Australian Antarctic Division for algal identifications. We also thank Dr. X. He and F. Althaus at CSIRO Marine Research and three anonymous reviewers whose constructive comments improved earlier versions of the paper. The study was supported by the Fisheries Research and Development Corporation of Australia (FRDC Project 94/040).

References

Bass, A.J., D'Aubrey, J.D., and Kistnasamy, N. 1973. Sharks of the east coast of southern Africa. I. The genus *Carcharhinus* (Carcharhinidae). South African Association for Marine Biological Research, Oceanographic Research Institute, 2 West St., Durban, South Africa. Investigational Report No. 33.

Bax, N.J. 1998. The significance and prediction of predation in marine fishery ecosystems. ICES J. Mar. Sci. **55**: 997–1030.

Bax, N.J., Williams, A., Davenport, S., and Bulman, C. 1999. Managing the ecosystem by leverage points: a model for a multispecies fishery. *In* Ecosystem approaches for fisheries management. Proceedings of the Symposium on Ecosystem Considerations in Fisheries Management, 30 Sept. – 3 Oct. 1998, Anchorage, Alaska. Alaska Sea Grant Program, AK-SG-99-01. pp. 283–303.

Bax, N., Burford, M., Clementson, L., and Davenport, S. 2001. Phytoplankton blooms and production sources on the south-east Australian continental shelf. Mar. Freshwater Res. **52**: 451–462.

Boutton, T.W. 1991. Stable carbon isotope ratios of natural materials: II. Atmospheric, terrestrial, marine, and freshwater environ-

© 2002 NRC Canada

ments. *In* Carbon isotope techniques. *Edited by* D.C. Coleman and B. Fry. Academic Press, San Diego.

Bulman, C., Althaus, F., He, X., Bax, N.J., and Williams, A. 2001. Diets and trophic guilds of demersal fishes of the south-eastern Australian shelf. Mar. Freshwater Res. **52**: 537–548.

Cliff, G., and Dudley, F.F.J. 1992. Sharks caught in the protective gill nets off Natal, South Africa. 6. The copper shark *Carcharhinus brachyurus* (Gunther). S. Afr. J. Mar. Sci. **12**: 663–674.

Collette, B.B., and Nauen, C.E. 1983. Scombrids of the world: an annotated and illustrated catalogue of tunas, mackerels, bonitos and related species known to date. FAO Species Catalogue. Vol. 2.

DeNiro, M.J., and Epstein, S. 1978. Influence of diet on the distribution of carbon isotopes in animals. Geochim. Cosmochim. Acta, **42**: 495–506.

France, R.L. 1994. Nitrogen isotopic composition of marine and freshwater invertebrates. Mar. Ecol. Prog. Ser. **115**: 205–207.

France, R. 1995. Stable nitrogen isotopes in fish: literature synthesis on the influence of ecotonal coupling. Estuar. Coast. Shelf Sci. **41**: 737–742.

France, R.L., and Peters, R.H. 1997. Ecosystem differences in the trophic enrichment of ^{13}C in aquatic food webs. Can. J. Fish. Aquat. Sci. **54**: 1255–1258.

Francois, R., Altabet, M.A., Goericke, R., McCorkle, D.C., Brunet, C., and Poisson, A. 1993. Changes in the $\delta^{13}C$ of surface water particulate organic matter across the Subtropical Convergence in the S.W. Indian Ocean. Global Biogeochem. Cycles, **7**: 627–644.

Fry, B., and Sherr, E.B. 1984. $\delta^{13}C$ measurements as indicators of carbon flow in marine and freshwater ecosystems. Contrib. Mar. Sci. **27**: 13–47.

Gales, R., and Pemberton, D. 1990. Seasonal and local variation in the diet of the little penguin, *Eudyptula minor*, in Tasmania. Aust. Wildl. Res. **17**: 231–259.

Gales, R., and Pemberton, D. 1992. Stomach contents of long-finned pilot whales (*Globicephala melas*) and bottlenose dolphins (*Tursiops truncatus*) in Tasmania. Mar. Mammal Sci. **8**: 405–413.

Gales, R., and Pemberton, D. 1994. Diet of the Australian Fur Seal in Tasmania. Aust. J. Mar. Freshw. Res. **45**: 653–664.

Hesslein, R.H., Hallard, K.A., and Ramlal, P. 1993. Replacement of sulfur, carbon and nitrogen in tissue of growing broad whitefish (*Coregonus nasus*) in response to a change in diet traced by $\delta^{34}S$, $\delta^{13}C$, and $\delta^{15}N$. Can. J. Fish. Aquat. Sci. **50**: 2071–2076.

Hutchings, P. 1982. Bristleworms (phylum Annelida). *In* Marine invertebrates of Southern Australia. Part I, Ch. 6. *Edited by* S.A. Shepherd and I.M. Thomas, Adelaide.

Klaer, N.L. 2001. Steam trawl catches from south-eastern Australia from 1918 to 1957: trends in catch rates and species composition. Mar. Freshwater Res. **52**: 399–410.

Last, P.R., and Stevens, J.D. 1994. Sharks and rays of Australia. CSIRO Publishing, Australia.

MacDonald, J.S., Waiwood, K.G., and Green, R.H. 1982. Rates of digestion of different prey in Atlantic cod (*Gadus morhua*), ocean pout (*Macrozoarces americanus*), winter flounder (*Pseudopleuronectes americanus*), and American plaice (*Hippoglossoides platessoides*). Can. J. Fish. Aquat. Sci. **39**: 651–659.

McConnaughey, T., and McRoy, C.P. 1979. Food-web structure and the fractionation of carbon isotopes in the Bering Sea. Mar. Biol. **53**: 257–262.

Minagawa, M., and Wada, E. 1984. Stepwise enrichment of ^{15}N along food chains: further evidence and the relation between $\delta^{5}N$ and animal age. Geochim. Cosmochim. Acta, **48**: 1135–1140.

Montague, T.L., and Cullen, J.M. 1988. The diet of the little penguin *Eudyptula minor* at Phillip Island, Victoria. Emu, **88**: 138–149.

Morton, B., Prezant, R.S., and Wilson, B. 1998. Class Bivalvia. *In* Mollusca: the southern synthesis. Fauna of Australia. Vol. 5. *Edited by* P.L. Beesley, G.J.B. Ross, and A. Wells. CSIRO Publishing, Melbourne. Part A, xvi. pp. 195–234.

Nichols, P.D., Klumpp, D.W., and Johns, R.B. 1985. A study of food chains in seagrass communities III. Stable carbon isotope ratios. Aust. J. Mar. Freshw. Res. **36**: 683–690.

Nichols, P., Mooney, B., Virtue, P., and Elliott, N. 1998. Nutritional value of Australian fish: oil, fatty acid and cholesterol of edible species. Final report, August 1988. FRDC Project 95/122. Report prepared for the Fisheries Research and Development Corporation (Australia). *Available from* Fisheries Research and Development Corporation, P.O. Box 222 ACT 2600, Australia.

Owens, N.J.P. 1987. Natural variations on ^{15}N in the marine environment. Adv. Mar. Biol. **24**: 389–451.

Peterson, B.J., and Fry, B. 1987. Stable isotopes in ecosystem studies. Annu. Rev. Ecol. Syst. **18**: 293–320.

Rau, G.H., Teyssie, J.-L., Rassoulzadegan, F., and Fowler, S.W. 1990. ^{13}C /^{12}C and ^{15}N /^{14}N variations among size-fractionated marine particles: implications for their origin and trophic relationships. Mar. Ecol. Prog. Ser. **59**: 33–38.

SAS Institute Inc. 1995. SAS/STAT user's guide, release 3.1 ed. SAS Institute Inc., Cary, N.C.

Schoeninger, M.J., and DeNiro, M.J. 1984. Nitrogen and carbon isotopic composition of bone collagen from marine and terrestrial animals. Geochim. Cosmochim. Acta, **48**: 625–639.

Schouten, S., Klein Breteler, W.C.M., Blokker, P., Schogt, N., Rijpstra, W.I.C., Grice, K., Baas, M., and Sinninghe Damsté, J.S. 1998. Biosynthetic effects on the stable carbon isotopic compositions of algal lipids: implications for deciphering the carbon isotopic biomarker record. Geochim. Cosmochim. Acta, **62**: 1397–1406.

Scott, R.J. 1997. Aspects of the biology of the introduced gastropod *Maoricolpus roseus*. Thesis submitted to Institute of Antarctic and Southern Ocean Studies, University of Tasmania. *Available from* IASOS Library, University of Tasmania, Australia.

Sholto-Douglas, A.D., Field, J.G., James, A.G., and van der Merwe, N.J. 1991. $^{13}C/^{12}C$ and $^{15}N/^{14}N$ isotope ratios in the Southern Benguela Ecosystem: indicators of food web relationships among different size-classes of plankton and pelagic fish; differences between fish muscle and bone collagen tissues. Mar. Ecol. Prog. Ser. **78**: 23–31.

Thomas, C.J., and Cahoon, L.B. 1993. Stable isotope analyses differentiate between different trophic pathways supporting rocky-reef fishes. Mar. Ecol. Prog. Ser. **95**: 19–24.

Tieszen, L.L., Boutton, T.W., Tesdahl, K.G., and Slade, N.A. 1983. Fractionation and turnover of stable carbon isotopes in animal tissues: implications for $\delta^{13}C$ analysis of diet. Oecologia, **57**: 32–37.

Wada, E., Kabaya, Y., and Kurihara, Y. 1993. Stable isotopic structure of aquatic ecosystems. J. Biosci. **18**: 483–499.

Watson, L. 1981. Sea guide to whales of the world. Hutchinson, London.

Williams, A., and Bax, N. 2001. Delineating fish-habitat associations for spatially-based management: an example from the south-eastern Australian continental shelf. Mar. Freshwater Res. **52**: 513–536.

Wong, W.W., and Sackett, W.M. 1978. Fractionation of stable carbon isotopes by marine phytoplankton. Geochim. Cosmochim. Acta, **42**: 1809–1815.

Young, J.W., and Blaber, S.J.M. 1986. Feeding ecology of three species of midwater fishes associated with the continental slope of eastern Tasmania, Australia. Mar. Biol. **93**: 147–156.

© 2002 NRC Canada

Appendix A

Table A1. Stable nitrogen and carbon values for fauna, flora, particulate organic matter (POM), and sediments from the southeastern continental shelf of Australia.

			$\delta^{15}N$				$\delta^{13}C$			
Species	Common name	*n*	Mean	SD	Min.	Max.	Mean	SD	Min.	Max.
Teleosts and elambobranchs										
Alopias vulpinus	Thresher shark	2	13.5	0.1	13.4	13.6	−17.1	0.1	−17.2	−17.1
Apogonops anomalus	Threespine cardinalfish	25	11.5	0.6	10.5	13.1	−18.7	1.1	−21.0	−16.0
Asymbolus analis	Grey spotted catshark	7	13.0	0.3	12.6	13.5	−16.1	0.2	−16.3	−15.8
Atypichthus strigatus	Mado	9	12.9	0.4	12.4	13.6	−18.0	0.8	−19.5	−16.8
Caelorinchus australis	Southern whiptail	5	13.9	0.3	13.4	14.2	−16.7	0.5	−17.4	−16.1
Caelorinchus mirus	Gargoylefish	5	13.6	0.3	13.3	14.0	−17.3	0.4	−17.8	−16.9
Caesioperca lepidoptera	Butterfly perch	19	11.4	0.3	10.8	12.0	−18.5	0.4	−19.2	−17.9
Caesioperca rasor	Barber perch	8	10.7	0.2	10.4	10.9	−18.3	0.4	−19.0	−17.8
Callorhinchus milii	Elephantfish	2	10.3	0.2	10.2	10.5	−16.8	0.1	−16.9	−16.8
Carcharhinus brachyurus	Bronze whaler shark	1	11.7				−16.7			
Centroberyx affinis	Redfish	68	12.7	0.5	11.8	13.8	−18.4	0.7	−19.9	−17.1
Cephaloscyllium laticeps	Draughtboard shark	30	13.6	0.6	12.1	14.4	−16.3	0.4	−17.5	−15.6
Cepola australis	Bandfish	1	10.5				−20.2			
Chlorophthalmus nigripinnis	Cucumber fish	18	12.3	0.4	11.6	13.3	−18.3	0.4	−19.1	−17.6
Conger verrauxi	Southern conger	6	13.9	0.1	13.8	14.0	−16.9	1.4	−19.6	−16.0
Cyttus australis	Silver dory	43	12.6	0.8	10.2	13.7	−18.1	1.0	−19.9	−16.6
Cyttus novaezelandiae	New Zealand dory	5	12.2	0.4	11.6	12.6	−18.6	0.5	−19.3	−18.2
Dasyatis brevicaudata	Smooth stingray	1	13.9				−16.8			
Diaphus danae	Dana lanternfish	7	9.6	0.7	8.8	10.7	−19.7	0.8	−21.0	−19.0
Dinolestes leweni	Longfin pike	10	14.3	0.2	13.9	14.8	−17.0	0.3	−17.5	−16.5
Diodon nichthemerus	Globefish	12	11.9	0.8	10.2	13.2	−17.6	0.8	−19.2	−16.8
Emmelichthys nitidis	Redbait	25	11.6	0.5	11.0	13.1	−18.1	0.5	−19.1	−17.2
Galeorhinus galeus	School shark	13	13.3	0.5	12.6	14.2	−17.0	0.6	−18.0	−15.9
Gasterochisma melampus	Butterfly mackerel	10	10.4	0.3	9.8	10.8	−19.0	0.9	−20.8	−17.9
Genypterus blacodes	Pink ling	18	13.1	0.7	12.1	14.3	−17.2	0.6	−18.9	−16.7
Gymnoscopelus piabilis	Family Myctophidae	1	11.7				−19.3			
Gymnothorax prasinus	Green moray	4	14.6	0.4	14.1	15.0	−15.9	0.3	−16.2	−15.5
Helicolenus percoides	Ocean perch	58	12.8	0.7	11.0	14.3	−17.2	0.4	−18.9	−16.4
Heterodontus portusjacksoni	Port Jackson shark	6	12.0	0.4	11.6	12.7	−15.2	0.3	−15.6	−14.6
Hypoplectrodes annulata	Blackbanded seaperch	3	13.9	0.2	13.8	14.0	−15.7	0.1	−15.8	−15.5
Hypoplectrodes maccullochi	Halfbanded seaperch	2	13.1	0.1	13.0	13.2	−17.2	0.4	−17.4	−16.9
Ichthyscopus barbatus	Fringed stargazer	1	13.4				−16.6			
Isurus oxyrinchus	Mako shark	3	13.5	0.3	13.2	13.7	−17.1	0.3	−17.4	−16.9
Kathetostoma canaster	Speckled stargazer	6	14.1	0.8	13.1	15.4	−16.6	0.4	−17.3	−16.1
Kathetostoma laeve	Common stargazer	5	12.7	0.8	12.0	13.6	−16.8	0.4	−17.2	−16.2
Lampanyctodes hectoris	Hector's lanternfish	10	10.6	0.4	10.1	11.3	−19.8	1.2	−21.2	−18.4
Latridopsis forsteri	Bastard trumpeter	10	13.6	0.4	12.7	14.5	−18.0	1.7	−19.8	−14.1
Latris lineata	Striped trumpeter	19	13.6	0.8	11.4	15.0	−16.9	1.2	−18.1	−12.4
Lepidoperca pulchella	Eastern orange perch	13	12.2	0.3	11.8	12.9	−18.3	0.5	−19.4	−17.5
Lepidotrigla modesta	Minor gurnard	29	12.7	0.5	11.8	14.0	−17.9	0.5	−18.6	−16.6
Lepidotrigla mulhalli	Deepwater gurnard	11	12.2	0.6	11.1	13.2	−17.7	0.3	−18.1	−17.1
Lophonectes gallus	Crested flounder	2	10.4	0.2	10.3	10.5	−17.5	0.7	−17.9	−17.0
Lotella rhacinus	Largetooth beardie	6	14.7	0.6	13.6	15.2	−16.1	0.5	−17.1	−15.6
Macrorhamphosus scolopax	Common snipefish	19	12.7	0.6	11.2	13.6	−18.0	0.5	−19.4	−17.5
Maurolicus muelleri	Pennant lightfish	5	10.2	0.3	9.8	10.4	−20.6	0.3	−21.0	−20.3
Meuschenia freycineti	Sixspine leatherjacket	8	12.7	1.1	10.8	14.2	−16.9	0.8	−18.8	−16.3
Meuschenia scaber	Velvet leatherjacket	10	11.7	0.3	11.2	12.1	−18.7	0.8	−19.8	−17.8
Muraenichthys sp.	Worm eel	3	11.1	1.2	10.2	12.5	−16.6	1.0	−17.6	−15.7
Mustelus antarcticus	Gummy shark	14	12.9	0.5	12.0	13.4	−16.2	0.3	−16.8	−15.7
Narcine tasmaniensis	Tasmanian numbfish	15	13.8	0.5	13.0	14.8	−14.6	0.4	−15.7	−14.0
Nemadactylus douglasi	Grey morwong	7	12.7	0.3	12.2	13.0	−17.4	0.4	−17.9	−16.6
Nemadactylus macropterus	Morwong	43	13.1	0.6	11.9	14.4	−17.9	0.9	−19.6	−16.5
Neoplatycephalus aurimaculatus	Toothy flathead	4	12.6	0.4	12.0	13.0	−16.6	0.2	−16.8	−16.3
Neoplatycephalus richardsoni	Tiger flathead	58	12.8	0.5	11.8	14.0	−17.4	0.5	−18.9	−16.5
Neosebastes scorpaenoides	Ruddy gurnard perch	5	12.8	0.3	12.4	13.2	−17.0	0.3	−17.4	−16.5
Notolabrus tetricus	Bluethroat wrasse	12	13.4	0.6	12.1	14.1	−16.6	0.4	−17.3	−15.9

© 2002 NRC Canada

Table A1 (*continued*).

Species	Common name	*n*	$\delta^{15}N$ Mean	SD	Min.	Max.	$\delta^{13}C$ Mean	SD	Min.	Max.
Opthalmolepis lineolata	Maori wrasse	13	13.1	0.3	12.6	13.4	−16.2	0.3	−16.9	−15.8
Pagrus auratus	Snapper	5	11.3	0.3	10.9	11.6	−16.4	1.2	−18.3	−15.1
Parascyllium ferrugineum	Rusty carpetshark	2	12.2	0.1	12.1	12.2	−16.2	0.2	−16.4	−16.1
Parma microlepis	White ear	5	12.7	0.4	12.2	13.1	−17.5	1.0	−19.0	−16.7
Pempheris multiradiata	Common bullseye	10	12.8	0.4	12.1	13.3	−17.7	0.4	−18.9	−17.4
Platycephalus bassensis	Sand flathead	23	12.2	0.8	10.0	13.3	−16.9	1.2	−20.3	−13.6
Pseudocaranx dentex	White trevally	21	12.3	0.7	10.6	13.1	−17.1	0.7	−18.7	−15.8
Pseudolabrus psittaculus	Rosy wrasse	10	12.9	0.3	12.4	13.3	−16.7	0.3	−17.0	−16.2
Pseudophycis bachus	Red cod	9	13.3	0.3	12.7	13.6	−17.5	0.2	−17.7	−17.1
Raja sp. A	Longnose skate	6	12.4	0.8	11.1	13.3	−16.9	0.8	−18.5	−16.3
Rexea solandri	Gemfish	9	13.5	0.4	12.9	14.0	−17.8	0.3	−18.3	−17.4
Sardinops neopilchardus	Pilchard	10	10.8	0.8	9.7	12.4	−19.3	0.7	−20.2	−17.7
Scomber australasicus	Blue mackerel	10	12.0	0.6	11.3	13.1	−18.2	0.7	−19.3	−17.6
Scorpis lineolata	Sweep	8	11.4	0.5	10.4	11.9	−18.2	0.3	−18.5	−17.5
Seriolella brama	Blue warehou	28	12.6	0.5	11.7	13.8	−18.7	1.0	−20.8	−15.3
Seriolella punctata	Silver warehou	40	12.2	0.8	11.1	13.9	−19.2	0.9	−21.3	−16.3
Sillago flindersi	Eastern school whiting	28	12.5	1.0	10.2	15.5	−17.2	0.7	−18.9	−15.3
Sphyrna zygaena	Smooth hammerhead	1	14.2				−16.8			
Squalus megalops	Spikey dogfish	6	13.3	0.4	12.8	13.9	−16.7	0.7	−17.9	−15.7
Squatina australis	Australian angel shark	5	12.5	0.7	11.4	13.4	−16.2	0.4	−16.5	−15.6
Squatina sp. A	Eastern angel shark	3	13.9	0.5	13.5	14.5	−16.5	0.2	−16.7	−16.3
Symbolophorus barnardi	Bullseye lanternfish	5	10.1	0.8	9.0	11.1	−19.4	0.7	−20.2	−18.4
Synchiropus calauropomus	Common stinkfsh	28	11.9	0.6	11.0	13.6	−17.6	0.6	−18.7	−16.5
Thyrsites atun	Barracouta	36	13.3	0.8	11.7	14.5	−18.4	1.0	−20.2	−16.8
Trachurus declivis	Jack mackerel	52	12.5	0.7	11.5	14.5	−18.4	1.1	−20.5	−12.8
Trygonorrhina sp.	Fiddler ray	9	12.8	0.8	11.4	14.0	−15.9	0.2	−16.2	−15.6
Urolophus cruciatus	Banded stingaree	13	11.9	0.5	11.2	12.9	−16.5	0.4	−17.2	−15.9
Urolophus paucimaculatus	Sparsely-spotted stingaree	23	12.0	0.5	11.0	12.8	−17.3	0.7	−18.7	−16.2
Urolophus viridis	Greenback stingaree	11	11.5	0.4	10.8	12.5	−17.3	0.5	−17.8	−16.1
Zenopsis nebulosus	Mirror dory	3	12.0	0.3	11.6	12.2	−17.6	0.1	−17.7	−17.5
Zeus faber	John dory	40	13.3	0.7	11.8	15.1	−17.3	0.8	−19.2	−15.8
Marine mammals										
Arctocephalus pusillus doriferus	Australian fur seal	2	15.8	0.4	15.5	16.1	−16.7	0.5	−17.0	−16.3
Balaenoptera acutorostrata	Minke whale	1	6.0				−27.0			
Delphinus delphis	Common dolphin	3	13.3	2.1	11.6	15.6	−19.3	0.8	−20.1	−18.4
Globicephala melas	Pilot whale	94	10.7	0.9	9.8	14.4	−19.6	0.4	−20.8	−18.8
Lissodelphis peronii	Southern right whale dolphin	1	10.6				−17.7			
Mesoplodon grayi	Gray's Scamperdown beaked whale	1	12.9				−19.0			
Mesoplodon sp. 1	Beaked whale	1	9.4				−22.6			
Orcinus orca	Killer whale	1	15.2				−18.7			
Phocoena dioptrica	Spectacled porpoise	1	9.9				−20.9			
Tursiops truncatus	Bottlenose dolphin	5	14.4	0.5	13.9	15.1	−20.1	0.1	−20.3	−20.1
Seabirds										
Eudyptula minor	Little penguin	19	13.0	1.2	9.1	15.1	−19.4	0.6	−20.4	−18.4
Invertebrates										
Phylum Porifera										
	Sponges	4	7.6	1.5	5.6	8.9	−17.6	2.1	−19.7	−15.0
Phylum Cnidaria										
	Anemone	1	11.7				−14.4			
Sarcoptilus grandis	Sea pen	1	7.9				−19.9			
Family Nephtheidae: *Capnella* sp.	Soft coral	1	8.8				−16.4			
Phylum Annelida										
Class Polychaeta										
Aphrodite australis	Sea mouse	2	8.4	0.3	8.2	8.6	−16.7	0.5	−17.1	−16.4
Family Eunicidae		4	11.9	0.3	11.6	12.2	−24.3	13.5	−44.4	−16.4
Family Lumbrinereidae: *Lumbrineris*		1	15.5				−15.8			
Family Lysaretidae		2	12.4	1.0	11.7	13.1	−17.5	0.1	−17.5	−17.4
Family Lysaretidae: *Oenone*		2	15.0	0.2	14.8	15.1	−18.6	0.4	−18.8	−18.3
Family Opheliidae		1	11.7				−11.5			

© 2002 NRC Canada

Table A1 (*continued*).

Species	Common name	*n*	$\delta^{15}N$				$\delta^{13}C$			
			Mean	SD	Min.	Max.	Mean	SD	Min.	Max.
Family Polynoidae		1	12.4				−17.7			
Family Polyodontidae		1	14.6				−14.5			
Family Onuphidae: *Rhanphobranchium*		1	10.3				−17.8			
Family Sabellidae	Fan worms	2	6.6	0.2	6.4	6.7	−18.1	0.2	−18.2	−18.0
Family Sigalionidae		2	8.7	0.4	8.5	9.0	−19.1	0.5	−19.4	−18.7
Phylum Bryozoa										
Bryozoa	Bryozoan	1	4.0				−14.1			
Bryozoa	Soft bryozan	1	8.1				−15.3			
Phylum Mollusca										
Class Gastropoda										
Amoria undulata	Wavy volute	1	10.2				−15.7			
Ericusa sowerbyi	Sowerby's volute	1	13.7				−13.6			
Fusinus novaehollandiae	Spindle shell	1	10.6				−18.1			
Maoricolpus roseus	New Zealand screw shell	4	5.3	0.2	5.0	5.5	−18.1	0.4	−18.5	−17.6
Sinum zonale	Ear snail	1	9.0				−18.1			
Family Doridida	Opisthobranch (nudibranch)	1	9.5				−18.2			
	Opisthobranch	1	9.4				−20.2			
Philine	Opisthobranch	1	8.1				−10.8			
Class Bivalvia										
Eucrassatella kingicola		5	8.9	0.3	8.6	9.2	−18.3	0.4	−18.9	−17.9
Glycymeris striatularis		4	6.8	0.2	6.5	6.9	−18.0	0.4	−18.6	−17.8
Myochama anomioides		1	7.8				−19.3			
Tucetona flabellata		1	6.2				−18.5			
Venericardia amabilis		1	6.5				−18.9			
Class Cephalopoda										
Nototodarus gouldi	Gould's squid	8	12.9	0.5	12.1	13.5	−17.8	0.6	−18.6	−17.1
Octopus berrima		1	9.0				−17.4			
Octopus maorum	Maori ortopus	4	12.6	0.3	12.2	13.0	−17.0	0.9	−18.4	−16.4
Sepia sp.	Cuttlefish	5	11.5	0.6	11.1	12.5	−17.9	0.3	−18.2	−17.5
Phylum Arthropoda										
Sub-phylum Crustacea	Crustacean zooplankton	1	7.4				−20.2			
Megalopa larva	Larval crab	1	7.9				−21.0			
Class Malacostraca										
Order Stomatopoda		2	9.7	0.5	9.3	10.1	−17.1	0.9	−17.8	−16.5
Order Mysidacea		1	7.6				−14.1			
Order Amphipoda	various amphipods	2	7.6	1.3	6.7	8.5	−18.2	0.9	−18.8	−17.6
Order Isopoda										
Family Seriolidae		1	8.1				−15.2			
Family Sphaeromatidae		1	7.6				−13.4			
Order Decapoda										
Family Aristeidae	Penaeoid prawns									
Aristaeomorpha foliacea	Giant red prawn	5	11.1	0.3	10.7	11.5	−18.7	0.5	−19.5	−18.4
Infra-order Caridea										
Aegaeon locazei	Carid shrimp	5	9.7	0.6	9.1	10.7	−16.9	1.0	−18.3	−15.4
	Carid shrimp	1	8.8				−20.1			
Chlorotocus sp.	Carid shrimp	2	6.9	0.6	6.5	7.3	−20.8	0.7	−21.3	−20.3
Pontophilus sp.	Carid shrimp	2	9.8	0.3	9.5	10.0	−16.5	0.5	−16.8	−16.1
Sicyonia australiense	Carid shrimp	2	9.9	1.4	8.9	11.0	−18.0	0.5	−18.3	−17.7
Family Alpheidae	Snapping shrimp	1	9.9				−17.5			
Family Palaemonidae	Shrimp	2	9.6	0.6	9.2	10.0	−18.8	1.6	−19.9	−17.6
Family Palinuridae										
Jasus edwardsii	Southern rock lobster	1	10.8				−15.3			
Jasus sp.	Rock lobster	5	13.4	0.2	13.2	13.6	−14.5	0.4	−14.8	−13.9
Family Scyllaridae										
Scyllarides sp.	Flat lobster	1	11.5				−16.7			
Ibacus alticrenatus		1	11.8				−17.4			
Infra-order Anomura										
Family Diogenidae	Hermit crabs									
Strigopagrus strigimanus		3	10.4	0.3	10.1	10.6	−18.3	1.8	−20.2	−16.8

© 2002 NRC Canada

Table A1 (*concluded*).

Species	Common name	*n*	$\delta^{15}N$ Mean	SD	Min.	Max.	$\delta^{13}C$ Mean	SD	Min.	Max.
Dardanus sp.		1	12.6				–16.1			
Family Paguridae	Hermit crabs: larvae	1	8.8				–15.1			
Family Galatheidae: *Munida* sp.	Craylets	4	8.6	0.2	8.4	8.8	–15.3	0.7	–15.8	–14.3
Infra-order Brachyura										
Family Dromiidae	Sponge crabs	1	10.7				–19.4			
Petalomera sp.		1	10.9				–14.5			
Family Raninidae	Spanner crab	1	9.5				–10.3			
Family Calappidae: *Mursia* sp.		1	10.0				–16.5			
Family Latreillidae:		1	9.4				–16.6			
Latreillopsis petterdi										
Family Portunidae: *Ovalipes molleri*		1	9.4				–17.8			
Family Goneplacidae: *Carcinoplax* sp.		1	7.9				–12.1			
Phylum Echinodermata										
Class Asteroidea										
Coscinasterias sp.	Eleven-armed seastar	1	8.8				–13.9			
Australiaster dubia	Seastar	1	8.9				–12.6			
Class Ophiuroidea	Various Ophiuroids	3	9.4	1.2	8.5	10.8	–9.8	3.0	–13.1	–7.1
Ophiocrossota multispina	Ophiuroid	1	9.2				–5.6			
Class Echinoidea										
Clypeaster virescens	Sea biscuit	1	8.3				–5.2			
Echinoidea		1	5.6				–10.2			
Class Holothuroidea	Holothurian	1	7.2				–17.6			
Class Crinoidea	Crinoid	1	7.7				–15.8			
	Crinoid	1	8.6				–10.9			
Phylum Chordata										
Class Ascidiacea										
Polycarpa sp.	Sea-squirt	2	8.2	0.5	7.9	8.5	–21.3	0.1	–21.4	–21.2
Polycarpa rigida	Sea-squirt	1	7.7				–22.3			
Class Thaliacea	Pyrosome	3	4.3	2.6	1.7	6.8	–22.0	2.2	–24.1	–19.7
Zooplankton from surface plankton tows										
	Mixed zooplankton	6	7.7	1.9	5.0	9.7	–21.3	0.5	–22.2	–20.9
	Amphipods	1	2.9				–22.9			
	Clupeid fish larvae	1	9.3				–20.3			
	Copepods	2	6.2	1.6	5.0	7.3	–21.5	1.0	–22.2	–20.8
	Euphausids	2	6.5	2.3	4.9	8.2	–21.1	1.5	–22.1	–20.0
	Fish eggs	1	10.2				–22.1			
	Larval fish	2	7.1	0.6	6.7	7.5	–22.8	1.2	–23.6	–21.9
Sediments		103	7.0	1.0	4.3	9.1	–21.8	1.7	–28.9	–15.6
Particulate organic carbon	n = 91 for $\delta^{13}C$; n = 81 for $\delta^{15}N$	81/91	6.1	2.5	2.3	18.2	–21.5	0.2	–25.2	–16.0
	With 4 outliers removed	77	5.7	1.4	2.3	8.4				
Algae										
Phytoplankton (zooplankton removed)	1994 Spring bloom	4	6.2	2.3	2.8	7.6	–20.5	0.9	–21.4	–19.3
Phytoplankton (with zooplankton)	1994 Spring bloom	4	5.9	2.3	2.4	7.5	–20.8	0.6	–21.4	–20.1
Ptilonia australasica	Red alga sp. 1	1	4.8				–24.6			
Craspedocarpus blepharicarpus	Red alga sp. 2	1	5.9				–31.8			
Rhodymenia australis	Red alga sp. 3	1	4.6				–29.7			
Gracilaria secundata	Red alga sp. 4	1	5.2				–21.7			
	Red alga sp. 5	1	5.5				–27.6			
Platoma australica	Red alga sp. 6	1	6.5				–31.7			
Family Zosteraceae	Seagrass sp. 1	1	3.5				–7.8			
Family Zosteraceae	Seagrass sp. 2	1	5.7				–14.6			
Phaeophyte alga	Macroalga	1	6.6				–25.5			

Note: SD, standard deviation.

© 2002 NRC Canada

Fleet dynamics of herring trawlers—change in gear size and implications for interpretation of catch per unit effort

Mika Rahikainen and Sakari Kuikka

Abstract: Catch per unit effort (CPUE) is widely used as an index of stock abundance. It is as widely acknowledged that CPUE can be a misleading index of abundance owing to a multitude of factors including fish behavior, fishing fleet interaction, and the increase in catchability over time caused by improvement in fishing technology. Based on information concerning the size of herring trawls manufactured in Finland since the early 1980s, an increase in fishing power of the fleet was postulated. Because we lacked direct information about the size of trawls aboard, we applied a model to estimate the changes over time. In the analysis, an analogy between fish and trawls was created by adopting the concepts and algorithms from fish stock assessment into assessment of the trawl "population", where both the total number of trawls and the size of individual trawls were being analyzed. The results indicate that the average gear size has nearly tripled in 20 years. Accepting the assumption that larger trawls are generally more effective than smaller ones, a substantial increase in fishing power has taken place. As a result, sequential population models calibrated with CPUE data will be severely biased as well.

Résumé : Les captures par unité d'effort (CPUE) sont souvent utilisées comme indices de l'abondance des stocks, mais il est aussi généralement admis que les CPUE sont parfois des indices erronés à cause d'une multitude de facteurs, dont le comportement des poissons, l'interaction entre la flotte de pêche et les poissons et le raffinement de la technologie des pêches avec le temps. Compte tenu de la taille des chaluts à harengs construits en Finlande depuis le début des années 1980, nous avons postulé un accroissement du pouvoir de capture de la flotte. Bien que nous n'ayons aucun renseignement direct sur la taille des chaluts à bord, nous avons utilisé un modèle pour estimer les changements dans le temps. Dans cette analyse, nous avons fait une analogie entre les poissons et les chaluts en appliquant les concepts et les algorithmes utilisés pour l'évaluation des stocks de poissons à l'évaluation de la «population de chaluts» dans laquelle le nombre total de chaluts et leurs tailles respectives ont été analysés. Les résultats révèlent que la taille moyenne des engins de pêche a presque triplé en 20 ans. S'il est vrai que les chaluts plus grands sont généralement plus efficaces que les plus petits, un accroissement important du pouvoir de capture s'est donc produit. Il en résulte que les modèles démographiques séquentiels calibrés à partir des données de CPUE donnent lieu à des erreurs importantes.

[Traduit par la Rédaction]

Introduction

Commercial catch per unit effort (CPUE) is used widely as an index of abundance in many fisheries, although it is known to be a potentially biased estimator. The relationship between abundance and capture success is a product of several processes that have the potential to break down proportionality, including schooling behavior of fish (Paloheimo and Dickie 1964), variable catchability (Cooke and Beddington 1984; Winters and Wheeler 1985), movements of vessels in response to changing catch rate (Gillis et al. 1993), and interactions of fishing vessels (Gillis and Peterman 1998). Hilborn and Walters (1992) give a summary of the potential biases on the CPUE–abundance relationship and factors inducing them.

Recognizing and quantifying the conditions and assumptions regarding CPUE data and catch rate analysis are important in deciding whether the analyses are valid. Criteria for use depend on the purpose for which the catch rate information is being applied and the importance of that information in the inference. In fish stock assessment, CPUE data have been applied as independent estimates of abundance (Mendelssohn and Cury 1989; Large 1992), as inputs in biomass dynamic models (Schaefer 1954), and as tuning series for sequential population analysis (SPA) (e.g., ICES 2000). Vessel movements and strategies have been inferred on the basis of commercial CPUE (Vignaux 1996) and in econometric research, CPUE provides an estimate of the income of fishermen and profitability of the fishery (Béné 1996; Campbell and Hand 1999). The tolerance limits of bias in CPUE with respect to applicability of that information may

Received 31 July 2001. Accepted 8 March 2002. Published on the NRC Research Press Web site at http://cjfas.nrc.ca on 17 April 2002.
J16473

M. Rahikainen.[1] University of Helsinki, Department of Limnology and Environmental Protection, P.O. Box 65, FIN-00014 University of Helsinki, Helsinki, Finland.
S. Kuikka. Finnish Game and Fisheries Research Institute, P.O. Box 6, FIN-00721 Helsinki, Finland.

[1]Corresponding author (e-mail: mika.rahikainen@helsinki.fi).

 DOI: 10.1139/F02-030 © 2002 NRC Canada

be estimated by sensitivity analysis or by simulation studies, and even by having a quantitative estimate of the bias if this bias is considerably large.

Violation of the assumption of constant catchability due to increased fishing power with time is a concern in fish stock assessment using CPUE as a tuning series for SPA (Marchal et al. 2001). Technical advancement is obvious in any commercial fishery characterized by increasing vessel size, engine power, and gear size. In particular, affordable electronic nautical charts combined with satellite navigation systems have introduced very accurate and easy navigation at all times and in all weather conditions. Moreover, echo sounders and sonars have continuously improved features with decreased cost, thereby increasing the capability of finding fish. Other indicators of technical advancement include communication electronics, such as the use of mobile phones instead of radiophones, which has improved cooperation within fleet fragments. Advances in fishing power are thus enhanced by several interactive factors.

In Finland, records of basic vessel attributes and gear types are accessible through vessel registers, but accurate information regarding gear characteristics is lacking. We believe that this is a common global feature of the data sets used as auxiliary information in stock assessment. However, the gear itself is the instrument directly interacting with fish and contributing significantly to capture success. During catch sampling, field staff of the national fisheries agency have observed a marked increase in trawl sizes of the Finnish herring fleet, mostly during the last 10 years. Although apparent, the magnitude of this increase was undocumented, raising a question of whether the effect on fishing power and thus catchability is of relevance with respect to using commercial CPUE as a tuning series for SPA.

The body of information held by fishers and other stakeholders has an important role to play in fisheries assessment (Neis et al. 1999). As there is scattered information of an increase in trawl sizes, it seems logical to pursue quantitative estimates. The objective is to get a measure of "average trawl size" that can be used to adjust effort for efficiency changes. Our approach is to use industry information, specifically fishers' and trawl manufacturers' knowledge base. It must be recognized, however, that the gear size itself may not be an adequate proxy for fishing power of a vessel or fleet. From the stock assessment viewpoint it is the fish depletion rate caused by the whole system including trawler warps, otterboards, the area swept by the trawl net, and trawl gear that is of concern (Dickson 1993). Moreover, schooling behavior of herring, weather conditions, and fishing area characteristics affect the way that gear is deployed, and thus fishing power.

Methods

The life of a trawl is analogous to that of a fish in that after recruitment, it has a certain probability of being removed from the population; for example, a trawl's removal due to break down of construction on a harsh bottom and a fish's removal by predation or disease. In addition to breakdowns, the causes for retirement of a trawl are mostly related to a skipper's discontent with the fishing performance of the gear and general deterioration of the gear materials. The size of the trawl "population" is controlled by recruitment and retirement rate. A trawl does not grow larger when it grows older and the change of the average size of gears in a trawl population is due to introduction of new gears of different size. These trivial observations imply certain dynamics of a trawl population, namely that the average size of gears in the fleet cannot be directly inferred from manufacturer data including amounts and sizes of trawls sold. Instead, we suggest that the essential dynamics of a trawl population may be captured by a virtual population analysis (VPA)-type model. The recruitment data, i.e., the information concerning sale of new herring trawls and their sizes, is accessible from gear manufacturers as we describe in the next section. Retirement rates can be inferred on the basis of service lives of trawls from the information held by herring trawler skippers. In our approach, the retirement estimates are obtained from a parametric distribution.

Proportional hazard models using the Weibull distribution have been applied in fisheries science to describe the probability of survival by capture (Neilson et al. 1989; Smith et al. 1994). The Weibull distribution (Evans et al. 1993) was used to describe the service life of trawls, since probability density and survival functions are defined for this theoretical distribution. By interviewing several trawler skippers, frequency data about the service life of gear were obtained. The probability density function of the Weibull distribution was then fitted to the data. These parameters also define the survival function describing retirement rate, i.e., the fraction of trawls in use as a function of time. Finally, retirement rate was converted to age-specific instantaneous mortality rates (Z) in the trawl VPA to calculate removals from the trawl population.

The overall framework is analogous to forward calculation from a VPA (Table 1), where the number of trawls in a specific cohort decreases with increasing age (service life) according to the estimated retirement rate. The total number of trawls in a specific size class is obtained by summing the amount of gears of different ages annually. By repeating these calculations for all size categories, a matrix including total number of trawls in all size classes is obtained for the study period.

The trawls have been assigned to a size class corresponding to their nominal size, defined as stretched circumference of the mesh in the trawl's "mouth". The nominal size of a typical modern midwater trawl is about 366–610 m. To estimate the change in trawl size as a function of swept area, the nominal size was transformed to dimension of square metres by the approximation described below and using a defined "fishing circle" as a measure for the gear size (Fig. 1). An average trawl size is calculated from estimates of the amount of trawls of different size in the fleet and interpreted as an index of fishing power.

Data and application

Trawl recruitment

Data concerning new trawls recruited into the herring fishery were obtained from three gear manufacturers who produce all commercially manufactured herring trawls in Finland. Telephone interviews provided information regarding changes,

© 2002 NRC Canada

Table 1. Recruitment (age 0), retirement rate (expressed as instantaneous mortality, Z), and change in trawl numbers in time in the size class 290–366 m during 1980–2000.

		Size class: 290–366 m													
Z	Trawl age	1979	1980	1981	1982	1983	1984	1985	1986	1987	1988	1989	1990	...	2000
0.05	0	5	4	6	6	9	9	3	12	15	15	8	20	...	1
0.09	1	5	5	4	6	6	9	9	3	11	14	14	8	...	8
0.11	2	5	5	5	4	5	5	8	8	3	11	13	13	...	11
0.13	3	4	4	4	4	3	5	5	7	7	2	9	12	...	8
0.15	4	4	4	4	4	4	3	4	4	6	6	2	8	...	12
0.17	5	3	3	3	3	3	3	2	4	4	5	5	2	...	8
0.19	6	3	3	3	3	3	3	3	2	3	3	4	4	...	12
0.20	7	2	2	2	2	2	2	2	2	2	2	2	4	...	9
0.22	8	2	2	2	2	2	2	2	2	2	1	2	2	...	5
0.23	9	1	1	1	1	1	1	1	1	1	1	1	2	...	5
0.24	10	1	1	1	1	1	1	1	1	1	1	1	1	...	4
...	...	...	...	...	...	...	...	...	...	...	...	...	...	...	...
0.39	25	0	0	0	0	0	0	0	0	0	0	0	0	...	0
Total		35	34	35	35	39	43	40	46	55	63	63	75	...	82

Note: The trawl population numbers for year 1979 are calculated from the average recruitment during 1980–1982 and are not based on direct observations. The row labeled Total sums up the annual amount of trawls of specific size class.

Fig. 1. The area of fishing circle as an approximation for the gear size.

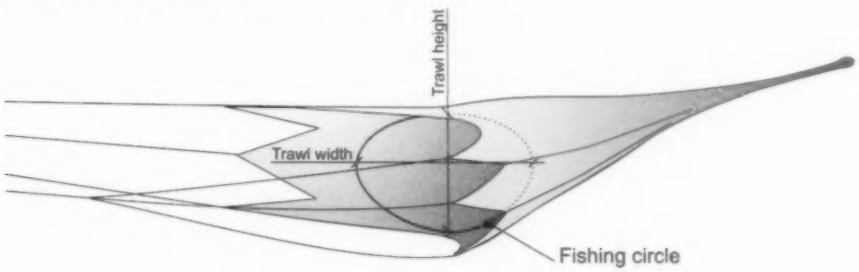

innovations, and trends in the gear construction and rigging. Each manufacturer also provided a detailed list of the amount, nominal sizes, and sweep mesh sizes of the herring trawls they sold in Finland from 1980 to 2000. A significant number of trawls have been imported from Denmark, and the Danish manufacturer known to sell herring trawls to Finland provided similar information to that provided by the domestic gear companies. These data are regarded as immigration enhancing trawl recruitment. It was not possible to quantify a small fraction of trawls made by fishers themselves.

A total of 837 midwater trawls were recruited into the Finnish herring fishery during 1980–2000. These midwater trawls were of 58 different nominal sizes ranging from 57 m to 914 m. Single and pair trawls were not segregated in the data.

Estimating trawl retirement rate

Interviews were conducted in person in 1999–2000 to obtain detailed attributes of herring trawlers related to fishing power and skippers' fishing strategies. As a part of the interview, the skippers were asked the minimum, average, and maximum service life of pelagic trawls during their fishing career. Answers related to the average service life were considered to give a frequency distribution describing retirement rates of the trawls in the fleet. The minima and maxima were not used analytically, but to check whether the tails of the fitted Weibull distribution appeared to be in accordance with the most extreme observations.

The target population of the interviews included fishing vessels operating under the Finnish flag, being at least 10 metres long, and reporting herring caught by trawl in 1997 or 1998. These criteria allowed us to extract herring trawlers from the vessel register. Because of the manner in which vessel and catch report registers are structured, the technical sampling unit is the vessel. The herring trawler fleet consists of 172 vessels. To exclude the least active fraction of the fleet from the interview, the trawlers were sorted in descending order according to their reported landings. The limit was set to vessels giving 99% of the total reported catch. This fraction included 122 vessels and the other 50 were removed from the study. Two of included vessels stopped herring trawling and another two were lost with their crew, leaving the final sampling population size 118 vessels (Table 2). This was further broken down into five strata according to the length, landings, and spatial fishing history of a vessel. (*i*) The "intensifiers" included trawlers of at least 28 m. In addition to the length-based selection, 10 trawlers having reported the largest landings during 1997–1998 were also in-

© 2002 NRC Canada

Table 2. The five strata according to the length, reported landings, and spatial fishing history of a vessel.

Stratum	No. trawlers	No. pair trawler units	No. sampling units	Sample size	Intended sampling ratio	Realized sample size	Realized sampling ratio
Intensifiers	19	2	17	17	1	13	0.76
SD 29	27	3	24	10	0.42	5	0.21
SD 30	30	5	25	11	0.44	10	0.40
SD 31	20	8	12	5	0.42	5	0.42
SD 32	22	5	16	7	0.44	6	0.38
Total	118	23	94	50	0.53	39	0.41

cluded. It was also required that the trawler had been operating in at least two separate International Council on the Exploration of the Sea (ICES) subdivisions to reflect mobility. (*ii*) Trawlers not belonging to stratum (*i*), and fishing exclusively or mainly in ICES subdivision 29 (Archipelago Sea). (*iii*) Trawlers not belonging to stratum (*i*), and fishing exclusively or mainly in ICES subdivision 30 (Bothnian Sea). (*iv*) Trawlers not belonging to stratum (*i*), and fishing exclusively or mainly in ICES subdivision 31 (Bothnian Bay). (*v*) Trawlers not belonging to stratum (*i*), and fishing exclusively or mainly in ICES subdivision 32 (Gulf of Finland).

The skipper, or in some rare cases, the owner, was interviewed. The intended sample size was not reached in all strata because of refusals to be interviewed (n = 7) and in ICES subdivision 29 stratum because of lack of personnel resources to reach skippers living in the most remote archipelago areas.

Skippers' answers were interpreted to be their subjective estimates of trawl service life on the vessels they had worked as a crew member or captain. The estimate was not only subjective, but also surrogative in that it should capture the properties of a distribution, which was unknown to the skipper. The location and shape of the distribution were possibly not adequately described by the subjective average. The questions posed to the interviewee had to be understandable in their own language and concepts, and thus the average was likely to be the best parameter to use. Consequently, answers were not obtained about the service life of unique trawls, but subjective and surrogative estimates about captains' observations pooled over several trawls during his career. Because of this, the answers were sensitive to the number of trawls a skipper had experience with.

The designed original stratification (Table 2) was not used in estimation of service life, but instead the data were post-stratified by size of trawl. The acquired frequency data suggested that trawl service lives should be considered in two classes, where service life is considerably shorter among large trawls compared to smallest ones. The boundary between these classes was somewhat equivocal, but 290 m was chosen as a limit (Fig. 2). Trawl size was, in the current context, defined as the most used trawl size on the vessel during the year of interview. The typical service life for trawls over 290 m was 3–5 years, whereas it was 10–15 years among smaller ones. This phenomenon was presumably a product of annual fishing effort, which affected the rate of deterioration. The structure of the commercial fishery has polarized in Finland in the 1980s and 1990s, indicated by a fraction of fishers intensifying and rationalizing their fishery, compared

Fig. 2. The average trawl service life according to interviewed skippers as a function of the most used trawl size of the vessel during the year of interview.

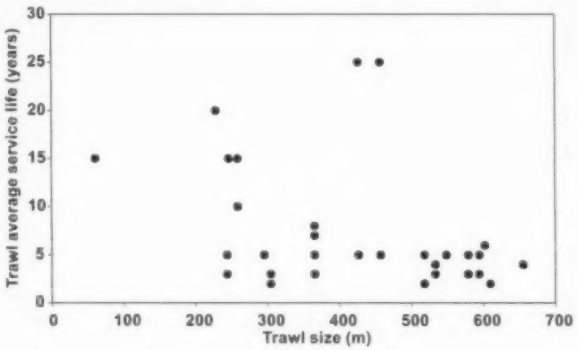

with the static fishing strategy by others (Salmi and Salmi 1998). A long average trawl service life is likely to display a lack of major investments on fishing and low fishing effort of the interviewed skipper. Two exceptional observations with 25-year average trawl service life for large gear sizes were the result of new trawls being acquired in the year when the interview was conducted. These skippers' strategies could be classified as passive, and these two observations were analyzed as a part of the <290-m trawl class.

A Weibull probability density function was fitted to the two sets of service life data using maximum-likelihood estimators (Palisade Corporation 1993). All observations in the >290-m group were located between ages 2 and 8 and this was reflected satisfactorily by the function (Fig. 3). In the smaller trawls group there were fewer observations, and the probability mass was more evenly distributed over the time range. The Kolmogorov–Smirnov test for goodness-of-fit could not reject H_0 at 10% risk for either of the size groups. Consequently, the Weibull distribution was considered an adequate parametric approximation for retirement rate and was applied in the analysis.

Having estimated parameters b and c, the Weibull survival functions provided the retirement rate of the trawls (Fig. 4). The retirement rate for the larger trawls was considerably faster; 50% of trawls were retired after four years of service, whereas it took 13.5 years to retire 50% of the smaller trawls. The age-specific instantaneous "mortality" (Z_a) was calculated from the retirement rate estimates by simply using eq. 1 giving the removals from the trawl population as a function of time (e.g., Ricker 1975).

© 2002 NRC Canada

Fig. 3. The Weibull probability density functions for average service lives for trawls (panel *a*) larger than 290 m and (panel *b*) smaller than 290 m. The fitted parameters are $b = 5.09$, $c = 1.91$, and $b = 16.04$, $c = 1.98$ for panels *a* and *b*, respectively.

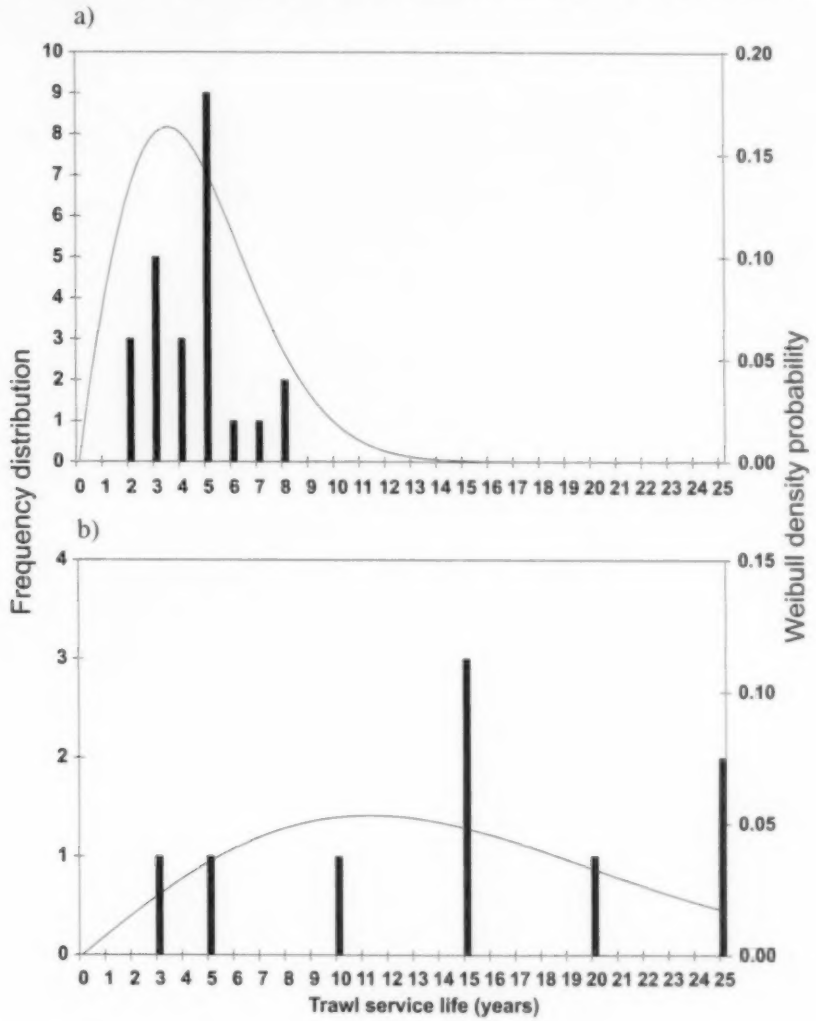

$$(1) \qquad Z_a = -\ln\left(\frac{N_{t+1,a+1}}{N_{t,a}}\right)$$

where $N_{t,a}$ is the number of age a trawls in year t. Transforming the survival function to Z was factually unnecessary, for the desired estimate of N_{t+1} is obtained directly from the survival function, or alternatively, from the Weibull hazard function at the midpoint of each service age. Z was calculated to achieve the full analogy to the conventional VPA.

Estimating area of net path

The nominal size of a trawl was defined as the theoretical circumference at the trawl mouth measured with meshes fully open. Because the true hanging ratio is near 0.5, the fishing circle should be about half of the size expressed by the nominal size. Moreover, meshes in the side panels and in the vicinity of selvedges are almost closed during towing, reducing the actual size of the trawl. According to information acquired from a trawl manufacturer, the actual circumference of the fishing circle during the capture process is typically about 25% of the nominal size of the trawl (K. Blomqvist, Scandi Net Ab, P.O. Box 70, FIN-66901 Uusikaarlepyy, Finland, personal communication).

The area of the fishing circle (Fig. 1) was estimated by assuming that (*i*) the actual circumference of a trawl was 25% of its nominal size, and (*ii*) the shape of fishing circle was adequately approximated by an ellipse of eccentricity rate 0.83. This rate implies that the maximum height of a trawl is about 60% of a trawl's maximum width. The eccentricity rate (e) was estimated from a typical pelagic trawl with known height and weight of the fishing circle during towing as provided by a trawl manufacturer (K. Blomqvist, Scandi Net Ab, P.O. Box 70, FIN-66901 Uusikaarlepyy, Finland,

© 2002 NRC Canada

Fig. 4. Survival functions for trawls smaller (solid line) and trawls larger than 290 m (dashed line) estimating the retirement rate.

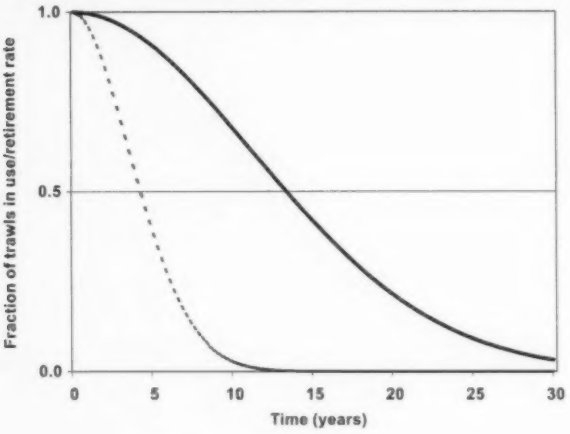

personal communication). The above assumptions allow for estimating the area (A) of fishing circle corresponding to the nominal size of a trawl. Let $2a$ be the width and $2b$ be the height of the trawl and let c designate the distance between the midpoint and the focus points of the trawl (ellipse). P designates the actual circumference of the trawl (size-class-specific average circumference). By definition, the mathematical formulation for an ellipse is

$$(2) \quad \frac{x^2}{a^2} + \frac{y^2}{b^2} = 1$$

and for the ratios associated with height, width, eccentricity, circumference, and area

$$(3) \quad b^2 + c^2 = a^2$$

$$(4) \quad e = \frac{c}{a}$$

$$(5) \quad P = 2\pi \frac{a+b}{2}$$

$$(6) \quad A = \pi ab$$

By first solving eq. 3 for c and substituting parameter c in eq. 4 by rearranging eq. 3, eq. 4 was solved for b. Then parameter b in eq. 5 was substituted by the previously modified eq. 4

$$(7) \quad \frac{P}{\pi} = a + \sqrt{a^2 - (ea)^2}$$

where the square root is eq. 4 solved for b.

Parameters P (Table 3), e, and p are constants and parameter a was solved numerically. After this, parameter b was easily obtained from eq. 5. Finally, size-class-specific fishing circle areas were calculated from eq. 6.

Skippers are able to rig their midwater trawls to be towed on soft bottoms. In these circumstances the height of the trawl can be decreased by 50% allowing the width of the trawl mouth to be increased. These possible modifications were excluded from our trawl size estimates.

The trawl population model

Trawls were aggregated by nominal size into eight categories (Table 3). The possible bias introduced to estimates by the aggregation was considered insignificant because the size distributions within each class were not severely skewed. Each size class had its own recruitment data and estimate of average fishing circle area. Two separate retirement rate estimates were used: the lower retirement rate for the four smallest trawl size classes and the higher retirement rate for the four largest ones.

The number of age $a + 1$ trawls in year $t + 1$ was calculated by a conventional fish stock assessment equation (e.g., Ricker 1975), also taking the size classes s into account

$$(8) \quad N_{t+1,a+1,s} = N_{t,a,s} e^{-Z_{a,s}}$$

The total number of trawls belonging to size class s in year t was calculated as a sum of trawls of all service ages a

$$(9) \quad N_{\text{tot},t,s} = \sum_{a=0}^{25} N_{t,s}$$

Because the first year in the acquired recruitment data was 1980, the VPA was initialized by creating an equilibrium trawl population for year 1979. The average recruitment of each size class during years 1980–1982 was used to get a starting value for $N_{1979,0,s}$; eq. 8 was then modified to calculate the trawl population size in 1979

$$(10) \quad N_{1979,a+1,s} = N_{1979,a,s} e^{-Z_s}$$

Year 1980 was used as the index year for gear size alteration of the fleet.

After calculating the total number of trawls by year t and size class s, an annual average gear size in the herring trawling fleet was estimated. This was done by calculating a weighted mean of fishing circle areas, the number of trawls in a size class as a weighting factor

$$(11) \quad P_t = \frac{\sum_{s=1}^{8} N_{\text{tot},t,s} A_s}{\sum_{s=1}^{8} N_{\text{tot},t,s}}$$

where the average gear size in the fleet in year t was denoted as P_t and the average area of fishing circle in the size class s as A_s. P_t described the increase in the technical fishing power through time.

Results

During the early 1980s the recruitment of new gears was in balance with the retirement of trawls smaller than 229 m (Fig. 5). While the retirement rate of the smallest gear size classes was low during the few first years of use, it increased in the older ages causing the number of trawls smaller than 229 m to decline steadily at the end of the 1980s. This decrease is a corollary of retirement rate being higher than recruitment rate, and the replacement of small trawls by larger ones, which was evident from the late 1980s onwards. At present, the fraction of trawls smaller than 229 m is about

© 2002 NRC Canada

Table 3. Trawl size classes in the VPA, the average trawl circumference in a size class, and corresponding area of a fishing circle.

	Size class, *s*							
	1	2	3	4	5	6	7	8
Nominal size (m)	<137	137–198	198–229	229–290	290–366	366–457	458–610	>610
Average circumference, P (m)	119	176	214	259	333	436	538	719
Average area, A (m^2)	66	142	211	308	509	876	1328	2378

Note: Gear manufacturers and fishers use exclusively feet as a measure of trawl size. They are approximated here in metric units.

Fig. 5. The number of trawls in the fleet by size class during 1980–2000.

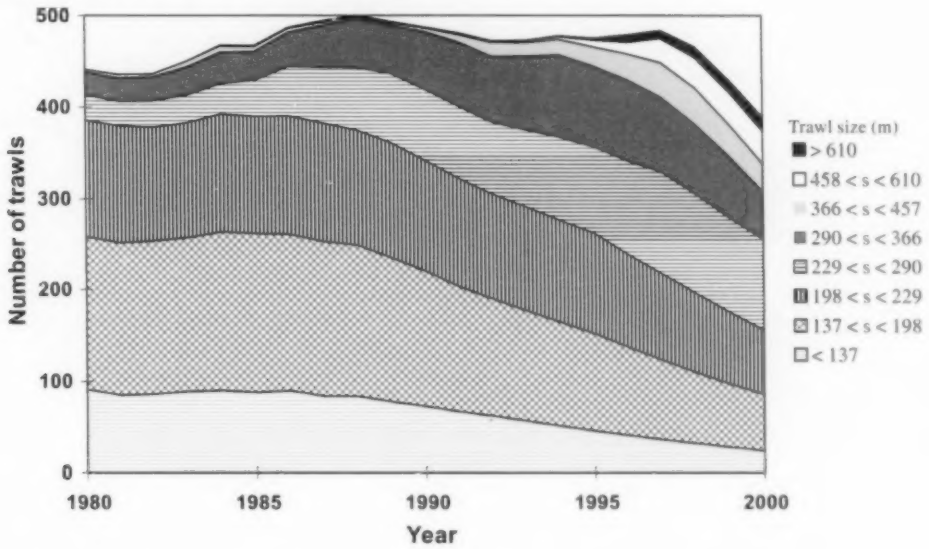

40% of the trawl population, whereas it was nearly 90% at the beginning of the 1980s. Trawls larger than 457 m appeared in the fishery in the mid-1990s. Since then the fraction of the largest size classes has increased continuously.

The average trawl size has increased by a factor of 2.7 during the 20-year study period (Fig. 6). The increase of the fishing circle area was a slow but continuous process during the 1980s. At that time the change in size was 26%. The rate of change increased at the beginning of the 1990s and has been particularly rapid from 1995 onwards. During the last eight years the increase of gear size has been 100%. The development is enhanced by the fact that the relationship between the circumference of the trawl (nominal size) and the fishing area is exponential. As a result, the rate of increase in fishing circle is higher when the nominal sizes are large.

The overall size of the gear population has been fairly stable at around 450 trawls. While there are about 170 trawlers in the fleet, the result implies an average of about 2.5 trawls per vessel. The estimate seems quite realistic, for according to the interview study, each skipper had used between one and five different trawls in the fishery during the year of interview. This independent estimate of the number of trawls in the fleet supports the results obtained from our modeling approach.

The recruitment data shows a dramatic increase in the average size of manufactured trawls; in 2000 the average size of recruiting trawls was 7.5 times larger than in 1980 (Fig. 7). From 1997 onwards, the number of purchased trawls has fallen considerably indicating lack of investment in gears. This may be an additional sign of polarization in the fleet, where only the wealthiest and most effective fishers continue investing in their livelihood.

Discussion

A substantial increase of the average trawl size of the fleet indicates that the increase in fishing power is of a magnitude that must be recognized and considered in stock assessment. Clearly, the doubling in gear size during the last eight years is bound to bias SPA using CPUE as tuning series if this event is ignored. For comparison, the Icelandic bottom trawling fleet for cod has annually increased efficiency by almost 5% from the mid-1970s to the mid-1990s (Stefánsson 1998). In Australia, the fishing power in the northern prawn fishery fleet increased by 12% within three years from the impact of global positioning systems (GPS) and plotters (Robins et al. 1998). In light of notorious failures in stock assessments in the past, worldwide, the bias in Finnish herring trawler CPUE would cause the classical flaw of an underestimate in fishing mortality and an overestimate of stock size. However, after the trend in the gear size was discovered, the CPUE time series was adjusted by the estimated increase in the recent assessments (ICES 1999, 2000, 2001). The adjustment was made by multiplying fishing effort by

© 2002 NRC Canada

Fig. 6. The index of trawl size in the fleet (-◆-) and the rate of change (—). The rate of change has been at least 1 during all years denoting increase in the average trawl size except 1985. The maximum rate of change has occurred in 1996 but since then it has decreased, probably reflecting that maximum advantage obtainable from the technical modification of trawl has already been used by the fleet.

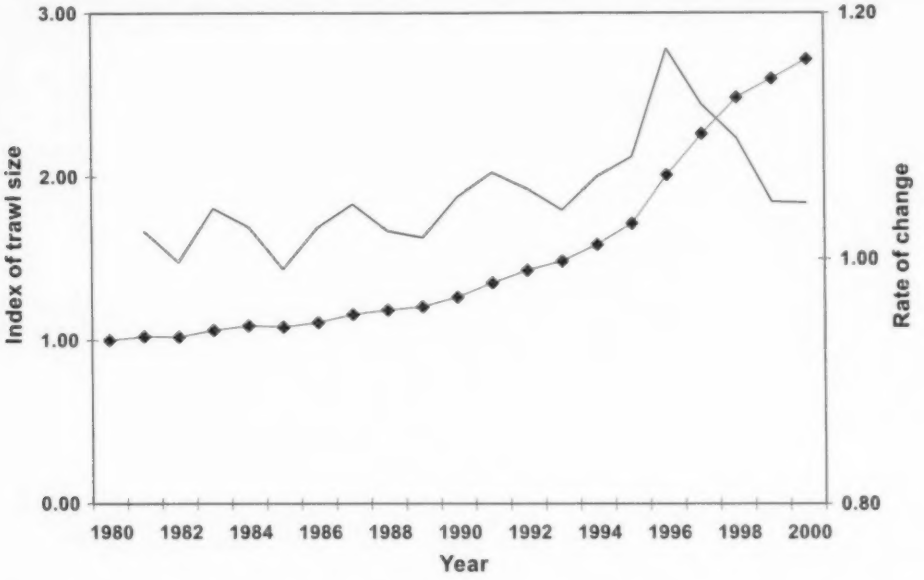

Fig. 7. New trawls in 1980–2000 (bars) and their relative average size (line) compared with year 1980.

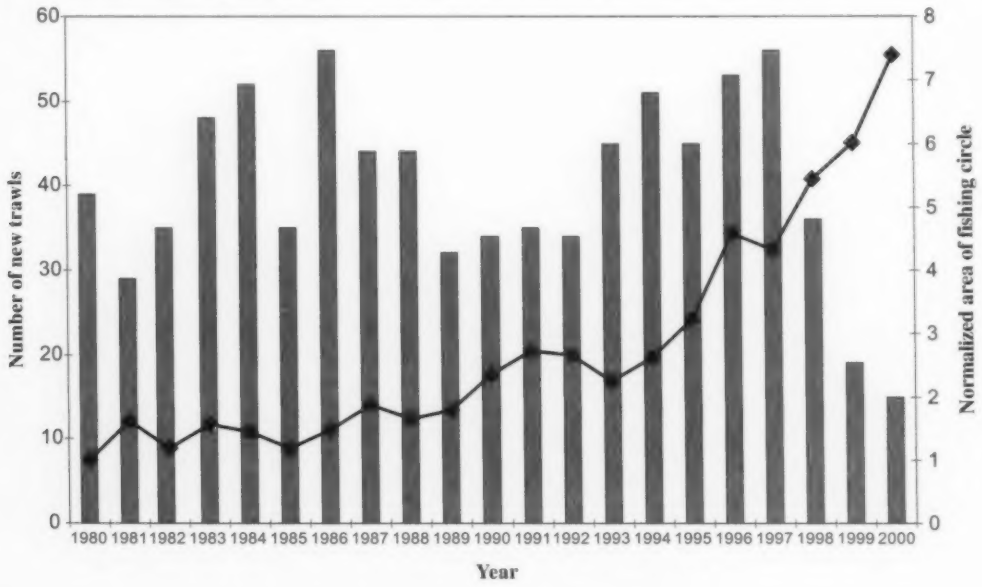

the gear size index. This had a considerable impact on the abundance index, it being just one third of the unadjusted abundance index for the last year in the data series and about one half in 1992. Although this adjustment is the simplest possible approach, it had an effect of removing the trend from catchability residuals in the SPA for ICES subdivision 30 herring stock (e.g., ICES 2000).

Trawl life is assumed to be modeled adequately using the parametric Weibull distribution in association with interview data. The tails of the fitted probability density distributions matched the reported minimum and maximum service lives of trawls confirming that the Weibull parameter estimates were realistic. The mode for minimum service life was zero years for both size groups, whereas there was more variation regarding the maximum service life. The reported maximum was 15 years for the trawls larger than 290 m and 30 years

© 2002 NRC Canada

for the smaller ones. An alternative approach could be to use the observed frequency of trawl service life and apply a nonparametric resampling scheme to get an empirical distribution of the average trawl size as well an estimate of uncertainty in results.

The average size of a trawl population may not be an adequate indicator of the fishing power. Our information does not allow us to conclude which trawls of the population have been used in fishery. As there are typically two trawls onboard each vessel, and as the newest gears are generally the largest ones, one would tend to assume that we are underestimating the true fishing power of the fleet. This statement implies that most of the effort is allocated to the largest and presumably the most efficient trawl. However, based on the interviews, we know that it is not always the largest trawl onboard which has been allocated most of the effort. Since skippers have described their fishing practices in detail, it is possible to understand why a smaller trawl is preferred in some fishing circumstances. Smaller trawls are easier to handle in fishing areas characterized by irregular bottom structure with abrupt underwater ridges and gullies. These areas attract herring aggregations intermittently, but are risky to harvest with respect to gear breakdowns. Successful fishing requires a high maneuverability of gear in conjunction with a very accurate navigation system. There are also practical reasons for not using the largest gear on the vessel: that gear may be under repair or has not appeared to be sufficiently workable. In addition, the behavior of herring schools, e.g., incidence of herring near bottom, affects the choice of which gear to use. The fact that skippers have used between one and five trawls in fishing annually makes deductions of the actual fishing power ambiguous. In spite of the concomitant uncertainty, a rational baseline is to assume that skippers are able to choose the most efficient gear, with respect to size and construction, for varying fishing circumstances.

From the fisher's viewpoint there can be several factors affecting investments on larger trawls. If their target is to maintain a level of income, then the adverse change in CPUE, in price of herring, or in fishing costs will act as an incentive to be more efficient. A profound change in the operational environment took place in 1995 when Finland integrated with the European Union. During one year the market price for herring to be processed dropped by 50% owing to withdrawal of subsidies (Stephenson et al. 2001). The price of herring on other human consumption and fodder markets decreased as well, but the price reduction was not as large. Moreover, stock assessments indicate a steady decrease of about 25% in herring abundance since 1993–1994 to present (ICES 2000). Consequently, there appear to be at least two factors encouraging or even compelling one to increase fishing power to stay in business.

According to Finnish trawl manufacturers, the increase in trawl size was facilitated by modification of the sweeps and the front section of the trawl. At the beginning of the 1980s, mesh size in the sweeps was typically 400–800 mm, whereas it is 1800–3600 mm at present. By using considerably larger mesh sizes in the sweeps and the front section, tensile stress directed at the vessel and in special to the vessel engine has not changed much in spite of the substantial increase in trawl size. As a result, fishers have been able to tow larger trawls with their present vessels and engines. Avoiding investments into larger vessels and more powerful engines is a significant advantage. Moreover, anecdotal information from one trawl manufacturer confirms that tailoring of trawl sweeps has changed during the late 1990s in that sweeps are now about 20% longer compared with trawls of the same nominal size, thereby increasing the area swept by the gear.

A single major technical innovation, the increase of sweep mesh size, has ratcheted up fishing power quite rapidly within less than 10 years to a substantially higher level. The event can be classified as sudden (stepped) rather than continuous (gradual) development. If future data were available, we likely would be able to observe when the utility of this innovation is fully exploited and the average trawl size begins to level out. The stepped innovation in the 1990s, contributing to increase in trawl size, justifies the equilibrium "warm-up" of the trawl VPA, because the results for small trawls are influenced by the initialization to the mid-1980s.

Interestingly, the increase in fishing power could not be observed from data concerning vessel size or engine power (vessel register data), and auxiliary fishery information was necessary to document the phenomenon. The vessel register was restructured in 1988 and 1995. In restructuring the register, the limit of vessel size to be included was first lowered to 12 m and then to 10 m. This results in a flawed impression that the average vessel length and engine power in the herring trawl fleet has decreased from the beginning of the 1980s to the present.

Research related to assessing changes in fishing power is generally focused on the catching technology. We assessed the change in the size of trawls, whereas the effects of alterations in the bridle path, i.e., the width swept by the otterboards, bridles, and sweeps, were not considered. The factors that determine the efficiency of a gear are complicated and trawl mouth area may be a poor approximator. It has been suggested that the profile of a fish stock at the otterboards determines the number of encounters with the gear (Dickson 1993). On the other hand, alteration in some technical measure (e.g., in trawl size) may not be the major issue. Changes in the way the gears are deployed may be more important, but this has not received as much attention. For instance, major escapement may take place during hauling (Misund et al. 1999) and hauling practices such as type of the vessel (side trawler versus stern trawler) may influence catch size. Also the density of fish ahead of the trawl mouth as well as diel vertical migrations (Arrhenius and Hansson 1993) may affect swimming behavior and catchability (Godø et al. 1999; Petrakis et al. 2001). Although basic stock assessment implications are straightforward, the actual increase in fishing power is not at the moment accurately quantifiable. The relationship between gear size and catchability is likely not to be proportional. Moreover, there are several currently immeasurable variables such as skipper skill (Hilborn 1985; Hilborn and Ledbetter 1985), fish behavior, and on-site dynamics of vessels, which also may bias the relationship between CPUE and abundance (Hilborn and Walters 1992).

It is evident that assumptions about fishing efficiency drive stock assessments. At present, the applied tuning method is extended survivors' analysis, XSA (Shepherd 1999). Because of lack of any survey index for tuning the SPA, methods rely-

© 2002 NRC Canada

ing on time series models and being capable of estimating mortality rates without reference to CPUE data (e.g., Gudmundsson 1998) might be worthy of further investigation.

Acknowledgments

We thank the representatives from Cosmos Trawl, Scandi Net, T-Trål, and Wasa Trawl for providing gear specifications and information about trawl construction. Esa Lehtonen pointed out the change in commercial gear size, provided fishing technology information, and together with Folke Halling helped access trawl manufacturer data. We acknowledge the many skippers who participated in interviews. John Neilson and John Wheeler provided useful reviews of the manuscript. We thank Rob Stephenson and Stratis Gavaris for many helpful comments on earlier versions of this paper.

References

Arrhenius, F., and Hansson, S. 1993. Food consumption of larval, young and adult herring and sprat in the Baltic Sea. Mar. Ecol. Prog. Ser. **96**: 125–137.

Béné, C. 1996. Effects of market constraints, the remuneration system, and resource dynamics on the spatial distribution of fishing effort. Can. J. Fish. Aquat. Sci. **53**: 563–571.

Campbell, H.F., and Hand, A.J. 1999. Modeling the spatial dynamics of the U.S. purse-seine fleet operating in the western Pacific tuna fishery. Can. J. Fish. Aquat. Sci. **56**: 1266–1277.

Cooke, J.G., and Beddington, J.R. 1984. The relationship between catch rates and abundance in fisheries. IMA J. Math. Appl. Med. Biol. **1**: 391–405.

Dickson, W. 1993. Estimation of the capture efficiency of trawl gear. I: Development of a theoretical model. Fish. Res. **16**: 239–253.

Evans, M., Hastings., N. and Peacock, B. 1993. Statistical distributions. 2nd ed. John Wiley & Sons, New York.

Gillis, D.M., and Peterman, R.M. 1998. Implications of interference among fishing vessels and the ideal free distribution to the interpretation of CPUE. Can. J. Fish. Aquat. Sci. **55**: 37–46.

Gillis, D.M., Peterman, R.M., and Tyler, A.V. 1993. Movement dynamics is a fishery: application of the ideal free distribution to spatial allocation of effort. Can. J. Fish. Aquat. Sci. **50**: 323–333.

Godø, O.R., Walsh, S.J., and Engås, A. 1999. Investigating density-dependent catchability in bottom-trawl surveys. ICES J. Mar. Sci. **56**: 292–298.

Gudmundsson, G. 1998. Joint time series analysis of catch-at-age and CPUE data. *In* Fishery stock assessment models. 15th Lowell Wakefield Fisheries Symposium, 8–11 Oct. 1997, Anchorage, Alaska. *Edited by* F. Funk, T.J. Quinn, II, J. Heifetz, J.N. Ianelli, J.E. Powers, J.F. Schweigert, P.J. Sullivan, and C.-I. Zhang. American Fisheries Society, 5410 Grosvenor Ln. Ste. 110, Bethesda, Md. pp. 199–217.

Hilborn, R. 1985. Fleet dynamics and individual variation: why some people catch more fish than the others. Can. J. Fish. Aquat. Sci. **42**: 2–13.

Hilborn, R. and Ledbetter, M. 1985. Determinants of catching power in the British Columbia salmon purse seine fleet. Can. J. Fish. Aquat. Sci. **42**: 51–56.

Hilborn, R., and Walters, C.J. 1992. Quantitative fisheries stock assessment. Choice, dynamics and uncertainty. Chapman & Hall, New York.

International Council on the Exploration of the Sea (ICES). 1999. Report of the Baltic Fisheries Assessment Working Group. ICES CM 1999/ACFM:15.

International Council on the Exploration of the Sea (ICES). 2000. Report of the Baltic Fisheries Assessment Working Group. ICES CM 2000/ACFM:14.

International Council on the Exploration of the Sea (ICES). 2001. Report of the Baltic Fisheries Assessment Working Group. ICES CM 2001/ACFM:18.

Large, P.A. 1992. Use of multiplicative model to estimate abundance from commercial CPUE data. ICES J. Mar. Sci. **49**: 253–261.

Marchal, P., Nielsen, J.R., Hovgård, H., and Lassen, H. 2001. Time changes in fishing power in the Danish cod fisheries of the Baltic Sea. ICES J. Mar. Sci. **58**: 298–310.

Mendelssohn, R., and Cury, P. 1989. Temporal and spatial dynamics of a coastal pelagic species, *Sardinella maderensis* off the Ivory Coast. Can. J. Fish. Aquat. Sci. **46**: 1686–1697.

Misund, O.A., Luyeye, N., Coetzee, J., and Boyer, D. 1999. Trawl sampling of small pelagic fish off Angola: effects of avoidance, towing speed, tow duration, and time of day. ICES J. Mar. Sci. **56**: 275–283.

Neilson, J.D., Waiwood, K.G., and Smith, S.J. 1989. Survival of Atlantic halibut (*Hippoglossus hippoglossus*) caught by longline and otter trawl gear. Can. J. Fish. Aquat. Sci. **46**: 887–897.

Neis, B., Schneider, D.C., Felt, L., Haedrich, R.L., Fischer, J., and Hutchings, J.A. 1999. Fisheries assessment: what can be learned from interviewing resource users? Can. J. Fish. Aquat. Sci. **56**: 1949–1963.

Palisade Corporation. 1993. BestFit—distribution fitting software for Windows. *Available from* Palisade Corporation, 31 Decker Rd., Newfield, NY 14867, U.S.A.

Paloheimo, J.E., and Dickie, L.M. 1964. Abundance and fishing success. Rapp. P.-v. Réun. Cons. Int. Explor. Mer. **155**: 152–163.

Petrakis, G., MacLennan, D.N., and Newton, A.W. 2001. Day–night and depth effects on catch rates during trawl surveys in the North Sea. ICES J. Mar. Sci. **58**: 50–60.

Ricker, W.E. 1975. Computation and interpretation of biological statistics of fish populations. Fish. Res. Board Can. Bull. No. 191.

Robins, C.M., Wang, Y.-G., and Die, D. 1998. The impact of global positioning systems and plotters on fishing power in the northern prawn fishery, Australia. Can. J. Fish. Aquat. Sci. **55**: 1645–1651.

Salmi, J., and Salmi, P. 1998. Livelihood and way of life: Finnish commercial fisheries in the Baltic Sea. *In* Northern waters: management issues and practice. *Edited by* D. Symes. Fishing News Books. pp. 175–183.

Schaefer, M.B. 1954. Some aspects of the dynamics of populations important to the management of commercial marine fisheries. Bulletin of the Inter-American Tropical Tuna Commission, **1**: 27–56.

Shepherd, J.G. 1999. Extended survivors' analysis: an improved method for the analysis of catch-at-age data and catch-per-unit-effort data. ICES J. Mar. Sci. **56**: 584–591.

Smith, S.J., Waiwood, K.G., and Neilson, J.D. 1994. Survival analysis for size regulation of Atlantic halibut. *In* Case studies in biometry. *Edited by* N. Lange, L. Ryan, L. Billard, D. Drillinger, L. Conquest, and J. Greenhouse. John Wiley & Sons, New York. pp. 125–144.

Stefánsson, G. 1998. Comparing different information sources in a multispecies context. *In* Fishery stock assessment models. 15th Lowell Wakefield Fisheries Symposium, 8–11 Oct. 1997, Anchorage, Alaska. *Edited by* F. Funk, T.J. Quinn, II, J. Heifetz, J.N. Ianelli, J.E. Powers, J.F. Schweigert, P.J. Sullivan, and C.-I. Zhang. American Fisheries Society, 5410 Grosvenor Ln. Ste. 110, Bethesda, Md. pp. 741–758.

Stephenson, R., Peltonen, H., Kuikka, S., Pönni, J., Rahikainen, M.,

© 2002 NRC Canada

Aro, E. and Setälä, J. 2001. Linking biological and industrial aspects of the Finnish commercial herring fishery in the northern Baltic Sea. Proceedings from the International Symposium Herring 2000: expectations for a new millennium, 18th Lowell Wakefield Fisheries Symposium, 23–26 Feb. 2000, Anchorage, Alaska. *Edited by* F. Funk, J. Blackburn, D. Hay, A.J. Paul, R. Stephenson, R. Toresen, and D. Witherell. University of Alaska Sea Grant, AK-SG-01-04, Fairbanks. pp. 741–760.

Vignaux, M. 1996. Analysis of vessel movements and strategies using commercial catch and effort data from the New Zealand hoki fishery. Can. J. Fish. Aquat. Sci. **53**: 2126–2136.

Winters, G.H., and Wheeler, J.P. 1985. Interaction between stock area, stock abundance, and catchability coefficient. Can. J. Fish. Aquat. Sci. **42**: 989–998.

© 2002 NRC Canada

Pacific herring respond to simulated odontocete echolocation sounds

Ben Wilson and Lawrence M. Dill

Abstract: There has been a long-running debate as to if and how clupeoid fish, such as herring (*Clupea* sp.), respond to anthropogenic sound. Anatomical and physiological investigations have shown that members of the clupeoid suborder have highly developed hearing extending into ultrasonic frequencies and behavioural studies suggest that they respond to many sounds. However, only recently have the selective forces that have driven the evolution of this keen sense and behavioural repertoire played a major part in the debate. One explanation is the adaptation to predation from echolocating cetaceans. In this study, we investigate the responses of adult Pacific herring (*Clupea pallasii*) to broadband biosonar-type sounds with high-frequency similarities to those produced by odontocete cetaceans. Exposures to these sounds in an indoor tank and sea cage caused feeding fish to cease, drop in the water column, and begin to school actively. Fish already schooling dropped in the water column and increased their swimming speed. Exposures to electronic silence and an acoustic deterrent device for marine mammals did not elicit such responses. We discuss the potential suitability of the observed manoeuvres for avoidance of foraging odontocetes and consider their relevance for human-related fishing activities.

Résumé : Il existe depuis longtemps un débat à savoir si et dans quelle mesure les poissons clupéoïdes, tels que les harengs (*Clupea* spp.), réagissent aux sons générés par l'activité humaine. Des études anatomiques et physiologiques révèlent que les poissons du sous-ordre des clupéoïdes possèdent une ouïe bien développée qui s'étend jusque dans les ultrasons; des études comportementales montrent qu'ils réagissent à plusieurs sons. Ce n'est cependant que récemment que l'on a fait intervenir de façon importante dans le débat les forces de sélection qui ont favorisé cette ouïe fine et la gamme des comportements associés. Une explication veut que ce soit une adaptation à la prédation par écholocation des cétacés. Nous examinons donc les réactions de harengs du Pacifique (*Clupea pallasii*) à des sons de type sonar à bande large qui ont des similitudes de haute fréquence avec les sons produits par les cétacés odontocètes. Des expositions à de tels sons dans un enclos de laboratoire et dans une cage en milieu marin causent un arrêt de l'alimentation, un mouvement vers le bas de la colonne d'eau et un regroupement actif en bande. Les poissons déjà en bande se déplacent vers le bas de la colonne d'eau et augmentent leur vitesse de nage. Des expositions à un silence électronique ou à des sons générés par un appareil de dissuasion des mammifères marins ne causent pas de telles réactions. La signification des comportements observés dans l'évitement des odontocètes en quête de nourriture et leur influence sur les activités de pêche commerciale font l'objet d'une discussion.

[Traduit par la Rédaction]

Introduction

There are many reports from the fishing and research communities that some fish species, particularly Atlantic and Pacific herring (*Clupea harengus* and *Clupea pallasii*) and other clupeoids, respond to the sounds made by boats, tackle, sonar equipment, and, most recently, acoustic deterrent devices for marine mammals (Mohr 1971; Misund et al. 1996; Kraus et al. 1997). Such observations have put into question the validity of acoustically derived abundance estimates (MacLennan and Simmonds 1992) and led directly to changes in fishing practices with, for example, the construction of quieter vessels (Mitson 1995; Fernandes et al. 2000). The aversive behavioural responses have also been exploited. For example, high-frequency sounds have been used to keep clupeoid fish from power plant water intakes (Nestler et al. 1992; Ross et al. 1996). Together, the potential consequences and opportunities raised by these responses have stimulated a diverse variety of anatomical, physiological, and ethological research studies.

Physiological investigations of a clupeoid (the American shad, *Alosa sapidissima*) have shown that its hearing spans an unusually broad frequency range that stretches high into the ultrasonic (Mann et al. 1997, 1998). The mechanism behind this specialization remains unclear (Mann et al. 1998), although the paired tubular extensions that reach from the physostomous swimbladder to the bony air-filled auditory bullae are likely to be involved (Blaxter et al. 1981). Because these structures are common to clupeoids, it is thought that the other members of this suborder have similar hearing

Received 16 January 2002. Accepted 28 February 2002. Published on the NRC Research Press Web site at http://cjfas.nrc.ca on 17 April 2002.
J16702

B. Wilson.[1,2] Bamfield Marine Sciences Centre, Bamfield, BC V0R 1B0, Canada.
L.M. Dill. Behavioural Ecology Research Group, Department of Biological Sciences, Simon Fraser University, Burnaby, BC V5A 1S6, Canada.

[1]Corresponding author (e-mail: bw9@st-andrews.ac.uk).
[2]Present address: Behavioural Ecology Research Group, Department of Biological Sciences, Simon Fraser University, Burnaby, BC V5A 1S6, Canada.

 DOI: 10.1139/F02-029 © 2002 NRC Canada

abilities. While permitting the detection of high-frequency far-field sounds, the single-receiver nature of the swimbladder-mediated reception system could possibly deny these fish the ability to perceive the bearing from which the sounds originated. Instead they would have to resort to behavioural tactics such as assessing spatial amplitude gradients. Indeed, in a limited behavioural experiment, herring did not show evidence of directionally informed responses to aversive noises at frequencies over 5 kHz (Olsen 1976).

The responses that clupeoids show to sound have received much attention. A wide variety of stimuli have been applied including low to high-frequency sine waves, square waves, recorded and actual vessel noises, sonar and echosounder outputs, and killer whale calls (Olsen 1971; Schwarz and Greer 1984; Nestler et al. 1992). The responses described generally fall into two categories: startle and avoidance. Short-duration, low-frequency sounds appear to elicit short-lived directional startle responses (Blaxter and Hoss 1981; Schwarz and Greer 1984). Higher-frequency or long-duration sounds produce avoidance responses including compaction and polarization of schools, sinking in the water column, leaving the vicinity of the sound, and being herded in front of a moving source (Schwarz and Greer 1984; Misund et al. 1996; Suuronen et al. 1997). Furthermore, reactions appear to be context specific. For example, schools of *Sardinella* reacted to vessel noise by diving but only when encountered above a depth of 20 m (Gerlotto and Freon 1988).

Despite the economic importance of these responses, their evolutionary relevance for the fish is unclear. Their hearing and behavioural repertoires have clearly not evolved as a response to human fishing activities (MacLennan and Simmonds 1992). Instead, an idea that has recently gained increasing interest is that the unusually high-frequency component of their hearing and their behaviour may be adaptations to predation from echolocating marine mammals, specifically odontocete cetaceans (Mann et al. 1997; Astrup 1999). Odontocetes typically produce intense, short duration directional signals that range in frequency from 0.3 kHz to as high as perhaps 325 kHz and durations from 40–600 μs (Au 1993; Richardson et al. 1995). Within this range, there are several so far unexplained, but potentially niche-related, patterns of variation. Dolphins in the genus *Cephalorhynchus* and the porpoises, for example, produce relatively high-frequency, narrowband clicks, whereas killer whales (*Orcinus orca*) produce low-frequency broadband signals (Au 1993). All of these sounds are potentially detectable to clupeoids; however, the behavioural responses that they might elicit have not been specifically assessed to determine if they are of any relevance to odontocete predation.

In this study, we investigate the responses of adult Pacific herring to broadband biosonar-type sounds with high-frequency similarities to those produced by odontocete cetaceans. A combination of different clicks varying in amplitude and interpulse interval were applied to determine if the fish's responses were generalized or specific to the nature of the sound that they experienced. Sound-exposure experiments were carried out on feeding and nonfeeding fish in a large indoor tank and in a sea cage. We discuss the potential relevance of the manoeuvres observed for avoidance of predation from foraging odontocetes as well as offering a possible explanation for the responses frequently described to human-related fishing activities.

In addition to the echolocation-type sounds, we exposed fish to an acoustic deterrent device designed to reduce bycatch of odontocete cetaceans in fishing nets. Trials at sea of the same device have given mixed results as to whether they also influence the catch of herring (Kraus et al. 1997; Trippel et al. 1999). By investigating how the sound produced by such devices impacts herring behaviour, we hoped to better understand why the results of separate but similar studies at sea have produced such different results.

Methods

Fish and maintenance

Adult Pacific herring were caught in early March of 1999 and 2000 during Canadian Department of Fisheries and Oceans spawning stock assessment surveys in Barkley Sound, B.C. (048°58′N, 125°22′W). Fish ranged in length from 14.9 to 26.2 cm, with the fish caught in 1999 being slightly larger than those caught in 2000 (mean fork length year 1999: 20.6 cm, standard error (SE) 1.4, n = 200; year 2000: 19.5 cm, SE 1.5, n = 200). Following capture, they were transferred to adjacent on-land holding facilities at the Bamfield Marine Sciences Centre, B.C. (048°50′N, 125°08′W). Fish were held in circular holding tanks (average 1.6 m diameter and 1 m deep), supplied with fresh seawater and fed on freeze-dried or frozen euphausiids.

Experiment 1: impacts of sound exposures on feeding behaviour

To evaluate the impacts of odontocete echolocation-type sounds on the feeding behaviour of adult herring, small groups were placed in a test tank and subjected to computer-generated sounds during feeding. Each trial was conducted in a large, circular, concrete, indoor test tank (9.18 m across and 2.15 m deep, Fig. 1*a*). Ten fish per trial were allowed to acclimate overnight before being tested the following day. During daylight hours, the water was illuminated from above with five ceiling-mounted 500-W lamps (maximum in-water light levels 16.2 $\mu mol \cdot m^{-2} \cdot s^{-1}$). During the hours of natural darkness, the lights were extinguished. Water temperatures ranged from 8 to 12°C during the study.

Immediately before each test, freeze-dried krill were delivered to the centre of the tank using a remotely operated pipe system running along the bottom (Fig. 1*a*). Once delivered, the food quickly rose through the water column to float at the surface. Behaviour of the fish was recorded using a Hi-8 video camera (Handycam CCD-V101, Sony Corporation, Japan) mounted on the ceiling 3.5 m above the centre of the tank. Fish were allowed to feed undisturbed for three minutes before a three-minute sound exposure was presented. Sounds were played through an Oceanears DRS-8 underwater speaker (Ocean Engineering Enterprises, North Canton, Ohio) powered by a 50-W amplifier and signals were generated with a laptop computer running Cooledit software (Syntrillium Software, Phoenix, Ariz.). The speaker was suspended at a depth of 1 m and held 2.3 m from the sidewall of the tank (Fig. 1*a*). Three sound types were presented as follows: (A) Control: a three minute flat waveform including the incidental noise generated by the computer,

© 2002 NRC Canada

Fig. 1. Experimental set-up. (*a*) Experiment 1. Fish in an indoor concrete tank were fed floating food in the centre via a delivery pipe (DP). Their behaviour was recorded with an overhead video camera (V) and sounds played through an underwater speaker (S). (*b*) Experiment 2. Fish circuiting the same tank were observed from a hide (H) and their time between gateways (formed by a baffle (B) and the tank walls) were recorded. Sounds were played with a speaker (S). (*c*) Experiment 3. Fish in a net pen tethered in open water were filmed (V) from a floating pontoon (FP) and observed from behind a hide (H). Sounds were played with an underwater speaker (S) 6 m from the outside perimeter of the net pen. For clarity, fish in (*a*), (*b*), and (*c*) are drawn larger than scale.

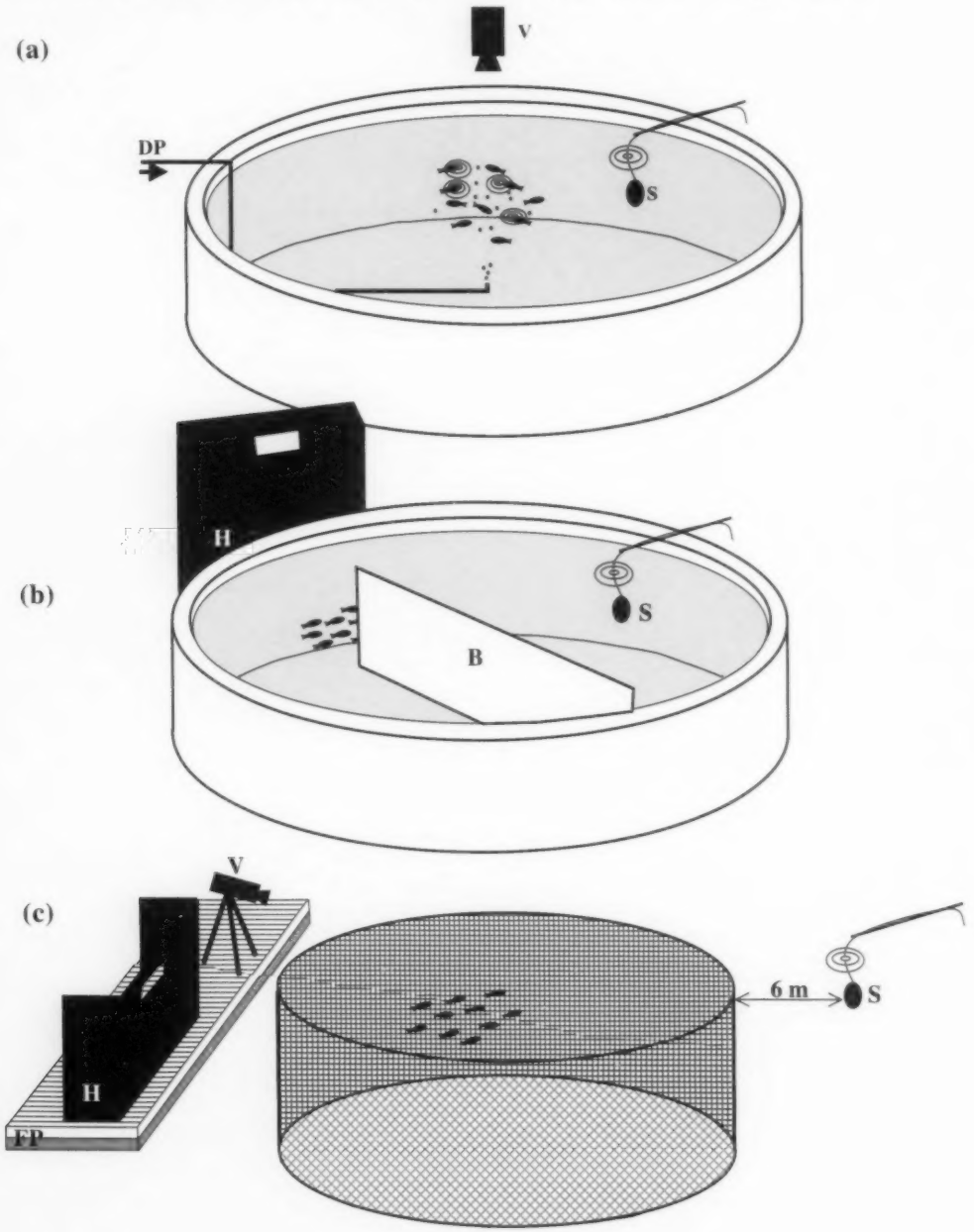

amplifier, and speaker. (B) Click trains: because tapes of foraging odontocetes recorded in the wild potentially contain sounds from other organisms and processes, tapes of foraging odontocetes could not be directly played to the fish. Instead, tapes of foraging schools of killer whales were used to determine a temporal distribution of echolocation clicks (inter-click intervals: mean = 0.2, max = 7.8, min = 0.03, SD = 0.35 s) and then simulated broadband echolocation-

© 2002 NRC Canada

type pulses (see below) of constant amplitude were created in the same temporal sequence. (C) Regular clicks: the same echolocation signals as the click trains were used, but with a regular time interval between each click. The inter-click interval was 0.2 s, which for a single odontocete would represent a foraging horizon of approximately 120 m (Au 1993).

To reduce the potential for pseudoreplication, three different versions of the click trains and regular clicks were constructed and used during the replicates (Hopp and Morton 1998). Ten groups of fish were tested in 1999 and the order of the sound exposures was assorted between trials in ABC, BCA, CAB, BAC, etc. fashion. Fish were allowed up to an hour between sound exposures to resume normal behaviour and each group was subjected to the sounds only once. The video tapes that resulted from these trials were used to document feeding rates, proximity to the food patch, rates of turning, and school polarization before and during the sound exposures (columns 1 and 2 in Table 1).

Click characteristics

Because of the interspecies variation in echolocation sound characteristics among odontocete cetaceans and the potential that these specializations developed as a counter to the evolving detection systems of their fish prey (analogous to the bat–moth arms race, Fenton et al. 1998), generalized broadband, medium-duration odontocete-type echolocation signals were constructed for this study. Again, three versions were generated to reduce potential pseudoreplication (Hopp and Morton 1998). These waveforms were modified slightly by both the sound production equipment and the tank itself. In consequence, the actual clicks that the fish received were composed of 370- to 390-μs broadband pulses with 2350–13 900 μs of subsequent reverberation (Fig. 2). In each click the initial pulse had energy in frequencies from 1.3 to 140 kHz with a peak at 6–7 kHz. Reverberation tended to be at frequencies below 20 kHz. Amplitudes were recorded with a calibrated hydrophone (Cetacean Research Technology, C50a) at 264 locations in the tank (over a grid of 88 points and at three depths (0.3, 1.0, and 1.7 m)). At 1 m, peak-to-peak sound-pressure levels (SPLs) of individual clicks ranged from 157 to 169 dB re 1 μPa (relative to one microPascal). On average, SPLs were 3 dB quieter on the side of the tank opposite the speaker; however, there was a complex pattern of troughs and peaks in SPL in different parts of the tank such that there was no relationship between SPL and proximity to the speaker for fish swimming around the perimeter (ordinary least squares regression $r^2 = 0.07$, $P = 0.1$, $n = 36$).

Experiment 2: impacts of sound exposures on nonfeeding behaviour

To quantify the impacts of the clicks on the nonfeeding behaviour of adult herring, small groups were subjected to sounds in the indoor test tank in the absence of food. The set-up was as for experiment 1, except for the following. An opaque vertical baffle was erected to bisect the tank leaving gateways (1.45-m wide) between the ends of the baffle and the tank walls (Fig. 1*b*). Instead of using a camera, behaviour was recorded by a seated observer concealed by a hide. In the absence of food, fish would circuit the perimeter of the tank passing through the two gateways on each circuit.

Table 1. Comparison of the behaviour of groups of feeding fish before and during sound exposures ($n = 10$).

Activity	Measure used	Control		Click trains		Regular clicks	
Feeding rate	Total no. of strikes at surface food per minute	$b = 26.3$ $d = 26.8$	$z = -1.066$ $P = 0.29$ (NS)	$b = 23.8$ $d = 0.3$	$z = -2.80$ $P < 0.01$ (**)	$b = 16.5$ $d = 0.5$	$z = -2.80$ $P < 0.01$ (**)
Residence at food patch	No. of fish in portion of tank where food was delivered	$b = 3.7$ $d = 5.3$	$z = -1.36$ $P = 0.17$ (NS)	$b = 4$ $d = 1.5$	$z = -2.60$ $P < 0.01$ (**)	$b = 3.2$ $d = 1.2$	$z = -2.80$ $P < 0.01$ (**)
Changes in direction	No. of direction changes (>20°) by randomly chosen fish over 2 s	$b = 1.7$ $d = 2.0$	$z = -0.8$ $P = 0.41$ (NS)	$b = 1.5$ $d = 0.0$	$z = -2.80$ $P < 0.01$ (**)	$b = 1.7$ $d = 0.3$	$z = -2.80$ $P < 0.01$ (**)
School polarization	Relative orientation of pairs of fish chosen at random (range 0–180°)	$b = 87.0$ $d = 71.3$	$z = -0.15$ $P = 0.88$ (NS)	$b = 83.8$ $d = 21.8$	$z = -2.70$ $P < 0.01$ (**)	$b = 78.5$ $d = 21.2$	$z = -1.99$ $P < 0.05$ (*)

Note: Comparisons performed using the Wilcoxon test for matched pairs with the before and during exposure values making up each pairing. The variables *b* and *d* represent median values before and during exposures, respectively. NS, not significant; *, significant at a 95% confidence level; **, significant at a 99% confidence level.

© 2002 NRC Canada

Fig. 2. (*a*) Time waveform and (*b*) spectral plots of a typical click recorded in the test tank. Measurement taken at 1 m from the speaker with a calibrated hydrophone (Cetacean Research Technology C50a, Seattle, Wash.) and data acquisition equipment (Digidata 1200B, Axon Instruments, Union City, Calif.). Sampling rate 333 kHz. Spectral plot analysis bandwidth 650 Hz.

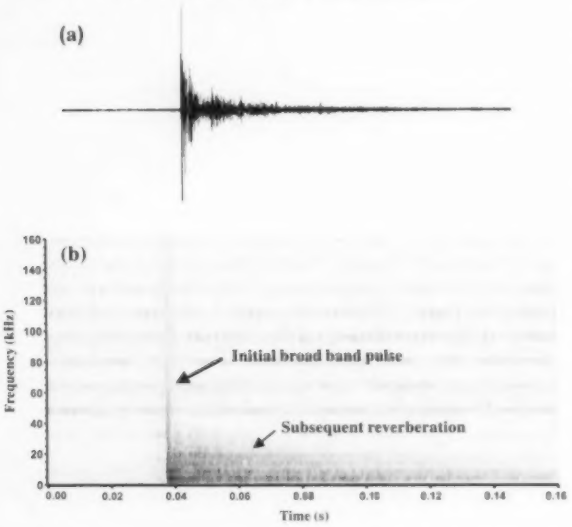

Each minute, the observer recorded their behaviour, specifically the number of schools formed, their estimated depth in the water column, and how many fish were on either side of the tank. Swimming speeds were calculated from the times that the lead fish in the fastest moving school passed between the two gateways on each circuit. The baffle was positioned so that the observer could see the fish at all times and so that the speaker (positioned as experiment 1) was centred on one side of the bisected tank.

In each trial, the behaviour of 10 fish 15 min before and 15 min after each sound exposure was recorded, as well as their behaviour during the transmission period. In the summer of 1999, the three sound types used in experiment 1 were played to 16 groups for durations of 15 min.

In the spring of 2000, five additional sounds were presented to 16 new groups. (D) Regular clicks short: as regular clicks, but played for 3 minutes; (E) increasing amplitude clicks: as regular clicks with a constant inter-click interval of 0.2 s, but clicks sequentially increasing in amplitude; initial clicks began at 130 dB re 1 μPa at 1m and steadily increased to reach 169 dB by the ninth minute and remained at 169 dB for a further 5 min; (F) decreasing amplitude clicks: reversed version of increasing amplitude clicks; (G) variable amplitude clicks: as increasing amplitude clicks, but clicks in random order so that the amplitude of each click was unrelated to those preceding or following; (H) pinger: an acoustic deterrent device (Dukane NetMark 1000), positioned by the speaker, turned on for 15 min. The pinger produced 0.3-s pulses at a peak frequency of 10–11 kHz every 4 s at an SPL of between 133 and 145 dB re 1 μPa at 1 m (Trippel et al. 1999). Batteries were replaced if their output dropped below 6 volts. As with Experiment 1, three versions of each sound exposure were constructed and three different pingers used to reduce any impacts of pseudoreplication (Hopp and Morton 1998).

Experiment 3: repetition of experiment 2 in a free-field environment

Because of the potential impact of the test tank on the acoustic characteristics of the sound exposures, the procedure used in experiment 2 was repeated in a free-field environment in the summer of 2000. A 2.9-m diameter, 1.5-m deep sea cage was constructed from 1-mm net twine (3-cm mesh) and 21-mm plastic hose and suspended in a sheltered inlet off Barkley Sound (Fig. 1*c*). Minimum water depth under the sea pen was 3 m and the bottom was soft mud. The behaviour of the fish was recorded both by a hidden observer and a Hi-8 video camera. Ten separate groups were filmed for 3 min without intervention, then subjected to a 3-min sound exposure of either click trains (n = 3) or regular clicks (n = 7). The speaker used in earlier experiments was held 1 m below the surface and 6 m from the outside of the cage to minimize near-field effects (Enger and Andersen 1967). Subsequent double-blind analyses of the videotape were carried out such that the analyst was unaware of the sound exposure type.

Results

Exposures to odontocete echolocation-type sounds elicited changes in the behaviour of both feeding and nonfeeding fish, whereas the control (electronic silence) and an acoustic deterrent device for marine mammals did not.

Experiment 1: impacts of sound exposures on feeding behaviour

In 1999, 10 separate groups of herring were exposed to sounds while feeding. No measurable changes in behaviour were detected in response to the control sound. The number of strikes at surface food, the number of individuals directly under the food patch, the frequency of sharp changes in direction, and the fishes' relative orientation to one another (polarization) showed no significant difference during exposure to the control sound as compared with before the production of the control sound (Table 1). In contrast, the behaviour of fish changed during the click trains and regular clicks. Some groups severely reduced their feeding activity while all others (8 out of 10 click trains; 7 out of 10 regular clicks) stopped feeding entirely (Fig. 3). Instead, fish appeared to actively school near the bottom of the tank and become more polarized (by converging their swimming trajectories; Fig. 4), turn less frequently, and spend less time in the part of the tank containing the surface food patch (Table 1).

Experiment 2: impacts of sound exposures on nonfeeding behaviour

None of the 1999 treatments (control, click train, or regular click sounds) had any significant impact on the number of schools the fish formed, the proportion of time spent on the with- or without-speaker sides of the tank, or the frequency with which fish changed from clockwise to counterclockwise swimming (Table 2). Neither fast-start startle responses nor the ejection of air bubbles was observed in any of the trials. However, in contrast to the controls, the click

© 2002 NRC Canada

Fig. 3. Frequency with which fish took food from the water surface before and during (*a*) control, (*b*) click train, and (*c*) regular click exposures. Mean ± 1 SE bars shown.

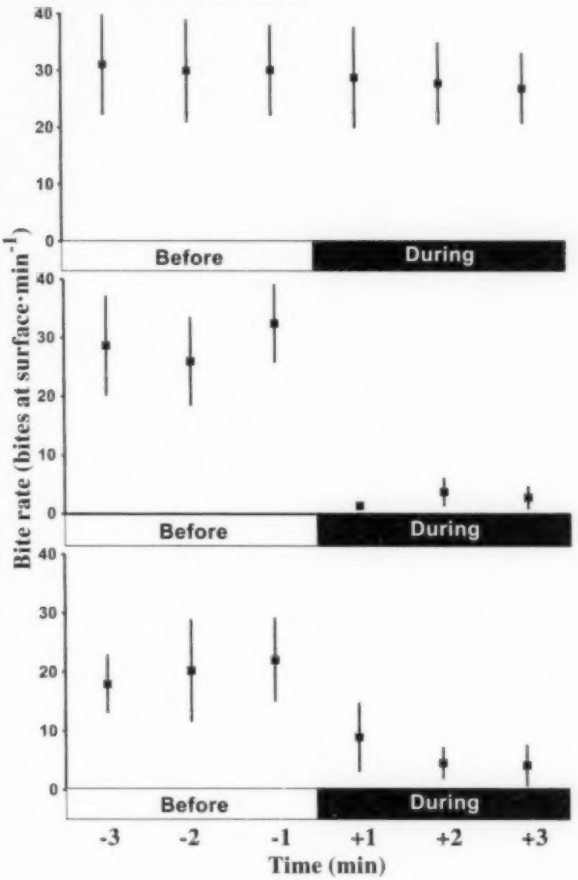

Fig. 4. Group polarisation before (left) and during (right) (*a*) control, (*b*) click train, and (*c*) regular click exposures. Once per minute in each trial, all fish visible on the video screen were assigned numbers and two chosen with a random number table. Their relative orientation to each other (0°, same; 180°, opposite trajectory) was then measured from the screen.

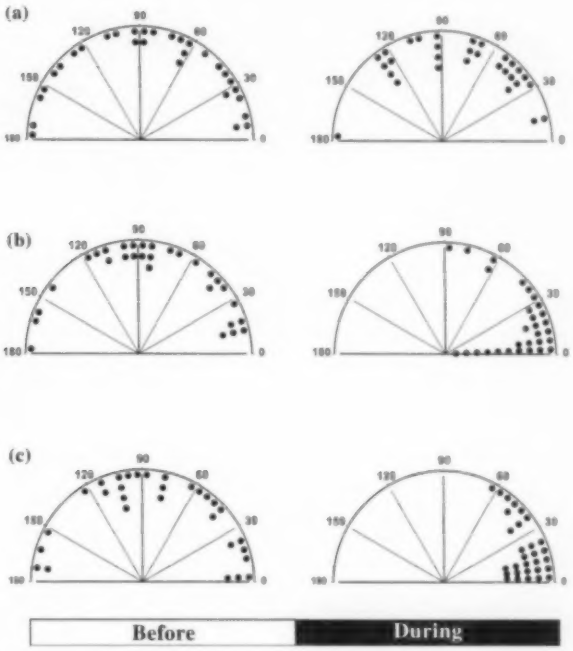

train and regular click exposures had a significant, sustained impact on swimming speeds and depths chosen by the fish (Table 2; Figs. 5*a*–5*c* and 6*a*–6*c*). In response to click trains, the fish increased their swim speeds within a minute of the start of the exposure, reaching peak speeds two minutes later and swimming 1.70 times faster than pretreatment. Swimming speeds during the rest of the exposure gradually declined towards those measured before the treatment. Speeds after the exposure were similar to those before it. The regular clicks elicited a similar response, although the maximal swim speeds were reached more abruptly (within two minutes of the start of the exposure) and the increase was slightly smaller in magnitude (1.45 times pretreatment). Changes in depth were equally dramatic (Fig. 6*a*–6*c*). Within two minutes of the start of the click train and regular click exposures all groups had left the water column to circuit the tank at its bottom. As the exposures continued, groups gradually re-entered the water column and reached pretreatment depths shortly after the exposures finished.

The 3-min exposures to regular clicks in 2000 elicited a similar response to the 15-min exposures to regular clicks; however, the duration of the changes in swim speed and depth differed (compare Figs. 5*c* versus 5*d* and 6*c* versus 6*d*). The elevation in swim speed continued past the end of the 3-min exposures, returning to normal levels approximately 4–5 min later and approximately nine minutes earlier than in the 15-minute exposures. The period of decrease in swimming depth was similarly foreshortened compared with the longer exposures. The magnitude of change in swimming speed was similar between the 3-min (year 2000) and the 15-min (year 1999) trials, at 1.32 versus 1.45 times pretreatment speeds, respectively. However, the actual pretreatment and during-treatment speeds were higher in 2000 (0.53 $m \cdot s^{-1}$) than in 1999 (0.43 $m \cdot s^{-1}$).

The exposures to clicks of varying amplitude, like those of constant amplitude, all had impacts on the swimming speeds and depth choices of the fish (Figs. 5*e*–5*g* and 6*e*–6*g*). The increasing-amplitude click exposures had the smallest impact, producing only minor changes, whereas the decreasing-amplitude click exposures had more effect, particularly in the first few minutes of treatment. The variable amplitude clicks exposures (which were composed of the same clicks as the previous two treatments but in a random order) elicited a major and sustained change in swimming speed (peaking at 1.43× pretreatment speed) and a

© 2002 NRC Canada

Fig. 2. (*a*) Time waveform and (*b*) spectral plots of a typical click recorded in the test tank. Measurement taken at 1 m from the speaker with a calibrated hydrophone (Cetacean Research Technology C50a, Seattle, Wash.) and data acquisition equipment (Digidata 1200B, Axon Instruments, Union City, Calif.). Sampling rate 333 kHz. Spectral plot analysis bandwidth 650 Hz.

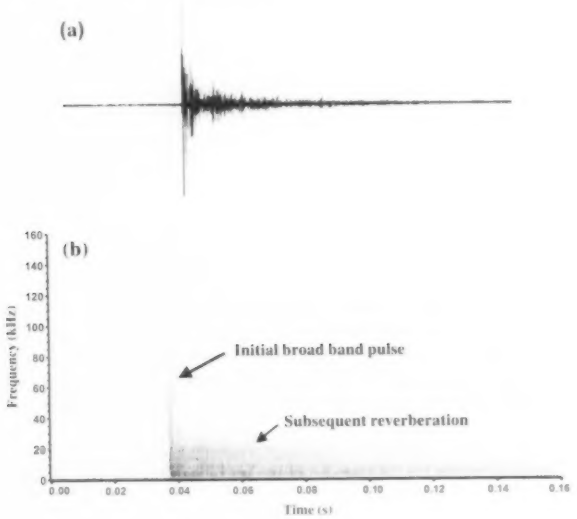

Each minute, the observer recorded their behaviour, specifically the number of schools formed, their estimated depth in the water column, and how many fish were on either side of the tank. Swimming speeds were calculated from the times that the lead fish in the fastest moving school passed between the two gateways on each circuit. The baffle was positioned so that the observer could see the fish at all times and so that the speaker (positioned as experiment 1) was centred on one side of the bisected tank.

In each trial, the behaviour of 10 fish 15 min before and 15 min after each sound exposure was recorded, as well as their behaviour during the transmission period. In the summer of 1999, the three sound types used in experiment 1 were played to 16 groups for durations of 15 min.

In the spring of 2000, five additional sounds were presented to 16 new groups. (D) Regular clicks short: as regular clicks, but played for 3 minutes; (E) increasing amplitude clicks: as regular clicks with a constant inter-click interval of 0.2 s, but clicks sequentially increasing in amplitude; initial clicks began at 130 dB re 1 μPa at 1m and steadily increased to reach 169 dB by the ninth minute and remained at 169 dB for a further 5 min; (F) decreasing amplitude clicks: reversed version of increasing amplitude clicks; (G) variable amplitude clicks: as increasing amplitude clicks, but clicks in random order so that the amplitude of each click was unrelated to those preceding or following; (H) pinger: an acoustic deterrent device (Dukane NetMark 1000), positioned by the speaker, turned on for 15 min. The pinger produced 0.3-s pulses at a peak frequency of 10–11 kHz every 4 s at an SPL of between 133 and 145 dB re 1 μPa at 1 m (Trippel et al. 1999). Batteries were replaced if their output dropped below 6 volts. As with Experiment 1, three versions of each sound exposure were constructed and three different pingers used to reduce any impacts of pseudoreplication (Hopp and Morton 1998).

Experiment 3: repetition of experiment 2 in a free-field environment

Because of the potential impact of the test tank on the acoustic characteristics of the sound exposures, the procedure used in experiment 2 was repeated in a free-field environment in the summer of 2000. A 2.9-m diameter, 1.5-m deep sea cage was constructed from 1-mm net twine (3-cm mesh) and 21-mm plastic hose and suspended in a sheltered inlet off Barkley Sound (Fig. 1*c*). Minimum water depth under the sea pen was 3 m and the bottom was soft mud. The behaviour of the fish was recorded both by a hidden observer and a Hi-8 video camera. Ten separate groups were filmed for 3 min without intervention, then subjected to a 3-min sound exposure of either click trains ($n = 3$) or regular clicks ($n = 7$). The speaker used in earlier experiments was held 1 m below the surface and 6 m from the outside of the cage to minimize near-field effects (Enger and Andersen 1967). Subsequent double-blind analyses of the videotape were carried out such that the analyst was unaware of the sound exposure type.

Results

Exposures to odontocete echolocation-type sounds elicited changes in the behaviour of both feeding and nonfeeding fish, whereas the control (electronic silence) and an acoustic deterrent device for marine mammals did not.

Experiment 1: impacts of sound exposures on feeding behaviour

In 1999, 10 separate groups of herring were exposed to sounds while feeding. No measurable changes in behaviour were detected in response to the control sound. The number of strikes at surface food, the number of individuals directly under the food patch, the frequency of sharp changes in direction, and the fishes' relative orientation to one another (polarization) showed no significant difference during exposure to the control sound as compared with before the production of the control sound (Table 1). In contrast, the behaviour of fish changed during the click trains and regular clicks. Some groups severely reduced their feeding activity while all others (8 out of 10 click trains; 7 out of 10 regular clicks) stopped feeding entirely (Fig. 3). Instead, fish appeared to actively school near the bottom of the tank and become more polarized (by converging their swimming trajectories; Fig. 4), turn less frequently, and spend less time in the part of the tank containing the surface food patch (Table 1).

Experiment 2: impacts of sound exposures on nonfeeding behaviour

None of the 1999 treatments (control, click train, or regular click sounds) had any significant impact on the number of schools the fish formed, the proportion of time spent on the with- or without-speaker sides of the tank, or the frequency with which fish changed from clockwise to counterclockwise swimming (Table 2). Neither fast-start startle responses nor the ejection of air bubbles was observed in any of the trials. However, in contrast to the controls, the click

© 2002 NRC Canada

Fig. 3. Frequency with which fish took food from the water surface before and during (*a*) control, (*b*) click train, and (*c*) regular click exposures. Mean ± 1 SE bars shown.

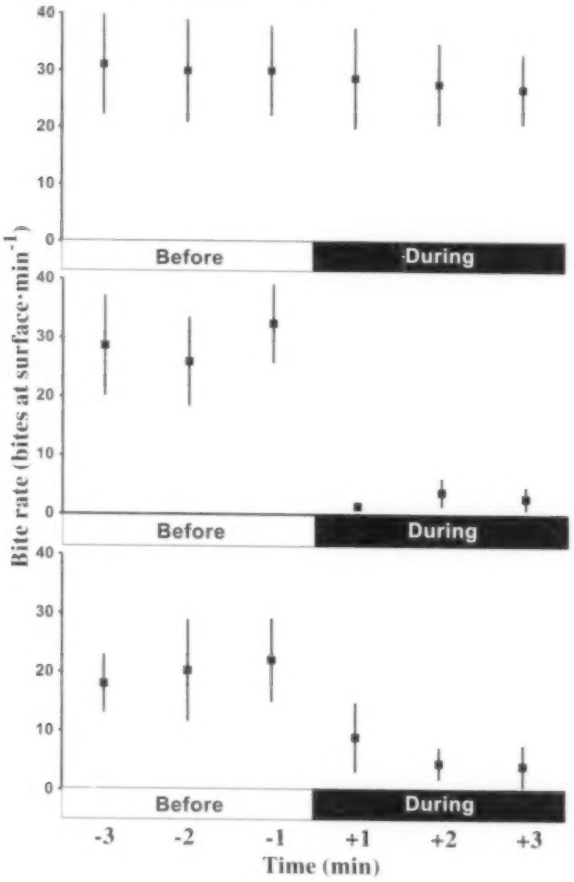

Fig. 4. Group polarisation before (left) and during (right) (*a*) control, (*b*) click train, and (*c*) regular click exposures. Once per minute in each trial, all fish visible on the video screen were assigned numbers and two chosen with a random number table. Their relative orientation to each other (0°, same; 180°, opposite trajectory) was then measured from the screen.

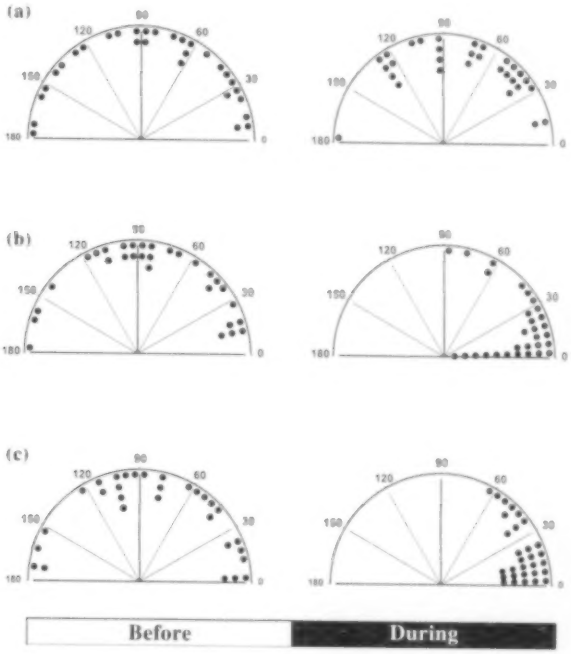

train and regular click exposures had a significant, sustained impact on swimming speeds and depths chosen by the fish (Table 2; Figs. 5*a*–5*c* and 6*a*–6*c*). In response to click trains, the fish increased their swim speeds within a minute of the start of the exposure, reaching peak speeds two minutes later and swimming 1.70 times faster than pretreatment. Swimming speeds during the rest of the exposure gradually declined towards those measured before the treatment. Speeds after the exposure were similar to those before it. The regular clicks elicited a similar response, although the maximal swim speeds were reached more abruptly (within two minutes of the start of the exposure) and the increase was slightly smaller in magnitude (1.45 times pretreatment). Changes in depth were equally dramatic (Fig. 6*a*–6*c*). Within two minutes of the start of the click train and regular click exposures all groups had left the water column to circuit the tank at its bottom. As the exposures continued, groups gradually re-entered the water column and reached pretreatment depths shortly after the exposures finished.

The 3-min exposures to regular clicks in 2000 elicited a similar response to the 15-min exposures to regular clicks; however, the duration of the changes in swim speed and depth differed (compare Figs. 5*c* versus 5*d* and 6*c* versus 6*d*). The elevation in swim speed continued past the end of the 3-min exposures, returning to normal levels approximately 4–5 min later and approximately nine minutes earlier than in the 15-minute exposures. The period of decrease in swimming depth was similarly foreshortened compared with the longer exposures. The magnitude of change in swimming speed was similar between the 3-min (year 2000) and the 15-min (year 1999) trials, at 1.32 versus 1.45 times pretreatment speeds, respectively. However, the actual pretreatment and during-treatment speeds were higher in 2000 (0.53 $m \cdot s^{-1}$) than in 1999 (0.43 $m \cdot s^{-1}$).

The exposures to clicks of varying amplitude, like those of constant amplitude, all had impacts on the swimming speeds and depth choices of the fish (Figs. 5*e*–5*g* and 6*e*–6*g*). The increasing-amplitude click exposures had the smallest impact, producing only minor changes, whereas the decreasing-amplitude click exposures had more effect, particularly in the first few minutes of treatment. The variable amplitude clicks exposures (which were composed of the same clicks as the previous two treatments but in a random order) elicited a major and sustained change in swimming speed (peaking at 1.43× pretreatment speed) and a

© 2002 NRC Canada

Table 2. Impacts of sound exposures (1999) and pinger (2000) on nonfeeding fish (n = 16).

Activity	Measure used	Control		Click trains		Regular clicks		Pinger	
No. of schools	No. of schools made by the 10 fish each minute	b = 1.0 d = 1.1	z = –1.07 P = 0.28 (NS)	b = 1.2 d = 1.3	z = –0.06 P = 0.95 (NS)	b = 1.2 d = 1.2	z = –0.77 P = 0.44 (NS)	b = 1.1 d = 1.1	z = –1.25 P = 0.21 (NS)
Avoidance of speaker	No. of fish each minute on non-speaker side of tank	b = 5.2 d = 5.1	z = –0.70 P = 0.49 (NS)	b = 5.0 d = 5.0	z = –0.88 P = 0.38 (NS)	b = 5.3 d = 4.8	z = –0.96 P = 0.34 (NS)	b = 4.9 d = 5.5	z = –0.54 P = 0.59 (NS)
Reversals in direction	Switches between clockwise and counter-clockwise swimming	tb = 13 td = 7	z = –0.84 P = 0.40 (NS)	tb = 7 td = 12	z = –1.18 P = 0.24 (NS)	tb = 15 td = 12	z = –0.34 P = 0.74 (NS)	tb = 3 td = 2	z = –0.44 P = 0.65 (NS)
Swimming speed	Time between gateways (converted to m·s^{-1})	b = 0.3 d = 0.2	z = –0.70 P = 0.48 (NS)	b = 0.2 d = 0.4	z = –2.74 P < 0.01 (**)	b = 0.3 d = 0.4	z = –3.39 P < 0.001 (**)	b = 0.5 d = 0.4	z = –0.31 P = 0.76 (NS)
Depth	Water column depth each minute (measured from tank bottom)	b = 1.4 d = 1.6	z = –1.6 P = 0.12 (NS)	b = 1.6 d = 1.0	z = –3.29 P = 0.001 (**)	b = 1.5 d = 1.1	z = –2.97 P < 0.005 (**)	b = 1.5 d = 1.7	z = –1.60 P = 0.11 (NS)

Note: Before and during exposure values were compared using the Wilcoxon test for matched pairs. The variables b and d represent median values before and during exposures, tb and td represent total numbers of reversals before and during, respectively. NS, not significant; **, significant at a 99% confidence level.

change in depth similar to the decreasing amplitude exposures.

The pinger had no demonstrable impact on the number of schools the fish formed, the proportion of time spent on either the with- or without-pinger sides of the tank, the frequency with which fish changed from clockwise to counterclockwise swimming, their swimming speed, or the depth they chose (Table 2; Figs. 5*h* and 6*h*).

Experiment 3: repetition of experiment 2 in a free-field environment

Ten groups with 10 fish in each were exposed to either click trains (n = 3) or regular click trials (n = 7) in the tethered net pen during the summer of 2000. As with the indoor tank experiments, fish swam significantly faster during the 3-min exposures than during the 3 min preceding the tests (median before = 0.16; median during = 0.22 m·s^{-1} (an increase of 1.36×), Wilcoxon test for matched pairs z = –2.803, P < 0.005, n = 10) and positioned themselves significantly deeper in the net pen (z = –2.80, P < 0.01). Again, no fast-start startle responses or bubble releases were observed. No tendencies to avoid the side of the pen nearest the speaker were apparent to the observer at the time or on reviewing the videotapes.

Discussion

These experiments have shown that Pacific herring do respond to broadband echolocation-type click sounds. The responses observed were both simple and overall relatively subtle. Feeding fish ceased striking at prey and took up more typical schooling behaviour, whereas already schooling fish increased both their swimming speed and their depth. The fish showed the ability to alter the magnitude of their response depending on the nature of the sound exposure. For example, clicks of variable amplitude produced a greater overall change in swim speed than the same clicks played in either increasing or decreasing amplitude order. Changes in swim speed for all trials typically represented an increase of between 130 and 170% compared with pre-exposure speeds. All swimming speeds, both before and during exposures, were cruising speeds sustainable over considerable periods for herring of this size (Blaxter and Dickson 1959). The durations of the speed elevations and depth increases were also variable and related to the duration of the exposure. The increase in swim speed and increase in depth resulting from the 3-min exposures lasted longer than the exposures themselves, but the swim speeds were not sustained throughout the 15-min exposures. However, the decay of elevated swimming speeds during the longer exposures does not appear to have signified exhaustion. Their close relationship with the types of exposure received rather than any particular duration or distance swum suggests a behavioural rather than energetic cause. Furthermore, the changes in depth were unlikely to require significant energetic expenditure but still returned to more normal levels during longer exposures suggesting either habituation or gradual abandonment of the response despite continued stimulation.

Although the feeding fish left the food patch during exposures, no avoidance of the speaker or its vicinity in either the indoor tank or net pen was observed. In the net pen, the predominant signal received by the fish would have been in the

© 2002 NRC Canada

Fig. 5. Swim speeds of nonfeeding fish before (open bar), during (solid bar), and after (open bar) exposures. The sound type is indicated in the solid bar. Mean ± 1 SE bars shown, n = 16 for each.

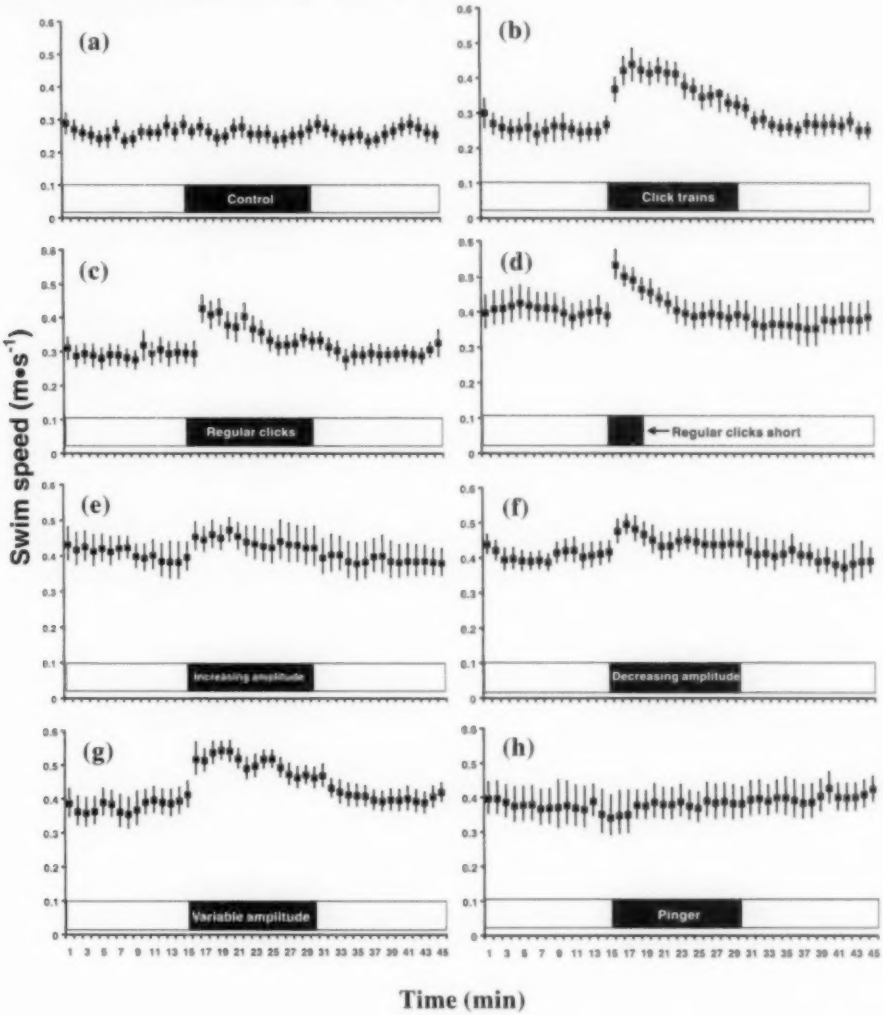

far-field and therefore potentially given them little directional information, however the absence of some spatial response in the indoor tank is somewhat surprising. On circuiting, fish would pass within at least 2.5 m of the speaker, usually nearer, and therefore potentially gain near-field stimulation with consequent directional information. However, their consistent swim speeds on the with- and without-speaker sides of the tank and their lack of increased turning suggests that they used a tactic of simply increasing speed. Furthermore, the similarity of results between the net pen and indoor tank suggests that near field and amplitude gradients were not essential components to elicit the responses observed.

The behavioural changes detected with exposures to odontocete-type echolocation sounds bear similarities with those found for anthropogenic sounds in other herring studies. Downward movements are reported almost universally both in enclosure and at-sea studies. Reported descent rates are generally rapid (up to 0.7–1 $m \cdot s^{-1}$), decrease with increasing depth, and can take fish from surface waters to as deep as 150 m (Olsen et al. 1983; Misund and Aglen 1992; Pitcher et al. 1996). However, Pitcher et al. (1996) noted that a downward movement in herring schools was not a response to all threats. Individual attacking cod and haddock did not elicit downward flight, whereas an approaching research vessel and a suspected school of saithe did.

Changes in swim speeds may be more common than reported. Avoidance responses are often described whereby fish appear to leave an area on commencement or approach of a stimulus. However, such a response need not actually require active avoidance. Hering (1969), for example, reported that escaping herring chose a direction to swim in and then kept it even if the heading took them directly toward the aversive stimulus. Thus, simply by increasing swim

© 2002 NRC Canada

Fig. 6. Swimming depths of nonfeeding fish before (open bar), during (solid bar), and after (open bar) exposures. The sound type is indicated in the solid bar. Mean ± 1 SE bars shown, n = 16 for each. Fish depth was recorded on each circuit and ascribed to bins (bottom, bottom–middle, middle, etc.). 1 represents the tank bottom and 3 represents the surface.

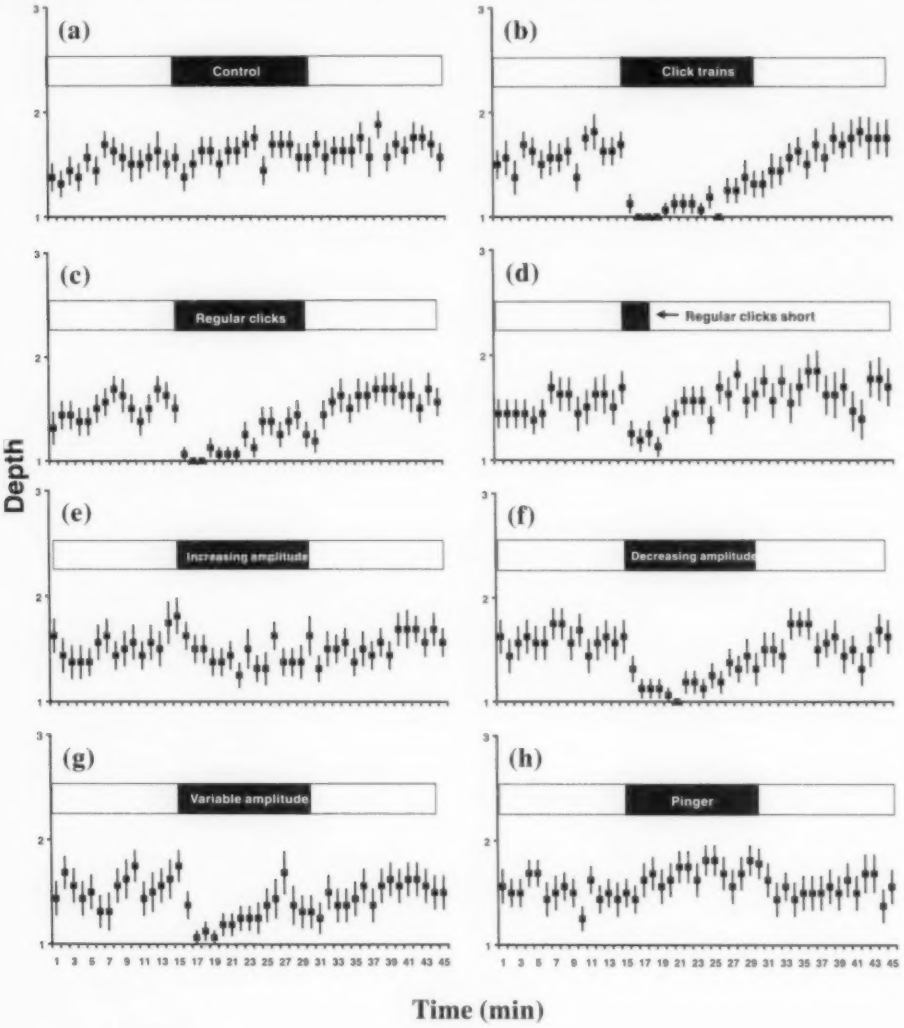

speeds and maintaining a straight trajectory, schools of fish receiving an acoustic stimulus would move horizontally and thus frequently appear to avoid a fixed or moving sound source. The increase in swim speed as a result of the 15-min variable amplitude click sound exposure in this study, for example, would have taken the average school of fish horizontally an extra 140 m. The duration of interactions and their consequent flight distances are likely to be shorter. In real fisheries interactions, a straight horizontal flight along random headings by ensonified fish would reduce the numbers occurring directly in the path of a net or sonar beam. A simple mechanism such as this could explain many of the "avoidance" responses that have been documented (Misund et al. 1996; Suuronen et al. 1997). Frequently, these events have been detected using ultrasonic echosounders. The recently discovered high-frequency hearing capabilities of clupeoids and their potential responses to transient sounds containing high frequencies could imply that the impacts of the echosounders themselves (rather than just the low frequencies produced by engines, warps, etc.) need to be considered. In a recent case where herring avoidance of a survey vessel was thought to have been disproven (Fernandes et al. 2000), the presence of the same echosounders (producing 38-kHz signals) on both the ship and the control appears to have been overlooked.

The absence of fast-start escape responses (Blaxter and Hoss 1981), fountain effects (Hall et al. 1986), or bubble emissions (Nøttestad 1998) in any of the experiments performed in this study suggest that the sound stimuli were not perceived as a sign of imminent danger (Astrup 1999). This raises the question of what evolutionary force could have driven the development of the subtler, potentially long-range

© 2002 NRC Canada

responses observed. No matter how appropriate, these behaviours have clearly not evolved in response to human-related fishing activities (MacLennan and Simmonds 1992). Their being a tactic to avoid predation from echolocating odontocetes has historically been excluded as a possibility (Bone and Marshall 1982), but has more recently gained interest and credibility (Mann et al. 1997; Astrup 1999). Odontocete echolocation systems bear similarities with man-made ship mounted sonar systems. Their sounds are predominantly high in frequency (ship, 0.4–500 kHz; cetacean 0.3–325 kHz), short in duration (ship, 1 µs to 1 s; cetacean 40 µs to 0.6 ms), and loud (ship, 180–230+ dB; cetacean, 135–230 dB re 1 µPa at 1 m; Richardson et al. 1995). Sonar beams from ships may be directed forward, downward or to the side, whereas odontocete biosonar sounds are directed forward.

For odontocetes hunting relatively small prey a tiny portion of their outgoing sounds return as echoes. The discrepancy between the intensity of the outgoing sound and the returning echoes produces a potential zone ahead of the hunting cetacean where prey sensitive to the appropriate frequencies can hear the echolocation sounds, but if their own acoustic reflectivity is small enough, will not provide echoes loud enough to be detectable to the odontocete (Astrup 1999). The nature of this zone is dependent on the hearing sensitivities of both the prey and the odontocete and the prey target strength. The existence of this spatio-temporal window may offer the opportunity for prey to escape before being perceived by the predator. We suggest that the avoidance responses observed in this and previous studies of clupeoid behaviour may represent just such an adaptation. The cessation of feeding, adoption of polarised schooling, and increases in swim-speed coupled with a lack of turning would help fish overtaken by the outer fringes of a hunting odontocete's sonar beam to move away before entering the zone where their own echoes would be detectable to the echolocator. Clearly, directional hearing capabilities would help fish take an optimal path of escape. However, even without accurate information on the bearing of the sound source, simply increasing speed in any direction would potentially help many schools dodge the relatively narrow sonar beam (<50°, Au 1993) operated by odontocete cetaceans. Similarly, changes in depth (either ascending or descending) could take fish out of the equally narrow vertical beam. Upward avoidance movements appear rare in clupeoids but downward trajectories are common and would be especially beneficial against air-breathing predators, such as odontocetes. By diving down, the fish would effectively increase the energetic costs of foraging for their predators and therefore encourage them to switch to shallower schools or other prey items (Boyd 1997). Furthermore, by descending, the increased pressure would reduce the fishes' swimbladder cross-sectional area and so reduce their own target strength (Ona 1990) thereby increasing their window of opportunity for undetected escape.

A situation where the active detection systems of the predator potentially provide information and possibilities of escape to prey is not unique. A similar but better-understood interaction occurs between echolocating bats and nocturnal insects, notably moths. As with other longstanding predator–prey dynamics, both parties appear to have engaged in an arms race with the evolution of a diverse array of tactics and counter-tactics (e.g., Fenton et al. 1998). A similar dynamic might have shaped the behaviour we observe today of both the fish and odontocetes. As with bats, different odontocete species produce echolocation clicks with different characteristics. Small delphinids from the genus *Cephalorhynchus* as well as the phocoenids (porpoises) produce convergent narrowband, high-frequency echolocation clicks centred between 110 and 140 kHz (Au 1993). It may prove fruitful in trying to understand why such narrow-band characteristics have been selected to specifically investigate what impact such precise sounds (in comparison to the broadband sounds used in this study) have on their preferred prey (often clupeoid fish). In addition to the characteristics of the echolocation sounds themselves, foraging behaviour in odontocetes is diverse and potentially reflective of the capabilities of their prey. For example, killer whales (*Orcinus orca*) hunting salmon echolocate for significantly more time than those feeding on marine mammals, probably because of the differing auditory abilities of salmonids and mammals (Barrett-Lennard et al. 1996). As clupeoid fish appear more similar to the latter in auditory ability, we might predict that whales searching for clupeoids use their echolocation more sparingly or differently than they do with other fish species. In any case, it is clear from the literature that the behaviour of prey has too frequently been ignored when trying to understand the foraging patterns and capabilities of cetaceans. Further, by understanding what strategies odontocetes might use to detect fish capable of detecting their own sounds, we may gain insight into methods to improve our own techniques to estimate abundance and to capture acoustically sensitive fish species.

The absence of a measurable response to the acoustic deterrent device (pinger) used in this study is interesting. Firstly, it suggests that not all noises produce the behavioural responses observed for the clicks. Secondly, it makes the significant (at the $P < 0.01$ level) reduction of herring catch in fishing nets equipped with similar pingers in the Kraus et al. (1997) sea trial even more curious. In attempting to explain the absence of a repeatable result during a similar trial in an adjacent sea area, Trippel et al. (1999) suggested that the longer deployment of pingers in the Kraus et al. (1997) study might have drained the batteries. This could have led to pingers that produced lower than normal frequency sounds and hence pushed the frequency away from a null in the clupeoid bimodal hearing range. Although feasible and relatively testable, it seems unlikely however that increased soak time and consequent gradual battery decline could lead to the 85% reduction in catch. Another possibility is that ambient noise levels could have differed between studies and thus raised or lowered the pinger signals either side of background. The ambient noise levels in the indoor tank in the current study proved too low to measure effectively, but were likely to be lower or at worst comparable with those experienced at sea. Furthermore, the proximity of the fish to the pinger (always less than 7 m) makes it unlikely that the pingers were less audible to the fish in this study than in the Kraus et al.'s (1997) sea trial. Therefore, the differences between these studies remain unexplained; however, because our detailed knowledge of the high-frequency hearing abilities of clupeoids are currently limited to just one species (the American shad; Mann et al. 1997), a better understanding of the auditory abilities of other members of the suborder, particularly the commercially and eco-

© 2002 NRC Canada

nomically important Atlantic and Pacific herring, would be extremely valuable. Among many other applications, such information coupled with behavioural studies would aid design of marine mammal acoustic deterrent devices for fishing nets that do not impact catches of clupeoids. Alternatively, if these fish were not the target, such information could aid the design of devices that both reduced unwanted bycatch of marine mammals and clupeoids.

Acknowledgements

The authors are indebted to Alex Fraser, Tom Greenacre (Dukane Corporation), Kristina Swerhun, Lisa Walker, Nathan Webb, Darren Witt, the crew of the *Ocean Provider* and the Bamfield Volunteer Fire Department for their skilled assistance with tanks, fish, and loan of equipment. We thank Carl Schilt, Sonam Bennett-Vasseux, Tara Law, and two anonymous reviewers for comments on the text. This work was carried out with the financial assistance of the U.K.'s Leverhulme Trust, the Natural Sciences and Engineering Research Council (NSERC Canada grant A6869 to L.M.D.) and a Bamfield Marine Sciences Centre Research Associate Award. Herring were caught under licence issued to the BMSC pursuant to the Canadian Fisheries Act RSC-1985 and held according to Canadian Council of Animal Care rules, under permit SFU 541B.

References

Astrup, J. 1999. Ultrasound detection by fish – a parallel to the sonar-mediated detection of bats by ultrasound-sensitive insects? Comp. Biochem. Physiol. A, **124**: 19–27.

Au, W.L. 1993. The sonar of dolphins. Springer-Verlag, New York, N.Y.

Barrett-Lennard, L.G., Ford, J.K.B., and Heise, K.A. 1996. The mixed blessing of echolocation: differences in sonar use by fish-eating and mammal-eating killer whales. Anim. Behav. **51**: 553–565.

Blaxter, J.H.S., and Dickson, W. 1959. Observations on the swimming speeds of fish. J. Cons. Int. Explor. Mer, **24**: 472–479.

Blaxter, J.H.S., and Hoss, D.E. 1981. Startle response in herring: the effect of sound stimulus frequency, size of fish, and selective interference with the acoustico-lateralis system. J. Mar. Biol. Assoc. U.K., **61**: 871–879.

Blaxter, J.H.S., Gray, J.A.B., and Denton E.J. 1981. Sound and startle response in herring shoals. J. Mar. Biol. Assoc. U.K., **61**: 851–869.

Bone, Q., and Marshall, N.B. 1982. Biology of fishes. Blackie, Glasgow, Scotland.

Boyd, I.L. 1997. The behavioural and physiological ecology of diving. TREE, **12**: 213–217.

Enger, P.S., and Andersen, R. 1967. An electrophysiological field study of hearing in fish. Comp. Biochem. Physiol. **22**: 517–525.

Fenton, M.B., Portfors, C.V., Rautenbach, I.L., and Waterman, J.M. 1998. Compromises: sound frequencies used in echolocation by aerial-feeding bats. Can. J. Zool. **76**: 1174–1182.

Fernandes, P.G., Brierley, A.S., Simmonds, E.J., Millard, N.W., McPhail, S.D., Armstrong, F., Stevenson, P., and Squires, M. 2000. Fish do not avoid survey vessels. Nature (London), **404**: 35–36.

Gerlotto, F., and Freon, P. 1988. Influence of the structure and behaviour of fish schools on acoustic assessment. ICES CM 1988/B:53.

Hall, S.J., Wardle, C.S., and Maclennan, D.N. 1986. Predator evasion in a fish school – test of a model for the fountain effect. Mar. Biol. **91**: 143–148.

Hering, G. 1969. Avoidance of acoustic stimuli by the herring. Int. Counc. Explor. Sea. ICES CM 1969/H:18. pp. 1–8.

Hopp, S.L., and Morton, E.S. 1998. Sound playback studies. *In* Animal acoustic communication: sound analysis and research methods. *Edited by* S.L. Hopp, M.J. Owren, and C.S. Evans. Springer-Verlag, Berlin, Germany. pp. 323–352.

Kraus, S.D., Read, A.J., Solow, A., Baldwin, K., Spradlin, T., Anderson, E., and Williamson, J. 1997. Acoustic alarms reduce porpoise mortality. Nature (London), **388**: 525.

MacLennan, D.N., and Simmonds, E.J. 1992. Fisheries acoustics. Chapman and Hall, London.

Mann, D.A., Lu, Z., and Popper, A.N. 1997. A clupeid fish can detect ultrasound. Nature (London), **389**: 341.

Mann, D.A., Lu, Z., Hastings, M.C., and Popper, A.N. 1998. Detection of ultrasonic tones and simulated dolphin echolocation clicks by a teleost fish, the American shad (*Alosa sapidissima*). J. Acoust. Soc. Am. **104**: 562–568.

Misund, O.A., and Aglen, A. 1992. Swimming behaviour of fish schools in the North Sea during acoustic surveying and pelagic trawl sampling. ICES J. Mar. Sci. **49**: 325–334.

Misund, O.A., Ovredal, J.T., and Hafsteinsson, M.T. 1996. Reactions of herring schools to the sound field of a survey vessel. Aquat. Living Resour. **9**: 5–11.

Mitson, R.B. 1995. Underwater noise of research vessels: review and recommendations. ICES Co-op. Res. Rep. **209**: 1–61.

Mohr, H. 1971. Behaviour patterns of different herring stocks in relation to ship and midwater trawl. *In* Modern fishing gear of the world. Vol. 3. *Edited by* H. Kristjonsson. Fishing News (Books) Ltd., London. pp. 368–371.

Nestler, J.M., Ploskey, G.R., Pickens, J., Menezes, J., and Schilt, C. 1992. Responses of blueback herring to high-frequency sound and implications for reducing entrainment at hydropower dams. N. Am. J. Fish. Manag. **12**: 667–683.

Nøttestad, L. 1998. Extensive gas bubble release in Norwegian spring-spawning herring (*Clupea harengus*) during predator avoidance. ICES J. Mar. Sci. **55**: 1133–1140.

Olsen, K. 1971. Influence of vessel noise on behaviour of herring. *In* Modern fishing gear of the world. Vol. 3. *Edited by* H. Kristjonsson. Fishing News (Books) Ltd., London. pp. 291–294.

Olsen, K. 1976. Evidence for localization of sound by fish schools. *In* Sound reception in fish. *Edited by* A. Schuijf and A.D. Hawkins. Elsevier Science Publishers, Amsterdam. pp. 257–270.

Olsen, K., Angell, J. Pettersen, F., and Løvik A. 1983. Observed fish reactions to a surveying vessel with special reference to herring, cod, capelin and polar cod. FAO Fish. Rep. **300**: 131–138.

Ona, E. 1990. Physiological factors causing natural variations in acoustic target strength of fish. J. Mar. Biol. Assoc. U.K., **70**: 107–127.

Pitcher, T.J., Misund, O.A., Ferno, A., Totland, B., and Melle,V. 1996. Adaptive behaviour of herring schools in the Norwegian Sea as revealed by high-resolution sonar. ICES J. Mar. Sci. **53**: 449–452.

Richardson, W.J., Greene, C.R., Malme, C.I., and Thomson, D.H. 1995. Marine mammals and noise. Academic Press, San Diego.

Ross, Q.E., Dunning, D.J., Menezes, J.K., Kenna, M.J., and Tiller, G. 1996. Reducing impingement of alewives with high-frequency sound at a power plant intake on Lake Ontario. N. Am. J. Fish. Manag. **16**: 548–559.

Schwarz, A.L., and Greer, G.L. 1984. Responses of Pacific herring, *Clupea harengus pallasi*, to some underwater sounds. Can. J. Fish. Aquat. Sci. **41**: 1183–1192.

© 2002 NRC Canada

Suuronen, P., Lehtonen, E., and Wallace, J. 1997. Avoidance and escape behaviour of herring encountering midwater trawls. Fish. Res. **29**: 13–24.

Trippel, E.A., Strong, M.B., Terhune, J.M., and Conway, J.D. 1999. Mitigation of harbour porpoise (*Phocoena phocoena*) by-catch in the gillnet fishery in the lower Bay of Fundy. Can. J. Fish. Aquat. Sci. **56**: 113–123.

© 2002 NRC Canada

Factors regulating nitrification in aquatic sediments: effects of organic carbon, nitrogen availability, and pH

Eric A. Strauss, Nicole L. Mitchell, and Gary A. Lamberti

Abstract: We investigated the response in nitrification to organic carbon (C) availability, the interactive effects of the C: nitrogen (N) ratio and organic N availability, and differing pH in sediments from several streams in the upper midwestern United States. In addition, we surveyed 36 streams to assess variability in sediment nitrification rates. Labile dissolved organic carbon (DOC) additions of 30 mg C·L^{-1} (as acetate) to stream sediments reduced nitrification rates ($P < 0.003$), but lower concentration additions or dilution of ambient DOC concentration had no effect on nitrification. C:N and organic N availability strongly interacted to affect nitrification ($P < 0.0001$), with N availability increasing nitrification most at lower C:N. Nitrification was also strongly influenced by pH ($P < 0.002$), with maximum rates occurring at pH 7.5. A multiple regression model developed from the stream survey consisted of five variables (stream temperature, pH, conductivity, DOC concentration, and total extractable NH_4^+) and explained 60% of the variation observed in nitrification. Our results suggest that nitrification is regulated by several variables, with NH_4^+ availability and pH being the most important. Organic C is likely important at regulating nitrification only under high environmental C:N conditions and if most available C is relatively labile.

Résumé : Nous avons étudié la nitrification en fonction de la disponibilité du carbone organique (C), les effets interactifs du rapport C:N et de la disponibilité de l'azote organique (N) ainsi que les différences de pH dans les sédiments de plusieurs cours d'eau du Midwest supérieur des États-Unis. De plus, nous avons inventorié 36 cours d'eau pour déterminer la variabilité des taux de nitrification dans les sédiments. L'addition de carbone organique dissous (DOC) labile à raison de 30 mg C·L^{-1} (sous forme d'acétate) aux sédiments des cours d'eau réduit les taux de nitrification ($P < 0{,}003$), mais l'addition de concentrations moindres ou la dilution des concentrations ambiantes de DOC restent sans effet sur la nitrification. Le rapport C:N et la disponibilité de N organique interagissent fortement pour affecter la nitrification ($P < 0{,}0001$) et c'est aux valeurs inférieures du rapport C:N que la disponibilité de N agit le plus sur la nitrification. La nitrification est aussi fortement influencée par le pH ($P < 0{,}002$), avec un taux maximal qui se situe à pH 7,5. Un modèle de régression multiple élaboré à partir des inventaires des cours d'eau contient cinq variables (température du cours d'eau, pH, conductivité, concentration de DOC et NH_4^+ total extractible) et explique 60% de la variation observée dans la nitrification. Il apparaît donc que la nitrification est contrôlée par plusieurs variables, dont les plus importantes sont la disponibilité de NH_4^+ et le pH. Le C organique n'a probablement de rôle important à jouer dans le contrôle de la nitrification que lorsque le rapport C:N dans l'environnement est élevé et que la plus grande partie du C disponible est relativement labile.

[Traduit par la Rédaction]

Introduction

Understanding the natural cycling of nitrogen (N) in freshwater ecosystems is of key importance, because N is an essential component of proteins, enzymes, and other biologically important compounds. Furthermore, low N availability can limit primary productivity, whereas excess N has been linked to eutrophication and health concerns (Carpenter et al. 1998). Great progress has been made in understanding N cycling in aquatic ecosystems (reviewed by Duff and Triska 2000), but many gaps in our knowledge persist. For example, a firm understanding of the factors regulating certain transformations, such as nitrification, remains elusive.

Nitrification, the chemoautotrophic conversion of NH_4^+ to NO_3^-, is a key transformation in the N cycle because it is the only natural process by which NH_4^+ can be converted to NO_3^-. Excess NO_3^- is an aquatic pollutant and a potential health risk. Furthermore, NO_3^- is an initial substrate for denitrification, the reduction of oxidized N forms (NO_3^-, NO_2^-, NO, or N_2O) to N_2. Because of the common link (NO_3^-) between nitrification and denitrification, these processes may be coupled (i.e., localized denitrification rates are dependent upon the NO_3^- produced by nearby nitrifying bacteria) (Duff and Triska 2000). Thus, a better understand-

Received 31 July 2001. Accepted 27 February 2002. Published on the NRC Research Press Web site at http://cjfas.nrc.ca on 17 April 2002.
J16470

E.A. Strauss,[1,2] N.L. Mitchell, and G.A. Lamberti. Department of Biological Sciences, University of Notre Dame, Notre Dame, IN 46556-0369, U.S.A.

[1]Corresponding author (e-mail: eric_strauss@usgs.gov).
[2]Present address: U.S. Geological Survey, Upper Midwest Environmental Sciences Center, 2630 Fanta Reed Road, La Crosse, WI 54603, U.S.A.

 DOI: 10.1139/F02-032 © 2002 NRC Canada

ing of the spatial and temporal patterns of nitrification in aquatic sediments can provide insight into observed denitrification patterns and eventual losses of N from ecosystems.

Previous studies in freshwater systems have suggested that nitrifying bacteria and nitrification rates in general may be regulated by several factors including NH_4^+ availability (Triska et al. 1990) or ammonification of organic matter (Jones et al. 1995), oxygen concentration (Triska et al. 1990; Kemp and Dodds 2001), and organic carbon (C) availability (Strauss and Dodds 1997; Strauss and Lamberti 2000). Nitrifying bacteria are autotrophic organisms, i.e., they utilize CO_2 (not organic C) as a C source; however, our previous research has resulted in the hypothesis that increases in organic C levels could reduce or even inhibit nitrification depending on the C concentration and source (Strauss and Lamberti 2000). Heterotrophic bacteria apparently can outcompete nitrifying bacteria for NH_4^+ when its availability is low and organic C is not limiting. Labile organic C also may be able to elicit a stronger negative effect on nitrification than more refractory C (Strauss and Lamberti 2002). To date, the only natural system in which the relationship between organic C and nitrification has been examined is for a northern Indiana stream (Strauss and Lamberti 2000, 2002). It is unknown whether or not such a relationship exists in other aquatic systems. Many studies have identified organic matter as a mineralizable source of NH_4^+ for nitrification (Duff and Triska 2000), but it is unclear if C content, N content, and C:N (total organic C : total N) of the organic matter can interact to affect nitrification rates.

Furthermore, few studies have examined how various factors regulate nitrification over a large spatial scale. One study of several sites in the Rhone River estuary (Mediterranean Sea) found that NH_4^+ availability alone accounted for 74% of the variability in nitrification rates (Bianchi et al. 1999). However, we are unaware of any study that has examined variables regulating nitrification rates across several distinct aquatic systems.

Our overall goal in this study was to quantify spatial variability in nitrification in stream sediments and explore factors potentially responsible for that variability. Specifically, we first tested if organic C, C:N, N availability, and pH regulate lotic nitrification by conducting a series of laboratory experiments using sediments and water from a variety of streams. Second, we measured sediment nitrification rates for 36 streams in Wisconsin and Michigan, and related rates to other physical and chemical variables that could influence nitrification.

Materials and methods

Dissolved organic carbon addition and reduction experiments

In July 1998, we tested the effect of dissolved organic carbon (DOC) on nitrification for six "focal" streams (Mill Creek, Pelton Creek, Scott and Howe Creek, Star Creek, Tamarack Creek, and Tenderfoot Creek) located in northern Wisconsin or the Upper Peninsula of Michigan (Fig. 1), which had different physical and chemical characteristics (Table 1). Three streams (Mill, Star, and Tenderfoot) were lake outlets and were sampled within 3 km of their source. The other three streams were sampled in forested areas and either drained wetlands (Pelton and Tamarack) or upland forest (Scott and Howe). One characteristic that all six streams shared was a relatively high DOC concentration (DOC > 10 mg $C \cdot L^{-1}$, Table 1) when compared with a global average of approximately 5 mg $C \cdot L^{-1}$ (Sedell and Dahm 1990). However, high DOC is typical of streams, rivers, and lakes in this geographic region (Gergel et al. 1999).

Initial nitrification rates were determined for each stream using the nitrapyrin method previously described in detail by Strauss and Lamberti (2000). Unfiltered stream water and sieved (0.64 cm) sediment were collected at each site and returned to the laboratory and stored in the refrigerator at 4°C. Sediments were collected in the mid-channel region of each stream and consisted of either a silt–sand (Pelton and Tenderfoot) or a sand–gravel mixture (Mill, Star, Tamarack, Scott, and Howe). Particulate organic matter was not abundant in any of the streams at the time of sampling. Within 24 h, nitrification incubations were started on four replicate samples for each stream. Each replicate consisted of two flasks, each containing 25 mL sediment and 85 mL stream water. Nitrification was inhibited in one flask by adding 10 mg $\cdot L^{-1}$ nitrapyrin (C-1930, Sigma Chemical Co. St. Louis, Mo.). Because nitrapyrin is not soluble in water, it was dissolved in dimethyl sulfoxide (DMSO) before addition. The other flask received DMSO only as a control. Neither flask received an NH_4^+ amendment. The flasks were then incubated at 23°C (mean temperature of streams) in the dark for three days on an orbital shaker (175 rpm). Dissolved oxygen (DO) and pH were measured for each replicate at the beginning and end of the incubation to identify potential shifts in environmental conditions. Flask contents were homogenized with vigorous shaking and subsamples removed at the beginning and end of the incubation, from which NH_4^+ was extracted using 1 M KCl. Nitrification rates over the incubation period were calculated by subtracting the observed mass change of total extractable NH_4^+ in the flasks containing only DMSO from the NH_4^+ increase in the flasks that contained nitrapyrin, which blocked ammonium oxidation.

In the DOC addition experiment, we added a labile C source, sodium acetate, at four C concentrations (0 (control), 2, 10, and 30 mg $C \cdot L^{-1}$) to flasks containing stream sediment (25 mL, sieved to < 0.64 cm) and unfiltered stream water (85 mL). Nitrification rates were measured as described above for four replicates of each of 24 treatment combinations (6 streams × 4 C concentrations).

In the DOC reduction experiment, we added 85 mL of undiluted or diluted (10%, 50%, or 80% diluted) stream water to flasks containing sediments (25 mL, sieved to <0.64 cm). Stream water was diluted with reverse osmosis treated water and micro- and macro-nutrients were re-amended by adding 100 µL of sterile NH_4^+-oxidizer media to each flask. The added media contained no organic C and was made according to Schmidt and Belser (1994). The undiluted treatment also received 100 µL of the NH_4^+ oxidizer media as a control. Nitrification rates were determined on four replicates of each treatment as described earlier. Results from both experiments were analyzed as a two-way analysis of variance (ANOVA) with stream and DOC treatment as factors.

© 2002 NRC Canada

Fig. 1. Map showing the location of stream sites sampled in Wisconsin and Michigan. Site numbers correspond to stream numbers listed in Table 2. The location of Juday Creek in northern Indiana is shown on the inset map.

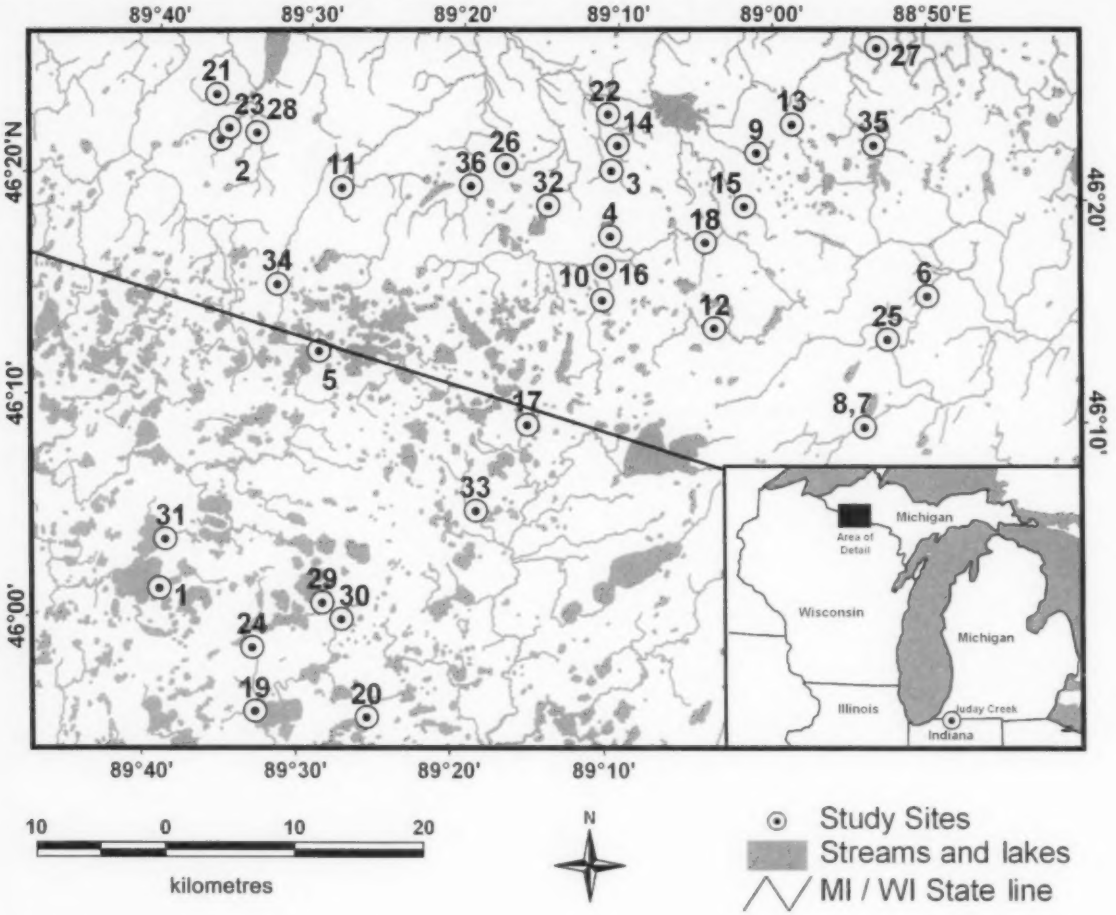

Table 1. Surface water characteristics of the six focal streams used in the dissolved organic carbon (DOC) addition and removal experiments.

Stream	Stream No.	Temperature (°C)	DO ($mg \cdot L^{-1}$)	pH	Velocity ($m \cdot s^{-1}$)	NH_4^+–N ($\mu g \cdot L^{-1}$)	DOC ($mg \cdot L^{-1}$)
Mill Creek	17	27.1	6.8	7.4	0.49	175	16.4
Pelton Creek	23	19.5	6.3	6.6	<0.03	54	33.0
Scott and Howe Creek	26	20.8	7.5	7.0	0.24	2	12.1
Star Creek	29	25.6	7.9	7.7	0.30	5	10.3
Tamarack Creek	33	22.6	7.4	6.7	0.79	<1	20.4
Tenderfoot Creek	34	25.9	4.1	7.0	0.27	<1	13.8

Note: Values shown are from samples collected at the time of the DOC addition experiment (13 July 1998). Stream No. corresponds to those shown in Fig. 1. DO, dissolved oxygen.

C:N and N availability experiment

To test the interactive effects of C:N and N availability on nitrification, we used stream water and sediments collected from a forested reach of Juday Creek, a third-order stream in north-central Indiana (Fig. 1). A detailed description of Juday Creek can be found in Lamberti and Berg (1995). Earlier studies on this stream have shown that nitrification is NH_4^+ limited and can be inhibited with organic C amendments (Strauss and Lamberti 2000). We amended stream sediments and water with organic C and N at three ratios (based on moles) as follows: 7:1, 23:1, and 70:1. In addition, three levels of organic N were tested within each C:N: 0.1, 1.0, and 10 mg $N \cdot L^{-1}$. All N (and some C) was added in organic form as L-lysine acetate, an organic amino salt with a C:N of 4.0. To achieve targeted C:N, additional C was added as sodium acetate. Nitrification rates were determined as before for nine replicates of each of the nine treatment combinations (3 C:N × 3 N levels) and a control (no C or N amendment). The C:N molar ratio of the sediments in Juday Creek has been previously determined to be around 21:1. (Strauss

© 2002 NRC Canada

Table 2. Stream water temperature, conductivity, and dissolved organic carbon (DOC) concentration of 36 streams sampled during the 1998 field survey.

Stream	No.	Date sampled	Temperature (°C)	Conductivity (μmhos·cm^{-1})	DOC (mg C·L^{-1})
Allequash Creek	1	26 July	20.7	92	14.8
Banner Creek	2	25 July	14.3	52	50.3
Bluff Creek	3	1 August	15.1	228	15.3
Boniface Creek	4	29 July	21.6	88	19.2
Brown Creek	5	11 August	21.0	191	13.4
Bush Creek	6	11 August	24.3	169	6.8
Cooks Run (A)	7	10 August	16.0	163	3.8
Cooks Run (B)	8	11 August	15.1	170	28.0
Deadman Creek	9	10 August	11.4	189	6.3
Duck Creek	10	21 July	22.4	185	7.4
Grosbeck Creek	11	19 July	20.8	158	26.0
Imp Creek	12	11 August	20.5	171	16.5
Jumbo River	13	10 August	22.9	225	8.5
Matheson Creek	14	21 July	26.1	92	17.0
McGinty Creek	15	10 August	20.3	215	24.7
Mid. Br. Ontanogan River	16	21 July	23.3	193	21.2
Mill Creek	17	6 August	21.8	98	19.4
Morrison Creek	18	10 August	20.8	233	9.2
Mud Creek	19	6 August	17.8	102	19.1
Muskellunge Creek	20	6 August	17.0	99	44.7
Nelson Creek	21	29 July	15.3	108	37.7
Paulding Creek	22	2 August	14.6	242	11.7
Pelton Creek	23	6 August	16.5	175	25.1
Plum Creek	24	2 August	24.3	108	10.6
S. Branch Paint River	25	11 August	22.1	193	8.7
Scott and Howe Creek	26	6 August	16.9	151	16.9
Shane Creek	27	10 August	16.4	133	22.3
Slate River	28	29 July	15.5	213	18.0
Star Creek	29	6 August	21.4	84	20.7
Stella Creek	30	6 August	19.4	112	10.7
Stevenson Creek	31	26 July	16.7	107	14.1
Sucker Creek	32	19 July	27.9	153	71.3
Tamarack Creek	33	6 August	16.0	109	18.6
Tenderfoot Creek	34	13 July	22.3	134	18.7
Tepee Creek	35	10 August	26.1	159	13.0
Twomile Creek	36	19 July	23.8	138	35.5

Note: Stream locations are shown in Fig. 1.

and Lamberti 2000). Data were analyzed using two-way ANOVA.

pH experiment

We determined the effect of pH on sediment nitrification rates in the laboratory. Stream sediments consisted of a sand–silt mixture collected from Juday Creek. Nitrification rates were determined in flasks containing 10 mL of stream sediment and 100 mL of 60 mM phosphate buffer (K_2HPO_4 and KH_2PO_4 with pH adjusted according to treatment) using the nitrapyrin method as before. Each flask also received an initial NH_4^+ addition of 0.5 mg N·L^{-1} (as NH_4Cl). Eight pH treatments were used: pH 5.9, 6.1, 6.5, 7.0, 7.5, 7.9, 8.4, and 8.7 (five replicates per treatment). Data were analyzed using one-way ANOVA.

Stream survey

During summer 1998, we sampled 36 "survey" streams in northern Wisconsin and the upper peninsula of Michigan, (Fig. 1; Table 2) to identify factors that potentially influence nitrification rates. Nitrification rates were measured (as described above) together with 12 additional variables on the same stream water or sediments: temperature, pH, dissolved oxygen, conductivity, DOC concentration, redox potential, salinity, sediment ash-free dry mass (AFDM), specific ultraviolet absorbance (SUVA), stream water NH_4^+ concentration, soluble reactive phosphorus concentration (SRP), and total extractable NH_4^+. Environmental variables were correlated (Spearman's r) with nitrification rates to search for significant associations. In addition, we used stepwise multiple regression to best predict nitrification rates based on the environmental variables. All statistical analyses were done using SAS v. 6.12 (SAS Institute Inc. 1990).

Analytical methods

Total extractable NH_4^+ (water column NH_4^+ plus sediment

© 2002 NRC Canada

extracted NH_4^+) and surface water NH_4^+ concentrations were determined colorimetrically on filtered samples (Whatman GF/F) using the phenol–hypochlorite method (Solorzano 1969). DOC concentration was determined on filtered (preashed Whatman GF/F) samples using a Shimadzu Model TOC-5000A high-temperature combustion carbon analyzer (Shimadzu Scientific Instruments, Inc., Columbia, Md.). SUVA, a measure of DOC quality, was determined by dividing the measured DOC concentration of a water sample by its ultraviolet absorbance measured at 254 nm (Ravichandran et al. 1998). SRP was measured colorimetrically on filtered (Whatman GF/F) water samples using the acid molybdate method (Strickland and Parsons 1972). All spectrophotometer measurements were conducted on a Spectronic Genesys 2 spectrophotometer (Thermo Spectronic, Rochester, N.Y.).

Results

Ambient nitrification rates for the six focal streams ranged from 0.08 to 1.1 μg N·mL sediment^{-1}·day^{-1} (Fig. 2*a*), with Mill and Tenderfoot Creeks exhibiting the highest nitrification rates and Star and Pelton Creeks having the lowest. DOC additions (as acetate) to sediments and water from the six streams revealed that DOC significantly reduced ($P \leq 0.003$) nitrification rates only when added at the highest level of 30 mg·L^{-1} (Fig. 2*b*). Nitrification reduction was not caused by the formation of anaerobic conditions or environmental pH shifts, because DO and pH were not appreciably different from control flasks that received no DOC amendments (e.g., post-incubation conditions for 30 mg C·L^{-1} addition treatment and control: $\bar{x}$ O_2 for treatment = 7.8 mg·L^{-1}, $\bar{x}$ O_2 for control = 7.3 mg·L^{-1}; $\bar{x}$ pH for treatment = 7.7, $\bar{x}$ pH for control = 7.5). Dilution of stream water to reduce DOC concentrations had no significant effect on nitrification (Fig. 2*c*). Nitrification rates observed in the DOC reduction experiment, in general, were higher than those initially measured and those in the DOC addition experiment, but this was likely a result of adding nitrifier media to counteract the effect of nutrient removal by dilutions. Neither experiment revealed statistically significant interaction between stream and DOC treatment. In both experiments, stream-specific mean nitrification rates exhibited patterns similar to those measured initially (i.e., Mill and Tenderfoot consistently had the highest nitrification rates, whereas Pelton always had the lowest).

The experiment examining the interactive effects of C:N and N availability on nitrification rates (Fig. 3) suggested that both factors were important in regulating nitrification (significant C:N and N availability interaction; $P < 0.0001$). However, this significant interaction was likely a result of the large nitrification response to the 10 mg N·L^{-1} addition at the 7:1 C:N. The C:N factor also was significant, with each of the three ratios being significantly different ($P < 0.0001$) from one another. The highest C:N generally decreased nitrification, whereas N concentration affected nitrification only at the lowest C:N. Environmental pH had a strong effect on nitrification (Fig. 4). Nitrification rates were highest at pH 7.5 ($P < 0.002$) and decreased more gradually with declining pH than with increasing pH.

Fig. 2. Results from (*a*) the initial nitrification measurements, (*b*) the dissolved organic caron (DOC) addition experiment, and (*c*) the DOC dilution experiment. Error bars ± 1 SE are shown. Lowercase letter combinations over bars in *a* and *b* denote significance among treatments; treatments containing the same lowercase letter were not significantly different ($P > 0.05$, LS means procedure). *F* statistic in *b* represents ANOVA results for DOC addition factor. Significant treatment differences were not observed in the DOC dilution experiment. Asterisk indicates that nitrification rate was below detection.

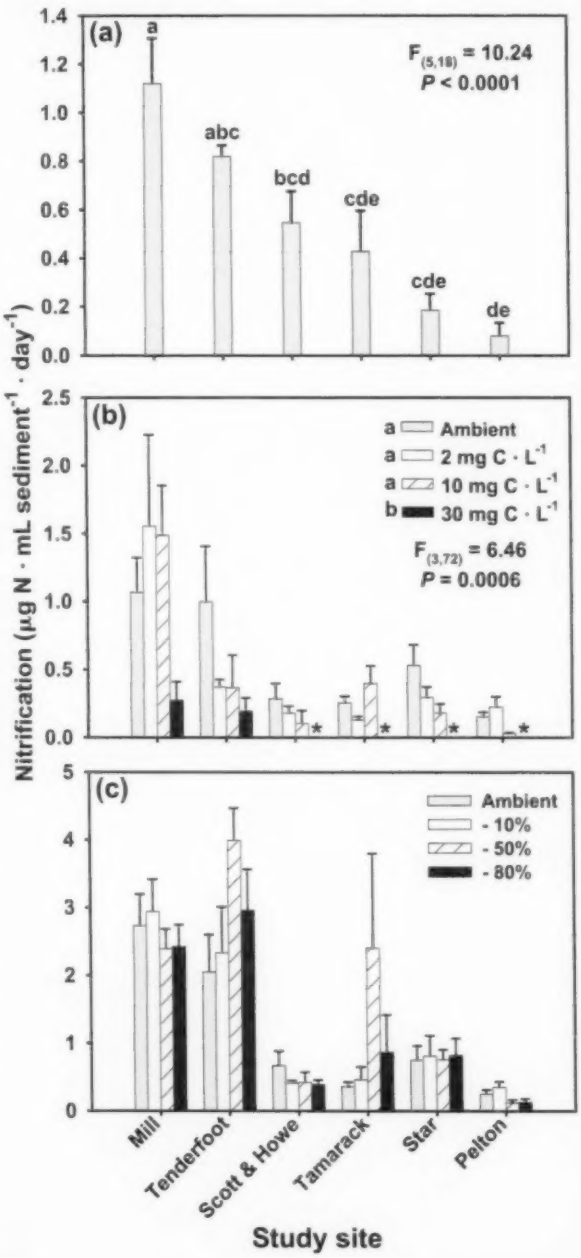

© 2002 NRC Canada

Fig. 3. Results from the experiment testing the interactive effects of C:N and N availability on nitrification rates in Juday Creek sediments. All N (and some C) was added in organic form as L-lysine acetate. Additional C was added as sodium acetate to reach the target C:N. The control was not amended with either N or C. Error bars ± 1 SE are shown. *F* statistic represents ANOVA results for the interaction among factors (C:N × N). Treatments containing the same lowercase letter were not significantly different ($P > 0.05$, LS means procedure).

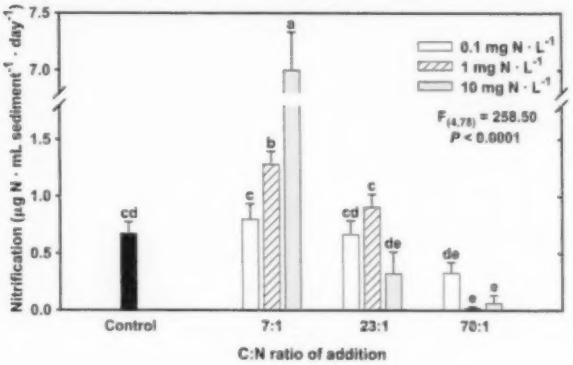

Fig. 4. Effect of pH on nitrification rate in stream sediments from Juday Creek. Error bars ± 1 SE are shown. Treatments containing the same lowercase letter were not significantly different ($P > 0.05$, LS means procedure).

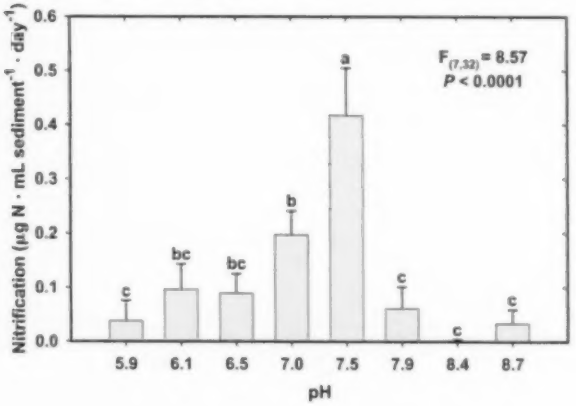

Nitrification rates for the 36 survey streams spanned over two orders of magnitude and ranged from below detection (Stella and Tepee Creeks) to over 2.7 µg N·mL sediment^{-1}·day^{-1} (Mill Creek and Cooks Run B). Cooks Run B is a diversion from the main Cooks Run channel (Cooks Run A) and is used as a trout-rearing facility for a high density of trout fingerlings that receive regular inputs of commercial trout feed. The only significant correlation found between nitrification and the 12 environmental variables measured was with stream water pH (Fig. 5*a*, $r = 0.440$, $P = 0.007$). A weak positive correlation also was found between nitrification and total extractable NH_4^+ (Fig. 5*b*, $r = 0.297$, $P = 0.079$). Both relationships showed the highest variation in nitrification rates at higher pH or NH_4^+ concentration. A multiple regression

Fig. 5. Linear correlations (Spearman's *r*) between nitrification rate in stream sediments and (*a*) stream water pH, and (*b*) total extractable NH_4^+. Each point represents a different stream from the 36-stream survey.

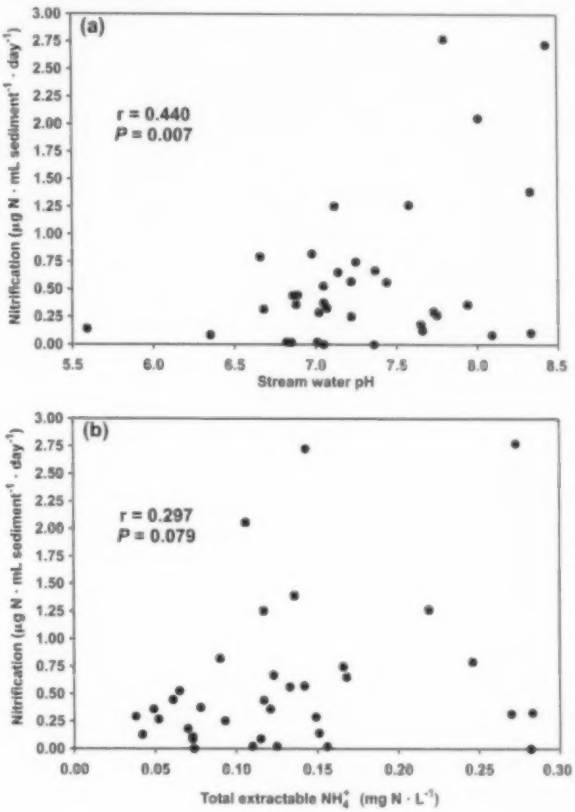

model consisting of five environmental variables (stream temperature, pH, conductivity, DOC concentration, and total extractable NH_4^+) explained 60% of the variation in nitrification rates (Table 3). Observed nitrification rates in the 36 streams fit well with predicted rates based on the multiple regression model (Fig. 6).

Discussion

Nitrification appears to be a ubiquitous N transformation in stream sediments, but our study demonstrates that rates are highly variable. Furthermore, this variability may be related to a multitude of factors in natural ecosystems. Previous studies have suggested that organic C can regulate nitrification in streams (Strauss and Lamberti 2000), forest soils (Paavolainen et al. 1998), and during wastewater treatment (Cheng and Chen 1994). Our DOC addition experiment clearly demonstrated that high DOC (30 mg C·L^{-1}) could significantly reduce nitrification rates. However, lower DOC additions (2 mg C·L^{-1} and 10 mg C·L^{-1}) had a less profound effect on nitrification, likely because of the high background DOC (10.3–33 mg C·L^{-1}) of the water. The mechanism responsible for reducing nitrification at high DOC amendment

© 2002 NRC Canada

Table 3. Multiple regression model used to predict ambient nitrification rates in stream sediments explaining 60% of the variability observed in nitrification rates (overall model $R^2 = 0.600$).

(*a*)

Source	df	Sum of squares	Mean square	*F* value	Prob. > *F*
Model	5	10.1081	2.0216	8.69	0.0001
Error	29	6.7464	0.2326		

(*b*)

Variable	df	Parameter estimate	Standard error	*t* for H_0: Param. = 0	Prob. > |*t*|	Partial R^2
Intercept	1	–5.7645	1.1476	–5.02	0.0001	—
pH	1	1.0148	0.1768	5.73	0.0001	0.1928
DOC	1	0.0181	0.0064	2.84	0.0081	0.1337
Total NH_4+	1	4.0952	1.1985	3.41	0.0019	0.1213
Temperature	1	–0.0591	0.0222	–2.66	0.0125	0.0584
Conductivity	1	–0.0052	0.0020	–2.60	0.0144	0.0935

Note: df, degrees of freedom; DOC, dissolved organic carbon; Param., parameter; Prob., probability.

Fig. 6. Relationship between nitrification rates measured in the 36 streams and those predicted by the multiple regression model presented in Table 3. The diagonal reference line plots a 1:1 relationship where observed rates would equal predicted rates.

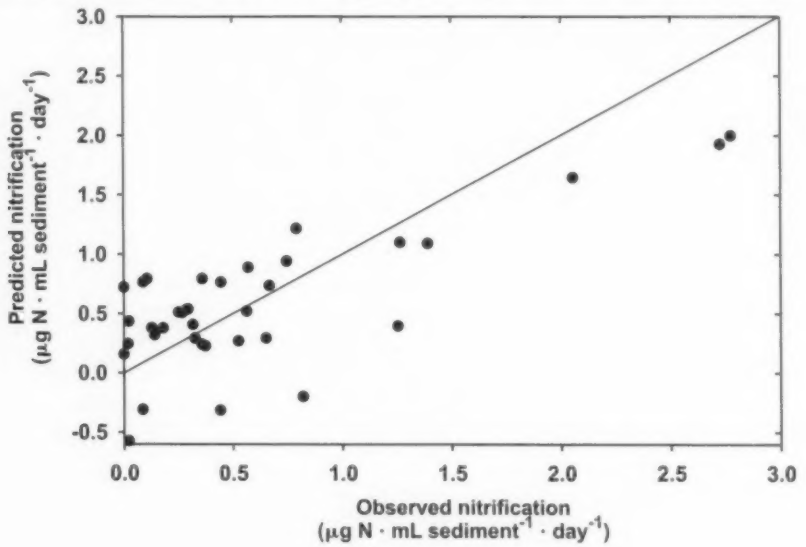

was likely stimulation of heterotrophic bacteria that outcompeted nitrifying bacteria for available NH_4^+ (Strauss and Lamberti 2000).

The results of the DOC removal experiment contrasted with those of the DOC addition experiment. If DOC availability regulated nitrification rates, nitrification rates should have increased with dilution. However, no significant effects were observed. Several possible explanations exist for these contrasting results. First, a large fraction of the organic C may have been particulate organic C or C bound to the sediments rather than DOC (Dahm 1981). Diluting stream water would not reduce these C pools, thereby limiting the effect on nitrification. Second, the positive effect from the inorganic nutrients in the nitrifying bacteria media (added to offset the loss of nutrients from dilution) may have offset any negative effect of higher DOC concentrations. Third, the quality or lability of the organic C reduced during dilution was not equal to that of the labile DOC (acetate) augmented during the addition. A recent study has shown that labile organic C has a stronger negative effect on nitrification than refractory organic C (Strauss and Lamberti 2002).

The C:N – organic N-availability experiment revealed two important relationships. First, nitrification was negatively affected by increasing the C:N. Low C:N (7:1) increased nitrification, whereas high C:N (70:1) inhibited nitrification, consistent with our organic C hypothesis (Strauss and Lamberti 2000). Under high environmental C:N, the metabolic requirement for N by bacteria is high, thus heterotrophic bacteria should out-compete nitrifying bacteria for mineralized organic N (NH_4^+), resulting in lower nitrification rates. Second, organic N availability influenced nitrification, but the effect depended on the C:N of the environment. The positive effect of organic N availability on nitrification was stronger at low C:N because heterotrophic bacteria were not favored. As the C:N of the environment increased, nitrifying bacteria did not effectively compete with

© 2002 NRC Canada

Fig. 7. Conceptual model of controls on nitrification in aquatic sediments. Certain physical and chemical variables of the environment (e.g., DO and pH) constrain nitrification (upper box). Under these constraints, regulation of nitrification depends on the environmental C:N and its relation to a critical value (C:N ~ 20) (middle box). Near and below this ratio (C:N < 20), maximum nitrification is determined by NH_4^+ availability (lower box, left) and follows Monod-type growth kinetics with reported half-saturation constants being as low as 600 μg $N{\cdot}L^{-1}$ (Denac et al. 1983). At C:N above the critical value (C:N > 20), nitrification rates are regulated by organic C quantity and quality (lower box, right). In general, nitrification decreases as organic C increases because of competition between heterotrophic and nitrifying bacteria for NH_3. High-quality C (line *a*) elicits a stronger negative effect than low-quality C (line *b*). Purely recalcitrant C would have no effect (line *c*).

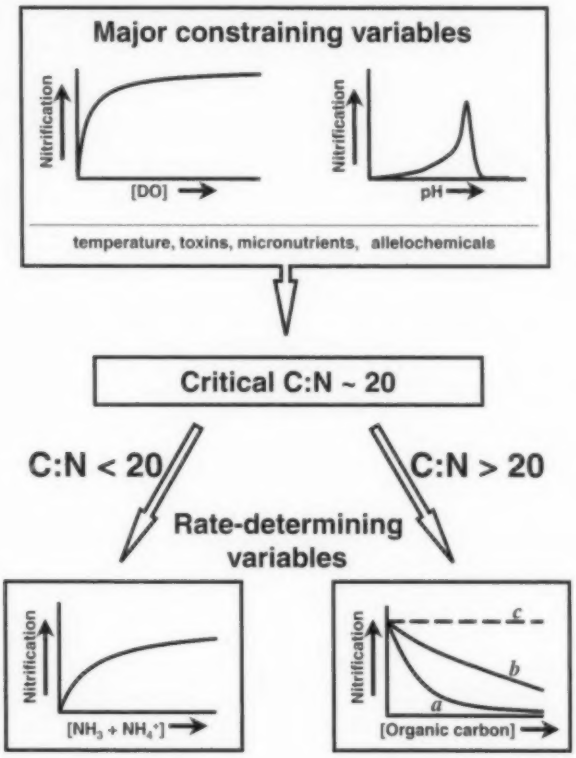

heterotrophic bacteria for biologically available NH_4^+. The average global C:N in riverflow is around 11.1 (Schlesinger 1997). Based on our study, nitrification rates should be more strongly influenced by NH_4^+ availability at C:N near and below this global average, whereas at C:N above this average nitrification should be influenced more by C availability (Fig. 7).

Our multiple regression model to predict field nitrification rates explained 60% of the variability in nitrification, but had a tendency to underestimate higher nitrification rates. The 36 streams in our survey probably had different combinations of factors regulating nitrification, whereas a single system likely will have a more restrictive set of constraints on nitrification. For instance, in a one-year nitrification study of an estuarine area of the Rhone River (Bianchi et al. 1999), 74% of the variability in nitrification was explained by a single variable, NH_4^+ availability. Of the five variables in our model, total extractable NH_4^+, DOC, and stream water pH explained the most variation, but no single variable explained more than 20% of the total variation. NH_4^+ availability and nitrification rates have been positively associated in streams (Triska et al. 1990; Jones et al. 1995), lakes (Hall 1986), groundwater (Strauss and Dodds 1997), and soil systems (Davidson and Hackler 1994). The results from our C:N – N-availability experiment also demonstrated a positive relationship between N and nitrification rates at low C:N.

The effect of pH on nitrification has not been studied in natural aquatic systems. However, pH has received considerable attention in soils, wastewater treatment, and pure cultures. For example, Paavolainen and Smolander (1998) reported increased nitrification through a pH gradient of 4.2–6.2 in a spruce-forest soil. In wastewater treatment sludge, the optimum pH for nitrification was approximately 7.8 over a range of 6.4–8.2 (Antoniou et al. 1990). Watson et al. (1989) recommend a media pH of 7.5–7.8 for culturing pure strains of NH_4^+-oxidizing bacteria. In our study, we observed an optimum pH of 7.5 consistent with previous studies. The positive relationship between pH (up to 7.5) and nitrification is related to the increasing availability of NH_3, unprotonated ammonia, which is believed to be the true substrate for oxidation (Suzuki et al. 1974). Both NH_3 and NH_4^+ occur in the environment with relative proportions dependent upon pH and temperature. As pH increases, the relative NH_3 concentration increases by nearly a full order of magnitude for each pH unit (Emerson et al. 1975). Above the optimum pH for nitrification, the advantages of increased availability of free NH_3 may be counterbalanced by the energy required to maintain the cytoplasmic pH below that of the external environment (Wood 1988). As pH falls below the optimum, evidence exists that enzyme activity is negatively affected, thereby reducing nitrification (Prosser 1989).

In the 36 streams we surveyed, the relationship between nitrification and pH was significant but somewhat variable. Nitrification rates were low at low pH, but variable at higher pH. This suggests that nitrification is inhibited at low pH, but is enhanced at circumneutral pH values. However, optimal pH is not enough to ensure high nitrification and therefore additional environmental factors must be involved (Fig. 7).

The regression model also revealed a positive relationship between DOC and nitrification, in apparent disagreement with our organic C hypothesis. However, because high DOC has been associated with increased primary productivity (Kaplan and Bott 1989), we believe that this positive relationship may reflect increased nitrification in more eutrophic streams rather than a direct effect of DOC on nitrification. The better controlled DOC addition and the C:N – N-availability experiments indicate that additions of labile C can dramatically reduce nitrification rates in stream sediments. In addition, previous research has shown that a range of C sources (labile glucose to less-labile leaf leachates) can reduce nitrification rates in stream sediments (Strauss and Lamberti 2000). Our conceptual model proposes that ambient organic C can reduce nitrification in natural systems if the environmental C:N is high (>20) and a reasonable frac-

© 2002 NRC Canada

tion of the available organic C is relatively labile. Unfortunately, little is known about the factors that regulate C:N in aquatic ecosystems except that ratios generally increase with time following inputs of organic matter because N-containing amino and proteinaceous compounds are used more rapidly than carbohydrate-based compounds (Wetzel 2001). Regardless, stoichiometric ratios of important elements can exert profound influences on aquatic ecosystem structure and function (Elser et al. 1996), as we also suggest for nitrification.

Predicting specific conditions that could result in high environmental C:N with a large fraction of relatively labile organic C, a scenario where nitrification should be inhibited by organic C, is difficult because of the following: (*i*) inter- and intra-system variability is inherent to organic C dynamics, and (*ii*) the relative fraction of labile DOC depends on the DOC source. However, we can make a few generalizations. In temperate forested streams, we might expect to find these conditions during annual leaf fall when potentially very large inputs of high C:N material are deposited into the stream (Meyer et al. 1998). These conditions could easily be present in small, localized areas adjacent to leaf packs or debris jams where the particulate matter is concentrated. In desert and other nonforested streams where organic C is primarily of autochthonous origin, periodic floods and subsequent periphyton sloughing often result in increased organic C export (Jones et al. 1996). During these periods, the quantity and quality of organic C may be high enough to initiate a temporary system-wide reduction in nitrification. In lakes, wetlands, and large rivers, high C:N conditions may occur in vegetated littoral zones, sloughs, or in backwater areas after macrophyte senescence and its microbial decomposition. Also, waterways that receive C-rich effluent (e.g., paper pulp processing) may exhibit these conditions. In general, conditions conducive to organic C inhibition of nitrification are possible at several spatial and temporal scales, and may help explain N cycling patterns when these conditions exist.

Our study demonstrates that nitrification is a complex transformation in the aquatic N cycle that is regulated by a suite of environmental variables. Clearly, however, NH_4^+ availability, pH, and organic C exert strong influences on nitrification rates. In aerobic environments, nitrification is positively associated with NH_4^+ availability, but the importance of NH_4^+ declines with increasing C:N as heterotrophic bacteria dominate N-uptake dynamics. Nitrification is maximized at a pH of 7.5–7.8, but rates of nitrification are likely determined by other environmental factors. If organic C is labile and the C:N is high, organic C may be a primary determinant of nitrification rates in aquatic ecosystems.

Acknowledgements

We thank J. Nelson, J. Engelhardt, and K. Engel for their valuable technical assistance during this study. We are also grateful to R.A. Hellenthal, J. Runde, and the staff at the University of Notre Dame Environmental Research Center for providing facilities and general assistance that made several aspects of this study possible. Two anonymous reviewers provided valuable comments on an earlier version of this manuscript. Funding for this research was provided by the National Science Foundation through a graduate research traineeship to EAS (Grant No. EHR9452655) and a dissertation improvement grant (Grant No. DEB9801090). This paper is a contribution from the University of Notre Dame Environmental Research Center.

References

Antoniou, P., Hamilton, J., Koopman, B., Jain, R., Holloway, B., Lyberatos, G., and Svoronos, S.A. 1990. Effect of temperature and pH on the effective maximum specific growth rate of nitrifying bacteria. Water Res. **24**: 97–101.

Bianchi, M., Feliatra, and Lefevre, D. 1999. Regulation of nitrification in the land-ocean contact area of the Rhone River plume (NW Mediterranean). Aquat. Microb. Ecol. **18**: 301–312.

Carpenter, S.R., Caraco, N.F., Correll, D.L., Howarth, R.W., Sharpley, A.N., and Smith, V.H. 1998. Nonpoint pollution of surface waters with phosphorus and nitrogen. Ecol. Appl. **8**: 559–568.

Cheng, S.-S., and Chen, W.-C. 1994. Organic carbon supplement influencing performance of biological nitrification in a fluidized bed reactor. Water Sci. Technol. **30**: 131–142.

Dahm, C.N. 1981. Pathways and mechanisms for removal of dissolved organic carbon from leaf leachate in streams. Can. J. Fish. Aquat. Sci. **38**: 68–76.

Davidson, E.A., and Hackler, J.L. 1994. Soil heterogeneity can mask the effects of ammonium availability on nitrification. Soil Biol. Biochem. **26**: 1449–1453.

Denac, M., Uzman, H., Tanaka, H., and Dunn, I.J. 1983. Modeling of experiments on biofilm penetration effects in a fluidized bed nitrification reactor. Biotechnol. Bioeng. **25**: 1841–1861.

Duff, J.H., and Triska, F.J. 2000. Nitrogen biogeochemistry and surface-subsurface exchange in streams. *In* Streams and ground waters. *Edited by* J.B. Jones and P.J. Mulholland. Academic Press, San Diego. pp. 197–220.

Elser, J.J., Dobberfuhl, D.R., MacKay, N.A., and Schampel, J.H. 1996. Organism size, life history, and N:P stoichiometry. BioScience, **46**: 674–684.

Emerson, K., Russo, R.C., Lund, R.E., and Thurston, R.V. 1975. Aqueous ammonia equilibrium calculations: effect of pH and temperature. J. Fish. Res. Board Can. **32**: 2379–2383.

Gergel, S.E., Turner, M.G., and Kratz, T.K. 1999. Dissolved organic carbon as an indicator of the scale of watershed influence on lakes and rivers. Ecol. Appl. **9**: 1377–1390.

Hall, G.H. 1986. Nitrification in lakes. *In* Nitrification. *Edited by* J.I. Prosser. IRL Press, Oxford. pp. 127–156.

Jones, J.B., Fisher, S.G., and Grimm, N.B. 1995. Nitrification in the hyporheic zone of a desert stream ecosystem. J. North Am. Benthol. Soc. **14**: 249–258.

Jones, J.B., Fisher, S.G., and Grimm, N.B. 1996. A long-term perspective of dissolved organic carbon transport in Sycamore Creek, Arizona, U.S.A. Hydrobiologia, **317**: 183–188.

Kaplan, L.A., and Bott, T.L. 1989. Diel fluctuations in bacterial activity on streambed substrata during vernal algal blooms: effects of temperature, water chemistry, and habitat. Limnol. Oceanogr. **34**: 718–733.

Kemp, M.J., and Dodds, W.K. 2001. Centimeter-scale patterns in dissolved oxygen and nitrification rates in a prairie stream. J. North Am. Benthol. Soc. **20**: 347–357.

Lamberti, G.A., and Berg, M.B. 1995. Invertebrates and other benthic features as indicators of environmental change in Juday Creek, Indiana. Nat. Areas J. **15**: 249–258.

Meyer, J.L., Wallace, J.B., and Eggert, S.L. 1998. Leaf litter as a source of dissolved organic carbon in streams. Ecosystems, **1**: 240–249.

© 2002 NRC Canada

Paavolainen, L., and Smolander, A. 1998. Nitrification and denitrification in soil from a clear-cut norway spruce (*Picea abies*) stand. Soil Biol. Biochem. **30**: 775–781.

Paavolainen, L., Kitunen, V., and Smolander, A. 1998. Inhibition of nitrification in forest soil by monoterpenes. Plant Soil, **205**: 147–154.

Prosser, J.I. 1989. Autotrophic nitrification in bacteria. Adv. Microb. Physiol. **30**: 125–181.

Ravichandran, M., Aiken, G.R., Reddy, M.M., and Ryan, J.N. 1998. Enhanced dissolution of cinnabar (mercuric sulfide) by dissolved organic matter isolated from the Florida Everglades. Environ. Sci. Technol. **32**: 3305–3311.

SAS Institute Inc. 1990. SAS/STAT User's Guide. Ver. 6. 4th ed. Vol. 2. SAS Institute Inc., Cary, N.C.

Schlesinger, W.H. 1997. Biogeochemistry: an analysis of global change. Academic Press, San Diego.

Schmidt, E.L., and Belser, L.W. 1994. Autotrophic nitrifying bacteria. *In* Methods of soil analysis. Part 2. Microbiological and biochemical properties. *Edited by* R.W. Weaver et al. Soil Science Society of America, Madison, Wis. pp. 159–177.

Sedell, J.R., and Dahm, C.N. 1990. Spatial and temporal scales of dissolved organic carbon in streams and rivers. *In* Organic acids in aquatic ecosystems. *Edited by* E.M. Perdue and E.T. Gjessing. John Wiley & Sons Ltd., Chichester, U.K. pp. 261–279.

Solorzano, L. 1969. Determination of ammonia in natural waters by the phenolhypochlorite method. Limnol. Oceanogr. **14**: 799–801.

Strauss, E.A., and Dodds, W.K. 1997. Influence of protozoa and nutrient availability on nitrification rates in subsurface sediments. Microb. Ecol. **34**: 155–165.

Strauss, E.A., and Lamberti, G.A. 2000. Regulation of nitrification in aquatic sediments by organic carbon. Limnol. Oceanogr. **45**: 1854–1859.

Strauss, E.A., and Lamberti, G.A. 2002. Effect of organic carbon quality on microbial decomposition of DOC and nitrification rates in stream sediments. Freshwater Biol. **47**: 65–74.

Strickland, J.D.H., and Parsons, T.R. 1972. A practical handbook of seawater analysis. 2nd ed. Bull Fish. Res. Board. Can. No. 167.

Suzuki, I., Dular, U., and Kwok, S.-C. 1974. Ammonia or ammonium ion as substrate for oxidation by *Nitrosomonas* cells and extracts. J. Bacteriol. **120**: 556–558.

Triska, F.J., Duff, J.H., and Avanzino, R.J. 1990. Influence of exchange flow between the channel and hyporheic zone on nitrate production in a small mountain stream. Can. J. Fish. Aquat. Sci. **47**: 2099–2111.

Watson, S.W., Bock, E., Harms, H., Koops, H.-P., and Hooper, A.B. 1989. Nitrifying bacteria. *In* Bergey's manual of systematic bacteriology. Vol. 3. *Edited by* J.T. Stanley. Williams and Wilkins, Baltimore, Md. pp. 1808–1834.

Wetzel, R.G. 2001. Limnology: lake and river ecosystems. 3rd ed. Academic Press, San Diego.

Wood, P.M. 1988. Monooxygenase and free radical mechanisms for biological ammonia oxidation. *In* The nitrogen and sulphur cycles. *Edited by* J.A. Cole and S.J. Ferguson. Cambridge University Press, Cambridge, U.K. pp. 219–243.

© 2002 NRC Canada

Regional patterns in periphyton accrual and diatom assemblage structure in a heterogeneous nutrient landscape

Eric B. Snyder, Christopher T. Robinson, G. Wayne Minshall, and Samuel R. Rushforth

Abstract: The effect of nutrient regime on periphyton community development in large rivers was examined (sites ranged from oligotrophic to eutrophic). Patterns in diatom community structure were examined at a large spatial scale (ultimate), whereas at the microhabitat scale (proximate), artificial nutrient-diffusing substrata were used to examine periphyton response to amendment with nitrogen, phosphorus, and N + P. Ratios of ambient dissolved inorganic nitrogen to total phosphorus were used to make predictions of nutrient limitation (molar total inorganic nitrogen (TIN) : total phosphorus (TP)), which matched experimental results in 8 of 12 sites. Two sites with highest ambient nutrient levels (mean NO_3 + NO_2 and TP, 1.49 and 0.081 mg·L^{-1}, respectively) possessed the highest diatom richness and diversity (mean richness = 42). Lowest diatom taxa richness (19) occurred in an impounded system with low TP (0.008 mg·L^{-1}). Principal components analysis (PCA) of diatom taxa structure among sites (control treatments only) and small-scale patterns among nutrient treatments using all sites and treatments combined indicated that sites were grouped according to drainage basin (r^2 = 0.79) and that there was no unified response to enrichment (r^2 = 0.43). Results suggest that large spatial scale factors are more important in determining the potential benthic diatom assemblage than small-scale, proximate variables provided by the diffusers.

Résumé : Nous avons étudié les effets du régime des nutriments sur le développement des communautés de périphyton de grandes rivières à des sites variant d'oligotrophes à eutrophes. Nous avons examiné les configurations des structures des communautés de diatomées à une grande échelle spatiale (éloignée); à l'échelle du microhabitat (immédiate), nous avons utilisé des substrats diffuseurs de nutriments pour étudier la réaction du périphyton à des amendements à l'aide d'azote, de phosphore et de N + P. Les rapports de l'azote inorganique dissout ambiant sur le phosphore total (azote inorganique molaire total (TIN) : phosphore total (TP)) ont servi à faire des prédictions sur l'importance des nutriments comme facteurs limitants; nos prédictions correspondaient aux résultats expérimentaux à 8 des 12 sites. Aux deux sites aux concentrations ambiantes les plus élevées de nutriments (NO_3 + NO_2 et TP moyens, respectivement de 1,49 et 0,081 mg·L^{-1}) prévalaient les valeurs les plus grandes de richesse et de diversité de diatomées (richesse moyenne = 42). La richesse taxonomique la plus basse en diatomées (19) a été observée dans des réservoirs à concentrations de TP faibles (0,008 mg·L^{-1}). Une analyse en composantes principales (PCA) de la structure taxonomique des diatomées aux différents sites (sites témoins seulement) et l'étude des configurations à petite échelle à tous les sites englobant toutes les manipulations des nutriments ont montré que les sites se regroupent en fonction de leur bassin versant (r^2 = 0,79) et qu'il n'y a pas de réaction commune à l'enrichissement (r^2 = 0,43). Nos résultats laissent croire que les facteurs qui agissent à grande échelle sont plus importants dans la détermination des communautés benthiques potentielles de diatomées que les variables immédiates à petite échelle que sont les diffuseurs de nutriments.

[Traduit par la Rédaction]

Introduction

Benthic algal assemblages are structured by the interaction of proximate or direct factors (nutrients and velocity) and intermediate (i.e., reach) and ultimate factors (climate, geology, and land use) (Biggs and Gerbeaux 1993; Biggs 1995; Stevenson 1997). Ultimate factors operate at the catchment scale over long time periods (e.g., identified as >1 year by Biggs and Gerbeaux (1993)) and determine the potential range of proximate factors that operate at smaller spatial and

Received 22 March 2001. Accepted 30 January 2002. Published on the NRC Research Press Web site at http://cjfas.nrc.ca on 17 April 2002.
J16277

E.B. Snyder.[1,2] Flathead Lake Biological Station, The University of Montana, 311 Bio Station Lane, Polson, MT 59860, U.S.A.
C.T. Robinson. Department of Limnology, EAWAG/ETH, Ueberlandstrasse 133, Duebendorf CH-8600, Switzerland.
G.W. Minshall. Department of Biological Sciences, Box 8007, Idaho State University, Pocatello, ID 83209, U.S.A.
S.R. Rushforth. Utah Valley State College, School of Science and Health, Orem, UT 84058, U.S.A.

[1]Corresponding author (e-mail: esnyder@selway.umt.edu).
[2]Mailing address: Department of Biological Sciences, Central Michigan University, Mt. Pleasant, MI 48859, U.S.A.

 DOI: 10.1139/F02-021 © 2002 NRC Canada

temporal scales. For example, climate influences flow and temperature regimes and the interaction of climate and catchment geology determines overall nutrient availability (Biggs 1995). Hierarchy theory (sensu Allen and Starr 1982) predicts that ultimate factors should influence benthic algae indirectly, whereas proximate factors should act directly. Thus, benthic algal biomass accrual is determined by the source pool of colonist and by the interaction of light, temperature, and availability of macro- and micro-nutrients (Bothwell 1988, 1989). Biomass loss is determined by the disturbance regime, mainly flood events and grazing by macroinvertebrates (for example, see Robinson and Minshall 1986). The interaction of these factors, particularly nutrients, was examined using artificial nutrient-diffusing substrata in a suite of river systems located throughout the state of Idaho, U.S.A., where nutrient regimes were quite variable as determined by parent geology.

Validation of nutrient limitation using artificial nutrient-diffusing substrata is particularly important given that many researchers have found variability in the transition point between nitrogen and phosphorus limitation (Rhee and Gotham 1980; Schanz and Juon 1983; Grimm and Fisher 1986). The inherent variability is due, in part, to differences in the algal species composition and variation in optimal ratios of N and P (Redfield 1958; Rhee and Gotham 1980). Ambient molar N–P ratios can be used to make initial predictions of limitation, allowing study sites to be placed into phosphorus, nitrogen, or co-limited groups (Grimm and Fisher 1986; Morris and Lewis 1988; Chessman et al. 1992).

Nutrient availability can influence both periphyton accrual and diatom community structure in streams and rivers (Pringle 1990; Stevenson et al. 1991; Chételat et al. 1999. Many researchers have noted that diatom communities varied along rivers in relation to differences in land use, geomorphology, and stream order, all ultimate factors indirectly influencing periphyton accrual and diatom community structure (Cushing et al. 1983; Leland 1995). Biggs and Gerbeaux (1993) found that mean annual periphyton accrual was associated with catchment geology, whereas monthly change in biomass was correlated with velocity. Biggs et al. (1998) observed that growth form (e.g., dense and coherent vs. long filamentous) is an important determinant of algal community responses to changes in velocity. Other research has demonstrated how proximate factors, such as enrichment with phosphorus and (or) nitrogen, differentially increase the abundance of *Achnanthes minutissima* and *Cocconeis placentula* (Lowe et al. 1986; Hill and Knight 1988; Burton et al. 1991). Pringle (1990) noted increased abundance of the two species above in addition to positive responses from *Navicula pelliculosa*, *Opephora martyi*, and *Nitzschia* spp.

Our objectives were (*i*) to examine the response of periphyton (as chlorophyll *a* (chl *a*) concentration and organic matter content) to nitrogen (N), phosphorus (P), and N + P addition at numerous sites in Idaho rivers (discharge ranged from 13 $m^3 \cdot s^{-1}$ to 430 $m^3 \cdot s^{-1}$) and (*ii*) to examine patterns in diatom assemblage structure among nutrient treatments and study sites and their correlation to physicochemical habitat variables. The sites selected were located within a diverse landscape that varied in geology and chemistry. Proximate-scale nutrient regimes were manipulated using artificial nutrient diffusers that were small, easily transported, cost effective, and replicable. This specific technique has been used in smaller systems (Gibeau and Miller 1989; Wold and Hershey 1999), but this is their first use in larger rivers. Most research using artificial diffusers has been conducted either in lentic systems (Fairchild et al. 1985; Barnese and Schelske 1994) or in smaller lotic systems (Pringle 1987; Wold and Hershey 1999), although Scrimgeour and Chambers (1997) used artificial diffusers of a different design in a large river in Alberta, Canada.

Materials and methods

Study sites

This research was conducted in the State of Idaho, U.S.A., located in the Pacific Northwest (Table 1; Fig. 1). Twelve study sites were selected, all on large rivers greater than 5th order (Strahler 1957) with molar total inorganic nitrogen (TIN) to total phosphorus (TP) ratios ranging from 1 to 49. The variation in ambient TIN:TP is determined in part by parent geology. For example, the central region is dominated by Cretaceous granite, quartz diorite, and Idaho batholith, which provide a limited source of nitrogen and phosphorus (Omernik 1977*a*, 1977*b*). The southern region is characterized by basalt flows of the Snake River Plain (south central) and the sedimentary structure of the basin and range (southeast), both of which provide higher sources of nitrogen and phosphorus (Omernik 1977*a*, 1977*b*). In the north, the region is principally underlain by metamorphosed Precambrian sedimentary rocks, which provide a limited source of nitrogen and phosphorus. Thus, ambient nutrient regimes were quite variable, emphasizing the natural variation in ultimate factors (e.g., catchment geology).

For the purpose of clarity in discussing predicted nutrient limitation, all sites were given a code name that consisted of the first letter of the river system and the longitudinal location within the system (upstream → downstream). For example, the downstream-most site on the Kootenai River was designated "K3". The Bear River system, flowing through basin and range topography, originates in northern Utah, flows north into Idaho, and then turns and flows back into Utah. Land use has degraded the lower reaches of the system where the study site was located, leading to slightly elevated ambient nutrient concentrations, higher temperatures, and higher turbidity, relative to other sites. The Snake River system originates in Wyoming (South Fork of the Snake) and Idaho (Henrys Fork) where topography is mainly mountainous. The upper three sites, particularly S1 and S3, are in relatively pristine reaches of the system, although S3 is located approximately 20 river-kilometres below a large hydropower dam. The second site (S2) is located within an agricultural region and is characterized by heavy *Cladophora* growth. The lower two Snake River sites, which flow through the Snake River Plain, were considered degraded because of numerous hydroelectric dams and eutrophication from upstream agricultural activity, wastewater effluent from the city of Twin Falls, and effluent from several large fish hatcheries. Nutrient concentrations at these two sites were elevated, turbidity was high relative to all other sites except the Bear River, and temperatures were relatively warm. The three Clearwater sites, which originate and flow through a mountainous National Wilderness Area, are slightly impacted by gravel roads, logging, and mining activities outside the wil-

© 2002 NRC Canada

Table 1. Study sites ranked according to predicted nutrient limitation based on molar ratio of total inorganic nitrogen to total phosphorus.

Site	Code	Latitude	Longitude	Predicted limitation (river system)
Kootenai	K1	116°10′41″	48°42′55″	P limited (Kootenai; Upper and Middle Snake)
Kootenai	K2	116°18′00″	48°41′56″	
Kootenai	K3	116°25′39″	48°53′19″	
Upper Snake	S2	111°31′59″	44°03′24″	
Middle Snake	S4	114°39′04″	42°39′38″	
Middle Snake	S5	115°13′05″	42°59′51″	
Selway	C1	115°29′13″	46°05′06″	Colimited (Clearwater; Bear; Upper Snake)
Clearwater	C3	115°29′47″	46°08′18″	
Bear	B1	111°08′24″	42°07′54″	
Upper Snake	S1	111°22′01″	44°29′30″	
South Fork Snake	S3	111°28′59″	43°35′50″	
Lochsa	C2	115°35′24″	46°09′52″	N limited

Fig. 1. Major river systems and study site locations in Idaho, U.S.A.

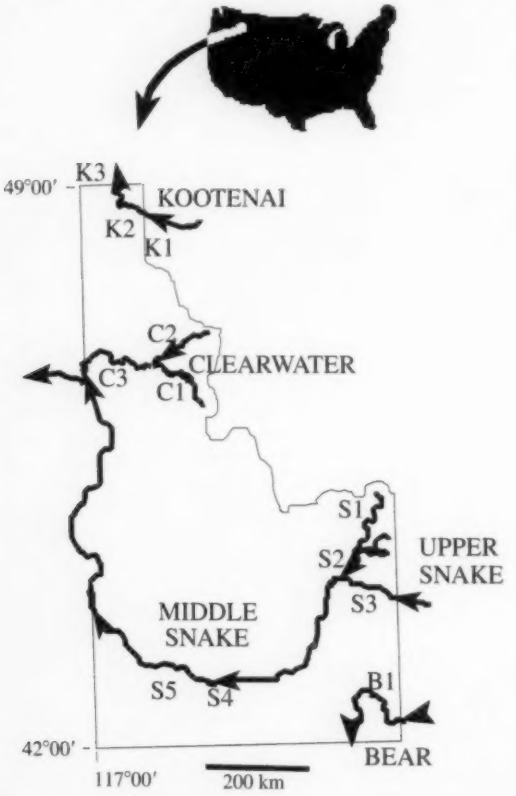

derness boundary. The Kootenai River originates in British Columbia, Canada, flows south into Montana and Idaho, and enters the Columbia River back in British Columbia. Impacts include some agriculture, a large hydroelectric dam, and extensive logging activity in catchments of the larger tributaries.

A suite of physical and chemical variables was measured once at each site (Table 2). Ambient nutrient samples were collected at the same time that diffusers were placed in the water. Unfiltered samples for total phosphorus and ammonia were immediately preserved with sulfuric acid, whereas nitrate and nitrite samples were filtered in the field (0.45-μm-pore-diameter, pre-rinsed membrane filter) and transported on ice within 24 h to a freezer. All analyses were conducted within 2 weeks with TP analyzed by persulfate autoclave digestion (250°F (121°C)), and concentration was determined by colorimetry (phosphomolybdate – ascorbic acid) (Friedman et al. 1985). Soluble nitrate and nitrite were analyzed by automated colorimetry (sulfanilimide – *N*-naphthylethylenediamine (NED) – dihydrochloride; EPA 1979). Soluble ammonia was determined by the automated colorimetric phenate method (EPA 1979).

The transitions between N, co-, and P limitation have been broadly defined as <10, 10–20, and >20 using molar ratios of NO_3 to total dissolved phosphorus (TDP) (Schanz and Juon 1983). In this study, we used molar ratios of dissolved inorganic nitrogen (DIN) to TP to classify sites based on expected limitation (where DIN = NO_3 + NO_2 + NH_4). This classification was based on a study by Morris and Lewis (1988), who tested nine indices for effectiveness in predicting phytoplankton limitation. Results indicated that the physiologically relevant fractions of N and P, namely DIN:TDP or DIN:TP, were the most successful metrics predicting nutrient limitation. They noted that TDP is externally available via (*i*) direct uptake of soluble reactive P (SRP) and (*ii*) via phosphatase-mediated hydrolysis of dissolved organic P (DOP). Internally available phosphorus can be estimated by particulate phosphorus concentration (PP). Nitrogen is mainly available as nitrate and ammonia, which together comprise the majority of the DIN fraction. Although their study was conducted on phytoplankton, we felt that the same arguments could be made for lotic periphyton, even given the added influence of effects of periphyton mat development on nutrient uptake and recycling (Bothwell 1989) and the variable interaction between velocity and nutrient concentration and form on algal specific growth rate (Borchardt 1994). Therefore, in a river with ambient molar DIN–TP > 12, we predicted that phosphorus addition would produce higher periphyton accrual than nitrogen addition or control treatments (Table 1). However, in rivers with intermediate DIN–TP ratios (i.e., 1–12), we were uncertain whether nitrogen, phosphorus, or both nutrients would be limiting.

© 2002 NRC Canada

Table 2. Physical and chemical characteristics of study sites.

Variable	B1	S1	S2	S3	S4	S5	C1	C2	C3	K1	K2	K3
Velocity at diffusers ($cm \cdot s^{-1}$)	29	26	34	26	1	9	29	22	17	58	28	1
Depth at diffusers (cm)	13	26	25	17	30	35	26	29	18	45	37	26
Solar radiation available (% shade-free sky)	96	94	97	94	93	93	76	87	87	94	88	97
Total global solar radiation ($W \cdot m^{-2} \cdot day^{-1}$)	3792	3792	3792	3792	5477	5477	4524	4524	4524	2650	4524	4524
Gradient (%)	1	1	2	1	1	1	2	2	1	2	1	0.2
Channel sinuosity	1.4	1.0	1.0	1.1	1.0	1.0	1.0	1.0	1.0	1.0	1.1	1.9
Mean water depth (m)	0.86	0.52	0.83	0.87	1.78	1.78	0.82	0.67	1.59	2.08	2.02	6.13
Mean width (m)	76	75	81	84	194	190	43	36	51	106	158	184
Width (m) : depth (m)	88	145	97	96	109	107	53	54	32	51	78	30
Median substrate size (cm)	7	2	11	11.5	0	13	40	27	24	12	12	0
Substrate embeddedness (%)	41	6	1	13	93	48	36	39	28	35	15	0
Macrophyte cover (%)	0	39	85	3	35	0	1	0	0	2	3	37
Alkalinity ($mg \cdot L^{-1}$ as $CaCO_3$)	126	34	36	68	100	98	4	12	12	60	42	49
Hardness ($mg \cdot L^{-1}$ as $CaCO_3$)	299	89	101	190	240	204	8	24	24	93	75	83
Conductivity ($\mu S \cdot cm^{-1}$)	480	115	121	302	505	500	17	17	17	240	225	225
$NO_3 + NO_2$ ($mg \cdot L^{-1}$ as N)	0.089	0.002	0.09	0.018	1.61	1.36	0.002	0.003	0.003	0.12	0.11	0.11
NH_4 ($mg \cdot L^{-1}$ as N)	0.021	0.01	0.017	0.012	0.037	0.02	0.01	0.006	0.02	0.005	0.04	0.009
TP ($mg \cdot L^{-1}$ as P)	0.024	0.009	0.014	0.012	0.1	0.062	0.014	0.016	0.028	0.007	0.013	0.009
Molar TIN:TP	10	3	17	6	36	49	2	1	2	39	26	29
pH	8.2	8.3	8.4	8.5	7.1	6.7	7.8	8.1	7.8	8.2	7.4	8
Turbidity (NTU, nephelometric turbidity units)	24.8	1.8	1.5	1.6	9.5	8.4	0.4	5.1	4.1	1.6	1.2	1.6

Note: "Zero" values for median substrate size indicate sand. Site designations as in Table 1. TIN, total inorganic nitrogen ($NO_2 + NO_3$, NH_4); TP, total phosphorus (unfiltered and digested).

Artificial nutrient diffusers were constructed after a technique devised by Gibeau and Miller (1989) in which 10-dram plastic vials (Leco Corporation) were filled with 4% agar (control treatment) amended with 0.1 $mol \cdot L^{-1}$ $NaNO_3$-N (N treatment), 0.1 $mol \cdot L^{-1}$ KH_2PO_4-P (P treatment), or 0.1 $mol \cdot L^{-1}$ $NaNO_3$ + 0.1 $mol \cdot L^{-1}$ KH_2PO_4 (N + P treatment) (sensu Hill and Knight 1988). After being filled with autoclaved agar–nutrient treatments, vials were sealed by heating porous, porcelain crucible covers (Dynalab Corporation) and fusing them into the tops of the plastic vials that then were inverted until the agar solidified. The covers (2.6 cm diameter), pre-cleaned by soaking in a 10% HCl solution and rinsing in distilled water, provided a surface conducive to periphyton accrual and growth (Gibeau and Miller 1989). Vials (n = 7 per treatment) were randomly glued into wooden racks (distance between vials = 7 cm) that were placed at a water depth of about 50 cm for 30 days. Virtually all vials contained no invertebrate grazers with the exception of the second Snake River site (S2), which had a total of 10 Brachycentridae (spp.) clinging to the tops of the diffusers (E.B. Snyder, personal observation).

Rates of diffusion were not measured in this experiment; however, previous research using identical design but with lower concentrations of nutrient treatments (Gibeau and Miller 1989) indicated that diffusion rates decrease with time in a negative exponential fashion. For example, after 21 days of incubation, release rates for ammonium (NH_4) and phosphate (PO_4) were only 2% and 7% of initial rates, respectively, and 93% and 77% of the NH_4 and PO_4 remained in respective vials. The concentrations of nutrients that we used were greater than those used by Gibeau and Miller (1989) (N treatment = 0.05 $mol \cdot L^{-1}$ NH_4Cl, P treatment = 0.005 $mol \cdot L^{-1}$ K_2HPO_4, and N + P = 0.05 and 0.005 $mol \cdot L^{-1}$, respectively) under the assumption that all treatments would still be releasing nutrients after 30 days.

Physical measurements were made when vials were placed and removed at each site. Riparian shading was estimated at each site using the Solar Pathfinder, and available solar energy, measured as Watts ($m^2 \cdot day^{-1}$), was used as a surrogate for photosynthetically active radiation and was estimated using weather data collected at major air fields in the vicinity of the sample sites. All other physical measurements were composed of mean values collected over 6 transects (20 equidistant measurements taken per transect) located within each study reach. On day 30, four of the nutrient-diffusing vials per treatment were placed on ice and transported to a laboratory freezer (–30°C) prior to determination of periphyton chl *a* and ash-free dry mass (AFDM). After freezing, periphyton was removed from each cover using a small bristle brush and filtered through a 0.45-µm, pre-ashed glass fibre filter (Whatman GF/F) that was placed in 100% reagent-grade methanol for 24 h in the dark. Chlorophyll *a* was determined spectrophotometrically (Gilford model 2200) (APHA 1992). AFDM was determined using the remaining extractant from each sample used in the chlorophyll analysis, thus slightly underestimating total AFDM. Differences in chl *a* and AFDM among treatments for each site were tested using analysis of variance (ANOVA) and Tukey's post-hoc repeated measures analysis (Zar 1984).

The remaining three vials per treatment were used for enumeration of the diatom community. Samples were placed in Lugol's iodine preservative, composited by treatment to facilitate analysis, and identified following the technique of St. Clair and Rushforth (1976). Minimum counts of 550–1000 diatom valves, primarily living (S.R. Rushforth, personal observation), were made for each composited sample to estimate relative density. Other biological metrics calculated included species richness and Simpson's dominance index.

Functional response to enrichment was inferred from periphyton standing crop as chl *a* and organic matter content,

© 2002 NRC Canada

both measures of diatom accrual and potential surrogates for productivity. Diatom assemblage structure was used to examine regional patterns (e.g., ultimate determinants of the diatom community) by comparing differences among sites using only the control treatments. These analyses included a comparison of richness and dominance (as Simpson's dominance index), a principal components analysis (PCA) of the top five taxa on control treatments, and a histogram of those species that contributed the most to site separation. Jaccard's Index (C_j), a similarity coefficient that provides a measure of β diversity, was calculated on control treatments using the 20 most abundant taxa to assess the similarity of diatom communities among sites. Finally, Spearman's rank correlations were used to identify relationships between the relative abundance of taxa that were identified in the PCA and the various physical and chemical habitat variables. All variables were ln or SQRT(asin) transformed prior to analysis; the latter was used for gradient, substrate embeddedness, and macrophyte cover. Significant relationships were considered to be those with coefficient scores greater than 0.50 (Kutka and Richards 1996).

The response of the diatom community to enrichment was used to examine patterns in proximate determinants (at the spatial scale of the reach or smaller) of assemblage structure. Specifically, richness and Simpson's dominance index were evaluated across all nutrient treatments. PCA was conducted using the 10 most abundant taxa in all treatments. Finally, a histogram was used to examine spatial patterns using the 5 most abundant taxa in all treatments.

Results

Periphyton standing crops—functional response to enrichment

Based on molar TIN–TP ratios, we predicted that the three Kootenai River, two Middle Snake River, and the upper Snake S2 sites would be phosphorus limited. This prediction was supported in two of the Kootenai River sites (K1 and K2) where chl *a* and AFDM concentrations on the P and N + P treatments were significantly higher than those of the control and N treatments (Fig. 2). The third Kootenai River site (K3) had significantly higher chl *a* and AFDM only on the N + P treatment, suggesting colimitation. All three Snake River sites showed no significant differences among treatments (Fig. 2). However, ambient nutrient concentrations were quite high, particularly at the Middle Snake sites (S4–S5) (Table 2), both of which were considered eutrophic. Sites predicted to be colimited by N and P included the Selway (C1) and Clearwater (C3) Rivers, the Bear River (B1), and the two upper Snake sites (S1 and S3). Patterns in periphyton accrual significantly supported these predictions in all five of the study reaches (Fig. 2). Finally, the Lochsa River (C2) was predicted to be nitrogen limited, and chl *a* concentration demonstrated this pattern, although AFDM did not follow this trend, being significantly higher on the N + P treatment (Fig. 2).

Ultimate determinants—regional patterns and site differences in diatom assemblage structure

Trends in community structure among sites were analyzed by examining only the control treatments, as these would provide a representation of the 30-day colonization pool in each river without the added effect of enrichment. Diatom richness ranged from 15 to 47, with the highest values in the nutrient-enriched Middle Snake sites and the lowest values in the South Fork of the Snake and the Kootenai rivers (Table 3). The 10 most abundant taxon at each site represented over 70% of the diatom community. Common taxa at the various sites included *Achnanthes minutissima* Kütz., *Nitzschia paleacea* Grun., *Nitzschia amphibia* Grun., *Cymbella affinis* Kütz., *Gomphonema ventricosum* Greg., *Cocconeis placentula* Ehr., *C. placentula* var. *euglypta* Ehr., and *Synedra rumpens* Kütz. Simpson's dominance index, which provides a measure of evenness (1.0 = complete dominance or complete unevenness), ranged from 0.91 (K3) to 0.08 (S5) (Table 3).

Principal components analysis (PCA) was used to determine whether patterns, based on diatom community structure, existed among sites and among nutrient treatments. Based on the top five taxa from control treatments, sites were grouped mainly by drainage basin, e.g., Middle Snake (S4–S5), Kootenai River (K1–K3), and Clearwater sites (C1–C3) (Fig. 3). The Kootenai River sites also were closely associated with the Upper Snake site (S3) and the Bear River (B1), whereas the three Clearwater sites were associated with the first and second Upper Snake sites (S1 and S2). The three Upper Snake sites were not closely associated with one another, although S1 and 2 were more closely grouped than S3, as would be predicted based on longitudinal linkage. PCA axis 1 was associated with *Nitzschia paleacea* (NIPA) and *Cocconeis placentula* (COPL); the second PCA axis was associated with *Nitzschia amphibia* (NIAM) (cutoff for rotated loadings = 0.8). These two axes explained 78.5% of the variation among sites.

Comparison of these five taxa indicated that *Nitzschia amphibia* was abundant at the two Middle Snake sites (S4–S5) and present, but rare, at the Clearwater River (C2) and Bear River (B1) sites. *Nitzschia paleacea* was commonly found at all sites except the Upper Snake site (S3) and was dominant at both S1 and S2. Similarly, *Cocconeis placentula* was common at many sites and dominated the community in the Upper Snake (S1) and Clearwater (C1–C3) sites.

The Middle Snake sites (S4–S5) were similar to one another (Jaccard's index (C_j) = 0.89; where 1.0 indicates identical diatom communities) and to the second Upper Snake site (S2) (C_j = 0.75 and 0.74, respectively), and the three Clearwater sites were quite similar (C_j ranged from 0.81 to 0.94) but also were similar to S1–S2 and S4–S5 (Table 4). Finally, K1 and K2 in the Kootenai River system were similar (C_j = 0.78). Diatom richness was positively correlated with total global solar radiation, NH_4, and TP based on Spearman's rank correlations (Table 5). Simpson's dominance was positively correlated with mean water depth and negatively correlated with width–depth ratio and TP. *Nitzschia paleacea*, an indicator of higher quality water, was positively correlated with width–depth ratio and negatively correlated with mean depth, nitrate plus nitrite ($NO_3 + NO_2$), and pH, whereas *Cocconies placentula* was negatively correlated with a number of physical–chemical variables. *Nitzschia amphibia*, a pollution-tolerant species often found

© 2002 NRC Canada

Fig. 2. Concentration of chlorophyll *a* (mg·m^{-2}) and organic matter content (ash-free dry mass (AFDM), g·m^{-2}) of periphyton on nutrient treatments (mean + 1 standard deviation). Sites are grouped according to predicted nutrient limitation based on molar total inorganic nitrogen to total phosphorus ratios where (*a*) was predicted to be limited by phosphorus, (*b*) colimited, and (*c*) nitrogen limited. Within a site, bars with different letters were significantly different ($p < 0.05$). Samples for AFDM at the Middle Snake sites (S4–S5) were lost. Within a site, treatments are represented as individual histogram bars from left to right as follows: control, open bars; N, fine-hatched bars; P, coarse-hatched bars; N + P, solid bars. Site locations and designations as in Table 1. Note that *y* axes are variable.

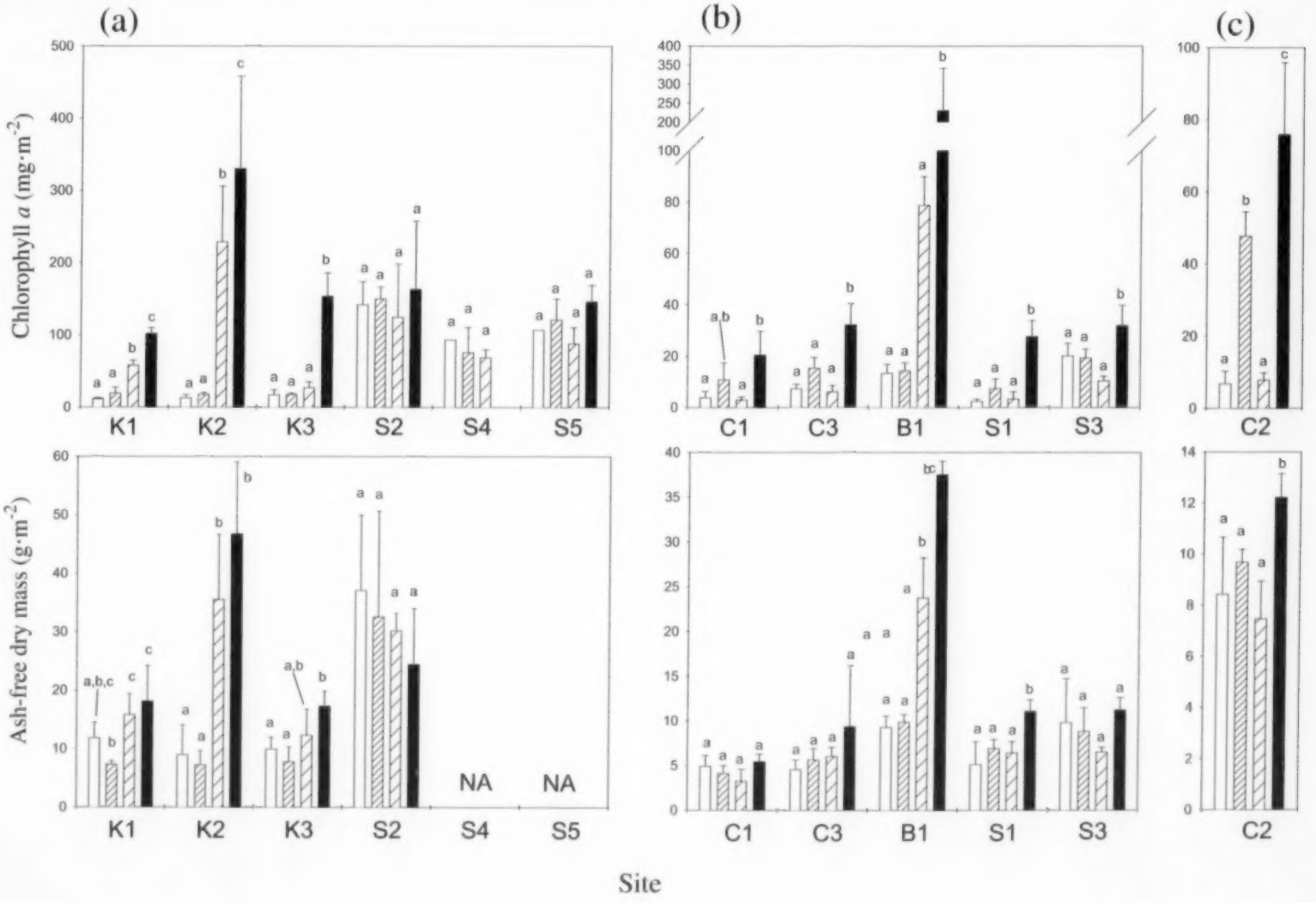

© 2002 NRC Canada

Table 3. Ambient chlorophyll *a* (chl *a*) and organic matter content of periphyton growing on natural substrate and taxa richness and Simpson's dominance on artificial diffusers.

Variable	B1	S1	S2	S3	S4	S5	C1	C2	C3	K1	K2	K3
Ambient periphyton chl *a* ($mg \cdot m^{-2}$)	31.2	27.5	146.8	39	108.8	79.9	38.5	32.9	19.6	30.2	34.6	0
Ambient periphyton AFDM ($g \cdot m^{-2}$)	19.7	16.7	39.6	20.2	26.1	32.9	17	13	8.5	41.3	38.5	0
Diatom taxa richness	25	33	37	15	47	36	25	38	35	19	27	19
Simpson's dominance	0.49	0.2	0.16	0.62	0.14	0.08	0.29	0.2	0.37	0.72	0.67	0.91

Note: "Zero" values for chl *a* at K3 are a function of sand substrate. AFDM, ash-free dry mass; site designations as in Table 1.

Fig. 3. Scatterplot of principal components analysis (PCA) based on the five most abundant diatom species in the control treatments. Code used for site location as in Table 1. Axis 1: NIPA, *Nitzschia paleacea*; COPL, *Cocconeis placentula*. Axis 2: NIAM, *Nitzschia amphibia*. Cutoff for rotated loadings = 0.80.

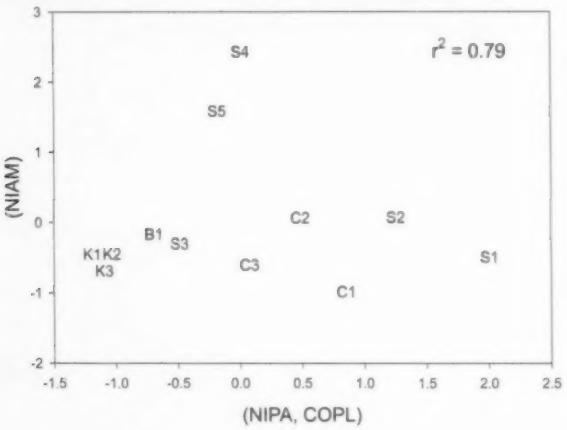

in eutrophic waters, was positively correlated with total global solar radiation, embeddedness, TP, and turbidity and negatively correlated with velocity.

Proximate determinants—response to enrichment

No significant differences were found in richness and Simpson's dominance index among nutrient treatments (ANOVA and Tukey's post-hoc tests). However, trends suggested that richness increased and dominance decreased with enrichment (Table 3).

Treatments were highly associated with site location and there was little directional response to a specific enrichment treatment (Fig. 4; PCA, all sites and treatments). Secondarily, sites and treatments were grouped according to drainage basin, as in the initial PCA conducted on control treatments. As such, the two Middle Snake sites (S4–S5) were well separated and closely associated with one another, as were the first two Kootenai Sites and the Clearwater sites. Study sites on the Upper Snake (S1–S3) were interspersed among the three Clearwater sites. Axis 1 (*Cocconeis placentula*) and axis 2 (*Nitzschia amphibia* and *Navicula menisculus*) explained 42.7% of the variation among treatments and sites (cutoff for rotated loadings = 0.7).

The top five taxa from all treatments combined included *Achnanthes minutissima*, *Nitzschia paleacea*, *Cocconeis placentula*, *C. placentula* var. *euglypta*, and *Nitzschia amphibia*. These taxa comprised >28% of the relative abundance of all taxa in all treatments. There were no significant responses to enrichment (control vs. three nutrient treatments; ANOVA and Tukey's post-hoc test; Fig. 5), although some trends at specific sites were apparent. For example, *Nitzschia paleacea* increased in response to enrichment in the Bear River (B1), Upper Snake (S1) and Middle Snake (S5), Clearwater (S1), and Kootenai (K1 and K2) sites (Fig. 5). *Achnanthes minutissima* generally did not respond to enrichment (the exception being the Bear River) and dominated the diatom community in the Snake (S3) site, and the Clearwater, Bear, and Kootenai systems (Fig. 5).

Discussion

We felt that there were three possible outcomes determining the mechanisms behind observed patterns in diatom community structure: (*i*) no difference among sites, (*ii*) similar diatom communities at sites with similar ambient nutrient regimes (e.g., same ecoregion), or (*iii*) similar communities at sites occurring within the same drainage basin (Fig. 6). As such, these hypotheses represent the hierarchical structure of factors that can influence algal assemblages (Stevenson 1997). Results of the PCAs and Jaccard's index of similarity indicated that sites tended to be grouped by drainage basin, what we are considering an intermediate determinant of algal assemblage structure. Furthermore, observed patterns showed that in most cases, diatom assemblages were structured based on location within a drainage basin. For example, the Kootenai River, Clearwater, and Middle Snake sites all tended to be closely associated to one another. This implies that basin characteristics, such as geomorphology and land use, are critical determinants of diatom community structure (Kutka and Richards 1996), a conclusion that is supported by the absence of a unified response to enrichment by diatom taxa. For example, in the Middle Snake, land use (an ultimate determinant of diatom assemblage structure) and subsequent eutrophication appear to be responsible for determining the structure of the diatom community. These patterns suggest that both intermediate and ultimate determinants were important in structuring the diatom communities (Fig. 6) and that proximate factors (as mediated by the nutrient diffusers) did not influence diatom community structure. High nutrient levels were associated with high diatom species diversity, whereas phosphorus limitation led to the lowest diatom species diversity in these large river systems.

Because this study was conducted over only 30 days, we were cautious about inferring the potential impacts of chronic nutrient addition (e.g., non-point sources) on the diatom community. However, in the Kuparuk River, Alaska, Peter-

© 2002 NRC Canada

Table 4. Jaccard's index of similarity based on 20 most abundant diatom taxa on control treatments.

	S1	S2	S3	S4	S5	C1	C2	C3	K1	K2	K3
B1	0.37	0.61	0.53	0.60	0.67	0.44	0.61	0.56	0.33	0.44	0.35
S1		0.61	0.35	0.60	0.58	0.63	**0.71**	**0.75**	0.33	0.53	0.53
S2			0.63	**0.75**	**0.74**	0.61	0.68	**0.72**	0.35	0.53	0.53
S3				0.45	0.50	0.44	0.44	0.47	0.31	0.43	0.43
S4					**0.89**	0.60	**0.75**	**0.70**	0.30	0.45	0.53
S5						0.58	**0.74**	0.68	0.26	0.42	0.50
C1							**0.81**	**0.87**	0.43	0.47	0.35
C2								**0.94**	0.35	0.53	0.44
C3									0.38	0.56	0.47
K1										**0.78**	0.50
K2											0.67

Note: Site codes as in Table 1.

Table 5. Significant ($p > 0.50$) Spearman's rank correlation coefficients for diatom species loading most heavily in the PCA (3 most abundant taxa in control treatments).

			Relative abundance of diatom taxa		
Variable	Richness	Simpson's dominance	NIPA (%)	COPL (%)	NIAM (%)
Velocity at diffusers ($cm \cdot s^{-1}$)					–0.59
Solar radiation available (% shade-free sky)				–0.54	
Total global solar radiation ($W \cdot m^{-2} \cdot day^{-1}$)	0.53				0.71
Channel sinuosity				–0.71	
Mean water depth (m)		0.49	–0.71	–0.73	
Mean width (m)				–0.60	
Width (m) : depth (m)		–0.70	0.50		
Substrate embeddedness (%)					0.72
Alkalinity ($mg \cdot L^{-1}$ as $CaCO_3$)				–0.69	
Conductivity ($\mu S \cdot cm^{-1}$)				–0.61	
$NO_3 + NO_2$ ($mg \cdot L^{-1}$ as N)			–0.65		
NH_4 ($mg \cdot L^{-1}$ as N)	0.55				
TP ($mg \cdot L^{-1}$ as P)	0.64	–0.58			0.77
Molar TIN:TP				–0.64	
pH			–0.57		
Turbidity (NTU, nephelometric turbidity units)					0.60

Note: Variables were all ln transformed before analysis with the exception of gradient, substrate embeddedness, and macrophyte cover, which were SQRT(asin) transformed. DIN, total nitrogen ($NO_2 + NO_3$, NH_4); TP, total phosphorus (unfiltered and digested); NIPA, *Nitzschia paleacea*; COPL, *Cocconeis placentula*; NIAM, *Nitzschia amphibia*.

son et al. (1993) observed no real change in diatoms as a result of nutrient addition over the course of 4 consecutive years of phosphorus addition, although there were dramatic changes in algal biomass and productivity and a shift from bottom-up nutrient limitation to top-down limitation by macroinvertebrates. This suggests that our results could be used to make initial predictions of short-term changes (e.g., = 4 years) in the periphyton community.

Periphyton standing crop—patterns in chlorophyll *a* and AFDM

Bothwell (1985) noted that molar N:P only identifies potential limitation and that it is the actual concentration that determines whether or not growth rate (μ) is limited. We used N:P as a tool to predict potential limitation and argue that the inherent utility of artificial diffusers is their ability to corroborate or refute these predictions. In part, this study was initiated to try to demonstrate the utility of artificial diffusers for determining potential nutrient limitation, the results of which could be used to direct more rigorous research given an increase, for example, in anthropogenic nutrient loading.

We utilized ambient N:P vs. cellular N:P for several reasons. Measurement of cell N and P is difficult to relate back to ambient concentrations of dissolved and total nutrients, which makes it difficult to apply from a management perspective (e.g., establishment of total maximum daily load (TMDL) criteria). In addition, if non-algal particles represent a significant fraction of the periphyton matrix, results will be biased, and because a digestion step is involved in the analysis, cost can be prohibitive (Biggs 2000). Bothwell (1985) observed good agreement between the phosphorus concentration of grab samples and most of the cellular physiological indicators of P nutrition, such as alkaline phosphatase activity, $^{32}PO_4^{-1}$ uptake velocity (V_{max}), cellular N : organic P, chl *a* : adenosine triphosphate (ATP), C:ATP,

© 2002 NRC Canada

Fig. 4. Scatterplot of principal components analysis (PCA) based on 10 most abundant diatom species in all treatments. Code used for site and treatment identification is as follows: 1st letter and number = river system and longitudinal location (as in Table 1); 2nd letter = treatment (C = control, N = nitrogen, etc). Axis 1: COPE, *Cocconeis placentula*. Axis 2: NIAM, *Nitzschia amphibia*; NAME, *Navicula menisculus*. Cutoff for rotated loadings = 0.70.

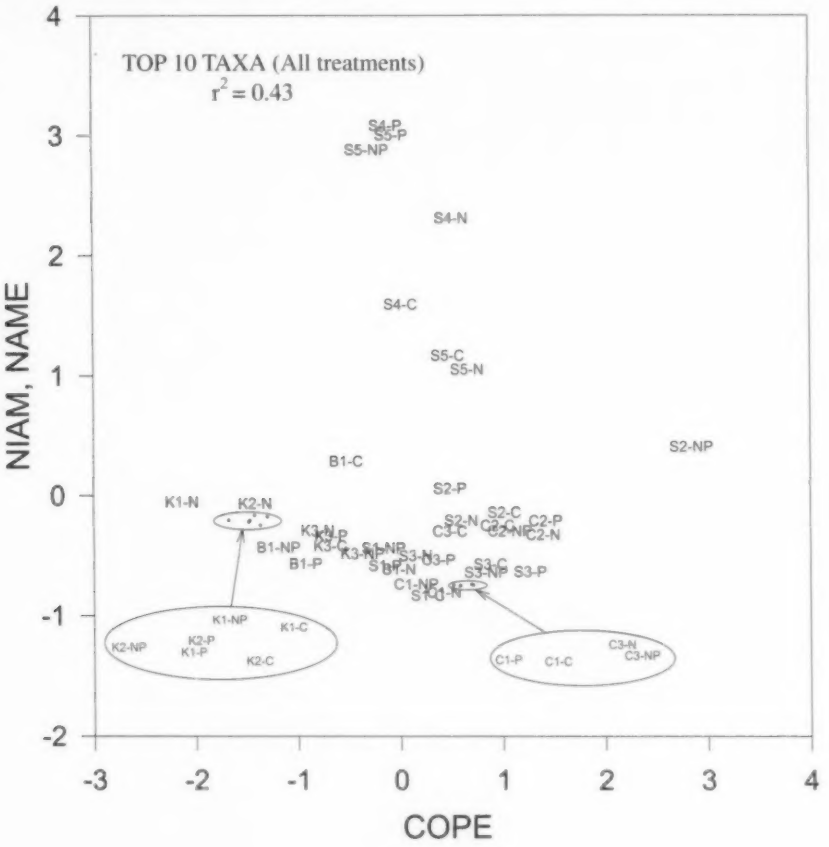

and C : organic P, suggesting that the use of ambient concentrations to predict nutrient limitation of algae is a useful exercise. This is not to suggest that measurement of cellular N:P is not a useful tool. Biggs (2000) noted that cellular N and P provides a direct measure of algal nutrient status that can be related to specific μ as well as providing an assessment of the historic nutrient regime by integrating alternative nutrient sources, such as mineralized organic particles in the periphyton matrix and nutrients supplied from upwelling groundwater.

Molar TIN:TP suggested that the three Kootenai River sites (K1–K3) and the two sites on the middle reach of the Snake River (S4–S5) should be phosphorus limited as TIN:TP (ranging from 26 to 49) likely exceed algal optima, an assertion based on limited lotic periphyton research (Schanz and Juon 1983; Grimm and Fisher 1986; Borchardt 1994) but well substantiated in the phytoplankton literature (Redfield 1958; Rhee and Gotham 1980). DIN:TP at the final site (S2) predicted to be phosphorus limited was 17, very similar to Redfield's ratio of 16 as the transition point between N and P limitation in the ocean (Redfield 1958) and also similar to the mean cellular N:P of 17.1 observed by Grimm and Fisher (1986) for desert periphyton. There was no evidence of limitation at S2, potentially as a result of the close match between optimum cellular and ambient N:P ratios.

Experimental results supported predictions only for upper Kootenai River sites (K1 and K2). The third Kootenai site (K3) appeared colimited even though molar N:P did not predict this (TIN:TP = 29). As an explanation, it is possible that input from extensive agricultural activity in this region could increase nutrient concentrations, although this was not apparent from ambient nutrient sampling. However, nutrients were only monitored synoptically and it is possible that pulses of nutrients associated with precipitation and runoff were influencing patterns of periphyton accrual (Humphrey and Stevenson 1992). The other two sites predicted to be phosphorus limited (S4 and S5) occurred in reaches heavily impacted by nutrification from sources such as agriculture, urbanization, and fish hatchery effluent. Concomitant with results obtained by others (Bushong and Bachmann 1989; Chessman et al. 1992; Scrimgeour and Chambers 1997), the lack of response to nutrient addition suggests that molar N:P does not provide reliable predictions in systems with high ambient nutrient concentrations because the absolute, rather

© 2002 NRC Canada

Fig. 5. Relative abundance (%) of top five most abundant diatom taxa in all treatments. Taxa include (*a*) *Achnanthes minutissima* (ACMN), (*b*) *Nitzschia paleacea* (NIPA), (*c*) *Cocconeis placentula* (COPL), (*d*) *Cocconeis placentula* var. *euglypta* (COPE), and (*e*) *Nitzschia amphibia* (NIAM). Within a site, treatments are represented as individual histogram bars from left to right as follows: control, open bars; N, fine-hatched bars; P, coarse-hatched bars; N + P, solid bars. Note that *y* axes are variable and samples were composited, thus no error bars. Key to site abbreviations as in Table 1.

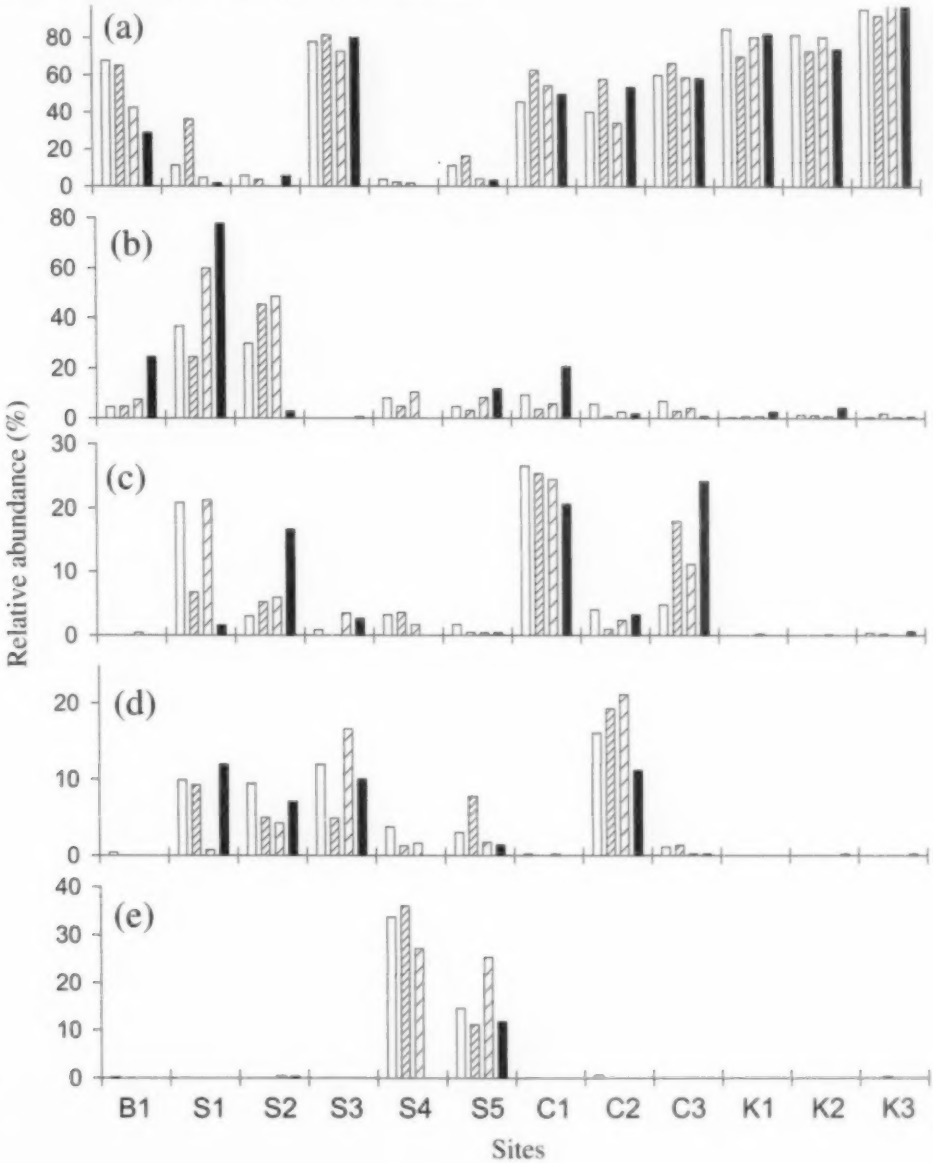

than the relative, amounts are of overriding importance at these saturated levels. In his study on the Thompson River, Bothwell (1985) noted that at temperatures less than 10°C, P limitation commenced around 3–4 $\mu g \cdot L^{-1}$ SRP. The lowest concentration for TP that we recorded occurred in the Kootenai River (7 $\mu g \cdot L^{-1}$) supported the prediction that this site would be P limited. Results of the diffusers substantiated this, as well as for other sites with low concentration of TP.

Predictions of colimitation (as concentration of chl *a*) were supported by experimental results in all five sites (C1, C3, B1, S1, S3). A significant increase in both chl *a* and AFDM on the N + P treatments was observed at S1 as predicted. In addition, S1 had lower nitrate-N concentrations (0.002 $mg \cdot L^{-1}$) than S2 (0.09 $mg \cdot L^{-1}$). Grimm and Fisher (1986) found that periphyton growth was saturated at nitrate-N concentrations of 0.055 $mg \cdot L^{-1}$. The other Upper Snake site, S3, had nutrient concentrations similar to those of S2 and showed a positive response to the N + P treat-

© 2002 NRC Canada

Fig. 6. Hierarchical conceptualization of factors that potentially determine algal assemblage structure and function. The emergent patterns represent experimental outcomes that we would predict given that ultimate, intermediate, or proximate variables were determining algal assemblages (largely taken from Stevenson (1997) and Minshall (1993)). Note that nutrients are listed at two hierarchical levels. This indicates that parent geology will determine overall ambient nutrient regime, whereas microhabitat variability can influence local (i.e., proximate) nutrient supply.

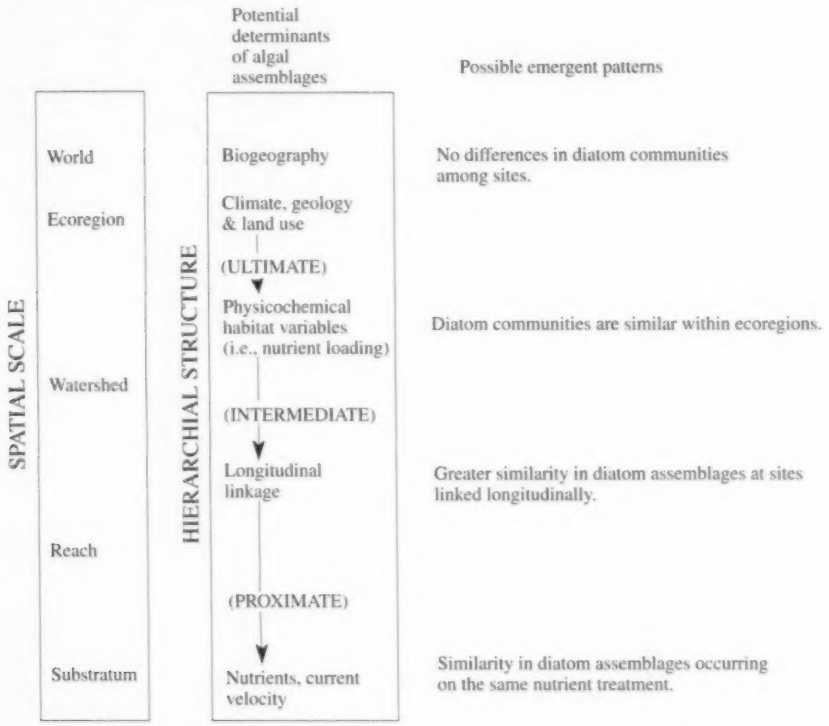

ment. However, S3 was located on a different tributary than S1 and subsequently may have differed along another environmental gradient (e.g., variation in micronutrients). Finally, the only site predicted to be N limited was C2 (NO_3 + NO_2 = 0.003 mg·L^{-1}), and experimental results supported these predictions, but only for chl *a*.

We found that experimental results matched predictions 8 of 12 times and 2 of 12 times for chl *a* and AFDM, respectively. This is likely because N:P does not provide sufficient information on ambient nutrient concentrations. This was well demonstrated in the Middle Snake sites where ambient concentrations were high enough to saturate enzymatic uptake and where no response to enrichment was observed. Given this lack of predictive ability, we found the diffuser technique to offer insight into patterns of nutrient limitation that otherwise would not have been apparent (Pringle 1987; Scrimgeour and Chambers 1997). We are uncertain as to why AFDM and chl *a* predictions were not corroborative. A longer study might yield different results. In addition, AFDM incorporates any non-algal organic detritus captured in the developing periphyton matrix, potentially leading to a less sensitive indicator of enrichment relative to chl *a*.

Diatom assemblage structure—patterns in richness and diversity

Diatom richness and diversity were highest at the nutrient-enriched Middle Snake sites. This is counterintuitive given that many other researchers have noted that an increase in resources above a threshold value led to competitive exclusion of some algal species (for example, see van Dam 1982; Lowe et al. 1986). This concept of competitive exclusion was described by Tilman (1982) and is characterized by the classic, bell-shaped curve of resource richness vs. species richness. In the Middle Snake, nutrient concentrations were well above threshold values reported in the literature. Thus, in the Middle Snake, the curve described by Tilman (1982) could be extended along the resource gradient axis leading to a sustained plateau in diversity (e.g., the predicted falling limb of the resource–species richness curve was not observed). In the Middle Snake, a broad range of relatively high nutrient concentrations appeared to be utilized by a variety of diatom taxa. This suggests that many diatom species should be able to coexist given a combination of superabundant nutrients and subsequent lack of competitive inhibition and assuming that other factors are not limiting (such as light or temperature) or toxic (as in high concentrations of ammonium).

Pringle (1990) found that diatom diversity increased when nutrients were added, a response attributed to the fact that nutrient enrichment occurred within the rising limb of the curve described above and that increasing nutrient concentrations beyond a given point would eventually lead to a

© 2002 NRC Canada

decline in richness and an increase in dominance. Stated another way, diatom diversity is maximized when resources are most heterogeneous (Connell 1978). However, the nutrient concentrations that Pringle (1990) recorded (ambient $NO_3 + NO_2$ and $TPO_4 = 0.041$ mg·L^{-1} and 0.008 mg·L^{-1}, respectively) were much lower than those experienced in the Middle Snake (ambient $NO_3 + NO_2$ and TP = 1.5 mg·L^{-1} and 0.081 mg·L^{-1}, respectively). Also, diffuser enrichment caused no change in either periphyton chl *a* and AFDM or diatom assemblage structure in the Middle Snake, indicating that the diatom community was adapted to the high ambient nutrient levels and was not a result of nutrient treatments. A study done by Marcus (1980) provides another example where increased resources (nutrients) were associated with increased algal diversity. Relatively high concentrations of ammonia (0.026 mg·L^{-1}) and phosphate-P (0.063 mg·L^{-1}) in a reservoir outflow increased diatom diversity and productivity relative to downstream locations, similar to patterns in productivity observed in the Middle Snake (S.A. Thomas, Virginia Tech, Biology Department, Blacksburg, VA 24060, personal communication). The concentrations of nutrients in the Middle Snake are higher than those of most other studies examining periphyton accrual in rivers and suggest that the resource gradient – species richness curve can be extended before competitive exclusion occurs, at least for benthic algae. Future studies hopefully will determine the point at which competitive exclusion would occur in the Middle Snake as well as specific mechanisms. Whether or not these results are applicable to other river systems with high ambient nutrient concentrations has yet to be determined.

Richness and diversity were lowest in the Kootenai sites (K1–K3) and in the Upper Snake site (S3). Both rivers are impounded and experience substantial alteration in nutrient, flow, and temperature regimes. Results from this study suggest that systems that are impounded and nutrient limited will have low diatom diversity, whereas the effects of impoundment may be offset by high ambient nutrient concentrations. In the case of the Kootenai River, research indicates that the reservoir severely limits the downstream transport of nutrients and organic matter. For example, Woods (1982) found that 63% and 25% of the influent total phosphorus and total nitrogen, respectively, were retained and that the reservoir had a sediment-trapping efficiency that exceeded 95%. Thus, the nutrient regime of the river system downstream of impoundment is severely altered and would represent a change at the ultimate scale.

Ultimate determinants—taxa-specific geographic patterns

At a regional scale (ultimate determinants; among-site analysis), emergent patterns influencing the algal community were examined using only the control treatments. Patterns from graphical analysis of the specific diatom taxa associated with the 1st and 2nd PCA axes (control treatments only) indicated that the Middle Snake sites were associated with a high abundance of *Nitzschia amphibia*, which is not unexpected given that it is considered to be a eutrophic species (Lowe 1974). Sites low in species richness and diversity (e.g., the Kootenai River and South Fork of the Snake (S3)) were characterized by the presence of *Nitzschia paleacea* (the only species present at all three Kootenai River sites) and *Cocconeis placentula*, which is considered to be cosmopolitan but generally found in unpolluted systems (Patrick and Reimer 1966; Lowe 1974). Wantanabe et al. (1986) observed that *Nitzschia paleacea* is an indicator of good water quality and is intolerant to organic pollution. The three Clearwater sites also were closely clustered in the PCA, and results from the graphical analysis indicated that two taxa, *Cocconeis placentula* and *Nitzschia paleacea*, were relatively abundant at all three of these sites. Thus, sites appeared to be clustered based on location within the same drainage basin. Exceptions, such as the separation of the Middle Snake sites, occurred when there was substantial alteration in various chemical and physical characteristics relative to sites located further upstream.

Spearman's rank correlations were conducted to identify positive and negative associations between richness, dominance, and the three diatom taxa (those that contributed heavily to site separation in the PCA) vs. the various physical and chemical measurements that were made at each site. Results of Spearman's rank correlations indicated that diatom richness was positively associated with total global solar radiation, NH_4, and TP. These correlations were, in part, a result of the high diatom richness recorded in the eutrophic and slow-moving Middle Snake (as discussed previously). The dominance index was negatively associated with TP and width–depth ratio and positively associated with water depth. Similar to the explanation above, we believe that high nutrient concentrations in the Middle Snake negated competition leading to a diverse and even algal community vs. sites with high dominance values (e.g., the Kootenai River) that were impounded and nutrient poor.

Correlation analysis, conducted using the relative abundance of taxa identified in the PCA (control treatments only), indicated that both *Nitzschia paleacea* and *Cocconeis placentula* were negatively correlated to numerous variables, both physical and chemical. As such, these two taxa were associated with smaller, more heavily shaded, and nutrient poor systems (e.g., the three Clearwater sites and the Upper Snake sites). Wantanabe et al. (1986) classified *Nitzschia paleacea* as oligosaprobic and an indicator of good water quality. *Cocconeis placentula*, although considered to be cosmopolitan and not a good indicator species, is generally found in unpolluted systems (Lowe 1974). *Nitzschia amphibia*, a taxon more tolerant of organic pollution and considered a eutrophic species, was positively associated with numerous physical and chemical variables (exception being a negative correlation to water velocity at the diffusers) and was found almost exclusively in the Middle Snake.

These three taxa have different tolerances to nutrient loading and, subsequently, contributed most strongly to site separation in the PCA. The Middle Snake sites were characterized by relatively slow water and high ambient nutrient concentrations, turbidity, and embedded substrate, variables positively correlated with the relative abundance of *Nitzschia amphibia*. Alternatively, the Clearwater sites were separated in the PCA by taxa negatively correlated to characteristics such as alkalinity, conductivity, nitrogen, and N:P, as well as channel sinuosity and water depth and width, indicating that these taxa occurred in smaller systems, low in ion and nutrient concentrations and having relatively rapid flow.

© 2002 NRC Canada

Proximate determinants—response to enrichment

Hierarchy theory predicts that ultimate factors should indirectly influence the periphyton community, whereas proximate factors (e.g., at the scale of the artificial diffusers) should directly influence the community. Directional responses to nutrient enrichment among all treatments and sites also were examined using PCA to determine if diatom communities clustered by site or by treatment. For example, if similar treatments tended to be grouped more closely than sites, this would indicate that our short-term additions were more important in structuring the diatom community than other habitat variables or resources. In other words, local nutrient supply, a proximate factor, would determine algal assemblages. Alternatively, given that treatments were grouped according to a site, we would have evidence that some other intermediate or ultimate variable, such as longitudinal linkage, was more important than local nutrient regime over the 30-day experiment. Many studies have demonstrated a species-specific response to enrichment. For example, *Stigeoclonium* spp. typically become predominant on nitrogen-enriched substrata (Fairchild et al. 1985; Chessman et al. 1992), and *Achnanthes minutissima*, *Synedra rumpens*, and *Cocconeis placentula* commonly increase in abundance following nutrient enrichment (Pringle 1990; Stevenson et al. 1991). However, we generally observed a lack of species-specific responses to nutrient addition, similar to results observed by Peterson et al. (1993) who found that diatom community composition changed little in four summers of phosphorus addition even though chl *a* and biomass greatly increased in the first 2 years of addition and then decreased as the result of top-down regulation by grazing chironomids. In our study, exceptions included the response of *Nitzschia paleacea*, which increased in abundance on nutrient treatments, and *Achnanthes minutissima*, which was dominant at most sites. Our results suggest that the ultimate and intermediate factors, such as drainage basin characteristics and longitudinal location within the same basin, are more important in determining the potential benthic diatom assemblage than small-scale, proximate variables provided by the diffusers.

Of the three predicted outcomes, we found that the diatom communities tended to be similar within the same drainage basin, what we are classifying as an intermediate determinant of the algal assemblage. This is supported by results from the PCAs and Jaccard's index of similarity. For example, the Middle Snake, Kootenai, and Clearwater sites all tended to be grouped together, although there were exceptions. Both the Bear River and the third Upper Snake site (S3) were closely associated with the Kootenai River sites. All of these sites (K1–K3, B1, and S3) were low in richness and diversity. This trend likely is related to the presence of impoundments in the Kootenai and South Fork of the Snake (S3). In the Middle Snake, land use, which we have classified as an ultimate determinant of diatom assemblage structure, and subsequent eutrophication appear to be responsible for determining the structure of the diatom community. These patterns suggest that both intermediate and ultimate determinants were important in structuring the diatom communities, and basin characteristics, such as geomorphology and land use, are critical determinants of diatom community structure (Kutka and Richards 1996), a conclusion supported by the absence of a unified response to enrichment by diatom taxa.

High nutrient levels were consistent with greatest diatom species diversity, whereas extreme phosphorus limitation, caused by the presence of a large dam, led to the lowest diatom species diversity in these large river systems. We found that predicted nutrient limitation, based on ambient molar TIN:TP, only matched experimental results about two thirds of the time. We believe that a combination of nutrient monitoring and artificial diffuser techniques provides the greatest insight into nutrient limitation and observed patterns of periphyton accrual and diatom community structure.

Acknowledgments

This study was funded by the Idaho Department of Health and Welfare, Division of Environmental Quality, and the Idaho Department of Fish and Game. We thank M.B. Overfield, M.M. Thornton, T.V. Royer, J. Varricchione, M.C. Beery, and S.A. Thomas for field and laboratory assistance.

References

Allen, T.F.H., and Starr, T.B. 1982. Hierarchy. Perspectives for ecological complexity. University of Chicago Press, Chicago.

American Public Health Administration (APHA). 1992. Standard methods for the examination of water and wastewater. American Public Health Administration, Washington, D.C.

Barnese, L.E., and Schelske, C.L. 1994. Effects of nitrogen, phosphorus and carbon enrichment on planktonic and periphytoc algae in a softwater, oligotrophic lake in Florida, U.S.A. Hydrobiologia, **227**: 159–170.

Biggs, B.J.F. 1995. The contribution of flood disturbance, catchment geology and land use to the habitat template of periphyton in stream ecosystems. Freshwater Biol. **33**: 419–438.

Biggs, B.J.F. 2000. Eutrophication of streams and rivers: dissolved nutrient–chlorophyll relationships for benthic algae. J. North Am. Benthol. Soc. **19**: 17–31.

Biggs, B.J.F., and Gerbeaux, P. 1993. Periphyton development in relation to macro-scale (geology) and micro-scale (velocity) limiters in two gravel-bed rivers, New Zealand. N.Z. J. Mar. Freshw. Res. **27**: 39–53.

Biggs, B.J.F., Goring, D.G., and Nikora, V.I. 1998. Subsidy and stress responses of stream periphyton to gradients in water velocity as a function of community growth form. J. Phycol. **24**: 598–607.

Borchardt, M.A. 1994. Effects of flowing water on nitrogen- and phosphorus-limited photosynthesis and optimum N:P ratios by *Spirogyra fluviatilis* (Charophycea). J. Phycol. **30**: 418–430.

Bothwell, M.L. 1985. Phosphorus limitation of lotic periphyton growth rates: an intersite comparison using continuous-flow troughs (Thompson River system, British Columbia). Limnol. Oceanogr. **30**: 527–542.

Bothwell, M.L. 1988. Growth rate responses of lotic periphytic diatoms to experimental phosphorus enrichment: the influence of temperature and light. Can. J. Fish. Aquat. Sci. **45**: 261–270.

Bothwell, M.L. 1989. Phosphorus-limited growth dynamics of lotic periphytic diatom communities: areal biomass and cellular growth rate responses. Can. J. Fish. Aquat. Sci. **46**: 1293–1301.

Burton, M.B., Oemke, M.P., and Molloy, J.M. 1991. Contrasting effects of nitrogen and phosphorus additions on epilithic algae

© 2002 NRC Canada

in a hardwater and a softwater stream in Northern Michigan. Verh. Int. Ver. Limnol. **24**: 1644–1654.

Bushong, S.J., and Bachmann, R.W. 1989. In situ nutrient enrichment experiments with periphyton in agricultural streams. Hydrobiologia, **178**: 1–10.

Chessman, B.C., Hutton, P.E., and Burch, J.M. 1992. Limiting nutrients for periphyton growth in sub-alpine, forest, agricultural and urban streams. Freshwater Biol. **28**: 349–361.

Chételat, J., Pick, F.R., Morin, A., and Hamilton, P.B. 1999. Periphyton biomass and community composition in rivers of different nutrient status. Can. J. Fish. Aquat. Sci. **56**: 560–569.

Connell, J.H. 1978. Diversity in tropical rain forests and coral reefs. Science (Washington, D.C.), **199**: 1302–1310.

Cushing, C.E., Cummins, K.W., Minshall, G.W., and Vannote, R.C. 1983. Periphyton, chlorophyll *a*, and diatoms of the Middle Fork of the Salmon River, Idaho. Holarct. Ecol. **6**: 221–227.

U.S. Environmental Protection Agency (EPA). 1979. Methods for chemical analysis of water and wastes. U.S. Environmental Protection Agency, Environmental Monitoring and Support Laboratory, EPA/600/4-79-020.

Fairchild, B.W., Lowe, R.L., and Richardson, R.B. 1985. Algal periphyton growth on nutrient-diffusing substrates: an *in situ* bioassay. Ecology, **66**: 465–472.

Friedman, L.C., Erdmann, D.E., and Duncan, S.S. 1985. United States Geological Survey, methods for the determination of inorganic substances in water and fluvial sediments. Book 5, Chap. A1. *Edited by* M.W. Skougstad et al. U.S. Government Printing Office, Washington, D.C.

Gibeau, G.G., Jr., and Miller, M.C. 1989. A micro-bioassay for epilithon using nutrient diffusing artificial substrata. J. Freshw. Ecol. **5**: 171–176.

Grimm, N.B., and Fisher, S.G. 1986. Nitrogen limitation in a Sonoran Desert stream. J. North Am. Benthol. Soc. **5**: 2–15.

Hill, W.R., and Knight, A.W. 1988. Nutrient and light limitation of algae in two northern California streams. J. Phycol. **24**: 125–132.

Humphrey, K.P., and Stevenson, J.R. 1992. Responses of benthic algae to pulses in current and nutrients during simulations of subscouring spates. J. North Am. Benthol. Soc. **11**: 37–48.

Kutka, F.J., and Richards, C. 1996. Relating diatom assemblage structure to stream habitat quality. J. North Am. Benthol. Soc. **15**: 469–480.

Leland, H.V. 1995. Distribution of phytobenthos in the Yakima River basin, Washington, in relation to geology, land use, and other environmental factors. Can. J. Fish. Aquat. Sci. **52**: 1108–1129.

Lowe, R.L. 1974. Environmental requirements and pollution tolerance of freshwater diatoms. U.S. Environmental Protection Agency, Environmental Monitoring Series, EPA-670/4-74-005.

Lowe, R.L., Golladay, S.W., and Webster, J.R. 1986. Periphyton response to nutrient manipulation in streams draining clearcut and forested watersheds. J. North Am. Benthol. Soc. **5**: 221–229.

Marcus, M.D. 1980. Periphytic community response to chronic nutrient enrichment by a reservoir discharge. Ecology, **6**: 387–399.

Morris, D.P., and Lewis, W.M. 1988. Phytoplankton nutrient limitation in Colorado mountain lakes. Freshwater Biol. **20**: 315–327.

Omernik, J.M. 1977*a*. Total phosphorus concentrations in streams from non-point sources. National Map, U.S. Environmental Protection Agency, Corvallis Environmental Research Laboratory, Corvallis, Oreg.

Omernik, J.M. 1977*b*. Total inorganic nitrogen concentrations in streams from non-point sources. National Map, U.S. Environmental Protection Agency, Corvallis Environmental Research Laboratory, Corvallis, Oreg.

Patrick, R., and Reimer, C.W. 1966. The diatoms of the United States. Vol. I. Academy of Natural Sciences of Philadelphia, Monogr. No. 13. (ISBN LCN 65-29113).

Peterson B.J., Deegan, L., Helfrich, J., Hobbie, J.E., Hullar, M., Moller, B., Ford, T.E., Hershey, A., Hiltner, A., Kipphut, G., Lock, M.A., Fiebig, D.M., McKinley, V., Miller, M.C., Vestal, J.R., Ventullo, R., and Volk, G. 1993. Biological responses of a tundra river to fertilization. Ecology, **74**: 653–672.

Pringle, C.M. 1987. Effects of water and substratum nutrient supplies on lotic periphyton growth: an integrated bioassay. Can. J. Fish. Aquat. Sci. **44**: 619–629.

Pringle, C.M. 1990. Nutrient spatial heterogeneity: effects on community structure, physiognomy, and diversity of stream algae. Ecology, **71**: 905–920.

Redfield, A.C. 1958. The biological control of chemical factors in the environment. Am. Sci. **46**: 205–221.

Rhee, G-Y., and Gotham, I.J. 1980. Optimum N:P ratios and coexistence of planktonic algae. J. Phycol. **16**: 486–489.

Robinson, C.T., and Minshall, G.W. 1986. Effects of disturbance frequency on stream benthic community structure in relation to canopy cover and season. J. North Am. Benthol. Soc. **5**: 237–248.

Schanz, F., and Juon, J. 1983. Two different methods of evaluating nutrient limitations of periphyton bioassays, using water from the River Rhine and eight of its tributaries. Hydrobiologia, **102**: 187–195.

Scrimgeour, G.J., and Chambers, P.A. 1997. Development and application of a nutrient-diffusing bioassay for large rivers. Freshwater Biol. **38**: 221–231.

St. Clair, L.L., and Rushforth, S.R. 1976. The diatom flora of the Goshen warm spring ponds and wet meadows, Goshen, Utah, U.S.A. Nova Hedwigia, **24**: 353–425.

Stevenson, R.J. 1997. Scale-dependent determinants and consequences of benthic algal heterogeneity. J. North Am. Benthol. Soc. **16**: 248–262.

Stevenson, R.J., Peterson, C.G., Kirschtel, D.B., King, C.G., and Tuchman, N.C. 1991. Density dependent growth, ecological strategies, and effects of nutrient and shading on benthic diatom succession in streams. J. Phycol. **27**: 59–69.

Strahler, A.N. 1957. Quantitative analysis of watershed geomorphology. Trans. Am. Geophys. Union, **38**: 913–920.

Tilman, D. 1982. Resource competition and community structure. Monogr. Popul. Biol. **17**.

van Dam, H. 1982. On the use of measures of structure and diversity in applied diatom ecology. Nova Hedwigia Beih. **73**: 97–113.

Wantanabe, T., Kazumi, A., and Houki, A. 1986. Numerical water quality monitoring of organic pollution using diatom assemblages. *In* Proceedings of the Ninth International Diatom Symposium. *Edited by* F.E. Round. Biopress Ltd., Bristol, and Koeltz Scientific Books, Koenigstein.

Wold, A.P., and Hershey, A.E. 1999. Spatial and temporal variability of nutrient limitation in 6 North Shore tributaries to Lake Superior. J. North Am. Benthol. Soc. **18**: 2–14.

Woods, P.F. 1982. Annual nutrient loadings, primary productivity, and trophic state of Lake Koocanusa, Montana and British Columbia, 1972–80. Geological Survey Professional Paper 1283. United States Government Printing Office, Washington, D.C.

Zar, J.H. 1984. Biostatistical analysis. 2nd ed. Prentice-Hall, Englewood Cliffs, N.J.

© 2002 NRC Canada

PERSPECTIVE

Perspectives on the age and distribution of large wood in riparian carbon pools

Richard P. Guyette, William G. Cole, Daniel C. Dey, and Rose-Marie Muzika

Abstract: Most knowledge of carbon budgets is derived from the productivity and sequestration of carbon in terrestrial and marine ecosystems. Less is known of carbon stored in riparian areas associated with lakes and rivers. Case studies of the age distribution of carbon in aquatic large wood (C_{lw}) from two different landscapes with different drainage patterns were established using tree-ring and ^{14}C dating. Cumulative negative exponential distributions of the age of C_{lw} ranged over periods from 1000 to 9485 years. Large woody debris had mean residence times of 261 years in small oligotrophic lakes and 350–800 years in a stream reach. Large wood can reside for an order of magnitude longer in freshwater–riparian ecosystems than in comparable above-ground terrestrial ecosystems. Although riparian areas make up only a small fraction of most landscapes, they may account for a relatively larger proportion of aged C_{lw} than is stored above ground in terrestrial ecosystems.

Résumé :
La connaissance des budgets de carbone provient en très grande partie des études sur la productivité et la séquestration de carbone dans les écosystèmes terrestres et marins. On possède moins de données sur le carbone emmagasiné dans les zones ripariennes des lacs et des rivières. Nous avons procédé à deux études de cas de la répartition du carbone dans du bois de grande taille (C_{lw}) en milieu aquatique, dans deux paysages différents à structures de drainage distinctes, à l'aide de datations basées sur les anneaux de croissance et sur le ^{14}C. La distribution cumulative exponentielle négative des âges du C_{lw} s'étend sur des périodes de 1000 à 9485 années. Les débris ligneux de grande taille ont un temps de séjour moyen de 261 ans dans les petits lacs oligotrophes et de 350 à 800 ans dans une section de cours d'eau. Le bois de grande taille peut demeurer 10 fois plus longtemps dans les écosystèmes d'eau douce et les écosystèmes ripariens que dans les écosystèmes terrestres épigées comparables. Bien que les zones ripariennes ne représentent qu'une faible fraction de la plupart des paysages, elles peuvent contribuer une proportion relativement plus importante du C_{lw} que celle qui s'accumule au-dessus du sol dans les écosystèmes terrestres.

[Traduit par la Rédaction]

Introduction

Despite considerable knowledge of carbon (C) storage in forests and soils (Dixon et al. 1994; Turner et al. 1995; Trumbore et al. 1996), few if any studies have quantitatively addressed the age distribution of C and its storage in the dead, large wood (>25 cm in diameter) associated with aquatic–terrestrial ecotones. While C storage in forests is often limited by the relatively rapid decay of wood after the death of a tree, C assimilated in trees that enter aquatic systems as large wood (LW) often decays very slowly in submerged or buried environments. This wood may represent a distinct type of carbon sink and can be an important source of aged particulate organic carbon in river systems (Becker 1993; Raymond and Bauer 2001), low-density substrate for invertebrates (Culp and Davies 1985; O'Conner 1991; Bowen et al. 1998), and aquatic structure and habitat (Mallory et al. 2000).

We assessed the age distribution of carbon sequestered in LW by sampling aquatic LW (>25 cm diameter) in two types of riparian ecotones: freshwater lake littoral zones adjacent to *Pinus–Tsuga–Thuja* forests in the Michigan–Huron and Lower St. Lawrence ecoregions (Abell et al. 2000) and stream channels flowing through *Quercus–Carya–Acer* gallery forests and prairie vegetation in the Middle Missouri freshwater ecoregion. The objectives of this perspective are to explore means of characterizing the temporal distribution of LW in several stream and lake aquatic ecosystems, and to characterize the age, decay rates, and distribution of aquatic LW with case studies from lake and stream riparian areas. This objective is a first step toward understanding ecosystem level carbon sequestration in freshwater. Specifically, our hypotheses are (*i*) that the age of carbon in LW of streams and

Received 28 August 2001. Accepted 5 March 2002. Published on the NRC Research Press Web site at http://cjfas.nrc.ca on 17 April 2002.
J16515

R.P. Guyette[1] **and R.-M. Muzika.** Department of Forestry, University of Missouri, Columbia, MO 65211, U.S.A.
W.G. Cole. Ontario Ministry of Natural Resources, Sault Ste. Marie, ON P6A 2E5, Canada.
D.C. Dey. U.S. Forest Service, Columbia, MO 65211, U.S.A.

[1]Corresponding author (e-mail: guyetteR@missouri.edu).

 DOI: 10.1139/F02-026 © 2002 NRC Canada

littoral zones can be characterized by negative exponential functions, and (*ii*) that LW is sequestered for much longer periods in riparian and littoral zones than is LW in terrestrial forest ecosystems.

Materials and methods

Four study lakes and a stream reach (Table 1) were chosen that were relatively free of recent anthropogenic disturbances (e.g., removal of aquatic wood, riparian structures) to best reflect the long-term temporal dynamics of aquatic LW. The location of the stream reach was chosen because of its availability as a research site, because the reach appeared to have LW that had recently entered the stream, and because it had LW of an unknown age in the water. The stream reach is in a floodplain of agricultural and forest lands and has been without recent logging. The stream channel is actively meandering in a broad floodplain, is composed of sediments of low hydrologic resistance (glacial till), is unconstrained by bedrock, and is low gradient. The LW of streams is potentially more mobile than that in lakes because it may move (Sickle and Gregory 1990) into a particular stream reach from an upstream source, be carried into a lower stream reach, be deposited on the floodplain as floodwaters recede, move into a downstream water body such as a lake, or be buried in fluvial sediments.

The forests bordering two of the study lakes were not logged, whereas the forests were selectively logged for *Pinus strobus* (eastern white pine) circa 1900 around the other two lakes. The aquatic–forest interface of the lake study sites is relatively stable and constrained by bedrock. Our study lakes represent relatively closed systems with respect to LW owing to the limited movement of LW between lakes.

We obtained samples and measurements for analysis from 67 specimens of aquatic LW (*Quercus* spp., *Juglans nigra*, *Acer* spp., *Betula* spp., *Populus* spp., *Salix* spp.) in a 0.5-km stream reach of Medicine Creek, Mo., U.S.A. We collected data and cross-sections from 256 specimens of LW (*Pinus strobus*) in the littoral zones of Scott, Dividing, and Swan lakes in Algonquin Provincial Park, and from McCulloch Lake in Lady Evelyn Smooth Water Provincial Park in Southern Ontario, Canada. Sampling of LW for age distributions was exhaustive at four sites and random at one lake site. Volume, mass, and C were calculated for each piece of LW. We sorted LW by age and summed the C mass beginning with the oldest dates. We divided cumulative values by the sum of all C to construct cumulative relative distributions.

We used both dendrochronology and radiocarbon dating to determine the age of LW. Wood and ring-width plots were visually matched for ring-width signatures and latewood characteristics (Baillie 1982; Stokes and Smiley 1996). Statistical verification of the ring-width dating was done using the computer program COFECHA (Grissino-Mayer et al. 1996) and Student's *t* tests as well as tree-ring chronologies derived from living, old trees (*Pinus strobus*, *Quercus alba*) in Ontario and Iowa (Duvick 1996; Guyette 1996*a*, 1996*b*). Carbon isotope measurements and radiocarbon age determinations for the samples in this project were conducted by Geochron Laboratories, Cambridge, Mass., U.S.A. The dates are based upon the Libby half-life (5570 years) for ^{14}C. All dates are corrected for ^{13}C. Wood samples of 20–30 g were treated with hot, dilute HCl to remove carbonates; with 0.1 N dilute NaOH to remove humic acids and organic contaminants, and a second time with dilute HCl. After washing and drying, the samples were combusted to recover carbon dioxide. We calibrated the radiocarbon ages using a calibration program (Stuiver et al. 1998). These ages are referenced to the year AD 2000 to be comparable with tree-ring dates. LW in the stream channel that was not tree-ring dateable and had intact leaves, bark, terminal growth rings, or small branches (<2 cm) was classed as "modern". Ten random samples from this category all ^{14}C-dated less than 100 years before present (BP) and verified this categorization. We randomly assigned modern dates (<100 years BP) to members of this class.

Results and discussion

The sequestration of C is a function of the time C is stored in both the living and dead components of the tree. Here we examined the age distribution of dead LW in lakes and streams and compared these with the decay of wood in terrestrial forest ecosystems. The age distribution of C_{lw} at all study sites took the form of negative exponential distributions (Figs. 1 and 2) such as has been hypothesized for LW (Harmon et al. 1986; MacMillian 1988). Equations 1 and 2 were fit to these cumulative distributions of mean ring dates as empirically derived probability density functions to determine the remaining proportion of C assimilated at a given age in the aquatic and riparian LW carbon pools. The equations describe the probabilistic fate of C assimilated in the boles of trees that are eventually incorporated into aquatic–forest ecotones as follows:

$$(1) \qquad C_{lw} = 100\ e^{-kt} \text{ (stream)}$$

$$(2) \qquad C_{lw} = 100\ (1 - e^{-kt})^{l} \text{ (lakes)}$$

where C_{lw} is carbon in LW, k represents decay constants (0.0065 for the lakes; 0.0015 for the stream), t is time (years BP), and $l = 5$ (a dimensionless exponent for C stored in living trees before entering the water).

The exponents ($-kt$) describe the release of carbon from aquatic LW. Additionally, where the duration of C storage is long in living trees relative to aquatic LW, an exponent (l) defines the time that C is held in living trees (Harmon et al. 1986). In eq. 2 we used half of the average life of a tree that falls into the lake (100 years) as a rough estimate of the average time that C is stored in living tree boles (Guyette and Cole 1999). The value of k for eq. 1 (used in Fig. 2) is based on the in-stream volume of wood only and does not include sections of wood buried in sediments (these are not measurable). In addition, there may be an "age shadow" effect in the age distribution of LW. An "age shadow" is defined as the unexpected absence of wood in the temporal distribution of wood possibly caused by the migration and return of a meander belt within the floodplain. An "age shadow" is created as the meander belt of a stream moves away from recently buried wood and into older buried wood. Thus, wood collected in natural stream channels may not be unbiased with respect to the age of wood stored in a flood plain. A much smaller value of k may more accurately reflect the age

© 2002 NRC Canada

Table 1. Site and temporal characteristics for large wood (LW), dated samples, and carbon. Water area is total lake or stream reach surface area.

Site name	Medicine	Swan	Scott	Dividing	McCulloch
Water body	Stream	Lake	Lake	Lake	Lake
Latitude	40°22′N	45°30′N	45°29′N	45°24′N	47°19′N
Longitude	93°18′W	78°43′W	78°43′W	78°36′W	80°45′W
Water area (ha)	0.1	87	27	53	42
Number LW dated	67	82	29	105	40
Mean length, diameter LW (m)	4.4, 0.36	10.7, 0.36	10.4, 0.35	15, 0.39	12.1, 0.32
Range of age C_{lw} (years BP)	<10 to 9485	107–1070	128–877	4–1050	2–1134
LW mean residence time by piece (years)	2212	333	271	196	279
Mean assimilation–release period for C_{lw} by mass (years)	389	443	368	295	341

Note: Mean LW residence time by piece is the mean age of all dated LW without respect to their mass, thus the stream reach had smaller, older pieces that account for the much longer residence time. The mean assimilation–release period for carbon in LW (C_{lw}) includes the time carbon is stored in living trees that enter aquatic systems. Time is in years before present (BP).

Fig. 1. The cumulative age distribution of carbon from the large wood (LW) of eastern white pine (*Pinus strobus*) in the littoral zones of four small oligotrophic lakes and the C remaining in terrestrial LW (Mattson et al. 1987; Turner et al. 1995). Goodness-of-fit for aquatic LW data (○) and the equation is 98%. Age corresponds to t in the equation. BP, before present.

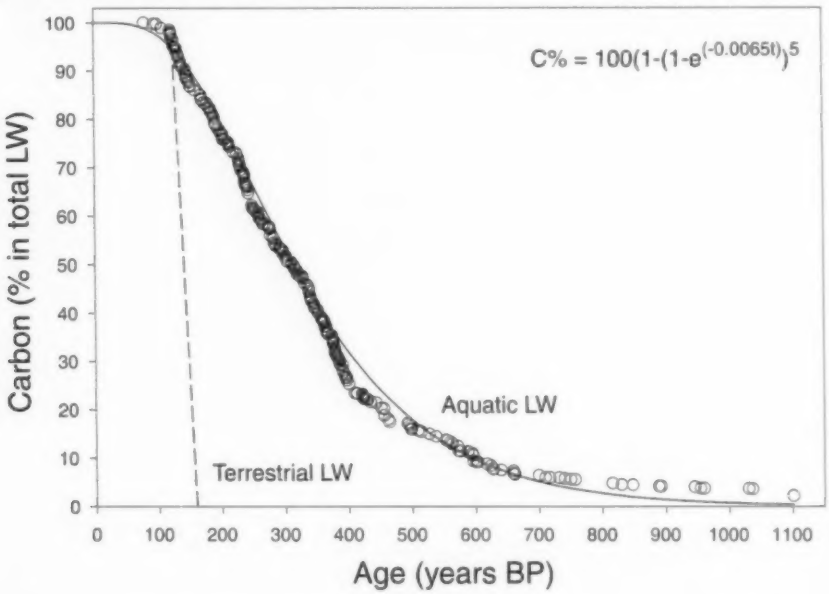

distribution of wood in the stream–floodplain–subterranean system of carbon storage.

Mean residence time for LW in the study lakes was 261 years and ranged from means of 350 years to 800 years in the study stream depending on the value of k used. These residence times are about 9–80 times greater than the mean residence time of wood in adjacent terrestrial forests (Table 2) (Nabuurs and Mohren et al. 1995; Jenkins and Parker 1997; Spetich et al. 1999). We found mean C assimilation–release periods (C in living and dead phases of LW) of 362 years in four Ontario lakes and 389–839 years for LW in the study stream.

Reductions in the specific gravity (G_b, the basic specific gravity based on the volume of wet wood) of wood with age reflect differences in decay processes, decay rates in terrestrial versus aquatic and subterranean–riparian ecosystems, and the effect of time on C storage and quality. LW on the ground in terrestrial ecosystems decays in an oxygen-rich and moist environment in eastern North America, where precipitation is abundant and well distributed throughout the year. Oxygen is more limiting to decay of LW when it is submerged in lake or stream waters, but wave action, currents, and lake turnover can deliver oxygen by mass flow to LW. In contrast, decay of LW is most limited when LW is subterranean, buried in water-saturated soils in floodplains and bogs, where anaerobic conditions prevail because the diffusion of oxygen is so slow.

The mean specific gravity of *Quercus* spp. (oak species) is reduced by half during about 6500 years of aquatic and subterranean storage (Fig. 3), whereas mean G_b of *Quercus* spp. LW on forest floors is reduced by half in approximately 40 years (Harmon et al. 1986; MacMillian 1988). In the lit-

© 2002 NRC Canada

Fig. 2. The cumulative age distribution of carbon in the aquatic large wood (LW) of a stream reach and C remaining in terrestrial coarse wood (Harmon et al. 1986; MacMillan 1988). Age data for LW are from calibrated radiocarbon dates and tree-ring dating (13). Goodness-of-fit for aquatic LW data (○) and the equations are 85% for $k = 0.0015$. The smaller value of k is based on the existence of an age shadow (see text). Age corresponds to t in the equation given for aquatic LW. BP, before present.

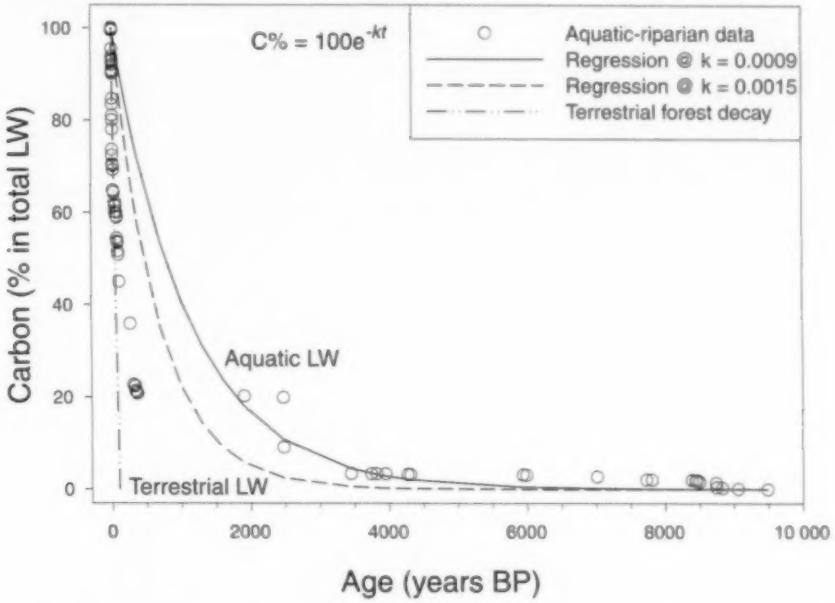

Table 2. Characteristics of large wood (LW) in the littoral zones of lakes and in a stream channel (with subterranean storage) compared with LW in terrestrial forest ecosystems.

Characteristics	Lake littoral	Stream channel	Forests
Mean $C_{1\infty}$ residence time (years)	261	350	10–40[a,b]
C assimilation–release (years)	362	389	49–140
G_b half life (years)	334	6500	35–40[c,d]
Decay constants	0.0065	0.0015	0.024–0.086[e,f,g,h,i]
Maximum ages dead LW (years)	1097	9485	60–160
LW volume / area ($m^3 \cdot m^{-2}$)	0.0212[j]	0.0045	0.0019–0.011[b,k,l,m]

Note: Data for terrestrial ecosystems are for forest tree species and ecosystems comparable to the study regions. The C assimilation–release period is the mean time from carbon fixation to its release from LW (years in living tree + years as dead wood). The specific gravity (G_b) half-life is for *Pinus* in lakes and *Quercus* in a stream reach. Maximum ages for forest are derived from decay constants. Data citations: a, Nabuurs and Mohren (1995); b, Spetich et al. (1999); c, MacMillian (1988); d, Mattson et al. (1987); e, Harmon et al. (1986); f, Turner et al. (1995); g, Chambers et al. (2000); h, Alban and Pastor (1993); i, Onega and Eickmeier (1991); j, Mallory et al. (2000); k, Jenkins and Parker (1997); l, Shifley et al. (1997); m, Muller and Liu (1991).

toral zones, in one of the study lakes the G_b of *Pinus strobus* (eastern white pine) decreased by half in 334 years (Guyette and Cole 1999). The cellulose–lignin ratio in wood is known to decline with time in water-saturated wood and may account for the recalcitrant nature of some particulate organic carbon in rivers as water further erodes structurally weakened old wood (Hedges 1990; Raymond and Bauer 2001).

The piece size of LW and the quantity of carbon per piece of LW are a function of time. Large wood becomes smaller with time from weathering, erosion of the exterior surface, and breakage. Consequently, the quantity of carbon decreases with decreasing piece size. The amount of carbon per piece was significantly ($p < 0.01$) reduced with time (Fig. 4) because of reductions in the volume of LW pieces. Time, however, explains less than 30% of variance (Fig. 4) in the quantity of carbon per piece. This relationship is weak at our study sites and may be weak in many freshwater ecosystems because of the great variability in tree size, the portion of the tree entering the water, and the integrity of the tree stem upon entry into the stream or lake.

Piece size may also have an effect on the movement of LW (Braudrick and Grant 2000) and carbon within aquatic systems. Small pieces of LW will be moved much more readily in streams, especially smaller streams. Wood may move into environments (e.g., subterranean, fluvial, and benthic sediments) where the rates of decay may be much different than those in the waters of streams and lakes. As LW in lakes becomes smaller, it may be incorporated into lake-

© 2002 NRC Canada

Fig. 3. A comparison of the specific gravity (G_b) of *Quercus* spp. that occurs with time in the aquatic–subterranean ecotones (○) of the study stream and large wood (LW) on a terrestrial forest floor (●) (MacMillian 1988). BP, before present.

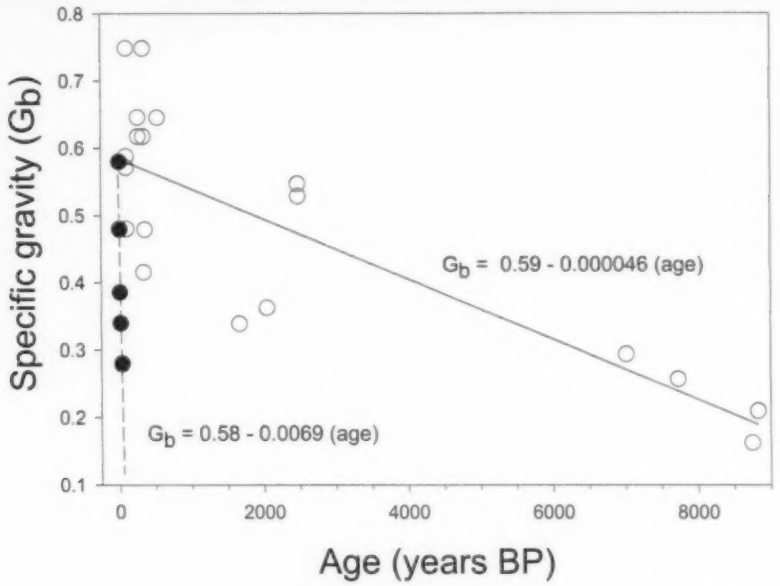

shore bogs or washed ashore by wave action. In streams, small wood may be incorporated into fluvial deposits or be deposited on the soils of floodplain forests. The movement and fate of LW in streams has been of particular interest in northwestern North America (Maser and Sedell 1994; McHenry et al. 1998; Wing et al. 1999) because of its contribution to aquatic habitat.

The age and distribution of C_{lw} illustrates the importance of riparian dynamics for the storage of C. Although we aged only wood in water, subterranean storage in both flood plains and along lakeshores may be important in long-term C storage. Wood in streams flowing through sediments of low hydrologic resistance is constantly being excavated, buried, reburied, and only slowly exported to downstream waters. About 65 percent of the LW mass was involved (partially buried) in fluvial sediments, and thus had reduced downstream mobility and a high probability of having been or being totally buried before contemporary export downstream. In lake systems, some species like *P. strobus* are potentially highly mobile because they may float for centuries.

Relative to terrestrial forests, carbon sequestration by LW in freshwater–forest ecotones may constitute only a small portion of carbon input because of the limited spatial dimensions of riparian ecotones, but may represent a large carbon sink because of the temporal duration of carbon storage. For example, there are about 1.1 million hectares of flood plain in a total area of about 7.5 million hectares in North Missouri, the region of our stream study site. Thus, riparian areas, including floodplains, represent about 15% of the landscape but may sequester carbon in LW 10 times longer (Table 2) than the landscape as a whole. There are about 250 000 lakes in Ontario, the location of our study lakes. Lakes in the vicinity of our study area averaged 8.6% of the area of the landscape and lake littoral zones were 1.3% of the total area of the landscape. However, this 1.3% may sequester carbon more than six times longer than the landscape as a whole. These estimates do not include areas with wood buried in lake bogs, rivers, lake bottoms, and wood in deep water. Thus, the role of carbon sequestration in aquatic environments may be large in proportion to area because the duration of carbon storage is greater in aquatic than in terrestrial environments.

The long-term storage of wood submerged or buried in streams and lakes has been noted elsewhere. Thousands of pieces of ancient LW (*Quercus* spp.) have been tree-ring dated from aquatic and riparian ecosystems in Germany and Western Europe (Pilcher et al. 1984; Becker 1993). Ancient (<4763 years BP) particulate organic matter has been reported in the waters of major rivers (Raymond and Bauer 2001). *Pinus sylvestris* (Scots pine) LW from lakes in Fennoscandia have been tree-ring dated and used to construct a continuous tree-ring chronology dating to 7500 years BP (Zetterberg et al. 1996). In addition to our case study sites, we found wood over 2000 years in age in 0.5-km survey reaches of 9 of 10 rivers in Missouri. Rarely, however, are sampling or collections of LW in aquatic systems conducted in a manner consistent with construction of statistical distributions (i.e., random or exhaustive) at the study or ecosystem level. Although we used random, stratified random, and exhaustive sampling in our case studies, these studies only allude to potential differences in residence times of C_{lw} in terrestrial and riparian areas.

Changes in the dynamics of C storage in lakes and streams may result from global climate change (King et al. 1999; Magnuson et al. 2000) and increases in human population density. Changes in temperature may result in changes in bacterial activity (Vaque et al. 1994; Trumbore et al. 1996) and degradation of LW in lake littoral zones stream waters.

© 2002 NRC Canada

Fig. 4. Two scatter plots illustrating a weak but significant relationship between age and the mass of carbon per piece of large wood (LW) (*a*) in a stream and (*b*) in lakes. The quantity of carbon in each piece of LW (*y* axis) is plotted against the duration (*x* axis) of carbon sequestering in LW. Note the order of magnitude of difference in the *x* axes for (*a*) stream and (*b*) lake wood. BP, before present.

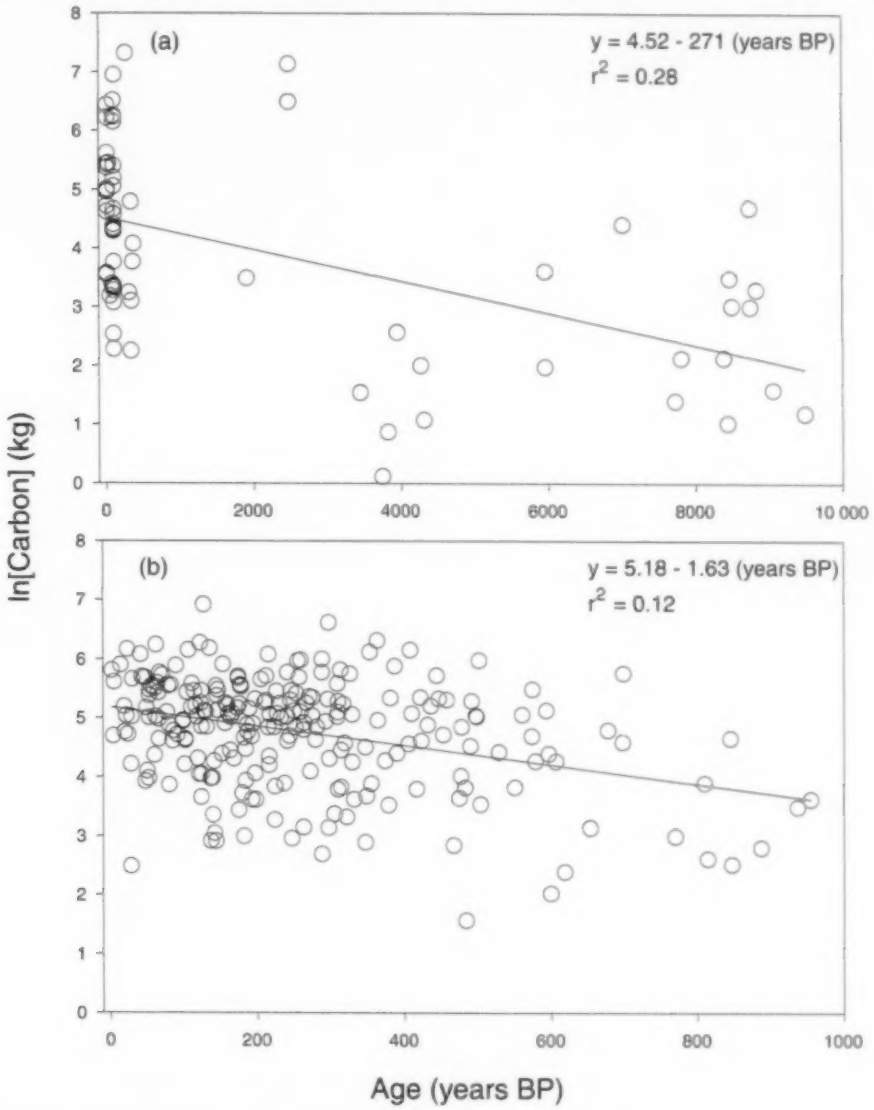

Biological activity, even under anoxic conditions, may be governed by temperature-dependent reaction rates as quantified by the Arrhenius equation (Vollhardt 1987). The long-term storage of C_{lw} in the subterranean components of riparian floodplains, however, may be less affected by increases in atmospheric temperature like those found in soils (Trumbore et al. 1996) because of the insulation provided by 3–6 m of floodplain sediments that lie over LW in North Missouri streams. The effects of increasing human population may be equally important as, if not more important than the effects of climate change on aquatic–forest ecotones. Stream bank stabilization, river channelization, navigation improvements, river impoundment, and riparian and lakeshore development (Christensen et al. 1996) will all influence riparian forests and the dynamics of LW and C storage in freshwater ecosystems.

Acknowledgements

The authors want to thank the Ontario Ministry of Natural Resources, the Center for Agroforestry at the University of Missouri, North Central Station USDA Forest Service, Algonquin and Lady Evelyn Smooth Water provincial parks, the Harkness Laboratory of Fisheries Research, Steve Peter-

© 2002 NRC Canada

son, Steve Pallardy, and Kevin Hosman for their support in this research.

References

Abell, R.A., Olson D.M., Dinerstein, E., Hurley, P.T., Diggs, J.T., Eichbaum, W. Walters, S., Wettengel, W., Allnutt, T., Loucks, C.J., and Hedao, P. 2000. Freshwater ecoregions of North America. Island Press, Washington, D.C.

Alban, D.H., and Pastor, J. 1993. Decomposition of aspen, spruce, and pine boles on two sites in Minnesota. Can. J. For. Res. **23**: 1744–1749.

Baillie, M.G.L. 1982. Tree-ring dating and archaeology. University of Chicago Press, Chicago.

Becker, B. 1993. An 11 000-year German oak and pine chronology for radiocarbon calibration. Radiocarbon, **35**: 201–213.

Bowen, K.L., Kaushik, N.K., and Gordon, A.M. 1998. Macroinvertebrate communities and biofilm chlorophyll on woody debris in two Canadian oligotrophic lakes. Arch. Hydrobiol. **141**: 257–281.

Braudrick, C.A., and Grant, G.E. 2000. When do logs move in rivers? Water Resour. Res. **36**: 571–583.

Chambers, J.Q., Higuchi, N., Schimel, J.P., Ferreira, L.V., and Melack, J.M. 2000. Decomposition and carbon cycling of dead trees in tropical forests of the central Amazon. Oecologia, **122**: 380–388.

Christensen, D.L., Herwig, B.R., Schindler, D.E., and Carpenter, S.R. 1996. Impacts of lakeshore residential development of coarse woody debris in north temperate lakes. Ecol. Appl. **6**: 1143–1149.

Culp, J.M., and Davies, R.W. 1985. Responses of benthic macroinvertbrate species to manipulation of interstitial detritus in Carnation Creek, British Columbia. Can. J. Fish. Aquat. Sci. **42**: 139–146.

Dixon, R.K., Brown, S., Houghton, R.A., Solomon, A.M., Trexler, M.C., and Wisniewski, J. 1994. Carbon pools and flux of global forest ecosystems. Science (Washington, D.C.), **263**: 185–190.

Duvick, D.N. 1996. Lake Ahquabi State Park. International Tree-Ring Data Bank. IGBP PAGES/World Data Center-A for Paleoclimatology Data Contribution No. IA025.CRN2-014. NOAA/NGDC Paleoclimatology Program, Boulder, Co., U.S.A.

Grissino-Mayer, H.D., Holmes, R.L., and Fritts, H.C. 1996. International Tree-Ring Data Bank program library version 2.0 users manual. International Tree-Ring Data Bank, Laboratory of tree-ring research, University of Arizona, Tucson.

Guyette, R. 1996*a*. Tree-ring data, Swan Lake, Ontario. International Tree-Ring Data Bank. IGBP PAGES/World Data Center-A for Paleoclimatology Data Contribution Series No. 96-013. NOAA/NGDC Paleoclimatology Program, Boulder, Co., U.S.A.

Guyette, R. 1996*b*. Tree-ring data, Ontario and Missouri. International Tree-Ring Data Bank. IGBP PAGES/World Data Center-A for Paleoclimatology Data Contribution Series No. 92-014. NOAA/NGDC Paleoclimatology Program, Boulder, Co., U.S.A.

Guyette, R.P., and Cole, W.G. 1999. Age characteristics of coarse woody debris (*Pinus strobus*) in a lake littoral zone. Can. J. Fish. Aquat. Sci. **56**: 496–505.

Harmon, M.E., Franklin, J.F., Swanson, F.J., Sollins, P., Gregory, S.V., Lattin, J.D., Anderson, N.H., Cline, S.P., Aumen, N.G., Sedell, J.R., Lienkaemper, G.W., Cromack, K, Jr., and Cummins, K.W. 1986. Ecology of coarse woody debris in temperate ecosystems. Adv. Ecol. Res. **15**: 133–302.

Hedges, J.I. 1990. The chemistry of archaeological wood. *In* Archaeological wood. *Edited by* R.M. Rowell and R.J. Barbour. American Chemical Society, Washington, D.C. Adv. Chem. Ser. 225. pp. 111–140.

Jenkins, M.A., and Parker, G.R. 1997. Changes in down dead wood volume across a chronosequence of silvicultural openings in southern Indiana forests. *In* Proceedings of the 11th Central Hardwood Forest Conference, 23–26 March 1997, University of Missouri, Columbia. *Edited by* S. Pallardy, R. Cecich, H. Garrett, and P. Johnson. GTR NC-188. pp. 162–169.

King, J.R. Shuter, B.J., and Zimmerman, A.P. 1999. Signals of climate trends and extreme events in the thermal stratification pattern of multibasin Lake Opeongo, Ontario. Can. J. Fish. Aquat. Sci. **56**: 847–852.

MacMillian, P.C. 1988. Decomposition of coarse woody debris in an old-growth Indiana forest. Can. J. For. Res. **18**: 1353–1362.

Magnuson, J.J., Robertson, D.M., Benson, B.J., Wynne, R.H., Livingstone, D.M., Arai, T., Assel, R.A., Barry, R.G., Card, V., Kuusisto, E., Granin, N.G., Prowse, T.D., Stewart, K.M., and Vuglinshki, V.S. 2000. Historical trends in lake and river ice cover in the Northern Hemisphere. Science (Washington, D.C.), **289**: 1743–1746.

Mallory, E.C., Ridgway, M.S., Gordon, A.M., and Kaushik, N.K. 2000. Distribution of woody debris in a small headwater lake, central Ontario, Canada. Arch. Hydrobiol. **148**: 587–606.

Mattson, K.G., Swank, W.T., and Waide, J.B. 1987. Decomposition of woody debris in a regenerating, clear cut forest in the Southern Appalachians. Can. J. For. Res. **17**: 712–721.

Maser, C., and Sedell, J.R. 1994. From forest to sea: the ecology of wood in streams, rivers, estuaries, and oceans. St. Lucie Press, Delray Beach, Fla.

McHenry, M.L., Shott, E., Conrad, R.H., and Grette, G.B. 1998. Changes in the quantity and characteristics of large woody debris in streams of the Olympic Peninsula, Washington, U.S.A. (1982–1993). Can. J. Fish. Aquat. Sci. **55**: 1395–1407.

Muller, R.N., and Liu, Y. 1991. Coarse woody debris in an old-growth deciduous forest on the Cumberland Plateau, southern Kentucky. Can. J. For. Res. **21**: 1567–1572.

Nabuurs, G.J., and Mohren, G.M.J. 1995. Modeling analysis of potential carbon sequestration in selected forest types. Can. J. For. Res. **25**: 1157–1172.

O'Conner, N.A. 1991. The effects of habitat complexity on the macroinvertebrates colonizing wood substrates in a lowland. Oecologia, **85**: 504–512.

Onega, T.I., and Eickmeier, W.G. 1991. Woody detritus inputs and decomposition kinetics in a southern temperate deciduous forest. Bull. Torrey Bot. Club, **118**: 52–57.

Pilcher, J.R., Baillie, M.G.L., and Schmidt, B. 1984. A 7272 year tree-ring chronology for Western Europe. Nature (London), **312**: 150–152.

Raymond, P.A., and Bauer, J.E. 2001. Riverine export of aged terrestrial organic matter to the North Atlantic Ocean. Nature (London), **409**: 497–500.

Shifley, S.R., Brookshire, B.L., Larson, D.R., and Herbeck, L.A. 1997. Snags and down wood in Missouri old-growth and mature second-growth forests. North. J. Appl. For. **14**: 165–172.

Sickle, J.V., and Gregory, S.V. 1990. Modeling inputs of large woody debris to streams from falling trees. Can. J. For. Res. **20**: 1593–1601.

Spetich, M.A., Shifley, S.R., and Parker, G.R. 1999. Regional distribution and dynamics of coarse woody debris in Midwestern old-growth forests. Forest Sci. **45**: 302–313.

Stokes, M.A., and Smiley, T.L. 1996. An introduction to tree-ring dating. University of Arizona Press, Tucson.

Stuiver, M., Reimer, P.J., and Braziunas, T.F. 1998. High-precision radiocarbon age calibration for terrestrial and marine samples. Radiocarbon, **40**: 1127–1151.

© 2002 NRC Canada

Trumbore, S.E, Chadwick, O.A., and Amundson, R. 1996. Rapid exchange between soil carbon and atmospheric carbon dioxide driven by temperature change. Science, **272**: 393–396.

Turner, D.P., Koerper, G.J., Harmon, M.E., and Lee, J.J. 1995. A carbon budget for forests of the conterminous United States. Ecol. Appl. **5**: 421–436.

Vaque, D., Gasol, J.M., and Marrase, C. 1994. Grazing rates on bacteria—the significance of methodology and ecological factors. Mar. Ecol. Prog. Ser. **109**: 263–274.

Vollhardt, P.C. 1987. Organic chemistry. W.H. Freeman Co., New York.

Wing, M.G., Keim, R.F., and Skaugset, A.F. 1999. Appling goestatistics to quantify distributions of large woody debris in streams. Comput. Geosci. **25**: 801–807.

Zetterberg, P., Eronen, M., and Lindholm, M. 1996. Construction of a 7500-year tree-ring record for Scots Pine (*Pinus sylvestris*, L.) in Northern Fennoscandia and its application to growth variation and paleoclimatic studies. *In* Growth trends in European Forests. *Edited by* H. Spiecker, K. Mielikainen, and M. Kohl. Springer-Verlag, Berlin. pp. 7–18.

© 2002 NRC Canada

ANNOUNCEMENT AND CALL FOR PAPERS

ICES symposium on

FISH BEHAVIOUR IN EXPLOITED ECOSYSTEMS

Bergen, Norway, 23–26 June 2003

The International Council for the Exploration of the Sea (ICES) will hold a symposium on Fish Behaviour in Exploited Ecosystems to deal with the following topics:

1. Observation techniques and experimental designs for the study of fish behaviour, including sampling schemes, tools and methods for observing and analyzing and quantifying behaviour.
2. Physiological mechanisms of sensory organs and their role in fish behaviour including the tools and methods used to measure morphological and physiological aspects of fish behaviour.
3. Reaction to stimulation, including basic behaviour determining the probability of contact with stimuli from vessels and fishing gear, motivational effects and conflicts between stimuli, ontogenetic effects, the role of learning in fish behaviour, and the effects of selection on response pattern.
4. Understanding temporal and spatial dynamics and their effect on fish behaviour and catchability, including the impact of site fidelity, homing, migrations (long distance and vertical), and habitat selection behaviours on accurate resource abundance estimation, monitoring studies, and fishery operations.
5. Influence of social behaviour and behavioural interactions on availability and catchability of fish in resource and monitoring surveys, fishery operations, and in the design of species-selective and ecosystem-friendly fishing gears.
6. Fish behaviour relevant to fish catchability, including quantifying fish reactions to fishing vessels and fishing gear, avoidance behaviour and their effect on resource surveys and monitoring studies.
7. Modeling fish behaviour including mechanistic and descriptive approaches, individual-based and other simulation models of natural and fishing gear induced behaviour.

The Symposium seeks to provide a broad international forum for global synthesis of the scientific knowledge of fish behaviour in exploited ecosystems, to review and discuss the advancements in technology and analytical methods used to study fish behaviour and to provide a forum for discussions on how objectives related to fish behaviour can be incorporated effectively into stock assessment and fisheries management. Special emphasis will be given to the use of direct studies in the field to measure natural behaviour and also behavioural responses to fishing gears. Papers reporting ongoing fish behaviour research in exploited stocks of demersal fish, small and large pelagics, and sharks and rays found in coastal, estuarine, semi-enclosed seas, continental shelves, and the deep sea are invited.

Anyone wishing to present a paper or poster should submit a title and abstract by 15 August 2002 by registering on the web page at http:www.imr.no/fishbehave

Stephanie R. Davenport and Nicholas J. Bax	**514–530**	A trophic study of a marine ecosystem off southeastern Australia using stable isotopes of carbon and nitrogen
Mika Rahikainen and Sakari Kuikka	**531–541**	Fleet dynamics of herring trawlers—change in gear size and implications for interpretation of catch per unit effort
Ben Wilson and Lawrence M. Dill	**542–553**	Pacific herring respond to simulated odontocete echolocation sounds
Eric A. Strauss, Nicole L. Mitchell, and Gary A. Lamberti	**554–563**	Factors regulating nitrification in aquatic sediments: effects of organic carbon, nitrogen availability, and pH
Eric B. Snyder, Christopher T. Robinson, G. Wayne Minshall, and Samuel R. Rushforth	**564–577**	Regional patterns in periphyton accrual and diatom assemblage structure in a heterogeneous nutrient landscape
		PERSPECTIVE
Richard P. Guyette, William G. Cole, Daniel C. Dey, and Rose-Marie Muzika	**578–585**	Perspectives on the age and distribution of large wood in riparian carbon pools

National Research Council Canada
Ottawa, Canada K1A 0R6

Conseil national de recherches Canada
Ottawa, Canada K1A 0R6

Postage paid at Ottawa
Publications mail
Registration No. 1240579

Port payé à Ottawa
Poste-publication
Enregistrement n° 1240579

Canadian Journal of Fisheries and Aquatic Sciences

Volume 59, Number 3, March 2002

Journal canadien des sciences halieutiques et aquatiques

Volume 59, numéro 3, mars 2002

ARTICLES

P. Apostolaki, E.J. Milner-Gulland, M.K. McAllister, and G.P. Kirkwood	**405–415**	Modelling the effects of establishing a marine reserve for mobile fish species
Kevin D.E. Stokesbury, Jay Kirsch, E. Vincent Patrick, and Brenda L. Norcross	**416–423**	Natural mortality estimates of juvenile Pacific herring (*Clupea pallasi*) in Prince William Sound, Alaska
Graham M. Pilling, Geoffrey P. Kirkwood, and Stephen G. Walker	**424–432**	An improved method for estimating individual growth variability in fish, and the correlation between von Bertalanffy growth parameters
Jon T. Schnute and A.R. Kronlund	**433–449**	Estimating salmon stock–recruitment relationships from catch and escapement data
Steven E. Campana, Lisa J. Natanson, and Sigmund Myklevoll	**450–455**	Bomb dating and age determination of large pelagic sharks
Franz J. Mueter, Randall M. Peterman, and Brian J. Pyper	**456–463**	Opposite effects of ocean temperature on survival rates of 120 stocks of Pacific salmon (*Oncorhynchus* spp.) in northern and southern areas
Andréa M. Weise, Maurice Levasseur, François J. Saucier, Simon Senneville, Esther Bonneau, Suzanne Roy, Gilbert Sauvé, Sonia Michaud, and Juliette Fauchot	**464–473**	The link between precipitation, river runoff, and blooms of the toxic dinoflagellate *Alexandrium tamarense* in the St. Lawrence
David J. Kelly and Max L. Bothwell	**474–482**	Avoidance of solar ultraviolet radiation by juvenile coho salmon (*Oncorhynchus kisutch*)
Rolf D. Vinebrooke, Sushil S. Dixit, Mark D. Graham, John M. Gunn, Yu-Wei Chen, and Nelson Belzile	**483–493**	Whole-lake algal responses to a century of acidic industrial deposition on the Canadian Shield
Björn Björnsson and Agnar Steinarsson	**494–502**	The food-unlimited growth rate of Atlantic cod (*Gadus morhua*)
Jack J. Piccolo and Mark S. Wipfli	**503–513**	Does red alder (*Alnus rubra*) in upland riparian forests elevate macroinvertebrate and detritus export from headwater streams to downstream habitats in southeastern Alaska?

Continued on inside back cover / Suite au verso

Canada

Printed in Canada by / Imprimé au Canada par
University of Toronto Press Inc.
Typesetting by / Typographie par
NRC Research Press / Presses scientifiques du CNRC

0706-652X(200203)59:3;1-G